

THE UNIVERSITY OF MICHIGAN  
INDUSTRY PROGRAM OF THE COLLEGE OF ENGINEERING

ANALYSIS AND DIGITAL SIMULATION OF CARBURETOR METERING

David L. Harrington

A dissertation submitted in partial fulfillment  
of the requirements for the degree of  
Doctor of Philosophy in  
The University of Michigan  
1968

December, 1968

IP-825

© David Lee Harrington 1968  
All Rights Reserved

## ACKNOWLEDGMENTS

I wish to express my appreciation to all of the members of the Doctoral Committee for their assistance and advice during this entire project. Special thanks are due to Professor Jay A. Bolt who provided leadership and inspiration in the course of countless project discussions. I also owe special thanks to Dean Gordon Van Wylen for his special support and counsel.

The financial support of the United States Public Health Service is gratefully acknowledged. Without this support, this project could not have been completed. The financial support of the Cummins Engine Co., through their Fellowship in the Mechanical Engineering Department, is also appreciated.

The assistance of Mr. Stephen Derezinski in obtaining accurate flow model data is greatly appreciated. In addition, his numerous comments and suggestions were invaluable in developing the over-all simulation program.

Acknowledgment is also made of the assistance given by Mr. Robert Olree, now of the Ethyl Corporation, in instrumenting and obtaining engine test data.

Thanks is also due to the various carburetor groups of the Ford Motor Company for providing numerous test carburetors, specification sheets, and road load curves.

The valuable assistance of Mrs. Joan Neagli and Miss Ruth Howard in preparing the original manuscript is gratefully acknowledged.

Thanks is also due to the personnel of the Office of Research Administration at The University of Michigan for their assistance in preparing this document.

## TABLE OF CONTENTS

	PAGE
LIST OF TABLES	viii
LIST OF ILLUSTRATIONS	x
NOMENCLATURE (non-computer)	xv
CHAPTER	
I INTRODUCTION	1
A. General	1
B. Reasons for Developing the Simulation	3
C. Overall Scope and Limitations of the Simulation	5
D. Brief Description and Goals of the Simulation	8
II. THEORETICAL ANALYSIS OF COMPRESSIBLE MIXTURE FLOW	11
A. Background	11
B. Mathematical Model of the Compressible Flow Path	15
C. Thermodynamic Properties of the Compressible Mixture	18
D. Throttle Plate Flow	21
E. Analysis of Total Mixture Flow and Engine Parameter Effects	25
F. Analysis of Compressible Flow Through Multiple Venturii	44
G. Analysis of Fuel Atomization and Spray Vaporization	50
III. FUEL FLOW THROUGH ORIFICES	66
A. Reasons for Orifice Flow Work	66
B. Background	67
C. Analysis and Correlation of Orifice Flow	76
D. Correlation of Fuel Properties	86
E. Results of Orifice Flow Bench Tests	90
F. Application of Orifice Coefficient Data to Actual Flow Situations	106

TABLE OF CONTENTS (continued)

	PAGE
IV. THEORETICAL ANALYSIS OF FUEL AND AIR BLEED FLOW	116
A. Background	116
B. Fuel Channel Model	121
C. Criteria for Solution	124
D. Pressure Losses in Fuel Channel Elements	127
E. Fuel Channel Iterative Technique	137
V. ENGINE AND VEHICLE ANALYSIS	142
A. Reasons for Relating The Engine and Vehicle to the Carburetor	142
B. Requirements For Road Load Carburetor Analysis	143
C. Vehicle Road Load Relationships	144
D. Correlation and Prediction of Engine Performance	148
E. Summary of Engine Data Correlation Technique	161
F. Iterative Technique For Obtaining Road Load Operating Points	164
VI. ON-ENGINE CARBURETOR TESTS	167
A. Reasons for Tests	167
B. Background	168
C. Experimental Equipment and Conditions	171
D. Carburetor Performance Over The Entire Operating Range	177
E. Special Experimental Programs	188
1. Suction profiles within the boost venturi	188
2. High speed movies of fuel discharge	190
3. Transient and pulsating flow study	195

TABLE OF CONTENTS (continued)

		PAGE
VII.	LUCITE FUEL CHANNEL MODEL TESTS	206
	A.    Reasons for Fuel Channel Model Tests	206
	B.    Lucite Fuel Channel Model	206
	C.    Flow Model Test Stand	211
	D.    Advantages of Using the Flow Model and Test Stand	216
	E.    General Test Techniques and Conditions	217
	F.    Results of Fuel Channel Flow Tests	221
	G.    Two-Phase Flow Observations	239
	H.    Comparison With Predictions of Subroutine FLOW	243
VIII.	OPERATION OF THE COMPLETE SIMULATION	246
	A.    General Description	246
	B.    Required Input Data	248
	C.    Basic Iterative Scheme	251
	D.    Carburetor Analysis At Constant Engine Speed or Constant Throttle Angle	255
	1.    Simulation predictions	255
	2.    Carburetor - engine operating map	260
	3.    Accuracy of the simulation predictions	262
	4.    Available computer plots	263
	E.    Carburetor Analysis At Road Load Operating Conditions	268
	F.    Carburetor Analysis With Production Variations In Dimensions	274
	G.    Auxiliary Subroutine Printouts	280
	H.    Computer Times Required	282
IX.	APPLICATIONS OF THE COMPLETE CARBURETOR SIMULATION	283
	A.    General Applications	283
	B.    Single Variable Effects	283
	C.    Additional Applications	284
	D.    Examples of Single Variable Effects	285

TABLE OF CONTENTS (continued)

	PAGE
X. RECOMMENDATIONS	296
APPENDICES	
A. ADDITIONAL SIMULATION PREDICTIONS	298
B. THROTTLE FLOW AREA	304
C. IDLE NEEDLE FLOW AREA	311
D. THERMODYNAMIC PROPERTIES OF AN AIR, WATER VAPOR, AND FUEL VAPOR MIXTURE	314
E. EXPLANATION OF SUBROUTINES	319
F. MULTI-PURPOSE INTERPOLATION SUBROUTINE	326
G. GENERAL CONVERGENCE TECHNIQUE	330
H. ANALYTICAL PREDICTION OF FUEL VAPORIZATION WITHIN THE CARBURETOR	333
I. LISTING OF MAIN COMPUTER PROGRAM	340
J. LISTING OF SUBROUTINES	363
K. ADDITIONAL FLOW MODEL CURVES AND DATA UTILIZED WITHIN THE SIMULATION	407
L. EXPLANATION OF SYMBOLS USED IN THE SIMULATION	417
BIBLIOGRAPHY	439

## LIST OF TABLES

TABLE	TITLE	PAGE
I.	Specifications of Test Orifices	92
II.	Computed Results For A Typical Flow Bench Test	94
III.	Orifice $C_d$ Data Used In The Simulation	105
IV.	The Percentage Of The Static Pressure Differential That Is Irrecoverable	112
V.	Head Loss Values For Non-Uniform Flow	133
VI.	Fuel Channel Analysis Results	140
VII.	Equipment Utilized in On-Engine Carburetor Tests	172
VIII.	Ranges Of Variables In Carburetor Tests	176
IX.	Reduced Data For On-Engine Carburetor Tests At Constant Engine Speed And Variable Throttle Angle	178
X.	Reduced Data For On-Engine Carburetor Tests At Constant Throttle Angle And Variable Engine Speed	181
XI.	Listing Of Fuel Channel Flow Tests	218
XII.	Typical Data Sheet For A Lucite Fuel Channel Flow Test Using Gasoline	222
XIII.	Reduced Data For A Lucite Fuel Channel Flow Test With Air Bleeds	224
XIV.	Reduced Data For A Lucite Fuel Channel Flow Test Without Air Bleeds	225
XV.	Required Input Data	249
XVI.	Simulation Predictions For A Constant Engine Speed - Variable Throttle Angle Analysis	256
XVII.	Simulation Predictions For A Constant Throttle Angle Analysis (Closed Throttle)	258



## LIST OF TABLES (continued)

TABLE	TITLE	PAGE
XVIII.	Simulation Predictions For A Constant Throttle Angle Analysis (26°)	259
XIX.	Simulation Predictions For Carburetor Operation At Road Load Conditions	270
XX.	Engine Input Data For Road Load Analysis	271
XXI.	Vehicle Input Data For Road Load Analysis	272
XXII.	Simulation Predictions For The Effects Of Production Tolerances On Carburetor Performance	276
XXIII.	Computer Prediction Of Main And Boost Venturi Parameters	281
XXIV.	Required Computer Times (Approximate)	282
XXV.	Simulation Predictions For Carburetor Performance at Altitude	286
XXVI.	Simulation Predictions For Carburetor Performance With Reduced Ambient Temperature	292
XXVII.	Simulation Predictions For The Effects of Production Tolerances on Carburetor Performance (Ford C4AFB-91 Carburetor)	300
XXVIII.	Reduced Data For A Lucite Flow Model Test Using Hot Mineral Spirits	408
XXIX.	Reduced Data For A Lucite Flow Model Test Using Cold Mineral Spirits	409
XXX.	Specifications and Experimental Values For A Typical Test Carburetor	413
XXXI.	Viscosity Conversions Utilized in The Simulation	415
XXXII.	Constants Utilized In The Simulation	416

## LIST OF ILLUSTRATIONS

FIGURE	TITLE	PAGE
1	Basic Model of the Compressible Flow Path	17
2	Computer Model of the Compressible Flow Path	19
3	Throttle Plate Discharge Coefficient Values	24
4	Illustration of Local $P_o$ and $T_o$ Values	29
5	Simultaneous Solution of Exhauster and Nozzle Equations	40
6	Computer Model Parameters for Boost Venturi	47
7	Methods of Illustrating Drop Size Distributions	53
8	Drop Size Distribution with Two Preferential Sizes	58
9	Illustration of Drop Vaporization Regimes	61
10	Variation in Ultimate $C_d$ with L/D Ratio	73
11	Boundary Layer Development within an Orifice	77
12	Ideal Flow in an Orifice	79
13	Nomenclature for Common Orifice Types	83
14	Iso-Octane Property Variations with Temperature	89
15	Specific Gravity Variations of Test Fuels	89
16	Schematic Diagram of Orifice Flow Bench	91
17	Gasoline Flow Rate vs. Pressure Drop for F-50 Orifice	96
18	$C_d$ vs. Pressure Drop for F-50 Orifice	97
19	Characteristic Discharge Coefficient Curve for F-50 Orifice	99

LIST OF ILLUSTRATIONS (continued)

FIGURE	TITLE	PAGE
20	The Effect of Fluid Type on the Discharge Coefficient	100
21	The Effect of L/D Ratio on the Orifice Characteristic Curve	102
22	Pressure Variations in the Vicinity of An Orifice	108
23	Typical Fuel Channel Geometry Near Air Bleed Well	119
24	Computer Model of Complete Carburetor Fuel Channel	121
25	Nodal Points in the Fuel Channel Flow Network	124
26	Total and Static Pressure Variations Within a Simple Fuel Channel	128
27	Dependence of the Engine IHP on the Air Mass Flow Rate	150
28	Slope of the IHP Curve as a Function of Fuel-Air Ratio	152
29	Constant Air Flow Curves for Varying Fuel-Air Ratios	154
30	Three-Dimensional Operating Surface for an Engine	155
31	FMEP Variations with Engine Speed and Intake Manifold Vacuum	159
32	Applications of Constant Air Mass Flow Rate Curves	163
33	Equipment Utilized in On-Engine Carburetor Tests	174
34	Equipment Utilized to Control and Monitor Carburetor Variables	175
35	Variations in Intake Manifold Vacuum With Throttle Angle and Engine Speed	182
36	Effect of Measured Air Flow Rate on The Metering Signal	184
37	Total Pressure Loss Through Venturi	185

LIST OF ILLUSTRATIONS (continued)

FIGURE	TITLE	PAGE
38	Brake Specific Fuel Consumption Curves For Various Engine Speeds	186
39	BSFC Variations At Constant Throttle Angle and Constant Engine Speed	187
40	Suction Distribution in Inches of Water Within A Typical Boost Venturi	189
41	Equipment Utilized in Obtaining High Speed Movies of Fuel Discharge	192
42	High Speed Photographs of Fuel Discharge Within The Boost Venturi - Low Fuel Flow	193
43	High Speed Photographs of Fuel Discharge Within The Boost Venturi - High Fuel Flow	194
44	Equipment Utilized in Obtaining Pressure - Time Traces Under Transient and Pulsating Conditions	196
45	Pressure Transients Within A Carburetor During A Sudden Throttle Opening	197
46	Pressure Transients Within A Carburetor During A Sudden Throttle Closing	198
47	Mean and Alternating Components of The Metering Signal At Various Operating Points	200
48	Waveforms For The Boost Venturi Suction And Main Metering Orifice Pressure Drop For Highly Pulsating Air and Fuel Flow	201
49	Effective Metering Signal For Pulsating And Steady Flow Conditions	204
50	Lucite Flow Model Of Complete Carburetor Fuel Channel	207
51	Cross-Section of Lucite Flow Model	209

LIST OF ILLUSTRATIONS (continued)

FIGURE	TITLE	PAGE
52	Flow Model Test Stand	210
53	Relative Position of The Lucite Flow Model On The Test Stand	212
54	Schematic Flow Diagram Of Fuel Channel Model Test Stand	214
55	Manometer Bank Utilized To Obtain The Static Pressure Distribution With The Fuel Channel	220
56	Experimental Values of Gasoline Flow Rate As A Function Of The Metering Signal	227
57	Log-Log Plot Of Total Gasoline Flow Rate Versus The Metering Signal	228
58	Measured Air Bleed Flow Rate As A Function Of The Metering Signal	230
59	Mass Flow Rate Of Cold Gasoline As A Function Of The Metering Signal	231
60	The Effect Of Numerous Operating Variables On The Mass Flow Rate of Mineral Spirits	233
61	The Effect Of Fluid Temperature On The Mass Flow Rate of Mineral Spirits	234
62	Illustrations Of The Rapid Change In The Main Channel Discharge Coefficient At Small Metering Signals	236
63	Air Bleed Flow Rate Variations For One And Two Operating Bleeds	237
64	The Effect Of Fluid Temperature On The Air Bleed Mass Flow Rate	238
65	High Speed Photographs Of Two-Phase Flow Within The Lucite Model	240
66	Total Pressure Loss Variations For Two-Phase Flow Within The Carburetor	242

LIST OF ILLUSTRATIONS (continued)

FIGURE	TITLE	PAGE
67	Comparison Of The Flow Rate Predictions Of Subroutine FLOW With Actual Fuel Channel Data	244
68	General Procedure Utilized In The Basic Iterative Scheme	252
69	Carburetor - Engine - Vehicle Operating Map	261
70	Predicted Fuel-Air Ratio Variations	265
71	Predicted Main Fuel Flow Rate Variations	266
72	Carburetor - Engine - Vehicle Operating Map With Expanded Scale	267
73	Predicted And Experimental Road Load Fuel Economy Values	273
74	Carburetor - Engine - Vehicle Operating Map At Altitude	290
75	Carburetor - Engine - Vehicle Operating Map For Reduced Ambient Temperature	295
76	Simulation Predictions Of Main Fuel Flow Rates	299
77	Variables In The Throttle Plate Flow Analysis	305
78	Idle Needle Flow Area Variables	312
79	Sample Difference Table Using Actual Square-Edged Orifice Data	327
80	Illustration Of The Newtonian Iteration Technique	330
81	Illustration Of Generalized Convergence Technique	331
82	Fuel Mass Flow Rate As A Function Of The Main Metering Orifice Pressure Differential In The Lucite Flow Model	410
83	Main Fuel Channel Discharge Coefficient Curve	411
84	Mass Flow Rate Of Hot Test Fluid Within The Lucite Flow Model	412

## NOMENCLATURE

### SYMBOLS (NON-COMPUTER)

A	=	Area
C	=	General constant
$C_d$	=	Discharge coefficient
$C_p$	=	Constant pressure specific heat
$C_v$	=	Constant volume specific heat
CC	=	Vena contracta coefficient
CR	=	Engine compression ratio
d	=	Throttle shaft diameter
D	=	Diameter or engine speed
$D_v$	=	Mass diffusion coefficient
E	=	Error
f( )	=	General functional relationship
$f_d$	=	Darcy friction factor
$g_c$	=	Mass conversion factor
h	=	Fuel hydrostatic head
H	=	Enthalpy of combustion
$\bar{H}_c$	=	Lower heating value of fuel
K	=	Specific heat ratio
$K^*$	=	Cavitation number
$K_L$	=	Head loss factor
L	=	Length
m	=	Mass

## NOMENCLATURE (continued)

$\dot{m}$	=	Mass flow rate
$M$	=	Mach number
$n$	=	Number of moles
$N$	=	Engine speed
$N_c$	=	Number of engine cylinders
$N_{cb}$	=	Number of cylinders per carburetor barrel
$N_{cyc}$	=	Number of strokes in an engine cycle
$N_{th}$	=	Number of threads per inch on idle needle
$N_u$	=	Nusselt number
$P$	=	Pressure
$q$	=	Moment of the drop size distribution
$\dot{q}$	=	Volume flow rate
$R$	=	Gas constant
$\bar{R}$	=	Universal gas constant
$R_e$	=	Reynolds number
$S_c$	=	Schmidt number
$t$	=	Time
$T$	=	Temperature
$V$	=	Velocity
$V_s$	=	Swept volume of engine cylinder
$W$	=	Molecular weight
$x$	=	Drop diameter or a general abscissa variable
$\bar{x}$	=	Mean drop diameter



## NOMENCLATURE (continued)

$\bar{x}_{vs}$	= Sauter mean drop diameter
$y$	= Mole fraction or a general ordinate variable
$z$	= Distance traveled by a fuel drop
$Z$	= General error parameter
$\alpha$	= Included angle of idle needle screw, or interpolation argument parameter
$\beta$	= Expansion ratio of venturi
$\delta$	= Air compressibility factor, or Sterling's divided difference
$\epsilon$	= Iterative error or surface roughness
$\Delta$	= Finite increment
$\theta$	= General throttle plate angle
$\theta_0$	= Completely closed throttle plate angle
$\eta$	= Vehicle drive train efficiency
$\phi$	= Relative humidity
$\Omega$	= Bend radius to channel radius ratio
$\rho$	= Density
$\psi$	= Pulsation factor
$\nabla$	= Surface tension or standard deviation of dimensions
$\Sigma$	= Summation
$\mu$	= Absolute viscosity
$\nu$	= Kinematic viscosity
$\omega$	= Mass ratio of water vapor to air

## NOMENCLATURE (continued)

### SUBSCRIPTS

a	=	Air
amb	=	Ambient
b	=	Air bleed system
cl	=	Clearance volume
corr	=	Corrected to zero approach velocity
e	=	Enrichment system
f	=	Fuel
fa	=	Fuel and air
$\text{h}_2\text{O}$	=	Water
i	=	Inlet or $i^{\text{th}}$ component or idle system
j	=	Main metering orifice (jet) flow
l	=	Local
m	=	Main system
man	=	Intake manifold
mix	=	Mixture of air, fuel vapor, and water vapor
n	=	Idle needle or normalized distribution
o	=	Stagnation conditions
r	=	Residual gases
rel	=	Relative
s	=	Static or surface
surf	=	Drop surface
surr	=	Surroundings

## NOMENCLATURE (continued)

t	=	Total flow or total (stagnation) conditions
th	=	Venturi throat
v	=	Fuel vapor
$v_{\infty}$	=	Fuel vapor at infinity
1	=	Fuel vapor or orifice approach channel
2	=	Air or orifice
3	=	Water vapor
$\nabla$	=	Surface tension
$\infty$	=	Infinity

## ABBREVIATIONS

A/F	=	Air-fuel ratio
BHP	=	Brake horsepower
BMEP	=	Brake mean effective pressure
BSFC	=	Brake specific fuel consumption
$^{\circ}\text{C}$	=	Degrees Centigrade
cm	=	Centimeter
R-55	=	Rochester main metering orifice of 0.055 inch diameter
cps	=	Cycles per second
$^{\circ}\text{F}$	=	Degrees Fahrenheit
FHP	=	Friction horsepower
FMEP	=	Friction mean effective pressure
F/A	=	Fuel - air ratio
F-50	=	Ford main metering orifice of 0.050 inch diameter

## NOMENCLATURE (continued)

ft	=	Feet
gm	=	Grams
in	=	Inches
IHP	=	Indicated horsepower
IMEP	=	Indicated mean effective pressure
ISFC	=	Indicated specific fuel consumption
lbf	=	Pound force
lbm	=	Pound mass
MPG	=	Miles per gallon
MPH	=	Miles per hour
psi	=	Pound force per square inch
psia	=	Pound force per square inch absolute
RPM	=	Engine revolutions per minute
$^{\circ}$ R	=	Degrees Rankine
S-E	=	Square-edged orifice
SG	=	Specific gravity
TORQB	=	Brake torque
TORQF	=	Friction torque
TORQI	=	Indicated torque
VACMAN	=	Intake manifold vacuum

## CHAPTER I

### INTRODUCTION

#### A. GENERAL

The modern carburetor is a complex assembly of subsystems, each with its specific function. The simple "ideal carburetor" as presented for analysis in textbooks bears little resemblance to the true hardware in either theory or operation. The theoretical analysis of carburetors is, in the case of textbooks, so greatly oversimplified that the resulting equations are of little or no value in predicting the operation of an actual carburetor. Even the published papers and theses in the field are very restrictive in terms of the assumptions made. These include:

1. assuming incompressible air flow
2. assuming constant coefficients of discharge for all orifices
3. ignoring viscous pressure losses in the fuel channels
4. ignoring the presence of the throttle plate and shaft
5. ignoring enrichment and idle systems
6. neglecting air bleed systems
7. ignoring engine parameter effects
8. ignoring heat and mass transfer effects in the vaporization of the fuel droplets.

In addition, the simplified analyses invariably predict a carburetor parameter such as total fuel flow as a function of air flow. This ignores the fact that any air flow is the result of a certain engine speed and throttle opening, and that there are an infinite number of combinations of the two which will give a specified air flow. Each combination will have a different intake manifold vacuum and thus a different total fuel flow. Therefore the simplified analyses are quite erroneous in assuming that if a total air flow is specified, the other carburetor parameters can be obtained. This concept has its corollary in the standard carburetor flow box test. This test presents the fuel-air ratio as a function of air flow and would seem to convey the fact, as mentioned above, that the fuel flow is fixed for a given value of air flow. This error is the result of neglecting the infinite number of engine speed-throttle opening combinations. As will be shown later, an accurate, comprehensive carburetor simulation must include, in addition to many other items, the interrelationships between the carburetor and the engine.

In the past, the theoretical analysis of carburetor operation has been hampered by the fact that closed form solutions were sought. An example of this type of solution is:<sup>70\*</sup>

$$F/A = \frac{A_{jet} C_{jet}}{A_{ven} C_{ven}} \sqrt{\frac{\rho_{fuel}}{\rho_{air}}}$$

The closed form solutions are obviously easy to work with but it should be evident that, in order to obtain a closed form equation describing a process which involves many interacting variables, a large number of

---

\* Superscript numbers refer to listings in the bibliography (Pages 439-444).

simplifying assumptions must be made. However, if the numerous complex relationships describing each variable are utilized in an iterative solution, numerical values may be obtained without oversimplifying.

The analogy to this is the solution of an  $n^{\text{th}}$  degree polynomial equation. For small  $n$ , closed form algebraic solutions of a general nature can be obtained, (such as the familiar quadratic formula) but for large  $n$  this becomes impossible. Yet numerical values can be obtained for large  $n$  by iterative techniques.

## B. REASONS FOR DEVELOPING THE SIMULATION

Most of the simplifying assumptions mentioned above were made because little is known of the complex interactions within and between carburetor systems. Thus, the analyses based on these assumptions yield predictions which do not correlate well with actual carburetor data. Therefore, one of the important reasons for developing a comprehensive simulation is to understand the complex phenomena that are known to occur during the operation of the carburetor. For example, it is known that carburetors deliver a richer mixture as altitude increases and as fuel temperature is decreased.

Almost every other carburetor variable from the main metering jet diameter to the throttle plate shaft diameter will affect the mixture ratio delivered to the engine. Since the fuel-air ratio is one of the most important variables in internal combustion engine work, accurate metering is extremely important. Numerous other variables, such as engine thermal

efficiency, unburned hydrocarbon emission, maximum brake mean effective pressure, rate of pressure rise, and dissociation losses are greatly influenced by this ratio. Many practical problems in internal combustion engine work, such as combustion instability under lean operation can be traced to variations in metering the fuel to the air. Also, the growing importance of the vehicle air pollution problem has given new and urgent incentives to improve all aspects of automotive carburetor and induction system performance. Foremost among these incentives is the desire for more precise carburetor metering under all engine and ambient conditions. This can only be accomplished if the metering processes are analyzed and understood more completely.

Another incentive for developing the carburetor simulation is based on economic considerations. If it is considered that millions of carburetors are manufactured annually and are used to meter billions of gallons of fuel, then the possible economic gain through more precise metering becomes evident. Another economic factor is related to the fact that there is still a great deal of art inherent in the design of carburetors. It is generally conceded that a great deal of practical carburetor experience and system prototype testing are required in the development of a new carburetor. In fact Stoltman<sup>52</sup> made the statement in a recent paper that ". . . . .the carburetor has more engineering hours per cubic inch than the majority of automotive components." This trial and error design, construction, and testing is expensive and time consuming, and the more



evaluation that is done by computer analysis, the less will be the trial and error design cost.

This points up the final reason for developing a comprehensive simulation and that is; to provide the engineer with an evaluation tool. If the simulation is accurate enough to replace some of the prototype construction and testing, the engineer can rapidly evaluate numerous proposed designs and can discard those that are unsuitable before they are constructed. Coupled with rapid computer plotting, the entire range of variables could be investigated and the simulation could be used to optimize systems and determine the effect of variables which would be too expensive to determine by actual test. An example of this might be; the effect of the fuel channel dimensional tolerances on the fuel-air ratio spread among hundreds of carburetors.

### C. OVERALL SCOPE AND LIMITATIONS OF THE SIMULATION

The purpose of this thesis was to perform a theoretical analysis of an actual carburetor, analyzing each system and phenomenon in terms of the fundamentals of fluid mechanics and thermodynamics and to combine these analyses into a comprehensive digital computer simulation. As few simplifying assumptions as possible were made and the following quantities were analyzed and incorporated into the simulation:

1. variations in ambient pressure, temperature, and humidity.
2. a fuel flow network containing main, idle, and a vacuum sensitive enrichment system.
3. variations in fuel specific gravity, viscosity, surface tension, and molecular weight with fuel type and temperature.
4. compressible flow of an air, fuel vapor, and water-vapor mixture through a primary and boost venturi in parallel.
5. variation in orifice coefficients of discharge with orifice type, L/D ratio, flow rate, and fuel properties.
6. effects of multiple air bleeds in both main and idle systems.
7. variations in operation due to mating with different engines and vehicles.
8. multiple passages which allow air to bypass the throttle plate.
9. flow of a wet mixture across a throttle plate (variable geometry throat) with a finite shaft size.
10. atomization of the fuel at discharge and vaporization of the fuel droplets in the air stream.

For reasons of maximum applicability and program readability, the simulation was written in the language most familiar to engineering groups in the industry, FORTRAN II. This was thought by the author to be a consideration outweighing the greater flexibility and ease of programming of FORTRAN IV and MAD. (The CALCOMP plotting subroutine is, however, written in the MAD language as will be seen later.) Although more statements are required to accomplish a given task in FORTRAN II

than in the newer, more flexible languages, it was the author's opinion that user adaptation should prevail over ease of programming.

The simulation was written for an air-bled, boost venturi carburetor with an enrichment valve which is sensitive to intake manifold vacuum. Each component of the compressible mixture (air, water vapor, and fuel vapor) was assumed to be an ideal gas and the equations describing the dynamics and thermodynamics of the compressible mixture were obtained by assuming one-dimensional, steady flow. (A pulsation parameter will be discussed later). Thus the simulation is not intended for transient air or fuel flow conditions such as occur with sudden throttle openings and closings or rapid engine speed increases or decreases. The fuel channel flow was analyzed on the basis of steady, incompressible flow in a branching network. Since no correlations existed for two-phase flow through orifices and since the standard two-phase pipeline pressure drop correlations gave very erroneous predictions, the air bleed system pressure drop was based on the average velocity of the fuel-air mixture foam in the passages. This velocity was based on the relative proportions of fuel and air by volume in each passage.

The simulation as written is essentially a comprehensive analysis of a carburetor barrel containing a primary and a secondary (boost) venturi. No air cleaner or choke is included, but as will be seen later, these devices could be included quite easily if desired, since their function can be described simply by a reduction in the incoming stagnation pressure.

In addition, the simulation as written is for two main fuel system air bleeds and two idle system air bleeds. However, as will be explained more fully in chapter eight, the program is flexible enough to account for variations in these numbers by a change in the input data. Many of the computer runs were for input data corresponding to a two-barrel carburetor with two main metering jets, because a significant portion of the experimental data used to verify the simulation accuracy was taken on carburetors of this type.

#### D. BRIEF DESCRIPTION AND GOALS OF THE SIMULATION

For a specified carburetor geometry, fuel, ambient conditions, engine, and vehicle, an analysis is made of the interactions between the various systems (taking into account the 10 items mentioned earlier) and values for nearly all important operating variables are calculated.

One of the most important goals of this simulation was to accurately predict, for any carburetor geometry, fuel type, fuel temperature, ambient conditions, engine, vehicle, and operating point, most of the significant carburetor, engine, and vehicle variables.

Some of these variables are:

1. total engine air flow
2. main system fuel flow
3. idle system fuel flow
4. enrichment system fuel flow
5. main and idle system air bleed flow

6. intake manifold pressure
7. boost and primary venturi signals
8. road load intake manifold pressure and throttle angle
9. vehicle miles per gallon
10. engine bhp, ihp, bsfc, and isfc

The road load and vehicle parameters were incorporated into the simulation because one of the original goals of the simulation was to analytically relate the carburetor, engine, and vehicle variables and to provide for computer evaluation of carburetor operation on a road load basis. This expands the usefulness and applicability of the simulation enormously. For example, any carburetor parameter can be varied over its limits and its effect on the road load miles per gallon predicted. The method of obtaining the large amount of engine data needed and the method of analytically predicting the road load throttle angle and air flow will be discussed in detail later.

Another goal of the simulation was to arrange the resulting computer predictions in such a way that many trial and error design tests could be eliminated. In other words, to have the computer predict the results of the test just as if it had been performed. This is applicable in many cases such as flow box tests and proving ground mileage tests where definite quantities are measured and recorded, but tests involving such subjective variables as "driveability" can obviously not be eliminated. However,

if the simulation is to eliminate a trial and error design test, it must produce as its output the accurately predicted values for all of the variables which would have been determined in the test. Also, if it is to evaluate any or all possible carburetor-engine-vehicle operating points, it must predict or calculate from the engine and vehicle input data nearly all the significant engine and vehicle parameters along with the carburetor values. This includes all the items listed on the previous page.

Thus the simulation and the computer plotting were developed with carburetor design and application in mind; that is, to assist the engineer in answering the inevitable questions which arise in design and operation:

1. How will a change in parameter "A" affect parameter "B"?
2. How will the operating variables such as ambient or fuel temperature affect the overall performance of the carburetor?
3. How will a particular carburetor design perform on a particular engine or engine-vehicle combination?
4. How do variations in carburetor dimensions due to production tolerances affect the metering?

## CHAPTER II

### THEORETICAL ANALYSIS OF COMPRESSIBLE MIXTURE FLOW

#### A. BACKGROUND

The analysis of the compressible flow of air, water vapor, and fuel vapor is an extremely important part of the over-all simulation. This is because all later fuel flow calculations are dependent upon the pressure losses and metering signals obtained from the compressible flow analysis.

The literature which exists on compressible flow through carburetors is mainly experimental in nature. That portion which is analytical involves, for the most part, many simplifying assumptions which results in an inadequate description of actual carburetor behavior.

Dodson, Booth, and Metsger<sup>1</sup> experimentally investigated the metering signals produced by double venturii combinations of various geometries. An analysis of the throttle plate flow was not made nor was the compressible air flow related to engine operation. Variations in metering signal with altitude were obtained experimentally and an altitude enrichment was calculated. This was not done by actually flowing fuel into the boost venturi but by describing the fuel flow as;

$$\dot{m}_{\text{fuel}} = \text{Constant} \sqrt{\Delta P_{\text{boost}}}$$

This is an extremely simplified description of the fuel flow, thus the resulting extension of measured boost venturi suction to fuel flow rates could be significantly in error. The chief contribution of

this work was the determination of the effect of geometry on the metering signal of double venturii.

Rogowski<sup>9</sup>, and Taylor and Taylor<sup>70</sup> gave analyses of compressible mixture flow which are suitable as an introduction to carburetor metering but which involved too many simplifying assumptions to give an accurate prediction of carburetor performance. The analyses involved only a single venturi with no throttle plate. In addition, the compressible mixture properties were assumed to be constant rather than varying with mixture ratio. In addition, the independent variable was the total air flow rather than engine speed and throttle angle. The errors associated with this assumption were stated in chapter one.

A very thorough experimental evaluation of nozzle and venturi design parameters was given by Shaffer.<sup>50</sup> This work represented an optimization of a triple venturi design. Various diameters, lengths, and profiles of primary, secondary, and tertiary venturii were used with the goal of obtaining a large, stable metering signal. Complete venturi drawings and test data were given for each series. The metering signals were obtained with long hypodermic needles inserted in the direction of flow. Some of the important conclusions were:

1. The maximum signal occurred near the inside wall of the boost venturi.
2. The signal was relatively insensitive to axial location within the throat of the primary venturi.
3. The signal was sensitive to throttle opening for low air flow and large throttle openings.



4. The maximum signal multiplication for the final triple venturi arrangement was 6.4

A few of the references on compressible mixture flow were concerned with the very involved phenomenon of pulsating air flow. Prien<sup>8</sup> reported an experimental study to determine the effect of air pulsations on metering. The metering device was a single venturi and nozzle system which was connected to a CFR engine. Steady flow tests were performed by drawing air through the engine cylinder with the valves open. Data on venturi suction, fuel flow, and air flow were taken. The pulsating air flow was obtained both by motoring and firing the engine. The results showed that the fuel/air ratio remained constant with increasing air flow for the steady flow case and increased with engine rpm for the pulsating case. Due to the complexity of the problem, no theoretical explanation of the data was given.

Another discussion of the difficulties encountered in pulsating air flow was given by Earles.<sup>33</sup> The main consideration of this paper was the measurement of the instantaneous mass flow rate for various pulsation waveforms. The data were correlated approximately by dimensionless groups involving the frequency and amplitude of the pulsations.

The application of pulsating flow measurement to engine air flow determination was discussed by Fries, et al.<sup>2</sup> This work was concerned with experimental techniques, and the theoretical analysis of pulsating air flow was not discussed.

Literature surveys related to the compressible mixture flow in the carburetor and induction system were given by Mirsky and Bolt,<sup>5</sup> and Oppenheim and Chilton.<sup>7</sup> Mirsky and Bolt were concerned with surveying a broad range of subjects dealing with the induction process in a spark ignition engine while Oppenheim and Chilton were concerned with the more specific problem of surveying the literature on the measurement of pulsating flow.

Hwa<sup>4</sup> reported a study of compressible flow through double venturis. This involved an experimental as well as an analytical investigation of the metering characteristics of the system. A one-dimensional compressible flow analysis was used with the additional restrictions of constant thermodynamic properties and no total pressure loss across the system. The following equation was derived for the velocity at the secondary venturi throat in terms of the system variables:

$$V_t^2 = \frac{\left(\frac{2g_c P_i}{\rho_i}\right) \left(\frac{K}{K-1}\right) \left[1 - \left[\frac{P_{th}}{P_i}\right]^{\frac{K-1}{K}}\right]}{1 - \left(\frac{A_{th}}{A_i}\right)^2 \left(\frac{P_{th}}{P_i}\right)^{2/K}}$$

The system was examined analytically and experimentally for nine combinations of area ratio and for two expansion angles. The important conclusions were:

1. A secondary venturi gave a lower over-all pressure loss for the same metering signal.
2. The experimental metering signal multiplication rose rapidly with increasing air flow up to a value of 5.0 where it leveled off. This was in all cases lower than the theoretical values.

3. The actual mass flow rate through the secondary venturi was less than predicted for all area ratios tested.

The general problem of compressible flow through restrictions was discussed by Greenland.<sup>34</sup> He classified the various types of flow as venturi, smooth orifice, and sharp-edged orifice and derived typical flow equations for each type. Also shown were coefficient of discharge curves and pressure versus length diagrams for various types of nozzles.

Fundamental relationships providing a foundation for the analysis of compressible mixture flow in the carburetor were given by Shapiro.<sup>10</sup> This included the thermodynamic and fluid mechanics aspects of steady, one-dimensional, compressible flow under various conditions of total pressure and total temperature change.

The variations in the thermodynamic properties of air with temperature and pressure reported by Gerhart, et al.<sup>3</sup> indicate that, for the normal range of values encountered in the carburetor and induction system, the specific heats and specific heat ratio of the air can be considered constant. Also, the assumption of ideal gas behavior is seen to be very good over the pressure and temperature ranges encountered in carburetor work.

## B. MATHEMATICAL MODEL OF THE COMPRESSIBLE FLOW PATH

In order to accurately simulate the complex behavior of an actual carburetor, an accurate mathematical model of each system must be obtained. To be able to adequately predict the mixture flow rates,

pressures, temperatures, and Mach numbers within the carburetor, the geometric flow path of the compressible mixture must be described accurately. This means that each flow path in the actual carburetor must have its counterpart in the model. Thus, if the carburetor has multiple venturii and bypasses around the throttle plate, these must be accounted for in the model.

The basic model of the compressible flow path consists of two fixed geometry converging-diverging nozzles in parallel, and in series with a variable geometry converging nozzle. The operating conditions within this system of nozzles is controlled by a variable rate exhaustor acting on an outlet plenum. The back pressure on the system is related to the exhaustor flow and the throat area of the variable geometry nozzle. The correspondence of this model with the actual carburetor is as follows: (See Figure 1) The two fixed geometry converging-diverging nozzles correspond to the primary and secondary (boost) venturi in an actual carburetor. This type of nozzle was chosen because the pressure recovery or conversion from static to total pressure in the expanding portion of the venturi is very high in typical carburetors. This is related to the expansion angle of the nozzle which is generally small. The variable geometry converging nozzle corresponds to the throttle plate. The variable geometry feature was incorporated to account for the large variation in throttle flow area with throttle angle, and the converging nozzle was chosen as the model because laboratory tests verified that the pressure recovery downstream of the throttle plate was

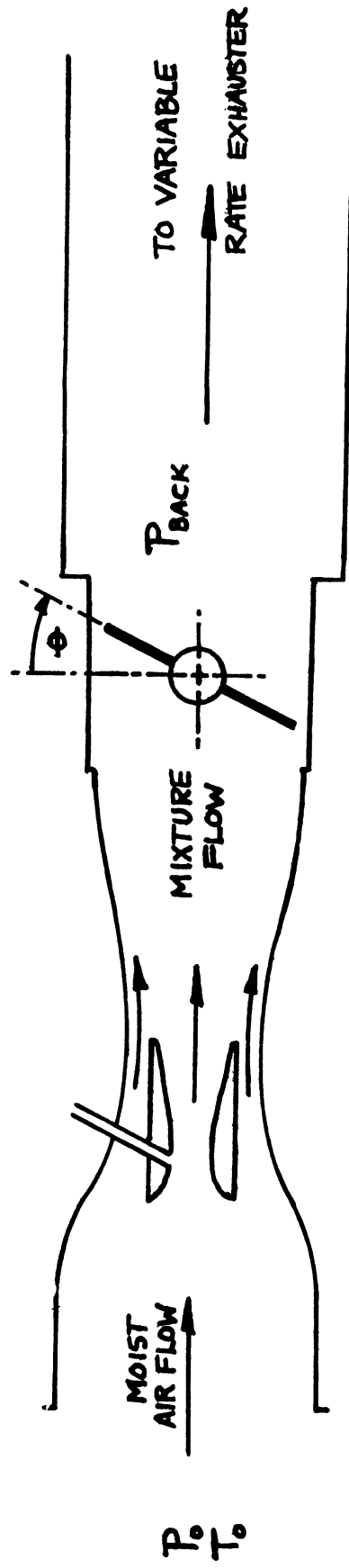


Figure 1. Basic model of the compressible flow path

very poor. This should be evident from the geometric arrangement of a typical throttle plate which is a complex sharp-edged restriction. The conversion of total to static pressure as the flow area decreases on the upstream side of the throttle plate is very good, but the expansion angle is much too great to permit good conversion of static to total pressure after the throttle plate minimum area. Thus the logical model is a converging nozzle with the throat area corresponding to the minimum throttle flow area. The plenum chamber corresponds to the intake manifold, and the back pressure acting on the nozzle system is the intake manifold pressure. The variable rate exhauster is the engine.

The basic model of the compressible mixture flow path is still inadequate for numerous reasons. These include the facts that bypasses exist around the throttle, fuel may be introduced at two places, and that the mixture properties are changing as it moves through the system. Thus the system must be divided into stations, which are the important points where areas must be calculated, pressures known, flow rates determined, or mixture properties evaluated. The numbering of these stations for the main venturi is shown in Figure 2. The boost venturi stations will be illustrated in Section 2-F.

### C. THERMODYNAMIC PROPERTIES OF THE COMPRESSIBLE MIXTURE

Any analysis of the compressible flow in carburetors will involve the thermodynamic properties of the mixture of air, water vapor, and fuel vapor. These properties include molecular weight, constant pressure and constant volume specific heats, and specific heat ratio. Since, in

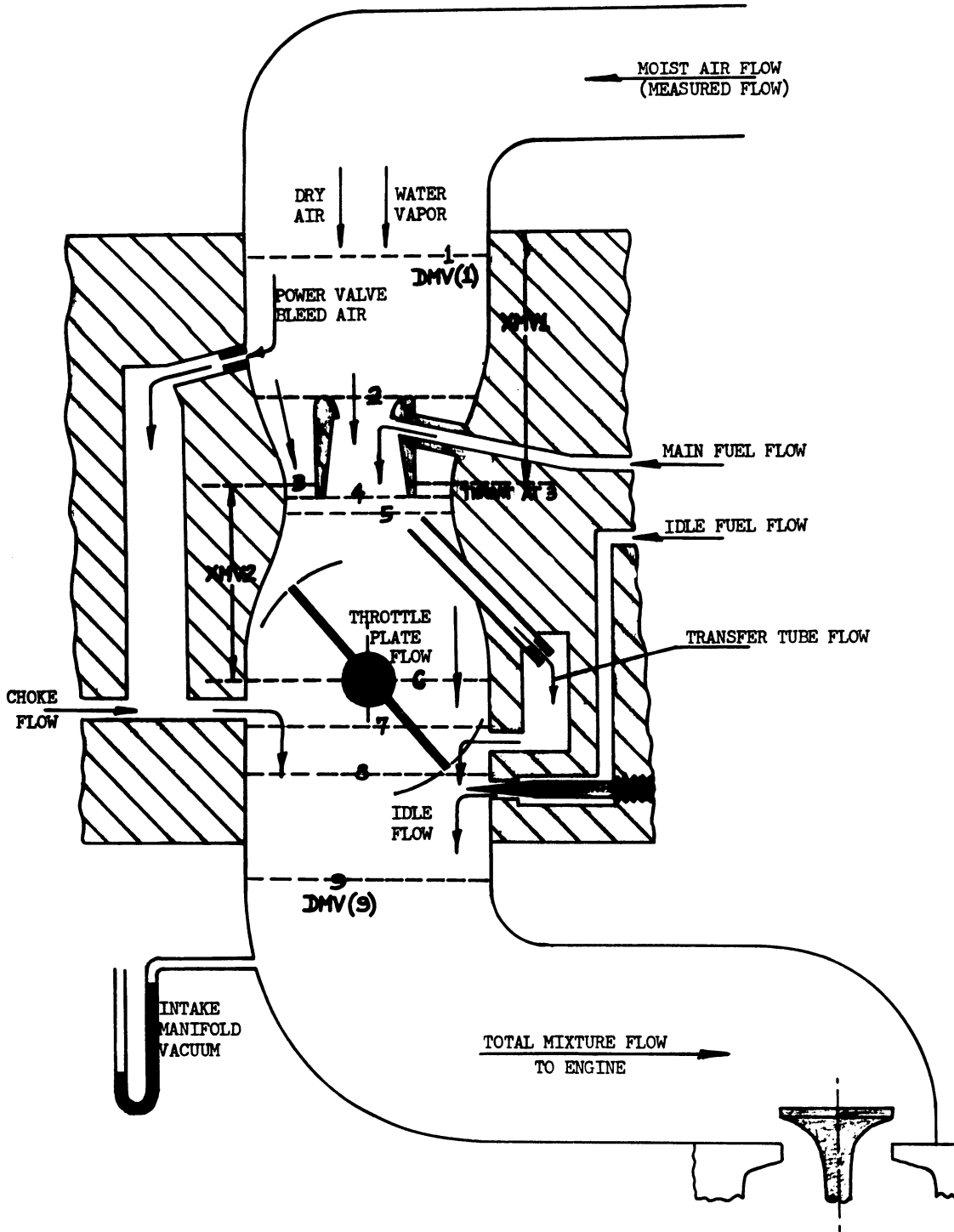


Figure 2. Computer model of the compressible flow path

general, the relative proportions of each component in the mixture will be changing as the mixture flows through the carburetor, general equations must be obtained for each property in terms of the individual component properties and the relative proportion of each in the mixture. This can be done by assuming that the mixture is composed of ideal gas components. Over the typical temperature and pressure ranges encountered in carburetors, this is an excellent assumption for the air. Also, since the partial pressures of the water vapor and fuel vapor in the mixture are almost always very low, the assumption of ideal gas behavior is justified for these components.

A complete derivation of the equations expressing the thermodynamic properties of the mixture is given in Appendix D. The final relationships in terms of the local fuel-air mass ratio ( $F/A$ ) and water-air mass ratio ( $\omega$ ) are:

Molecular weight  $W$ :

$$W_{\text{mix}} = \frac{1 + F/A + \omega}{\frac{F/A}{W_{\text{fuel}}} + \frac{1}{W_{\text{air}}} + \frac{\omega}{W_{\text{H}_2\text{O}}}} \quad \text{EQN 2.1}$$

Specific Heats :

$$C_p \text{ mix} = \frac{(C_p)_{\text{air}} + \omega (C_p)_{\text{H}_2\text{O}} + F/A (C_p)_{\text{fuel vapor}}}{1 + \omega + F/A} \quad \text{EQN 2.2}$$

$$C_v \text{ mix} = \frac{(C_v)_{\text{air}} + \omega (C_v)_{\text{H}_2\text{O}} + F/A (C_v)_{\text{fuel vapor}}}{1 + \omega + F/A} \quad \text{EQN 2.3}$$



Specific Heat Ratio:

$$K_{\text{mix}} = \frac{C_{p \text{ mix}}}{C_{v \text{ mix}}} = \frac{(C_p)_{\text{air}} + \omega (C_p)_{\text{H}_2\text{O}} + F/A \cdot (C_p)_{\text{fuel vapor}}}{(C_v)_{\text{air}} + \omega (C_v)_{\text{H}_2\text{O}} + F/A \cdot (C_v)_{\text{fuel vapor}}}$$

EQN. 2.4

It should be emphasized that the local values of  $W$  and  $F/A$  (at each station) are used to calculate the local thermodynamic properties.

#### D. THROTTLE PLATE FLOW

The throttle plate is an extremely important item in the compressible flow path. Under typical road load conditions about 95% of the total pressure loss occurs across the throttle plate. It usually provides the minimum flow area in the entire system although this area range is quite large, varying typically from about 0.010 to well over 1.0 square inches per barrel. This will obviously give a very large range in mixture flow rate through the throttle restriction.

As mentioned earlier, the model of the throttle plate was chosen to be a converging nozzle of varying throat area. This, however, creates the problem of calculating this flow area for any throttle plate and shaft size and for any throttle angle. There are four additional practical considerations which cannot be avoided in a comprehensive simulation.

These are:

1. The throttle plate shaft is almost always of significant diameter and must be considered.
2. To prevent binding in the throttle bore the throttle plate is, in most cases, completely closed at some angle to the

horizontal (usually 5 to 15°)

3. The coefficient of discharge of the throttle plate will be lower than that of a smoothly converging nozzle at the same pressure ratio. This coefficient will be a function of the throttle angle.
4. Due to the manufacturing tolerances involved, there is some minimum leakage area even at completely closed throttle. This leakage area becomes important at small throttle angles.

The above four considerations complicate the calculation of the throttle flow area and flow rate significantly, but ignoring them would result in an inaccurate simulation. In Appendix B, a complete analysis of the throttle flow area is given. This analysis includes 1 and 2 above and the following equation for the throttle flow area was obtained by evaluating an elliptic integral:

$$A_{\text{flow}} = \frac{\pi D^2}{4} \left[ 1 - \frac{\cos \theta}{\cos \theta_0} \right] + \frac{d}{2 \cos \theta} \sqrt{D^2 \cos^2 \theta - d^2 \cos^2 \theta_0} \\ + \frac{D^2 \cos \theta}{2 \cos \theta_0} \sin^{-1} \left[ \frac{d \cos \theta_0}{D \cos \theta} \right] - \frac{d}{2} \sqrt{D^2 - d^2} + \frac{D^2}{2} \sin^{-1} \left[ \frac{d}{D} \right]$$

EQN 2.5

where: d is the throttle shaft diameter  
 D is the throttle bore diameter  
 $\theta_0$  is the minimum closing angle  
 $\theta$  is the throttle plate angle

This complex relationship is easily evaluated as a computer sub-routine for any value of the parameters.

Item number 3 above was evaluated by actual engine tests. For numerous throttle angles, the values of air mass flow rate and pressure

ratio were determined with all throttle bypasses plugged. Equation 2.5 was used to calculate the throttle flow area corresponding to a given throttle angle. The coefficient of discharge was then calculated as the ratio of the actual flow rate to the ideal flow rate based on the flow area and pressure ratio. The throttle plate discharge coefficient values are shown in figure 3. Note that the discharge coefficient is lowest at the completely closed position as might be expected since the throttle plate is simply a sharp edged restriction. At greater throttle openings the coefficient rises, reaching a maximum at  $90^\circ$  from the horizontal, the point of minimum throttle turbulence. This data was incorporated into the simulation program and used to calculate accurate mass flow rate values for any operating point.

Item number 4 above was accounted for quite well by allowing  $\theta_o$ , the completely closed throttle angle, to be slightly smaller than the actual value. In other words, since there is some small leakage area  $A_1$  at the actual closed throttle angle, say  $5.0^\circ$ , then if we let  $\theta_o$  as used in the calculation be slightly smaller, (for example  $4.0^\circ$ ) then when the throttle angle is completely closed at  $5.0^\circ$ , the area calculated by equation 2.5 will be the actual leakage area. Thus what is needed is a relationship between  $(\theta_o)_{\text{actual}}$  and  $\theta_o$  as used in the program to accurately account for the leakage area. This relationship was determined empirically on the basis of measurements on numerous carburetors and is:

$$(\theta_o)_{\text{pseudo}} = (\theta_o)_{\text{actual}} - 3.800^\circ - 0.100(\theta_o)_{\text{actual}} \quad \underline{\text{EQN 2.6}}$$

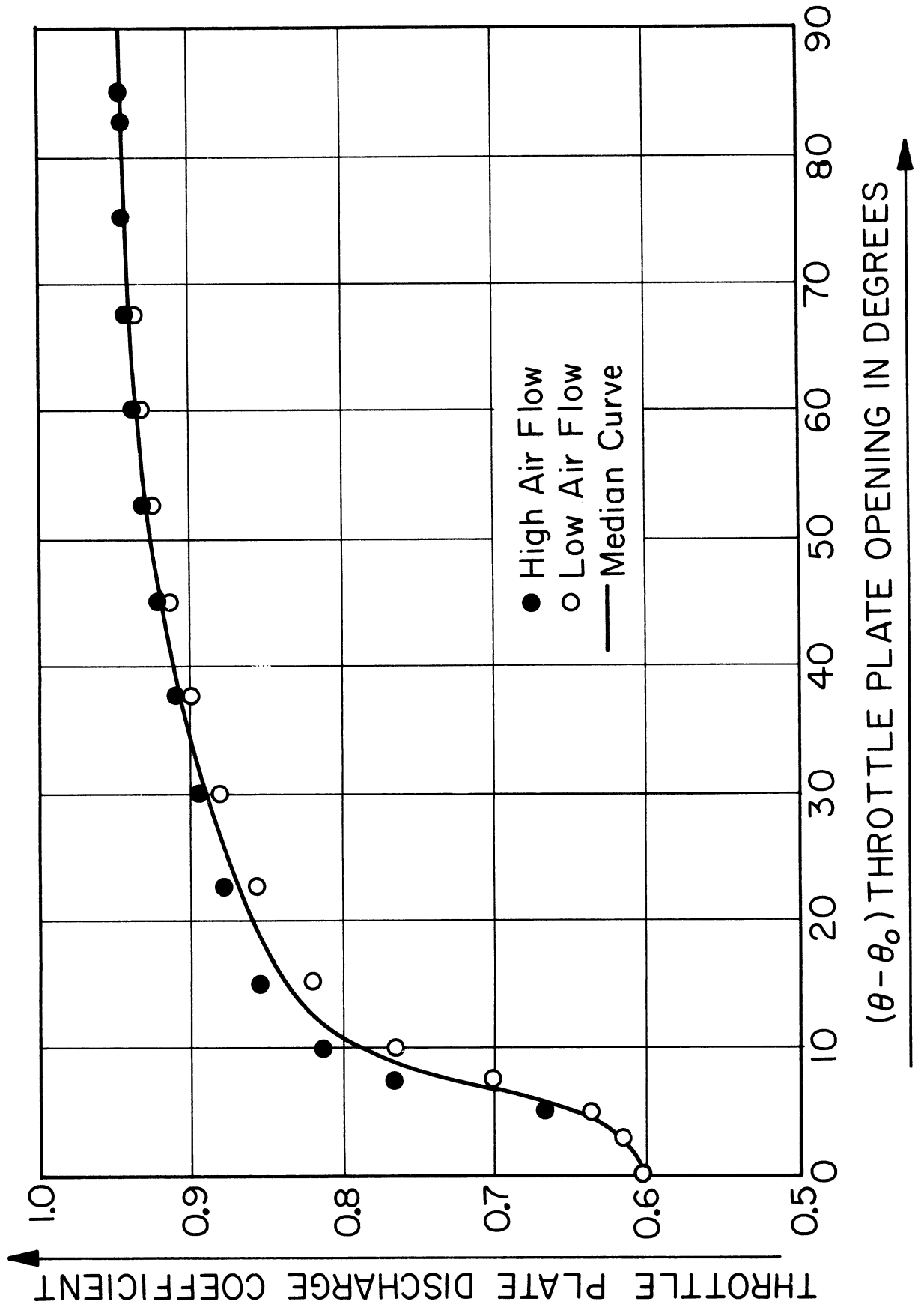


Figure 3. Throttle plate discharge coefficient values

This relationship is valid for completely closed throttle angles from  $5.0^{\circ}$  to  $15.0^{\circ}$ .

#### E. ANALYSIS OF TOTAL MIXTURE FLOW AND ENGINE PARAMETER EFFECTS

The flow of the compressible mixture in an actual carburetor is a very complex phenomena. The mass flow rate is determined by an engine volumetric flow rate and the density of the fuel-air mixture in the cylinder when the intake valve closes. This density is mainly a function of the ambient conditions, total pressure loss across the throttle plate, and the fuel-air ratio being delivered. Additional factors which affect this density are total pressure losses in the venturi section, air bypasses around the throttle, total pressure losses across the intake valve, heat addition in the intake manifold, and the mixing of hot residual exhaust gases with the incoming fuel-air mixture. The relative importance of these additional factors is directly related to the amount of throttling which occurs at the throttle plate. Thus, as will be shown in equation form later, the main variables determining the operating conditions in a carburetor are the engine volumetric flow rate and the amount of throttling present. This of course is directly related to the engine speed and throttle angle.

What are the goals in analyzing the compressible mixture flow and why is it of primary importance to the simulation? To answer this question one has only to consider the logical order of events in the actual carburetor: the mixture mass flow rate through the carburetor and

to the engine is established by engine speed and throttle angle (along with many secondary factors.) This flow rate is a value that will satisfy the throttle flow equations for the given area and pressure ratio, and will also satisfy the engine (exhauster) flow relationships. Once the total mixture mass flow rate has been calculated, the pressure distribution within the venturi section can be analyzed and the metering signals determined. Since the total fuel rate (the sum of the main and idle fuel flow rates) is a function of the boost venturi suction and the intake manifold vacuum, the following air flow parameters must be determined before any fuel rate interactions are performed.

1. Total air flow rate
2. Main venturi flow rate
3. Boost venturi flow rate
4. Venturi Mach numbers
5. Throttle plate Mach numbers
6. Intake manifold pressure
7. Boost venturi throat pressure

Thus the total mixture flow rate is given by the simultaneous (and iterative) solution of the flow equations for the throttle and the engine. General relationships will now be derived which describe the flow in each element. The physical meaning of these equations is as follows: The relationships describing the throttle plate flow correspond to flow at constant engine speed and variable throttle angle. That is, the exhauster conditions are fixed and the minimum area of the converging nozzle is changing. The relationships describing the engine flow correspond to flow at constant throttle angle and variable engine speed. That is, the minimum area of the converging nozzle is constant but the exhauster

volumetric flow rate is changing. These are very distinct relationships because a variable flow area nozzle with fixed exhaust volume flow rate will have greatly different operating characteristics than a fixed geometry nozzle with variable exhaust conditions. The latter is much easier to visualize since the flow rate will be increased as the back (downstream) pressure is lowered, finally choking at some low back pressure and high mass flow rate. However, the variable geometry nozzle with fixed exhaust volume flow rate operates in a much more complex manner. The main variable is flow area at the throat and the flow is choked for very low flow rates. As the flow area increases, the flow rate and back pressure increase. Thus, let us consider an extremely small flow area with the downstream plenum connected to a constant volume flow rate pump. There will be a large pressure drop associated with this small flow and the flow will be choked. If the flow area is now made quite large, the pressure ratio will be small, the flow rate large, and the flow will be non-choked for that particular area.

These equations will yield distinct curves, the intersection being the correct value of intake manifold vacuum (which controls idle flow) and air mass flow rate (which can be related to boost venturi suction).

Thus for the throttle plate flow with:

$$\begin{aligned}
 A &= \text{Flow area in square inches} \\
 P_o &= \text{Local stagnation pressure in } \text{lb}/\text{in}^2 \\
 T_o &= \text{Local stagnation temperature in } ^\circ\text{R} \\
 \bar{R} &= \text{Universal gas constant} = 1545.4 \frac{\text{ft lbf}}{\text{lbm mol } ^\circ\text{R}} \\
 g_c &= 32.174 \frac{\text{ft lbm}}{\text{lbf sec}^2} \\
 W &= \text{Molecular weight } \frac{\text{lbm}}{\text{lbm mol}}
 \end{aligned}$$

- $\dot{m}$  = Mass flow rate in lbm/Hour  
 $M$  = Mach number where area is  $A$   
 $K$  = Specific heat ratio of mixture  
 $P$  = Local static pressure in lbf/in<sup>2</sup>  
 $T$  = Local static temperature in °R  
 $\rho$  = Local fluid density in lbm/Ft<sup>3</sup>

Starting with the 1 dimensional, steady, compressible flow of an ideal gas mixture, the following equation can be easily obtained:<sup>10</sup>

$$\frac{\dot{m}_{mix}}{A} = (3600.0) P \sqrt{\frac{Kgc W}{R T_o}} M \sqrt{1 + \left(\frac{K-1}{2}\right) M^2} \quad \text{EQN 2.7}$$

This equation is actually the continuity relationship for the above assumptions and does not involve the assumption of isentropic flow. Now to eliminate  $P$  in terms of  $P_o$ , the isentropic relationship must be used:

$$\frac{P}{P_o} = \left(\frac{T_o}{T}\right)^{\frac{k}{k-1}} \quad \text{or} \quad P = \frac{P_o}{\left(\frac{T_o}{T}\right)^{\frac{k}{k-1}}} \quad \text{EQN 2.8}$$

When equation 2.8 is substituted into equation 2.7, the following relationship results for the mass flow rate through an area  $A$ :

$$\dot{m}_{mix} = (3600.0) A P_o \sqrt{\frac{Kgc W}{R T_o}} \frac{M}{\left[1 + \frac{K-1}{2} M^2\right]^{\frac{k+1}{2(k-1)}}} \quad \text{EQN 2.9}$$

The isentropic assumption is not as restrictive as it might seem because the flow can be evaluated from a point just ahead of the throttle plate to the point of minimum throttle flow area. In other words, by saying that there is some  $P_o$  loss in the carburetor (due to friction and turbulence) up to station  $X^*$  (see Figure 4), and that there is some  $T_o$  loss in the carburetor due to fuel vaporization, the isentropic relations can



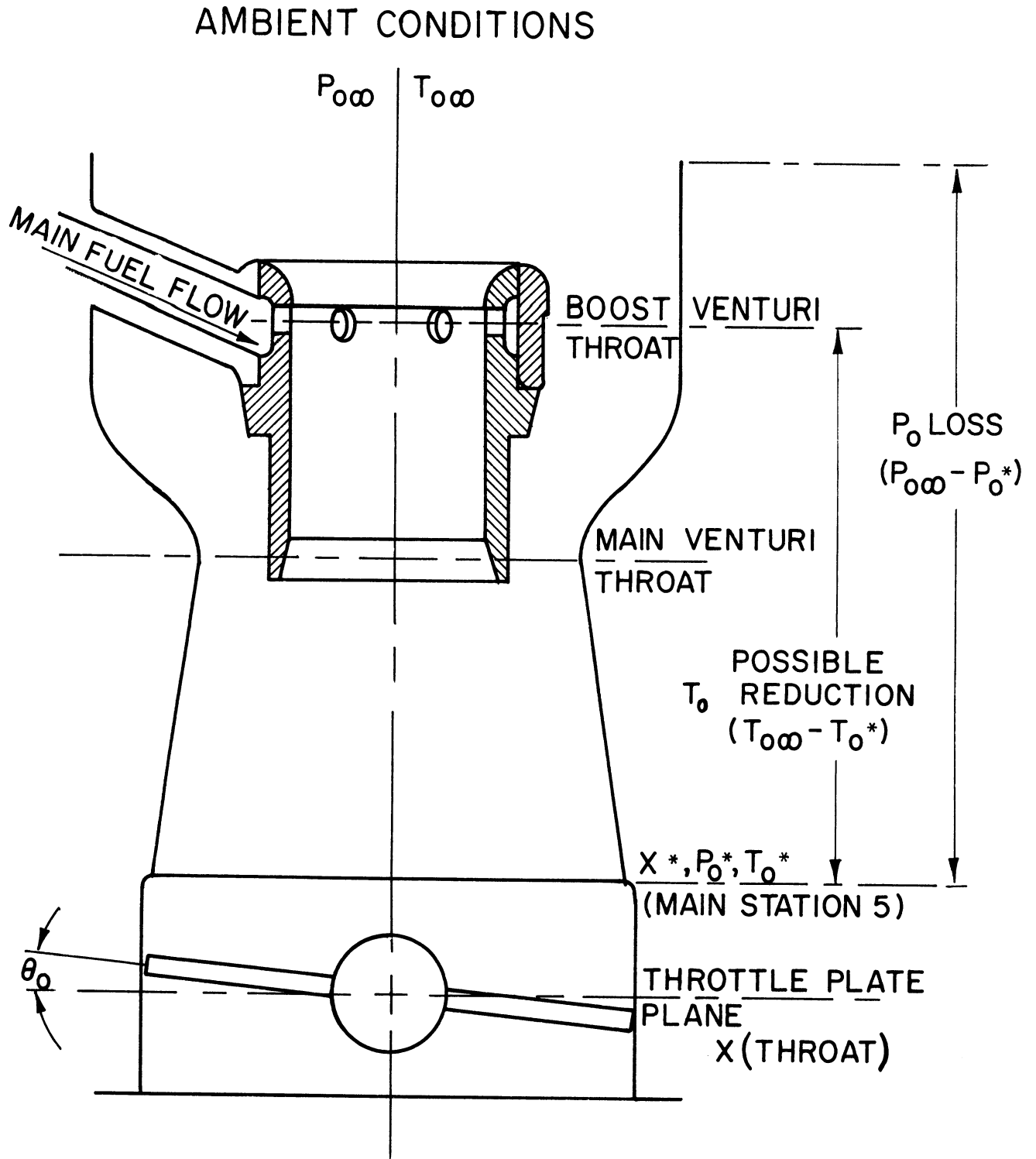


Figure 4. Illustration of local  $P_0$  and  $T_0$  values

still be used with little error between  $X^*$  and  $X$  throat if the values of  $P_O$  and  $T_O$  are the values at  $X^*$ . Thus what is needed in conjunction with the flow equations is the relationship between  $(P_O)_{local}$  and  $(P_O)_{ambient}$  as well as  $(T_O)_{local}$  and  $(T_O)_{ambient}$ . These can be easily obtained in terms of the total mixture flow rate and the amount of fuel vaporized up to a given station. The statement that there is very poor pressure recovery after the throttle restriction is equivalent to saying that the intake manifold pressure is the pressure at the throat of the converging nozzle. Note that the driving force for flow in the nozzle is the pressure ratio,  $\frac{P}{P_O}$ . For throttle flow it is much more convenient to work with the equations in terms of the pressure ratio rather than the Mach number. Thus let us eliminate the Mach number in terms of the pressure ratio across the nozzle  $\frac{P_{throat}}{P_O}$ .

$$\frac{P_O}{P} = \left[ 1 + \left( \frac{K-1}{2} \right) M^2 \right]^{\frac{K}{K-1}}$$

Now noting that  $X$  is merely a substitution variable ;

$$\text{Thus let: } X = 1 - \frac{K-1}{2} M^2 \quad \text{Then } \frac{P_O}{P} = X^{K/(K-1)}$$

$$\text{or } X = \left( \frac{P_O}{P} \right)^{K-1/K} \quad \text{also } M^2 = \frac{2}{K-1} (X-1)$$

$$\text{or } M = \sqrt{\frac{2}{K-1} (X-1)}$$

Now eliminate  $M$  from equation 2.9:

$$\dot{m}_{mix} = 3600.0 \sqrt{\frac{K g_c W}{R T_O}} (A_{flow}) \frac{P_O \sqrt{\frac{2}{K-1}} \sqrt{\left( \frac{P_O}{P} \right)^{\frac{K-1}{K}} - 1}}{\left( \frac{P_O}{P} \right)^{\frac{K+1}{2K}}} \frac{\text{LBM}}{\text{Hour}}$$

The throttle plate Mach number is thus given by:

$$M_{\text{throttle}} = \text{X MACH} = \sqrt{\frac{2}{K-1}} \sqrt{\left(\frac{P_o}{P}\right)^{\frac{K-1}{K}} - 1} \quad \text{EQN 2.11}$$

and the throttle plate flow will be critical (choked)

$$\text{when } \frac{P_o}{P} = \frac{1}{\left[\frac{2}{K+1}\right]^{\frac{K}{K-1}}}$$

at which point the throttle plate Mach number will be unity.

The flow rate under this condition will be given by:

$$\dot{m}_{\text{mix}} = (3600.0) A_{\text{flow}} P_o \sqrt{\frac{K}{R} \frac{g_c}{T_o} W} \frac{1}{\left[\frac{K+1}{2}\right]^{\frac{K+1}{2(K-1)}}} \quad \text{EQN 2.12}$$

For the special case of dry air ( $K = 1.40$ ) the choked flow rate will be given by:

$$\dot{m}_{\text{mix}} = (1913.1) \frac{A_{\text{flow}} P_o}{\sqrt{T_o}}$$

It should be emphasized that since this is a variable throat area nozzle, the choked flow value does not indicate the flow capacity of the throttle but only the maximum flow for the current area. It will turn out that the throttle plate mach number is 1.0 only for very low mass flow rates which correspond to very small flow areas.

Another useful relationship is obtained by introducing the intake manifold vacuum, VACMAN.

$$\text{VACMAN} = \text{Ambient pressure} - \text{intake manifold pressure}$$

or

$$\text{VACMAN} = P_{\infty} - P$$

$$\text{thus } \frac{P_{0\infty}}{P} = \frac{P_{0\infty}}{P_{0\infty} - \text{VACMAN}}$$

In terms of the throat Mach number instead of the nozzle pressure ratio, the special cases of equation 2.9 are:

For the special case of air only:  $K = 1.400$

$$W = 28.95 \frac{\text{lbm}}{\text{lb.mol}}$$

$$\dot{m}_{\text{pure air}} = \frac{A P_0}{\sqrt{T_0}} (.9189) \frac{M}{\left[1 + \frac{M^2}{5}\right]^3} \quad (3600.0)$$

or

$$\dot{m}_{\text{pure air}} = (3308.1) \frac{A P_0}{\sqrt{T_0}} \frac{M}{\left[1 + \frac{M^2}{5}\right]^3}$$

For the special case of a stoichiometric air-gasoline vapor mix:

$$K = 1.35$$

$$W = 30.3 \frac{\text{lbm}}{\text{lb.mol}}$$

$$\dot{m}_{\text{mix}} = (3324.0) \frac{A P_0}{\sqrt{T_0}} \frac{M}{\left[1 + \frac{M^2}{5.715}\right]^{3.357}} \quad \sim C_8 H_{17}$$

Next, the flow relationships for the engine must be obtained.

This will relate the engine variables to the mixture flow rate. The throttle and engine relationships will be coupled by means of the pressure ratio.

This is because the pressure on the downstream side of the throttle (exhauster side) is controlled by the exhauster. The pressure may be less than, equal to, or greater than the critical pressure, depending on

the exhauster flow. If the exhauster volume flow is such that the downstream (manifold) pressure is critical ( $.528 P_0$  for air alone), the Mach number at the throttle plate will be unity and the maximum mixture mass flow rate will exist for that particular flow area. If the exhauster volume flow rate is then increased, as by increasing engine speed, the downstream pressure will drop (manifold vacuum will increase) but the mass flow rate will not change significantly. (Slight changes in mass flow rate can occur even under choked conditions as a result of fuel-air ratio changes which affect the thermodynamic properties of the mixture.) Thus many values of manifold vacuum may exist for the same throttle setting and air mass flow rate.

To analytically predict the value of this downstream pressure, the exhauster flow must be analyzed. Now if we let:

$N_{cb}$  = number of cylinders per carburetor barrel

$N$  = engine revolutions per minute

$N_c$  = number of cylinders in engine

$P_0$  = atmospheric pressure lbf/in<sup>2</sup>

POHG = atmospheric pressure in inches of mercury

$V_s$  = swept volume of cylinders - in<sup>3</sup>

$D$  = displacement of engine - in<sup>3</sup>

$V_{cl}$  = clearance volume - in<sup>3</sup>

CR = compression ratio of engine

$T_{cl}$  = temp. of mixture in clearance volume - °R

$T_{man}$  = temp. of mixture in intake manifold °R

$P_{cl}$  = pressure of mixture in clearance volume - lbf/in<sup>2</sup>

$P_{man}$  = pressure of mixture in intake manifold - lbf/in<sup>2</sup>

$W_m$  = mixture molecular weight - lbm/lb mol

$V_{total}$  = total volume of cylinder - in<sup>3</sup>

VACMAN = manifold vacuum in inches of mercury

$m$  = mass of mixture inducted into cylinder - lbm

The mass of mixture added per intake stroke will be:

$$m_{added} = \frac{\text{total mass in cylinder when intake valve closes} - \text{mass in clearance volume when exhaust valve closes}}$$

however, the mass may be expressed as:

$$m = \frac{PVW}{\bar{R}T}$$

therefore:

$$m_{added} = \frac{(0.4912) P_{cyl} V_{total} W_{mix}}{(12.0) \bar{R} T_{final}} - \frac{(0.4912) P_{cl} V_{cl} W_{cl}}{(12.0) \bar{R} T_{cl}}$$

$T_{final}$  is the absolute temperature of the mix ( $^{\circ}R$ ) in the cylinder at the end of flow into the cylinder and results from a mixing of the hot residual gases with the cool intake gases. Inherent in this formulation is the assumption that the mass of mixture which enters the cylinder and immediately exits through the exhaust valve is insignificant. If, in a

particular engine, this is known to be significant, as in engines with large valve overlap at high loads, then an additional lost mass term would have to be included in the above equation.

The pressure in the cylinder when the inflow of fresh mixture ceases is the intake manifold pressure minus a pressure differential which is related to the average intake valve flow area and the mass flow rate of the mixture over the intake stroke. The clearance volume pressure at the end of the exhaust stroke is the ambient pressure plus a pressure differential which is related to the average exhaust valve flow area and mass flow rate of the exhaust gases over the exhaust stroke. These pressures, in equation form, are given by:

$$P_{\text{cyl}} = P_{\text{man}} - \Delta P_i \quad P_{\text{cl}} = P_o + \Delta P_{\text{ex}}$$

The pressure differentials are complex functions of valve design, valve timing, and mixture instantaneous velocity. Fortunately, under most operating conditions, these pressure differentials are on the order of a few inches of water and may be neglected in the expressions for  $P_{\text{cyl}}$  and  $P_{\text{cl}}$  (For example,  $P_o$  is typically on the order of 400 inches of water.)

Thus the following equation is obtained for the mass added per intake stroke; (the pressure units will be carried as lbf/in<sup>2</sup> until the final equation is obtained.)

$$m_{\text{added}} = \frac{P_{\text{man}} V_{\text{total}} W_{\text{mix}}}{(12) \bar{R} T_{\text{final}}} - \frac{P_o V_{\text{cl}} W_{\text{cl}}}{(12) \bar{R} T_{\text{cl}}} \quad \text{EQN 2.13}$$

$$\text{But } V_{\text{total}} = V_s + V_{\text{cl}}$$

$$\text{and } P_{\text{man}} = P_o - \text{VACMAN}$$

$$\text{Thus: } m_{\text{added}} = \frac{(P_o - \text{VACMAN}) (V_s + V_{\text{cl}}) W_m}{(12) \bar{R} T_{\text{final}}} - \frac{P_o V_{\text{cl}} W_{\text{cl}}}{(12) \bar{R} T_{\text{cl}}}$$

$$\text{EQN 2.14}$$

Now, for convenience, let us define C5 as the ratio of the absolute temperature of the mixture in the cylinder when mixture in-flow ceases, to the absolute intake manifold temperature. Let us also define C6 as the ratio of the absolute temperature of the gases in the clearance volume when exhaust outflow ceases, to the absolute intake manifold temperature.



or in equation form:

$$C5 = \frac{T_{\text{final}}^{\circ R}}{T_{\text{man}}^{\circ R}}$$

$$C6 = \frac{T_{\text{cl}}^{\circ R}}{T_{\text{man}}^{\circ R}}$$

Substituting these definitions into equation 2.14 and factoring, the following equation is obtained:

$$m_{\text{added}} = \frac{1}{(12) \bar{R} T_{\text{man}}} \left[ \frac{(P_o - \text{VACMAN}) (V_s + V_{\text{cl}}) W_m}{C5} - \frac{P_o V_{\text{cl}} W_{\text{cl}}}{C6} \right]$$

EQN 2.15

Now let us eliminate the cylinder volumes in terms of the common engine variables. Note that:

$$CR = \frac{V_{\text{total}}}{V_{\text{cl}}} = \frac{V_{\text{cl}} + V_s}{V_{\text{cl}}} \quad \text{EQN 2.16}$$

but :

$$V_s = \frac{D}{N_c}$$

thus :

$$V_{\text{cl}} = \frac{D}{N_c(CR-1)} \quad \text{EQN 2.17}$$

Substituting equation 2.16 into equation 2.15 and noting that  $W_{\text{cl}}$  differs very little from  $W_m$ , the resulting relationship is:

$$m_{\text{added}} = \frac{V_{\text{cl}} W_m}{(12) \bar{R} T_{\text{man}}} \left[ \frac{(P_o - \text{VACMAN}) (CR)}{C5} - \frac{P_o}{C6} \right]$$

or by rearrangement:

$$m_{\text{added}} = \frac{V_{\text{cl}} W_m (CR)}{(12) (C5) \bar{R} T_{\text{man}}} \left[ P_o \left( \frac{CR - C5/C6}{CR} \right) - \text{VACMAN} \right]$$

Now eliminate  $V_{c1}$  by using equation 2.17:

$$m_{\text{added}} = \frac{D W_m}{(12) (C5) N_c \bar{R} T_{\text{man}}} \left( \frac{CR}{CR-1} \right) \left[ P_o \left( \frac{CR - C5/C6}{CR} \right) - \text{VACMAN} \right]$$

EQN 2.18

This is, of course, the mass of mixture added per intake stroke. Of greater and more practical interest is the total mixture mass flow rate.

This mass flow rate is related to the mass added per intake stroke by:

$$\dot{m} \frac{\text{LBM}}{\text{Hour}} = \left( m_{\text{added}} \frac{\text{LBM}}{\text{intake}} \right) \left( \frac{\text{intakes}}{\text{Hour}} \right)$$

$$\text{and: } \frac{\text{intakes}}{\text{Hour}} = \left( N \frac{\text{Revs}}{\text{Minute}} \right) \left( 60 \frac{\text{Min}}{\text{Hour}} \right) \left( \frac{N_c}{2} \frac{\text{intakes}}{\text{Rev}} \right) = 30 N_c N$$

$$\text{thus: } \dot{m} \frac{\text{LBM}}{\text{Hour}} = \frac{30 N_c N D W_m}{(12) (C5) N_c \bar{R} T_{\text{man}}} \left( \frac{CR}{CR-1} \right) \left[ P_o \left( \frac{CR - C5/C6}{CR} \right) - \text{VACMAN} \right]$$

or further simplifying:

$$\dot{m} \frac{\text{LBM}}{\text{Hour}} = \frac{DN}{\left[ \frac{(0.40) (C5) \bar{R} T_{\text{man}} (CR-1)}{W_m (CR) (0.4912)} \right]} \left[ \text{POHG} \left( \frac{CR - C5/C6}{CR} \right) - \text{VACMAN} \right]$$

EQN 2.19

Where the 0.4912 enters if POHG and VACMAN are in the common units of inches of mercury.

Substitution of typical values shows that the ratio of  $C5/C6$  does not exert a great influence on the result, thus a sophisticated theoretical cycle analysis is not justified to obtain this ratio. The technique was to analyze various fuel-air cycles by means of the combustion charts and obtain reasonable correlations for the clearance volume and final temperature variations as a function of the fuel-air ratio. These correlations, in

piecewise form over various fuel-air ratio ranges, are listed in subroutine AIRMAS. It should be emphasized that the variables which greatly influence the mass flow rate are the engine displacement and speed and the intake manifold pressure. The engine compression ratio and the various temperature ratios have a much smaller influence on the mixture flow. (For hand calculations C5 can be taken as approximately 1.2 and C6 can be taken as about 2.4).

Thus we have obtained a theoretical equation relating the exhaust (engine) flow rate to the manifold vacuum in terms of ambient pressure, mixture properties, engine rpm, displacement, and compression ratio.

When a correlation of all the engine data taken in the carburetor-engine tests was attempted, the agreement with this theory was found to be excellent. The resulting theoretical equation for the values;

$$\begin{aligned}
 P_o &= 29.00 \text{ "Hg.} & CR &= 8.5 \\
 D &= 289.0 \text{ in.}^3 & T_{\text{man}} &= 600 \text{ }^\circ\text{R} \\
 \bar{R} &= 1545.4 \frac{\text{ft. lbf.}}{\text{lbm } ^\circ\text{R}} & C5/C6 &= T_{\text{final}}/T_{\text{cl}} = 1/2 \\
 W_m &= 30.3 \text{ LBM/LB MOL}
 \end{aligned}$$

is the following:

$$\dot{m} \frac{\text{lbm}}{\text{hr.}} = \frac{N}{95.50} \left[ 27.26 - \text{Vacman} \right]$$

When this theoretical exhaust analysis is coupled with the throttle flow area analysis;

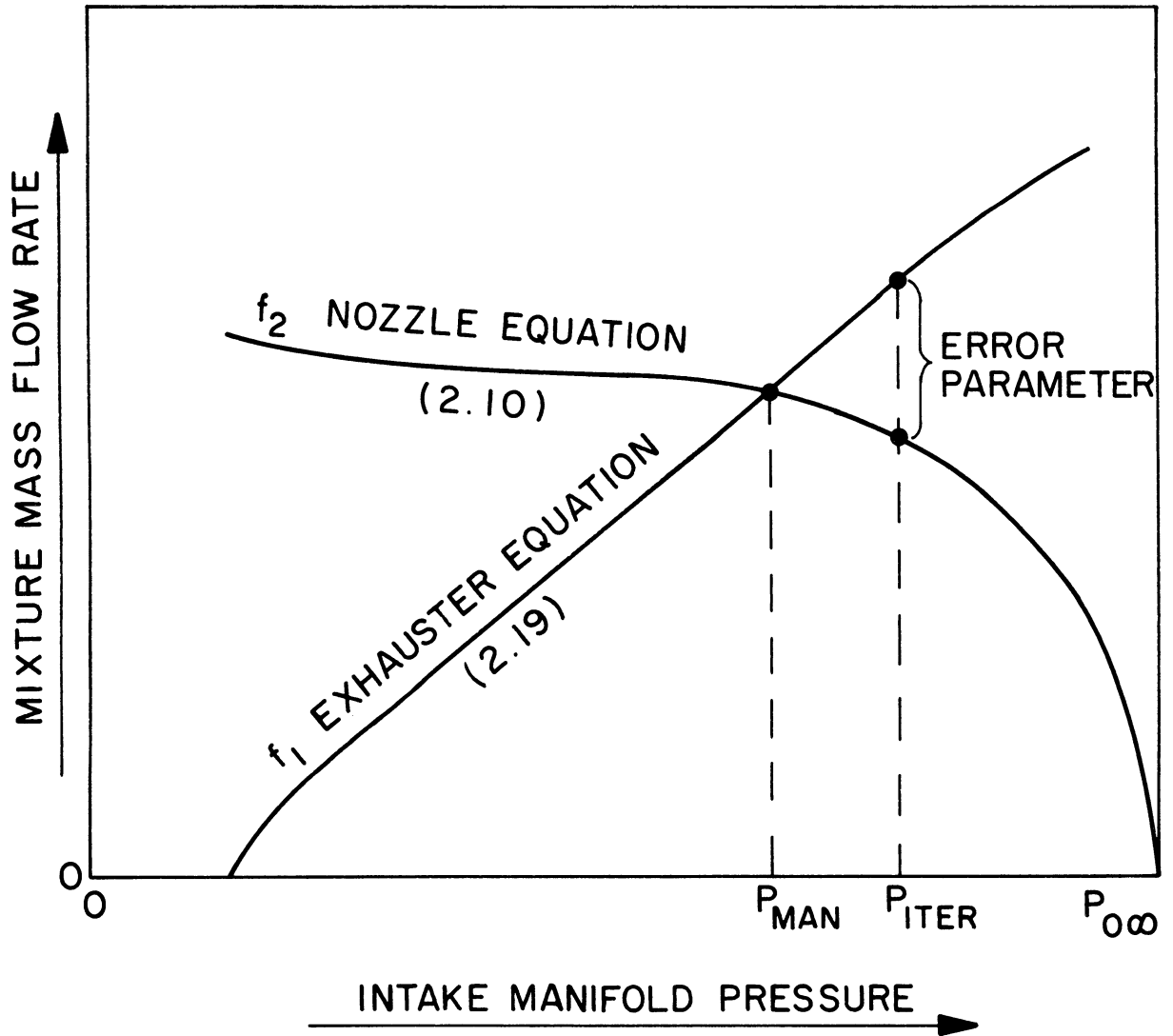


Figure 5. Simultaneous solution of exhaustor and nozzle equations

$$\dot{m}_{\text{exhauster}} = f_1 (\text{VACMAN}, P_o, D, N, W_m, CR)$$

$$\dot{m}_{\text{throttle}} = f_2 (\text{VACMAN}, P_o, A_{\text{flow}}, K, W_m, T_o)$$

The simultaneous solution will be the intersection of the two curves as shown schematically in Figure 5, with the result being an accurate prediction of mixture flow rate and intake manifold vacuum.

The importance of this result is that:

1. Engine-carburetor variables are mated theoretically. For example, this indicates the quantitative effect of engine displacement, speed, and compression ratio on the carburetor air flow.
2. All engine-carburetor operating points (combinations of engine speed and throttle angle) can be shown on a single graph as opposed to a standard carburetor flow box curve which does not directly involve the engine variables.

This analysis can also be utilized to determine the dilution of the fresh fuel-air mixture by the exhaust residual gases. The fractional dilution is defined as:

$$\text{dilution fraction} = \frac{\text{mass of residual gases}}{\text{total mass in cylinder when intake valve closes}} = \frac{m_{cl}}{m_{cl} + m_{\text{added}}}$$

But the mass of the residual gases in the clearance volume and the total mass of the mixture in the cylinder are given in equation 2.13.

Substituting these relations into the expression for the dilution fraction, the following equation is obtained:

$$\text{dilution fraction} = \frac{\left[ \frac{P_o V_{cl} W_{cl}}{(12) \bar{R} T_{cl}} \right]}{\left[ \frac{P_{\text{man}} V_{\text{total}} W_{\text{mix}}}{(12) \bar{R} T_{\text{final}}} \right]} = \frac{P_o V_{cl} T_{\text{final}}}{P_{\text{man}} V_{\text{total}} T_{cl}}$$

Now noting that  $T_{\text{final}}/T_{\text{cl}}$  is defined as  $C5/C6$ , that  $V_{\text{total}}/V_{\text{cl}}$  is the compression ratio of the engine, and that the intake manifold pressure may be expressed as  $P_o - \text{VACMAN}$ , the above expression may be written as:

$$\text{dilution fraction} = \frac{P_o (C5/C6)}{\text{CR} (P_o - \text{VACMAN})} \quad \text{EQN 2.20}$$

where the ambient pressure,  $P_o$ , and the intake manifold vacuum,

$\text{VACMAN}$ , are both in inches of mercury. This equation predicts the effects of ambient pressure, engine compression ratio, intake manifold vacuum, and fuel-air ratio on the dilution fraction. (The fuel-air ratio effect is given by the variation in  $C5/C6$ , which is small under steady firing conditions.) The most influential variable in affecting the dilution fraction is the intake manifold vacuum. The magnitude of this effect is tabulated below for the following variables:

$$\begin{aligned} P_o &= 29.00 \text{ "Hg.} \\ \text{CR} &= 8.5 \\ \left(\frac{C5}{C6}\right) &= 0.5 \end{aligned}$$

<u>VACMAN</u>	<u>dilution fraction</u>
0.00 "Hg	0.0588
5.00	0.0708
10.00	0.0863
15.00	0.1215
18.00	0.1545
23.00	0.2833
27.28 (max)	1.0000

Note from the above values that the dilution fraction will be unity (100% dilution) when the intake manifold vacuum has the following value:

$$\text{VACMAN (max.)} = \text{VACMAN (for 100\% dilution)} = P_o \left[ \frac{\text{CR} - (\text{C5/C6})}{\text{CR}} \right]$$

this value of intake manifold pressure corresponds to zero fresh mixture added to the cylinder. This can be verified by substituting the above expression for VACMAN into equation 2.19. This is theoretically the maximum intake manifold vacuum and, under these conditions, the intake stroke consists of the expansion of the hot exhaust residual gases from the clearance volume to the total volume. At this point the pressure has been reduced from slightly over one atmosphere to the value;  $P_o (1/\text{CR})^{k_r}$ , where  $k_r$  is the specific heat ratio of the residual gas mixture. No fresh mixture flows into the cylinder because the cylinder pressure during the intake stroke is always greater than the intake manifold pressure. This means that the same residual gases are continuously being compressed, expanded into the intake manifold through the intake valve, drawn back into the cylinder, and recompressed. Since no combustion is occurring under these maximum dilution conditions, the value of C5/C6 will be given by:

$$\left( \frac{\text{C5}}{\text{C6}} \right)_{\text{motoring}} = \left( \frac{T_{\text{final}}}{T_{\text{cl}}} \right) = \left[ \frac{V_{\text{cl}}}{V_{\text{total}}} \right]^{(k_r - 1)} = \left( \frac{1}{\text{CR}} \right)^{k_r - 1}$$

For a compression ratio of 8.5 and a specific heat ratio of 1.40, the minimum value of C5/C6 for these high dilution (non-firing) conditions is 0.427.

In operation the theoretical maximum intake manifold vacuum is not obtained, due to the fact that the mass of mixture added is never

zero. Since there is a throttle plate leakage area and bypasses around the throttle, the mixture mass flow rate will be small at the closed throttle position, (25 to 45 lbm/hour) but never zero. This means that the dilution is never 100% and that the intake manifold vacuum is always less than the theoretical maximum even at closed throttle.

All of the foregoing results and relationships were incorporated into subroutine AIRMAS which accurately predicts, for any combination of variables, the intake manifold vacuum and mass flow rates of each mixture component.

#### F. ANALYSIS OF COMPRESSIBLE FLOW THROUGH MULTIPLE VENTURII

After the total dry air and water vapor flow rates have been predicted for any specified operating condition, the next problem is to analyze the manner in which this flow passes through the main and boost venturii and to determine all significant pressure parameters. The questions to be resolved analytically include:



1. What fraction of the total flow passes through the boost venturi?
2. What are the metering signals at the throats of the main and boost venturii?
3. How does the introduction of fuel into the boost venturi air stream affect the metering signal?

The fraction of the total moist air flow that passes through the boost venturi is extremely important since the boost venturi throat depression (or metering signal) is very sensitive to air mass flow rate. The first step in the analysis of flow through nozzles in parallel is to establish the criterion for flow division. This criterion is that the static pressure at the outlet of the boost venturi be equal to the static pressure at the corresponding position in the main venturi. If we then define a parameter  $X_F$  as the fraction of the total moist air flow that passes through the main venturi, we have a very convenient iteration parameter.

$$X_F = \frac{\text{Primary venturi mass flow rate}}{\text{Total venturi mass flow rate}} = \frac{PVFLO}{VENFLO}$$

For a given value of total moist air mass flow rate (resulting from sub-routine AIRMAS) and an assumed  $X_F$  value, the flow rates through each venturi are specified. With this known, a compressible flow analysis can be performed on each venturi and the Mach numbers at each station calculated. This analysis will be for moist air only in the main venturi, and for a changing mixture of air, water vapor, and fuel vapor in the boost venturi. The static pressures at the boost venturi outlet and at

the corresponding main venturi position can thus be determined. They should be equal but, if  $XF$  is too high, the flow rate through the main venturi will be too great a fraction of the total flow and the boost outlet pressure will be greater than the corresponding main venturi pressure. (note that as the flow rate increases, the pressure at each station decreases.) Thus, a convenient error parameter for use in the generalized convergence technique (Appendix G) is :

$$\text{Iterative error parameter} = E1 = PB5W - PM4W \quad \underline{\text{EQN 2.21}}$$

where:

PB5W = Boost venturi pressure at boost station 5

PM4W = Main venturi pressure at main station 4

The main venturi stations were shown earlier in Figure 2 and the corresponding boost venturi stations are shown in Figure 6. Note that boost station 5 is at the outlet and that main venturi station 4 corresponds to the annular flow area in the plane of the boost venturi outlet. Note also that boost venturi station 3 is the throat of the converging - diverging nozzle and that fuel is discharged at 4. This means that the suction at boost station 4 is the metering signal. Thus, if the value of  $XF$  is continuously adjusted at each iteration until the error parameter  $E1$  becomes very small, the resulting flow rate in the boost venturi can be used to calculate a pressure at boost stations 2, 3, 4, and 5.

Recall that the compressible flow rate equation obtained earlier (equation 2.9) was:

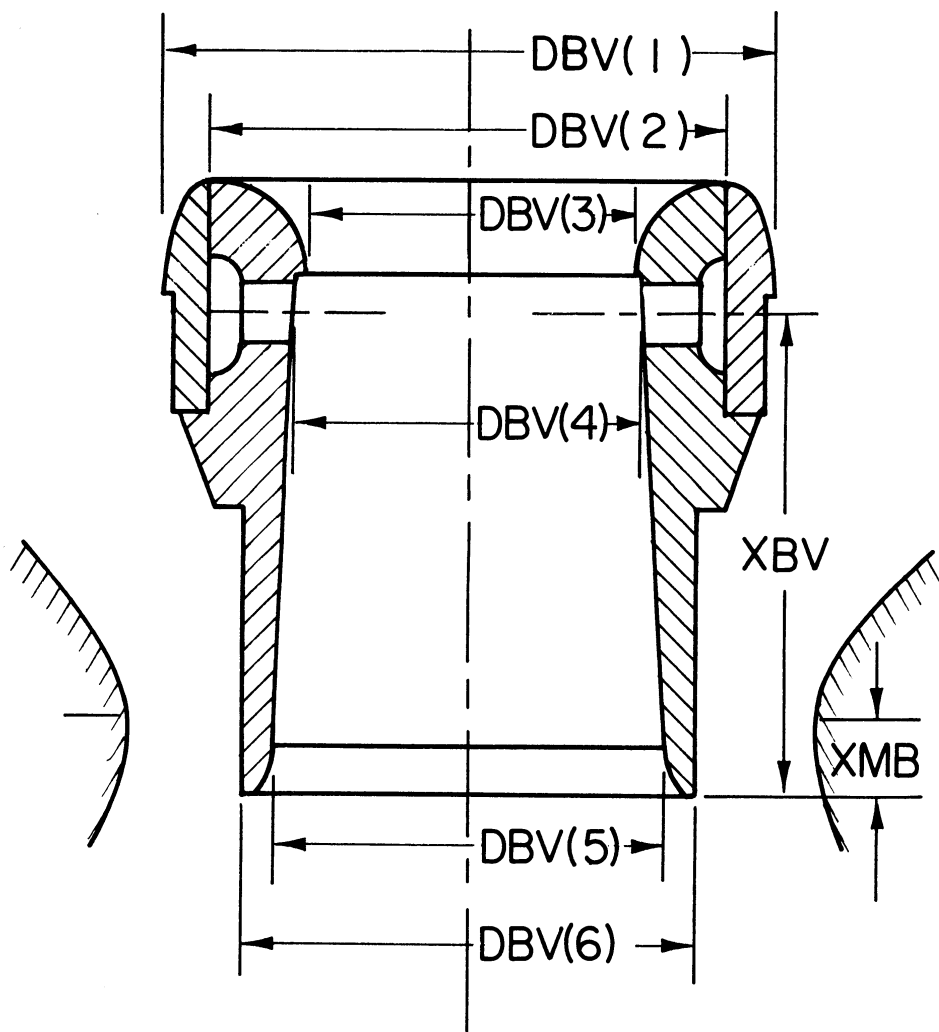


Figure 6. Computer model parameters for boost venturi

$$\dot{m} = (3600.0) A P_o \sqrt{\frac{K g_c W}{R T_o}} \frac{M}{\left[1 + \frac{K-1}{2} M^2\right]^{\frac{K+1}{2(K-1)}}}$$

Thus if  $\dot{m}$ ,  $A$ ,  $P_o$ ,  $T_o$ ,  $K$ , and  $W$  are specified, it should be possible to calculate the mach number  $M$ . However, the equation is not explicit in  $M$ , thus a direct solution is not obtainable. The Newton-Rhapson method may be employed to iteratively obtain the Mach number for any combination of variables. This technique may be written <sup>69</sup>as:

$$M_{i+1} = M_i - \frac{f(M_i)}{f'(M_i)} \quad \text{EQN 2.22}$$

where:

$$f(M_i) = \left\{ \frac{\dot{m} \left[1 + \frac{K-1}{2} M_i\right]^{\frac{K+1}{2(K-1)}}}{(3600.0) A P_o \sqrt{\frac{K g_c W}{R T_o}}} \right\} - M_i \quad \text{EQN 2.23}$$

$$f'(M_i) = \frac{d f(M_i)}{d M_i} = \left(\frac{K+1}{2}\right) \frac{\dot{m} M_i \left[1 + \frac{K-1}{2} M_i\right]^{\frac{3-K}{2(K-1)}}}{(3600.0) A P_o \sqrt{\frac{K g_c W}{R T_o}}} - 1.0$$

EQN 2.24

By assuming an initial guess for the mach number  $M_i$ , the values of  $f(M_i)$  and  $f'(M_i)$  can be calculated. The Newton-Rhapson iteration formula can then be used to calculate the next guess  $M_{i+1}$ . These equations as well as all of the other compressible flow relationships for isentropic, Fanno, and Rayleigh type flow have been incorporated into subroutine SOLVE. This subroutine performs the desired analysis by making a proper initial guess, performing the iterations, checking for

stability and errors, and returning the pressure, temperature, density, and Mach Number. The initial guess (for the isentropic case), and a check to see if the specified mass flow rate exceeds the maximum are made by noting that:

$$\dot{m}_{\max} = (3600.0) A P_o \sqrt{\frac{K g_c W}{R T_o}} \frac{1.0}{\left[ \frac{K+1}{2} \right]^{\frac{K+1}{2(K-1)}}} \quad \text{EQN 2.25}$$

and that a logical initial guess is:

$$M_{\text{initial}} = (3600.0) A P_o \sqrt{\frac{K g_c W}{R T_o}} \left\{ 1.0 + \frac{\dot{m}}{\dot{m}_{\max}} \left[ \left( \frac{K+1}{2} \right)^{\frac{K+1}{2(K-1)}} - 1 \right] \right\}$$

EQN 2.26

Once the Mach number has been calculated for the given conditions, the mixture density, temperature, pressure, and suction are calculated from the following relationships:

$$\rho_{\text{local}} = \frac{(\rho_o)_{\text{local}}}{\left[ 1 + \frac{K-1}{2} M^2 \right]^{\frac{1}{K-1}}} \quad \text{EQN 2.27}$$

$$P_{\text{local}} = \frac{(P_o)_{\text{local}}}{\left[ 1 + \frac{K-1}{2} M^2 \right]^{\frac{K}{K-1}}} \quad \text{EQN 2.28}$$

$$T_{\text{local}} = \frac{(T_o)_{\text{local}}}{\left[ 1 + \frac{K-1}{2} M^2 \right]} \quad \text{EQN 2.29}$$

$$\text{local suction} = (P_o)_{\text{ambient}} - P_{\text{local}} = (P_o)_{\text{amb.}} \left\{ 1 - \frac{P}{P_o \text{ local}} \cdot \left[ \frac{(P_o)_{\text{local}}}{(P_o)_{\text{amb.}}} \right] \right\}$$

The distinction between local and ambient total pressures and temperatures must be made because of  $P_o$  losses due to friction, and  $T_o$  decreases due to fuel vaporization. For example, if the dry air flow rate through the boost venturi is  $\dot{m}_b$ , the main system fuel flow rate is  $\dot{m}_f$ , and the fraction of fuel that has vaporized up to the station being analyzed is FRACTB, then the fuel-air ratio at that station is:

$$\text{boost fuel-air ratio} = \text{BFA} = (\dot{m}_f) (\text{FRACTB}) / \dot{m}_b \quad \underline{\text{EQN 2.30}}$$

The total temperature of the mixture at that station is given by:

$$(T_o)_{\text{local}}^{\circ R} = (T_o)_{\text{ambient}} + \text{BFA} * \text{HVAPOR} / (C_p)_{\text{mix}} \quad \underline{\text{EQN 2.31}}$$

where HVAPOR is the enthalpy of vaporization or latent heat of the fuel and  $(C_p)_{\text{mix}}$  is the constant pressure specific heat of the mixture at that station.

Subroutine SIGNAL contains the venturi flow analysis and iterates on XF for any venturi geometry, atmospheric conditions, fuel type, and total air flow rate. It calls on subroutine SOLVE at each main and boost station to obtain the flow parameters. When XF has converged to the proper value for the specified conditions, these flow parameters will represent the predicted performance of the main and boost venturi system.

## G. ANALYSIS OF FUEL ATOMIZATION AND SPRAY VAPORIZATION

The extremely complex processes of fuel atomization and spray vaporization were analyzed for two basic reasons. The first reason is that we would like to determine which variables affect these processes and to what extent. The second reason is that the thermodynamic properties

of the flowing mixture will be changing as the liquid fuel vaporizes. Thus the mixture flow will be affected by the vaporization rate within the carburetor. This effect will turn out to be slight because the relative amount of fuel in the air is small, thus the mixture properties will vary only slightly from those of pure air. It should be emphasized that we are concerned only with vaporization within the carburetor, from the point of main fuel introduction (boost venturi) to the throttle plate minimum area. This is the section of the carburetor where the thermodynamic properties of the mixture are utilized in the compressible flow analyses, and vaporization after the throttle plate (which is the bulk of the vaporization) does not affect the mixture properties within the carburetor. The amount of fuel vaporized after the throttle plate minimum area is important for other considerations such as unburned hydrocarbon emissions but will have little influence on the flow within the venturi and throttle sections. However, the vaporization equations which were derived could be extended to encompass this additional vaporization even though it was not necessary for this simulation.

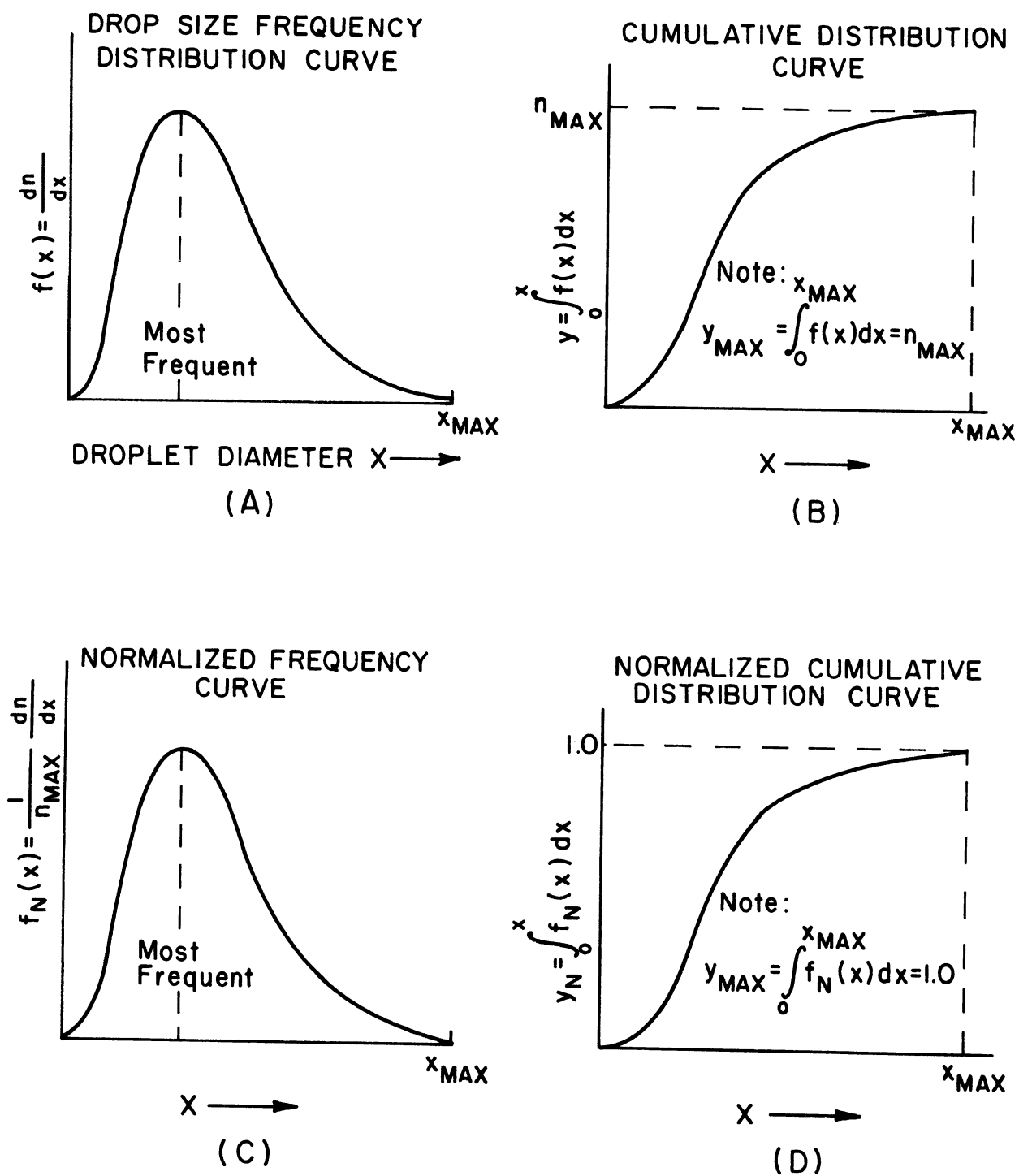
First let us categorize the analyses to be performed. The atomization analysis, which logically must precede the vaporization analysis, is basically a droplet size distribution study. The problem is one of predicting parameters which will adequately describe the characteristics of the spray in terms of the system variables.

The vaporization analysis consists fundamentally of predicting the mass and heat transfer between the droplets and the gaseous stream, taking into account the acceleration of the droplets in the stream (which affects the droplet Reynolds number.)

Let us first consider the atomization process in the carburetor. The fuel stream in the typical carburetor is drawn into a high velocity air stream by means of a slightly reduced air pressure at the throat of the boost venturi. This fuel stream is then broken into many droplets by the relative motion of the air stream. This type of atomization is termed "pneumatic atomization"<sup>18</sup> and the drop size distributions resulting from this method have been investigated experimentally by various workers. One other type of atomization occurs to a very slight degree in carburetors and that is "impingement atomization" which is the breaking up of a fuel stream by the action of fuel striking an object in the flow path (the throttle plate.) This has been studied very little and was not analyzed in this simulation.

Before discussing the investigations of pneumatic atomization, a few definitions and concepts basic to drop size distribution studies must be introduced. Figure 7 shows four curves which can be used to describe the distribution of droplet sizes within the spray. Curve  $7_a$  is a droplet size frequency curve and indicates the number of drops of a given diameter  $X_d$ . Curve  $7_c$  is the normalized frequency curve which is obtained by dividing the number of drops of a given diameter by the total number of





## DROP SIZE DISTRIBUTION CURVES

Figure 7. Methods of illustrating drop size distributions

drops in the spray  $n_{\max}$ . Curve 7<sub>b</sub> illustrates another technique for describing the distribution. This is denoted as the cumulative distribution curve and represents the number of drops having a size less than  $X_d$ . Note that there is always a maximum droplet size in the practical case. (It will be seen that many of the mathematical approximations to the distribution curves will not predict any maximum droplet size.) Curve 7<sub>d</sub> is the normalized cumulative distribution curve and is probably the most useful representation of the droplet sizes.

The various moments of the normalized frequency distribution curve (7<sub>c</sub>) have important physical meanings:

$$\text{moment } q = \int_0^{X_{\max}} X^q f_n(X) dx$$

The spray volume is proportional to the 3rd moment with  $\pi/6$  being the proportionality constant:

$$\frac{\pi}{6} \int_0^{X_{\max}} X^3 f_n(X) dx$$

The spray surface area is proportional to the 2nd moment:

$$\pi \int_0^{X_{\max}} X^2 f_n(X) dx$$

The Sauter volume -surface mean diameter is given by the ratio of the 3rd moment to the 2nd moment<sup>15</sup>:

$$\frac{1}{X_{vs}} = \frac{\int_0^{X_{\max}} X^3 f_n(X) dx}{\int_0^{X_{\max}} X^2 f_n(X) dx}$$

Thus  $\bar{X}_{vs}$  represents a droplet diameter which has the same ratio of volume to surface area as the total spray (when the proportionality factor of  $1/6$  is introduced.) This parameter is very important in calculating rates of evaporation.

$$\text{Thus: } \frac{\text{spray volume}}{\text{spray surface area}} = \frac{\bar{X}_{vs}}{6} \text{ microns} \quad \text{EQN 2.33}$$

Nukiyama and Tanasawa<sup>19</sup> studied the pneumatic atomization of alcohol-glycerine mixtures in air nozzles. They developed an empirical equation correlating the effects of the operating variables on the Sauter mean droplet size. This may be used where an experimental frequency distribution curve is not available, although the experimental data should be used if available.

$$\bar{X}_{vs} = \frac{1410.0 \sqrt{\sigma}}{V_A \sqrt{\rho_l}} + 191.0 \left[ \frac{\mu}{\sqrt{\sigma \rho_l}} \right] \frac{1000.0 \dot{Q}_L}{\dot{Q}_A} \quad \text{EQN 2.34}$$

where:

$\bar{X}_{vs}$  = Sauter mean drop diameter (microns)

$\sigma$  = liquid surface tension in contact with air  $\frac{\text{dynes}}{\text{cm.}}$

$\mu$  = liquid viscosity in centipoise

$V_A$  = relative velocity between air and liquid  $\frac{\text{ft}}{\text{sec}}$

$\rho_l$  = liquid density LBM / ft<sup>3</sup>

$\dot{Q}_L / \dot{Q}_A$  = ratio of liquid volume flow rate to air volume flow rate

This equation is applicable to the atomization of a liquid by a high velocity air stream when the liquid properties are in the following range:

$$\rho_l \quad 43 \text{ to } 75 \quad \text{LBM/FT}^3$$

$$\sigma \quad 19 \text{ to } 75 \text{ Dynes/cm}$$

$$\mu \quad 0.3 \text{ to } 50 \text{ centipoise}$$

$$V_A \quad \text{up to sonic}$$

In addition they proposed an empirical frequency distribution correlation of the form:

$$f(x) = \frac{dn}{dx} = b x^2 e^{-cx} \quad \text{EQN 2.35}$$

Where b and c are constants to be experimentally determined for a given geometry and fluid. Their distribution correlation has not found wide acceptance but their empirical relationship for the Sauter mean droplet diameter is used extensively. It was used in the atomization and vaporization analyses in this simulation. From the available literature, the accuracy of the Sauter mean diameter predicted with the N-T equation is probably about  $\pm 20\%$  for hydrocarbons in air. However much larger errors have occurred for gases other than air and for more viscous liquids.<sup>15</sup>

Some final comments on droplet size frequency distribution equations are justified when one considers the maximum drop size. Note that equation 2.35 predicts a decreasing frequency of occurrence as the drop size goes to infinity. Thus the frequency of occurrence is very small but non-zero for all huge drops. A more involved though physically more

realistic distribution function is the upper limit log normal distribution as discussed and utilized by Rice.<sup>21</sup> This predicts a limiting maximum droplet size as opposed to the Rosin-Rammler<sup>15</sup> and Nukiyama-Tanasawa<sup>19</sup> relations which do not limit the maximum droplet size.

Benson,<sup>12</sup> et al, state, on the basis of their work in determining droplet size distributions, that the assumption of a smooth curve having a single maximum may not be valid in all instances. This means that there may be, in some nozzles, preferential clustering of droplet sizes at two or more sizes, yielding a curve as shown in Figure 8. This complicates the analytical determination of mean droplet parameters to the point where numerical integration of the experimental distribution data would be the most accurate technique.

or:

$$\bar{X}_{vs} = \frac{\sum_0^{X_{MAX}} X^3 f_n(X) \Delta X}{\sum_0^{X_{MAX}} X^2 f_n(X) \Delta X} \quad \text{EQN 2.36}$$

where  $f(X)$  is obtained by interpolation from the experimental frequency curve.

The evaporation of the fuel droplets in the air stream is an extremely complex process. Each droplet diameter will have its own drag coefficient and mass and heat transfer rates. The acceleration of each droplet will be different and the time required to travel a distance downstream, or residence time, will be different for each droplet size. In addition, from studies of pneumatic atomization it may be stated that the droplets are not

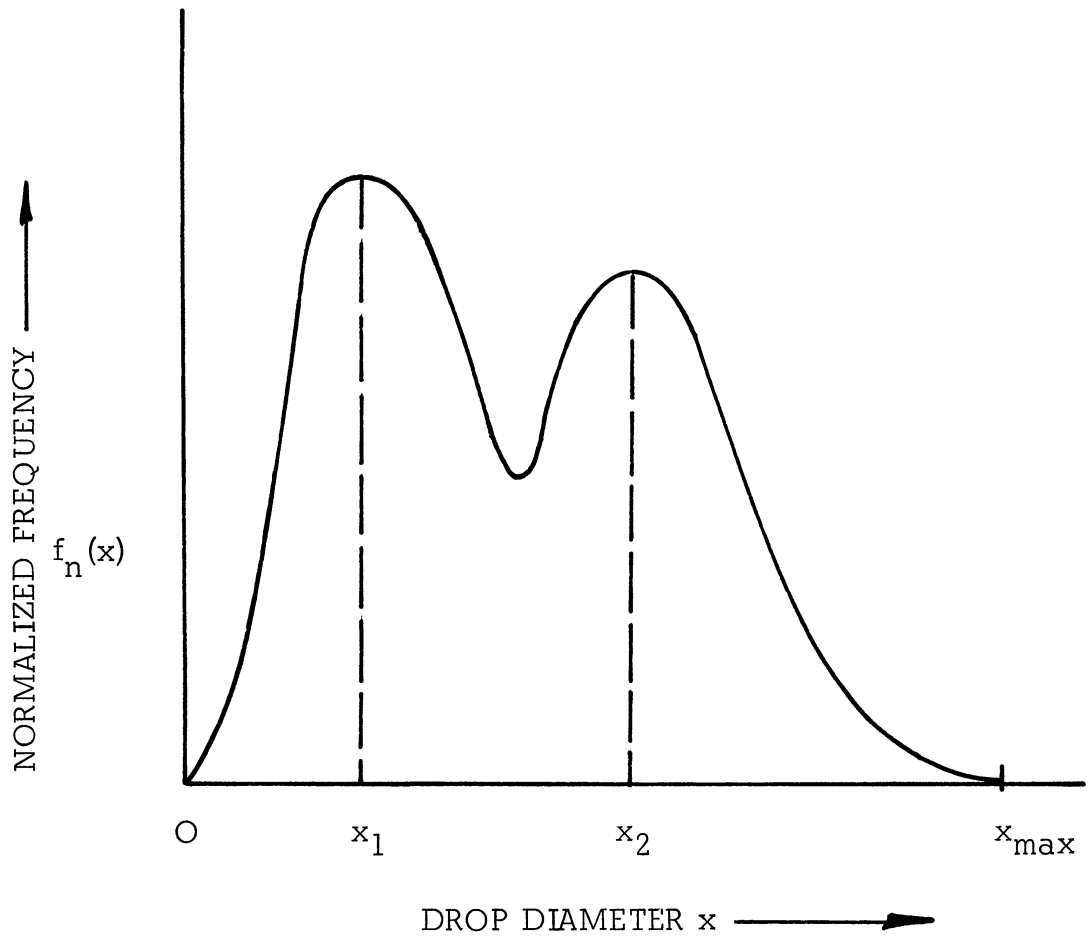


Figure 8. Drop size distribution with two preferential sizes

spherical but are actually highly irregular in shape.<sup>15, 18</sup> These facts should indicate that a mathematic description of the process is nearly impossible unless certain simplifying assumptions are made.

The droplet vaporization studies reported in the literature consist of experimental investigations of vaporization rates from single droplets and sprays, and analytical work on the heat and mass transfer rates from a single droplet. Bahr<sup>11</sup> reported an experimental investigation of the vaporization of isooctane sprays. The isooctane was injected under a pressure of 25 to 85 psia into a moving air stream. The air velocity was varied from 100 to 350 feet per second. The effect of the system variables on the per cent vaporized was indicated by the exponents in the correlating equations. The per cent vaporized was found to vary as:

Air Temperature to the + 4.40 power

Air velocity to the + 0.80 power

Air pressure to the - 1.20 power

Injection pressure to the + 0.42 power

Distance downstream to the + 0.84 power

The injection pressures were much higher than occur in typical carburetors (55 psia as compared to 25 inches of water) thus the data have little application to fuel vaporization within carburetors. The work of Ingebo<sup>16</sup> was performed at conditions more related to those in carburetors. Isooctane sprays were investigated at room temperature and pressure. Vaporization rates and droplet velocities were obtained by high speed photography. The

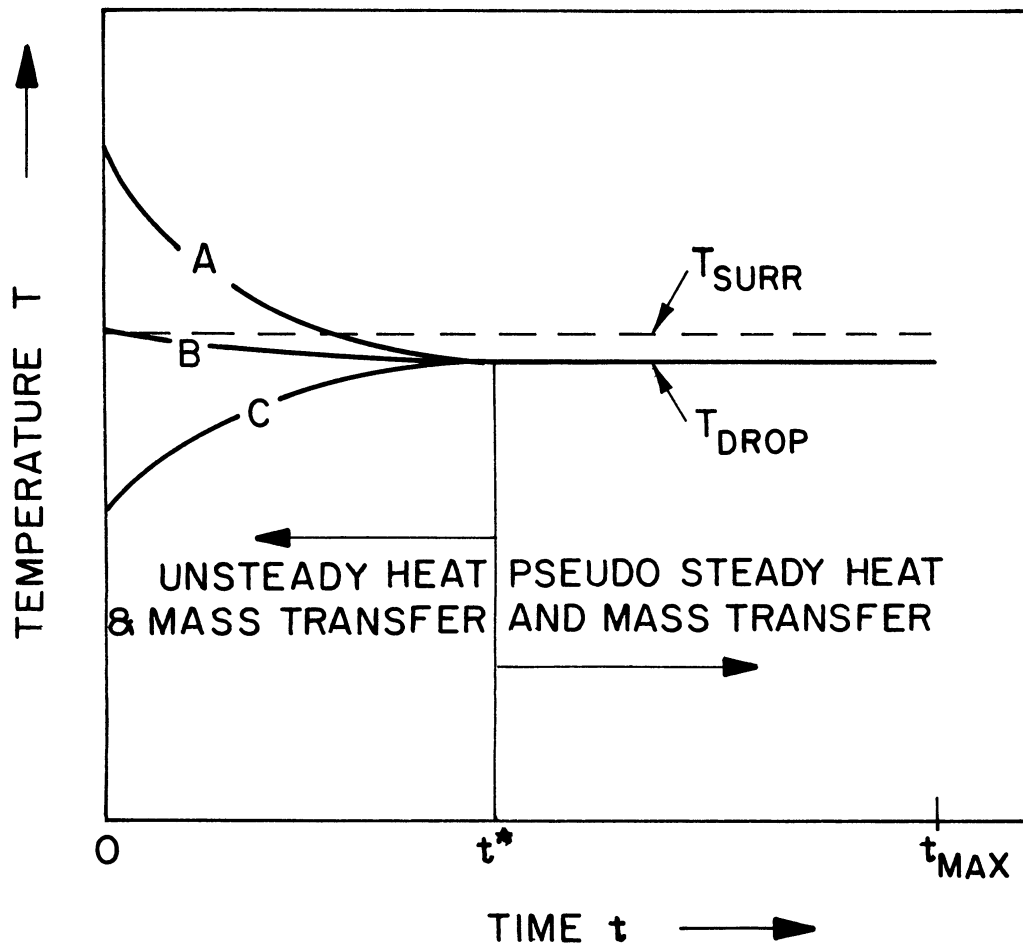
analytical portion of the study was based upon vaporization from a single spherical droplet of a mean diameter.

An excellent discussion of the experimental and analytical work that has been done was given by Graves and Bahr.<sup>15</sup> They described the problems and reviewed the existing literature extensively. They began their chapter on the evaporation of sprays by stating;

"Extension of single drop data to sprays is difficult, since both drop-size distribution of the spray and relative velocities between the air and the drops must be known. In addition, there are such complicating factors as drop distortion, unsteady state vaporization, and interactions between drops."

The vaporization of a liquid drop in the absence of relative motion with the surroundings is basically a diffusional mass transfer problem. The driving force for mass transfer will be the concentration gradient of the component comprising the droplet. The vaporization process will consist of two distinct portions, the relative importance of which will depend upon the initial difference between the droplet temperature and that of the surroundings. The quantitative variation in temperatures for the droplet (fuel) and the infinite, stagnant, surrounding medium (air) is illustrated in Figure 9. Note that the initial vaporization occurs with unsteady heat and mass transfer, that is, the droplet temperature is changing rapidly with time. This will continue until the droplet temperature reaches an equilibrium value slightly lower than that of the surroundings. This occurs at time  $t^*$  as shown in the figure. This portion of





- Curve A Initial drop temperature greater than  $T_{\text{surr}}$   
 Curve B Initial drop temperature equal to  $T_{\text{surr}}$   
 Curve C Initial drop temperature less than  $T_{\text{surr}}$

Figure 9. Illustration of drop vaporization regimes

the vaporization process is important in cases where the droplet is part of a liquid that is sprayed into surroundings which are at a much higher temperature, as in diesel engine injection. Due to the large changes in droplet temperature, the specific heats of the liquid fuel and fuel vapor become significant. The same is true for the upper curve which shows the case of initial droplet temperature much greater than that of the surroundings. However, if the initial temperatures of the droplets and the surroundings do not differ greatly, the time  $t^*$  will be a small portion of the total vaporization time,  $t_{\max}$ , and the unsteady portion can be neglected with little error. Such is the usual case in carburetor work where the fuel temperature does not differ greatly from the air stream temperature.

The pseudo steady portion of the vaporization is characterized by a relatively constant droplet temperature, with the energy transferred to the droplet (by means of the temperature difference) being equal to the enthalpy flux of the vapor leaving the droplet. In the actual situation, the surroundings are not infinite, thus the temperature of the surroundings (air temperature) must decrease as energy is supplied to the droplets. This would give a slight downward trend to the curves rather than a constant temperature.

The analysis of droplet vaporization is based upon the mass transfer from a single spherical droplet of an initial diameter equal to the Sauter

mean diameter. The equations are derived and the variables and units listed in Appendix H. Only the important results will be shown here. First, for the diffusion of a vapor,  $v$ , through a non-diffusing gas from a spherical droplet, the following equation for the rate of mass transfer was obtained:

$$\frac{\dot{m}_v}{A} = \frac{(12192.0) 2 D_v W_f}{\bar{R} T_f d_f} (P_s - P_{v\infty}) \frac{\text{LBM}}{\text{sec ft}^2} \quad \underline{\text{EQN 2.37}}$$

Equation 2.37 expresses the mass transfer rate only for zero relative motion between the droplet and the surrounding medium.

The droplet diameter at a time  $t$  after vaporization begins was obtained in terms of the system variables:

$$d_f^2 = d_{\text{sauter}}^2 - (12192)(304,800) \left[ \frac{8 D_v W_f (P_s - P_{v\infty})}{\rho_f \bar{R} T_f} \right] t \text{ microns}^2$$

EQN 2.38

For mass transfer with relative motion between the drop and the surrounding medium, the vaporization equations must be modified by the mass transfer Nusselt number. On the basis of their investigations on the evaporation of water drops in air streams, Ranz and Marshall<sup>20</sup> proposed the following correlation for the Nusselt number:

$$(N_u)_m = 2.0 + 0.60 (R_e)^{1/2} (S_C)^{1/3} \quad \underline{\text{EQN 2.39}}$$

where  $R_e$  is the droplet Reynolds number and  $S_C$  is the Schmidt number.

(See Appendix H) This resulted in the following equation for vaporization

with relative motion:

$$\frac{\dot{m}_v}{A} = (12192.0) \frac{D_v W_f}{\bar{R} T_f d_f} (P_{\text{surf}} - P_{\text{voo}}) \left[ 2.0 + 0.60 (Re)^{1/2} (Sc)^{1/3} \right]$$

EQN 2.40

By introducing the Sauter mean diameter as a description of the atomization that occurs, the single drop equations were extended to obtain relationships describing the vaporization of the entire spray. If  $\dot{m}_{\text{spray}}$  is the total mass flow rate of the spray, the spray surface area being formed can be expressed as:

$$A_{\text{spray}} = \frac{(304,800) (6) \dot{m}_{\text{spray}}}{\rho_f d_{\text{sauter}}} \frac{\text{ft}^2}{\text{sec}} \quad \text{EQN 2.41}$$

For small changes in drop diameter and thus for only the first 20 to 25% of the spray vaporization, the fraction of the spray vaporized in  $\Delta t$  seconds was found to be:

$$\text{FRACT} = (6)(12192)(304800) \left[ \frac{D_v W_f}{\bar{R} T_f \rho_f (d_{\text{sauter}})^2} \right] (P_s - P_{\text{voo}}) (Nu)_m \Delta t$$

EQN 2.42

It was found to be quite useful and informative to express the vaporization fraction in terms of downstream distance in the carburetor,  $\Delta Z$ , rather than in terms of time. This was an additional complexity since the droplet velocity is constantly changing and is related to the droplet diameter and Reynolds number. The result of this analysis was

the following equation, again valid only for the first 20 to 25% of the spray vaporization:

$$\text{FRACT} = (12192) \sqrt{304,800} \sqrt[8]{\frac{D_v W_f (P_s - P_{v\infty})}{\rho_f \bar{R} T_f (d_{\text{sauter}})^2}} (\text{Nu})_m \sqrt{\frac{\rho_f d_{\text{sauter}} \Delta Z}{\rho_{\text{air}} (V_{\text{rel}})^2 C_{\text{drag}}}}$$

EQN 2.43

Any extension of the equations to encompass the entire vaporization process would have to account for the droplet diameter decreasing significantly, with correspondingly large changes in Reynolds number and drag coefficient.

## CHAPTER III

### FUEL FLOW THROUGH ORIFICES

#### A. REASONS FOR ORIFICE FLOW WORK

The analysis of orifice flow is extremely important to the overall carburetor simulation. This is true because of the large number of orifices in series and parallel within the typical carburetor, and the control they exert over the main and idle fuel flows. The air bleed orifices are also extremely important in influencing the pressure losses within the fuel channels. If the coefficients of discharge of the orifices are assumed to be unity (or any constant value) then a very inaccurate description of fuel flow will result. A comprehensive simulation must determine the pressure drop across any orifice in terms of the orifice geometry, fluid properties, and fluid mass flow rate. This is equivalent to saying that the true variation in discharge coefficient with geometry, fluid properties, and flow rate must be known for each orifice in the carburetor.

Since the purely theoretical prediction of orifice discharge coefficients is a nearly impossible task, (as will be discussed in section 7c) each orifice type must be tested on an orifice flow stand over a wide flow rate range. Then the flow data must be correlated in a reasonable manner to facilitate the calculation of the coefficient of discharge for any operating conditions.

## B. BACKGROUND

There are numerous papers in the literature concerned with fluid flow through orifices. In general they are concerned with one or more of the following problems:

1. The experimental determination of orifice discharge coefficients
2. Correlation techniques for orifice  $C_d$  data
3. The effect of cavitation and fluid properties
4. The effect of orifice  $L/D$  ratio

Some of the literature on orifice flow is related to the calibration of standard orifice meters for pipe line flow measurement and does not have a direct bearing on carburetor fuel flow. Thus, the papers which are discussed here are, for the most part, concerned with the discharge characteristics of small, submerged orifices.

Bond<sup>32</sup> determined the variation in discharge coefficient with fluid properties and mass flow rate for a thin square-edged orifice with an  $L/D$  ratio of 0.051. Various mixtures of glycerine and water were used to obtain the effect of fluid properties. The data points were plotted as a function of  $\sqrt{\frac{\pi}{4} (Re)}$  and illustrated the fact that  $C_d$  reached a maximum value of 0.69 at a Reynolds number of about 180, then dropped slightly to a constant value of about 0.66 for higher Reynolds numbers.

The experimental work of Spikes and Pennington<sup>41</sup> was related to the variation in discharge coefficient with L/D ratio and with cavitation. The Reynolds number range investigated was generally higher than that encountered in carburetor fuel flow. The L/D ratios studied were from 0.142 to 2.00 and it was concluded that L/D ratios of about 1/2 gave  $C_d$  values which oscillated markedly with Reynolds number. It was also concluded that the discharge coefficient was constant for L/D ratios of 0.142 and less. (This would be true for the Reynolds number range investigated, which was from about 7000 to 40,000 but in the typical carburetor flow range from about 500 to 9000 this is not necessarily true.) In addition, the method of plotting the discharge coefficient data leaves much to be desired in this paper, as well as in numerous other orifice papers. The plot size, axis scales, and axis parameters used in many reports make it extremely difficult to read  $C_d$  values or distinguish different data sets.

Zucrow<sup>43</sup> reported the results of an extensive test program to study the variation in discharge coefficients of submerged orifices. The only fluid used was Benzol, however many orifices were tested with various L/D ratios, chamfer angles, chamfer depths, and mass flow rates. The Reynolds number range was fairly limited but was within the region of interest for carburetor orifice flow. Zucrow claimed that by plotting the coefficient of discharge against the orifice Reynolds number, a characteristic curve would be obtained for each orifice which would be independent



of fuel properties. This would be true if the only important variables were the ones involved in the Reynolds number, however there are many other factors which influence orifice flow and it has been found by numerous workers, including the author, that the Reynolds number does not completely correlate the fluid properties. Three additional variables which probably influence the flow are; the fuel surface tension in contact with the orifice material, the orifice surface roughness, and small cavitation bubbles at the leading edge of the orifice. These would tend to give different orifice performance even for the same Reynolds number.

Mirsky and Bolt<sup>39</sup> reported test results and a photographic flow study of a metering rod orifice system. They performed an inlet chamfer angle study and reported that a 40° included angle gave the optimum discharge coefficient. (Spikes<sup>41</sup> reported 50° and Zucrow<sup>43</sup> showed a peak in the coefficient of discharge at 40° to 60°.) Mirsky and Bolt correlated the flow data by means of dimensional analysis parameters and did not show coefficient of discharge values directly.

Ishikawa<sup>25</sup> attempted to find an orifice configuration which would compensate for changes in air and fuel temperature. This is admittedly an extremely difficult problem and could only be accomplished on an approximate basis. This was done by assuming the air flow was incompressible, the fuel kinematic viscosity decreases linearly with temperature, and that the viscous pressure loss in the fuel channel does not

change with flow rate. An orifice having a specific decrease in the coefficient of discharge with Reynolds number was needed and various configurations were tested until the desired characteristics were obtained. This study illustrates an important point: the manner of change in the orifice discharge coefficient is one of the controlling factors in the variation of the F/A ratio due to changes in fuel and ambient conditions.

The flow characteristics of short capillary tubes were studied by Kreith and Eisenstadt.<sup>37</sup> They were concerned with pressure drops and flow rates for small diameter tubes of varying L/D ratios. The interesting fact about this study is the variation in the flow exponent "n" in the equation:

$$\dot{Q} = \text{constant } (\Delta P)^n$$

It was known that for orifices (very low L/D values) the value of n was 1/2 and for flow in pipes (very large L/D values) the value was 1. The L/D range from 0.50 to 20.0 was investigated and the n value plotted versus L/D. A pressure drop correlation was found by using the dimensionless variable  $\frac{L/D}{(R_e)}$  which was first suggested by Langhaar.<sup>27</sup>

Kastner and McVeigh<sup>36</sup> were chiefly concerned with investigating the discharge coefficients of orifices in the Reynolds number range below 5000. Their Reynolds numbers were based upon the upstream pipe diameter rather than the orifice diameter. This is usually done in pipeline metering

work but since the pipe Reynolds number loses its significance when the orifice flow area is much smaller than the pipe flow area, the orifice Reynolds number is much preferred for carburetor work. They tested square-edged orifices with L/D ratios from 0.267 to 2.67 and all having a nominal orifice diameter of 0.375 inch. The fluids utilized in their investigation were water, oil, and air. Since the ratio of the orifice flow area to the upstream pipe flow area was 0.035, the conversion of their pipe Reynolds numbers to the more meaningful orifice Reynolds numbers will be:

$$(R_e)_{\text{orifice}} = \frac{(R_e)_{\text{pipe}}}{0.035} = 5.33 (R_e)_{\text{pipe}}$$

Since their reported data for square-edged orifices was over the pipe Reynolds number range from 150 to 3000, the corresponding orifice Reynolds number range was 800 to 16,000. Since there are significant  $C_d$  changes at orifice Reynolds numbers less than 800, ( $C_d$  will go to zero at zero Reynolds number) the results are only partially applicable to carburetor work.

Lichtarowicz, Duggins, and Markland<sup>38</sup> gave an excellent review of the literature on square-edged orifice studies. They also presented discharge coefficient data for L/D ratios from 0.50 to 10.0 over an orifice Reynolds number range from 1 to 10,000. Because these are the ranges of interest in carburetor work, this paper is a valuable reference. The coefficient of discharge curve for an L/D ratio of 0.50 was of an

oscillatory nature with a peak value of 0.72 at a Reynolds number of about 700. This phenomenon was also mentioned by Spikes and Pennington<sup>41</sup> although their curves did not clearly show it. The  $C_d$  data in the paper by Lichtarowicz was plotted on semi-log coordinates with the x axis as the logarithm of the orifice Reynolds number. The data points of numerous other workers were also plotted, which gave an indication of the magnitude of the scatter. A plot of the ultimate coefficient of discharge,  $C_{du}$  versus L/D ratio was also given. (The ultimate  $C_d$  value is the asymptotic value at high Reynolds numbers.) This data is of interest because it provides an easy check of any experimental results, and because the orifices with small L/D values reach their ultimate  $C_d$  values at low Reynolds numbers, after which the coefficient of discharge is constant. Figure 10 illustrates the variation in  $C_{du}$  with L/D ratio for square-edged orifices. Both the data points of various workers as plotted in reference 38 and the data points obtained in this project are shown. Note that the maximum value of  $C_{du}$  occurs at an L/D ratio of about 2.0, and that  $C_{du}$  is 0.61 for very thin orifices.

Empirical relationships which fit the experimental  $C_d$  data have been proposed by various workers. Nakayama,<sup>40</sup> on the basis of his experiments on 24 square-edged orifices with L/D ratios from 0.799 to 16.520, suggested the following relationship for the ultimate coefficient

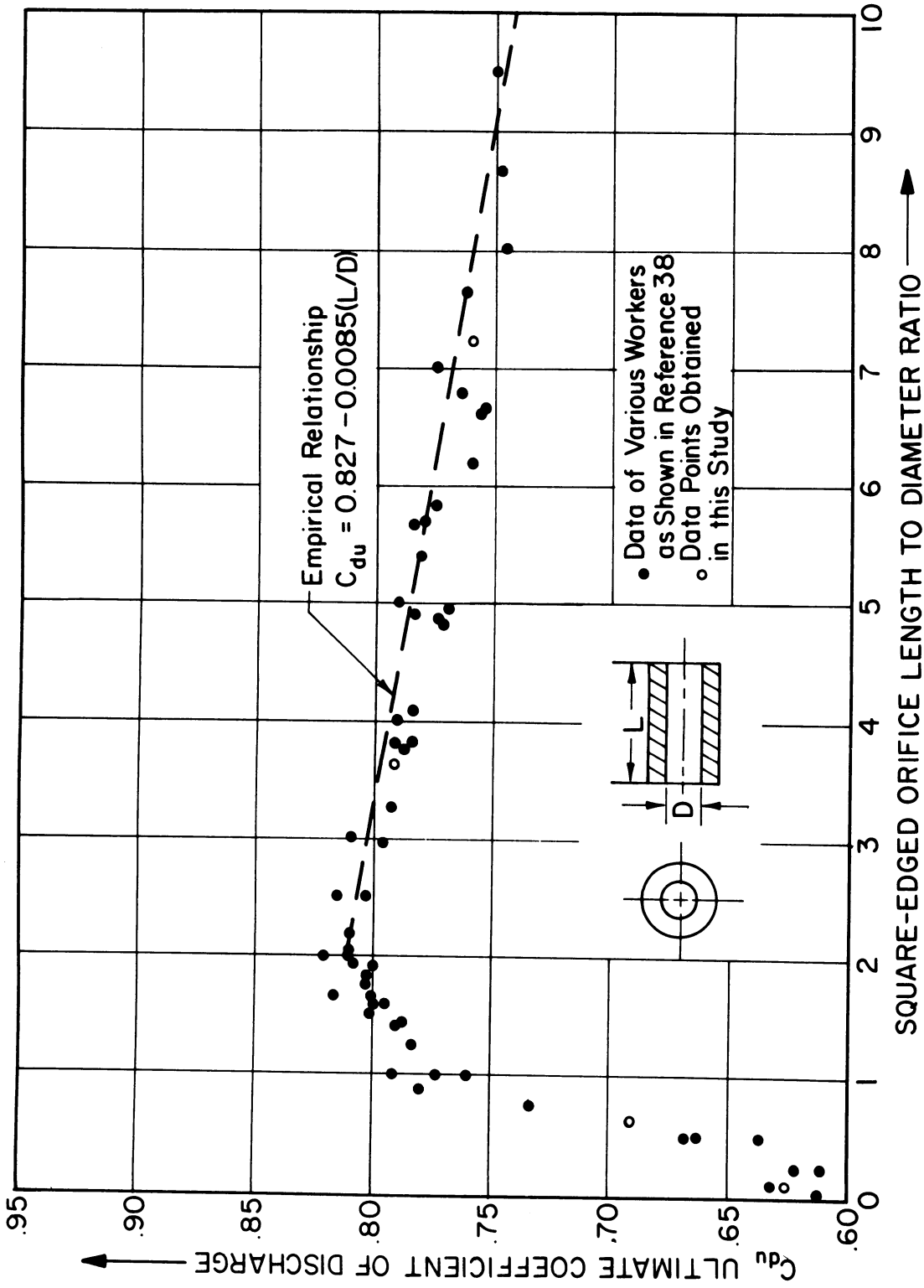


Figure 10. Variation in ultimate  $C_d$  with  $L/D$  ratio

of discharge:

$$C_{du} = 0.868 - 0.0425 \sqrt{L/D} \quad \text{EQN 3.1}$$

He also proposed an empirical equation for the coefficient of discharge in general. This would be suitable for use where specific test data for a given square - edged orifice are not available. This relationship is:

$$C_d = \frac{(R_e)^{5/6}}{17.11 (L/D) + 1.65 (R_e)^{0.8}} \quad \text{EQN 3.2}$$

An accuracy of  $\pm 2.8\%$  is claimed over an  $L/D$  range of 1.5 to 17.0 and a Reynolds number range of 550 to 7000. Another empirical relationship for  $C_{du}$  was proposed in reference 38 and is plotted on figure 10 . This equation is:

$$C_{du} = 0.827 - 0.0085 (L/D) \quad \text{EQN 3.3}$$

One of the few papers dealing with the theoretical analysis of the flow through square-edged orifices was given by Hall.<sup>35</sup> He analyzed the flow in terms of a developing turbulent boundary layer within the orifice and included the effect of a stable separation region near the inlet. In the model, the separation region results in a boundary layer which is thicker than it would be without the recirculation near the inlet. Hall proposed the concept of a virtual origin or a point upstream of the orifice from which the boundary layer would reach the given thickness. He then analyzed the movement of the virtual origin as a function of the Reynolds number based on orifice length. (The distance from the

leading edge of the orifice is the logical choice for the significant length in the Reynolds number. This is because the boundary layer thickness is related to the distance from the point of development, which in this case is the distance from the inlet to the orifice.) The result of this analysis was the following equation for the coefficient of discharge as a function of L/D ratio and Reynolds number based on orifice diameter:

$$C_d = 1.0 - \frac{0.184}{(R_e)^{0.2}} \left[ L/D - 1.0 + 1.11 (R_e)^{0.25} \right]^{0.80} \quad \text{EQN 3.4}$$

While many simplifying assumptions had to be made in the analysis, this work was certainly an initial step toward predicting the behavior of orifices.

Starrett, Halfpenny, and Nottage<sup>42</sup> were concerned with the effects of various approach conditions on the coefficients of discharge of standard metering orifices. While these standard pipe orifice plates are not important for the carburetor simulation, this paper was included because it illustrates the factors which may affect the coefficient of discharge when the orifice is in place (in the fuel channel.) When conditions are not exactly the same as the orifice flow stand, the  $C_d$  value may be affected to some degree. An example of this might be that the surface roughness of the fuel channel could be different from the inlet tube of the orifice flow stand. This could result in a different  $C_d$  value in the carburetor than in the flow stand. The paper of Starrett,

et al, examined the relative effects of various nonstandard approach conditions on the  $C_d$  values. These conditions were:

1. different approach area
2. different upstream velocity profile
  - a. swirl introduced by upstream elbows
  - b. skewed profile introduced by upstream obstructions
3. different upstream wall roughness

The effects of nonstandard approach conditions would be very difficult to evaluate for carburetor work (except for number one above) but the possibility of uncorrelated  $C_d$  variations due to these conditions should be kept in mind. The magnitude of these variations can be obtained only by testing the entire fuel channel and determining the discharge coefficient of each orifice in place.

### C. ANALYSIS AND CORRELATION OF ORIFICE FLOW

The general problem of the evaluation of the coefficient of discharge for any orifice configuration, fluid, and mass flow rate is, as stated earlier, a very important part of the overall simulation. However, while it is possible to analyze and predict the compressible flow through variable geometry nozzles in terms of fundamentals, the general problem of fluid flow through orifices is much more involved. The theoretical prediction of the fluid mass flow rate, pressure drop, and velocity distribution in an orifice is an exceedingly involved if not impossible task. This would involve the solution of the boundary layer equations with complex



exit conditions and with an increasing main stream velocity. The main stream velocity increases with orifice length because the annular boundary layer increases in thickness along the orifice. Continuity thus requires that the inner core of fluid increase in velocity as the boundary layer thickness increases. (The mass flow rate at any  $x$  must be the same as is shown below in Figure 11.)

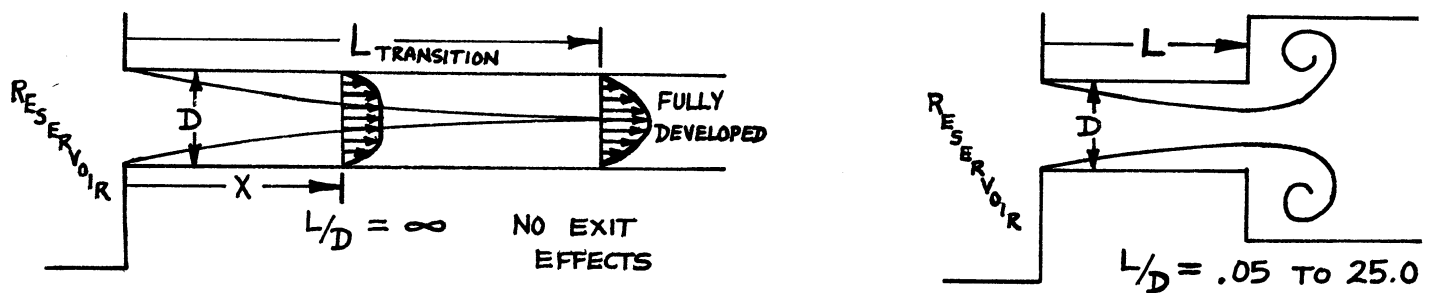


Figure 11. Boundary layer development within an orifice

One complication is that the increase in the boundary layer thickness depends upon the variation in main stream velocity with  $x$ , and this variation depends upon the thickness of the boundary layer. This problem has been solved theoretically for the special case of laminar flow in the inlet to an infinite pipe connected to a reservoir. It is a most involved solution consisting of the simultaneous solution of two infinite series with unknown coefficients. The correct coefficients yield the main stream velocity variation, the transition length required for fully developed parabolic flow, and the pressure variation with length.

Any attempts to extend this type of theoretical analysis to orifice flow, even for the simple geometry of the square edged orifice, soon encounter the fact that the flow never becomes fully developed. Thus the mating of two series at the point of parabolic velocity profile is meaningless. Added to this is the fact that there is a sudden expansion at a point where the boundary layer is only partially developed and that the velocity profile at the exit plane of the orifice is dependent on the L/D ratio and the Reynolds number. When it is also considered that boundary layer separation and cavitation occur in many orifice flow situations, it should be obvious that the theoretical prediction of orifice performance is nearly impossible.

We are thus faced with utilizing a more simplified flow situation in conjunction with experimentally determined coefficients. (Even this one-dimensional orifice flow model will become quite complex in the actual application of predicting pressure losses as will be seen later.) The experimental coefficients are referred to as discharge coefficients and they indicate the deviation from performance based on steady, one-dimensional, inviscid flow. Figure 12 illustrates an orifice flow situation with this type of flow, that is, the ideal conversion of pressure head to velocity head. Since there are no energy losses between 1 and 2 in the ideal case, we may write Bernoulli's equation between those two points assuming steady, one dimensional, incompressible flow.

$$Z_1 + \frac{P_1}{\rho_f} + \frac{V_1^2}{2g_c} = Z_2 + \frac{P_2}{\rho_f} + \frac{V_2^2}{2g_c}$$

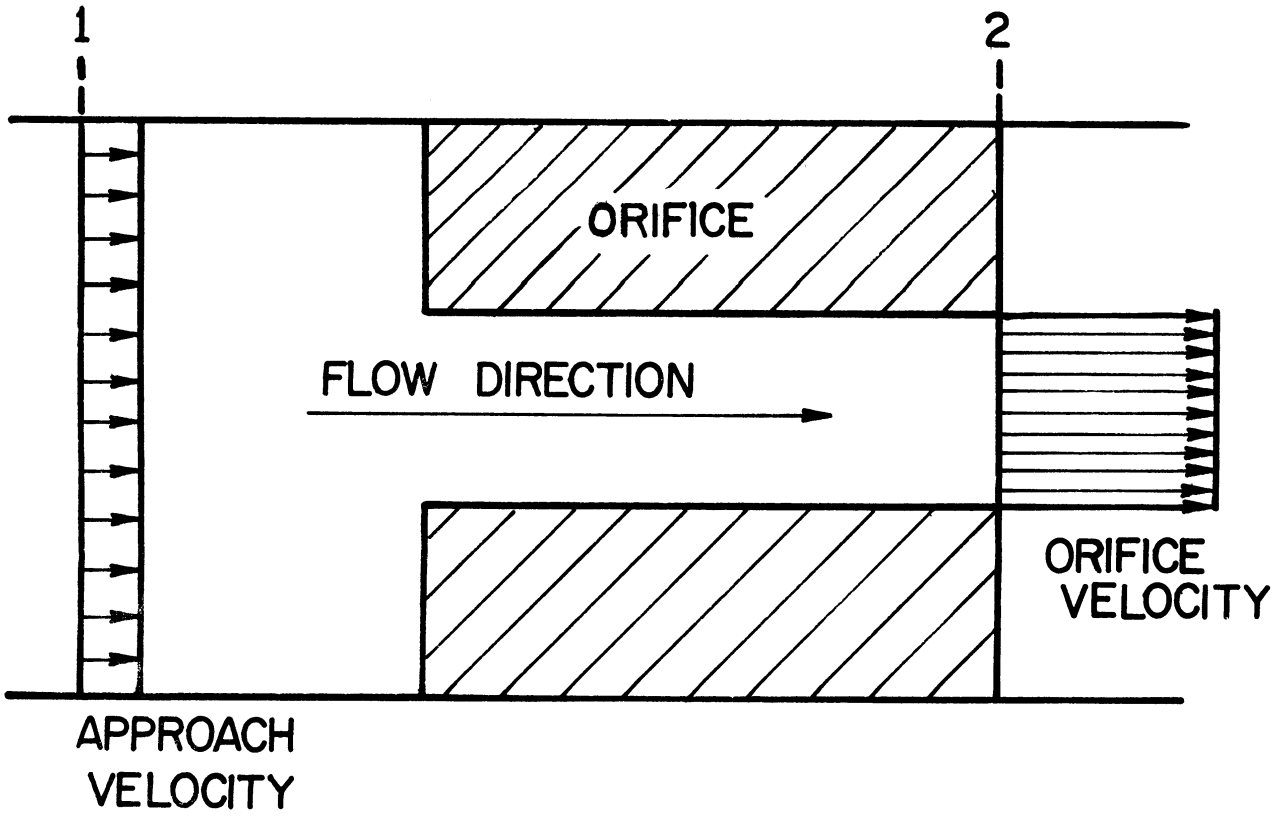


Figure 12. Ideal Flow in an Orifice

By noting that  $Z_1$  is equal to  $Z_2$  and that the head of a fluid is related to the pressure by:

$$\text{Head} = h = \frac{P}{\rho_f}$$

we obtain:

$$\frac{V_2^2 - V_1^2}{2g_c} = \frac{P_1 - P_2}{\rho_f} = \Delta h$$

By utilizing continuity,  $V_1$  and  $V_2$  are found to be related by  $A_1 V_1 = A_2 V_2$ , thus the ideal velocity is given by:

$$V_2(\text{ideal}) = \sqrt{\frac{2g_c (\Delta P / \rho_f)}{1 - \left(\frac{A_2}{A_1}\right)^2}} = \sqrt{\frac{2g_c (\Delta h)}{1 - \left(\frac{A_2}{A_1}\right)^2}} \quad \text{EQN 3.5}$$

Since the mass flow rate through the orifice is given by  $\dot{m} = \rho_f A_2 V_2$ , the following equation may be written for the ideal case:

$$\dot{m}(\text{ideal}) = \rho_f A_2 \sqrt{\frac{2g_c \Delta P / \rho_f}{1 - \left(\frac{A_2}{A_1}\right)^2}} \quad \text{EQN 3.6}$$

at this point the definition of the discharge coefficient is introduced.

This coefficient, which is denoted as  $C_d$ , is an experimentally determined parameter which compares the actual flow situation to the ideal case; that is:

$$C_d = \frac{\dot{m}(\text{actual})}{\dot{m}(\text{ideal})} \quad \text{or:} \quad \dot{m}(\text{actual}) = (C_d) \dot{m}(\text{ideal}) \quad \text{EQN 3.7}$$

if the units are as follows;

$$\rho_f = \text{lbm/ft}^3$$

$$A_2 = \text{inches}^2$$

$$g_c = \text{ft lbm/lbf sec}^2$$

$$\Delta h = \text{inches of fluid}$$

$$V = \text{ft/sec}$$

$$\dot{m} = \text{lbm/hour}$$

then the expression for the actual mass flow rate becomes:

$$\dot{m} \text{ (actual)} = \frac{3600.0 \rho_f A_2 C_d \sqrt{2 g_c \Delta h / 12}}{144.0 \sqrt{1 - (A_2/A_1)^2}} \frac{\text{lbm}}{\text{hr}} \quad \text{EQN 3.8}$$

The static pressure differential across the orifice is given by substituting equation 3.7 into equation 3.6 and converting to the desired units. The resulting equation for this pressure differential in inches of water is:

$$\Delta P = \frac{(406.62) (144.0)}{(3600.0) (3600.0) (14.696)} \left[ \frac{\dot{m}^2}{2 g_c \rho_f A_2^2 C_d^2} \right] \left[ 1 - (A_2/A_1)^2 \right]$$

inches H<sub>2</sub>O

EQN 3.9

Note that the complex flow effects have not been evaluated by introducing  $C_d$ . This has merely transferred the problem to one of determining the variation in  $C_d$  with fuel type, mass flow rate, and orifice type. As previously mentioned, this must be done experimentally by measuring the fluid mass flow rate and the pressure differential across the orifice.

Since the coefficient of discharge represents all deviations from ideal flow, we might expect that  $C_d$  would be influenced by many factors. This is in fact the case. The coefficient of discharge is affected to some extent by the following variables:

1. Fluid mass flow rate
2. Orifice L/D ratio
3. Orifice to approach area ratio
4. Fluid specific gravity
5. Fluid viscosity
6. Fluid surface tension
7. Orifice surface area
8. Orifice surface roughness
9. Orifice inlet and exit chamfers

The problem of correlating coefficient of discharge data is one of accounting for these effects experimentally and obtaining parameters from which  $C_d$  values can be predicted for other orifices of different geometries or fluids. It should be obvious that the correlation of all nine operating variables listed above would be exceedingly difficult. Fortunately, some of the variables are much less influential than others in the actual flow situation. This permits us to correlate only the most important variables and still obtain an accurate value for the discharge coefficient for nearly all operating conditions.

There are two distinct methods which can be used in correlating orifice discharge coefficient data. The first is to obtain a generalized correlation for all orifices of a given type. Ten common orifice types are shown in Figure 13. (The types of greatest interest in carburetor fuel channel flow analysis are 1, 2, and 6.) This correlation for an orifice type such as 1, the square-edged orifice, would be of the form:

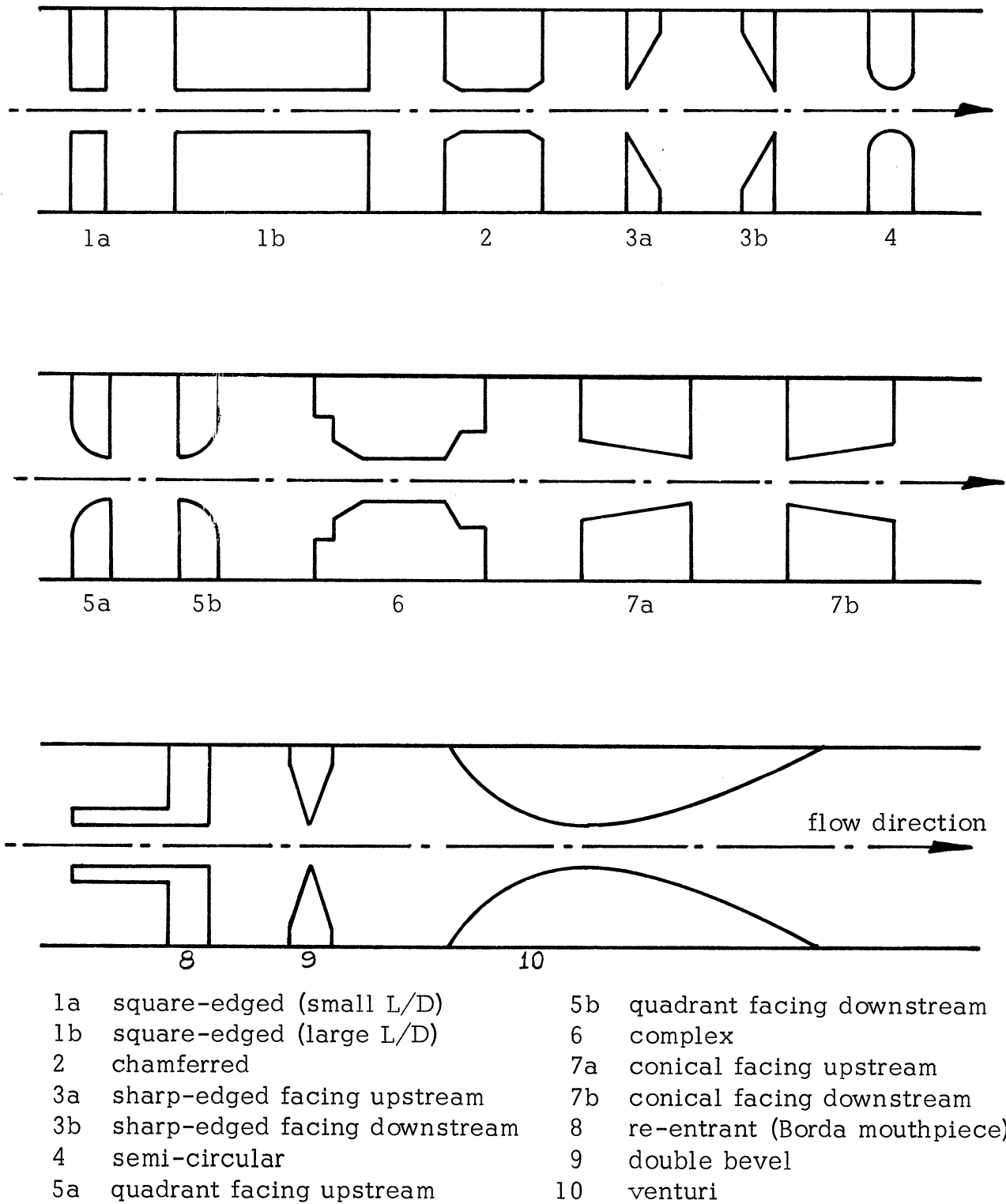


Figure 13. Nomenclature for common orifice types

$$C_d \text{ (type 1)} = f(\dot{m}_f, L/D, \rho_f, \mu_f, \nabla_f, A_1/A_2, A_{\text{surf}}, \epsilon)$$

The second technique involves a correlation for each orifice of a given geometry. More correlations are needed but they are of a simpler form. For example, consider the coefficient of discharge of a square-edged orifice with an  $L/D$  ratio of 3.63. The orifice geometry is fixed (except for the approach area), thus the correlation does not involve the  $L/D$  ratio. If the orifice for which a  $C_d$  value is to be predicted is geometrically the same as the orifice from which the correlation was obtained, then the surface area and roughness are not variables. This correlation is of the form:

$$C_d \text{ (specific geometry)} = f(\dot{m}_f, \rho_f, \mu_f, \nabla_f, A_1/A_2)$$

The second method is useful for carburetor fuel channel analysis. The application of this method is to obtain a correlation of the above form for each orifice in the fuel channel. This correlation is then used to obtain the coefficient of discharge for any fuel property values, mass flow rate, and approach area. This will be discussed in detail in Section 3f.

In obtaining the correlation from the experimental discharge coefficient data, the use of dimensional analysis has been found to be quite useful. Zucrow<sup>43</sup> was one of the first to propose a coefficient of discharge correlation utilizing the orifice Reynolds number,  $Re$ :

$$Re = \frac{\rho_f VD}{\mu_f} = \frac{VD}{\nu_f} = \frac{4\dot{m}}{\pi D \rho_f \nu_f}$$



where  $D$  is the orifice diameter in inches and  $\nu_f$  is the fluid kinematic viscosity in centistokes. In these units the orifice Reynolds number is given by:

$$\text{Re} = \frac{(12.0)(92903.0)(4.0)}{(3600.0) \pi} \left[ \frac{\dot{m}}{D \rho_f \nu_f} \right] \quad \text{EQN 3.10}$$

The use of the Reynolds number as a correlation parameter accounts for the effects of  $\dot{m}$ ,  $\rho_f$ , and  $\nu_f$  to a good first approximation. Since the Reynolds number represents the ratio of the inertial forces to the viscous shear forces, and these forces are based upon the shear of a Newtonian fluid, the Reynolds number does not completely correlate orifice flow. This will be obvious when actual  $C_d$  data are shown in Section 3e.

The orifice surface area and fluid surface tension in contact with the orifice material are not accounted for by the Reynolds number. These variables can be included in the dimensional analysis, resulting in the dimensionless number  $\rho_f V^2 D / \sigma_f$ . This number represents the ratio of the inertia forces to the capillary or surface tension forces and is known as the Weber number,  $W$ . An additional dimensionless number, known as the cavitation number, should be included if the orifice pressure drop and fuel vapor pressure,  $P_{fv}$ , are such that cavitation is likely. This number,  $K^*$ , is given by:

$$K^* = \frac{P_1 - P_2}{P_2 - P_{fv}}$$

Since cavitation does <sup>NOT</sup> occur under most normal fuel channel operating conditions, the cavitation number can usually be excluded. However,

cavitation effects can occur under conditions of high flow rates with hot fuel of low Reid vapor pressure.

Thus, the correlation of discharge coefficient data for a given orifice is of the form:

$$C_d \text{ (specified geometry)} = f(R_e, W, A_1/A_2)$$

The Weber number effect was found to be very small for typical fuels and orifice sizes, exerting only a slight influence at very low flow rates.

Fuel surface tension was found to exert a significant effect on the fuel discharge orifice pressure drop (where fuel is drawn into the air stream) and was included in that case. For other orifices, the final form of the  $C_d$  correlation becomes:

$$C_d \text{ (specified geometry)} = f(R_e, A_1/A_2)$$

#### D. CORRELATION OF FUEL PROPERTIES

It has just been shown that the correlation of orifice discharge coefficient data is very dependent on fuel property values. These values must be known for each possible fuel over a wide temperature range. This includes absolute viscosity, kinematic viscosity, density, and surface tension in contact with air. In addition, from the compressible mixture flow analysis in chapter two, it was found that numerous fuel property values were needed including specific heats, specific heat ratio, latent heat of vaporization, and molecular weight. Thus, the

goal of the fuel property correlation work was to provide all needed values for many possible fluids. This was accomplished by putting all values and correlations in a subroutine called FPROP. This subroutine may be called for a specified fuel type and temperature any time fuel properties are needed. Numerous fluids are listed in this subroutine including ASTM Iso-octane, ethyl alcohol, mineral spirits, four brands of gasoline, and water.

The experimental work on fuel properties consisted of determining kinematic viscosity and specific gravity variations with temperature for each of the fuels. The kinematic viscosity measurements were obtained with Cannon-Fenske capillary viscometers in conjunction with a Neslab constant temperature bath. A typical temperature range was 10° F to 110° F in 10° F increments, with three viscosity measurements made at each temperature. The experimental Kinematic viscosity data was correlated by an equation of the form:

$$\nu = A + \frac{B}{T+C} \text{ centistokes}$$

Where T is the temperature in degrees Fahrenheit and A, B, and C are constants to be determined for the best data fit. The correlating equation for the Kinematic viscosity of Standard regular gasoline was, for example:

$$\nu = 0.0830 + \frac{135.79}{T + 132.5} \text{ centistokes} \quad \text{EQN 3.11}$$

The specific gravity tests were run just after the viscosity tests for each fluid. In this manner all necessary test data were obtained for a given

temperature before the bath temperature was changed to a new value. The specific gravities of all fluids were determined with calibrated H-B Instrument Company hydrometers. The bath temperature was held to the nominal value  $\pm 0.1$  F in all cases.

The values of surface tension in contact with air were taken from the literature (chiefly from references 66 and 67). The variation in surface tension with temperature of a pure liquid can be adequately described by a correlating equation of the form;

$$\nabla = \nabla_0 (1 - T/T_c)^{11/9} \text{ dynes/cm} \quad \text{EQN 3.12}$$

Where T is the liquid temperature and  $T_c$  is the critical temperature, both in degrees Rankine, and  $\nabla_0$  is an empirical constant to be determined from the data. The conversion factor of ;

$$1 \text{ lbm/foot} = 14550.0 \text{ dynes/cm}$$

must be used when substituting surface tension values into equations with English units. The surface tension of most hydrocarbons (in the presence of air at one atmosphere) was found to lie between 16.0 and 23.0 dynes per centimeter at 70<sup>o</sup> F. A typical variation in surface tension with temperature is that of normal octane which decreases from 23.7 at 32<sup>o</sup> F to 19.8 dynes per centimeter at 104<sup>o</sup> F.

The effect of temperature on specific gravity, kinematic viscosity and surface tension is shown in Figure 14 for ASTM iso-octane. The gravity and viscosity data were obtained in this project and the surface tension values were obtained from reference 67. Similar curves exist for each fuel type. The important thing to notice is that significant

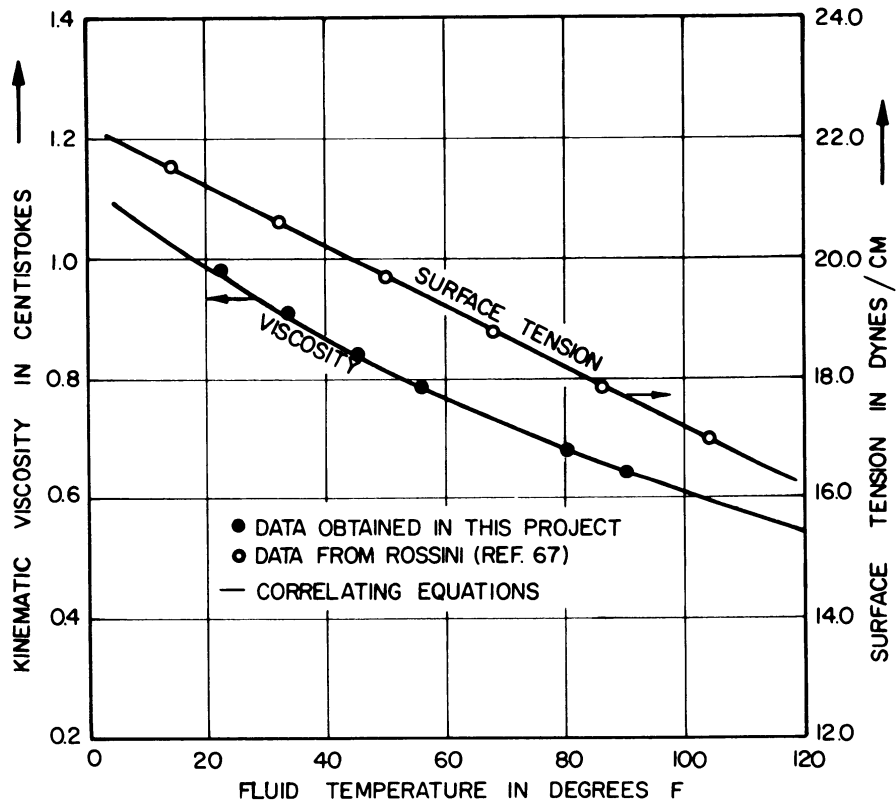


Figure 14. Iso-Octane Property Variations With Temperature

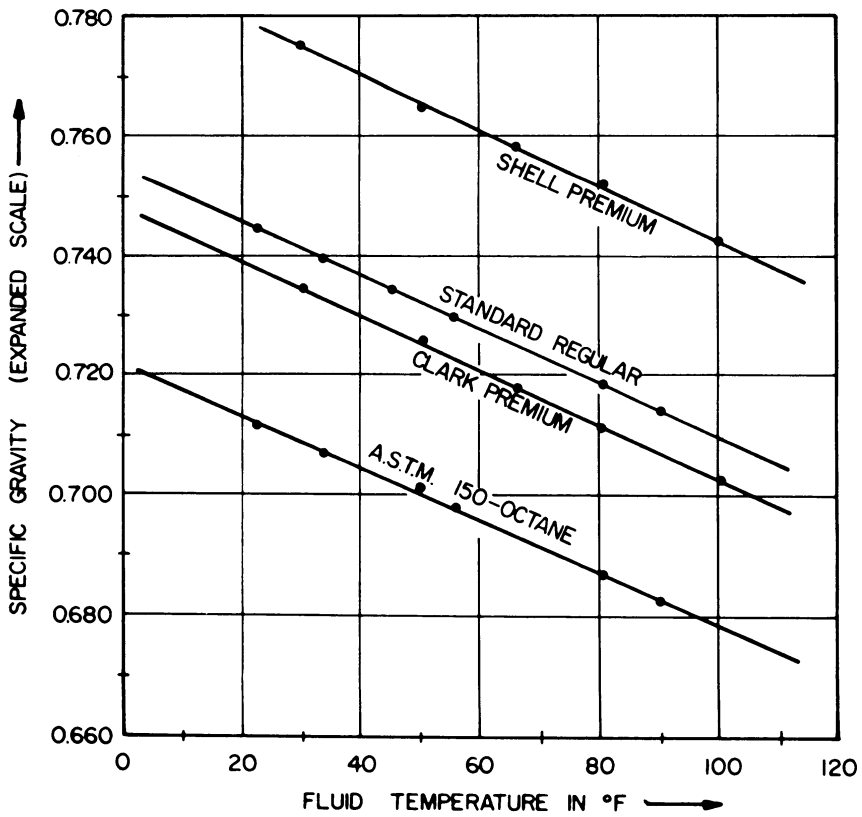


Figure 15. Specific Gravity Variations of Test Fuels

variations in these properties occur over the normal range of fuel temperature. In addition, the experimental data indicate that significant differences in kinematic viscosity and specific gravity can occur among various brands of gasolines, even at the same temperature. This is illustrated in Figure 15 which is a plot of the gravity data for three pump gasolines and ASTM iso-octane.

The numerical values for liquid specific heat, vapor specific heats, vapor specific heat ratio, latent heat of vaporization, lower heating value, and molecular weight were also obtained from the literature. These values, as well as the experimental correlations, are listed under each fluid in subroutine FPROP, in Appendix J.

#### E. RESULTS OF ORIFICE FLOW BENCH TESTS

A large scale orifice testing program was carried out on an orifice flow bench. The goal of this testing program was to provide accurate correlations of orifice discharge coefficients for use in the simulation. Approximately 100 tests on numerous orifice configurations were run on the flow bench using iso-octane, mineral spirits, and various gasolines as test fluids. A schematic diagram of the experimental apparatus is shown in Figure 16. The static pressure difference across the orifice was measured with a vernier manometer, accurate to within 0.02 inches of the fluid. The downstream pressure tap essentially measured the static pressure at the exit plane of the orifice. Test runs consisted of approximately 35 points taken over a pressure drop range

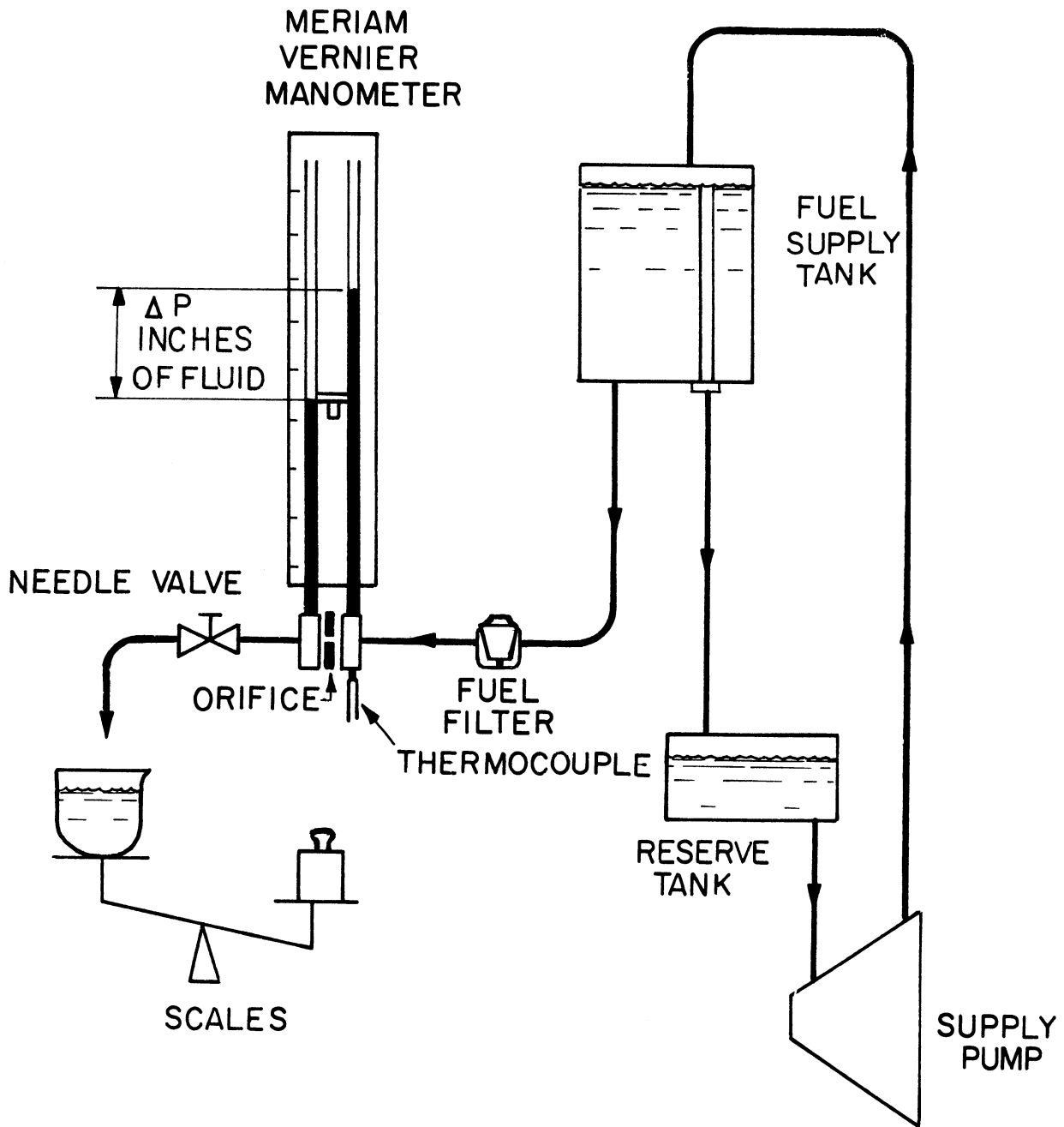


Figure 16. Schematic diagram of orifice flow bench

of 0.20 to 55.0 inches of fluid. Most of the orifices were tested for each fluid at various temperatures. This provides a check on the validity of the  $R_e$  correlation. A description of all of the orifices used in the tests is given in Table I. Note that typical automotive main metering jets were tested as were square-edged orifices with an L/D range from 0.100 to 7.230.

TABLE I  
ORIFICE TEST INFORMATION

ORIFICE NUMBER	TYPE	DIAMETER inches	LENGTH inches	L/D RATIO	REASON FOR TESTING
1	Ford F-50	0.0502	0.1837	3.660	to obtain $C_d$ curves for typical main metering orifices
2	Ford F-51	0.0514	0.1837	3.574	
3	Roch. R-55	0.0553	0.1765	3.191	
4	Square edged (Brass)	0.0518	0.0052	0.100	to obtain characteristic curves for orifices with various L/D ratios
5	Square edged (Brass)	0.0518	0.0319	0.616	
6	Square edged (Brass)	0.0518	0.1880	3.630	
7	Square edged (Brass)	0.0518	0.3745	7.230	
8	Square edged (Brass)	0.1015	0.0625	0.616	to determine the effect of orifice surface area (compare with orifice 5)
9	Square edged (Teflon)	0.0506	0.0323	0.638	to determine the effect of orifice material. (compare with orifice 5)

In Section 3C the discharge coefficient correlation for a given orifice was found to be of the form;

$$C_d (\text{specified geometry}) = F (R_e, A_2/A_1)$$

where  $A_2$  is the orifice flow area and  $A_1$  is the approach area. The



experimental data in these tests consisted of mass flow rate and static pressure differential values (in inches of test fluid) for a specified orifice and fluid. The Reynolds number was obtained by utilizing the relation:

$$R_e = 394.2 \left[ \frac{\dot{m}}{D \rho_f v_f} \right] \quad \text{EQN 3.13}$$

The observed coefficient of discharge can be calculated from the following equation:

$$C_d \text{ (observed)} = \frac{\dot{m} \text{ actual}}{\dot{m} \text{ ideal}} = \frac{(144.0) \dot{m}}{(3600.0) \rho_f A_2 \sqrt{2g_c \Delta h/12}} \quad \text{EQN 3.14}$$

The effect of the finite approach area  $A_1$  may be correlated by multiplying the observed coefficient of discharge by the factor  $\sqrt{1 - (A_2/A_1)^2}$ . This yields a discharge coefficient which is corrected to zero approach velocity.

$$\text{Thus: } C_d \text{ (corrected)} = \sqrt{1 - (A_2/A_1)^2} C_d \text{ (observed)} \quad \text{EQN 3.15}$$

Since the diameter of the approach channel in the flow bench was 0.375 inch, and the flow diameter of the orifices was about 0.051 inch, the velocity of approach correction factor was very nearly unity.

$$\sqrt{1 - (A_1/A_2)^2} = \sqrt{1 - (D_1/D_2)^4} = \sqrt{1 - (0.136)^4} \cong 1$$

The corrected  $C_d$  data is then plotted as a function of the orifice Reynolds number. (Note that the orifice diameter is used as the characteristic dimension in the Reynolds number.) The resulting curve of  $C_d$  versus  $R_e$  for a specific orifice will be referred to as the "Characteristic Curve" for that orifice. If the orifice Reynolds number

TABLE II

## RESULTS OF A TYPICAL ORIFICE FLOW STAND TEST

TEST NUMBER: 914661

ORIFICE: FORD F-50 MAIN METERING JET

FLUID: STANDARD REGULAR GASOLINE AT 77°F

Run Number	$\Delta P$ Inches of Fluid	$\Delta P$ Inches of Water	Fluid Flow Rate lbm/hr.	Orifice Reynolds Number	$C_d$	Ideal Flow Rate lbm/hr.
1	.030	.022	.329	99.8	.3643	.903
2	.080	.058	.717	217.6	.4858	1.475
3	.120	.088	.877	266.8	.4855	1.806
4	.210	.154	1.302	396.2	.5448	2.389
5	.300	.220	1.651	502.8	.5781	2.856
6	.400	.293	2.003	615.5	.6079	3.295
7	.500	.367	2.259	695.6	.6134	3.684
8	.590	.433	2.502	770.6	.6252	4.001
9	.700	.514	2.779	856.6	.6377	4.358
10	.790	.580	2.987	920.6	.6451	4.630
11	.940	.690	3.275	1009.4	.6484	5.050
12	1.040	.764	3.499	1078.6	.6587	5.312
13	1.520	1.116	4.531	1395.7	.7055	6.422
14	2.050	1.506	5.346	1645.8	.7167	7.459
15	2.520	1.851	5.997	1842.6	.7250	8.271
16	2.990	2.196	6.603	2027.7	.7329	9.010
17	3.650	2.681	7.518	2305.7	.7552	9.955
18	4.040	2.968	7.918	2423.7	.7559	10.475
19	4.500	3.306	8.418	2576.9	.7614	11.055
20	5.030	3.695	9.043	2768.3	.7737	11.688
21	5.520	4.055	9.540	2920.5	.7792	12.244
22	6.050	4.444	10.197	3121.5	.7955	12.819
23	6.540	4.804	10.574	3236.8	.7934	13.328
24	7.000	5.142	11.058	3385.1	.8020	13.789
25	7.530	5.532	11.499	3520.1	.8041	14.301
26	8.100	5.951	12.076	3696.7	.8142	14.832
27	8.390	6.164	12.213	3731.5	.8089	15.098
28	8.910	6.546	12.749	3893.0	.8194	15.559
29	9.530	7.001	13.147	4012.0	.8170	16.092
30	9.520	6.994	13.238	4034.7	.8230	16.085
31	10.020	7.362	13.585	4135.1	.8231	16.504
32	11.120	8.170	14.485	4406.3	.8331	17.387
33	12.070	8.868	15.138	4604.9	.8357	18.114
34	13.030	9.573	15.734	4786.2	.8360	18.821
35	14.060	10.330	16.425	4993.2	.8401	19.552
36	15.060	11.065	17.085	5190.7	.8443	20.236
37	16.050	11.793	17.696	5372.7	.8470	20.891
38	17.080	12.550	18.327	5557.3	.8503	21.553
39	18.050	13.263	18.853	5709.6	.8508	22.159
40	19.050	13.998	19.420	5874.1	.8530	22.766
41	20.040	14.725	19.940	6027.4	.8539	23.352
42	26.450	19.483	22.828	6885.8	.8620	26.531
43	29.620	21.766	24.647	7426.6	.8680	28.396
44	35.210	25.874	27.094	8143.3	.8750	30.966
45	40.510	29.769	29.131	8749.9	.8770	33.216
46	45.170	33.194	30.902	9270.2	.8810	35.078
47	50.000	36.745	32.524	9738.0	.8811	36.911
48	54.840	40.303	34.275	10243.0	.8866	38.661
49	58.040	42.655	35.264	10524.9	.8865	39.777

completely correlated the flow, the test data for all fluids would lie on the same curve. This claim was made by Zucrow when he proposed the Reynolds number correlation, but subsequent investigations, including the orifice work in this project, have shown that  $C_d$  data for different fluids, or for a given fluid at various temperatures, do not always lie on the same  $C_d$  versus  $R_e$  curve. This is likely due to phenomena which are not accounted for in the orifice Reynolds number correlation such as surface tension effects, non-Newtonian flow, boundary layer separation (which should be correlated with distance from the inlet edge of the orifice), and cavitation. It will be seen, however, that for the orifices, fuels, and flow rates normally encountered in carburetor work, the orifice Reynolds number does an adequate job of correlating fuel property and mass flow rate effects. It should be emphasized that the effects which have been neglected may be of great significance and could, in fact, predominate in other orifice flow situations.

All test data were reduced by a digital computer program and the resulting values were plotted on a CALCOMP plotter. Table 2 shows the test results for a typical run (number 914661) which was an orifice flow bench test of a Ford F-50 main metering jet using Standard regular gasoline as the fluid. The important parameters from this test are plotted in Figures 17 through 21. (computer plots of this type were obtained for each test). The variation in gasoline flow rate with static pressure differential across the orifice is shown in Figure 17. Note that this flow rate rises smoothly with pressure differential, yielding a

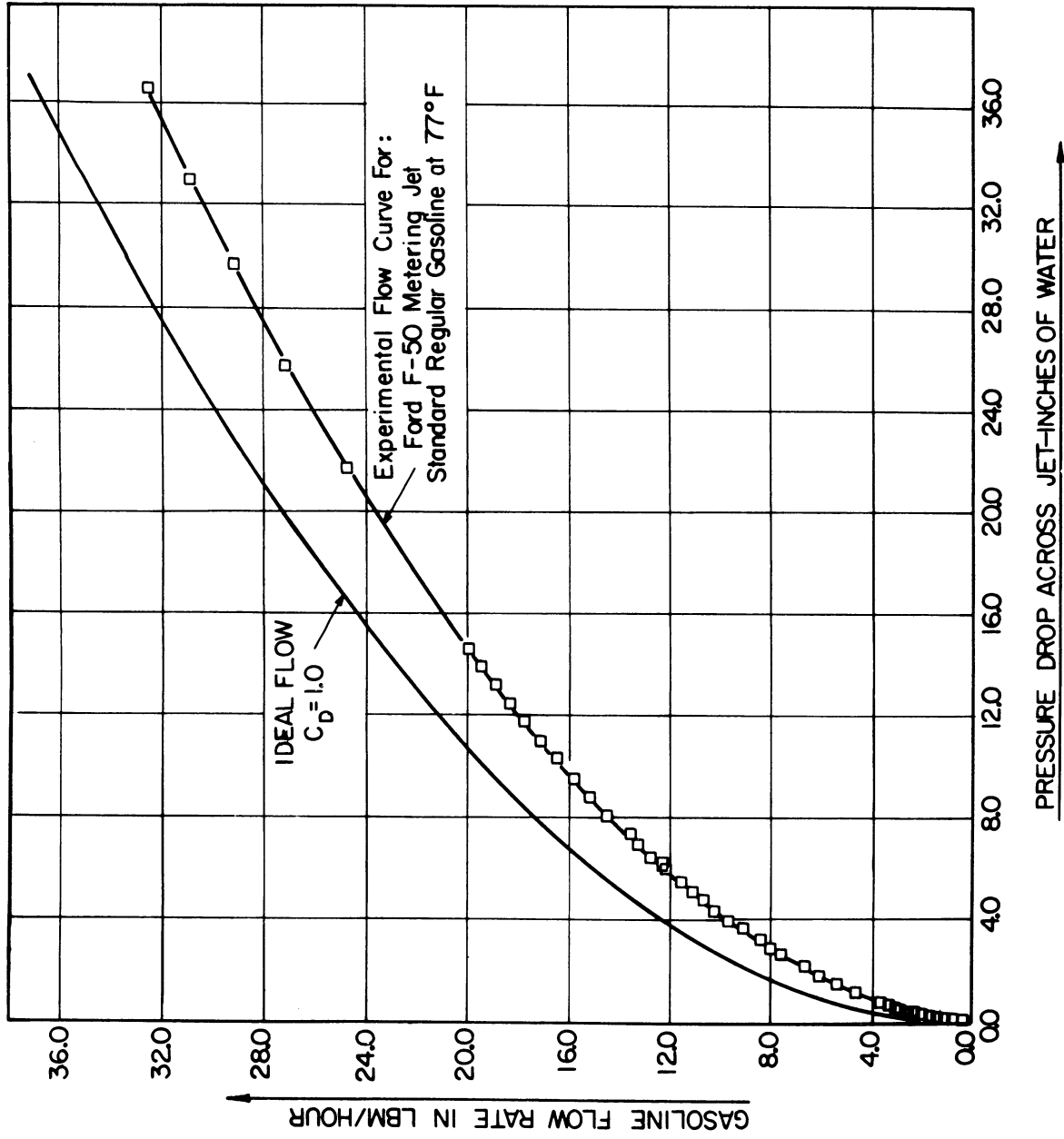


Figure 17. Gasoline flow rate vs. pressure drop for F-50 orifice

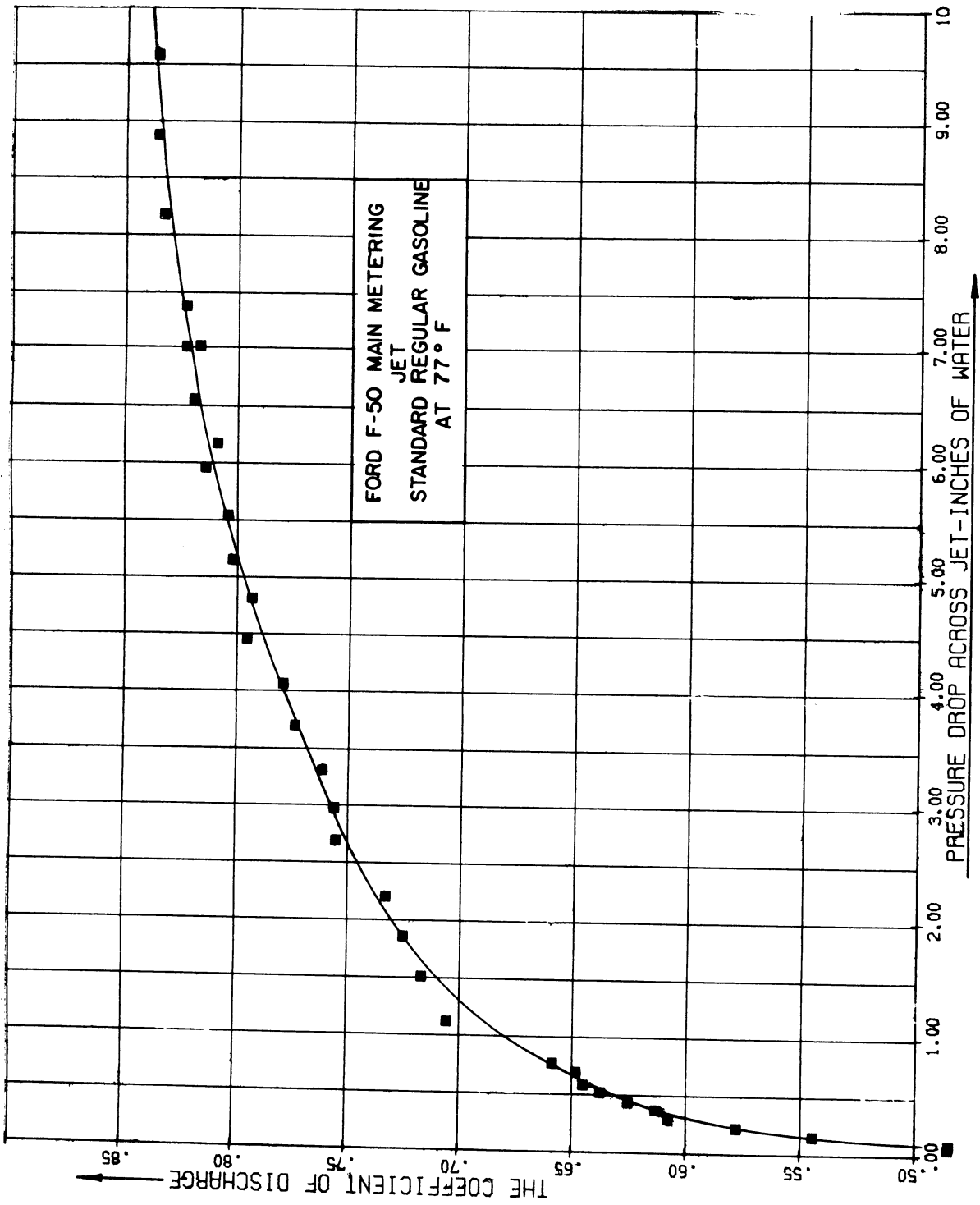


Figure 18.  $C_d$  vs. pressure drop for F-50 orifice

mass flow rate of 16.20 lbm/hour at a  $\Delta P$  value of 10.0 inches of water. Figure 18 illustrates the variation in the coefficient of discharge with the static pressure differential across the orifice. The important fact shown on this graph is that significant changes in the orifice discharge coefficient do occur over the normal operating range of pressure drops. For this particular orifice, the operating discharge coefficient will vary between 0.63 and 0.84. This verifies the statement made earlier that large errors in predicting fuel flow rates can result from assuming the discharge coefficient to be constant.

The characteristic or correlated curve for the orifice is shown in Figure 19. In this curve the orifice discharge coefficient is represented as a function of orifice Reynolds number. Note that the discharge coefficient rises smoothly with Reynolds number which is the usual case for orifices with  $L/D$  ratios greater than about 2.0. This data was obtained for a specified orifice (Ford F-50) and a specified fluid and temperature (Standard regular gasoline at 77° F.) If Figure 19 is actually a characteristic curve for that orifice, that is, if the  $R_e$  correlation is exact, then the discharge coefficient data for all other fluids and for Standard regular gasoline at other temperatures would lie on the same curve. Since many tests were performed on each orifice using fluids of various viscosities and densities, all that was required to check the validity of the Reynolds number correlation was to plot  $C_d$  curves for various fluids on the same grid. A typical set of these curves is shown in Figure 20. Note that the orifice Reynolds number

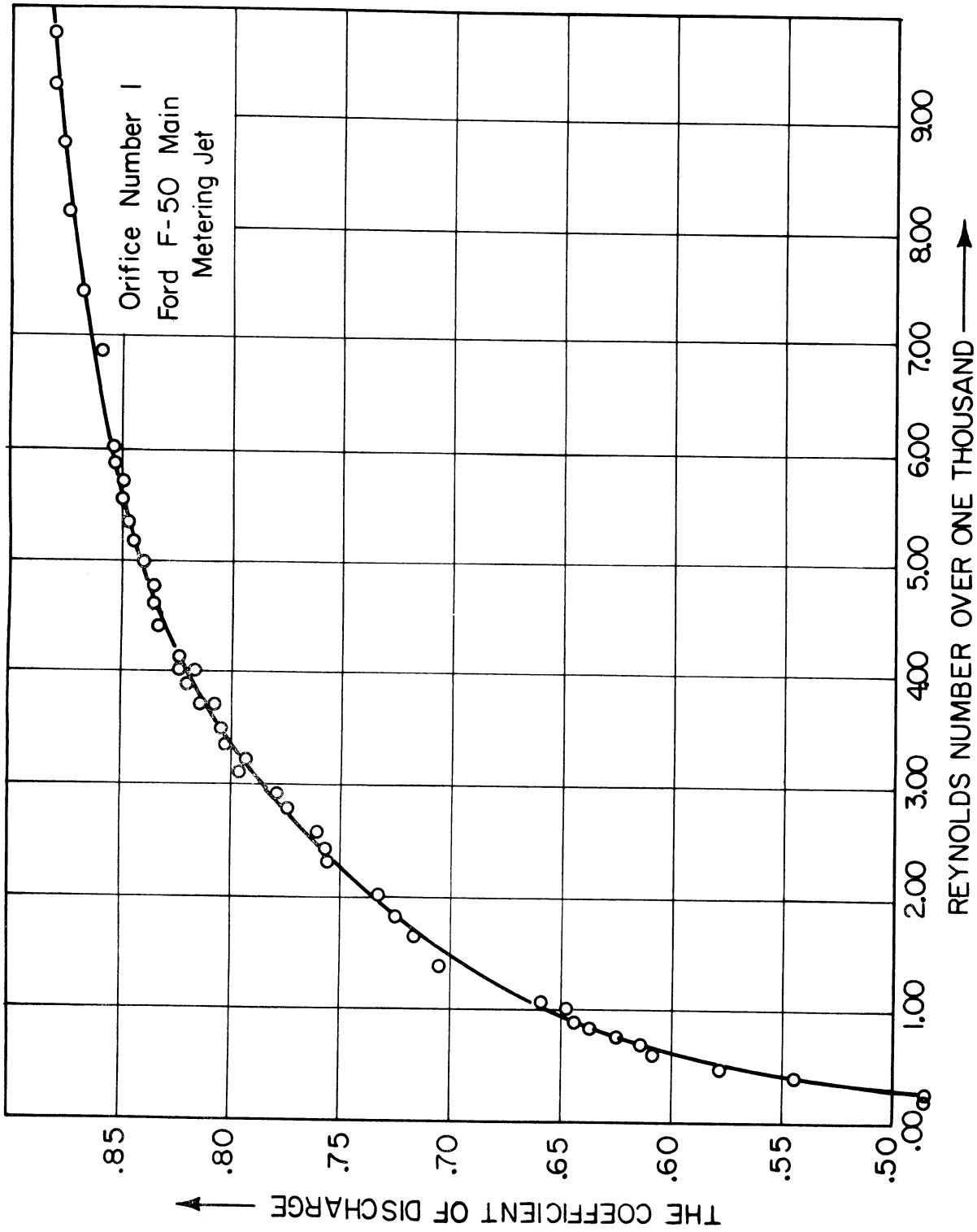


Figure 19. Characteristic discharge coefficient curve for F-50 orifice

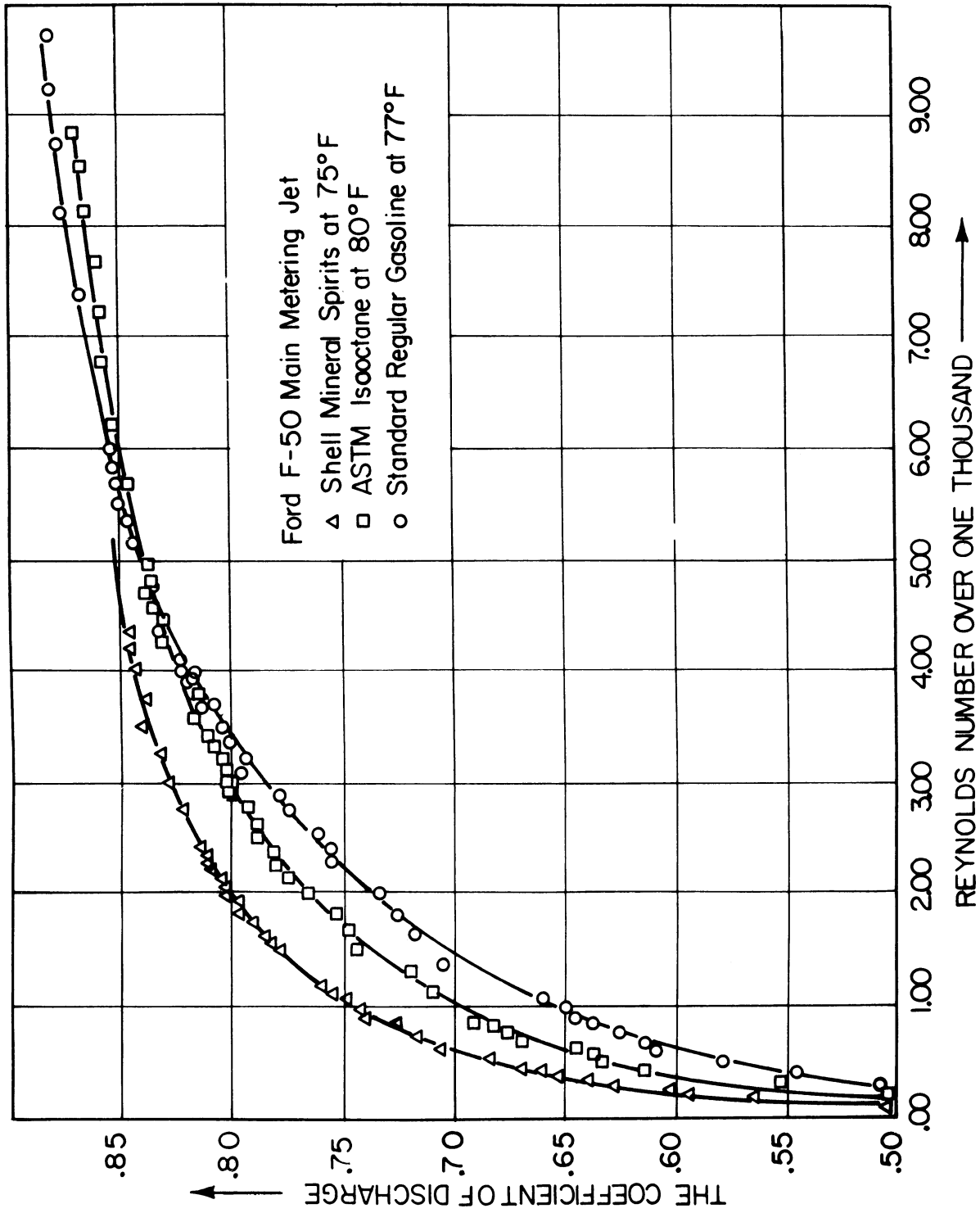


Figure 20. The effect of fluid type on the discharge coefficient



did not completely correlate the data because different  $C_d$  values were obtained at the same value of  $R_e$  (for  $R_e$  less than 5000). The higher  $C_d$  values were obtained with fluids of higher viscosity and surface tension. For this particular orifice, the spread between the curve for Standard regular gasoline and Shell mineral spirits at a Reynolds number of 1000 was 0.10 (0.55 to 0.65). The spread among gasoline brands was much smaller, being 0.64 to 0.67. For orifice Reynolds numbers greater than 5000, the discharge coefficient was correlated to within  $\pm 1\%$  for all fluids tested.

One of the important reasons for conducting the orifice flow tests was to obtain accurate data on the manner in which the characteristic curve is affected by orifice  $L/D$  ratio. Another reason was to compare the characteristic curves of various square-edged orifices with those of typical main metering orifices. This information can be ascertained by inspecting Figure 21 which contains the characteristic curves for three square-edged orifices and one main metering orifice. Notice that the  $L/D$  ratio exerts a large influence on the shape of the characteristic curve. The coefficient of discharge variation for orifice number four, with an  $L/D$  ratio of 0.100, is very similar in form to that of a sharp-edged orifice. This type of orifice yields a  $C_d$  value which reaches a maximum at a low Reynolds number (less than 1000) and then remains relatively constant or decreases slightly as the Reynolds number is increased. This similarity in performance is due to the fact that the square-edged orifice geometry approaches that of the sharp-

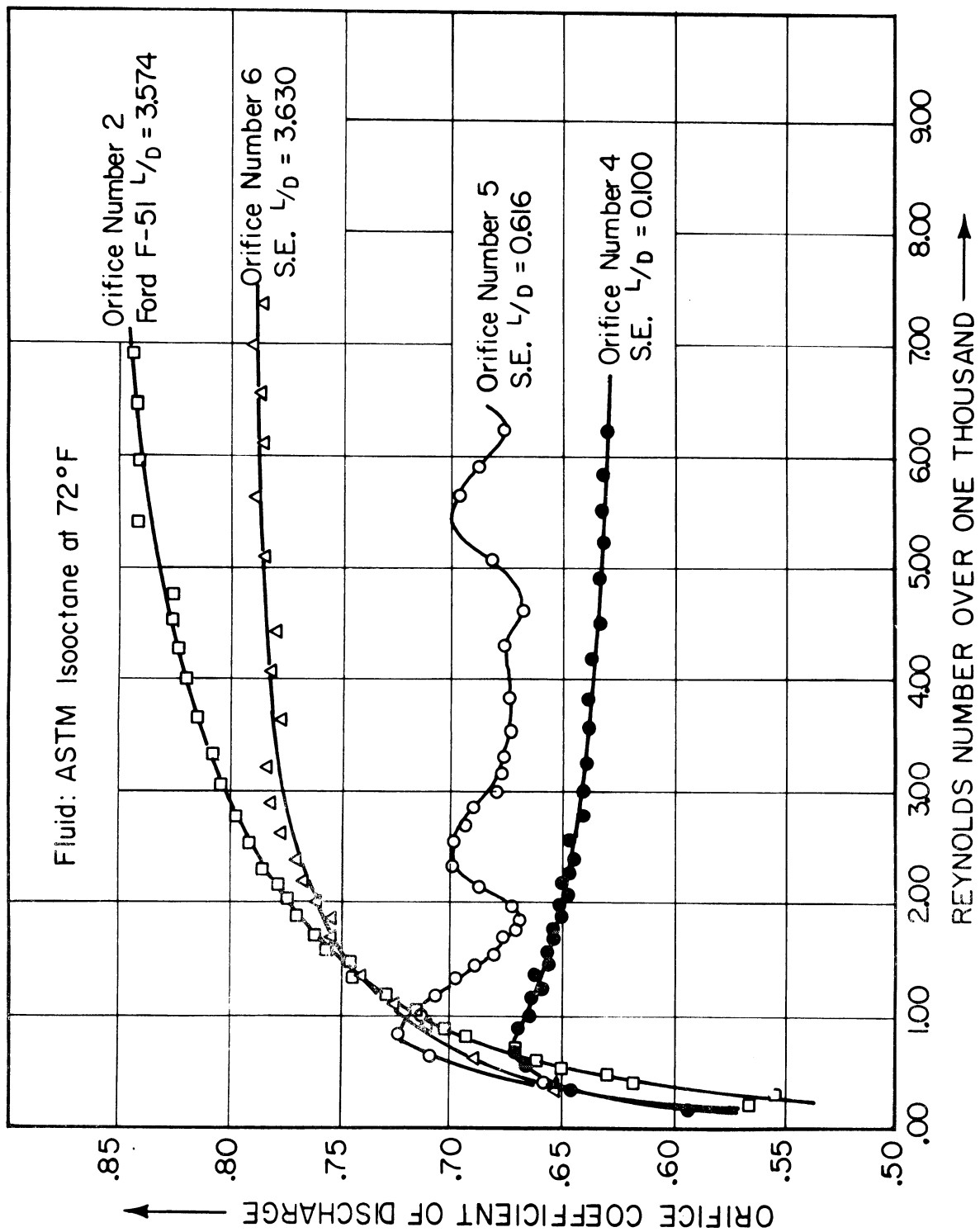


Figure 21. The effect of  $L/D$  ratio on the orifice characteristic curve

edged orifice as the length becomes very small.

Note that flow instabilities are inherent in orifice number 5, which has an  $L/D$  ratio of 0.616. The instability of square-edged orifices with  $L/D$  ratios between 0.25 and 1.0 has been noticed by numerous workers as mentioned previously. This instability is most predominate at  $L/D$  ratios near 0.50 and orifice Reynolds numbers greater than 800, and is characterized by difficulties in obtaining steady mass flow rates and pressure differentials during a flow bench test. These parameters tend to undergo step changes at various times during a flow test, indicating that the instabilities may result from a detachment and reattachment of a separation bubble near the upstream edge of the orifice.

Square-edged orifices with  $L/D$  ratios greater than about 1.0 yield a discharge coefficient which increases smoothly with Reynolds number as illustrated by orifice numbers 2 and 6 in Figure 21 (there is always a positive slope to the characteristic curve.) The ultimate value of the discharge coefficient for these orifices is reached, for all practical purposes, at Reynolds numbers in the 8000 to 10,000 range. The value of  $C_{du}$  decreases slightly as  $L/D$  increases because the viscous dissipation within the orifice is increasing. In fact, this is the predominate mechanism for total pressure losses as the  $L/D$  ratio approaches 40 (approximately), which is the beginning of the pipe flow regime.

The data points describing the characteristic curves of the orifices are listed in Table III. These points were read in as data for use by the interpolation subroutine STERL. The data for all L/D ratios which were previously listed in Table I were obtained in this project. The data for the remaining L/D ratios were obtained by reducing and plotting the original data of Zucrow.<sup>43</sup>

Table III Orifice  $C_d$  data used in the simulation

POINT	INPUT DATA FOR ORIFICE COEFFICIENTS OF DISCHARGE										RE	L/D RATIO	RE	F-50 L
	F-50	0.100	0.616	1.426	3.629	4.726	7.230	10.58	10.58	10.58				
1	.300	.000	.000	.000	.300	.000	.000	.000	.000	.000	0	0	.000	
2	.577	.663	.690	.737	.574	.623	.570	.525	.525	.525	100	100	.361	
3	.656	.665	.720	.766	.715	.580	.647	.620	.620	.620	200	200	.467	
4	.702	.654	.677	.770	.739	.710	.688	.660	.660	.660	300	300	.513	
5	.734	.648	.668	.774	.759	.727	.711	.685	.685	.685	400	400	.550	
6	.761	.644	.700	.788	.768	.741	.724	.703	.703	.703	500	500	.577	
7	.783	.641	.675	.790	.772	.750	.729	.712	.712	.712	600	600	.597	
8	.804	.638	.677	.790	.776	.756	.730	.720	.720	.720	700	700	.614	
9	.820	.635	.675	.793	.779	.751	.734	.726	.726	.726	800	800	.629	
10	.832	.633	.670	.796	.781	.764	.739	.729	.729	.729	900	900	.643	
11	.840	.631	.678	.798	.783	.766	.743	.732	.732	.732	1000	1000	.656	
12	.848	.629	.698	.800	.785	.768	.746	.734	.734	.734	1100	1100	.665	
13	.854	.627	.686	.802	.786	.770	.747	.736	.736	.736	1200	1200	.675	
14	.860	.626	.676	.804	.787	.771	.749	.737	.737	.737	1300	1300	.684	
15	.865	.625	.713	.805	.788	.772	.751	.738	.738	.738	1400	1400	.693	
16	.869	.624	.705	.806	.789	.773	.753	.739	.739	.739	1500	1500	.702	
17	.873	.623	.700	.807	.790	.774	.755	.740	.740	.740	1600	1600	.709	
18	.876	.622	.690	.808	.791	.775	.757	.741	.741	.741	1700	1700	.716	
19	.879	.621	.682	.809	.792	.776	.759	.742	.742	.742	1800	1800	.722	
20	.881	.620	.680	.810	.793	.777	.760	.743	.743	.743	1900	1900	.728	
21	.883	.620	.680	.810	.793	.778	.761	.743	.743	.743	2000	2000	.734	

## F. APPLICATION OF ORIFICE COEFFICIENT DATA TO ACTUAL FLOW SITUATIONS

The preceding sections have been devoted to methods of formulating and obtaining orifice flow correlations. Even after this has been accomplished, many questions must be answered in connection with the application of orifice flow stand data to actual flow situations.

These questions are:

1. How can the total and static pressure differentials across an orifice be calculated from its characteristic curve?
2. How can orifice performance be predicted when using fluids and approach area geometries which differ from those used to obtain the characteristic curve?
3. How can the pressure differentials be calculated for an orifice with an L/D ratio for which a characteristic curve has not been obtained.

These questions arise because the typical carburetor fuel channel contains numerous orifices of various types (square-edged, chamfered, and complex) and L/D ratios. The properties of the fluid flowing through these orifices will vary over a wide range due to variations in fuel brand and ambient temperature. In addition, the orifices will be installed in fuel channel branches having various diameters, giving various approach area ratios.

The characteristic curve for a particular orifice is, as mentioned in the previous section, a plot of the discharge coefficient (corrected to zero approach velocity) versus the Reynolds number based on orifice diameter. Once this has been obtained for a particular orifice type and L/D ratio, the discharge coefficient and pressure differentials can

be obtained for any mass flow rate by the following technique:

A mass flow rate, fuel type, and fuel temperature will be specified. (The mass flow rate is the iteration variable in the fuel channel analysis as will be explained in the next chapter.) Subroutine FPROP is called and the fuel properties determined. The orifice Reynolds number can then be calculated by using the relationship:

$$R_e = \frac{4 \dot{m} (309.6)}{\pi \rho v D}$$

The coefficient of discharge is obtained by interpolation within the characteristic curve. This is accomplished by the multi-purpose interpolation subroutine, STERL (Appendix F). The characteristic curve for the given orifice is supplied to the subroutine by reading in the  $C_d$  and  $R_e$  values. For example, for a square-edged orifice with an  $L/D$  ratio of 3.630, twenty  $C_d$  versus  $R_e$  points were obtained by a flow stand data reduction program. These points were read in and stored for use by the interpolation subroutine. Whenever a  $C_d$  value is required for this orifice at a certain  $R_e$  argument, subroutine STERL performs an accurate  $n^{\text{th}}$  degree interpolation on the data. Briefly, this is accomplished by generating a difference table from the data points and using Sterling's interpolation technique, which is a combination of the Gauss forward formula and the Gauss backward formula.

This  $C_d$  value is one which corresponds to zero approach velocity, as would be obtained in an orifice at the exit of a reservoir. In the general case of a fuel channel orifice, there is a finite approach area which will vary with the channel diameter. This must be taken into

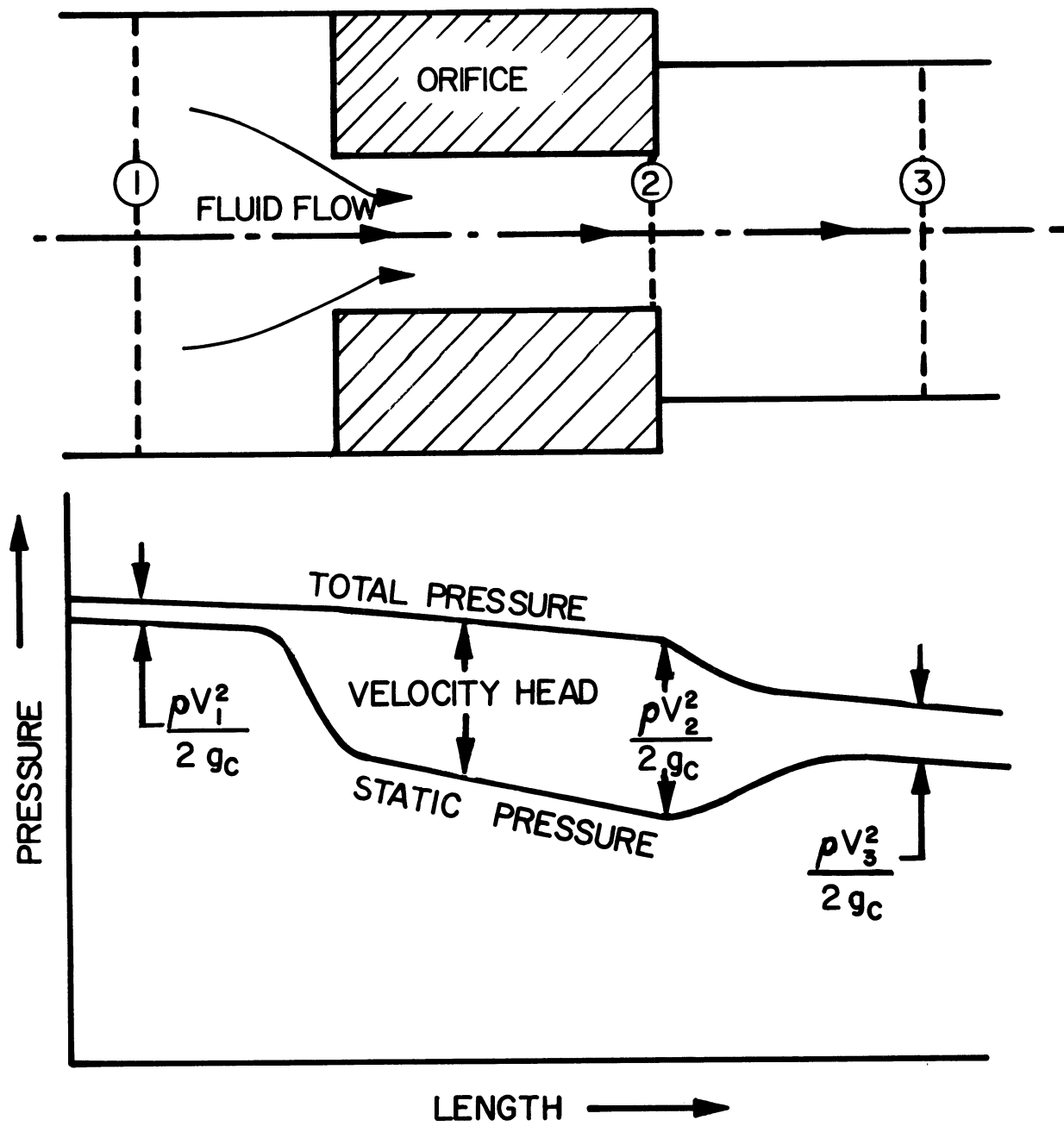


Figure 22. Pressure Variations in the Vicinity of an Orifice



consideration in utilizing flow stand data to calculate orifice pressure differentials.

Figure 22 illustrates the areas involved in the approach velocity correction as well as a schematic representation of the static and total pressure variations in the vicinity of the orifice. It should be realized that the calculation of the coefficient discharge is only an intermediate step in the analysis of orifice flow. The parameters of greatest interest are actually the static and total pressure differentials across the orifice as installed in the fuel channel. Note that areas  $A_1$  and  $A_3$  will, in general, be different from those of the orifice flow stand, and that only the static pressure differential is measured, although the total pressure differential is a more significant parameter in the analysis. Thus, expressions for these pressure differentials will now be obtained.

Let us define the following additional variables:

- $P_{1t}$  = total pressure at station 1 in inches of water
- $P_{2t}$  = total pressure at orifice exit in inches of water
- $P_{1s}$  = static pressure at station 1 in inches of water
- $P_{2s}$  = static pressure at orifice exit in inches of water
- $\Delta P_t$  = total pressure differential across orifice in inches of water
- $\Delta P_s$  = static pressure differential across orifice in inches of water
- $A_1$  = approach area in square inches (in this case the cross-sectional area of the fuel channel containing the orifice.)
- $A_2$  = orifice flow area in square inches

The total and static pressure differentials may be written as:

$$P_{1t} = P_{2t} + (\Delta P_t)_{1-2} \quad \text{and} \quad P_{1s} = P_{2s} + (\Delta P_s)_{1-2}$$

But the relationships between the static and total pressures are:

$$P_{1t} = P_{1s} + \frac{C^* \rho V_1^2}{2g_c} \quad \text{and} \quad P_{2t} = P_{2s} + \frac{C_p^* \rho V_2^2}{2g_c} \quad \text{EQN 3.16}$$

where  $C^*$  is a units conversion factor of  $406.62/2116.6$ . Now eliminating the total pressure values  $P_{1t}$  and  $P_{2t}$ , and factoring out the term  $C^* \rho / 2g_c$ , the following equation is obtained.

$$(P_{1s} - P_{2s}) = \frac{C^* \rho}{2g_c} (V_2^2 - V_1^2) + (\Delta P_t)_{1-2} \quad \text{EQN 3.17}$$

but, from the continuity equation for one-dimensional, steady, incompressible flow (which is the flow situation upon which coefficient of discharge analyses are based);

$$\dot{m} \frac{\text{lbm}}{\text{hr}} = (25.0) \rho A_1 V_1 = (25.0) \rho A_2 V_2 \quad \text{or} \quad V_1^2 = (A_2/A_1)^2 V_2^2 \quad \text{EQN 3.18}$$

Eliminating the approach velocity in the fuel channel,  $V_1$ , the following relationship is obtained:

$$V_2^2 = \frac{2g_c}{C^* \rho [1 - (A_2/A_1)^2]} \left\{ (P_{1s} - P_{2s}) - (\Delta P_t)_{1-2} \right\} \quad \text{EQN 3.19}$$

If there is no total pressure loss between 1 and 2 (ideal flow), then  $(\Delta P_t)_{1-2}$  is zero and the discharge velocity would be the theoretical maximum for the particular value of static pressure differential:

$$\text{or:} \quad (V_2)^2 \text{ (theoretical)} = \frac{2g_c (P_{1s} - P_{2s})}{C^* \rho [1 - (A_2/A_1)^2]} \quad \text{EQN 3.20}$$

For an actual orifice, the coefficient of discharge represents the efficiency of converting pressure (potential) energy to velocity (kinetic) energy. That is:

$$C_d = \frac{V_2 \text{ (actual)}}{V_2 \text{ (theoretical)}} \quad \text{or} \quad V_2 = C_d (V_2)_{\text{theor}} \quad \text{EQN 3.21}$$

Thus the fluid mass flow rate may be written as:

$$\dot{m} \frac{\text{lbm}}{\text{hr}} = (25.0) \rho A_2 C_d (V_2)_{\text{theor}} = (25.0) \rho A_2 C_d \sqrt{\frac{2g_c (P_{1s} - P_{2s})}{C^* \rho [1 - (A_2/A_1)^2]}} \quad \text{EQN 3.22}$$

or, solving equation 3.22 for the static pressure differential;

$$(P_{1s} - P_{2s}) = \frac{(406.62) \dot{m}^2 [1 - (A_2/A_1)^2]}{(2116.6) 2g_c \rho A_2^2 C_d^2 (625.0)} \quad \text{EQN 3.23}$$

Now an expression for the static pressure differential has been obtained in terms of the installed approach area ratio,  $A_2/A_1$ , and the interpolated flow bench data,  $C_d$ . To obtain an expression for the total pressure differential, equation 3.23 may be substituted into equation 3.17 to give:

$$(P_{1t} - P_{2t}) = \frac{C^* \dot{m}^2 [1 - (A_2/A_1)^2]}{2g_c \rho A_2^2 C_d^2 (625.0)} - \frac{C^* \rho}{2g_c} (V_2^2 - V_1^2) \quad \text{EQN 3.24}$$

Eliminating  $V_1$  by using equation 3.18 and factoring out  $\rho/2g_c$  and the area ratio term, the following relationship is obtained:

$$(P_{1t} - P_{2t}) = \frac{C^* \rho}{2g_c} [1 - (A_2/A_1)^2] \left\{ \frac{\dot{m}^2}{\rho^2 A_2^2 C_d^2 (625.0)} - V_2^2 \right\} \quad \text{EQN 3.25}$$

Next let us eliminate  $V_2$  by using the continuity equation, then factor out an additional  $\dot{m}^2/\rho^2 A_2^2 C_d^2$  term to obtain:

$$(P_{1t} - P_{2t}) = \frac{(406.62) \dot{m}^2}{(2116.6) 2g_c \rho A_2^2 C_d^2 (625.0)} [1 - (A_2/A_1)^2] (1 - C_d^2) \quad \text{EQN 3.26}$$

Thus, the total (irrecoverable) pressure loss for the orifice has been obtained as a function of the interpolated flow bench data, fuel channel geometry, and fluid mass flow rate. Note that from equations 3.23 and 3.26, the relationship between the static and total pressure differentials for the orifice can be written as:

$$(\Delta P)_{\text{total}} = (\Delta P)_{\text{static}} [1 - C_d^2] \quad \text{EQN 3.27}$$

Therefore, the coefficient of discharge indicates the fraction of the static pressure differential that is irrecoverable (cannot be reconverted to total pressure.)

This ratio is tabulated in Table IV for various values of the discharge coefficient.

TABLE IV  
THE PERCENTAGE OF THE STATIC PRESSURE  
DIFFERENTIAL THAT IS IRRECOVERABLE

<u><math>C_d</math></u>	<u><math>\Delta P_t / \Delta P_s</math></u>	<u>% IRRECOVERABLE</u>
0.00	1.000	100.0%
0.25	0.875	87.5%
0.50	0.750	75.0%
0.75	0.438	43.8%
0.80	0.360	36.0%
0.90	0.190	19.0%
1.00	0.000	0.0%

It should be emphasized here that all of the fuel properties will have some effect on the static and total pressure differentials, although only the fuel density appears in equations 3.23 and 3.26. The viscosity influence will occur by virtue of changing the Reynolds number for a given flow rate, resulting in a different  $C_d$  value. The magnitude of the viscosity effect will depend upon the shape of the characteristic curve for a particular orifice. The fuel surface tension exerts an effect which is related to the orifice surface to volume ratio, and to the fuel mass flow rate. As mentioned earlier this effect was found to be very slight for typical carburetor orifices over normal flow rate ranges, and

was therefore not included in the orifice flow correlation.

Next let us direct our attention to the problem of predicting the performance of an orifice with an  $L/D$  ratio for which no characteristic curve was obtained. This, for example, might be a square-edged orifice with an  $L/D$  ratio of 6.232. In the case of square-edged orifices, characteristic curves were obtained for many  $L/D$  ratios from nearly zero to over 10.0. Thus, a fairly accurate  $C_d$  value can be obtained by interpolating between the  $L/D$  ratios (on either side of the desired value) for the specified Reynolds number. This was the technique utilized in the simulation for any specified  $L/D$  ratio and Reynolds number. Similarly, each chamfered fuel channel orifice should be tested if possible. If this cannot be done, a reasonable approximation to their characteristic curves will be given by the  $C_d$  versus  $R_e$  plot for the square-edged orifice with an  $L/D$  ratio of 7.230. These chamfered orifices generally have smoothly increasing  $C_d$  versus  $R_e$  curves with approximately the magnitude of the above orifice. If the orifice is of complex profile, a characteristic curve must be obtained if accurate pressure differentials are to be predicted. This is especially true for main metering orifices, whose characteristic curves exert a substantial effect on the flow characteristics of the fuel channel.

A final question related to the selection of orifices for use in actual flow channel flow situations will now be discussed. This question may be stated as; what is the optimum shape for an orifice characteristic curve? This will depend upon the criterion for which

optimization is desired, such as minimizing fuel property variation effects. Stable orifice operation that is unaffected by variations in fuel properties will be obtained when the two following criteria are satisfied:

1. The orifice has a smoothly increasing mass flow rate versus pressure differential curve.
2. The orifice mass flow rate at a given pressure differential is the same for all fuel brands and fuel temperatures.

The above criteria immediately rule out square-edged orifices with L/D ratios between 0.25 and 1.00. Orifices with nearly constant coefficient of discharge values (L/D ratios less than 0.25) are also ruled out by the following reasoning:

Since it is desired to maintain the fuel mass flow rate constant (for a given pressure differential) as the fuel density and viscosity change, the coefficient of discharge must also change. This should be obvious from the expression for the fuel mass flow rate through the orifice as a function of the operating variables, with the pressure differential in inches of water:

$$\dot{m} \frac{\text{lbm}}{\text{hour}} = 93.90 C_d D^2 \sqrt{\rho_f \Delta P} \quad \text{EQN 3.28}$$

or for fixed values of D and  $\Delta P$ , the variation in the coefficient of discharge required to maintain a constant mass flow rate is:

$$C_d \text{ (required)} = \text{constant} (\rho_f)^{-0.5} \quad \text{EQN 3.29}$$

therefore, the orifice coefficient of discharge must increase as the fuel density decreases. The orifice Reynolds number is given by equation

3.13, which is rewritten here for reference:

$$R_e = 394.2 \left[ \frac{\dot{m}}{D \rho_f \nu_f} \right]$$

The characteristic curve shape required to eliminate the effect of variations in fuel properties must be one in which  $C_d$  increases with  $R_e$ . Let us consider an example of this, an increase in fuel temperature. As the temperature of a given fuel increases, its density and viscosity decrease. This increases the orifice Reynolds number and, from equation 3.28, would decrease the mass flow rate if  $C_d$  did not change. However, if  $C_d$  increases in the manner given by equation 3.29, the orifice flow will be unaffected by changes in fuel temperature. The locus for all values of pressure differential will yield the  $C_d$  versus  $R_e$  curve shape for minimal fuel property variation effects. The exact shape will depend upon the fuel viscosity and density variations with temperature, but for typical gasoline brands the square-edged orifice with an L/D ratio of 7.230 showed very little effect of fuel properties. Thus, for this type of fuel, the characteristic curve for this orifice is very near to the required curve.

## CHAPTER IV

### THEORETICAL ANALYSIS OF FUEL AND AIR BLEED FLOW

#### A. BACKGROUND

The multiplicity of analyses presented in the preceding chapters has resulted in equations which predict the intake manifold vacuum and venturii pressures for a wide range of operation. The next step in obtaining a comprehensive simulation of the air bled, boost venturi carburetor is to predict the fuel and air bleed flow parameters for the fuel channel. This includes the fuel and air bleed flow rates in the idle, main, and enrichment system branches of the fuel channel. In order to predict these variables accurately, the entire fuel channel must be analyzed as a Reynolds number dependent flow network, taking into account the interactions between individual branches. The driving force for flow in each branch will be the pressure differential acting on that branch, which can be related to the intake manifold vacuum and boost venturi suction.

There is very little published information concerning the analysis of actual carburetor fuel channels. There are, of course, textbook analyses in which the main metering orifice is the entire fuel channel and its discharge coefficient is assumed to be constant.<sup>9,70</sup> This neglects the pressure losses due to the numerous other elements of the fuel channel, the effects of other systems, such as enrichment and idle, and the effects of air bleeds. One of the few references which considered some of the complexities of carburetor fuel channel analysis



is that of Ting.<sup>30</sup> He analyzed fuel channel models which contained only a main system (no enrichment or idle system) but which contained an air bleed at various locations downstream from the main metering orifice. For that particular geometry, he obtained equations which expressed the fuel flow rate as a function of the fuel properties, pressure differential, and air bleed orifice diameter. The pressure loss for the two-phase flow downstream from the air bleed was calculated by assuming one-dimensional flow and using the average density and velocity of the fuel-air foam. A study not directly related to carburetion, but which has some application to fuel channel air bleeds was conducted by Weir.<sup>31</sup> He measured the mass flow rates and pressure differentials associated with sonic air flow through various square-edged orifices. Schlieren photographs were also obtained for the flow in the vicinity of the orifice. Although the flow rates and Reynolds numbers were higher than those encountered in carburetor air bleed flow, this study does provide limiting discharge coefficients for various L/D ratios.

Ishikawa and Ito<sup>25</sup> were concerned with minimizing the effects of fuel property variations on fuel channel flow by optimizing the main metering orifice design. However, their fuel channel model did not include air bleeds, idle, or enrichment systems, which would make the extension of their results to an actual carburetor a large extrapolation. (In fact, they reported that a main metering orifice which has a coefficient of discharge that decreases with Reynolds number in a specific manner would compensate for fuel property variations. It was found in this

project that the effect of variations in fuel properties was minimized with an orifice in which  $C_d$  increased smoothly with Reynolds number.)

There are numerous references dealing with the analysis of two-phase flow in long pipes. The analyses of Baker<sup>22</sup>, Lockhart and Martinelli<sup>23</sup>, and Huey and Bryant<sup>24</sup> were concerned with methods of predicting the pressure drop in a pipe under various two-phase flow conditions. These conditions, or flow regimes, are related to the relative mass velocities and fluid properties of each component, and are denoted as bubble, stratified, spray, slug, wave, and plug flow. Since these methods and correlations were intended for use in long pipes, (pipelines in many cases) they yielded very erroneous pressure drops when applied to the very short, bending, small diameter passages of the carburetor. This will be discussed in more detail in section 4c.

Fundamental relationships describing the pressure losses in conduits, orifices, bends, sudden expansions, and sudden contractions were stated by Daily and Harleman,<sup>23</sup> Kay<sup>26</sup>, and Streeter<sup>29</sup>. Streeter also gave an excellent discussion of the solution of complex pipe network problems which was quite applicable to the analysis of the carburetor fuel channel. The application of these relationships allow one to divide the fuel channel into discrete elements and determine the contribution of each element to the overall pressure differential of a given branch. These equations will be given in section 4c for each channel type and flow situation.

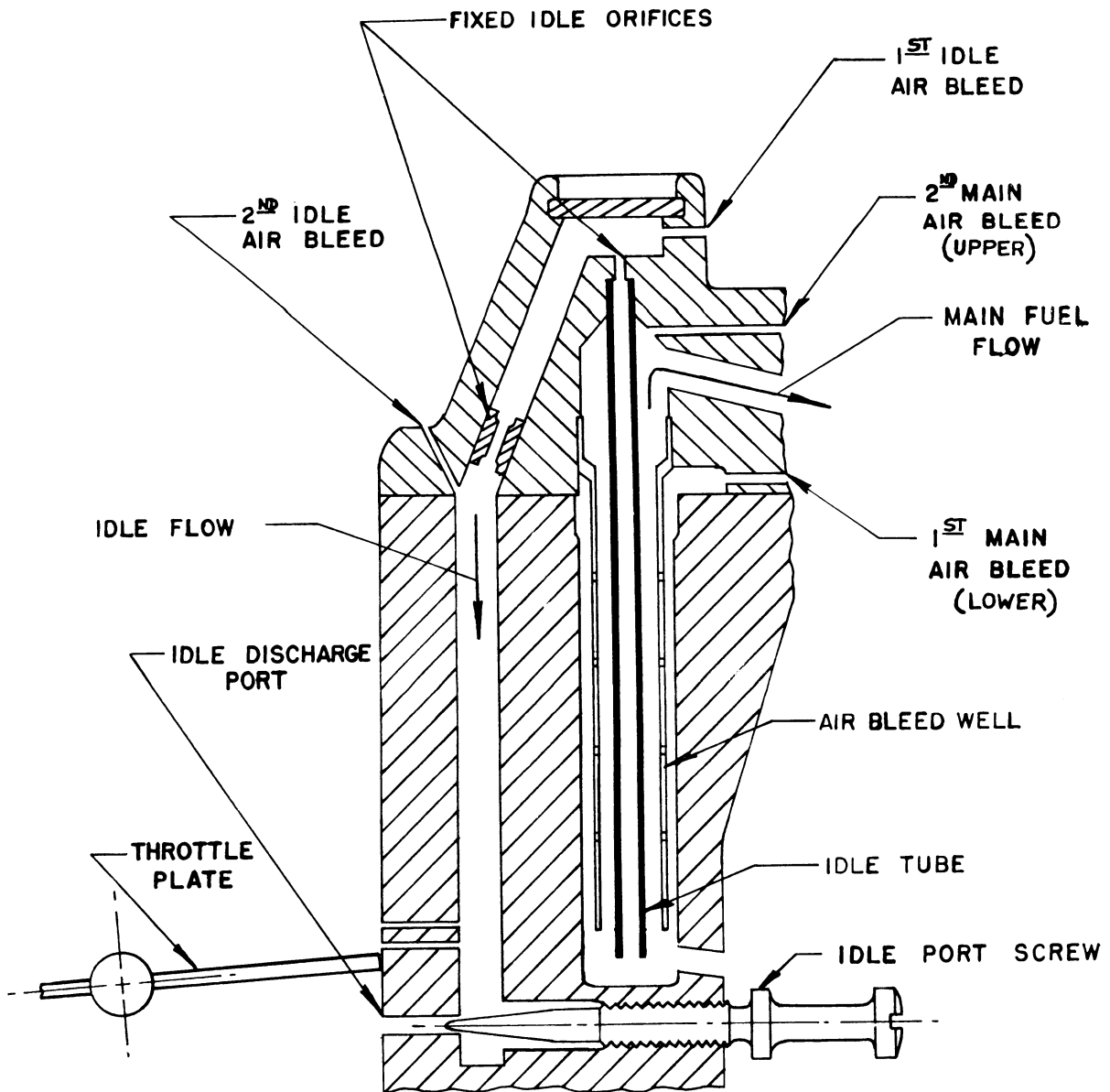


Figure 23. Typical Fuel Channel Geometry Near Air Bleed Well

## B. FUEL CHANNEL MODEL

From a fluid mechanics standpoint, the typical carburetor fuel channel is geometrically very complex. A portion of one of these channels is shown in figure 23. (The main metering orifice and enrichment systems have been omitted for clarity.) Note that there are numerous drilled passages of various diameters, giving rise to sudden expansions and contractions as well as bends and elbows. Also note that there are many fixed and variable area orifices installed in these passages. The enrichment valve and idle needle screw represent orifices in which the flow area may change. Another complexity is introduced by the fact that the fuel may or may not flow in different branches of the fuel channel, depending on the engine speed and load conditions. For example, at wide open throttle, fuel will flow in the enrichment system but not in the idle system. When the throttle is nearly closed, just the opposite is true. Further complexity is encountered due to the addition of air to the flowing fuel by means of multiple air bleeds. These bleed orifices typically supply ambient air to the main (boost venturi) and idle fuel flows, resulting in two-phase flow in that portion of the channel downstream from the initial bleed.

In order to accurately predict the operation of the fuel channel as one portion of the overall simulation, a model must be chosen which considers all of the above factors and yet is amenable to analysis. Such a computer model was constructed and is illustrated in Figure 24. The important thing to note is that each element of the actual fuel



channel has its counterpart in the model which means that each orifice, sudden expansion, and bend can be accounted for in the overall pressure distribution. In addition, each fuel channel system (or branch) in the actual carburetor has its equivalent in the model. These are:

1. Main system
2. Idle system
3. Enrichment system
4. Main air bleed system
5. Idle air bleed system

Each passage and orifice is numbered according to the numerical iteration sequence beginning with number 1, the main metering orifice. Each element has a length, diameter, manufacturing tolerance, angle from the preceding element, and type code which is read into the computer. The type code indicates the type of analysis that is to be applied to that particular element to determine the pressure and flow rate parameters. If the element is a drilled passage, the analysis will be different from that used for a square-edged orifice. Thus, an  $L/D$  ratio and a random passage diameter can be calculated for each element. A sudden expansion or contraction can be accounted for by comparing adjacent elements such as 8 and 9. If the diameter of element 9 is greater than the diameter of element 8, then a sudden expansion exists and the appropriate equations can be utilized.

In an actual carburetor, the enrichment system operation is related to the engine load, and the idle system operation may be adjusted by means of the idle needle screw. This is accounted for in the model by allowing the flow area of element 3 to be a function of intake

manifold vacuum and by obtaining the flow area of element 20 as a function of the idle needle geometry and the number of turns (See Appendix C.) The idle needle parameters, as well as the intake manifold vacuum at which the enrichment valve begins to open, are read in as data.

One final item to notice concerning the flow channel model is that the flow potentials for the network are provided by the boost venturi suction and the intake manifold vacuum, as is the case in the actual carburetor. If the boost venturi suction is high and the intake manifold vacuum is low, (as with large throttle openings) then most or all of the flow will pass through the main system. As the intake manifold vacuum increases and the boost venturi suction decreases, more and more fuel will pass through the idle system and the main fuel flow will go to zero. The values of boost venturi suction and intake manifold vacuum must be determined before a fuel channel analysis can be performed. This is accomplished by calling on subroutines THROTL and AIRMAS.

### C. CRITERIA FOR SOLUTION

The next consideration after the establishment of a geometric and iterative model is that of determining the criteria for obtaining the correct fuel flow rates in each system. These criteria are based upon the conservation of mass and energy and the relationship between the total and static pressure at a point in a moving fluid. Referring again to Figure 24, it is obvious that there are 5 distinct fuel mass flow rates, 4 air bleed mass flow rates, and 4 total mass flow rates to consider in

the model. These are as follows:

1.  $\dot{m}_j$  The main metering jet (orifice) mass flow rate
2.  $\dot{m}_e$  The enrichment system mass flow rate
3.  $\dot{m}_t$  The total fuel mass flow rate
4.  $\dot{m}_m$  The main system fuel mass flow rate
5.  $\dot{m}_i$  The idle system fuel mass flow rate
6.  $\dot{m}_{mb1}$  The first main air bleed mass flow rate
7.  $\dot{m}_{mb2}$  The second main air bleed mass flow rate
8.  $\dot{m}_{ib1}$  The first idle air bleed mass flow rate
9.  $\dot{m}_{ib2}$  The second idle air bleed mass flow rate
10.  $\dot{m}_{m1}$  The total flow rate between idle bleeds 1 and 2
11.  $\dot{m}_{i1}$  The total flow rate between main bleeds 1 and 2
12.  $\dot{m}_{mt}$  The total main system flow rate (fuel + air)
13.  $\dot{m}_{it}$  The total idle system flow rate (fuel + air)

Note in figure 25 below that there are six nodal points, or intersections of two or more network branches, in the total flow network.

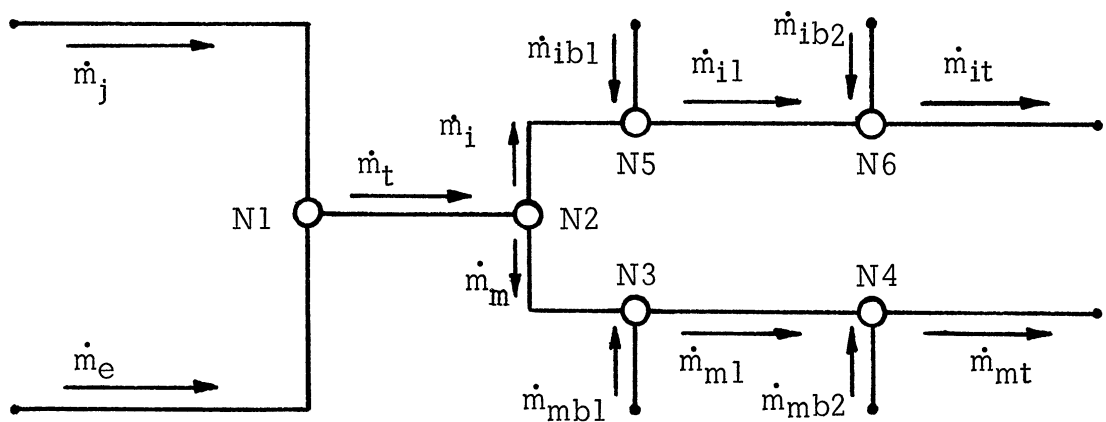


Figure 25. Nodal points in the fuel channel flow network



The application of the continuity equation to each node yields the following relationships:

$$\text{Node 1} \quad \dot{m}_j + \dot{m}_e - \dot{m}_t = 0 \quad \text{EQN 4.1}$$

$$\text{Node 2} \quad \dot{m}_t - \dot{m}_m - \dot{m}_t = 0 \quad \text{EQN 4.2}$$

$$\text{Node 3} \quad \dot{m}_m + \dot{m}_{mbl} - \dot{m}_{ml} = 0 \quad \text{EQN 4.3}$$

$$\text{Node 4} \quad \dot{m}_m + \dot{m}_{ml} - \dot{m}_{mt} = 0 \quad \text{EQN 4.4}$$

$$\text{Node 5} \quad \dot{m}_i + \dot{m}_{ibl} - \dot{m}_{il} = 0 \quad \text{EQN 4.5}$$

$$\text{Node 6} \quad \dot{m}_i + \dot{m}_{il} - \dot{m}_{it} = 0 \quad \text{EQN 4.6}$$

The above relationships control the iterative flow rates within the program, thus assuring that the 13 values currently being evaluated satisfy continuity at every nodal point. This avoids additional iterations on the mass flow rates to satisfy these criteria.

There are an infinite number of flow rates that will satisfy continuity for a given flow network, but only one set of these will also satisfy the energy requirements. These requirements may be generally stated as; the sum of total pressure losses of each element in a branch, plus the net fluid velocity head and height change between the inlet

and exit to the branch, must be equal to the imposed pressure differential across that particular branch. A specific example of this, for the carburetor fuel channel model, is that the sum of the total pressure losses for elements 1, 2, 8, 9, 10, 11, 12, and 13, plus the velocity head of element 13, plus the height change between the fuel bowl level and the outlet of element 13, plus the pressure differential at the outlet of element 13 due to the fuel surface tension, must be equal to the boost venturi suction. (With all units converted to inches of water.) In equation form, with BVSUCW meaning the boost venturi suction (metering signal) in inches of water, SPILL1 denoting the height differential discussed above, which is commonly referred to as the spill point of the carburetor, and VHEADW(I) and DELPTW(I) denoting the velocity head and total pressure loss in the I<sup>th</sup> element;

$$\sum_I \text{DELPTW}(I) + \text{VHEADW}(13) + \text{SPILL1} + \Delta P_{\sigma} - \text{BVSUCW} = E(\dot{m})$$

EQN 4.7

where I takes on the values 1, 2, 8, 9, 10, 11, 12, and 13. The symbol  $\Delta P_{\sigma}$  denotes the pressure differential due to surface tension, and  $E(\dot{m})$  is the iterative error parameter which is a function of the iterative flow rates. (When the 13 fuel and air bleed flow rates approach the correct values, the error parameters become very small.) It should be obvious from equation 4.7 that, for a specified value of BVSUCW, values of  $\dot{m}_J$ ,  $\dot{m}_t$ , and  $\dot{m}_{mt}$  which are too large will result in a large system pressure loss and give a positive error term.

Equations similar in form to that of equation 4.7 can be written for each branch of the network. For example the relationship for the enrichment system can be expressed as:

$$\sum_{I=3,4,5,6,7} \text{DELPTW (I)} + \text{VHEADW (7)} - \sum_{I=1,2} \text{DELPTW (I)} - \text{VHEADW (2)} = E(\dot{m}_e)$$

EQN 4.8

In this case the enrichment system flow rate,  $\dot{m}_e$  is adjusted iteratively while the main metering jet flow rate,  $\dot{m}_j$ , is held constant at its current value. This is continued until equation 4.8 is satisfied, which means that the correct relationship between  $\dot{m}_j$  and  $\dot{m}_e$  has been obtained. This means that each time the main metering jet flow rate is changed iteratively, a new iteration must be performed on  $\dot{m}_e$ . It should be noted here that enrichment flow exists, and the enrichment iteration is performed, only if the specified intake manifold vacuum is less than the value at which the enrichment system begins to operate (commonly 6 to 7 inches of mercury.) Otherwise the flow area of element number 3 is zero and  $\dot{m}_e$  is zero.

#### D. PRESSURE LOSSES IN FUEL CHANNEL ELEMENTS

The foregoing equations express the interrelationships among the various energy quantities but they do not relate the pressure terms to the physical channel variables such as mass flow rate, element diameter, and element length. The evaluation of these pressure terms will now be considered.

The evaluation of the pressure versus distance traveled along the

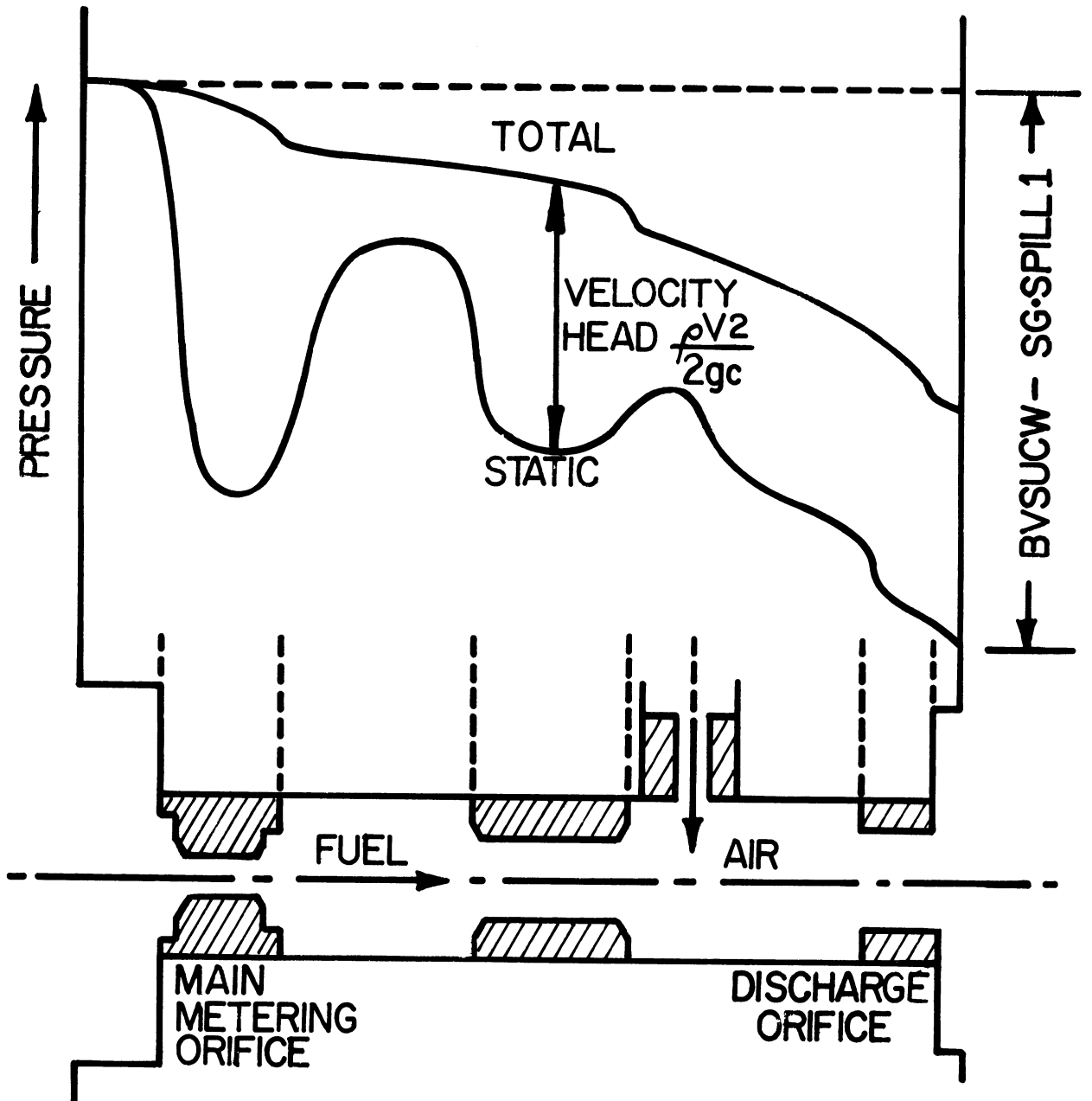


Figure 26. Total and Static Pressure Variations Within a Simple Fuel Channel

fuel channel must take into consideration both the static and total pressure changes. These values are not only required for the flow channel evaluation but are very useful in comparing the predicted fuel channel pressures to actual model test data, where the pressure taps measure the static pressure at various points in the fuel channel.

Figure 25 is a schematic representation of the total and static pressure variations in the fuel flowing through a simple main fuel system with 1 air bleed and 5 elements (from main metering orifice to discharge into the boost venturi.) Note that the difference between the total and static pressure at any point within the fuel channel is denoted as the velocity head and is related to the density and velocity of the fuel (or fuel-air mixture) at that point. The total pressure decreases continuously along the fuel channel while the static pressure decreases and increases at numerous points in the flow path. The static pressure will decrease markedly wherever the fluid encounters a decrease in flow area such as an orifice. Air that is bled into the flowing fuel stream will both decrease the average density of the stream and increase the velocity. This will increase the velocity head and also result in an increased slope for the total pressure curve (a greater energy loss per unit length of fuel channel.) The static pressure at the channel outlet will be the pressure that exists in the boost venturi at that position, minus the pressure differential required to lift the fuel up to the spill point which is, in inches of water, the spill point height multiplied by the fluid specific gravity. Figure 26 clearly illustrates how static pressure measurements

at various positions in a actual carburetor fuel channel can yield widely fluctuating values that should be corrected for local velocity effects.

The velocity in channel element I will be given by:

$$V(I) = \frac{(144) \dot{m}}{(3600) \rho A} \quad \text{ft/sec} \quad \text{EQN 4.9}$$

The velocity head of the fluid in channel element I, in inches of water, may be expressed as;

$$VHEADW(I) = (C3) \rho [V(I)]^2 \quad \text{EQN 4.10}$$

where the units conversion constant is given by:

$$C3 = \frac{406.62}{(2116.6) (2.0) (32.174)}$$

The pressure losses associated with fuel flow within the carburetor are a function of element type, as well as fuel properties and mass flow rate. Within FLOW, which is the subroutine that evaluates the fuel channel flow network for any specified conditions, the type of channel element is designated by the variable CTYPE(I). This designation is as follows:

C TYPE (I) = 0.0	A simple drilled passage
C TYPE (I) = 1.0	A standard carburetor main metering orifice
C TYPE (I) = 2.0	A square-edged orifice
C TYPE (I) = 3.0	A variable area orifice

For example, C TYPE (7) = 2.0 indicates to subroutine FLOW that channel element number 7 is a square-edged orifice. Thus the correct analysis

can be applied to that element during the iteration.

For the simple passage, the total pressure loss may be divided into distinct quantities. These quantities are :

1. Entrance Losses
  - a. Sudden contraction
  - b. Sudden expansion
  - c. Bends
2. Viscous Dissipation Losses
  - a. Laminar Flow
  - b. Turbulent Flow

Thus the total pressure loss for the  $I^{\text{th}}$  element,  $\Delta P_t(I)$ , may be written as:

$$\Delta P_t(I) = \Delta P_{\text{area change}} + \Delta P_{\text{direction change}} + \Delta P_{\text{friction}} \quad \text{EQN 4.11}$$

One point that should be mentioned here is that sudden expansion or contraction and bend losses are systematically accounted for in this program as entrance losses. Thus the total pressure loss due to the difference in diameter between elements 8 and 9 (refer to Figure 24) is evaluated in subroutine FLOW as an entrance loss for element 9.

Once it has been determined that element I is a simple passage with a given length and diameter, the entrance losses can be evaluated by using the following relationships, in which the variables have the meanings:

DPENTR = Entrance loss (total) in inches of water  
 DPW = Frictional loss (total) in inches of water  
 CC = Vena contracta coefficient  
 F1 = Sudden expansion or contraction factor  
 F2 = Bend loss factor  
 FDARCY = Darcy friction factor

The total entrance loss is given by :

$$DPENTR = C3 \rho (F1 + F2) [V (I-1)]^2 \quad \text{EQN 4.12}$$

where the relationship for F1 is:

$$\begin{array}{ll} \text{if } A(I) > A(I-1) & \text{Sudden expansion} \\ F1 = \left[ 1 - \frac{A(I-1)}{A(I)} \right]^2 & \end{array} \quad \text{EQN 4.13}$$

$$\begin{array}{ll} \text{if } A(I) < A(I-1) & \text{Sudden contraction} \\ F1 = \left( \frac{1}{CC} - 1 \right) \left[ \frac{A(I-1)}{A(I)} \right]^2 & \end{array} \quad \text{EQN 4.14}$$

Where the vena contracta coefficient, CC, has been experimentally determined<sup>23</sup> as:

$$CC = 0.62 + 0.38 \left[ \frac{A(I)}{A(I-1)} \right]^3 \quad \text{EQN 4.15}$$

The value of F2, the bend loss factor may be determined by curve fitting, as a function of angle, the experimental data for  $K_L$  in the equation:

$$\Delta P = K_L \rho V^2 / 2g_c$$

This data is available in numerous references, such as Streeter<sup>29</sup>.

Some of the more applicable values for  $K_L$  are listed below in table 5, with  $\Omega$  denoting the ratio of the bend radius to the element radius.



TABLE V

## HEAD LOSS FACTORS FOR NON-UNIFORM FLOW

TYPE OF FLOW	$K_L$		
	$45^\circ$	$90^\circ$	$180^\circ$
Smooth Bend ( $\Omega = 15$ )	$\frac{0.18}{0.18}$	$\frac{0.28}{0.28}$	$\frac{0.52}{0.52}$
Smooth Bend ( $\Omega = 5$ )	0.26	0.50	0.96
Right angle bend	1.10		
Sudden expansion	$[1 - A(I-1)/A(I)]^2$		
Sudden contraction	$[(1/CC) - 1]^2$		
Standard Tee	1.5 to 1.8		
Standard Elbow	0.7 to 1.0		

The viscous dissipation in the passage of length  $L$  and diameter  $D$  may be obtained by evaluating the general pressure loss equation involving the Darcy friction factor. This relationship, which is actually a definition of the friction factor, is as follows:

$$\Delta P_t = f_d \left( \frac{L}{D} \right) \left[ \frac{\rho V^2}{2g_c} \right] \quad \text{EQN 4.16}$$

or in computer nomenclature, with the total pressure loss in inches of water:

$$DPW = FDARCY \cdot [XLD(I)] \cdot [VHEADW(I)] \quad \text{EQN 4.17}$$

The value of  $FDARCY$  is dependent upon the element Reynolds number based on the diameter,  $D$ :

$$R_e = \frac{92903DV}{12\nu} \quad \text{EQN 4.18}$$

Where  $D$  is in inches,  $V$  in feet per second, and  $\nu$  is in centistokes. For element Reynolds numbers in the range from zero to approximately 2100 (the laminar range), the Darcy friction factor may be obtained analytically by considering the Hagen-Poiseuille equation<sup>23</sup>. This equation can be rearranged to express the mass flow rate as a function of the system variables;

$$\dot{m} \frac{\text{lbm}}{\text{hr}} = \frac{3600 \pi \rho D^4 \Delta P}{128 \mu L} \quad \text{EQN 4.19}$$

This relationship can be combined with the definition of the Darcy friction factor, equation 4.16, to obtain:

$$\text{for } R_e < 2100$$

$$f_{\text{DARCY}} = f_d = 64/R_e \quad \text{EQN 4.20}$$

for element Reynolds numbers greater than 2100, the friction factor must be obtained from empirical relationships. The correlating equation chosen for this turbulent flow regime is<sup>23</sup>:

$$\text{for } R_e > 2100$$

$$f_{\text{DARCY}} = 0.3164/(R_e)^{0.25} \quad \text{EQN 4.21}$$

The pressure differential across a fuel drop due to surface tension must be considered at fuel discharge points. This may be expressed in terms of the element diameter in inches,  $D$ , and the surface tension of the fuel in contact with air,  $\sigma$ , in dynes per centimeter.

Or in the usual pressure units of inches of water:

$$\Delta P_{\sigma} = 0.000634 \sigma / D \text{ inches of water} \quad \text{EQN 4.22}$$

If the element is not a simple passage, but is an orifice of some

type, the analysis utilized in subroutine FLOW is based upon the equations obtained in Chapter 3. Subroutine STERL is called to interpolate on the characteristic curve of the orifice for the particular element Reynolds number. After the interpolated value for  $C_d$  has been obtained, the approach area factor, which is denoted by ADUM within subroutine FLOW, is obtained in terms of the orifice flow area and the element area immediately upstream from the orifice. If  $A(I)$  is the flow area of the orifice under consideration:

$$ADUM = 1.0 - \left[ A(I)/A(I-1) \right]^2 \quad \text{EQN 4.23}$$

An additional factor that is evaluated is the relationship between the total and static pressure differentials across the orifice. This factor was obtained in chapter 3 and, in computer nomenclature, may be expressed as:

$$CDUM = 1.0 - C_d^2 \quad \text{EQN 4.24}$$

Thus the total pressure differential for any orifice under any flow condition may be written as;

$$DELPTW(I) = \frac{(C4) (\dot{m})^2 (ADUM) (CDUM)}{\rho C_d^2 A(I)^2} \text{ inches of water} \quad \text{EQN 4.25}$$

where C4 is a units conversion constant given by:

$$C4 = \frac{(406.62) (144)}{(3600) (3600) (14.696) (2) (32.174)}$$

Note that this is the only equation that must be evaluated if element I is an orifice, since all pressure loss factors are included in the

coefficient of discharge value.

The final item to be considered in evaluating the pressure losses in fuel channel elements is that of two-phase flow. This type of flow exists in the fuel channel at all points downstream from the first main or idle system bleed. The two-phase flow in the channel, as will be discussed in chapter 6, is usually in either the stratified or bubble regime. The standard correlations for predicting pressure losses with these flow types gave very erroneous values. This is in all probability due to the geometry of the channel. The short, bending passages of small diameter differ significantly from the long, large diameter pipelines from which much of the correlated data was obtained. The two alternative procedures were to utilize experimental flow channel data (which, of course, would be valid only for the geometry being used) or to use the equations presented earlier in this section, based on an average fuel-air mixture density and velocity. Since the first alternative also has the disadvantage of using data from the device that is being simulated, and thus detracts from the value of the computer predictions for other geometries, the second alternative was tried. (This method of evaluating the simultaneous flow of fuel and air was utilized by Ting in his analysis of air bleed flow.) For a given element downstream from an air bleed, such as elements 11, 12, 13, and 16 through 20 in Figure 24, the iterative mass flow rates of fuel and air were utilized to obtain a weighted average for the mixture velocity and density.

The density is given by;

$$\rho_{fa} = \frac{\dot{m}_f + \dot{m}_a}{\frac{\dot{m}_f}{\rho_f} + \frac{\dot{m}_a}{\rho_a}} \quad \text{lbm/ft}^3 \quad \text{EQN 4.26}$$

and the velocity is given by:

$$V_{fa} = \frac{144 (\dot{m}_f + \dot{m}_a)}{3600 \rho_{fa} A} \quad \text{ft/sec} \quad \text{EQN 4.27}$$

When these weighted averages were utilized in conjunction with equations 4.10 through 4.25, the resulting pressure predictions agreed surprisingly well with actual flow model data. Thus, it was not necessary to incorporate two-phase flow data into the simulation.

#### E. FUEL-CHANNEL ITERATIVE TECHNIQUE

The general iterative scheme utilized in subroutine FLOW is closely related to the actual flow situation in the fuel channel. The subroutine is called with the following quantities specified:

1. Number of elements and their type code.
2. Length, diameter, and angle of each element.
3. Fuel type and temperature.
4. The spill point and enrichment valve parameters.
5. Boost venturi suction and intake manifold vacuum.
6. Reasonable initial guesses for all system flow rates with continuity satisfied at every node point.

The initial guesses are obtained by calling subroutine ASSUME

(Appendix E ) with the given values of boost venturi suction and intake manifold vacuum, and are very helpful in reducing the number of iterations required. On the basis of the assumed system flow rates, the average densities, velocities, mass flow rates, Reynolds numbers, etc., can

be calculated for each element. The boost venturi suction is then checked to ascertain if it is sufficient to lift the fuel from its level in the air bleed well to the main system discharge point. This height is always greater than or equal to the spill point height. (With zero idle flow, the fuel level in the air bleed well is a maximum, and as the idle flow increases, this level is lowered). This means that a larger boost venturi suction is required to initiate flow in the main system. If the boost venturi suction is less than this minimum value, the fuel and air bleed flow rates in the main system elements 10, 11, 12, 13, 21, 22, and 23 are set to zero (no main flow.) It should be mentioned at this point that back flow is not considered in subroutine FLOW. This complex phenomena can occur in carburetor fuel channels under certain operating conditions, and consists of air (no fuel) flowing in the idle or main system in a direction opposite to that of normal fuel flow.

After determining whether main flow exists, the next step is to check the intake manifold vacuum and determine the enrichment valve opening, A(3). If the intake manifold vacuum is greater than the opening value then the flow rates in elements 3, 4, 5, 6, and 7 are set to zero (no enrichment flow.) If the intake manifold vacuum is less than the opening value, then the enrichment valve flow area is calculated from its geometry and opening rate, and the flow rates in elements 14 through 20, plus elements 24 and 25 are set to zero. The initial guesses are then adjusted such that continuity is satisfied at every node point. The network analysis utilized in subroutine FLOW, in

which the iterative flow rates are always chosen to satisfy continuity, is based upon the Hardy Cross method.<sup>29</sup>

The pressure losses for each element are evaluated utilizing the equations in the preceding section. The error terms are evaluated for each system, and new values are assumed for the 13 system mass flow rates on the basis of these terms. New velocities, Reynolds numbers, densities, coefficients of discharge, and friction factors are then computed for the elements. The iterations continue until all error terms are negligibly small. At this point, all of the important fuel channel parameters have been predicted for the specified values of boost venturi suction and intake manifold. This includes:

1. The pressure loss contribution of each element.
2. The fuel flow rates in each element and system.
3. The flow rate for each air bleed.
4. The velocity, Reynolds number, friction factor or coefficient of discharge value for each element.

In addition, the main and total (main + idle) fuel-air ratios can now be calculated since the air flow rates were previously determined by subroutine AIRMAS, and the main and idle fuel flow rates are known.

The fuel channel parameters calculated for various values of boost venturi suction and intake manifold vacuum are shown in Table 6. Note that the idle flow rate is zero for the first two cases, ( $VACMAN = 0.22$  and  $0.78$ ) and that the enrichment flow rate is zero for the last two cases.

**TABLE VI**  
**FUEL CHANNEL ANALYSIS RESULTS**

INITIAL SPILL POINT = 0.30 INCHES  
IDLE NEEDLE SCREW TURNS = 1.25

ENRICHMENT VALVE OPENING = 6.00 INCHES HG.

FOR: BVSUCW = 14.19 "H<sub>2</sub>O

VACMAN = 0.22" HG.

ELEMENT	$\dot{M}$ $\frac{\text{LBM}}{\text{HR}}$	$\Delta P_f$	VELOCITY HEAD	$R_o$	VELOCITY	DIAMETER	L/D
1	17.661	2.664	8.463	5551.4	7.94	.0502	3.6454
2	17.661	7.290	.044	1490.3	.57	.1870	1.6684
3	8.143	.267	.265	1586.2	1.41	.0810	1.3086
4	8.143	.231	.001	411.2	.09	.3125	.4000
5	8.143	.019	.019	823.6	.38	.1560	2.5000
6	8.143	.006	.034	951.7	.51	.1350	1.5259
7	4.071	4.828	4.647	2794.4	5.88	.0280	4.4643
8	21.732	2.551	.174	2332.8	1.14	.1470	6.3776
9	21.732	.185	.011	1178.4	.29	.2910	.8591
10	21.732	.083	.131	2170.4	.99	.1580	6.3291
11	21.964	.012	.121	9937.1	2.64	.2700	1.2593
12	22.267	.439	2.123	35763.2	16.05	.1600	5.0750
13	22.267	.281	.543	10000.0	8.12	.2250	.6000
14	.000	.000	.000	.0	.00	.0610	31.6393
15	.000	.000	.000	.0	.00	.0260	3.6077
16	.000	.000	.000	.0	.00	.1400	5.0429
17	.000	.000	.000	.0	.00	.0940	8.2979
18	.000	.000	.000	.0	.00	.0420	2.5238
19	.000	.000	.000	.0	.00	.0940	21.2766
20	.000	.000	.000	.0	.00	.0004	297.0645
21	.232	8.757	3.152	2145.5	122.47	.0370	3.3784
22	.232	4.148	1.493	1779.9	84.28	.0446	.6996
23	.302	14.909	5.366	2799.5	159.80	.0370	3.7838
24	.000	.000	.000	.0	.00	.0280	4.4643
25	.000	.000	.000	.0	.00	.0292	3.6301

FOR: BVSUCW = 9.04" H<sub>2</sub>O

VACMAN = 0.78" HG.

1	13.896	1.907	5.239	4367.8	6.25	.0502	3.6454
2	13.896	4.514	.027	1172.5	.45	.1870	1.6684
3	6.488	.169	.168	1263.9	1.12	.0810	1.3086
4	6.488	.147	.001	327.6	.08	.3125	.4000
5	6.488	.012	.012	656.2	.30	.1560	2.5000
6	6.488	.005	.022	758.3	.40	.1350	1.5259
7	3.244	3.065	2.950	1828.1	4.59	.0280	4.4643
8	17.140	1.613	.108	1839.8	.00	.1470	6.3776
9	17.140	.115	.007	929.4	.23	.2910	.8591
10	17.140	.047	.081	1711.7	.78	.1580	6.3291
11	17.324	.008	.076	7900.2	2.10	.2700	1.2593
12	17.565	.284	1.332	29444.7	12.77	.1600	5.0750
13	17.565	.176	.341	10000.0	6.46	.2250	.6000
14	.000	.000	.000	.0	.00	.0610	31.6393
15	.000	.000	.000	.0	.00	.0260	3.6077
16	.000	.000	.000	.0	.00	.1400	5.0429
17	.000	.000	.000	.0	.00	.0940	8.2979
18	.000	.000	.000	.0	.00	.0420	2.5238
19	.000	.000	.000	.0	.00	.0940	21.2766
20	.000	.000	.000	.0	.00	.0004	297.0645
21	.194	5.540	1.997	1728.0	97.42	.0370	3.3784
22	.184	2.620	.946	1416.9	47.10	.0446	.6996
23	.241	9.436	3.397	2227.2	127.13	.0370	3.7838
24	.000	.000	.000	.0	.00	.0280	4.4643
25	.000	.000	.000	.0	.00	.0292	3.6301



TABLE VI (Continued)  
FUEL CHANNEL ANALYSIS RESULTS

INITIAL SPILL POINT = 0.30 INCHES  
IDLE NEEDLE SCREW TURNS = 1.25

ENRICHMENT VALVE OPENING = 6.00 INCHES HG.

FOR: BVSUCW = 5.04" H<sub>2</sub>O

VACMAN = 7.78" HG.

ELEMENT	$\dot{M}$ LBM/HR	$\Delta P_f$	VELOCITY HEAD	$R_o$	VELOCITY	DIAMETER	L/D
1	11.215	1.505	2.413	3525.2	5.04	.0502	3.6454
2	11.215	2.941	.018	946.3	.36	.1870	1.6684
3	.000	.000	.000	1722.2	.00	.0004	297.2645
4	.000	.000	.000	192.0	.00	.3125	.4000
5	.000	.000	.000	384.5	.00	.1560	2.5000
6	.000	.000	.000	444.3	.00	.1350	1.5250
7	.000	.000	.000	1071.2	.00	.0280	4.4643
8	11.215	.016	.046	1203.8	.59	.1470	6.3776
9	11.215	.049	.003	608.1	.15	.2910	.8591
10	9.042	.022	.023	903.0	.41	.1580	6.3291
11	9.203	.002	.033	6530.8	1.74	.2700	1.2593
12	9.410	.130	.603	24047.5	10.79	.1600	5.0750
13	9.410	.080	.154	10000.0	5.46	.2250	.6000
14	2.173	.234	.059	562.1	.55	.0610	31.6393
15	2.173	1.792	1.700	1318.7	3.64	.0260	3.6077
16	2.173	3.265	.002	244.9	.13	.1400	5.0429
17	2.299	.110	.465	15402.4	11.77	.0940	8.2979
18	2.299	11.666	11.672	10000.0	58.95	.0420	2.5238
19	2.557	3.602	1.561	46491.0	35.52	.0940	21.2766
20	2.557	40.279	40.254	10000.0	180.36	.0417	2.5410
21	.161	3.091	1.514	1487.2	84.89	.0370	3.3784
22	.161	1.464	.717	1233.8	58.42	.0446	.6996
23	.207	5.138	2.517	1917.4	109.45	.0370	3.7838
24	.126	6.539	2.769	1521.7	114.78	.0280	4.4643
25	.258	23.139	10.005	3016.7	218.10	.0292	3.5301

FOR: BVSUCW = 0.47" H<sub>2</sub>O

VACMAN = 21.78" HG.

1	4.151	.370	.467	1304.7	1.87	.0502	3.6454
2	4.151	.403	.002	350.3	.13	.1870	1.6684
3	.000	.000	.000	1722.2	.00	.0004	297.2645
4	.000	.000	.000	192.0	.00	.3125	.4000
5	.000	.000	.000	384.5	.00	.1560	2.5000
6	.000	.000	.000	444.3	.00	.1350	1.5250
7	.000	.000	.000	1071.2	.00	.0280	4.4643
8	4.151	.006	.006	445.6	.22	.1470	6.3776
9	4.151	.007	.000	225.1	.06	.2910	.8591
10	.000	.000	.000	93.5	.00	.1580	6.3291
11	.000	.000	.000	2896.2	.00	.2700	1.2593
12	.000	.000	.000	10799.2	.00	.1600	5.0750
13	.000	.000	.000	7679.4	.00	.2250	.6000
14	4.151	.404	.214	1073.7	1.26	.0610	31.6393
15	4.151	6.540	6.497	2519.1	6.96	.0260	3.6077
16	4.151	11.909	.008	467.8	.24	.1400	5.0429
17	4.268	.257	1.174	20900.0	15.97	.0940	8.2979
18	4.268	29.438	29.452	10000.0	79.99	.0420	2.5238
19	4.602	7.696	4.633	76523.5	58.47	.0940	21.2766
20	4.602	119.526	119.451	10000.0	296.87	.0417	2.5410
21	.000	.000	.000	705.6	.00	.0370	3.3784
22	.000	.000	.000	585.3	.00	.0446	.6996
23	.000	.000	.000	869.6	.00	.0370	3.7838
24	.117	7.734	2.622	1480.8	111.60	.0280	4.4643
25	.335	53.967	16.802	3900.4	232.76	.0292	3.5301

## CHAPTER V

### ENGINE AND VEHICLE ANALYSIS

#### A. REASONS FOR RELATING THE ENGINE AND VEHICLE TO THE CARBURETOR

In this chapter the engine and vehicle parameters related to the operating point of the carburetor will be analyzed. There are sound reasons for performing this type of analysis within the framework of a carburetor simulation. The first reason is that carburetor operation is directly related to certain engine parameters, as was discussed in Chapter 2. Thus, in the rigorous sense, the carburetor must be analyzed with these interrelating engine parameters taken into consideration. Another important reason for relating the engine and vehicle to the carburetor is that the value and application of the simulation is greatly extended. This results from the fact that in numerous tests, carburetor performance is evaluated on the basis of engine or vehicle data such as brake specific fuel consumption, fuel-air ratio, and miles per gallon. Therefore, it would be very advantageous to be able to predict many of the important engine and vehicle parameters along with those associated with the carburetor.

It should be obvious that the carburetor simulation program would represent a much more powerful evaluation tool if the effect of any one carburetor variable on the engine brake specific fuel consumption or the vehicle miles per gallon could be predicted analytically.

This would allow the simulation program to evaluate a proposed carburetor design on the basis of predicted results for numerous standard tests. The engineer would then be able to evaluate the design not simply on how it will perform at various air flow rates, but also on the basis of what specific fuel consumptions and miles per gallon would be expected over a wide engine or vehicle speed range.

#### B. REQUIREMENTS FOR ROAD LOAD CARBURETOR ANALYSIS

The key to relating the engine and vehicle to the operation of the carburetor is to relate the respective operating points. The vehicle operating point may be based on many considerations, the most important of which is probably that of road load operation. This is defined as vehicle operation under conditions such that vehicle speed is maintained at a specified velocity,  $V$ , on a level roadway with no prevailing wind. These conditions are then referred to as those corresponding to the road load at the velocity,  $V$ .

One of the most important operating lines to consider is that given by the locus of all vehicle road load operating points, which is the road load curve for a given carburetor or engine parameter. The basis of this importance is that the carburetor-engine operating points (which are combinations of throttle angle and engine speed) will be on or near the road load operating curve the majority of the time.

In order to evaluate carburetor performance at points which correspond to operation along the road load line for a given vehicle and

engine, the vehicle velocity must first be related to the carburetor-engine operating point. This means that the engine speed and throttle angle corresponding to a given vehicle velocity,  $V$ , must be ascertained before road load carburetor operation can be simulated. Obtaining the engine speed in terms of the vehicle parameters is reasonably simple, but determining the throttle angle corresponding to road load operation for a specified vehicle velocity is much more involved, as will be evident later in this chapter.

### C. VEHICLE ROAD LOAD RELATIONSHIPS

In the relationships presented in this section, the following variables are defined as:

$V$	Vehicle velocity in miles per hour
$A_f$	Vehicle frontal area in square feet
ROLL	Rolling resistance coefficient
DRAG	Drag resistance coefficient
WEIGHT	Vehicle weight in lbm
BHP	Required engine brake horsepower
RHP	Road (rear wheel) horsepower
$N$	Engine speed in revolutions per minute
$N_{\text{tire}}$	Tire revolutions per mile
$G_d$	Differential gear ratio
$G_t$	Transmission gear ratio
$C_{1,2,3}$	Correlation constants
$\eta_d$	Total drive train efficiency

In terms of the specified vehicle parameters, including the differential and transmission gear ratios along with the tire revolutions per mile, the engine speed is;

$$N = N_{\text{tire}} G_d G_t V/60.0 \quad \text{EQN 5.1}$$

therefore the engine speed corresponding to any vehicle velocity may be obtained by using the above equation. The road or rear wheel

horsepower that is required for a specified vehicle at a velocity,  $V$ , may be obtained by a suitable correlation of vehicle proving ground data. There are numerous forms of this correlation available, and the relationship utilized in this simulation is:

$$\text{RHP} = (\text{ROLL} \cdot \text{WEIGHT} + \text{DRAG} \cdot A_f V^2) (V/375) \quad \text{EQN 5.2}$$

The rolling and drag resistance coefficients are obtained by curve fitting actual vehicle road horsepower data. Representative values for a typical American sedan are:

$$\text{ROLL} = 0.0150 \quad \text{DRAG} = 0.00125$$

These values could be used as an approximate representation of the road horsepower requirements for a vehicle if actual proving ground data were not available.

The engine brake horsepower that is required at any vehicle speed is a function of the road horsepower and the total drive train efficiency. This efficiency, expressed as a fraction, indicates the fraction of the input power that is dissipated in the entire drive train as a function of the vehicle velocity. This must also be obtained by correlating actual vehicle data for these power losses. The correlating equation used to describe the drive train efficiency of any vehicle is of the form:

$$\eta_d = C_1 - V/C_2 + V^2/C_3 \quad \text{EQN 5.3}$$

Typical values for the three constants in the above correlation are:

$$\begin{aligned} C_1 &= 0.86 \\ C_2 &= 1210.0 \\ C_3 &= 333300.0 \end{aligned}$$

Thus the brake horsepower output (of any engine) that is required to maintain a specified vehicle velocity may be written as:

$$\text{REQUIRED ENGINE BHP} = \text{ROADHP} / \eta_d \quad \text{EQN 5.4}$$

The engine speed and required engine brake horsepower have now been expressed for any vehicle velocity in terms of the vehicle parameters only. (No engine or carburetor parameters involved.)

The next step in the analysis, that of determining the specific operating point of a certain carburetor and engine that corresponds to the above vehicle velocity, is a complex one. There are an infinite number of combinations of throttle angle, engine air flow, and fuel-air ratio that will satisfy the vehicle road load requirements (a specified engine brake horsepower output at a specified engine speed). The complexity of this situation can be illustrated by considering the throttle angle required to produce 20 engine brake horsepower at a vehicle velocity of 25 miles per hour. (Assuming for the moment that this is the road load requirement for the specified vehicle.) The engine speed is therefore fixed and is related to the vehicle speed, tire revolutions per mile, differential gear ratio, and transmission gear ratio. The required engine air flow and throttle angle will be very dependent on the particular carburetor geometry and the manner in which the performance of the particular engine that is being used is affected by the overall fuel-air ratio. If the specified carburetor geometry is such that the fuel-air ratio curve is generally very rich, (as would occur if the main metering orifice diameter were large) and the engine

performance was poor at these overall fuel-air ratios, then a large air flow, low manifold vacuum, and hence a large throttle angle would be required. If the carburetor design, as specified by all the dimensions on the input data cards, were such that the resulting fuel-air ratio curve was in the range which yields high engine thermal efficiency values, then the required engine air flow and carburetor throttle angle would be much less. If the carburetor design being evaluated produced fuel-air ratios that were outside the flammability limits of the engine (richer than the rich limit or leaner than the lean limit) then the engine brake horsepower would be zero or negative for all air flow values. In this case even wide open throttle angles would be insufficient and road load operation could not be maintained.

The above examples were cited to illustrate that the road load operating parameters will be affected by a large number of vehicle, engine, carburetor, fuel, and ambient variables. Each proposed carburetor design and fuel type will result in a particular set of fuel-air ratio values. Each engine will utilize these fuel-air ratio values in a different manner, producing a particular set of brake specific fuel consumption curves and exhibiting a variation in performance with fuel-air ratio and speed that is particular to that engine. The road load requirements themselves will vary with the particular set of vehicle variables that are being used. Thus the complete simulation results for a road load carburetor analysis apply to one particular carburetor-engine-vehicle combination. This is especially valuable for evaluating

variations in carburetor operation due to mating with various combinations of engine and vehicle.

#### D. CORRELATION AND PREDICTION OF ENGINE PERFORMANCE

It is evident from the above discussion that in order to analyze carburetor operation at road load operating points, the brake horsepower output, as well as numerous other engine operating parameters, must be known for any engine speed, throttle angle, air flow, manifold pressure, and fuel-air ratio. This would obviously involve the determination of a tremendous amount of actual engine data if a universal correlation were not utilized. In addition, it would be quite advantageous to obtain most of the engine brake, indicated, and friction variables during the road load analysis. These important engine parameters are listed below with their corresponding symbols.

IHP	Indicated horsepower
BHP	Brake horsepower
FHP	Friction horsepower
IMEP	Indicated mean effective pressure in psi
BMEP	Brake mean effective pressure in psi
FMEP	Friction mean effective pressure in psi
ISFC	Indicated specific fuel consumption in lbm/IHP hr
BSFC	Brake specific fuel consumption in lbm/BHP hr
THERMI	Indicated thermal efficiency in %
THERMB	Brake thermal efficiency in %
TORQI	Indicated torque in foot pounds
TORQB	Brake torque in foot pounds
TORQF	Friction torque in foot pounds

One important goal in finding a universal engine data correlation technique was to be able to determine all of the above parameters for a particular engine for any engine speed, intake manifold pressure, air



mass flow rate, and fuel-air ratio, without conducting the hundreds of dynamometer tests that would be required. It was felt that in order to make the road load carburetor analysis feasible in an actual case, not over 2 dynamometer tests should be required to generate all of the needed data. No suitable correlation technique could be found in the literature, therefore a significant effort was expended to develop a method which would enable the computer to develop complete engine data maps from the results of two dynamometer tests. This technique was successfully developed and is based upon the following logic:

It is well known that, all other quantities being equal, the indicated horsepower of an engine is proportional to the air mass flow rate supplied to that engine. This is illustrated very well in figure 27, which is a plot of the results of approximately fifty engine tests for a specific engine (Ford 289 cubic inch V-8) over a wide range of speed and load conditions. The indicated horsepower is linearly related to the air mass flow rate by means of the slope of the line. A very important point to emphasize here is that the fuel-air ratio for these runs was always near stoichiometric. If the fuel-air ratio were to nominally be some other value, there would be no reason to expect the slope to remain the same. In fact, if the fuel-air ratio supplied to the engine were to be outside its particular flammability limits for spark ignition, the indicated horsepower would be zero for all values of air flow. (This is what occurs during a motoring test.) In those cases the proportionality constant would be zero. For fuel-air ratios near the

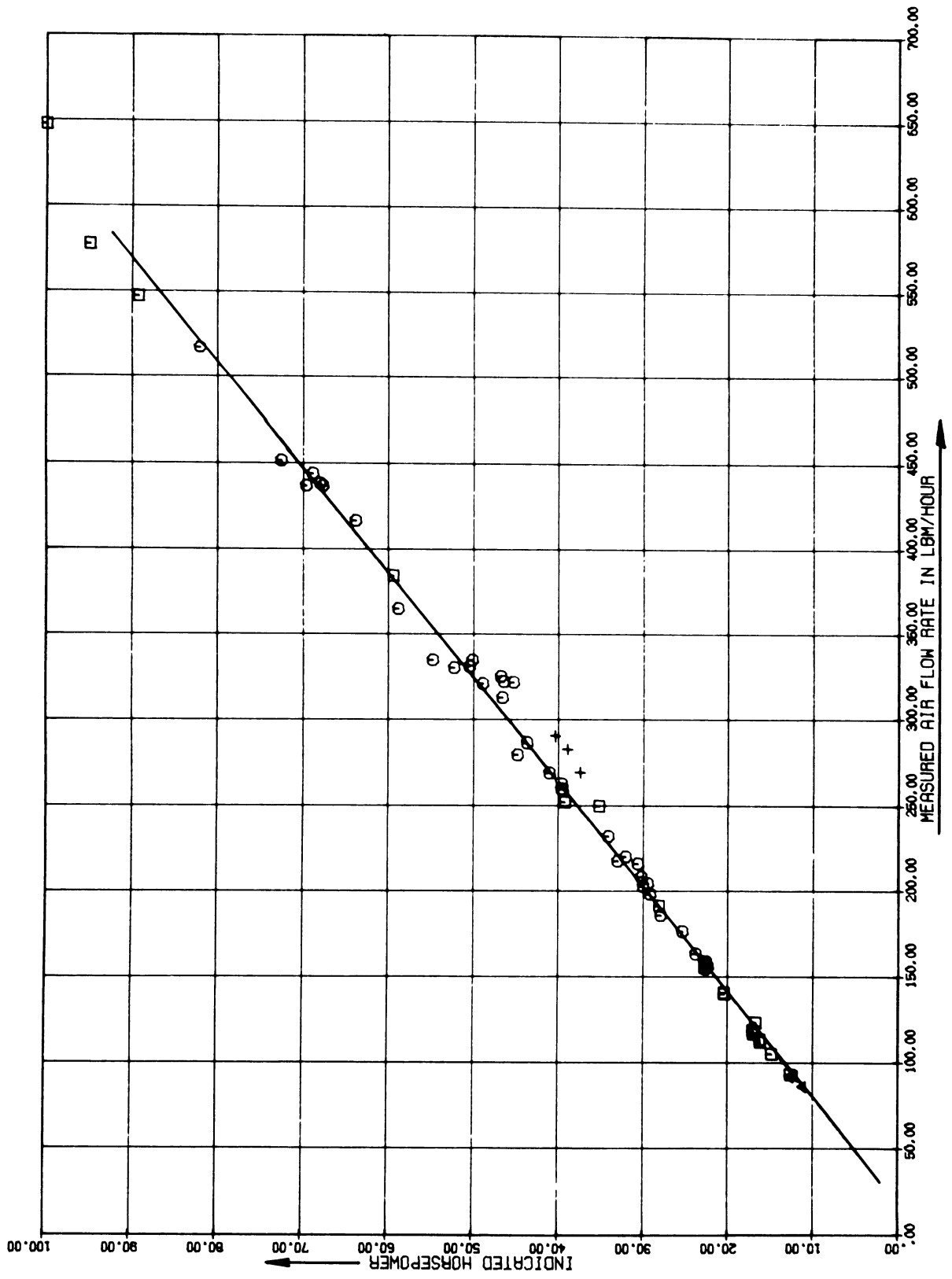


Figure 27. Dependence of the Engine IHP on the Air Mass Flow Rate

maximum power value of approximately 0.085, the slope will be a maximum, indicating that the greatest indicated horsepower per unit air mass flow rate is being obtained. For all other fuel-air ratios, both richer and leaner, the slope will be less, finally reaching zero at the lean and rich limits.

Since this suggested a possible technique for correlating engine data on the effect of fuel-air ratio, many engine tests were conducted at various nominal fuel-air ratios to determine the variation in this slope. Some of these test results are plotted in Figure 28, which has precisely the same coordinates as Figure 27. These curves were obtained by overriding the normal operation of a carburetor by applying an artificial pressure or vacuum to the float bowl until any desired fuel-air ratio was obtained. (The test equipment and procedures will be discussed in Chapter 7. This discussion will only be concerned with testing relevant to the development of the engine data correlation.) Note that the slope of the curve for a fuel-air ratio of 0.061 is very close to that in Figure 27, since 0.061 is also near stoichiometric. The fuel-air ratio of 0.080 yields a significantly greater slope than the test series conducted with the 0.061 fuel-air ratio. It is also evident that the rich (0.103) and lean (0.054) fuel-air ratios resulted in much lower slopes than those of the tests utilizing fuel-air ratios near the power ratio and stoichiometric. At fuel-air ratios richer than 0.103, and leaner than 0.054, the slope decreased rapidly. The significance of this slope becomes evident if one considers a constant air flow value.

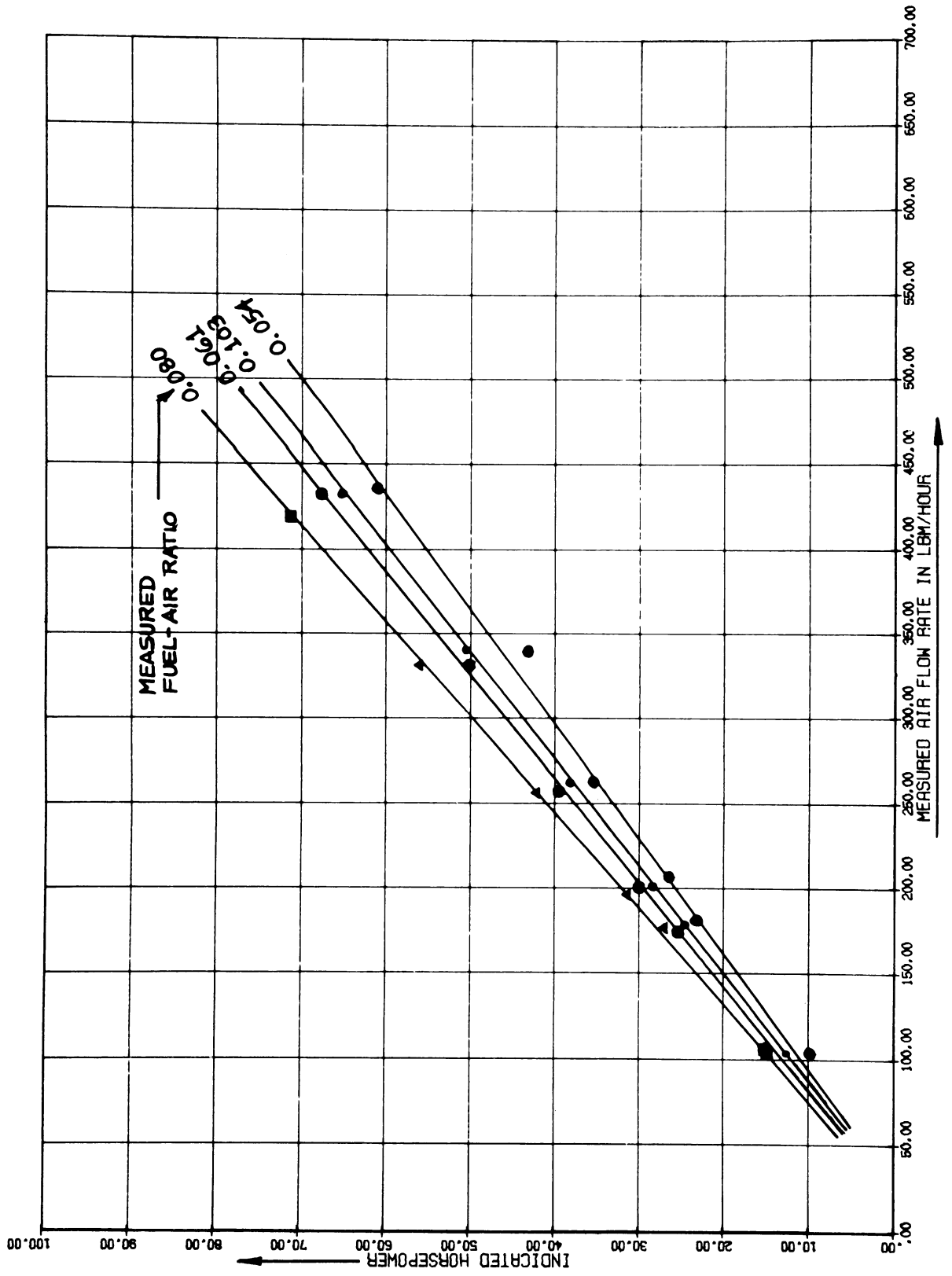


Figure 28. Slope of the IHP Curve as a Function of Fuel-Air Ratio

If the air mass flow rate to the engine is maintained constant in some manner while the fuel-air ratio is varied from zero to a value greater than the rich limit, the indicated horsepower will increase from zero, reach a maximum at the power ratio (which changes with air flow rate), and then decrease to zero again. The exact manner in which this occurs is particular to a given engine. If many such tests are conducted at various nominal air flow values, the results will be as shown in Figure 29. Note that the indicated horsepower decreases rapidly at fuel-air ratios less than 0.050, indicating a lean ignition limit of around 0.040. (This will in fact be a slight function of the air mass flow rate.) The curves also tend to flatten out for the lower air flow values, indicating less of an effect of fuel-air ratio on engine operation.

If Figures 28 and 29 are studied carefully, it will become evident that each is merely a cross section of a general 3-dimensional plot which describes the entire operation of the engine. An approximate sketch of this general plot is given in Figure 30. Note that Figure 28 may be generated by taking cross-sections of this volume at various fuel-air ratios, and that Figure 29 may be generated by taking cross sections at various air mass flow rates. The importance of this concept, along with the linearity of the indicated horsepower versus air mass flow rate curves, is that only two dynamometer tests need be run to establish the entire surface of Figure 30 which represents the variation in indicated horsepower (for that particular engine) for all possible fuel-air ratios and air flow rates. These two tests consist of two con-

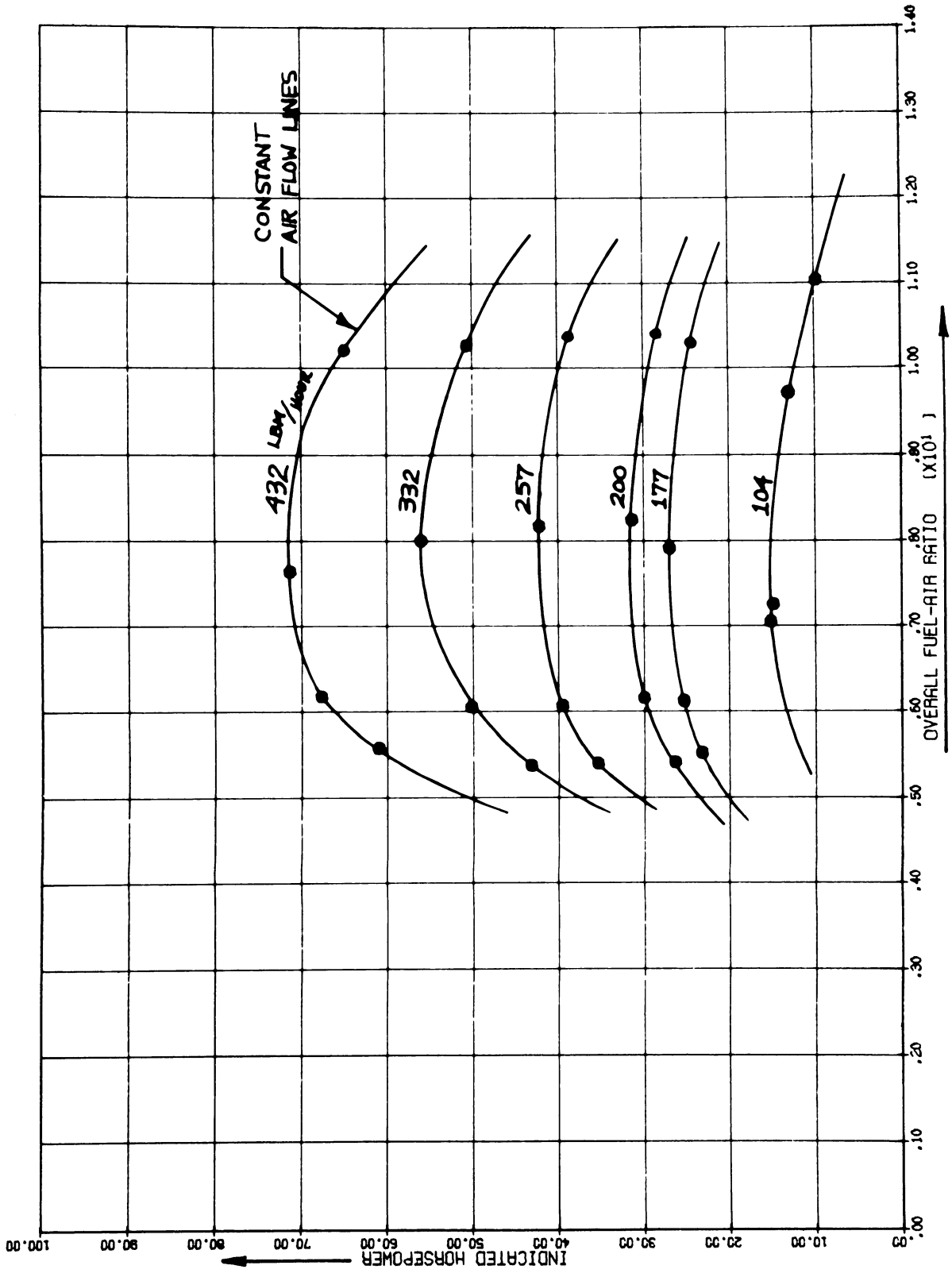


Figure 29. Constant air flow curves for varying fuel-air ratios

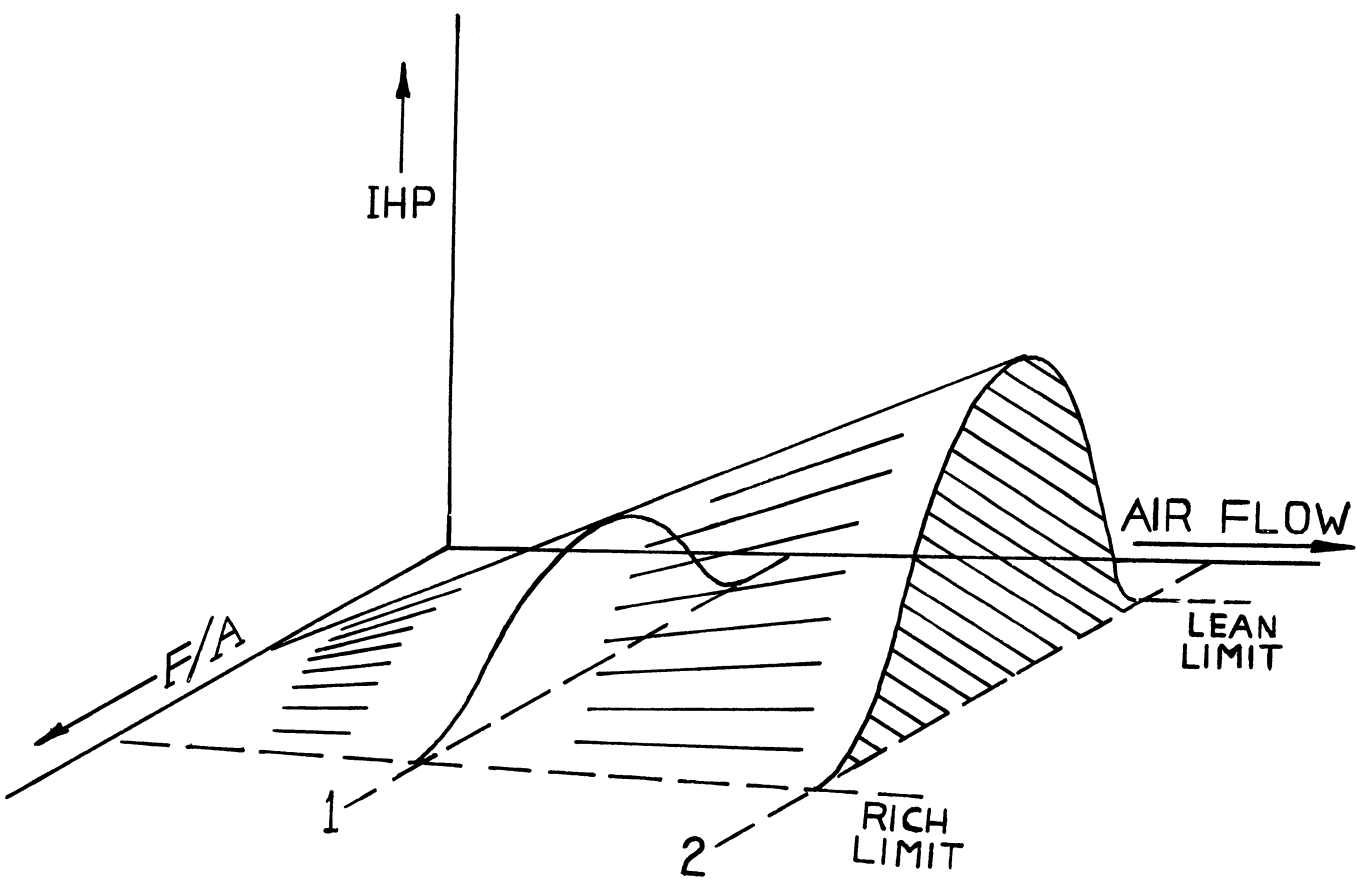


Figure 30. Three-dimensional operating surface for an engine

stant air mass flow rate tests such as the 200 and 432 lbm/hour curves shown in Figure 29. After the fuel-air ratio has been varied over the entire range from the lean to the rich limit and the indicated horsepower has been determined at each fuel-air test point, the IHP can be calculated for any other fuel-air ratio and air mass flow rate. This is accomplished by first supplying the computer with the IHP versus F/A data points for both air mass flow rate values, (two data sets) which will be denoted by AIRFL1 and AIRFL2. Then the indicated horsepower corresponding to each air flow rate for the desired fuel-air ratio is determined by calling the generalized interpolation subroutine STERL for each data set. These two indicated horsepower values corresponding to the desired fuel-air ratio will be denoted as XIHP1 and XIHP2. Since the curves are linear for all air flow rate values, the slope may be calculated by utilizing the following equation:

$$\text{SLOPE} = \frac{\text{XIHP2} - \text{XIHP1}}{\text{AIRFL2} - \text{AIRFL1}} \quad \text{EQN 5.4}$$

It was not found necessary to restrict the IHP versus air flow rate curve to pass through the origin. (In much of the data, the curves tended to intersect the air flow axis at small positive values such as +20 lbm per hour.) Thus the IHP relationship was left in the more general form;

$$\dot{m}_{\text{air}} \frac{\text{lbm}}{\text{hour}} = A_0 + \text{IHP}/\text{SLOPE} \quad \text{EQN 5.5}$$

where  $A_0$  represents the air flow rate at which the curve would intersect the axis if extended. This value may be expressed as:



$$A_o = \text{AIRFL}^2 - \text{XIHP}^2/\text{SLOPE} \quad \text{EQN 5.6}$$

For any desired air mass flow rate value, denoted as AIRFLO, the corresponding indicated horsepower value is given by the relationship:

$$\text{IHP} = (\text{AIRFLO} - A_o)(\text{SLOPE}) \quad \text{EQN 5.7}$$

Once the indicated horsepower has been determined for a specified fuel-air ratio and air flow rate, all of the other indicated engine parameters can be readily obtained. If the engine speed in revolutions per minute is denoted by  $N$ , the displacement in cubic inches is  $D$ , and the fuel mass flow rate in lbm per hour is  $\dot{m}_f$ , the indicated torque, specific fuel consumption, and mean effective pressure are;

$$\text{IMEP} = (5252.0)(150.8) \text{ IHP}/(N)(D) \text{ psi} \quad \text{EQN 5.8}$$

$$\text{ISFC} = \left[ \dot{m}_f/\text{IHP} \right] \text{ lbm/BHP hr} \quad \text{EQN 5.9}$$

$$\text{TORQI} = (\text{IMEP})(D)/150.8 \text{ ft lbf} \quad \text{EQN 5.10}$$

where the fuel mass flow rate is given by:

$$\dot{m}_f = (\text{AIRFLO})(F/A) \text{ lbm/hr} \quad \text{EQN 5.11}$$

The engine friction and brake values must now be obtained in terms of the indicated values and the friction parameters for any engine that is being utilized. The important point to note here is that the friction values (torque, horsepower, and mean effective pressure) are functions of the engine speed and intake manifold pressure for a given engine. The variation in these frictional values must be correlated for all possible engine speeds and intake manifold vacuums, since any combination might have to be evaluated during a carburetor simulation run. The goal of this study was to find a correlation technique that

could be easily implemented using friction data obtained from a simple test or tests, preferably tests that could be performed during the IHP tests discussed previously.

A successful technique was found to simply correlate the variations in engine friction with intake manifold pressure (pumping work variations) and with engine speed. This correlation can be obtained from two simple motoring tests on the dynamometer, and is conducted in the following manner. With the engine at a normal operating temperature, the engine is motored with the throttle wide open to give a very low intake manifold vacuum and consequently a minimum pumping work situation. The engine speed is varied from zero to the upper limit of the operating range, with friction load values recorded at suitable speed increments such as 500 RPM. This test run is then repeated with the throttle plate completely closed, which provides a maximum intake manifold vacuum and maximum pumping work situation. When the friction data are converted to mean effective pressure values by using the equation;

$$\text{FMEP} = (150.8)(\text{TORQF})/D \text{ psi} \qquad \text{EQN 5.12}$$

the values for a particular engine are as shown in figure 31. The lower curve, which corresponds to the minimum pumping work situation, is denoted as the FMEP1 data set, and the upper curve is the FMEP2 data set. All possible friction values will lie on or within the region bounded by the two curves. If the intake manifold vacuum is increased as the engine speed is kept constant, the friction mean effective pressure

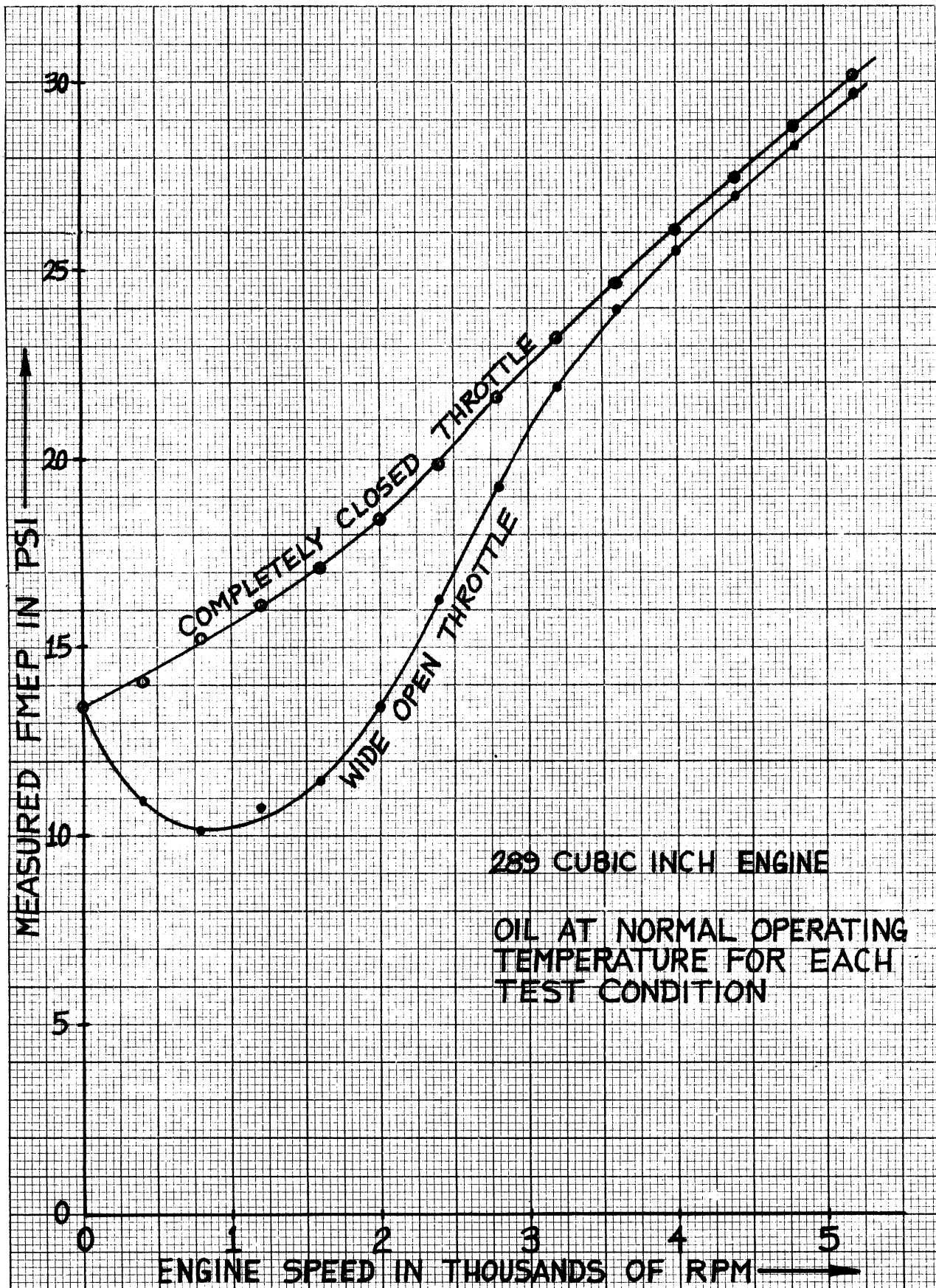


Figure 31. FMEP Variations with engine speed and intake manifold vacuum

will move from the lower curve value toward the upper curve.

The determination of the engine frictional values is quite similar in form to that utilized in obtaining the indicated values. If the engine speed and intake manifold vacuum are specified, the generalized interpolation subroutine STERL is called to return the upper and lower curve values for the given RPM, which are denoted as FMAX and FMIN. Then the FMEP corresponding to the actual intake manifold vacuum is obtained by noting that the pumping work will be proportional to the intake manifold vacuum at a given engine speed.

or:

$$\text{FMEP} = \text{FMIN} + (\text{FMAX} - \text{FMIN}) \left[ \frac{\text{VACMAN}}{\text{POHG} - 3.0} \right] \text{ psi} \quad \text{EQN 5.13}$$

In equation 5.13 the symbol POHG denotes the atmospheric pressure in inches of mercury, and the value 3.0 represents a very good approximation to the absolute intake manifold pressure (in inches of mercury) when the throttle is completely closed.

Once the friction mean effective pressure has been obtained, all of the important friction and brake values can be calculated from the following equations:

$$\text{FHP} = (\text{TORQF})(\text{N})/5252.0 \quad \text{EQN 5.14}$$

$$\text{BHP} = \text{IHP} - \text{FHP} \quad \text{EQN 5.15}$$

$$\text{BMEP} = \text{IMEP} - \text{FMEP} \text{ psi} \quad \text{EQN 5.16}$$

$$\text{BSFC} = \left[ \dot{m}_f / \text{BHP} \right] \text{ lbm/BHP hr} \quad \text{EQN 5.17}$$

$$\text{THERMI} = 2545.0 / (\text{ISFC}) \bar{H}_c \quad \text{EQN 5.18}$$

$$\text{THERMB} = 2545.0 / (\text{BSFC}) \bar{H}_c \quad \text{EQN 5.19}$$

Where  $\bar{H}_c$  is the lower heating value of the fuel being utilized. By utilizing the above relationships in conjunction with the carburetor analysis, nearly all of the important operating variables of numerous standard tests can be predicted.

#### E. SUMMARY OF ENGINE DATA CORRELATION TECHNIQUE

An accurate method of correlating numerous engine operating parameters on the basis of two simple dynamometer tests was developed for utilization within the simulation program. This correlation technique is not an engine simulation, but merely provides a method for efficiently employing actual engine data for the particular engine that is being used. Strictly speaking, the actual engine IHP data should be obtained using the same fuel, fuel temperature, and inlet air temperature as will be specified in the carburetor simulation. In the practical sense however, it was found from numerous engine tests that the indicated horsepower curves for a given engine are affected only slightly by variations in fuel and air temperature and gasoline brand. Thus, unless the fuel to be specified in the simulation differs markedly from that used to obtain the IHP data, or unless the temperature values to be specified differ greatly from those of normal test cell conditions, the IHP curves may be used as a good approximation of engine performance under many specified simulation conditions. The FMEP curves are affected even less than the IHP curves, therefore they may be used for all simulation runs.

Four parameters must be specified with this method in order to obtain values for all of the engine operating parameters listed in the preceding section. These are:

1. Engine speed
2. Dry air mass flow rate
3. Intake manifold vacuum
4. Total fuel-air ratio

This corresponds very well with the carburetor simulation since subroutine AIRMAS predicts all mixture flow rates and the intake manifold vacuum. Then, after the carburetor parameters have been analyzed and predicted in the simulation (including the total fuel-air ratio), the analyses presented in the preceding sections are utilized to determine how a particular engine would perform for the predicted carburetor behavior.

The method of acquiring data along constant air flow rate curves with varying fuel-air ratio, and the general correlation technique both have numerous other applications within the automotive industry. Figure 32 illustrates the significance of lines and points when the indicated (or brake) horsepower data are obtained along constant air mass flow rate lines and are plotted on the coordinates shown. Note that the fuel rate will be exactly linear and that a straight line through the origin that is tangent to the IHP (or BHP) curve, as denoted by point A, will be tangent at the point of minimum indicated (or brake) specific fuel consumption. Any other straight line through the origin will intersect a constant air flow rate at points of equal specific fuel

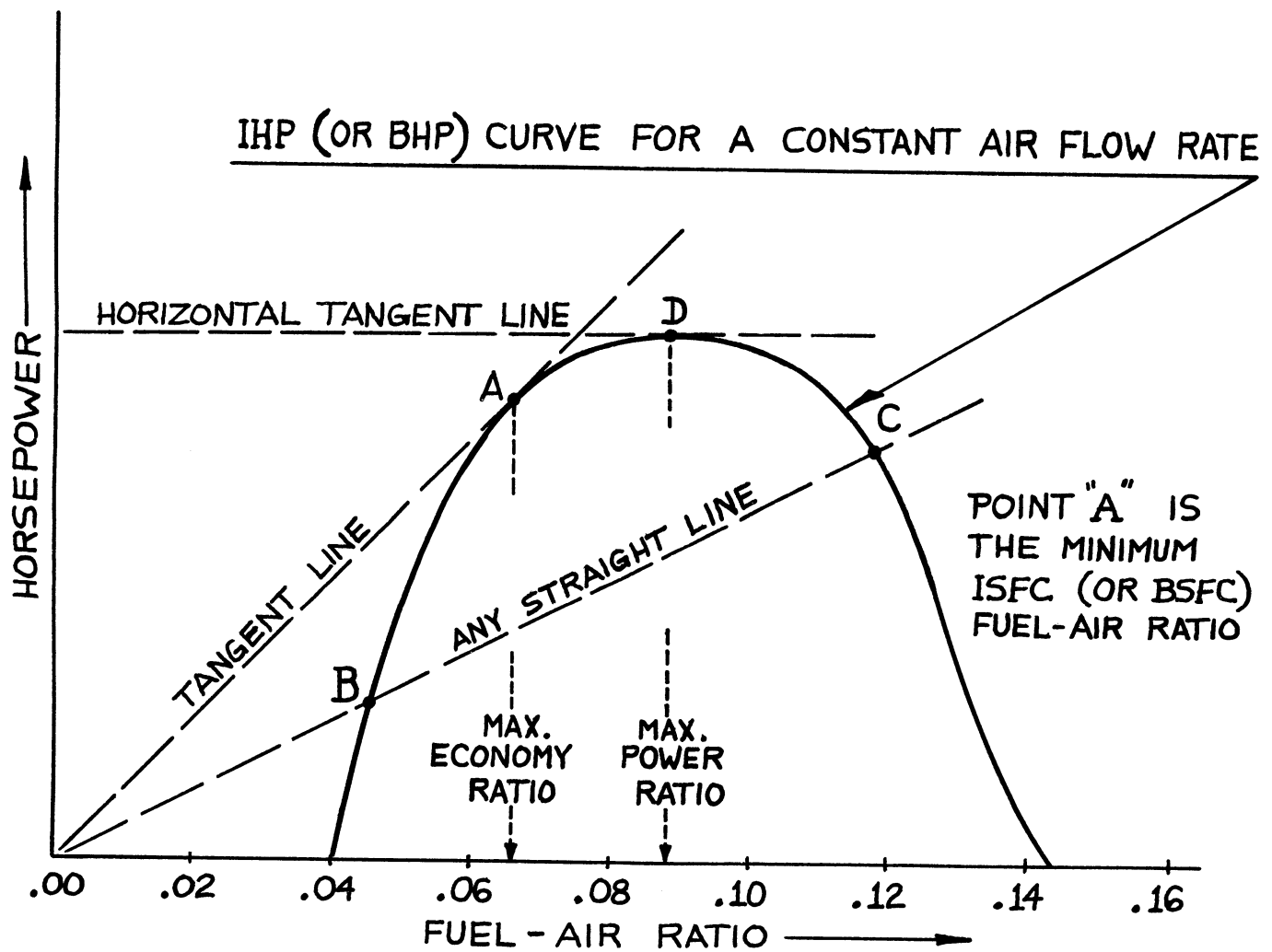


Figure 32. Applications of constant air mass flow rate curves

consumptions, as shown by points B and C. A horizontal line that is tangent to the curve (point D) will do so at the fuel-air ratio which represents the maximum power ratio for that particular engine and air flow rate. The general data correlation analysis has application wherever numerous engine parameters must be known over the entire operating range.

#### F. ITERATIVE TECHNIQUE FOR OBTAINING ROAD LOAD OPERATING POINTS

The engine data correlation technique, when combined with the road load considerations of the vehicle, makes possible the analysis of the carburetor at operating points which correspond to road load conditions for the particular carburetor, engine, and vehicle combination. Since the carburetor design is analyzed on the basis of specified operating points which are determined by engine speed and throttle angle, these parameters must be specified before the carburetor analysis is performed. The engine speed corresponding to any vehicle velocity may be calculated directly by means of the equations in section 3c, but the throttle angle corresponding to a given road load situation is much more difficult to obtain. This throttle angle is the one which will yield the fuel-air ratio, intake manifold vacuum, and air mass flow rate that results in the required brake horsepower. Therefore, the following iterative technique is utilized in obtaining the correct throttle angle and the resulting analysis for the road load conditions:



1. The vehicle velocity is specified and the corresponding engine speed and required engine BHP are calculated.
2. A reasonable initial guess is made for the throttle angle, thus the operating point is specified.
3. A complete carburetor analysis is performed utilizing all the relationships presented in the preceding chapters. This results in an air mass flow rate, intake manifold vacuum, and total fuel-air ratio.
4. Now the four parameters needed for the complete engine data calculations are known. Therefore all of the engine parameters presented in this chapter may be calculated, including the brake horsepower output.
5. If the engine BHP output for the assumed throttle angle is not equal to the required road load BHP value, a new throttle angle is assumed according to the general convergence technique (Appendix G) and the magnitude of the difference.
6. Another complete carburetor analysis is performed and the new engine brake horsepower output is calculated. This continues until convergence is obtained or the iterative throttle angle exceeds  $90^{\circ}$ . The latter indicates that the given carburetor-engine combination cannot provide the road load requirements of the specified vehicle and velocity.

This procedure can be applied over the entire velocity range from zero to the maximum value. In the carburetor simulation, if an analysis is requested under road load operating conditions, the above procedure is utilized at 5 miles per hour increments until the maximum vehicle velocity is reached, which corresponds to a throttle angle of  $90^{\circ}$ . Typical IHP, FMEP, and vehicle input data, as well as the computer output for a road load analysis will be presented in Chapter 8.

Once the throttle angle iterations have converged to the road load value, the vehicle miles per gallon can be calculated for each

velocity from the equation;

$$\text{MPG} = \frac{(231.0) \rho_f V}{(1728.0) (\text{BSFC}) (\text{BHP})} \quad \text{EQN 5.20}$$

thus, for any proposed carburetor design, the results of steady speed fuel economy tests can be predicted, as well as the results of numerous engine tests.

## CHAPTER VI

### ON-ENGINE CARBURETOR TESTS

#### A. REASONS FOR TESTS

Numerous dynamometer tests were performed on specific carburetor-engine combinations during this project. These tests were carried out for many important reasons, the first of which was to obtain a general understanding of the processes that occur within the carburetor over a wide range of operation. Another basic reason for conducting the on-engine carburetor tests was to obtain precise data for use in developing the engine data correlation technique which was presented in the previous chapter.

One of the most important reasons for conducting these tests was to obtain accurate data on the performance of individual carburetor systems. These data, such as the variation in metering signal with air mass flow rate, the choked mixture flow rates at various throttle angles, and the minimum air flow values for completely closed throttle angles, were necessary to check the analytical predictions of individual computer subroutines, as well as the complete simulation. Thus, it was possible to debug each subroutine separately and to assure that the analytical predictions were in good agreement with actual data before combining all subroutines into one carburetor simulation.

## B. BACKGROUND

Some experimental data on the effect of specific carburetor operating variables may be found in the literature. The data that have application to the overall computer simulation and the associated carburetor-engine test program will now be discussed.

In the area of overall carburetion, the problems of enrichment with altitude, variation in fuel/air ratio with fuel properties, and enrichment under deceleration are of current interest. This is mainly because of the air pollution problem and the relation between variations in mixture ratio and the emission of unburned hydrocarbons.

Bolt and Boerma<sup>44</sup> studied the effect of altitude on the mixture ratio delivered by three different carburetors. They showed a definite enrichment of the mixture with a decrease in ambient pressure, amounting to a 30% enrichment at an inlet pressure of 18.0 inches Hg. absolute. They also derived a theoretical enrichment equation:

$$\frac{F/A^*}{F/A} = \frac{\delta}{\delta^*} \sqrt{\frac{\rho_{air}}{\rho_{air}^*}} \quad \text{EQN 6.1}$$

where  $\delta$  is a compressibility parameter and the \* superscript denotes the reduced pressure conditions. This equation gives a reasonable correlation of the experimental data down to inlet pressures of 20 inches of mercury absolute. In the derivation of the equation, some terms had to be neglected due to lack of information. This included the manner in which fuel channel frictional pressure losses vary with flow rate and the variation in the main metering orifice discharge coefficient as a

result of changes in venturi suction.

Wahrenbrock<sup>56</sup> discussed the effect of fuel density variations on carburetion. The actual test data involved on-engine determinations of the fuel-air ratio for ten different fuel types. These fuels ranged from toluene to catalytically cracked fuels, and represented a density range from 31.6 to 71.9 A.P.I. degrees. Two carburetor types were tested at various throttle settings. The data showed an increase in the fuel-air ratio for increasing fuel density, however the effect was not large and the scatter was quite pronounced. A very simple analytical equation, relating the fuel-air ratio to the fuel specific gravity, was obtained for the special case of constant air mass flow rate:

$$F/A = \text{constant} \sqrt{SG_{\text{fuel}}} \quad \text{EQN 6.2}$$

However, the assumption of constant coefficients of discharge with increasing fuel flow rate, and the fact that the constant in equation 6.2 involves many complicated factors, reduces the validity of the equation. Also neglected was the fact that all of the metering signal is not lost across the main metering orifice in an actual carburetor. The analyses presented in the preceding chapters should convey the fact that the fuel-air ratio cannot be expressed simply as a function of specific gravity alone. Numerous other factors such as the viscosity of the fuel must be considered since the viscous pressure losses in the fuel channel are related to viscosity. In fact, for a given fuel, a decrease in specific gravity due to a temperature increase will be accompanied

by a reduction in viscosity. Thus, an important effect that is not considered in equation 6.2 is the change in the coefficient of discharge of the main metering orifice with viscosity.

The experimental data due to Goetsch, et al,<sup>47</sup> provided a useful reference because the carburetor used in the study was one of the types used in this experimental program (Ford C4AF-DE). The data included fuel-air ratio versus air mass flow rate, as well as pressure differentials at various locations in the carburetor fuel channel, including:

1. boost (secondary) venturi
2. main metering orifice
3. fuel discharge nozzle

The fuel specific gravity and viscosity were not given, nor was the fuel temperature, nevertheless the experimental trends shown in the report provided useful comparisons with the data obtained in this project.

Additional experimental data on the effect of fuel type on overall carburetion was given by Smith.<sup>51</sup> The tests were concerned with the separate effects of changes in specific gravity, viscosity, and vapor pressure. The results were as follows:

1. Increasing the fuel specific gravity from .70 to .74 increased the fuel mass flow rate 2.7%, and decreased the fuel volume flow rate 2.7%.
2. Increasing the kinematic viscosity from 0.582 to 2.35 centistokes by using eight different fuels gave a fuel mass flow rate decrease of about 1.0% per 0.1 centistoke increase. By using fuels with the same specific gravity but viscosities from .730 to 8.30 centistokes, a mass flow rate decrease of 0.4% per 0.1 centistoke change was obtained.

TABLE VII

## EQUIPMENT UTILIZED IN ON-ENGINE CARBURETOR TESTS

## CARBURETORS

Ford C6AFB-C6FC 2-barrel  
Ford C6AF-9510-B 2-barrel  
Rochester 2MV 2-barrel  
Rochester 4MV quadrajet model 7027135  
Ford C4AF-9510-DE 2-barrel  
Ford C7AF-9510-BZ 2-barrel  
Carter YF single barrel

## ENGINES

1966 Ford 289 cubic inch V-8  
1967 Chevrolet 283 cubic inch V-8

## INSTRUMENTATION

General Electric dynamometer model 26G51  
Meriam micromanometer (10 inch) model A-750  
Meriam manometer (30 inch) model 30W  
King manometer (6 tubes-60 inch) model ASC 6FF30  
Honeywell 8 channel Visicorder model 508  
General Motors standard air orifice plate (5 hole)  
Hewlett-Packard automatic fuel burette system model 521A  
Neslab constant temperature bath model PBC-5  
Statham strain gage pressure pickups ( $\pm 2.5$ ,  $\pm 5.0$ ,  $\pm 15.0$  psi)  
Beckman-Whitley movie camera (3000 frames/sec)  
Brown Instruments multi-point potentiometer model Y156X62-P18  
Carrier strain gage amplifiers  
Tectronix dual beam oscilloscope 502A  
Honeywell galvanometer amplifier

The viscosity effect seemed to be reduced at higher orifice pressure differentials but this was not investigated in detail. The test procedures, engines, carburetors, and orifice types were not given, thus the value of the data is significantly reduced. It may be that for a different orifice type the trend would be just the opposite.

### C. EXPERIMENTAL EQUIPMENT AND CONDITIONS

The on-engine carburetor test program was conducted at the University of Michigan Automotive Laboratory. A large number of tests were made utilizing various test conditions, carburetors, fuels, and engines. The bulk of the tests were performed on two-barrel, air-bleed, fixed venturi carburetors using gasoline as the fuel. However other carburetor types and fuels were also tested.

The equipment and instrumentation used in these tests consisted of the items listed in Table 7. Note that in addition to the normal air rate, fuel rate, and load measuring devices, numerous special items such as strain gage pressure transducers, a high speed movie camera, and a constant temperature bath were utilized to obtain additional information on carburetor operation.

Tests were performed on both a 1966 Ford 289 cubic inch V-8 engine and a 1967 Chevrolet 283 cubic inch V-8 engine, with the majority of the tests being run on the Ford engine. Various standard and modified carburetors were tested on these engines. The modifications consisted of such items as:



1. Internal pressure transducers installed
2. Enrichment system made inoperative
3. Idle system and air bleeds plugged
4. Float chamber pressurized
5. Choke and acceleration pump removed
6. Part of main and boost venturi cut away

One or more of these modifications were made for a given test in order to obtain information on specific carburetor variables. For example, modification number 4 was used in a test to determine the effect of fuel flow rate on the reduction in boost venturi suction.

An overall view of the equipment used for many of the tests is shown in Figure 33. Note that the air flow rate is measured by calibrated orifices and a micromanometer, and that the fuel flow rate is obtained by an automatic burette system. Figure 34 shows the carburetor pressure chamber and the protractor used to accurately position the throttle plate at any desired angle. The pressure chamber was used only for those tests with reduced carburetor inlet pressure (simulated altitude). For all other runs it was removed. A constant temperature bath provided a controlled fuel temperature over a wide range of values. A liquid nitrogen bath was used in conjunction with the constant temperature bath whenever very cold fuel temperatures were desired. This system was capable of holding the fuel temperature at any value down to the freezing point of the fuel being used. The types of tests run were:

1. constant engine speed, varying throttle angle
2. constant throttle angle, varying engine speed
3. constant air flow rate, varying fuel flow rate
4. varying fuel type and temperature
5. varying inlet air pressure
6. tests with no idle, enrichment, or air bleed flow

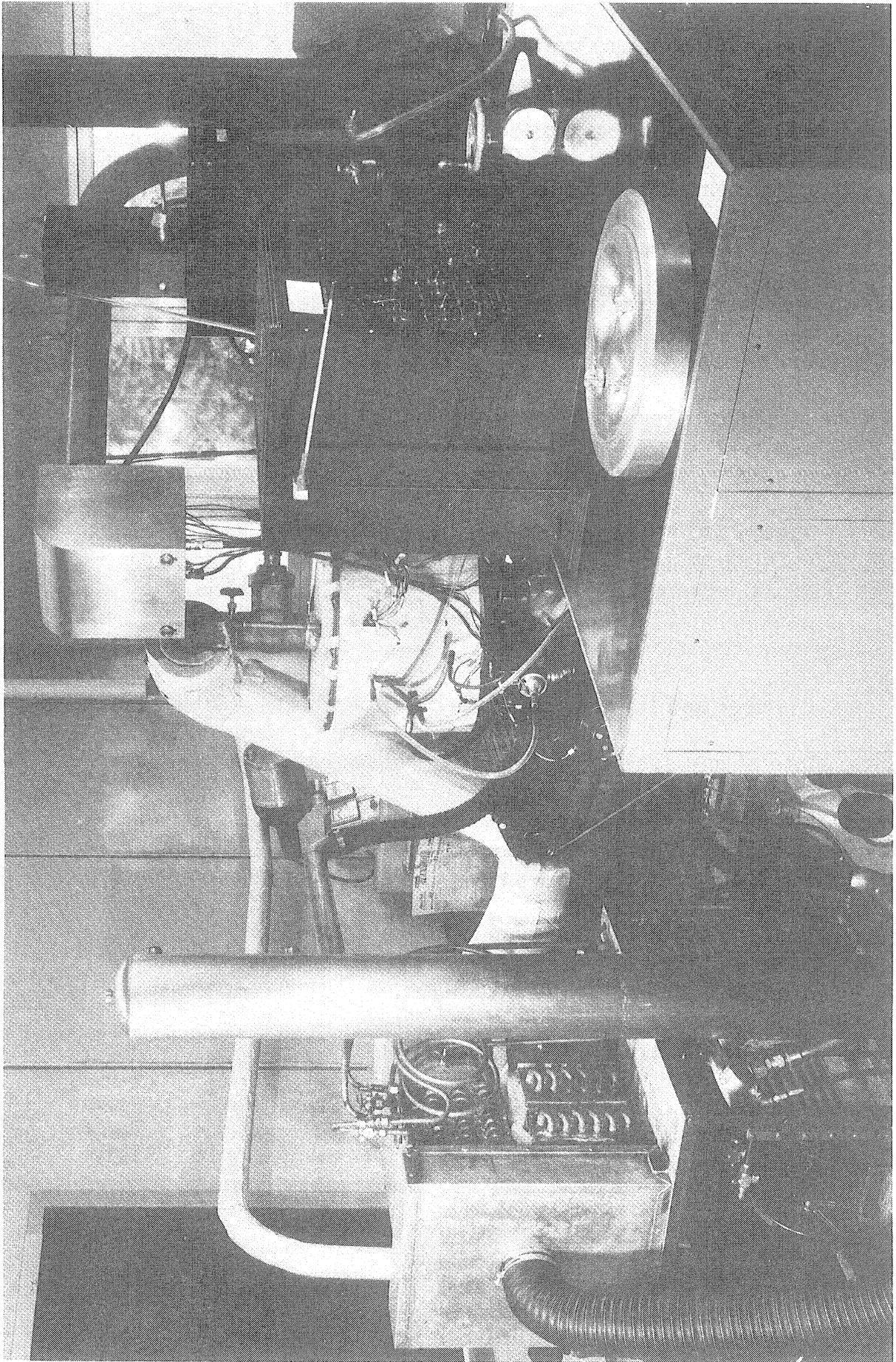


Figure 33. Equipment utilized in on-engine carburetor tests

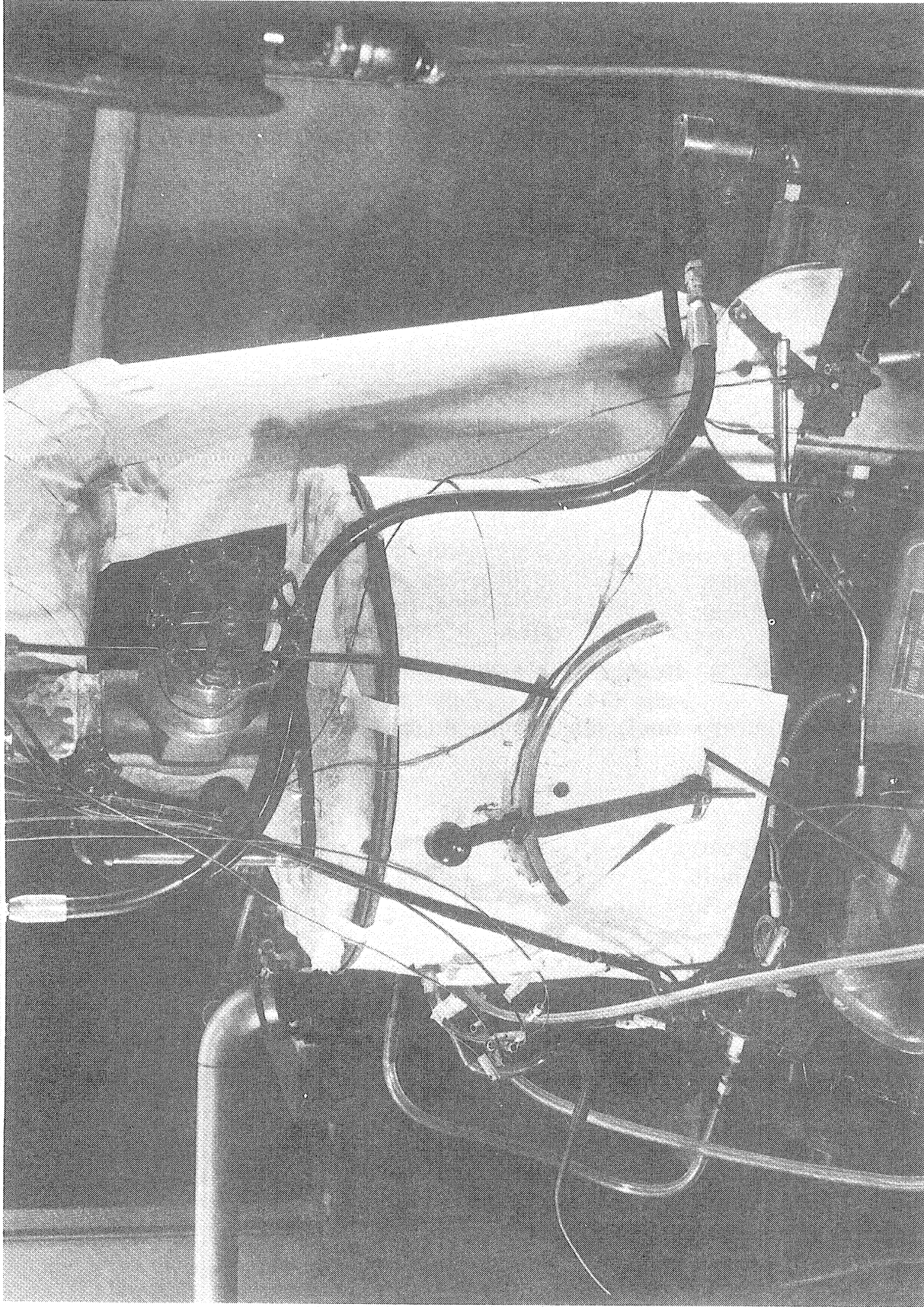


Figure 34. Equipment utilized to control and monitor carburetor variables

## 7. tests with engine motoring (no fuel flow)

The ranges of the important variables in these tests are listed in Table 8. Note that the humidity was measured for each test but was not controlled.

TABLE VIII

## RANGES OF VARIABLES IN CARBURETOR TESTS

VARIABLE	RANGE
Throttle Angle	Completely Closed to Fully Opened
Engine Speed	500 to 4500 RPM
Ambient Pressure	24.00 to 29.86 inches of mercury
Ambient Temperature	70.0 to 100.0 ° F
Fuel Type	3 gasoline brands and isooctane
Fuel Temperature	0.0 to 120.0 ° F
Relative Humidity	25 to 90% (uncontrolled)

The data obtained in these tests included all important variables related to the carburetor analyses and the engine data correlation.

Some of these variables are:

1. engine speed
2. throttle angle
3. intake manifold vacuum
4. air mass flow rate
5. total fuel mass flow rate
6. carburetor air inlet pressure
7. brake, indicated, and friction torque,  
mean effective pressure, and horsepower
8. brake and indicated specific fuel consumption  
and thermal efficiency
9. primary and secondary (boost) venturi suction
10. temperatures of the inlet air, fuel bowl,  
throttle plate, and intake manifold  
(inlet and outlet)

The throttle angle was obtained by fitting each throttle shaft with a protractor and pointer. The pointer was set in each case such that 90° corresponded to the venturi axis. This pointer was also equipped

with a special lever to allow the throttle plate to be set and locked in any desired position.

The carburetor air inlet pressure for simulated altitude runs was obtained from the pressure differential between the ambient and the inside of the chamber surrounding the carburetor. Both the chamber and the throttle angle lever are shown in Figure 34.

#### D. CARBURETOR PERFORMANCE OVER THE ENTIRE OPERATING RANGE

Series of tests were conducted with the engine speed held constant and the throttle angle varying in small increments from completely closed to wide open. The series was then repeated with the throttle angle held constant, while the engine speed was varied from 500 to 4500 RPM. Typical results from these test series are presented in Tables 9 and 10. Note that the test data have been reduced by a digital computer, and that all of the important variables have been tabulated. From these (and additional) results the next five figures were obtained. Figure 35 illustrates the observed variation in intake manifold vacuum with throttle angle for various engine speeds. Since the intake manifold vacuum was previously shown to be one of the controlling factors in determining both the idle and enrichment system flow rates, its relationship to the operating point variables is quite important. Plots of data illustrating the relation between air flow, intake manifold pressure, engine speed, and throttle angle will be presented in Chapter 8, where they can be compared to the simulation predictions.

TABLE IX  
 REDUCED DATA FOR ON-ENGINE CARBURETOR TESTS AT  
 CONSTANT ENGINE SPEED AND VARIABLE THROTTLE ANGLE

DATA REDUCTION PROGRAM FOR ENGINE TESTS

\*\*\*\* PROGRAM RESULTS FOR THIS TEST \*\*\*\*

THE TEST NUMBER IS 16 TO 26  
 THE TEST DATE IS 9/16/66 TO 10/15/67  
 THE AMBIENT AIR DENSITY IS .0716 TO .0635 LBM/FT<sup>3</sup>  
 THE SAE CORRECTION FACTOR IS 1.010 TO 1.022  
 THE ENGINE DISPLACEMENT IN CUBIC INCHES IS 288.52

ENGINE : FORD 289 V-8  
 CARBURETORS : VARIOUS FORD,  
 ROCHESTER, CARTER  
 FUEL : STANDARD REG. GASOLINE

RUN	RPM	SCALE	PMAN	BHP	FHP	RATEF	RATEA	F/A	BSFC	EFFVOL	THERMB
1	1195.0	27.5	9.8	6.28	6.35	7.215	92.91	.0777	1.1492	21.61	11.55
2	1202.7	46.8	11.7	10.72	6.18	7.932	117.99	.0672	.7401	27.36	17.93
3	1194.7	73.5	15.1	16.72	5.82	9.605	158.85	.0605	.5745	37.08	23.10
4	1200.5	104.5	18.7	23.89	5.53	12.121	204.24	.0593	.5074	47.45	26.15
5	1189.4	150.5	25.3	34.08	4.87	16.437	282.91	.0581	.4823	66.34	27.52
6	1226.3	179.5	28.8	41.91	4.67	18.520	312.75	.0592	.4419	71.13	30.03
7	1195.6	21.0	8.9	4.78	6.31	6.957	86.03	.0809	1.4553	20.07	9.12
8	1197.8	44.0	11.1	10.03	6.18	7.817	113.50	.0689	.7790	26.43	17.03
9	1198.8	73.0	14.6	16.66	5.91	9.690	157.77	.0614	.5815	36.71	22.82
10	1195.6	110.0	19.3	25.13	5.48	12.750	215.64	.0591	.5074	50.13	26.15
11	1202.1	155.0	25.4	35.48	4.92	16.943	290.38	.0583	.4776	67.37	27.79
12	1201.1	183.0	28.7	41.85	4.57	19.100	322.15	.0593	.4564	74.81	29.07
13	1588.9	23.0	9.1	6.96	9.20	7.682	112.06	.0686	1.1041	19.67	12.02
14	1595.8	45.2	11.4	13.73	8.93	9.610	154.92	.0620	.6997	27.08	18.96
15	1600.7	71.0	14.6	21.64	8.53	12.477	208.02	.0600	.5766	36.24	23.01
16	1603.4	117.0	19.2	35.72	7.97	17.152	286.63	.0598	.4802	49.86	27.63
17	1602.5	140.5	22.0	42.87	7.60	19.984	330.89	.0604	.4662	57.59	28.47
18	1603.5	203.5	28.5	62.13	6.72	27.826	443.91	.0627	.4479	77.21	29.63
19	1595.9	18.0	8.3	5.48	9.32	7.543	105.05	.0718	1.3757	18.31	9.65
20	1602.4	54.0	12.4	16.48	8.85	10.678	176.20	.0606	.6481	30.67	20.47
21	1600.2	70.0	14.0	21.33	8.62	12.345	202.55	.0609	.5789	35.30	22.92
22	1598.0	103.0	17.3	31.34	8.18	15.591	259.72	.0600	.4975	45.33	26.67
23	1603.0	139.0	21.7	42.44	7.66	20.048	334.66	.0599	.4724	58.20	28.09
24	1600.4	200.0	28.5	60.94	6.70	26.713	436.95	.0611	.4383	76.15	30.27
25	2601.3	20.5	8.7	7.81	12.57	8.946	140.82	.0635	1.1452	19.63	11.59
26	1598.3	44.5	11.2	16.93	12.21	11.968	197.94	.0605	.7068	27.63	18.77
27	2001.1	73.0	14.3	27.81	11.81	15.808	263.03	.0601	.5683	36.66	23.35
28	2001.4	118.0	17.9	44.97	11.36	20.491	334.66	.0612	.4557	46.64	29.12
29	2000.0	139.0	21.6	52.93	10.85	24.627	416.54	.0591	.4653	58.09	28.52
30	2002.5	208.0	28.2	75.31	9.91	35.147	547.26	.0642	.4432	76.22	29.94
31	2125.1	8.0	7.2	3.24	13.43	8.316	123.49	.0673	2.5689	16.21	5.17
32	2100.8	24.0	8.9	9.60	13.20	9.958	155.58	.0640	1.0373	20.66	12.79
33	2076.5	55.0	12.3	21.75	12.34	13.941	231.83	.0601	.6411	31.14	20.70
34	2104.6	81.0	14.1	32.46	12.38	16.943	279.76	.0606	.5220	37.07	25.42
35	2115.1	116.0	18.4	46.71	12.12	22.685	364.94	.0622	.4856	48.12	27.33
36	2152.6	148.0	22.3	60.66	11.89	27.627	451.54	.0612	.4554	58.50	29.14
37	2146.2	206.0	28.1	84.18	10.71	36.946	577.36	.0640	.4389	75.03	30.23
38	2503.2	21.0	7.0	10.01	17.87	11.437	185.64	.0616	1.1426	20.68	11.61
39	2502.2	47.0	11.7	22.39	17.25	15.808	259.72	.0609	.7060	28.95	18.80
40	2502.8	74.0	14.5	35.26	17.01	20.152	330.10	.0610	.5714	36.79	23.22
41	2500.0	111.5	18.5	53.08	16.57	26.658	436.95	.0610	.5023	48.75	26.42
42	2504.7	138.0	21.7	65.81	16.26	30.913	517.28	.0598	.4697	57.60	28.25
43	2505.5	195.0	27.9	93.03	15.46	40.981	647.67	.0633	.4405	72.10	30.12

TABLE IX (continued)

RUN	IMEP	TEGCF	TORQI	BMEP	IMP	BHPC	IHPC	SG	A/F	ISFC	THERMI
44	1213.6	26.5	9.3	6.12	6.47	7.300	91.75	.0796	15.1920	21.09	11.13
45	1198.9	47.5	11.3	10.85	6.21	7.974	118.80	.0671	.7348	27.61	18.06
46	1203.1	71.5	14.4	16.38	5.96	9.450	156.07	.0606	.5770	36.18	23.00
47	1201.3	116.0	19.6	26.53	5.49	13.211	219.87	.0601	.4979	51.05	26.65
48	1204.2	141.0	23.5	32.33	5.11	15.719	269.37	.0584	.4862	62.39	27.29
49	1213.2	183.0	28.7	42.17	4.61	19.193	325.15	.0590	.4552	74.93	29.15
50	1605.7	25.0	8.8	7.64	9.32	8.111	116.89	.0694	1.0612	20.50	12.50
51	1605.2	48.5	11.6	14.82	8.96	10.007	163.43	.0612	.6751	28.40	19.66
52	1602.8	80.0	14.8	24.41	8.58	13.479	217.22	.0621	.5521	37.80	24.04
53	1605.0	107.5	17.7	32.85	8.22	16.411	268.13	.0610	.4995	46.77	26.56
54	1601.1	135.0	20.9	41.16	7.74	19.593	320.94	.0610	.4761	55.91	27.87
55	1605.0	200.5	28.5	61.27	6.72	26.535	438.22	.0606	.4331	76.15	30.64
56	1205.2	24.5	9.8	5.64	6.40	7.422	92.30	.0804	1.3158	21.29	10.09
57	1205.9	62.8	13.5	14.42	5.74	9.344	140.24	.0666	.6480	32.44	20.48
58	1205.6	97.5	17.8	22.34	5.74	12.314	191.16	.0644	.5513	44.22	24.07
59	1205.0	130.5	22.6	29.94	5.23	15.894	249.71	.0637	.5309	57.80	25.00
60	1200.1	178.0	28.4	40.67	4.64	20.085	321.68	.0624	.4938	74.76	26.87
61	1602.5	101.5	17.1	30.97	8.24	16.263	252.12	.0645	.5251	43.88	25.27
62	1606.8	171.0	25.2	52.12	7.28	24.596	384.28	.0635	.4681	66.95	28.35
1	28.90	27.80	55.30	14.37	12.62	6.41	12.75	.7247	12.88	.571	23.22
2	38.57	27.00	73.80	24.46	16.90	10.89	17.07	.7243	14.88	.469	28.27
3	51.80	25.60	99.10	38.42	22.54	16.95	22.77	.7243	16.54	.426	31.14
4	67.27	24.20	128.70	54.62	29.42	24.19	29.72	.7243	16.85	.412	32.21
5	89.90	21.50	172.00	78.66	38.95	34.48	39.35	.7258	17.21	.422	31.45
6	104.27	20.00	199.50	93.82	46.58	42.38	47.05	.7262	16.89	.428	33.38
7	25.45	27.70	46.70	10.98	11.09	4.89	11.20	.7254	12.37	.628	21.15
8	37.16	27.10	71.10	23.00	16.22	10.20	16.38	.7254	14.52	.482	27.53
9	51.69	25.90	98.90	38.15	22.57	16.89	22.80	.7258	16.28	.429	30.91
10	70.04	24.00	134.00	57.49	30.61	25.44	30.92	.7262	16.91	.417	31.86
11	92.25	21.50	176.50	81.01	40.40	35.89	40.81	.7265	17.14	.419	31.64
12	106.10	20.00	203.00	95.65	46.42	42.32	46.90	.7265	16.87	.411	32.25
13	27.91	30.40	53.40	12.02	16.15	7.12	16.32	.7251	14.59	.476	27.90
14	38.99	29.40	74.60	22.67	22.67	13.96	22.90	.7262	16.12	.424	31.30
15	51.74	28.00	99.00	37.11	30.17	21.95	30.48	.7265	16.67	.414	32.09
16	74.79	26.10	143.10	61.15	43.69	36.16	44.13	.7276	16.71	.393	33.80
17	86.45	24.90	165.40	73.43	50.47	43.38	50.98	.7273	16.56	.396	33.51
18	117.86	22.00	225.50	106.36	68.85	62.83	69.55	.7276	15.95	.404	32.83
19	25.40	30.60	48.60	9.41	14.80	5.63	14.96	.7258	13.93	.510	26.04
20	43.38	29.00	83.00	28.22	25.32	16.73	25.58	.7258	16.50	.422	31.47
21	51.38	28.30	98.30	36.59	29.95	21.63	30.25	.7258	16.41	.412	32.19
22	67.89	26.90	129.90	53.83	39.52	31.74	39.93	.7258	16.66	.394	33.64
23	85.77	25.10	164.10	72.65	50.11	42.95	50.61	.7265	16.69	.400	33.17
24	116.03	22.00	222.00	104.53	67.65	61.63	68.33	.7267	16.36	.395	33.60
25	27.96	33.00	53.50	10.71	20.39	8.02	20.59	.7262	15.74	.439	30.24
26	40.04	32.10	76.60	23.26	29.15	17.23	29.44	.7262	15.54	.411	32.32
27	54.36	31.00	104.00	38.15	39.63	28.22	40.03	.7254	16.64	.399	33.26
28	77.25	29.80	147.80	61.67	56.32	45.54	56.90	.7262	16.33	.364	36.47
29	87.55	28.50	167.50	72.65	63.79	53.58	64.43	.7258	16.91	.386	34.37
30	122.30	26.00	234.00	108.71	89.22	80.21	90.12	.7258	15.57	.394	33.68
31	21.53	33.20	41.20	4.18	16.67	3.41	16.84	.7251	14.85	.499	26.60
32	29.79	33.00	57.00	12.54	22.80	9.83	23.03	.7251	15.62	.437	30.38
33	45.05	31.20	86.20	28.75	34.08	22.09	34.43	.7251	16.63	.409	32.44
34	58.49	30.90	111.90	42.34	44.84	32.91	45.30	.7265	16.51	.378	35.12
35	76.36	30.10	146.10	60.63	58.84	47.31	59.43	.7280	16.09	.386	34.42
36	92.51	29.00	177.00	77.35	72.55	61.40	73.28	.7280	16.34	.381	34.84

TABLE IX (continued)

37	121.36	26.20	232.20	107.67	94.89	85.14	95.85	.7288	15.63	.389	34.08
38	30.58	37.50	58.50	10.98	27.88	10.29	28.17	.7254	16.23	.410	32.35
39	43.49	36.20	83.20	24.57	39.64	22.79	40.04	.7254	16.43	.399	33.27
40	57.34	35.70	109.70	38.68	52.28	35.80	52.81	.7254	16.38	.385	34.42
41	76.47	34.80	146.30	58.28	69.64	53.78	70.35	.7254	16.39	.383	34.66
42	89.95	34.10	172.10	72.13	82.07	66.65	82.91	.7254	16.73	.377	35.23
43	118.85	32.40	227.40	101.92	108.48	94.13	109.58	.7262	15.80	.378	35.13
44	28.48	28.00	54.50	13.85	12.59	6.25	12.72	.7265	12.57	.580	22.89
45	39.04	27.20	74.70	24.83	17.07	11.03	17.24	.7262	14.90	.467	28.40
46	50.96	26.00	97.50	37.37	22.33	16.60	22.56	.7262	16.51	.423	31.36
47	73.17	24.00	140.00	60.63	32.02	26.86	32.35	.7262	16.64	.413	32.16
48	85.35	22.30	163.30	73.70	37.44	32.71	37.82	.7262	17.14	.420	31.61
49	106.10	20.00	203.00	95.65	46.78	42.64	47.25	.7262	16.94	.410	32.34
50	29.01	30.50	55.50	13.07	16.97	7.82	17.14	.7258	14.41	.478	27.76
51	40.66	29.30	77.80	25.35	23.78	15.06	24.02	.7251	16.33	.421	31.53
52	56.50	28.10	108.10	41.81	32.99	24.75	33.33	.7251	16.12	.409	32.48
53	70.25	26.90	134.40	56.19	41.07	33.27	41.49	.7251	16.40	.400	33.21
54	83.83	25.40	160.40	70.56	48.90	41.65	49.40	.7254	16.38	.401	33.12
55	116.29	22.00	222.50	104.79	68.00	61.96	68.69	.7254	16.51	.390	34.00
56	27.34	27.80	52.30	12.81	12.04	5.76	12.16	.7311	12.44	.616	21.53
57	46.52	26.20	89.00	32.82	20.43	14.63	20.64	.7311	15.01	.457	29.02
58	63.92	25.00	122.30	50.85	28.07	22.62	28.36	.7299	15.52	.439	30.25
59	80.12	22.80	153.30	68.21	35.17	30.30	35.53	.7296	15.71	.452	29.56
60	103.64	20.30	198.30	92.03	45.31	41.14	45.77	.7284	16.02	.443	29.94
61	67.16	27.00	128.50	53.05	39.21	31.37	39.61	.7284	15.50	.415	31.99
62	101.87	23.90	194.90	89.37	59.41	52.73	60.01	.7280	15.75	.411	32.31

ENGINE DATA REDUCTION ... D. HARRINGTON



TABLE X  
 REDUCED DATA FOR ON-ENGINE CARBURETOR TESTS AT  
 CONSTANT THROTTLE ANGLE AND VARIABLE ENGINE SPEED

DATA REDUCTION PROGRAM FOR ENGINE TESTS

\*\*\*\* PROGRAM RESULTS FOR THIS TEST \*\*\*\*

THE TEST NUMBER IS 46

THE TEST DATE IS 101667

THE AMBIENT AIR DENSITY IS .0709 LBM/FT<sup>3</sup>

THE SAE CORRECTION FACTOR IS 1.00999

THE ENGINE DISPLACEMENT IN CUBIC INCHES IS 288.52 IN<sup>3</sup>

ENGINE: FORD 289 V-8

CARBURETOR: C6 AFB

CLOSED THROTTLE : 10.0°

FUEL : STANDARD REGULAR  
 GASOLINE @ 77°F

RUN	RPM	SCALE	PMAN	BHP	FHP	RATEF	RATEA	F/A	BSPC	EFFVOL	THRRMB	THROTTLE ANGLE
1	800.3	146.0	25.9	22.25	3.03	11.427	189.07	.0604	.5136	66.55	25.84	26.0
2	1028.0	134.0	24.3	26.23	3.95	13.418	225.82	.0594	.5116	61.88	25.94	26.0
3	1199.9	128.0	22.8	29.24	4.98	14.947	249.95	.0598	.5111	58.68	25.96	26.0
4	1601.6	117.5	19.8	35.83	7.78	18.013	291.96	.0617	.5027	51.35	26.40	26.0
5	1863.7	98.5	17.1	34.95	11.57	19.375	303.53	.0638	.5543	45.88	23.94	26.0
6	2504.6	68.5	14.3	32.67	17.80	20.122	315.84	.0637	.6160	35.52	17.13	26.0
7	3001.6	51.0	12.6	29.15	24.06	22.573	327.09	.0690	.7745	30.70	21.54	26.0
8	1602.1	184.0	27.0	56.13	6.77	25.173	409.45	.0615	.6485	71.99	29.59	26.0
9	1608.5	164.0	25.5	50.23	7.01	23.060	387.54	.0595	.4551	67.87	28.90	31.0
10	1557.7	142.0	22.9	43.20	7.30	20.544	342.58	.0600	.4756	60.37	27.90	31.0
11	1585.2	139.5	21.2	42.21	7.47	20.636	319.28	.0646	.4889	56.59	27.14	28.0
12	1603.3	114.0	19.4	34.80	7.69	17.340	283.48	.0612	.4983	49.81	26.63	25.5
13	1604.8	67.0	14.0	20.47	8.40	12.469	199.42	.0625	.6091	35.01	21.79	20.6
14	1601.7	63.5	13.9	19.37	8.39	11.920	196.62	.0606	.6156	34.58	21.56	20.6
15	1595.5	40.0	11.0	12.18	8.80	9.767	150.10	.0651	.8017	26.44	16.55	18.1
16	1598.5	18.0	8.6	5.48	9.13	9.111	107.57	.0847	1.6631	18.96	7.98	15.6
17	1558.9	3.0	7.2	.91	9.29	7.737	81.73	.0947	8.4712	14.40	1.57	13.6
18	1594.1	2.0	6.0	.61	9.71	7.264	57.73	.1258	11.9655	10.20	1.11	11.6
19	1594.5	1.2	5.2	.36	10.08	6.355	41.91	.1516	17.4428	7.40	.76	10.0

RUN	IMEP	TORQF	TORGI	BNEP	IMP	BHPC	IHPC	SG	A/F	ISFC	THERMI
1	86.71	19.90	165.90	76.31	25.28	22.50	25.53	.7265	16.55	.452	29.36
2	80.59	20.20	154.20	70.04	30.18	26.53	30.48	.7265	16.83	.445	29.85
3	78.29	21.80	149.80	66.90	34.22	29.59	34.57	.7262	16.72	.437	30.38
4	74.74	25.50	143.00	61.41	43.61	36.27	44.04	.7262	16.21	.413	32.12
5	68.52	32.60	131.10	51.48	46.52	35.42	46.99	.7262	15.67	.416	31.86
6	55.40	37.50	106.00	35.80	50.55	33.17	51.05	.7262	15.70	.398	33.34
7	48.66	42.10	93.10	26.66	53.21	28.68	53.74	.7262	14.49	.424	31.28
8	107.77	22.20	206.20	96.17	62.90	56.76	63.53	.7296	16.27	.400	33.16
9	57.69	22.90	186.90	85.72	57.24	50.80	57.81	.7284	16.81	.403	32.94
10	86.76	24.00	166.00	74.22	50.50	43.70	51.00	.7284	16.67	.407	32.62
11	85.82	24.70	164.20	72.91	49.69	42.71	50.18	.7280	15.47	.415	31.95
12	72.75	25.20	139.20	59.58	42.49	35.22	42.92	.7284	16.35	.408	32.52
13	49.39	27.50	94.50	35.02	28.87	20.76	29.16	.7284	15.99	.432	30.73
14	47.56	27.50	91.00	33.19	27.75	19.64	28.03	.7280	16.49	.430	30.89
15	36.01	28.90	68.90	20.91	20.98	12.39	21.19	.7276	16.49	.465	28.51
16	25.09	30.00	48.00	9.41	14.61	5.62	14.76	.7265	11.81	.624	21.28
17	17.51	30.50	33.50	1.57	10.20	1.02	10.30	.7269	10.56	.759	17.49
18	17.77	32.00	34.00	1.05	10.32	.71	10.42	.7269	7.95	.704	18.85
19	17.98	33.20	34.40	.63	10.44	.47	10.55	.7269	6.59	.608	21.81

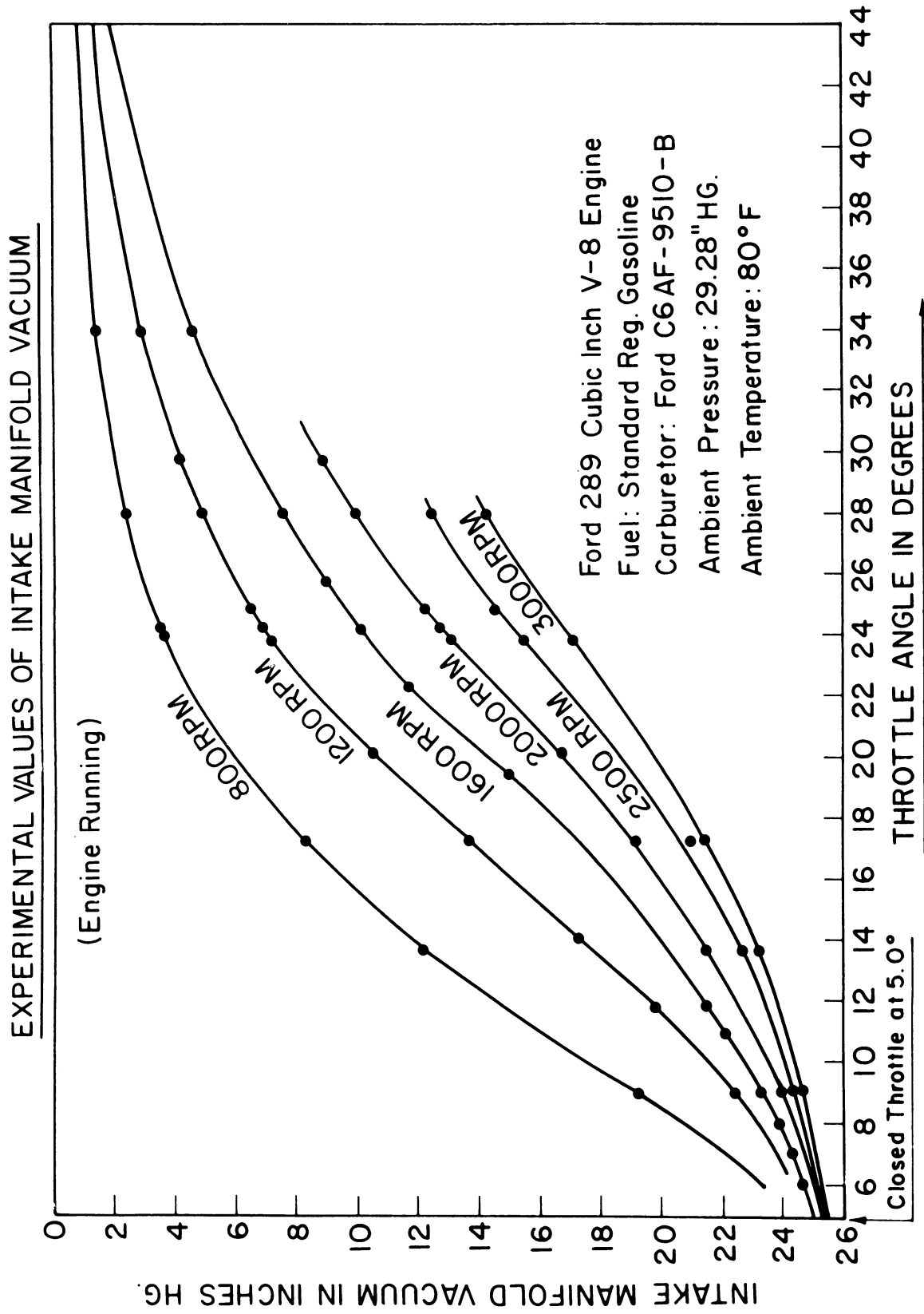


Figure 35. Variations in intake manifold vacuum with throttle angle and engine speed

The boost venturi suction provides the potential for fuel flow within the main system, thus it is an important quantity within the simulation. In order to provide an experimental verification of the predicted metering signal values, the boost and main venturi suction of typical carburetors were measured as a function of the total moist air mass flow rate. The results from one of these tests are presented in Figure 36. Note that the metering signal is slightly higher with no main system fuel flowing.

Another experimentally determined parameter was the wide open throttle pressure loss across typical carburetors. This is the minimum intake manifold vacuum, and the values were determined as a function of the measured air flow rate. The data are shown plotted in Figure 37. Note that the pressure loss increases rapidly as the air flow increases, reaching a pressure loss of 1 inch of mercury at an air flow of about 700 lbm/hour.

Brake specific fuel consumption curves are very important to the road load carburetor analysis and also to the engine data correlation technique. A series of these curves for a typical engine and a modified carburetor is shown in Figure 38. The carburetor modification consisted of a blocked enrichment system which prevented an increase in the fuel-air ratio at low intake manifold vacuums. This is the reason the curves do not slope upward at the high load end. These values were obtained along constant engine speed curves. A comparison of the curve shapes for constant throttle angle and constant engine speed is given in Figure

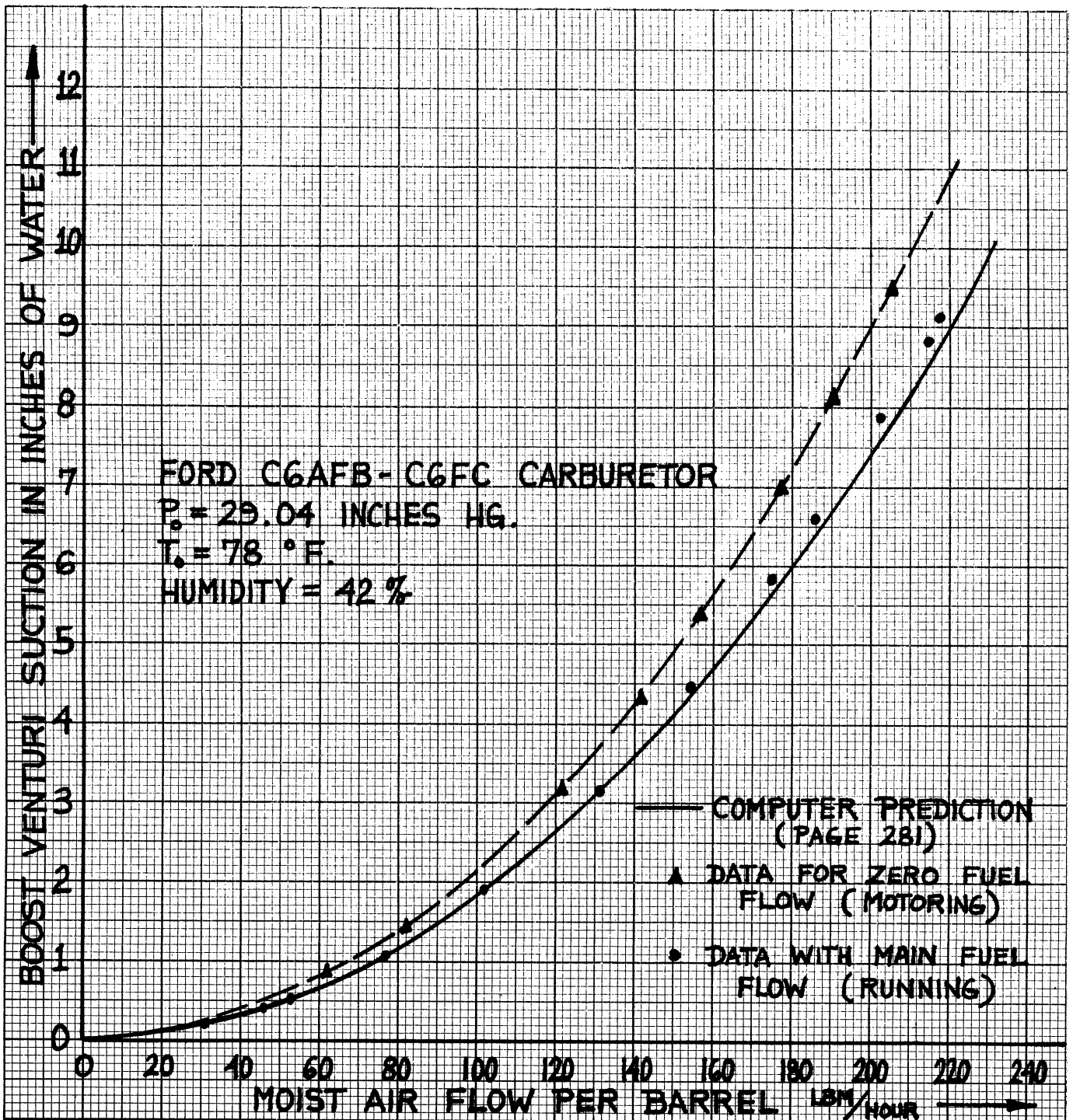


Figure 36. Effect of measured air flow rate on the metering signal

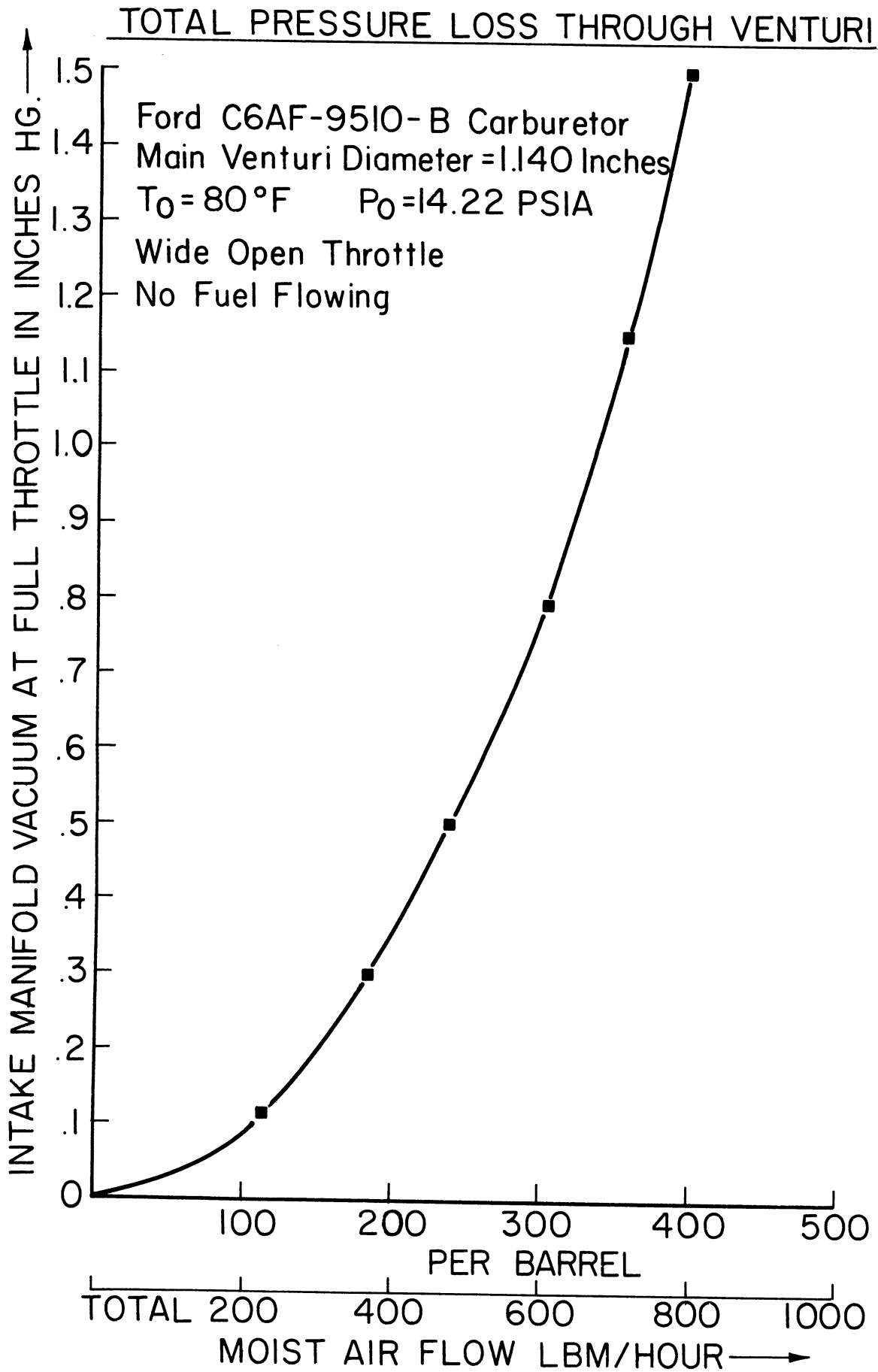


Figure 37

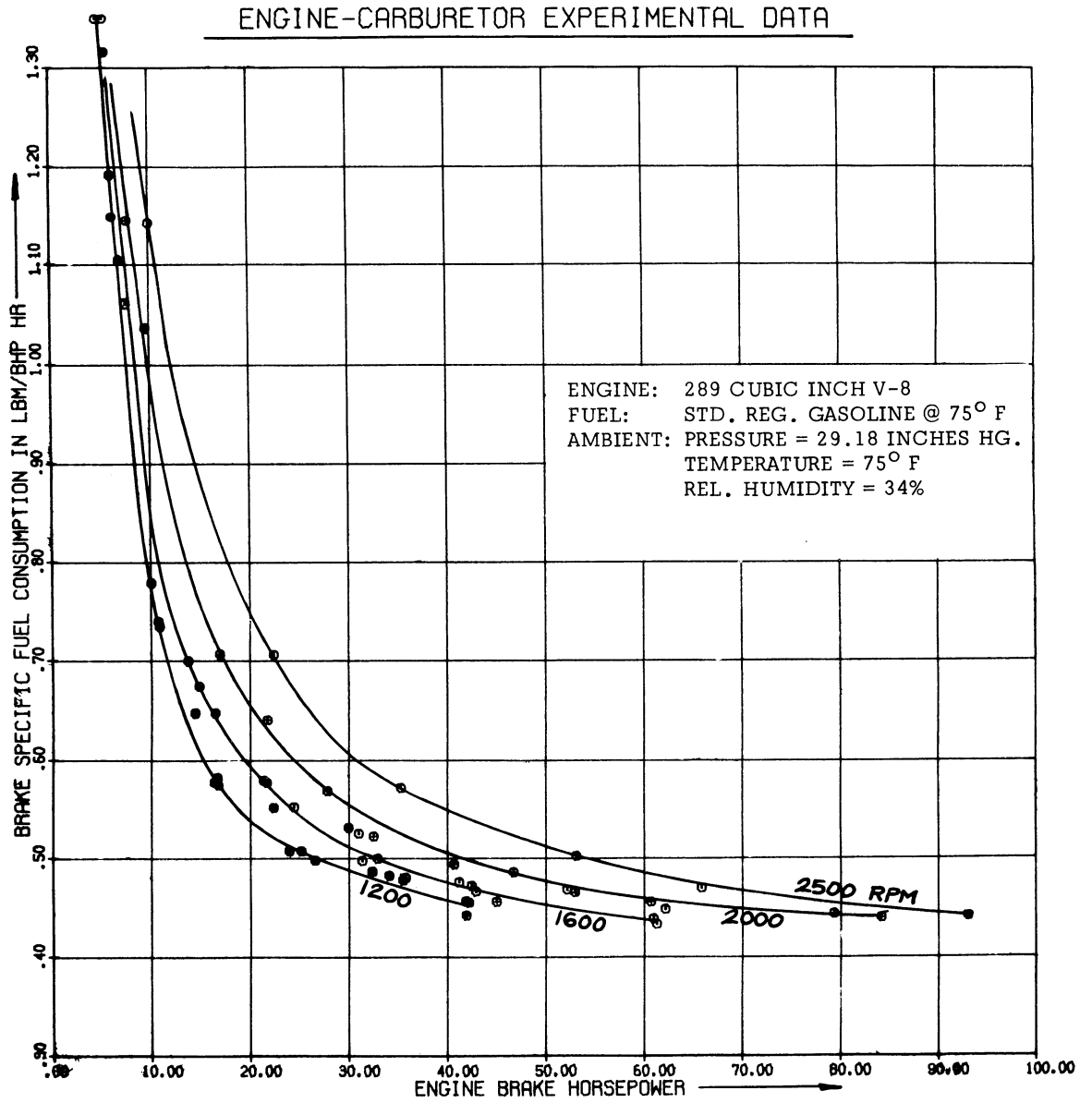


Figure 38. Brake Specific Fuel Consumption Curves For Various Engine Speeds

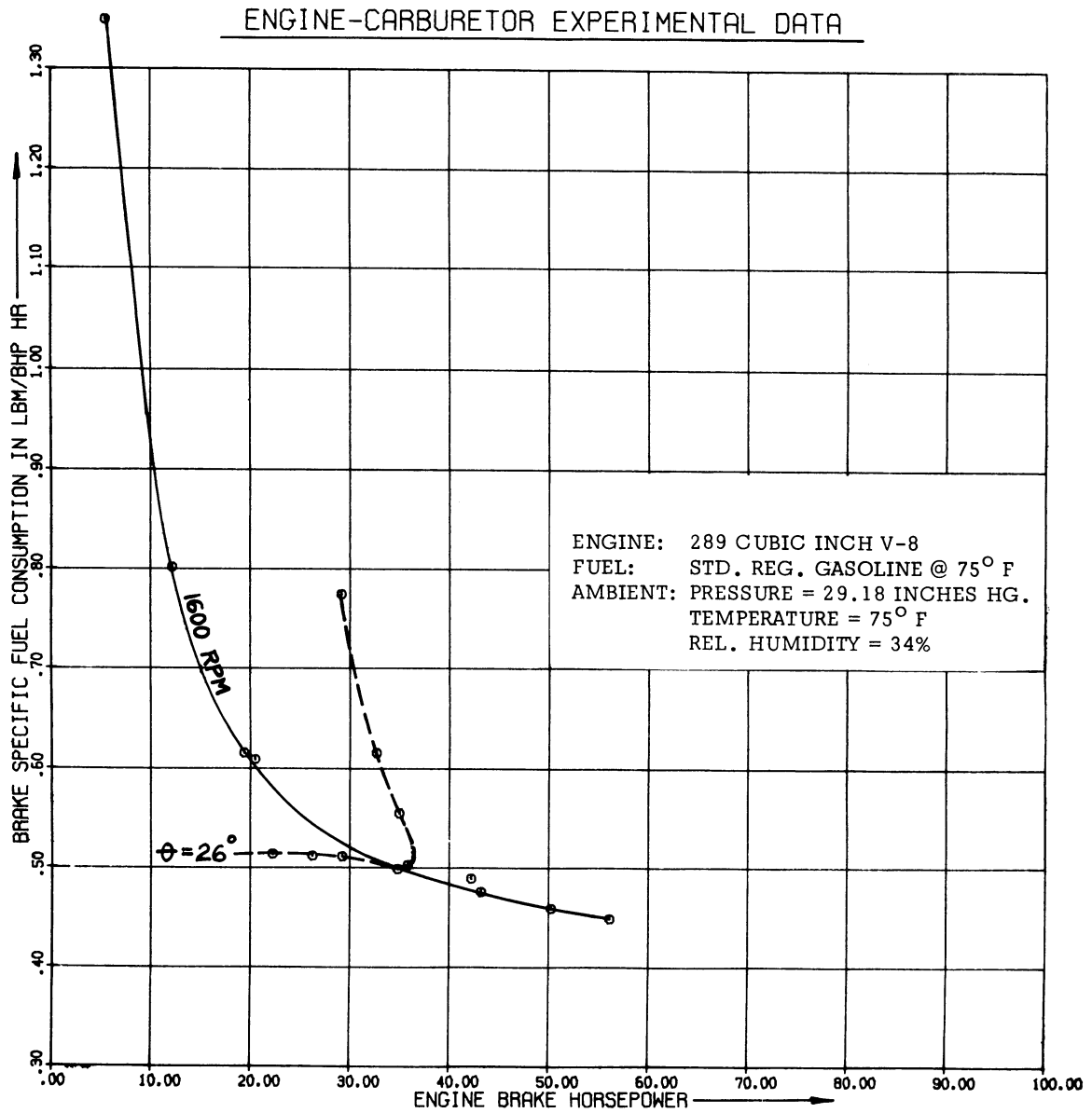


Figure 39. BSFC Variations At Constant Throttle Angle and Constant Engine Speed

39. The intersection of the curve for a given engine speed, and the curve for a given throttle angle will be the brake specific fuel consumption and brake horsepower corresponding to that particular operating point. In the case shown, the operating point of  $26^\circ$  and 1600 RPM would result in a BHP output of 35.0 and a BSFC value of 0.50.

#### E. SPECIAL EXPERIMENTAL PROGRAMS

##### 1. Suction Profiles Within the Boost Venturi

An experimental program was conducted to determine the pressure (actually the suction) variation with position within the boost venturi for typical operating points. The goal was to determine both the radial and axial variations in venturi suction and thus check the validity of the one-dimensional assumption. Some of this data is shown in Figure 40, and the conclusions are as follows:

1. The one-dimension flow assumption is reasonable for the main and boost venturi, except in the region of the boost venturi throat.
2. In order to use a one-dimensional compressible flow analysis to predict suction at the fuel discharge nozzle, the increase in suction due to any sudden expansions or contractions in area must be included.
3. The maximum suction occurs near the inner walls in the vicinity of the fuel discharge nozzle.

These conclusions helped to clear up some of the difficulties in the compressible mixture flow subroutine as it was originally written. Initially the subroutine evaluated the one-dimensional compressible mixture flow relationships and analytically predicted boost venturi



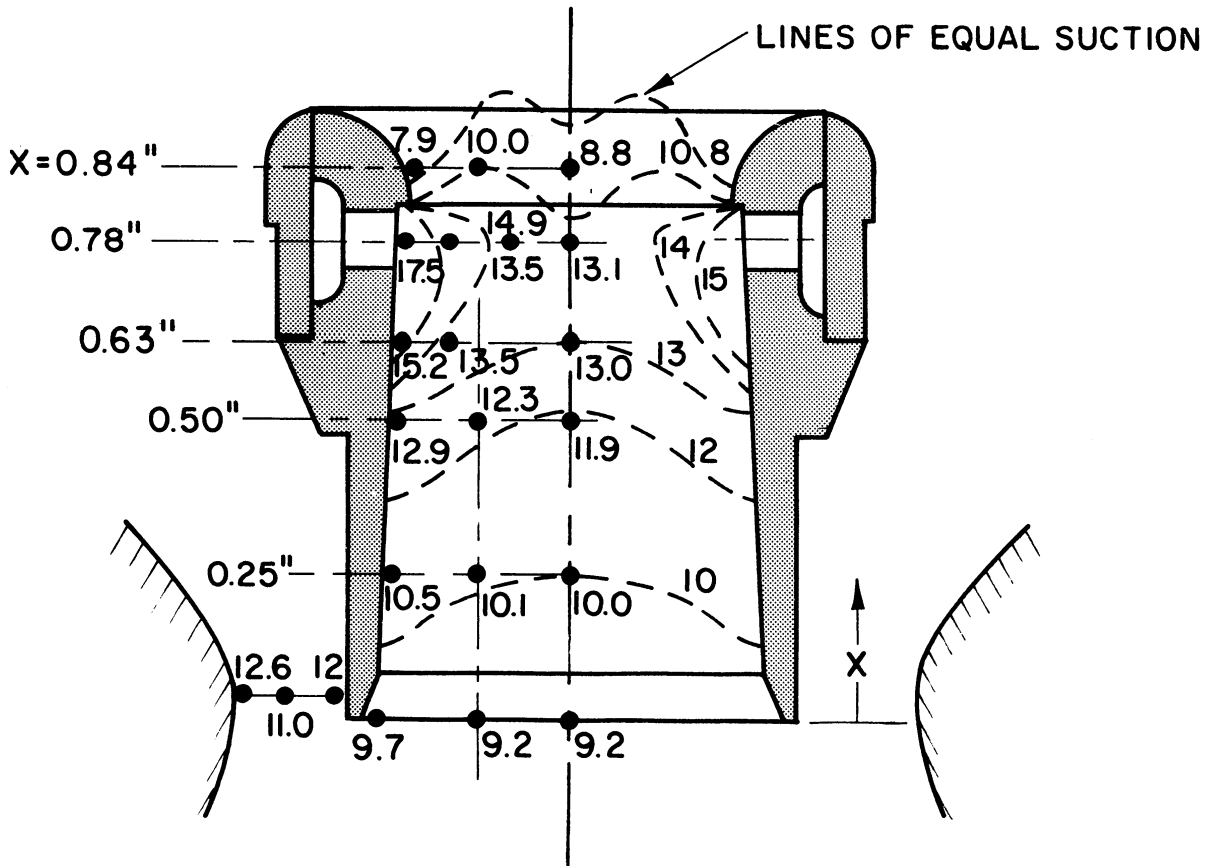


Figure 40. Suction distribution in inches of water within a typical boost venturi

suctions that were significantly lower than the measured values. For example, 14.0 instead of 17.5 inches of water for the conditions in Figure 40. The results from the study of the suction variation within the boost venturi pointed out the fact that subroutine SIGNAL was predicting an average suction at each axial position, when in fact the suction acting on the fuel discharge nozzle was significantly higher than the average in boost venturi designs having sudden expansions or contractions, due to the sudden area change in that region. By including an additional pressure loss due to this sudden area change (where applicable), the predicted boost suction values agreed very well with the experimental data.

## 2. High Speed Movies of Fuel Discharge

A standard Ford C6AF-9510-B 2-barrel carburetor was modified to permit visual observation of the fuel discharging into the air stream within the boost venturi. This was accomplished by making a vertical cut through the carburetor and exposing a cross section of the venturi (very similar to the cross section shown in Figure 4 on Page 29.) The section exposed by cutting was covered with a flat Lucite plate, thus giving an uninterrupted air flow path. High speed movies (3000 frames per second) were taken of the fuel discharge under many operating conditions, from the point at which the main fuel system begins to function, to conditions resulting in very high main fuel flow rates.

A view of the experimental equipment associated with this

particular project is given in Figure 41. This particular view shows the camera mounted in the vertical position to observe the fuel discharge in a Rochester Quadrajet carburetor. The camera was mounted in the horizontal position to obtain the movies of the Ford carburetor.

A single frame was taken from each of four movies and enlarged. (The enlarging process brought out some graininess of the film that is not noticeable in the movies.) The enlargements are presented in Figures 42 and 43, in the order of increasing fuel flow. The conditions corresponding to each photograph are:

<u>PHOTOGRAPH</u>	<u>FILM SPEED</u>	<u>ENGINE SPEED</u>	<u>INTAKE MANIFOLD VACUUM</u>	<u>FUEL FLOW PER BARREL</u>
	frames/sec	RPM	inches Hg	lbm/hour
42a	3000	1100	8.1	3.32
42b	3000	700	0.4	3.75
43a	3000	1500	7.8	4.90
43b	3000	3000	5.0	9.90

Note in photograph 42a that there are fuel droplets of various sizes leaving the boost venturi. Note also that the droplets are fairly large as compared to those in photograph 43b, where they form more of a mist, which indicates a greater degree of atomization. The throttle plate is apparent in photographs 42b and 43b, near the bottom of each picture. There is a distinct division of the atomized fuel stream at the throttle plate in photograph 43b, which is shown even more clearly in the movies.

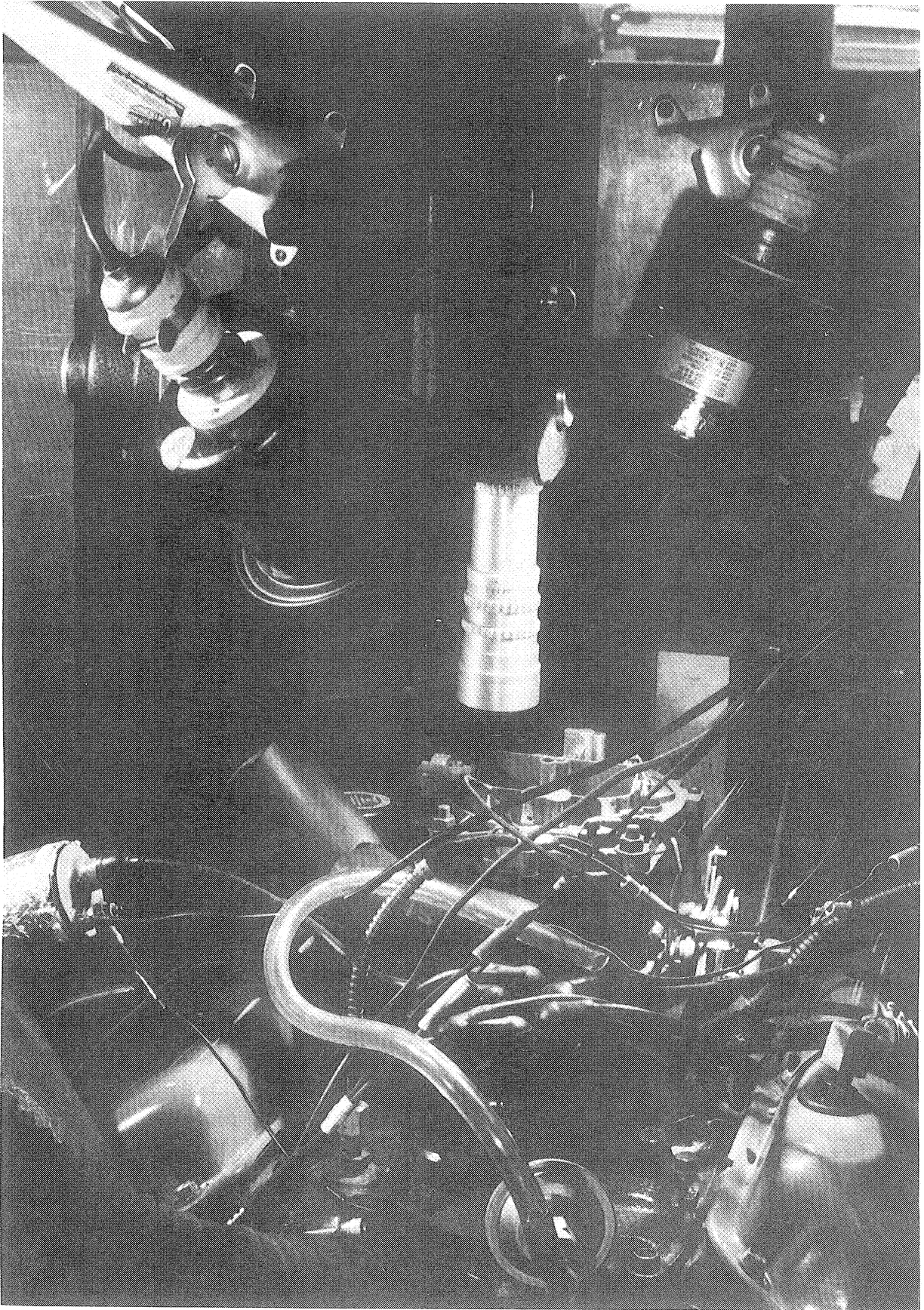
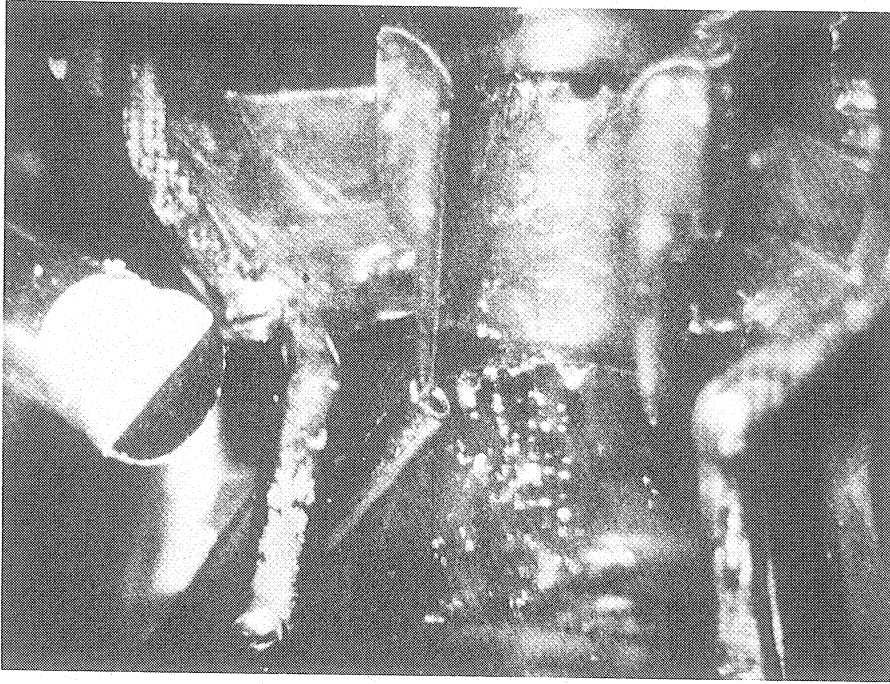
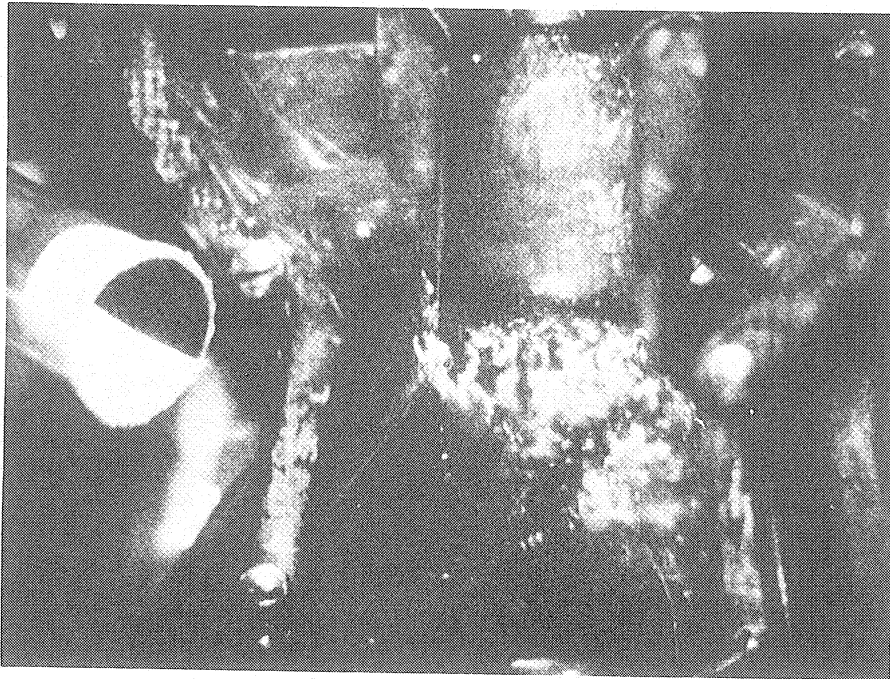


Figure 41. Equipment utilized to obtain high speed movies of fuel discharge

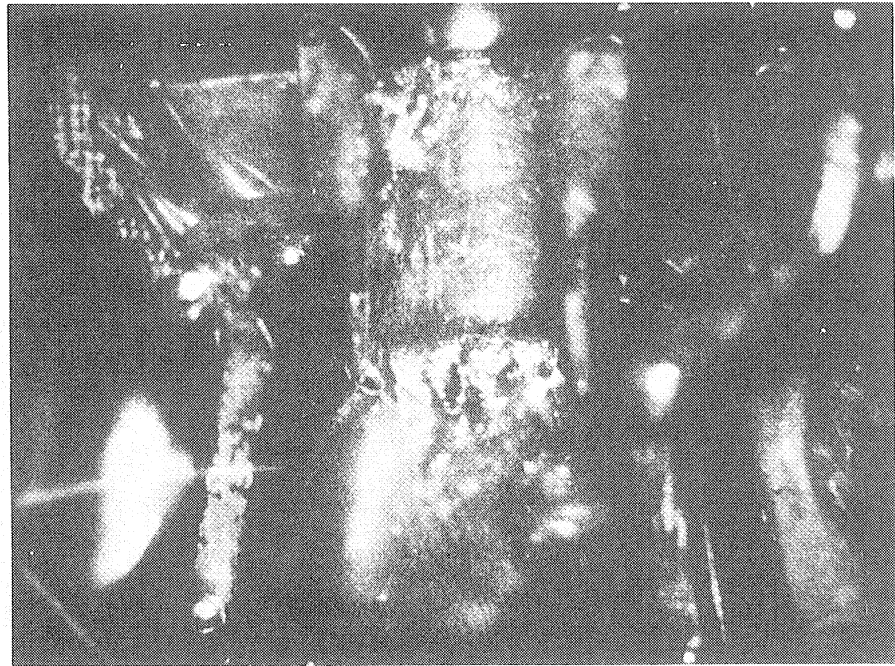


PHOTOGRAPH A

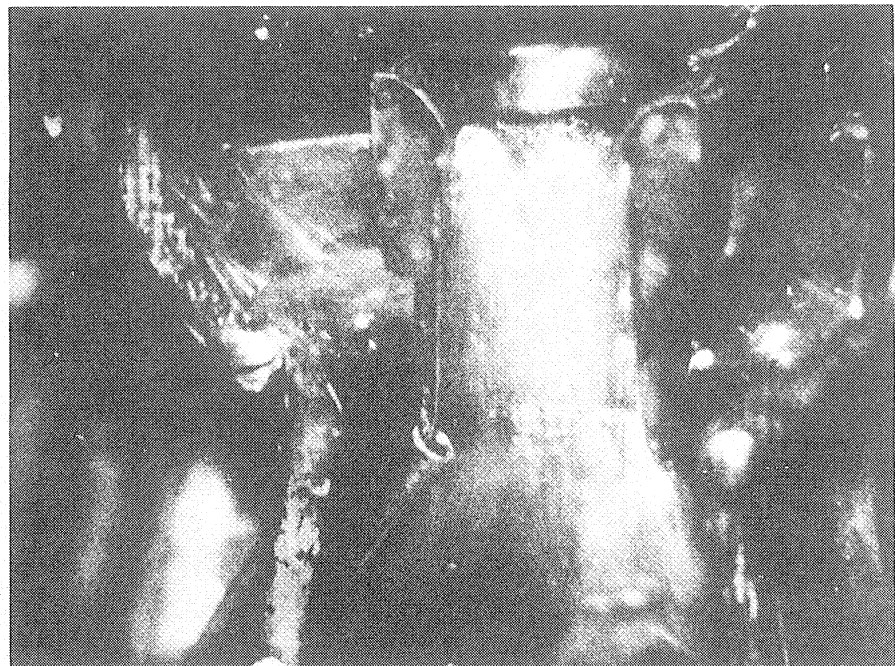


PHOTOGRAPH B

Figure 42. High speed photographs of fuel discharge within the boost venturi - Low fuel flow



PHOTOGRAPH A



PHOTOGRAPH B

Figure 43. High speed photographs of fuel discharge within the boost venturi - High fuel flow

### 3. Transient and Pulsating Flow Study

In the initial phases of this carburetor simulation project, an experimental study of the pressure variations in a carburetor under transient and pulsating conditions was conducted. This was done mainly to gain an understanding of the effects of rapid transients and to set bounds, if possible, on the steady flow region of operation.

A Ford C4-AFB 2-barrel carburetor was completely instrumented with Statham strain gage pressure transducers. These transducers, which varied in range from  $\pm 1$  psi to  $\pm 15$  psi, were calibrated and installed in the boost venturi, the fuel channel below the main metering orifice, and below the throttle plate (in communication with the intake manifold vacuum). A wirewound potentiometer was connected to the throttle shaft, and was calibrated in terms of millivolts per degree of throttle angle. The carburetor was then installed on a Ford 289 cubic inch engine, and the potentiometer and strain gage pressure transducers were connected to the associated amplifying and recording equipment, which is shown in Figure 44.

The transient portion of this test series consisted of sudden throttle openings and closings. This was accomplished by allowing conditions within the carburetor to stabilize at some engine speed and throttle angle and then rapidly opening or closing the throttle as far as possible. Just before the transient, the Visicorder chart was started and the pressure-time traces were recorded. Figures 45 and 46 show the pressure variations for the three pressure transducers, along with

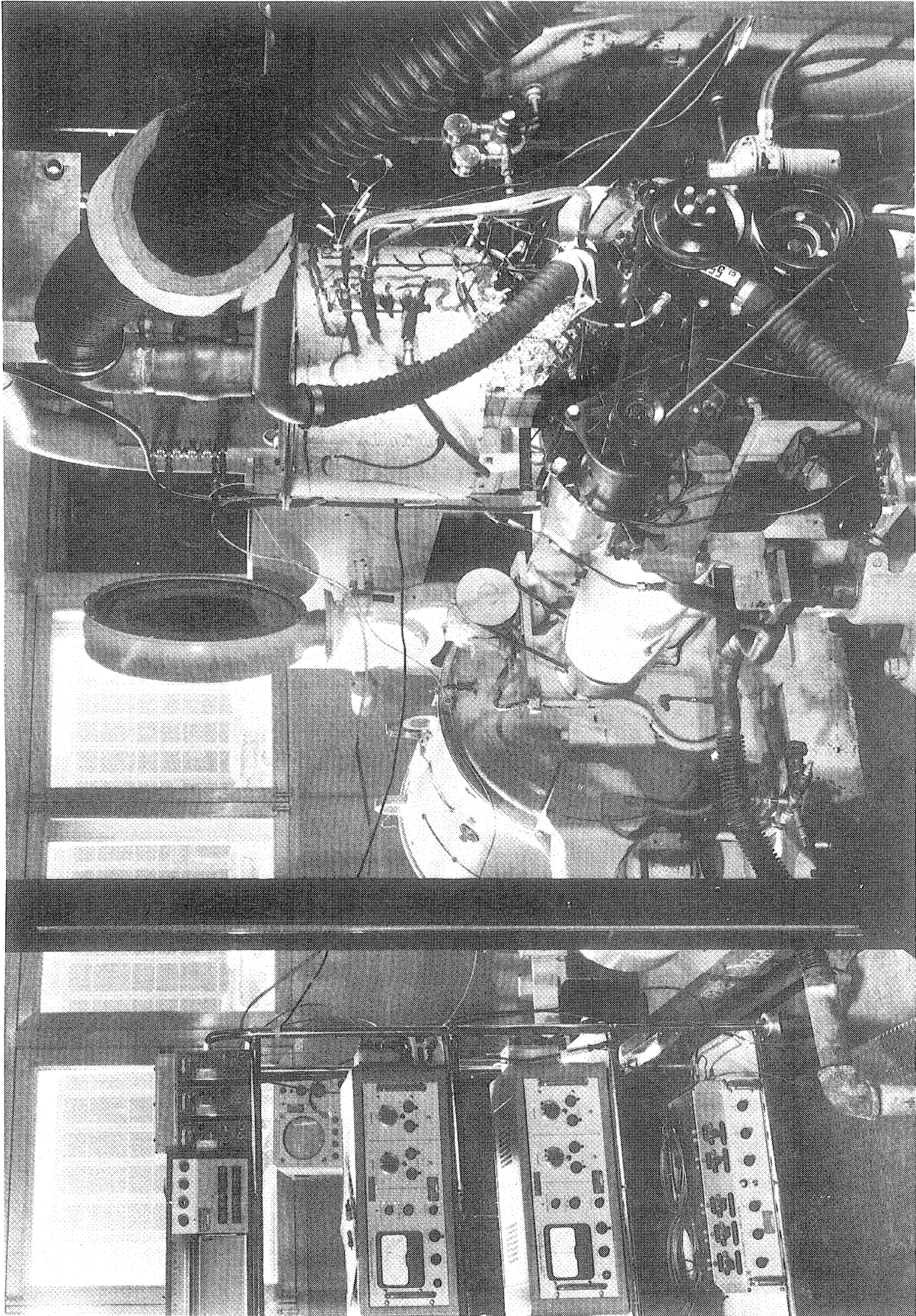


Figure 44. Equipment utilized in obtaining pressure - time traces under transient and pulsating conditions



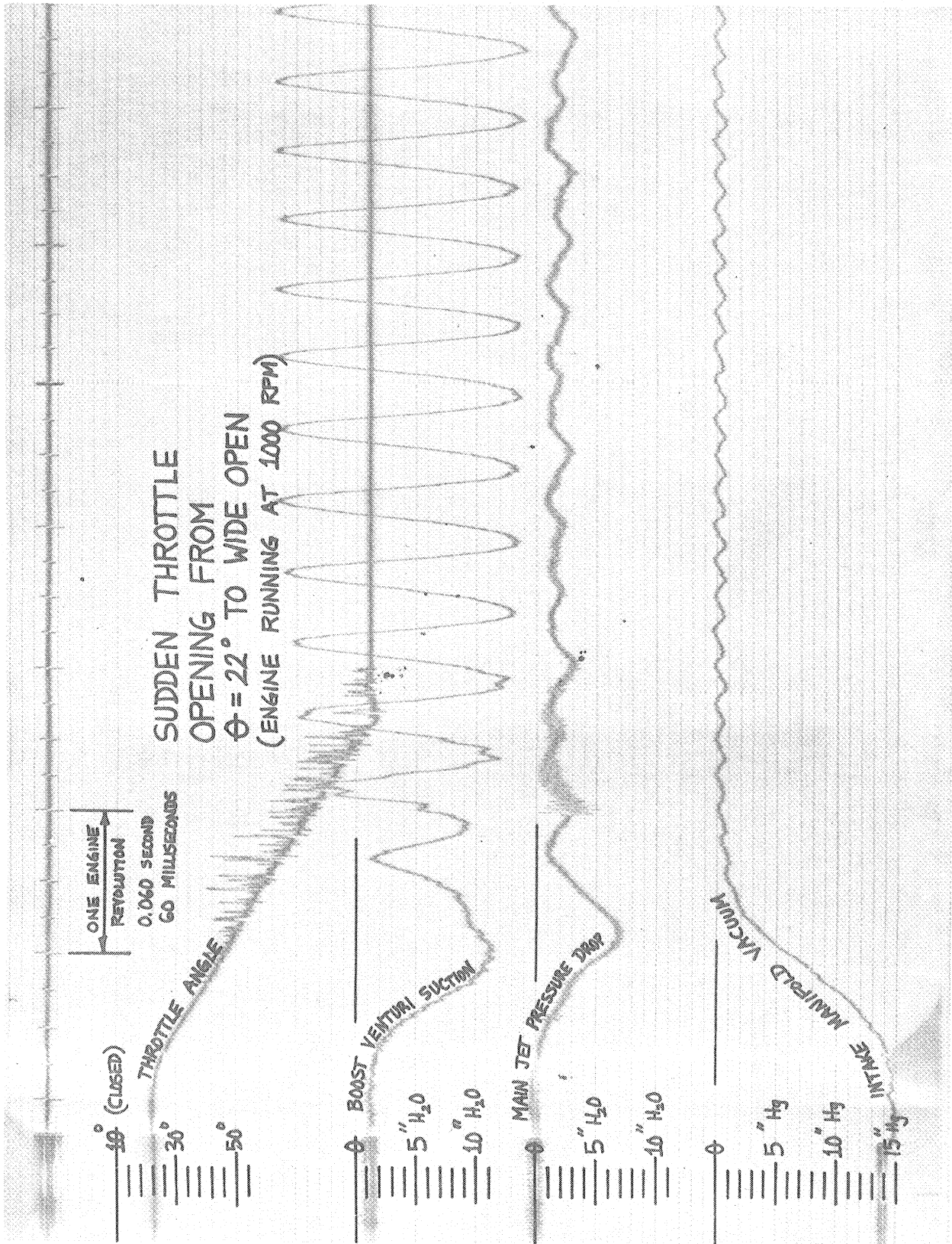


Figure 45. Pressure Transients Within A Carburetor During A Sudden Throttle Opening

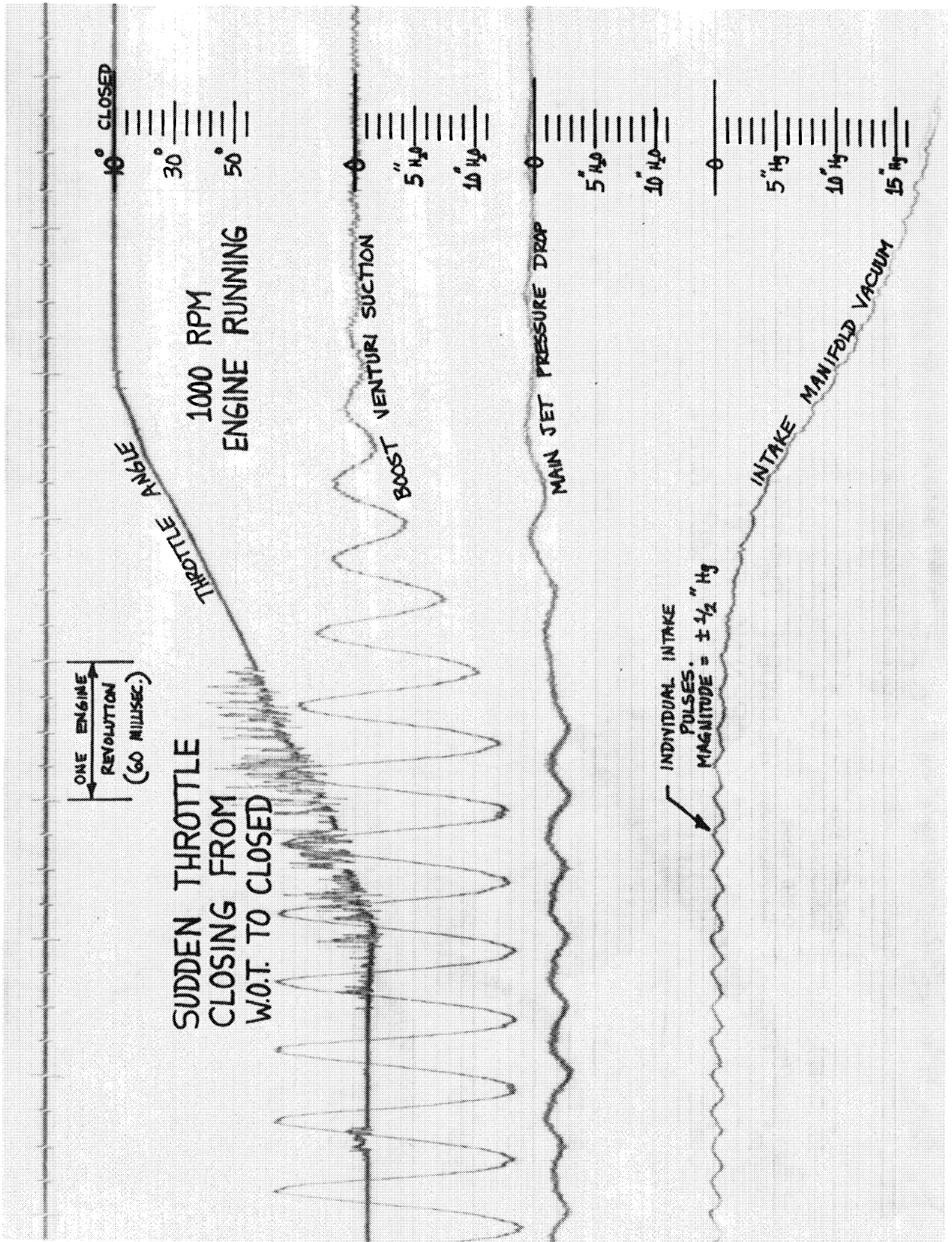


Figure 46. Pressure Transients Within A Carburetor During A

the throttle angle and crankshaft revolution indicators. Note the rapid increase in boost venturi suction in the case of the sudden throttle opening. This results from the large increase in the air flow rate and the corresponding increase in air velocity within the boost venturi. Also note that the pressure fluctuations decayed rather rapidly and within a few engine revolutions had stabilized at the periodic values associated with the new throttle angle.

Another type of test that was performed using this equipment was the pulsating flow case in which the engine speed and throttle angle were fixed. This case is of more importance to the carburetor simulation since it indicates the pulsation amplitude for various pseudo-steady operating points.

Figures 47 and 48 show typical visicorder traces from this test series. The data were obtained for various specified engine speeds and throttle angles by allowing conditions to stabilize, running the visicorder, and then changing the throttle angle by  $\Delta\theta^\circ$  and again letting the conditions stabilize. This resulted in mean and alternating pressures for each operating point. Note that the alternating (pulsating) component of the boost venturi suction is not large compared to the mean value except for large throttle angles.

On the basis of these tests, an empirical pulsation factor was developed. This factor is related to the amplitude and frequency of the intake pulses, as well as the damping effect of the throttle plate. These wave parameters can be related to the physical variables of the

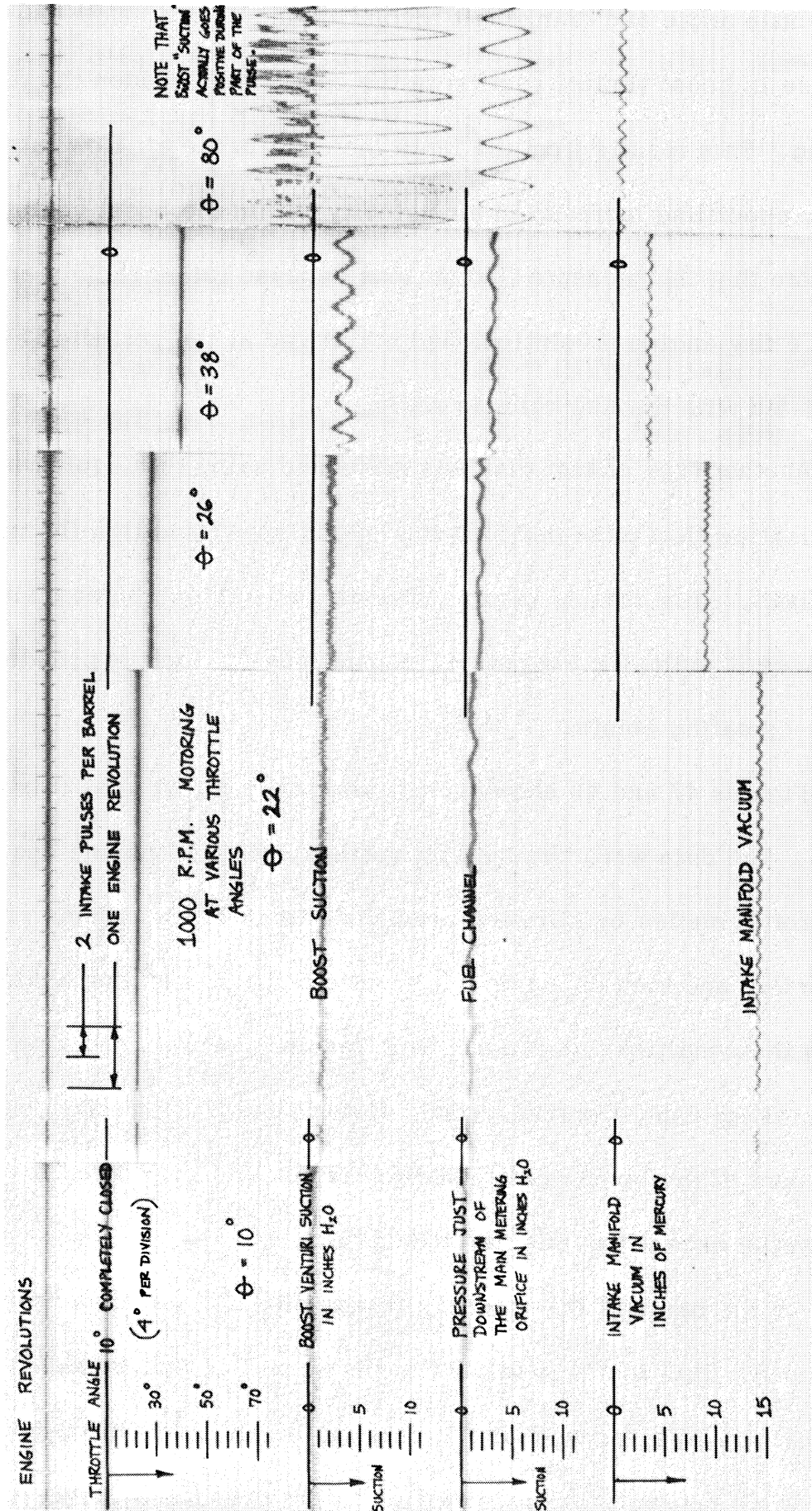


Figure 47. Mean and Alternating Components of The Metering Signal At Various Operating Points

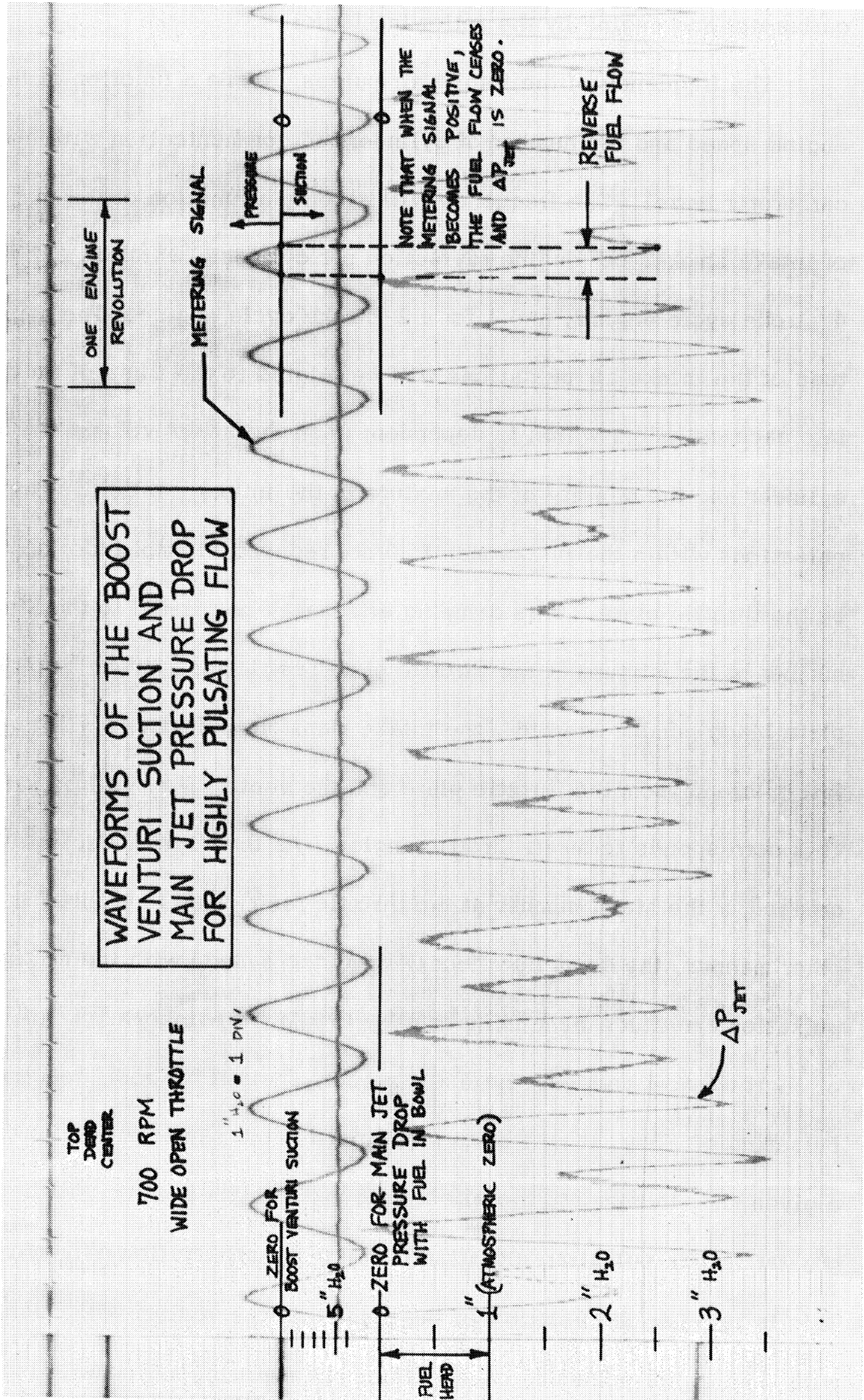


Figure 48. Waveforms For The Boost Venturi Suction And Main Metering Orifice Pressure Drop

carburetor and engine by the following logic:

The frequency of the intake air pulses will be a function of the engine speed and the number of cylinders in communication with each carburetor barrel. The frequency will also be a function of the number of intake strokes per engine revolution per cylinder, which is  $1/2$  for a 4-stroke cycle engine, and 1 for a 2-stroke cycle engine. The amplitude of the intake air pulsations will be related to the mass of air drawn into each cylinder, which is dependent upon the swept volume of the cylinder and the density of the mixture in the intake manifold. The pulsations within the intake manifold are reduced in amplitude (damped) by the throttle plate. This damping effect may be related to the Mach number of the mixture at the throttle plate restriction. If the throttle plate Mach number is unity, the intake manifold pulsations will not be felt upstream from the throttle plate and the venturi flow will be steady. This corresponds to small throttle angles. As the throttle angle is increased, or the Mach number at the throttle restriction is reduced in any other manner, the damping effect will be decreased, with the maximum pulsation amplitude occurring at very low Mach numbers.

If we now consider the boost venturi suction for both steady and pulsating air flow, it will be evident that for the same net air flow over a given time increment, the effective boost venturi suction will be greater for the pulsating situation than for the steady flow situation. This is because the velocity of the air within the venturi will fluctuate with time in the pulsating case. Since the metering signal will increase

as a function of the instantaneous air velocity squared (approximately), it is easily shown that the effective metering signal, averaged over a pulse cycle, will be greater than that for steady air flow.

Let us denote the ratio of the effective metering signal for a pulse cycle, to the metering signal for steady air flow at the same average mass flow rate, as  $1 + \Psi$ .

or:

$$1 + \Psi = \frac{\text{BVSUCW (pulsating)}}{\text{BVSUCW (steady flow)}} \quad \text{EQN 6.3}$$

The physical meaning of the pulsation factor is illustrated by the two sketches in Figure 49. Note that the effective metering signal becomes greater than that for steady flow at the same air mass flow rate. This difference is a maximum at the wide open throttle point for each engine speed. At the air flow rate indicated by the vertical line in Figure 49, the maximum value of  $\Psi$  would be given by the difference in metering signal between points P and S, divided by the metering signal at S.

The empirical equation developed for the pulsation factor,  $\Psi$ , in terms of known variables within the simulation is:

$$\Psi = (\text{constant}) \frac{(1 - M)(P_{\text{man}}) N_{\text{cyc}}}{N N_{\text{cb}}} \quad \text{EQN 6.4}$$

where  $N_{\text{cyc}}$  is either 2 or 4 for a 2 or 4 stroke cycle.

The constant must be evaluated for each carburetor geometry and engine, but typical values obtained in this project gave a correlation constant of about 25.

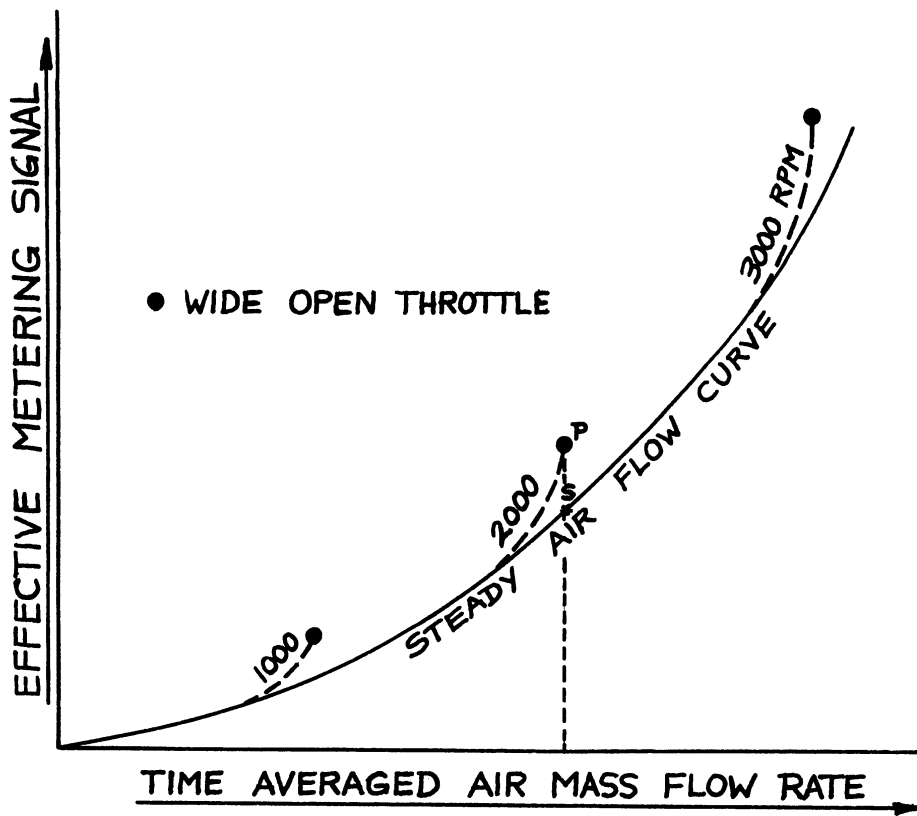
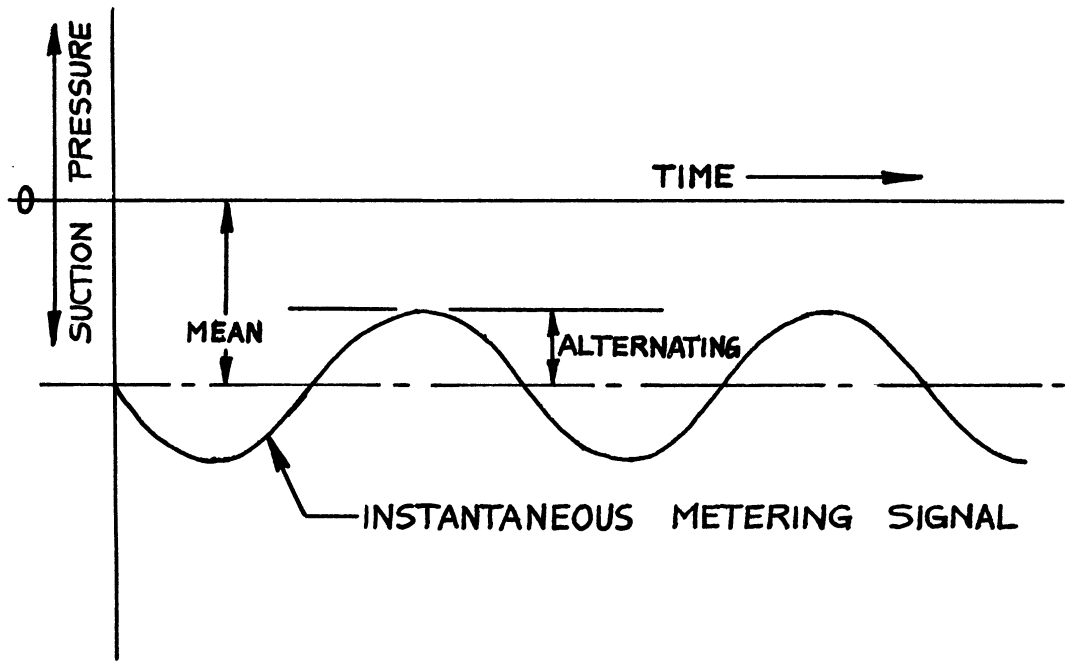


Figure 49. Effective metering signal for pulsating and steady flow conditions



It should be emphasized here that this only considers the effective metering signal, and not the greater complexities of pulsating 2-phase flow in the fuel channel, which results from the periodic metering signal. The determination of the fuel flow situation under these conditions would require a knowledge of orifice discharge coefficient variations with fuel flow pulsation amplitude and frequency, which would obviously require an extensive testing and correlation project.

## CHAPTER VII

### LUCITE FLOW MODEL TESTS

#### A. REASONS FOR FUEL CHANNEL MODEL TESTS

The bulk of the experimental work conducted during this project was directly related to carburetor fuel channel flow tests. These tests were necessary for three basic reasons:

1. To observe the overall operation of typical fuel channel configurations under many flow conditions, and from this to formulate a comprehensive computer model.
2. To accurately determine the effects of numerous important operating variables including fuel type, fuel temperature, and air bleed orifice diameters.
3. To obtain fundamental pressure and flow rate data for use in checking the carburetor simulation predictions.

All fundamental fuel channel tests were conducted using a transparent flow model in conjunction with a test stand, rather than with an actual carburetor mounted on an engine. There are numerous arguments that can be presented in favor of this, but they will be more meaningful if a description of the fuel channel flow model is first given.

#### B. LUCITE FUEL CHANNEL MODEL

The fuel channel flow model, as illustrated in Figure 50, represents an actual, complete carburetor fuel channel in nearly every respect. The basic geometry corresponds precisely to that of one-half of the Ford Cx - AF 2-barrel carburetor series, where the x designates the model year. This series was selected on the basis that it represented a typical fuel channel configuration and because a large amount

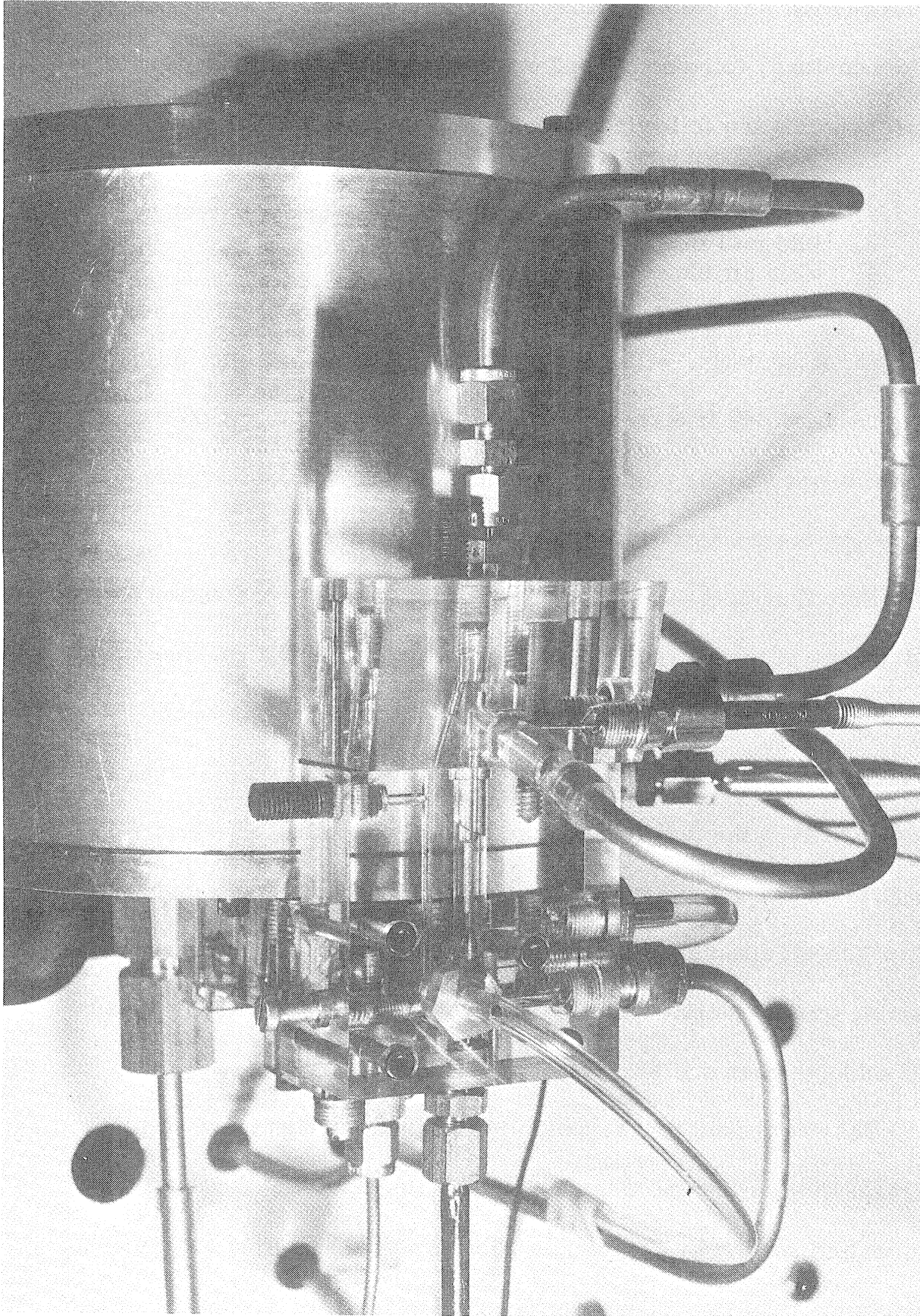


Figure 50. Lucite Flow Model Of Complete Carburetor Fuel Channel

of information was readily available for this type of carburetor, including dimensions, tolerances, and performance specifications. The flow model contains the following systems, all in Lucite:

1. main fuel flow system
2. enrichment fuel flow system (with enrichment valve)
3. idle fuel flow system (with idle needle)
4. main air bleed flow system
5. idle air bleed flow system

These systems, with the exception of the idle system, are shown in Figure 51, which is a cross-section of the actual lucite flow model. The circles at various points in the channel represent static pressure taps which are connected to a large manometer bank.

Note that the Lucite flow model permits visual observation and photography of the fuel and air bleed flow pattern in the passages. It also provides complete channel pressure measurements by means of the six pressure taps at strategic points along the fuel channel. Thermocouples monitor the fuel temperature from bowl to discharge nozzle. The main metering and air bleed orifice sizes may be easily changed or blocked off completely. This is accomplished by means of main metering orifice adaptors and set screws in which precision air bleed orifices have been drilled.

The enrichment valve, which is merely a vacuum closed valve in a bypass channel around the main metering orifice, may be opened to any desired setting by adjusting a micro-valve controlling the vacuum acting upon it. This vacuum corresponds to the engine intake manifold vacuum at the operating point being run on the flow model. The idle

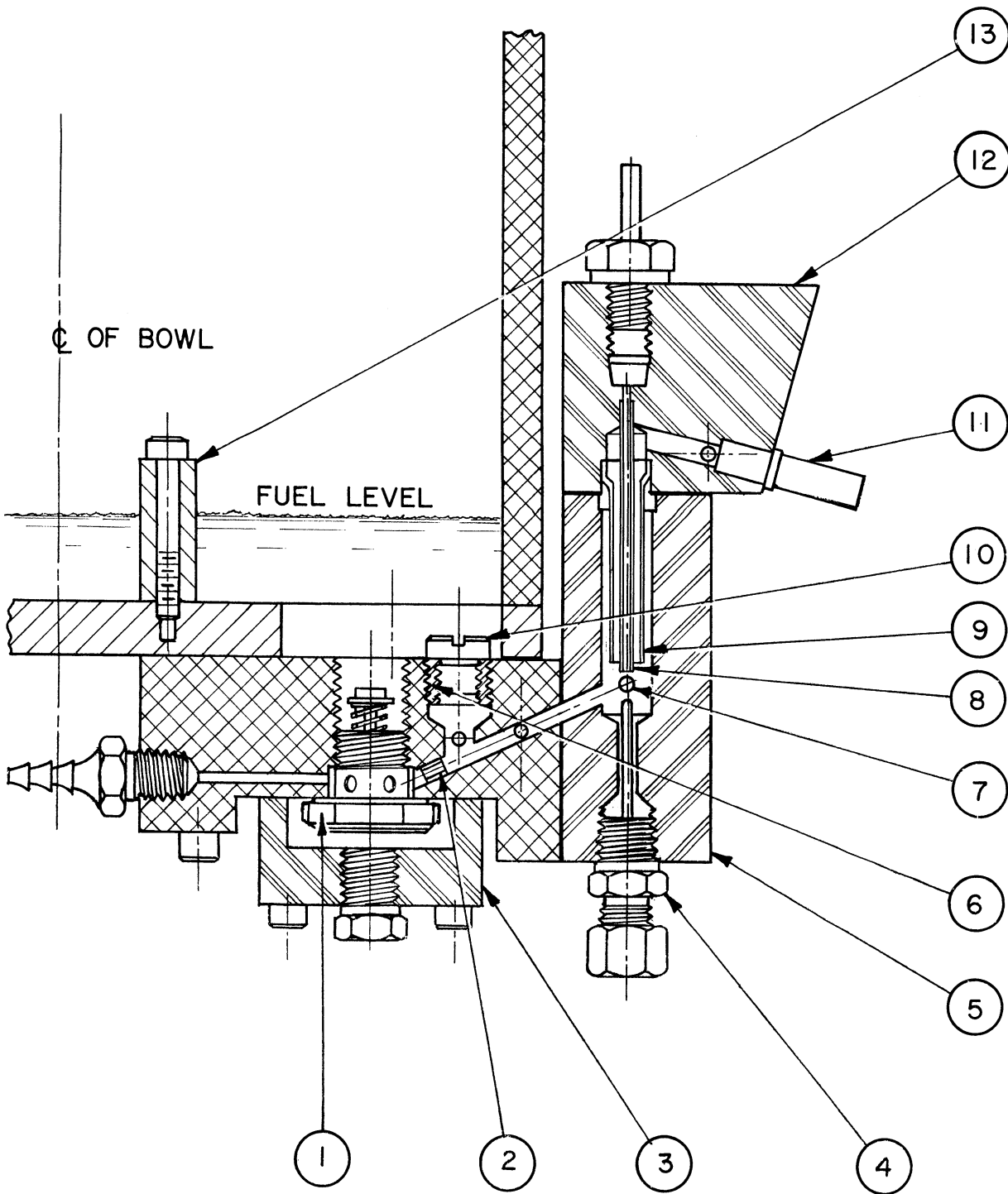


Figure 51. Cross-Section of Lucite flow model (to scale)

- |                                  |                                 |
|----------------------------------|---------------------------------|
| 1. Enrichment (Power) Valve      | 8. Idle Tube (Brass)            |
| 2. Enrichment Metering Orifice   | 9. Emulsion Tube (Lucite)       |
| 3. Enrichment Valve Vacuum Body  | 10. Main Metering Orifice       |
| 4. Lower Well Thermocouple       | 11. Fuel Discharge Tube         |
| 5. Air Bleed Well Body           | 12. Upper Air Bleed Body        |
| 6. Main Metering Orifice Adaptor | 13. Anti-Swirl Baffle (In Bowl) |
| 7. Pressure Tap (Typical)        |                                 |

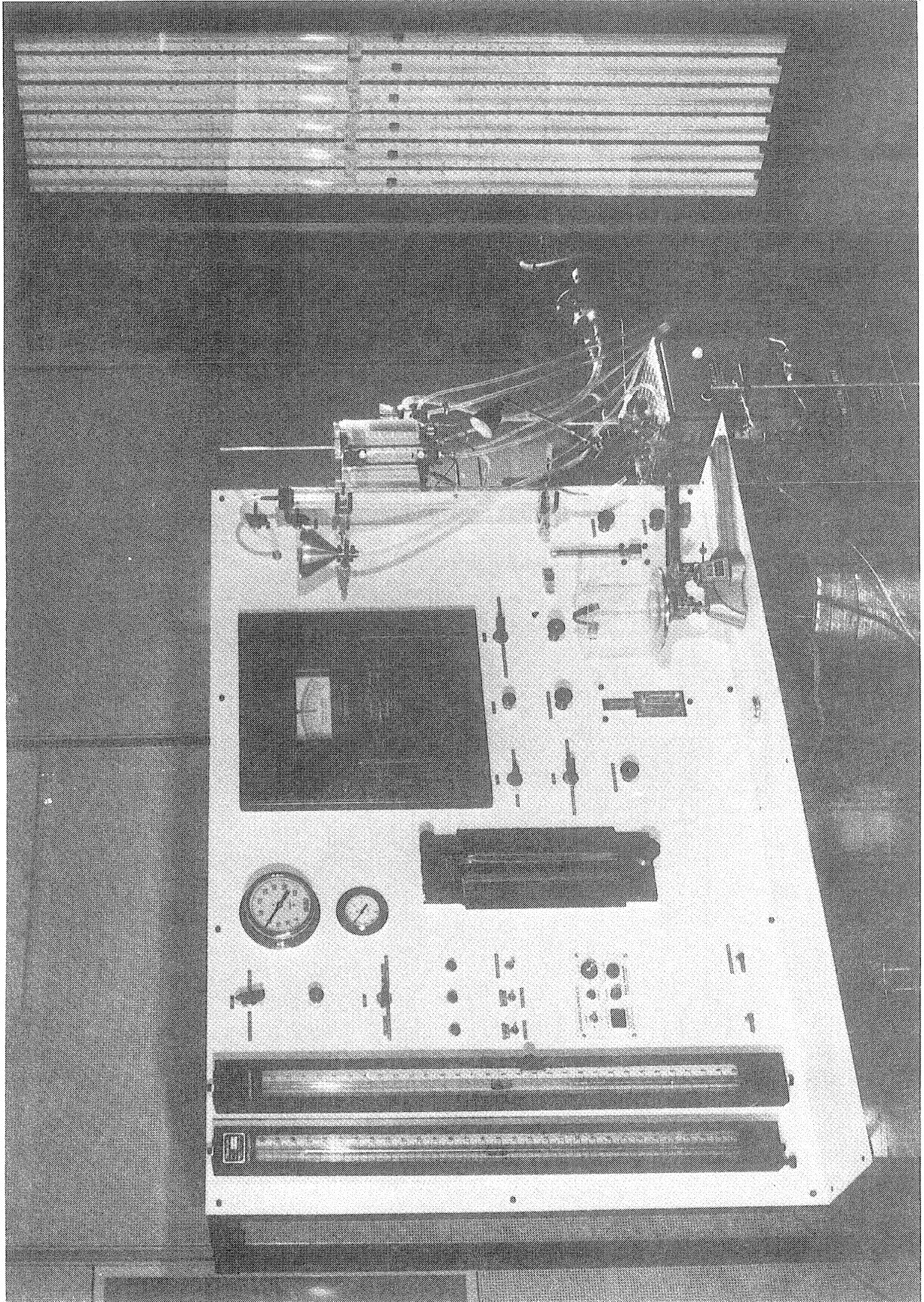


Figure 52. Flow Model Test Stand

system contains an adjustable needle screw, as in the actual carburetor.

### C. FLOW MODEL TEST STAND

A flow model test stand shown in Figure 52 is used in conjunction with the Lucite flow model. Complete fuel flow, air bleed flow, temperature, and pressure measurements can be made with this test stand over a very wide range of fuel flow rates and fuel temperatures. Nearly all operating variables can be accurately controlled and easily changed. This includes:

1. fuel type and temperature
2. fuel bowl head
3. boost venturi suction
4. orifice types and sizes
5. intake manifold vacuum

Figure 53 shows the position of the Lucite flow model in relation to the test stand. The instrument at the bottom of the figure is the constant temperature bath and the glass burette on the left is one of the bubble flowmeters. The functions of both of these items are as follows:

The Neslab constant temperature bath both controls and circulates the fuel in the bowl. The circulation is accomplished by means of build-in force and suction pumps. The force pump is used to deliver the fuel to the constant head fuel bowl, and the suction pump, which is of greater capacity than the force pump, continually removes fuel from the bowl by means of an adjustable stand pipe. This gives a constant fuel head and excellent temperature control, since the fuel in the chamber is being changed continuously. For test runs at fuel

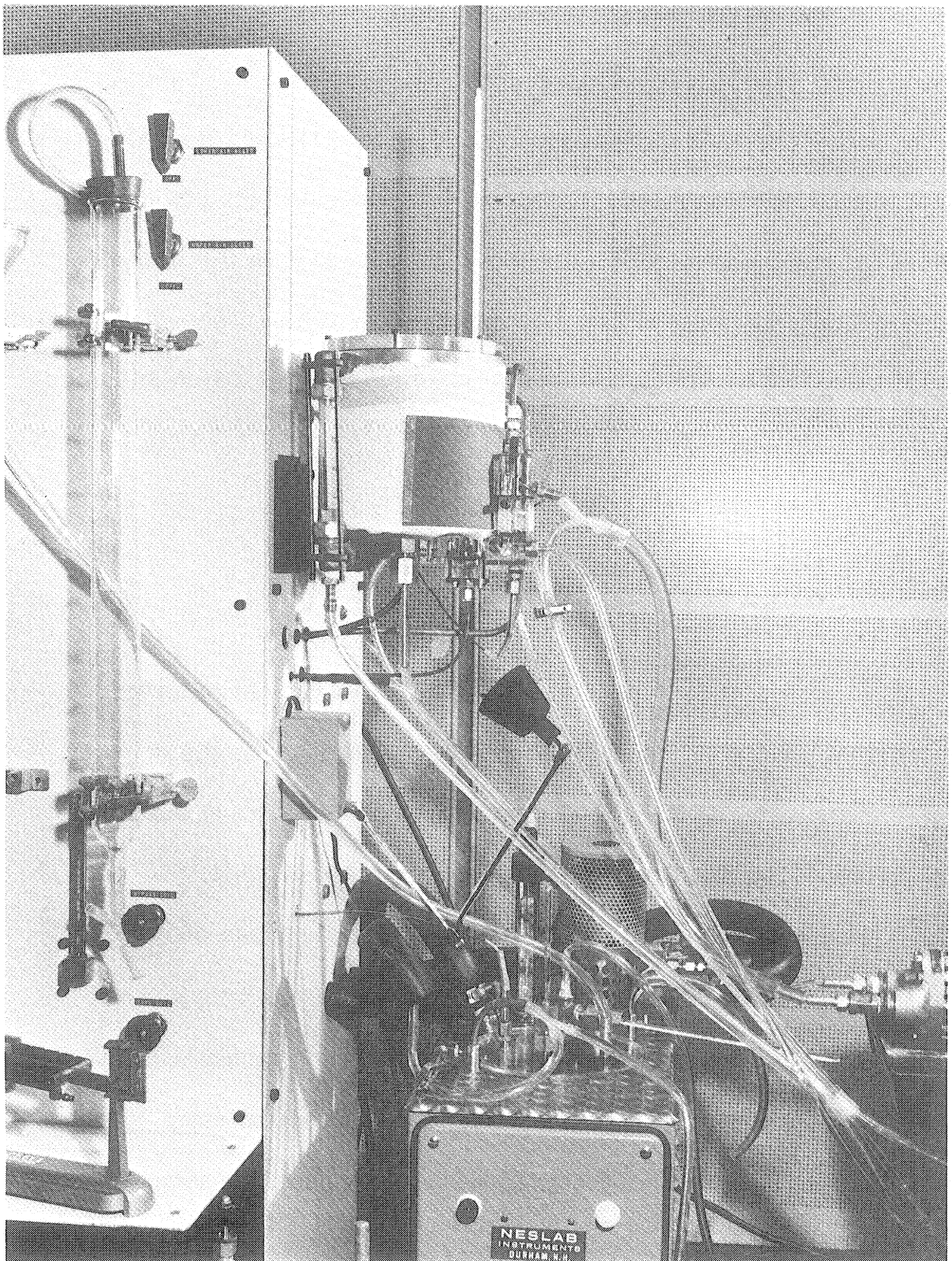


Figure 53. Relative Position of The Lucite Flow Model On The Test Stand



temperatures below 40° F, liquid nitrogen is used for supplementary cooling of the bath fluid. This is accomplished by means of a variable speed pump which continuously pumps bath fluid through a copper tube immersed in a liquid nitrogen dewar, and then back to the bath. The temperature at the tube outlet is monitored to prevent freezing of the bath fluid.

The extremely low air bleed flow rates (less than 1.0 lbm/hour) are measured by means of a bubble flowmeter. This flowmeter consists of a dispensing burette, open at both ends, with the provision for injecting a small soap or Photoflow solution bubble at the bottom of the burette. As the air is drawn into the air bleed system through the top of the burette, the bubble rises. If the time required for the bubble to displace 100 milliliters is obtained with a stopwatch, the flow rate can be easily calculated. This system has the following advantages:

1. It is extremely simple
2. It is a positive displacement meter (the most accurate type of air flow meter)
3. It has a very wide flow range and extends down to less than .001 lbm air/hour

By having both 100 and 500 milliliter burettes available, the flow rate range can be increased even more. One other important fact is that this system costs less than twenty five dollars.

The schematic flow diagram in Figure 54, shows that the fuel flows through the Lucite fuel channel model, through a variable speed pump, and to a 3-way valve. This valve will ordinarily be in the position which results in a recirculation of the test fluid through a bubble

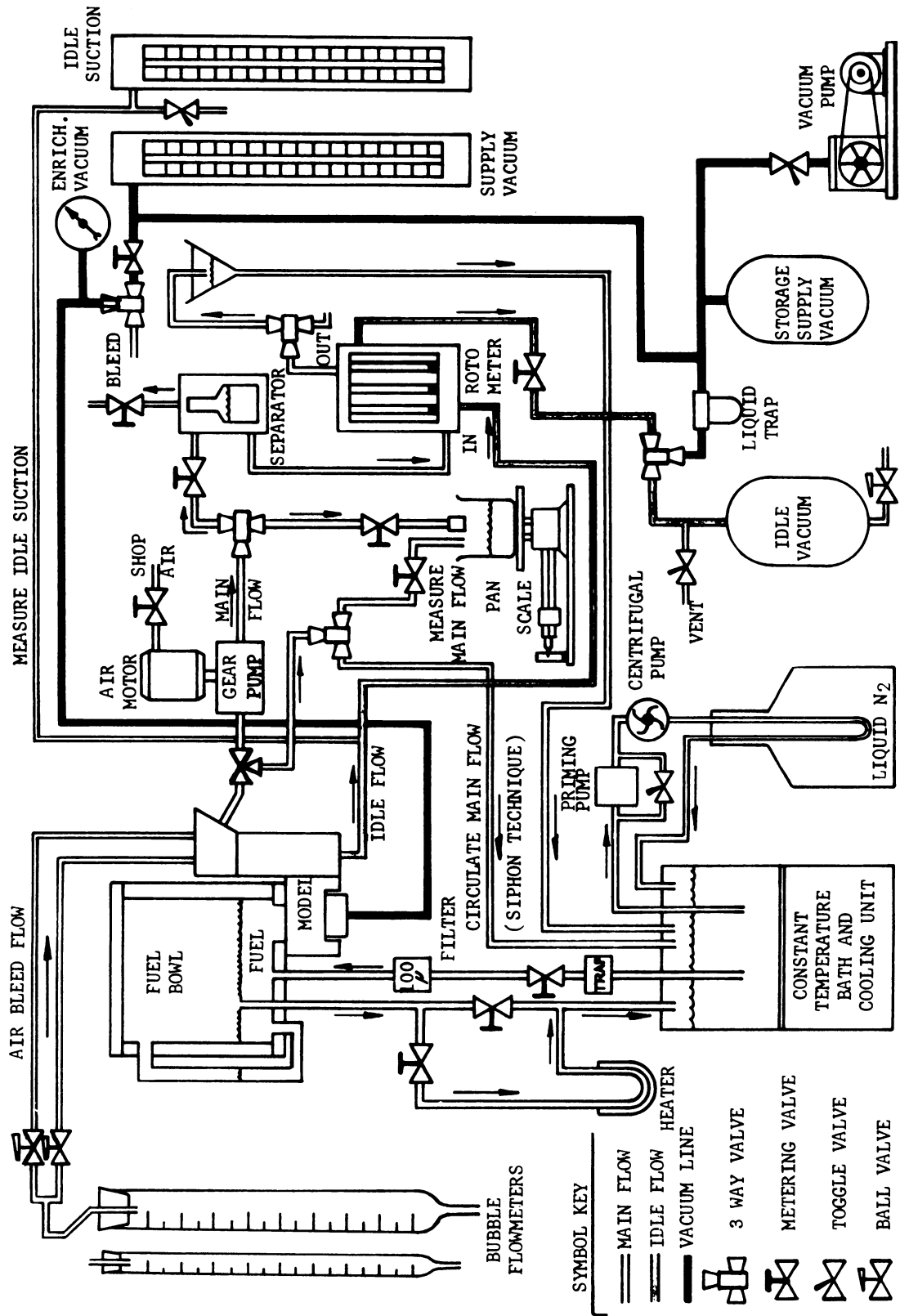


Figure 54. Schematic Flow Diagram Of Fuel Channel Model Test Stand

elimination chamber, a rotameter, and back to the constant temperature bath.

A centrifugal pump, driven by a variable speed DC motor, was originally selected to generate the required boost venturi suction. Note that venturi air flow is not actually needed in the fuel channel flow model since its only function is to produce a suction at the outlet of the fuel channel, and this can be accomplished by a pump. This results in a system in which the test fluid is easily recirculated through a constant temperature bath, and in which the fuel flow rate can be measured quite accurately with a scale and pan arrangement. One operational difficulty was that under certain conditions the air bleed flow rate was sufficient to unprime the centrifugal pump. Therefore, a variable speed, positive displacement pump and depulsing circuit were substituted for the centrifugal pump, and the operation of the flow stand proved to be quite stable.

The rotameter, a Cox 3-tube unit which was modified for this particular flow stand, is used only to establish approximate system flow rates. The smaller tube (0.6 to 5.0 lbm/hour) was isolated from the other two tubes, and is used to monitor the idle system fuel flow rate. When conditions have stabilized, the flow rates are accurately determined by turning a 3-way valve, thus diverting the flow into a scale and pan system instead of into the rotameter. This provides a fuel mass flow rate accuracy which is independent of fuel specific gravity, air bubble content, viscosity, or temperature of fuel in the

pan. When the measurement is obtained, the valve is turned to its original position and the fluid once more recirculates.

Any operating point can be reproduced on this model by varying the speed of the boost suction pump, and by adjusting an idle flow valve at the inlet to the idle vacuum storage tank. These parameters fix the simulated boost venturi suction and intake manifold vacuum which, as was shown in Chapter 2, fix the carburetor-engine operating point. Therefore, by utilizing this fuel channel model and flow stand, fundamental carburetor flow studies can be conducted.

#### D. ADVANTAGES OF USING THE FLOW MODEL AND TEST STAND

Now that the general features of the flow model and test stand have been outlined, numerous advantages over actual carburetor fuel channel tests should be evident. The first advantage is that it permits comprehensive tests to be conducted on the fuel channel. It would be very difficult if not impossible to instrument an actual carburetor for on-engine tests in which system fuel flow rates, air bleed flow rates, temperatures, and pressure profiles were to be accurately measured. In addition, many operating variables on the flow model, such as air bleed diameters, can be easily changed, whereas on an actual carburetor this would be much more involved. The operating variables can be controlled more closely with the flow model than with the actual carburetor. Temperatures can be held to close tolerances by means of the fuel recirculation system and there is no vibration and sloshing of fuel in the bowl with the model.

One of the important advantages of the Lucite flow model is that the flow in the entire fuel system may be observed and photographed. The two-phase flow downstream from the air bleeds, as well as cavitation at orifices, and system back flow may be studied visually. Vapor lock phenomena and the effects of ice crystals and water drops in the fuel (due to moist air bleeding into cold fuel) can also be observed. These types of observations are invaluable in formulating a solution to a given problem.

#### E. GENERAL TEST TECHNIQUES AND CONDITIONS

Fuel channel flow tests were performed using the Lucite flow model and test stand described in the preceding sections. Thirty one data sets were obtained for a wide range of operating conditions.

The fuel types utilized in these tests were:

1. Shell Woodriver mineral spirits.
2. Standard regular gasoline.
3. ASTM isooctane

In order to ascertain the effect of fuel properties on the channel flow, the fuel temperature was varied from 25<sup>o</sup> F to 135<sup>o</sup> F. In each data set the boost venturi suction was varied from zero to thirty inches of fluid in approximately one inch intervals. At each value of boost venturi suction the fuel flow rate, air bleed flow rate, channel pressure distribution, and fuel temperature changes were determined.

A list of the Lucite flow model tests is given in Table 11. Note that in addition to various fuel types, fuel temperatures, and flow rates, tests were performed with the main metering or enrichment

TABLE XI

## LISTING OF FUEL CHANNEL FLOW TESTS

<u>TEST NUMBER</u>	<u>FLUID TYPE</u>	<u>FLUID<sup>o</sup> TEMP. °F</u>	<u>MAIN JET OPEN</u>	<u>ENRICH. SYSTEM OPEN</u>	<u>LOWER BLEED OPEN</u>	<u>UPPER BLEED OPEN</u>
524671	M.S.	70 <sup>o</sup>	YES			
525671	M.S.	70 <sup>o</sup>	YES	YES		
526671	M.S.	70 <sup>o</sup>	YES		YES	
61671	M.S.	70 <sup>o</sup>	YES			
67671	M.S.	70 <sup>o</sup>	YES			
68671	M.S.	70 <sup>o</sup>		YES		
612671	M.S.	40 <sup>o</sup>		YES		
614671	M.S.	90 <sup>o</sup>		YES		
616671	M.S.	90 <sup>o</sup>	YES	YES		
616672	M.S.	90 <sup>o</sup>	YES			
619671	M.S.	48 <sup>o</sup>	YES			
621671	M.S.	100 <sup>o</sup>	YES			
622671	M.S.	100 <sup>o</sup>	YES	YES		
622672	M.S.	100 <sup>o</sup>		YES		
623671	M.S.	48 <sup>o</sup>		YES		
711671	M.S.	80 <sup>o</sup>	YES		YES	YES
721671	M.S.	120 <sup>o</sup>	YES			
919671	M.S.	135 <sup>o</sup>	YES			
922671	M.S.	135 <sup>o</sup>	YES			YES
922672	M.S.	135 <sup>o</sup>	YES		YES	
926671	M.S.	45 <sup>o</sup>	YES			
102671	M.S.	40 <sup>o</sup>	YES		YES	
104671	M.S.	40 <sup>o</sup>	YES		YES	YES
1011671	M.S.	135 <sup>o</sup>	YES		YES	YES
117671	GAS.	80 <sup>o</sup>	YES			
117672	GAS.	80 <sup>o</sup>	YES		YES	YES
1110671	GAS.	32 <sup>o</sup>	YES			
1113671	GAS.	32 <sup>o</sup>	YES		YES	YES
115671	ISO.	25 <sup>o</sup>	YES			
1116671	ISO.	80 <sup>o</sup>	YES		YES	YES
1118671	ISO.	80	YES			

orifices blocked, and with some or all of the air bleeds closed. Other parameters that were varied in certain tests were:

1. Initial fuel spill point.
2. Enrichment valve vacuum.
3. Idle needle screw turns.

The tests performed with the main metering or enrichment orifice blocked were conducted to obtain basic flow data for a single system. This data was utilized to check the predictions of subroutine FLOW. This assured that subroutine FLOW was correctly predicting the parameters for single-phase flow in one system before it was expanded to predict two-phase flow parameters in a network. For reasons of safety, most of the tests were conducted with mineral spirits as the test fluid. This solvent is also utilized by many automotive companies in flow testing production carburetors, also for reasons of safety.

The pressure distribution in the fuel channel was obtained, as mentioned earlier, by six static pressure taps along the fuel channel. The important operating feature of this method is that the taps were connected to a six tube manometer bank in the order of length along the channel. This arrangement is shown in Figure 55. The connecting tubing and the manometer well and tubes contained the same fluid that was flowing in the model. This avoided the problems of moving two-fluid interfaces, and the filling of dial manometer pressure lines. By having the connecting tubing slope downward toward the manometer bank, the pressure distribution during two-phase flow was easily obtained. (The air bubbles remained in the fuel channel, rather than

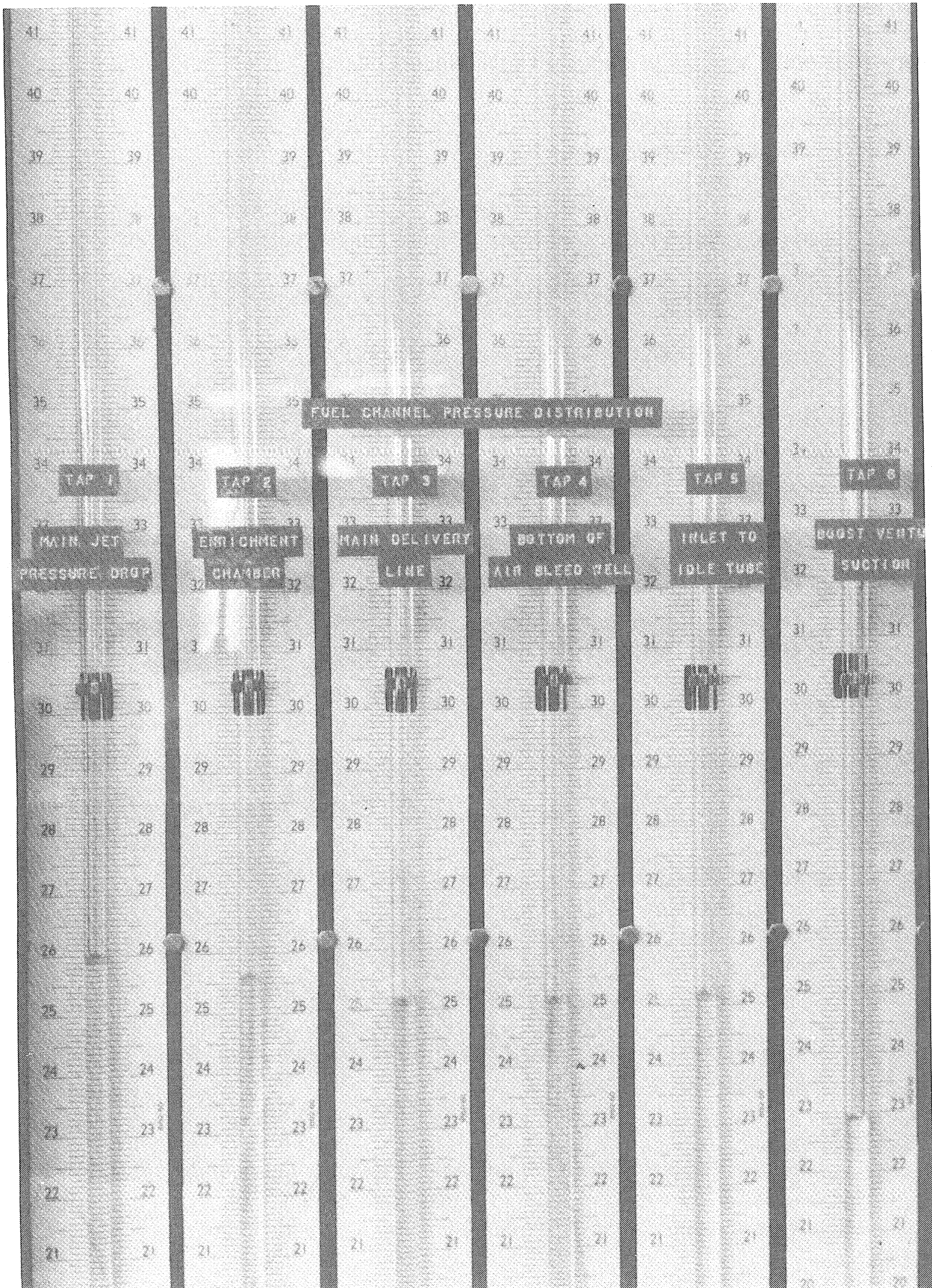


Figure 55. Manometer Bank Utilized To Obtain The Static Pressure Distribution With The Fuel Channel



entering the manometer tubing). Note that if there is no flow in the model, the fluid level in all six manometer tubes will be equal to the level in the fuel bowl. This was set at thirty inches on the manometer bank. The pressure loss from the fuel bowl to each pressure tap is indicated by the depression in the manometer reading below thirty inches. Therefore, the pressure distribution for any fuel flow rate was immediately evident.

One test technique that was utilized for runs without air bleeds was to connect a long tube to the main outlet of the Lucite flow model. The fuel was then allowed to exit from the tube at a point about thirty inches lower than the model discharge level. This created a siphon with corresponding channel pressures that were exceedingly steady (as compared to creating the suction at the model outlet with a pump, which always resulted in some minor pulsations.) All single phase flow tests were conducted utilizing this siphon technique.

#### F. RESULTS OF FUEL CHANNEL FLOW TESTS

Typical data obtained in one of the Lucite flow model tests is presented in Table 12. This data was obtained during test number 117672, which was a flow test utilizing Standard regular gasoline at 80° F. Both main air bleeds, each of 0.037 inch diameter, were open, and the enrichment valve was closed. Note that the upper well temperature, which is the temperature of the fuel-air foam leaving the emulsion section, was about 75° F. The 5° decrease in fuel temperature



indicates that about 1.6% of the fuel by weight was vaporized in the emulsion section of the fuel channel.

A complete data reduction program was written to process the model flow data. This program operated on the pressure tap, flow rate, and temperature data, and calculated all of the important parameters for each of the 31 data sets. The computer names for these variables and their meanings follow. (All are experimental values except VIDELA and WIDELA).

BLEDPH	Total air bleed mass flow rate
RATEPH	Total fuel mass flow rate
RE	Reynolds number of main metering orifice
CDCHAN	Discharge coefficient of entire main channel
BVSUCW	Boost venturi suction
CDJET	Discharge coefficient of main metering orifice
PDROPW	Static pressure differential of main metering orifice
DELPBW	Total pressure loss in bends
DELPXW	Total pressure loss in sudden area changes
QDOTF	Volume flow rate of fuel
RATIOM	Mass flow rate ratio (fuel to air)
RATIOV	Volume flow rate ratio (air to fuel)
QDOTA	Volume flow rate of bleed air
AIRVEL	Velocity of bleed air in 2nd main bleed
VIDELA	Ideal air velocity in 2nd main bleed
WIDELA	Ideal air mass flow rate in 2nd main bleed
SUMERR	Estimated total manometer reading error
DELAW	Static pressure differential across 2nd main air bleed

The reduced data from two of the thirty-one tests (number 117672) are presented in Tables 13 and 14. There are numerous interesting values in these tables, and also in the reduced data for the twenty-nine additional tests. In order to present these values in a meaningful way, a special CALCOMP plotting routine was written for the flow stand data reduction program. This made possible the automatic plotting of any of seven groups of six different graphs, each available in four

TABLE XIII  
 REDUCED DATA FOR A LUCITE FUEL CHANNEL FLOW TEST  
 WITH AIR BLEEDS

LUCITE FLOW MODEL TEST

THIS DATA IS FOR TEST NUMBER 117672      THIS TEST IS FOR LAB GAS AT A MEAN TEMP OF 80.0 °F

THE JET HAS A DIAMETER OF .0502 INCHES AND A LENGTH OF .1830 INCHES  
 THE FLUID VISCOSITY IN CENTISICKES IS .556  
 THE FLUID SPECIFIC GRAVITY IS .721  
 THE MAIN JET IS OPEN  
 THE LOWER MAIN AIR BLEED IS OPEN  
 THE UPPER MAIN AIR BLEED IS OPEN  
 THE INDEPENDENT PLOTTING VARIABLE IS THE ROOST VENTURI SUCTION  
 THE REYNOLDS NUMBER IS BASED ON THE MAIN CRIFICE DIAMETER

\*\*\* PROGRAM RESULTS FOR THIS RUN \*\*\*

RUN	Q FUEL G/HR	m FUEL / RATEPH	MAIN JET REYNOLDS NO. RE	CHANNEL DISCHARGE COEFFICIENT CUCFAN	BOOST SUCTION BVSUCH	MAIN JET C <sub>d</sub>	ΔP <sub>JET</sub> PDRPM	ΔP <sub>BEND</sub> DELPM	ΔP <sub>SUPPLY EXHAUST</sub> DELPM	ΔP <sub>2-THREE</sub> EMUL	PERCENT	% OF METERING SIGNAL LOST ACROSS MAIN JET (TOTAL PRESSURE)
1	.159	4.91	1541.6	.5268	2.36	.7023	1.33	.07	.00	1.03	44.1	
2	.202	6.41	2012.3	.6165	2.93	.7703	1.88	.10	.00	1.09	51.4	
3	.273	8.22	2581.5	.6469	4.38	.7746	3.06	.12	.04	1.43	58.9	
4	.305	9.08	2850.3	.6516	5.27	.7715	3.76	.21	.04	1.58	61.4	
5	.357	10.89	3417.3	.6963	6.63	.8162	4.82	.28	.04	1.95	63.4	
6	.381	11.39	3574.1	.6909	7.36	.8086	5.38	.32	.07	2.10	64.1	
7	.404	11.86	3723.7	.6771	8.32	.7924	6.08	.43	.07	2.28	64.8	
8	.426	12.19	3826.7	.6795	8.73	.7999	6.30	.57	.07	2.39	64.1	
9	.442	13.12	4117.7	.6967	9.61	.8166	7.00	.43	.07	2.69	65.0	
10	.460	13.43	4215.2	.6874	10.35	.8087	7.48	.50	.07	2.98	64.8	

RUN	Q FUEL G/HR	m FUEL / RATIO	Q AIR / RATIO	Q AIR / RATIO	V AIR BLEED AIRVEL	IPDIAL V <sub>air</sub> VICELA	UPPER m <sub>air</sub> WIDELA	ΣMERR	ΔP AIR BLEED DELAN	C <sub>d</sub> AIR BLEED CDAIR	R <sub>air</sub> AIR BLEED REAIRB
1	.11	30.88	15.95	2.18	40.5	96.0	.38	-.20	1.48	.422	1044.8
2	.14	31.75	19.40	2.76	51.4	108.5	.43	-.22	1.89	.474	1326.4
3	.18	30.10	20.46	3.74	69.6	133.8	.53	-.20	2.88	.520	1794.6
4	.20	25.43	20.93	4.22	78.6	147.3	.58	-.19	3.49	.533	2027.1
5	.24	30.47	20.21	4.89	91.0	165.5	.65	-.14	4.40	.550	2346.8
6	.25	29.91	20.59	5.21	96.9	174.7	.69	-.13	4.91	.555	2500.7
7	.26	29.38	20.57	5.53	102.8	186.1	.73	-.12	5.57	.552	2652.9
8	.27	28.61	21.53	5.83	108.5	190.6	.75	-.07	5.84	.569	2798.9
9	.29	25.66	20.77	6.05	112.6	199.8	.78	-.16	6.42	.564	2905.5
10	.30	29.20	21.09	6.29	117.1	207.0	.81	-.06	6.89	.566	3020.6

TABLE XIV  
 REDUCED DATA FOR A LUCITE FUEL CHANNEL FLOW TEST  
 WITHOUT AIR BLEEDS

PIN	THIS DATA IS FOR TEST NUMBER 117671		THIS TEST IS FOR LAR GAS AT A MEAN TEMP OF 80.0 °F		NO AIR BLEEDS						
	BOOST SUCTION RV/SUIC	FUEL FLOW RATE G/ALPH	RT	CHANEL C <sub>J</sub> CDCHAN	BOOST SUCTION RV/SUICW	ΔP <sub>JET</sub> DELPW	ΔP <sub>BLD</sub> DELPPH	ΔP <sub>EXHAUSTION</sub> DELPXW	2-PHASE ΔP EMULW	MAIN JET C <sub>D</sub> COJET	% OF METERS SIGNAL LOST ACROSS MAIN JET PERCFN
1	6.7	2.30	751.1	.5612	.49	.35	.01	.02	.15	.6742	41.8
2	10.4	3.40	1048.4	.6409	.76	.65	.04	.03	.15	.6228	60.0
3	20.4	5.00	1431.2	.6984	1.50	1.34	.10	.04	.19	.7364	45.4
4	20.76	6.40	2009.9	.7400	2.03	1.91	.13	.05	.20	.7625	76.3
5	30.35	7.13	2236.4	.7474	2.44	2.34	.15	.07	.24	.7572	78.5
6	30.00	7.03	2489.1	.7623	2.93	2.79	.16	.08	.26	.7811	75.9
7	50.14	9.06	2967.8	.7845	3.78	3.62	.15	.08	.30	.8000	82.3
8	50.07	10.00	3158.4	.7908	4.30	4.27	.26	.08	.32	.8073	84.2
9	70.76	11.03	3560.2	.8037	5.34	5.20	.32	.09	.37	.8144	85.5
10	80.26	12.16	3809.7	.8100	6.07	5.90	.38	.09	.41	.8224	86.0
11	90.79	13.45	4009.3	.8160	6.30	6.13	.38	.09	.44	.8286	94.1
12	100.25	13.84	4362.8	.8208	7.54	7.27	.42	.10	.51	.8452	86.1
13	110.65	14.79	4661.0	.8390	8.42	8.16	.42	.11	.54	.8591	87.1
14	120.87	15.77	5051.3	.8490	9.34	9.05	.45	.13	.59	.8634	87.4
15	140.15	16.76	5250.2	.8552	10.41	10.07	.53	.12	.64	.8699	87.8
16	150.79	17.63	5549.7	.8543	11.61	11.24	.64	.13	.68	.8685	88.2
17	170.75	18.73	5836.5	.8563	13.05	12.71	.73	.13	.72	.8677	89.3
18	190.36	19.81	6117.8	.8646	14.03	13.90	.81	.13	.75	.8740	89.9
19	210.00	20.78	6400.0	.8664	15.44	15.38	.90	.13	.82	.8760	90.1
20	230.57	21.63	6725.4	.8664	14.40	14.28	.90	.15	.82	.8743	90.2
21	250.00	22.05	6920.4	.8674	17.52	17.13	.95	.13	.82	.8770	90.8
22	250.00	22.75	7140.6	.8724	18.44	18.08	1.00	.14	.92	.8808	91.2
23	270.64	22.93	7410.6	.8755	20.25	19.82	1.09	.15	1.01	.8850	91.2

ONLY 1 PHASE IN THIS TEST

INCHES OF WATER

INCHES OF WATER

LB/HR

INCHES OF GAS

\*\*\* PROGRAM RESULTS FOR THIS RUN \*\*\*

THE JET HAS A DIAMETER OF .0502 INCHES AND A LENGTH OF .1830 INCHES  
 THE FLUID VISCOSITY IN CENTISTOKES IS .556  
 THE FLUID SPECIFIC GRAVITY IS .721  
 THE MAIN JET IS OPEN  
 THE INCREASING PLOTTING VARIABLE IS THE MAIN JET PRESSURE DROP  
 THE SPANNING NUMBER IS BASED ON THE MAIN ORIFICE DIAMETER

different scales. These computer plots were used to evaluate each test.

Figure 56 illustrates the variation in total fuel mass flow rate with the static pressure differential across the main fuel system which, in an actual carburetor, would be the boost venturi suction. Note that the mass flow rate increases smoothly with boost suction, and that the actual flow rate is below the ideal value, which is based on ideal flow for the given pressure differential. The ratio of the actual mass flow rate to the ideal flow rate is the effective discharge coefficient for the entire main channel. The same data is illustrated in Figure 57 on log-log coordinates. This has the distinct advantage of representing the ideal flow curve as a straight line. It will also be recalled from Chapter 3 that constant discharge coefficient values will appear as straight lines on these coordinates. The method of plotting flow data on these log-log coordinates was utilized by Kreith and Eisenstadt<sup>37</sup>, who related the value of the slope to the orifice L/D ratio.

There is a deviation from the general slope of the flow data at both the low and high head regions of the curve. Note that the slope of the mass flow rate data in Figure 57 begins to increase at pressure differentials less than 2.0 inches of water. Also, although it is not shown in this particular data set, the slope begins to decrease in the region of 60 inches of water. (It must do so or it would eventually cross the ideal line.)

The air bleed flow rates were measured over a wide range of boost venturi suction. The experimental values for the total main

## FLUID FLOW RATE VS PRESSURE DROP

MAIN ORIFICE NUMBER = F-50      AVERAGE TEMP = 80.0 °F  
 RUN NUMBER = 117671      TEST FLUID = GASOLINE  
 (STD. REG.)

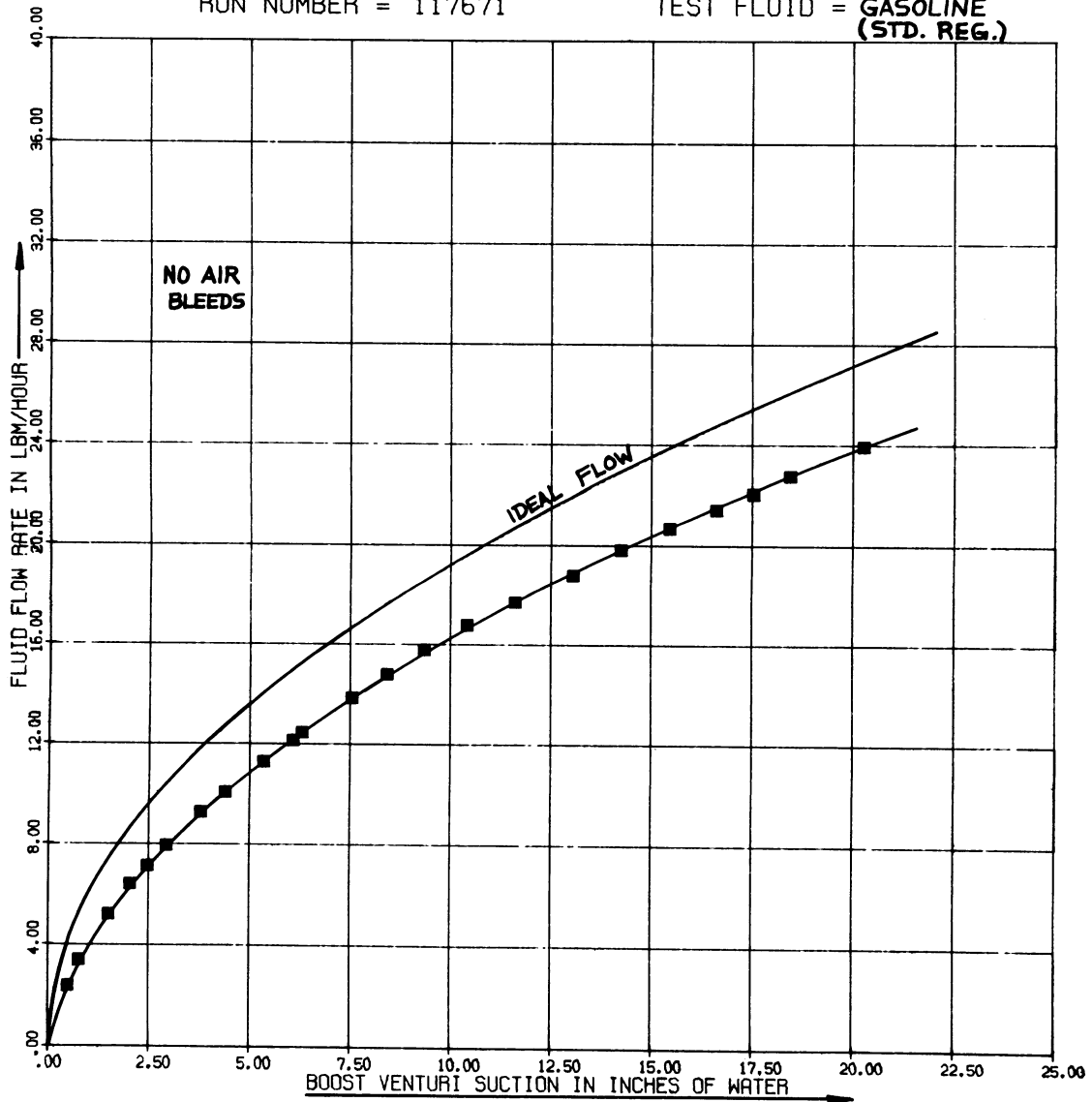


Figure 56. Experimental Values of Gasoline Flow Rate As A Function Of the Metering Signal

### LOG-LOG PLOT OF SYSTEM FLOW PARAMETERS

MAIN ORIFICE NUMBER= **F-50**     AVERAGE TEMP = 80.0 °F  
RUN NUMBER = 117671     TEST FLUID = **GASOLINE**  
(STD. REG.)

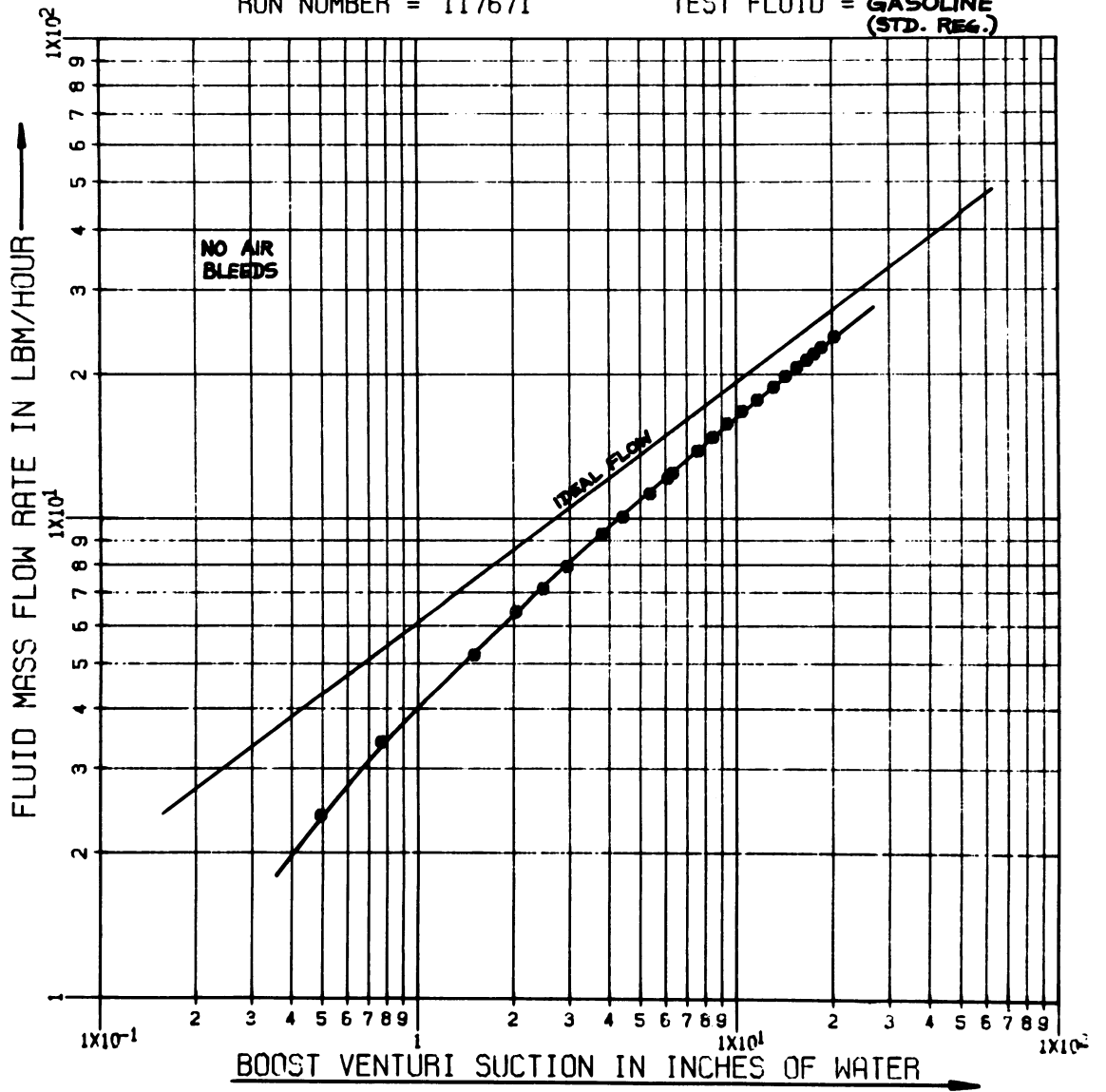


Figure 57. Log Plot Of Total Gasoline Flow Rate Versus The Metering Signal



system air bleeds are shown in Figure 58. These data were obtained utilizing 0.037 inch diameter air bleed orifices for both main bleeds. (The bleed orifices were square-edged with an L/D ratio of 3.63.) Note that the bleed air mass flow rate is very small, being generally less than 0.5 pound per hour. Referring again to Table 13, it will be noted that the fuel mass flow rate is about 30 times that of the bleed air, but that the volume flow rate of the bleed air is about 20 times that of the fuel. It is this large volume flow rate of air within the channel that increases the velocity of the fuel-air foam, and increases the total pressure loss over that for single phase flow.

Figure 59 illustrates the fuel mass flow rate data for run number 1110671, which was a test utilizing 32° F gasoline. Note that the measured fuel flow rates are very nearly equal to those obtained with 80° F gasoline (Figure 56). Actually the mass flow rates are slightly higher with the 32° F gasoline than the 80° F gasoline. The ideal mass flow rate curve is noticeably higher for the cold gasoline however. This is due to the increased density of the cold gasoline and to the fact that the ideal mass flow rate will increase as the square root of the fluid density for a given pressure differential (Chapter 3).

The effect of fluid temperature on the fuel mass flow rate is a complex relationship involving the precise variations in the discharge coefficients with Reynolds number for each of the orifices being used, and the variation in density and viscosity with temperature for the particular fuel being used. (This was discussed in Chapter 3.) Thus,

## AIR BLEED FLOW VS VENTURI SUCTION

AIR BLEED DIAMETERS =  $\frac{.037}{.037}$ "      AVERAGE TEMP = 80.0°F

RUN NUMBER = 117672

TEST FLUID = **GASOLINE**  
(STANDARD REG.)

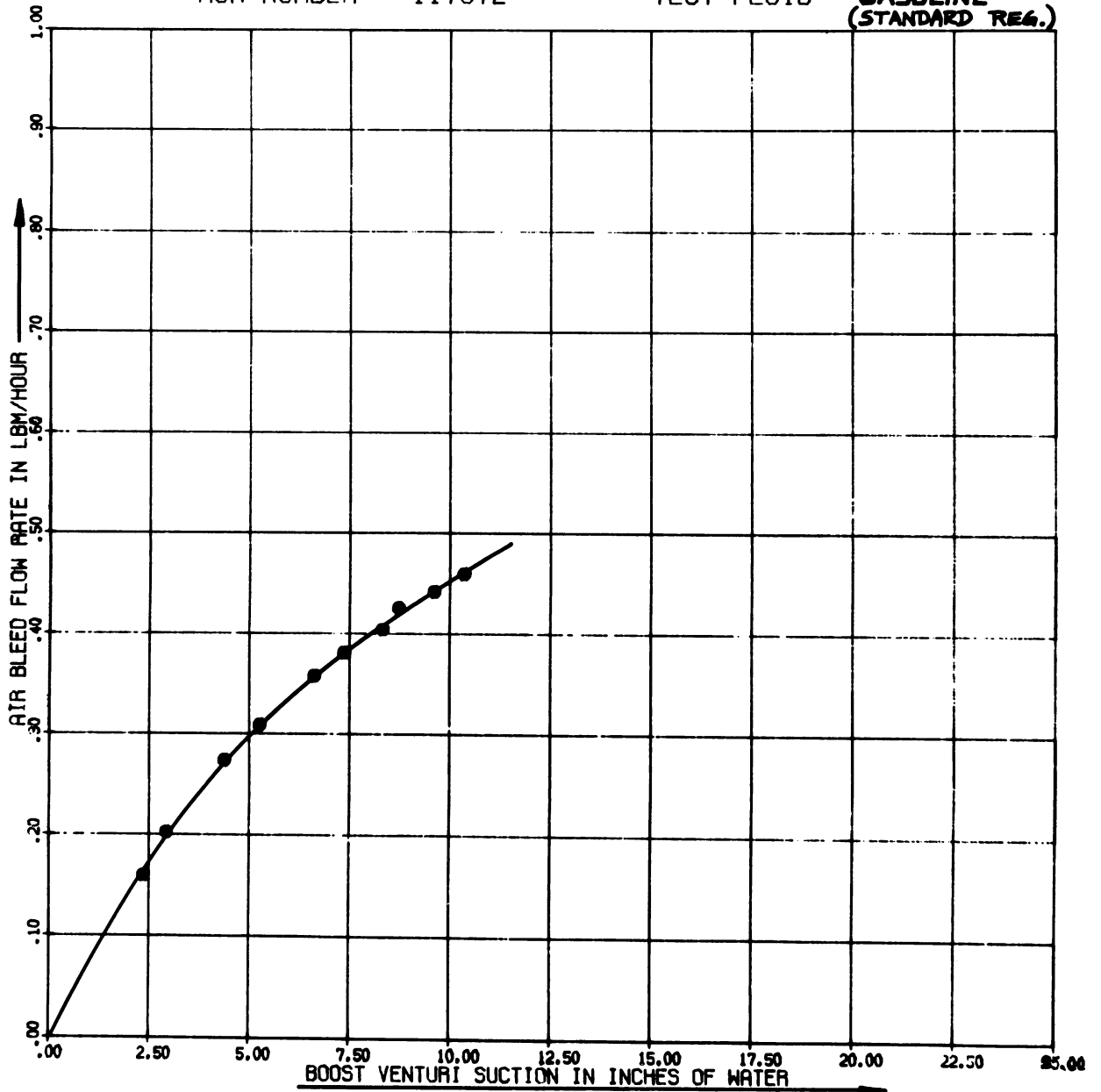


Figure 58. Measured Air Bleed Flow Rate As A Function Of  
The Metering Signal

## FLUID FLOW RATE VS PRESSURE DROP

MAIN ORIFICE NUMBER= F-50    AVERAGE TEMP = 32.0 °F  
 RUN NUMBER = 1110671    TEST FLUID = STANDARD REG. GASOLINE

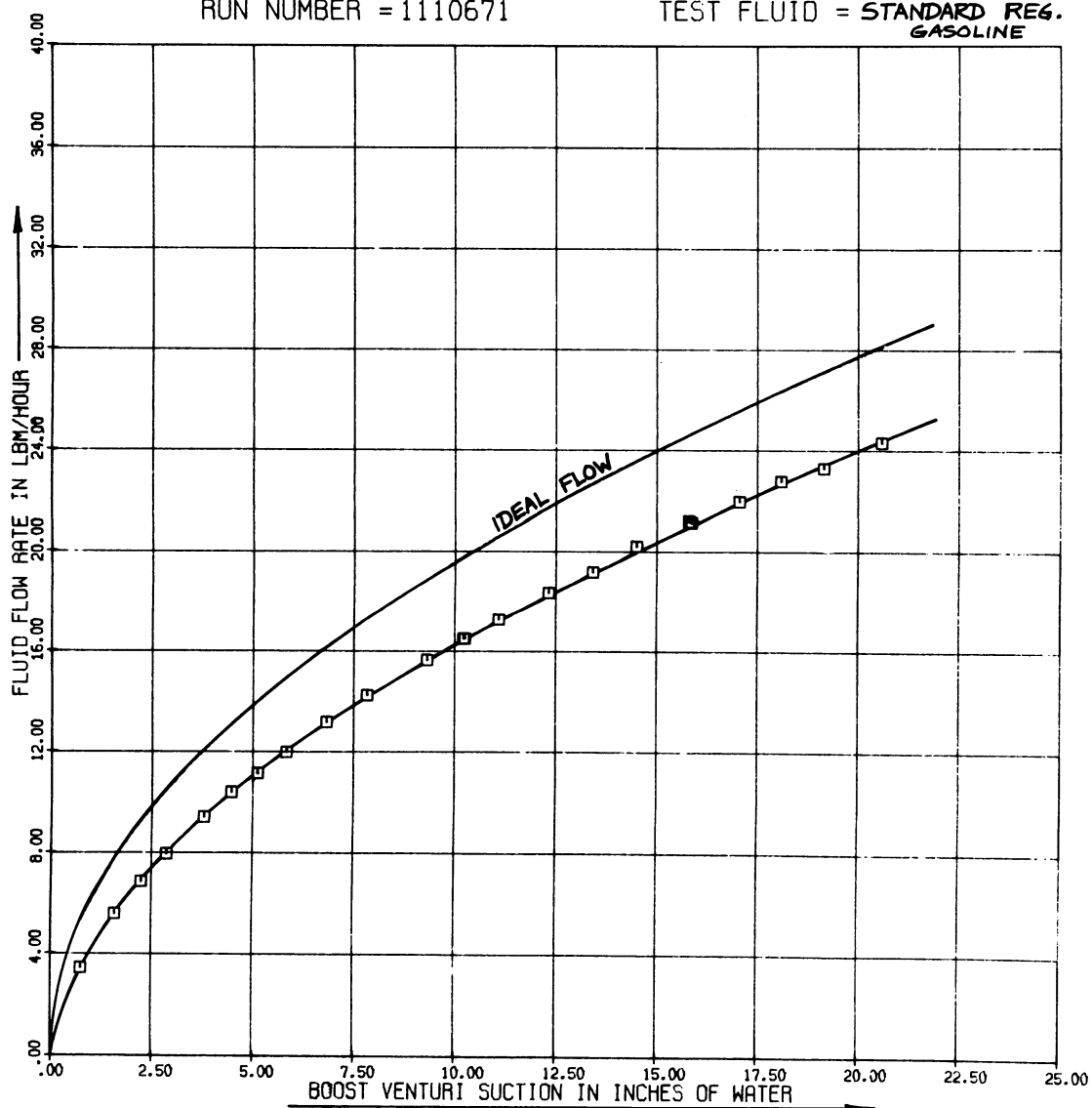


Figure 59. Mass Flow Rate Of Cold Gasoline As A Function Of The Metering Signal

for this particular fuel channel geometry and fuel type, the effect of increasing the fuel temperature was to decrease the fuel mass flow rate very slightly (less than 1%.) For mineral spirits the effect of temperature was quite different, as will be seen in the next series of graphs.

The effect of numerous variables on the mass flow rate of mineral spirits is shown in Figure 60. First notice that the flow rate increases significantly as the temperature is increased from 48° F to 120° F. This amounts to an 8.5% increase in mass flow rate for a 72° F increase in fuel temperature. This is for no air being bled into the fuel channel. Opening the main system air bleeds reduces the fuel mass flow rate at a given boost venturi suction by about 10%. Opening the enrichment valve, which in this case was a 0.052 inch diameter orifice in parallel with the main metering orifice, resulted in the mass flow rates shown by the upper curves in Figure 60.

The fuel mass flow rates obtained in two other tests, using mineral spirits at 45° F and 135° F respectively, are shown in Figure 61. Note the effect of fuel temperature, which becomes more pronounced at very low flow rates. There is a greater flow rate change per degree temperature change at small pressure differentials than at large pressure differentials. This results from the greater slope of the orifice characteristic curve in the low head region. Thus, the region of increasing sensitivity to fuel temperature corresponds to the region in which the slope of the mass flow rate curve begins to increase, which



## LOG-LOG PLOT OF SYSTEM FLOW PARAMETERS

MAIN ORIFICE NUMBER= F-50    AVERAGE TEMP = 135.0°F <sup>AND</sup> 45°F  
 RUN NUMBER = 919671 = ○ (135°F)    TEST FLUID = MIN. SPIRITS  
 926671 = ● (45°F)

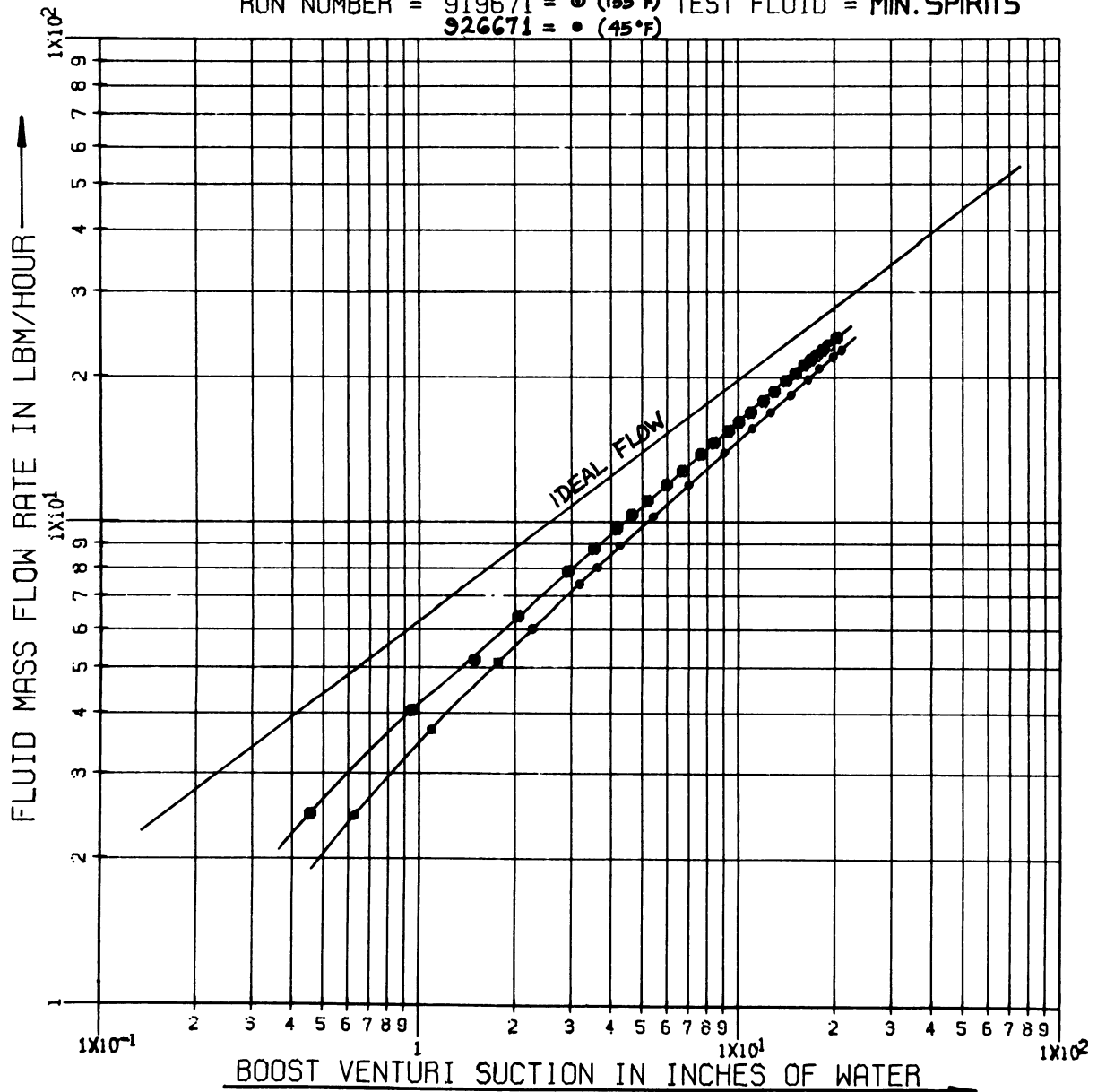


Figure 61. The Effect Of Fluid Temperature On The Mass Flow Rate of Mineral Spirits

indicates a more rapid change in discharge coefficient. Figure 62 illustrates this concept quite well. Note that lines of constant discharge coefficient have been drawn on the log-log coordinates, and that the discharge coefficient is changing more rapidly in the low head, low flow rate region.

The effect of various parameters on the air bleed mass flow rate is shown in Figures 63 and 64. These data were obtained using mineral spirits as the test fluid. Figure 63 illustrates the air bleed flow rate variations for both one and two air bleeds in the main system. Both curves increase smoothly with boost venturi suction, with the curve for two main air bleeds being slightly less than double that for one air bleed. If this data is compared to that in Figure 58, it will be evident that the air bleed mass flow rate curves are practically identical for gasoline and mineral spirits, although the two fluids have significantly different properties. Thus the air bleed flow rate is quite insensitive to fuel type.

The effect of fluid temperature on the air bleed mass flow rate is evident in Figure 64, which is a plot of the air bleed flow data obtained in two tests at significantly different fluid temperatures. It may be noted that the air bleed mass flow rate is relatively insensitive to fluid temperature in addition to fuel type. This may explain one interesting fact that became evident during the Lucite flow model tests. It was found that the addition of air bleeds resulted in a fuel flow rate curve that was less sensitive to fuel temperature changes. By introducing

LOG-LOG PLOT OF SYSTEM FLOW PARAMETERS

MAIN ORIFICE NUMBER = **SE-188** AVERAGE TEMP = 48.0°F  
 RUN NUMBER = 623671 TEST FLUID = **MIN.SPIRITS**

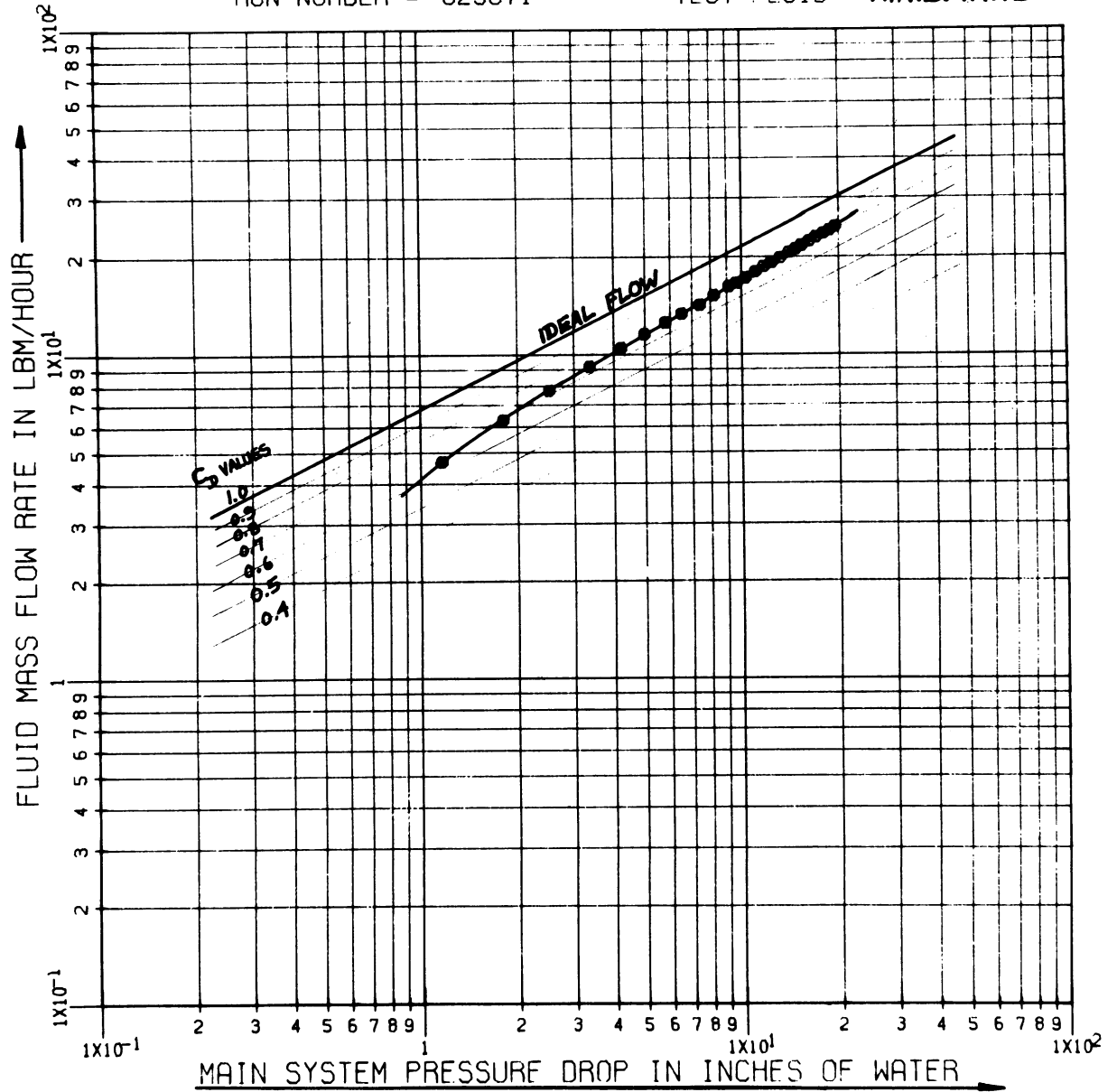


Figure 62. Illustrations Of The Rapid Change In The Main Channel Discharge Coefficient At Small Metering Signals



AIR BLEED FLOW VS VENTURI SUCTION

AIR BLEED DIAMETERS =  $\frac{0.037}{0.37}$   
 RUN NUMBER = 711671

AVERAGE TEMP = 80.0°F  
 TEST FLUID = MINERAL SPIRITS

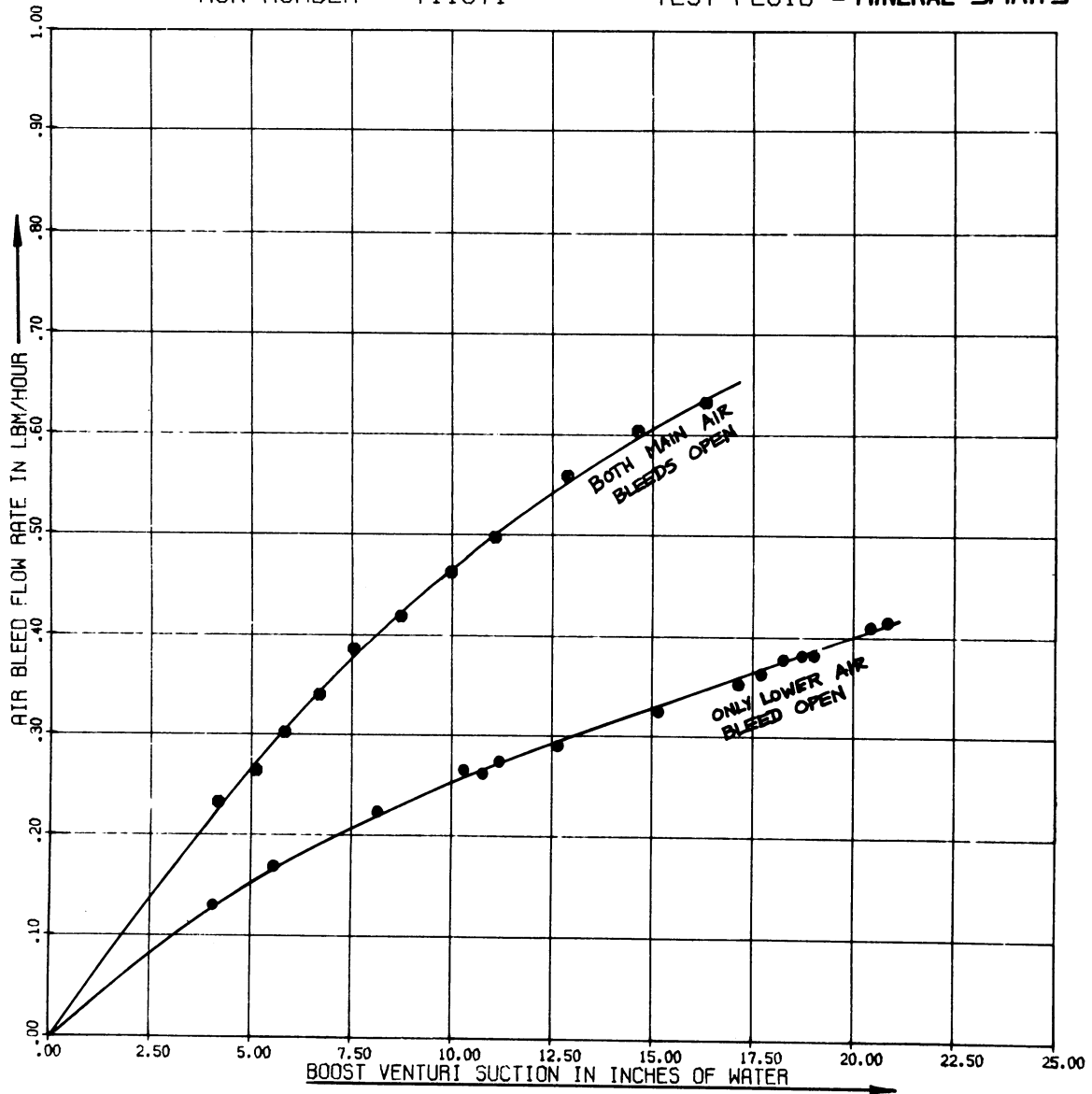


Figure 63. Air Bleed Flow Rate Variations For One And Two Operating Bleeds

### AIR BLEED FLOW VS VENTURI SUCTION

AIR BLEED DIAMETERS = 0.037"      AVERAGE TEMP = 135.0 ° F  
 0.037"      40.0 ° F  
 RUN NUMBER = 104671 (40 ° F) ●      TEST FLUID = SHELL WOODRIVER  
 1011671 (135 ° F) ●      MINERAL SPIRITS

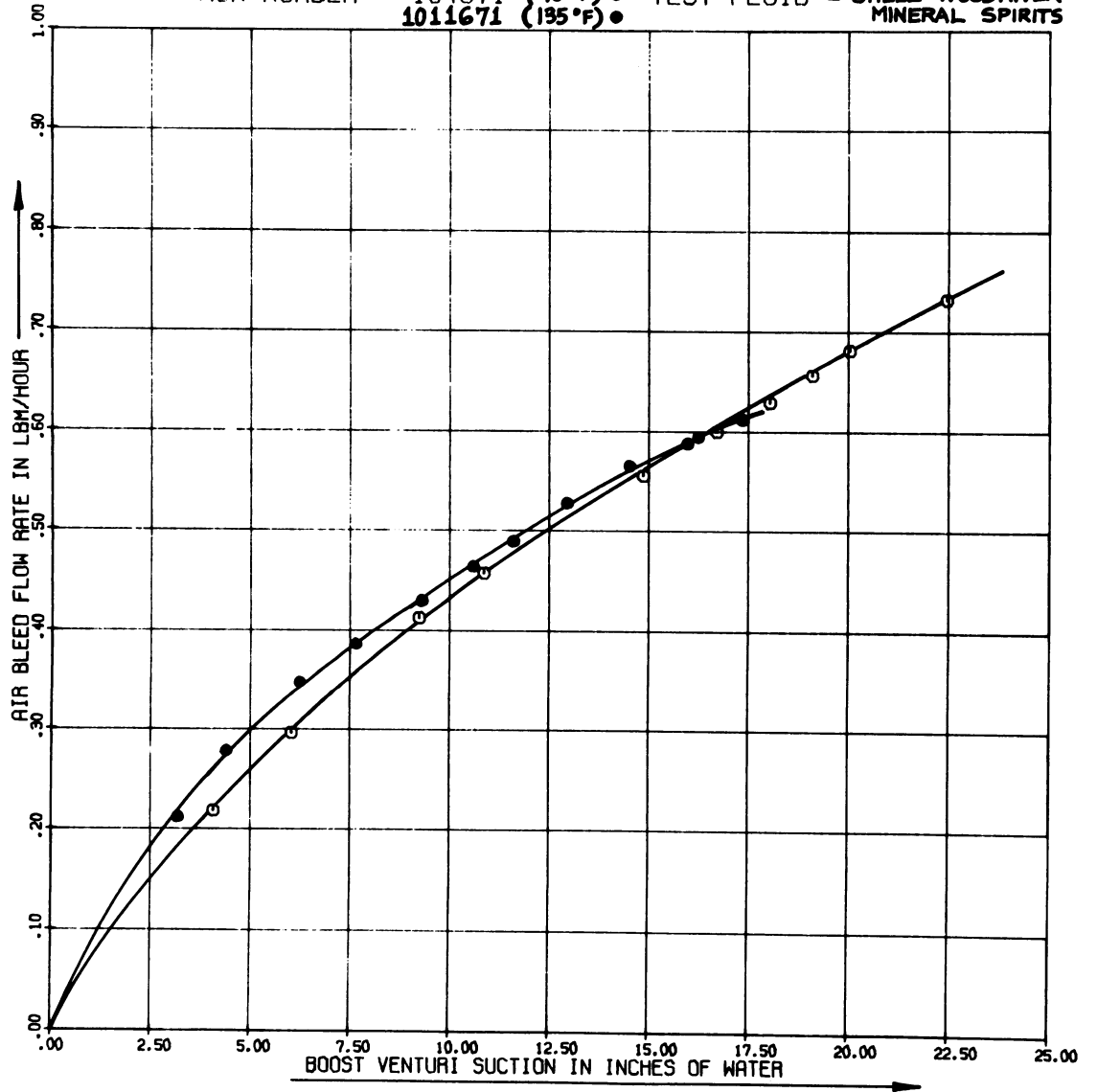


Figure 64. The Effect Of Fluid Temperature On The Air Bleed Mass Flow Rate

into the channel an air bleed flow which is relatively insensitive to fuel type or temperature, the overall sensitivity of the fuel flow rate to temperature change is decreased. For mineral spirits, the fuel mass flow rate increase was 1.2% per  $10^{\circ}$  F increase without air bleeds and 0.5% per  $10^{\circ}$  F with air bleeds.

#### G. TWO-PHASE FLOW OBSERVATIONS

As stated earlier, one of the advantages of the lucite model was that the two-phase flow within the fuel channel could be observed and photographed. This characteristic of the flow model was utilized to some extent in every flow test. It was discovered that occasionally, when using warm, highly volatile fuels, a vapor bubble would form below the main metering orifice, and would remain in that position until the fuel flow rate became sufficiently large to carry it away. While it remained in that position the metering characteristics of the channel were slightly altered.

One of numerous other phenomena that were observed was the condensation of water from moist bleed air when the fuel temperature was less than about  $40^{\circ}$  F. These water droplets, being heavier than the fuel, would fall to the bottom of the air bleed well and collect there. Under certain conditions, this ball of water would be drawn into the idle tube, which would certainly result in a rough engine idle, if not a complete stall.

High speed movies (300 frames per second) were taken of the two-phase flow in the emulsion section of the fuel channel. A few

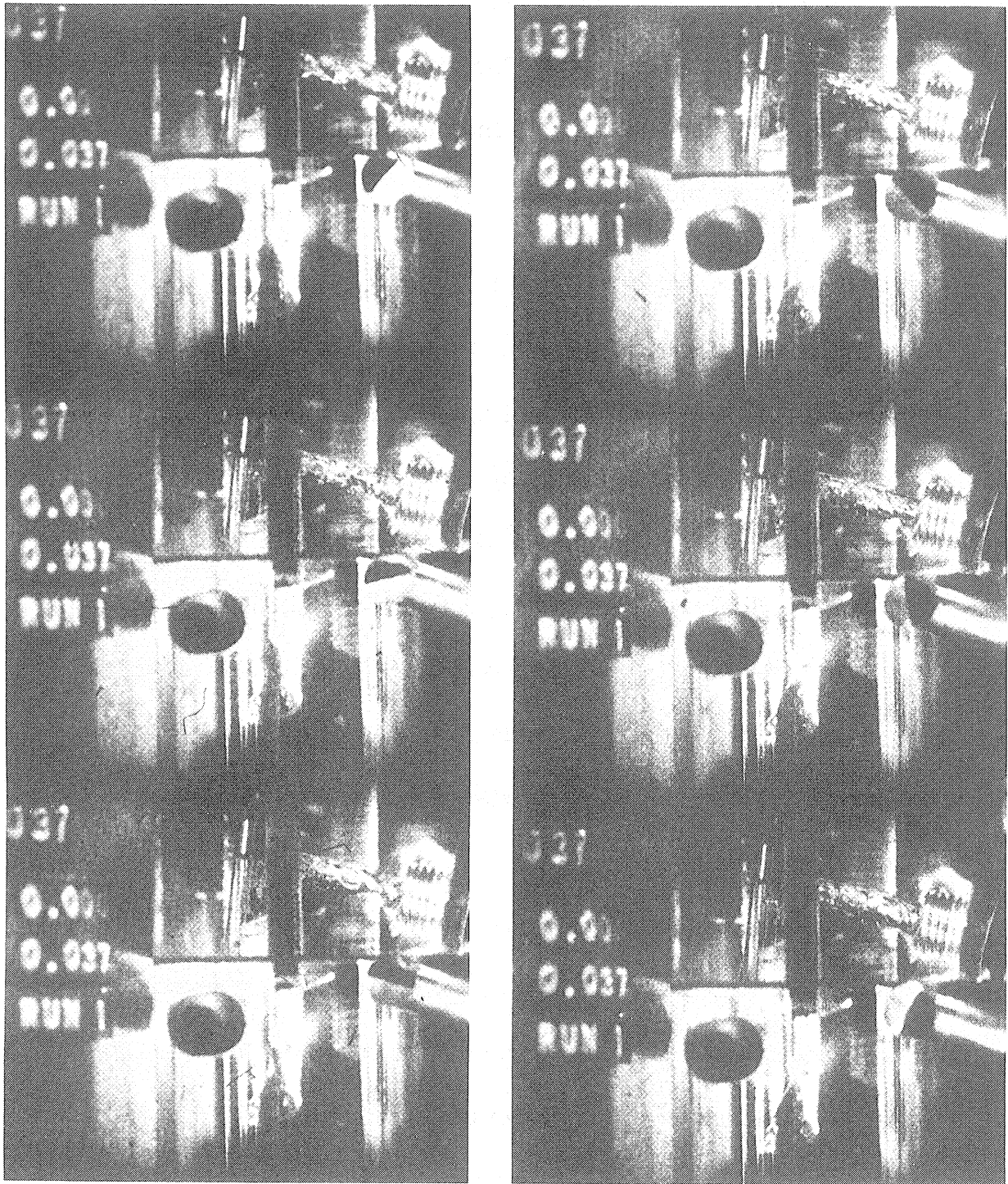


Figure 65. High Speed Photographs Of Two-Phase Flow  
Within The Lucite Model

consecutive frames from one of these movies were enlarged and are shown in figure 65. The view is that of the air bleed well and discharge tube, similar to the cross-sectional view shown in Figure 51. While the movies show significantly more detail than these enlarged frames, the bubble-type flow in the discharge tube is quite evident.

The two-phase flow within the fuel channel was found to be in a few distinct regimes in nearly all cases. The flow in the emulsion section was in the bubble-flow regime, and the flow regime in the main discharge tube was either bubble or stratified, depending on the fuel flow rate. At low main system fuel flow rates the discharge tube flow was stratified, with the air flowing in the upper portion of the tube. As the fuel flow rate increased, the two-phase flow regime changed from stratified to bubble flow. The flow in the idle system was mainly slug flow, changing to bubble flow only at the highest idle fuel flow rates.

The total pressure loss due to two-phase flow in the emulsion section of the fuel channel was determined experimentally, and is plotted in Figure 66 as a function of the boost venturi suction. There are three important facts inherent in this data on the two-phase total pressure loss:

1. This pressure loss increased linearly with boost venturi suction
2. This pressure loss was not significantly affected by fuel type or temperature
3. This pressure loss was related to the volume of air bled in, but for typical air bleed orifice sizes the two-phase pressure loss was about 4.5 times that for fuel flow alone

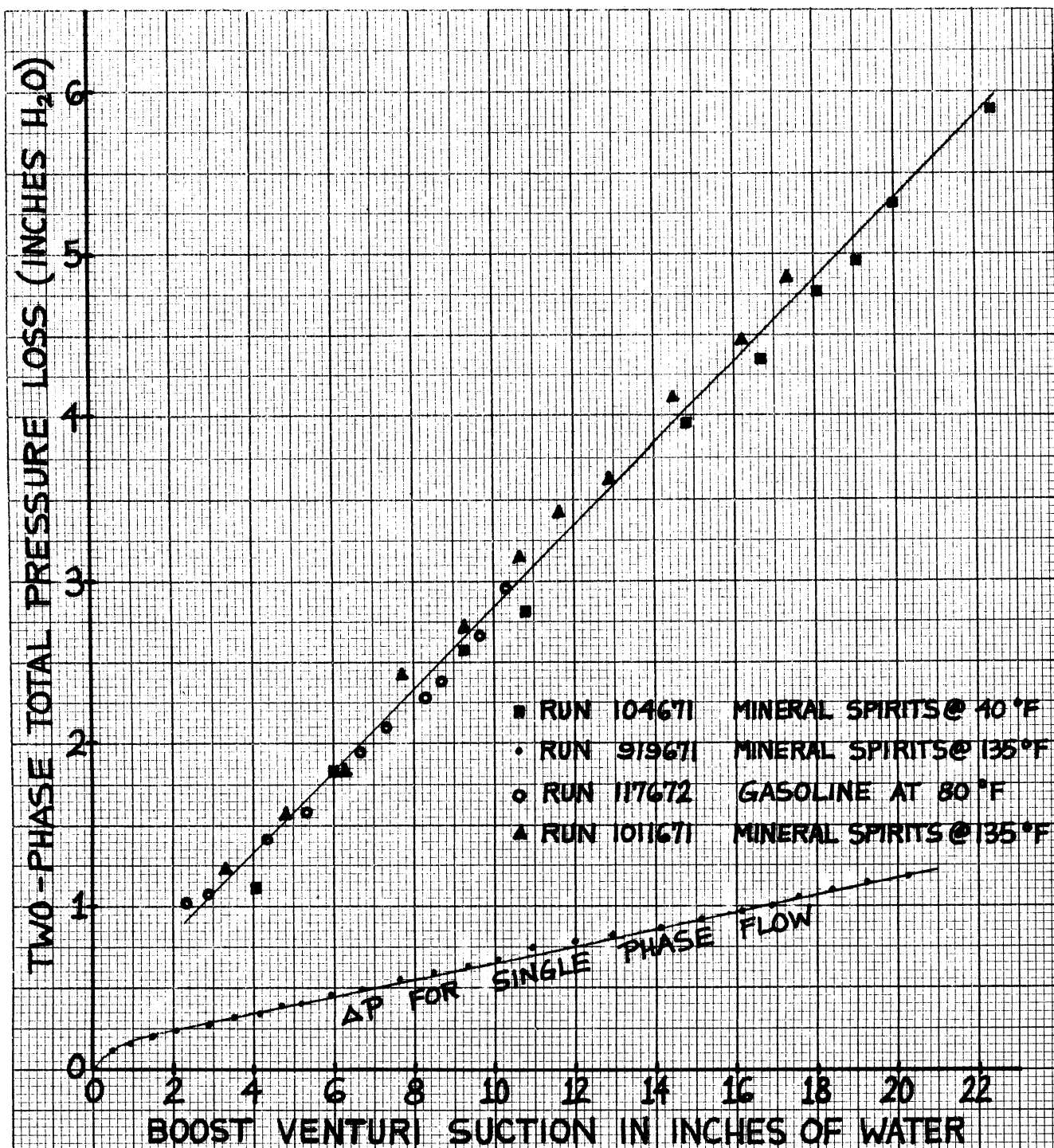


Figure 66. Total pressure loss variations for two-phase flow within the carburetor

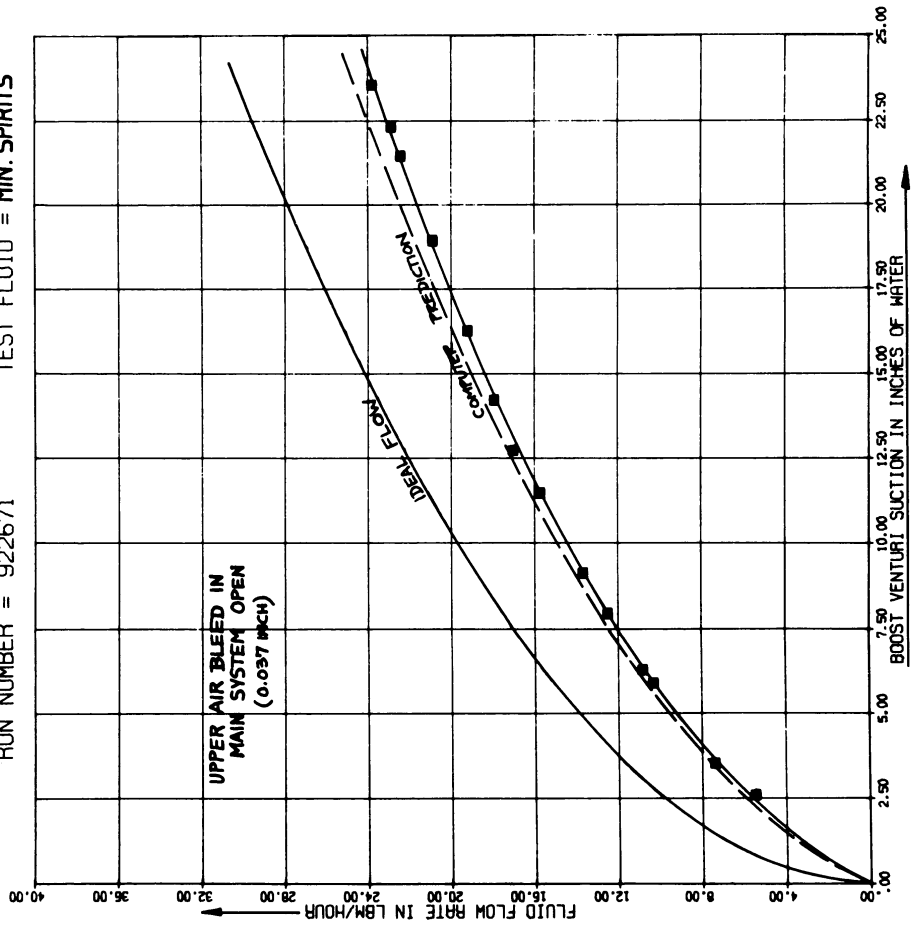
## H. COMPARISON WITH PREDICTIONS OF SUBROUTINE FLOW

As mentioned in Section 7A, one of the reasons for conducting the fuel channel flow tests was to obtain fundamental flow data with which to check the operation of subroutine FLOW, which is the fuel channel analysis subroutine. A small main program was written to check the predictions of subroutine FLOW by supplying the geometric values, fuel properties, and other conditions corresponding to an actual fuel channel flow test. These values were operated on by the subroutine for each specified operating condition of the actual test, and corresponding lists of flow rates and pressure differentials were predicted (similar to the values in Table 6.) These values were plotted by the computer and could readily be compared to the experimental data. The plots in Figure 67 illustrate the comparison between the measured and predicted fuel and air bleed mass flow rates for a typical test. The first plot in this figure is for the main fuel mass flow rate as a function of the metering signal. Note that the predicted values were about 3 or 4% higher than the experimental values, and that the predicted curve follows the same trend as the actual data.

The main air bleed mass flow rate values are shown in the second part of Figure 67. The experimental and predicted values in this case were for tests with 40° F Shell mineral spirits as the channel fluid. It may be seen that the air bleed flow rate predictions were about 10% high for both 1 and 2 air bleeds open. On the basis of numerous comparisons such as those in Figure 67, the following general conclusions may be stated concerning the accuracy of the fuel channel flow predictions:

FLUID FLOW RATE VS PRESSURE DROP

MAIN ORIFICE NUMBER= **F-50** AVERAGE TEMP = 135.0 °F  
 RUN NUMBER = 922671 TEST FLUID = **MIN. SPIRITS**



AIR BLEED FLOW VS VENTURI SUCTION

AIR BLEED DIAMETERS= **.037** AVERAGE TEMP = 40.0 °F  
 RUN NUMBER = 102671 TEST FLUID = **MINERAL SPIRITS**

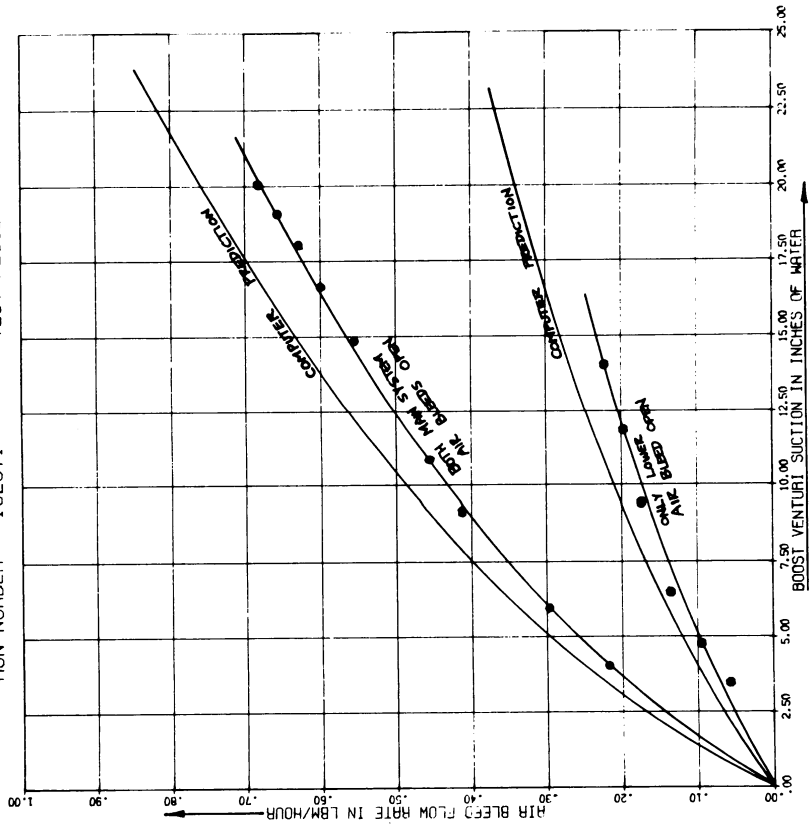


Figure 67. Comparison of The Flow Rate Predictions of Subroutine FLOW With Actual Fuel Channel Data



1. The fuel mass flow rate predictions were nearly always within 4% of the actual values with no air bleeds, and within 8% with air bleed flow.
2. In numerous cases where no air bleed flow existed, the fuel mass flow rates were predicted within 2% of the actual values.
3. The air bleed mass flow rate predictions were nearly always within 12% of the actual values, and in the majority of cases were within 8%.

The greater accuracy of the predictions for single-phase flow situations is to be expected, due to the increased complexities encountered in describing the effects of two-phase flow within the channel.

## CHAPTER VIII

### OPERATION OF THE COMPLETE SIMULATION

#### A. GENERAL DESCRIPTION

All of the foregoing analyses, in the form of their respective sub-routines, were combined into one general carburetor simulation program. This was achieved by developing a main calling program that utilized each of the subroutines in a logical order of solution which was directly related to the actual metering process within the carburetor.

The basic iterative scheme of the simulation is to determine the carburetor parameters corresponding to one fixed operating point, which is determined by a particular throttle angle and engine speed. However, the simulation program is able to evaluate carburetor performance over a wide range of operating conditions. In other words, if the simulation program can evaluate the performance of a carburetor for any one specified operating point, it is possible to perform the simulation repeatedly for various operating points, which correspond to certain physical situations. This is in fact what was incorporated into the simulation.

Based on the ideas discussed above, the simulation was written to provide for seven types of carburetor analyses, each invoking the basic iterative scheme for one specified operating point many times. These analysis types actually represent various sequences of operating points which correspond to specific physical situations that are encountered in carburetor and engine work. The seven sequences of

operating points for which the carburetor can be analyzed are:

1. analysis at a specified operating point which is read as data (RPM and  $\Theta$ )
2. analysis at constant engine speed and variable throttle angle
3. analysis at constant throttle angle and variable engine speed
4. analysis for the complete carburetor-engine operating map
5. analysis at road load operating conditions
6. analysis for the carburetor-engine-vehicle operating map
7. analysis with production variations in dimensions

Each of the above analysis types utilizes the basic iterative scheme. This can be illustrated by briefly considering the second analysis technique above, the constant engine speed, variable throttle angle analysis. This consists of a series of repeated simulations, one for each operating point, with the operating point incremented each time. The engine speed remains constant at some specified value (which is read in as data), but the throttle angle is automatically incremented from completely closed to fully opened, in  $2^\circ$  increments. In this case simulations will be performed for about 35 separate operating points, all corresponding to operation at the specified engine speed.

Since all of the analysis techniques utilize repeated applications of the single operating point simulation, the basic iterative scheme of the main program will be discussed. (A complete listing of the main program is given in Appendix I.) However, the analysis cannot begin until the operating conditions have been completely specified by means of the input data. Thus, let us first consider the required input data before discussing the basic iterative scheme in detail.

## B. REQUIRED INPUT DATA

On the basis of the number of analyses presented in the preceding chapters, and the number of parameters to be evaluated, it should be evident that a substantial amount of input data is required for the simulation. The input parameters required by the complete simulation may be divided into the following categories:

1. orifice characteristic curve data
2. vehicle data
3. engine correlation data
4. carburetor geometric data
5. carburetor functional data
6. fuel data
7. ambient conditions data
8. data indicating the type of analysis desired, the printout level, and the particular computer plots to be drawn

The actual data are read in the above order according to the formats listed in the main program. Table 15 shows a typical data set for a complete simulation run. These values should be compared to the formats given on the first and second pages of the main program.

The first group of input data represents the characteristic curves for square-edged orifices with a wide range of  $L/D$  ratios, as well as for the actual main metering orifice being used. This data was listed previously at the conclusion of Chapter 3. Also included in this data group are the throttle plate discharge coefficient values.

The second input data group consists of the parameters for the vehicle being used. Such items as the differential gear ratio, tire revolutions per mile, vehicle weight, and frontal area are included in this group.

TABLE XV  
REQUIRED INPUT DATA

26.0	26.0	1.0	CONSTANT THROTTLE ANGLE ANALYSIS DATA			
1600.0	1600.0	1.0	CONSTANT RPM ANALYSIS DATA			
0.0	0.0	0.0	0.0	1.0	4.0	PRINTOUT CONTROL CARD
F/A VS. DRY AIR FLOW			6.0	1.0		PLOT CARD
COMPLETE OPERATING MAP			6.0	1.0	4.0	ANALYSIS CARD
0.0	1.0	1	AMBIENT CONDITIONS CARD			
29.00	80.0	0.500	1.0	80.0	0.400	FUEL CARD
STANDARD REG. GASOLINE			0.001	0.001	0.000	
0.0730	0.0730	0.0000	0.001	0.001	6.00	1.00
0.140	0.093	0.010	2.0	2.0	10.00	1.4370
FORD 2 BBL. C6AF-9510-B F-50			2.0	2.0	10.00	0.375
TO DETERMINE CARBURETOR PERFORMANCE OVER A WIDE OPERATING RANGE			0.0010	0.0010	0.0100	0.0100
1.250	1.000	0.780	0.0010	0.0010	0.0010	0.0100
0.0010	0.0010	0.0010	0.0010	0.0010	0.0010	0.0100
1.030	0.875	0.538	0.596	0.650	0.750	TOLERANCES
0.0010	0.0010	0.0010	0.0010	0.0010		BOOST VENTURI DIAMETERS
1.930	1.930	1.145	1.160	1.400		TOLERANCES
0.0000	0.0000	0.0000	0.0000			MAIN VENTURI DIAMETERS
0.0000	90.000	75.000	0.0000	15.000	90.000	0.0000
64.000	64.000	0.0000	0.0000	75.000	0.0000	0.0000
0.0000	0.0000	0.0000	0.0000	90.000	0.0000	26.000
2.0000	2.0000	2.0000	2.0000			ELEMENT ANGLES
2.0000	0.0000	0.0000	2.0000	0.0000	3.0000	2.0000
0.0000	0.0000	0.0000	0.0000	0.0000	2.0000	0.0000
1.0000	0.0000	3.0000	0.0000	2.0000	0.0000	2.0000
0.0312	0.1400	0.1250	0.1060			ELEMENT TYPES
0.0938	0.7060	0.7800	0.1060	2.0000	0.1060	0.1250
0.9375	0.2500	1.0000	0.3400	0.8120	0.1350	1.9300
0.1830	0.3120	0.1060	0.1250	0.3900	0.2060	0.1250
0.0010	0.0010	0.0010	0.0010			CHANNEL LENGTHS
0.0005	0.0020	0.0030	0.0010	0.0030	0.0010	0.0010
0.0020	0.0030	0.0020	0.0050	0.0020	0.0010	0.0035
0.0005	0.0020	0.0020	0.0020	0.0020	0.0020	0.0010
0.0446	0.0270	0.0390	0.0350			TOLERANCES
0.0260	0.1400	0.0940	0.0420	0.0940	0.0590	0.0310
0.1470	0.2910	0.1580	0.2700	0.1600	0.2250	0.0610
0.0502	0.1870	0.0810	0.3125	0.1560	0.1350	0.0280
0.330	0.936	0.941	0.943	0.945	0.946	0.946
0.600	0.734	0.840	0.870	0.890	0.906	0.920
14.0	0.0	7.5	5	6	25	FIRST CARBURETOR GEOMETRY CARD
10.00	2.500	00.00	00.00	00.00	00.00	00.00
71.10	68.70	65.50	60.50	51.40	38.00	22.80
71.50	72.70	73.20	73.50	73.30	72.90	72.10
5.000	12.00	34.50	49.60	59.80	66.10	69.50
00.00	00.00	00.00	00.00	00.00	00.00	00.00
4.000	1.000	00.00	00.00	00.00	00.00	00.00
29.00	27.60	26.20	23.80	20.80	16.40	10.05
31.00	31.20	31.20	31.10	31.00	30.60	29.90
2.000	3.000	14.00	21.60	26.10	29.00	30.50
00.00	00.00	00.00	00.00	00.00	00.00	00.00
21.60	23.20	24.72	26.05	27.13	28.85	30.20
13.40	14.09	15.30	16.18	17.10	18.40	19.86
19.30	21.95	24.00	25.53	27.00	28.35	29.65
13.40	10.95	10.16	10.82	11.48	13.45	16.32
200.0	432.0	35.0	0.0000	0.0050	14.0	000.0
9.30	1.00	1.670	0.375	0.001	0.001	0.050
1966 FORD 289 V-8	289 V-8	1.000	1.000	2.870	8.0	400.0
3.000	1.000	1.000	1.000			ENGINE CARD
1966 FORD FAIRLANE 500	FAIRLANE 500	3435.0	30.70	775.0	0.0150	0.00121
0.738	0.739	0.740	0.741	0.742	0.743	0.743
0.720	0.726	0.724	0.732	0.734	0.736	0.737
10.58	0.000	0.525	0.620	0.660	0.685	0.703
0.751	0.753	0.755	0.757	0.759	0.760	0.761
0.730	0.734	0.739	0.743	0.746	0.747	0.749
7.230	0.000	0.570	0.647	0.688	0.711	0.724
0.772	0.773	0.774	0.775	0.776	0.777	0.778
0.756	0.761	0.764	0.766	0.768	0.770	0.771
4.726	0.000	0.623	0.680	0.710	0.727	0.741
0.782	0.783	0.790	0.791	0.792	0.793	0.793
0.776	0.779	0.781	0.783	0.785	0.786	0.787
3.629	0.000	0.674	0.715	0.739	0.759	0.768
0.805	0.806	0.807	0.808	0.809	0.810	0.810
0.790	0.793	0.796	0.798	0.800	0.802	0.804
1.426	0.000	0.737	0.766	0.770	0.774	0.788
0.713	0.705	0.700	0.690	0.682	0.680	0.680
0.677	0.675	0.670	0.673	0.698	0.686	0.676
0.616	0.000	0.690	0.720	0.677	0.668	0.700
0.625	0.624	0.623	0.622	0.621	0.620	0.620
0.638	0.635	0.633	0.631	0.629	0.627	0.626
0.100	0.000	0.663	0.665	0.654	0.648	0.644
0.699	0.702	0.709	0.716	0.722	0.728	0.734
0.614	0.629	0.643	0.656	0.665	0.675	0.684
F 50 L	0.000	0.361	0.467	0.513	0.550	0.577
0.865	0.869	0.873	0.876	0.879	0.881	0.883
0.804	0.820	0.832	0.840	0.843	0.854	0.860
F-50	0.000	0.577	0.656	0.702	0.734	0.761
21.0	21.0	21.0	300.0	100.0	500.0	ORIFICE DATA CONTROL CARD
XNCDJ	XNCDJL	XNCDSE	DELXJ	DELXJL	DELXSE	

The engine correlation data that is read in consists of two indicated horsepower curves and two friction mean effective pressure curves, as discussed in Chapter 5. These curves are read in as discrete points, as a function of the fuel-air ratio and engine speed respectively. Additional engine specifications that are required include bore, stroke, compression ratio, number of cylinders, and valve dimensions.

The required carburetor geometric data is extensive, since this is the means by which a given carburetor design is specified for the simulation. This data includes :

1. the number of carburetor barrels, main metering orifices, and enrichment systems
2. the number of stations to be used in the main venturi and in the boost venturi
3. the number of elements in the complete fuel channel
4. the length, diameter, angle, and production tolerance of each fuel channel element
5. the diameter and production tolerance at each main and boost venturi station, as well as the throttle bore and shaft
6. the spill point, closed throttle angle, enrichment valve opening vacuum, idle needle included angle, and number of turns
7. all throttle bypass and choke restriction diameters and tolerances

The fuel and ambient conditions data consists of the fuel type code (corresponding to those in subroutine FPROP), fuel temperature, ambient pressure, ambient temperature, and relative humidity.

The required simulation control data consists of switches which select the type of analysis to be performed, the order of interpolation to be utilized in the general interpolation subroutine, STERL, the print-out levels of the main program and subroutines, and the number and type

of CALCOMP plots to be drawn.

The arrangement of the above data is such that the less frequently changed parameters are read in first, and the control data, which is changed quite often, are read in last. Thus, in many cases it is not necessary to reread all of the input data for consecutive simulation runs, but only the last one or two data groups.

### C. BASIC ITERATIVE SCHEME

After the required data has been supplied to the main program, the determination of the values for the multitude of carburetor variables corresponding to a given operating point can begin. The basic iterative scheme for a carburetor simulation at one specified operating point may be best explained by referring to Figure 68, which is a diagram that illustrates the logical order in which the main program calls each of the subroutines, and the results of each call. It is by no means a flow chart for the main program or any of the individual subroutines. The diagram merely indicates the general procedure used in analyzing carburetor system performance and in evaluating the interactions of these systems.

Note that the analysis begins with a specified operating point. This operating point may correspond to one in a series based on any of the seven analysis types listed in section 8A. Regardless of how the operating point is obtained, the basic analysis formally begins by calling subroutine THROTL for the specified throttle angle, throttle bore

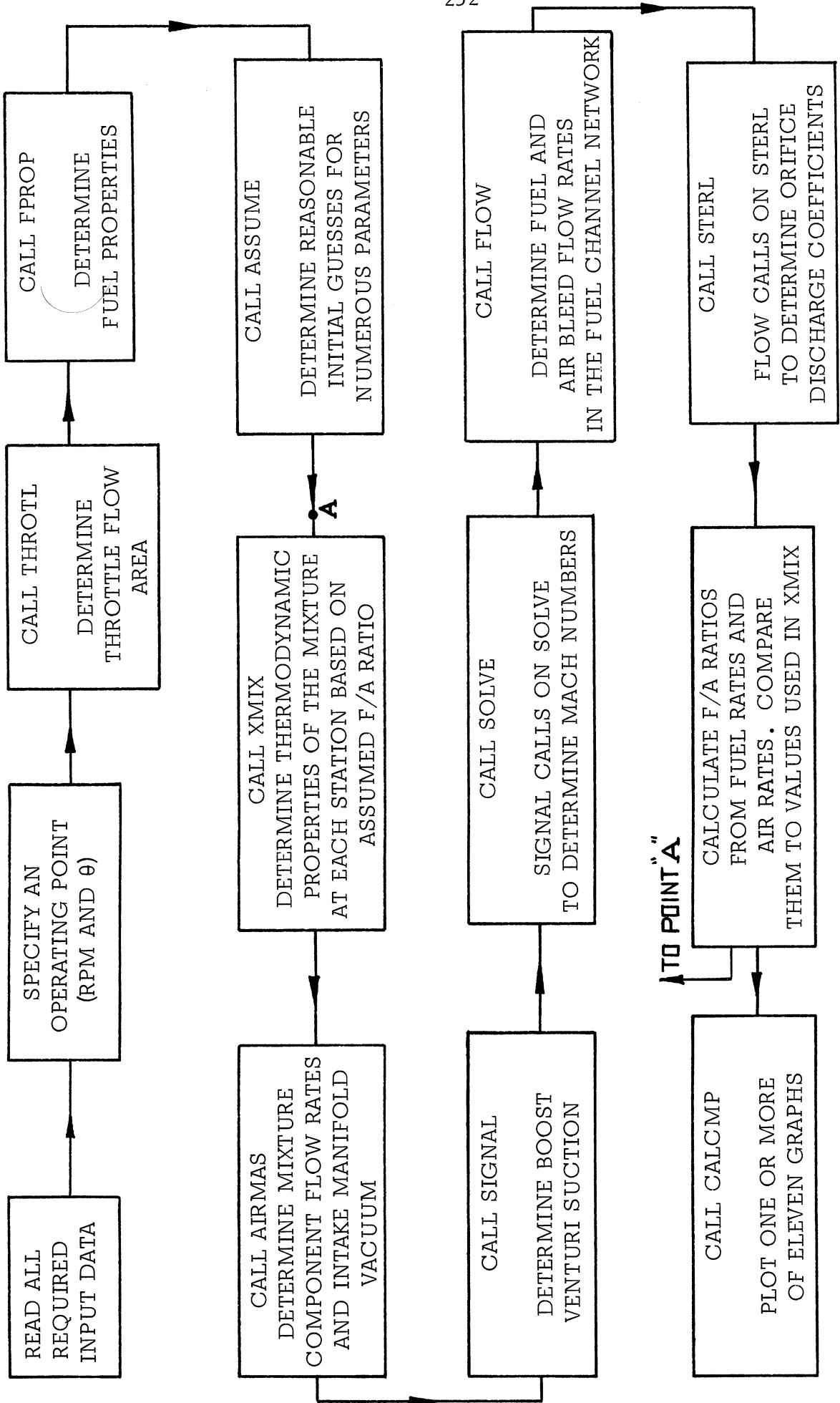


Figure 68. General Procedure Utilized in the Basic Iterative Scheme



diameter, and throttle shaft diameter. This subroutine evaluates the corresponding throttle flow area and returns it to the main program.

Subroutine FPROP is then called for the specified fuel type and temperature. This subroutine calculates and returns to the main program all needed fuel properties, including density, viscosity, surface tension, vapor specific heats, molecular weight, and latent heat of vaporization.

The next step in the procedure is to call subroutine ASSUME. This particular subroutine assigns reasonable initial guesses to numerous variables, including the main and total fuel-air ratios, and the fuel flow rates in each fuel channel branch. These initial guesses are based on a typical carburetor flow curve, and are used chiefly to reduce the number of iterations required within the simulation.

The values of humidity, fuel properties, and the assumed fuel-air ratio are now utilized by calling subroutine XMIX. This subroutine evaluates all needed thermodynamic properties of the mixture at each station within the main and boost venturii. Included in this list of properties are the mixture molecular weight, specific heats, and specific heat ratio.

Once the thermodynamic properties of the mixture are known at all strategic locations within the carburetor, a comprehensive compressible flow analysis (chapter 2) involving the interactions between the throttle plate pressure ratio and the engine air flow can be applied. This is accomplished by calling subroutine AIRMAS. Numerous parameters are calculated iteratively by this subroutine, the most important

of which are the mass flow rates of the mixture components, the intake manifold vacuum, and the throttle plate Mach number.

The next operation in the analysis is to utilize the mixture flow rates supplied by AIRMAS, along with the specified venturii geometry, to obtain the boost venturi suction. Subroutine SIGNAL is called, and a general compressible flow analysis is applied to the venturii system. Subroutine SOLVE is called by SIGNAL numerous times to evaluate Mach numbers at various stations. When the multiple iterative parameters within signal have converged, the boost venturi suction is known, as are the pressures, temperatures, Mach numbers, and suctions at all other stations.

At this point the intake manifold vacuum and boost venturi suction are known. Thus, the driving potentials for flow within the fuel channel network are known. Subroutine FLOW, the fuel channel analysis portion of the simulation, is then called. A comprehensive network flow analysis is performed iteratively, using the initial guesses for the system flow rates as a starting point. When convergence has been obtained, a large amount of information is known for each element in the fuel channel, including mass flow rate, total pressure loss, Reynolds number, velocity, and velocity head. In addition, the system flow rates are known, including the main, idle, and total (main + idle) flow rates. Many calls are made to STERL, the general purpose interpolation subroutine, during this network flow analysis. This is done to obtain discharge coefficient values for each orifice and iterative Reynolds number. The interpolation

is performed upon the characteristic curve data which was initially read in.

Since the air flow rate and the main, idle, and total fuel flow rates have now been obtained, the next logical step is to calculate the main, idle, and total fuel-air ratios, and to compare them to the values that were initially assumed. A convenient error parameter is defined as the current fuel-air ratio minus the previous iterative fuel-air ratio. If any of the error parameters are greater than 0.0001, then new thermodynamic properties are calculated for the mixture and another iteration is performed. If all of the fuel-air ratio error parameters are very small, the iterations are terminated for that particular operating point, and the appropriate values are stored for later computer plotting.

#### D. CARBURETOR ANALYSIS AT CONSTANT ENGINE SPEED OR CONSTANT THROTTLE ANGLE

##### 1. Simulation Predictions

The theoretical analysis of carburetor performance for constant engine speed-variable throttle angle conditions, or for constant throttle angle-variable engine speed conditions, is a useful extension of the basic iteration technique. In the first case, the throttle angle is automatically incremented from completely closed to fully opened, and in the second case the engine speed is incremented over the range from zero to 5000 RPM.

The simulation predictions for a typical constant engine speed analysis are listed in Table 16. Note that of the hundreds of carburetor

TABLE XVI  
SIMULATION PREDICTIONS FOR A CONSTANT ENGINE SPEED -  
VARIABLE THROTTLE ANGLE ANALYSIS

UNIVERSITY OF MICHIGAN  
MECHANICAL ENGINEERING DOCTORAL THESIS  
DIGITAL SIMULATION OF CARBURETOR METERING  
CARBURETOR-ENGINE-VEHICLE OPERATING MAP  
DAVID L. HARRINGTON

THE TYPE OF ANALYSIS REQUESTED IS.....COMPLETE OPERATING MAP  
THE TYPE OF PLOT(S) REQUESTED ARE.....F/A VS. DRY AIR FLOW  
THIS SIMULATION PERFORMED ON.....12 MAR 1968  
PURPOSE OF THIS SIMULATION RUN.....TO DETERMINE CARBURETOR PERFORMANCE OVER A WIDE OPERATING RANGE

AMBIENT CONDITIONS			CARBURETOR			FUEL			ENGINE			VEHICLE		
ENGINE RPM	THROTTLE ANGLE	THROT FLOW AREA	INTAKE MAN. PRESS	MOIST AIR FLOW	DRY AIR FLOW	BOOST VENTURI SUCTION	MAIN VENTURI SUCTION	THROT MACH NO.	MAIN F/A RATIO	TOTAL F/A RATIO	TOTAL FUEL FLOW	MAIN FUEL FLOW	THROT TOTAL TEMP	AIR BLEED FLOW
1600.0	10.0	.0179	4.98	41.21	40.76	.06	.03	1.0000	.0000	.1560	6.359	.000	80.0	.000
1600.0	12.0	.0286	5.34	60.81	60.14	.14	.07	1.0000	.0000	.1050	6.314	.000	80.0	.000
1600.0	14.0	.0413	6.83	85.64	84.70	.28	.15	1.0000	.0000	.0728	6.162	.000	80.0	.000
1600.0	16.0	.0559	8.77	115.74	114.47	.53	.28	1.0000	.0000	.0519	5.944	.000	80.0	.000
1600.0	18.0	.0724	10.86	149.61	147.97	.89	.47	1.0000	.0120	.0500	7.405	1.782	77.2	.176
1600.0	20.0	.0907	13.13	186.95	184.90	1.41	.74	1.0000	.0263	.0536	9.916	4.872	73.9	.240
1600.0	22.0	.1109	15.61	227.86	225.37	2.12	1.11	.9829	.0367	.0565	12.736	8.275	71.4	.300
1600.0	24.0	.1329	17.91	265.86	262.94	2.91	1.52	.8575	.0446	.0587	15.459	11.734	69.6	.352
1600.0	26.0	.1567	19.93	299.18	295.90	3.70	1.94	.7495	.0502	.0603	17.853	14.850	68.3	.400
1600.0	28.0	.1822	21.60	326.80	323.22	4.44	2.33	.6586	.0545	.0617	19.930	17.603	67.3	.450
1600.0	30.0	.2094	22.96	349.36	345.53	5.10	2.67	.5817	.0579	.0629	21.777	20.010	66.5	.486
1600.0	35.0	.2848	25.26	388.70	384.44	6.37	3.33	.4389	.0598	.0659	26.844	26.844	63.7	.453
1600.0	40.0	.3700	26.59	410.80	406.30	7.15	3.73	.3393	.0705	.0705	28.662	28.662	63.5	.481
1600.0	45.0	.4641	27.35	423.43	418.79	7.62	3.98	.2700	.0710	.0710	29.724	29.724	63.4	.497
1600.0	50.0	.5662	27.80	430.92	426.19	7.91	4.13	.2205	.0712	.0712	30.348	30.348	63.4	.506
1600.0	55.0	.6749	28.07	435.57	430.75	8.09	4.22	.1842	.0714	.0714	30.761	30.761	63.3	.512
1600.0	60.0	.7884	28.25	438.45	433.65	8.21	4.28	.1572	.0715	.0715	31.018	31.018	63.3	.516
1600.0	70.0	1.0135	28.44	441.61	436.77	8.34	4.35	.1217	.0717	.0717	31.297	31.297	63.3	.520
1600.0	80.0	1.0896	28.48	442.24	437.39	8.37	4.36	.1129	.0716	.0716	31.297	31.297	63.3	.520

CARBURETOR-ENGINE OPERATION AT CONSTANT ENGINE SPEED-VARIABLE THROTTLE OPENING

1966 FORD FAIRLANE  
VEHICLE WEIGHT=3435.0  
REAR AXLE RATIO= 3.00  
TIRE REVS/MILE =775.0

1966 FORD 289 V-8  
DISPLACEMENT=289.2 C.I.  
COMP. RATIO = 9.3  
VALVE FLOW AREA=6.87 IN2

STANDARD REG. GASOLINE  
TEMPERATURE = 80.0 F  
SPECIFIC GRAVITY = .721  
VISCOSITY = .556 CS

and engine variables that were calculated, only the most important parameters were listed. (All of the others may be obtained if desired.) The results of this particular simulation run indicate that the mixture flow at the throttle plate is choked (Mach number of unity) up to a throttle angle of  $20^{\circ}$ . The air flow rate increases significantly in this range however, because the throttle flow area is increasing. Also note that the main system fuel begins to flow at a throttle angle of  $18^{\circ}$ , which corresponds to an air flow of about 75 pounds per hour in each carburetor barrel. The total temperature of the mixture at the throttle plate is equal to the ambient temperature until main system fuel begins to flow (the idle fuel flow does not affect the thermodynamic properties of the mixture at the throttle restriction, since it is discharged slightly downstream). Once the main fuel system begins to function, and fuel enters the air stream at the boost venturi, the total temperature of the stream is reduced due to fuel vaporization.

It may also be observed from the predictions that the enrichment valve opened at a throttle angle of about  $35^{\circ}$ , at which point the total fuel-air ratio increased abruptly. It is also obvious that this particular carburetor geometry (which had significantly different idle system dimensions than the production carburetor, in order to check the operation of the simulation) would result in a very lean, off-idle fuel-air ratio at this engine speed.

The results of two constant throttle angle analyses are shown in Tables 17 and 18. The dimensions read in to the program in this case

TABLE XVII  
SIMULATION PREDICTIONS FOR A CONSTANT THROTTLE ANGLE  
ANALYSIS (CLOSED THROTTLE)

AMBIENT CONDITIONS			CARBURETOR			FUEL			ENGINE			VEHICLE		
PRESSURE = 29.28 INCHES HG	FORD 2 BARREL C6AFB	STANDARD REG. GASOLINE	1964 FORD 289 V-8	DISPLACEMENT=288.5 C.I.	1964 FORD FAIRLANE	VEHICLE WEIGHT=3650.0								
TEMPERATURE = 92.0 DEGREES F	MAIN JET = F-50	TEMPERATURE = 80.0 F	MAIN VENTURI=1.145 IN.	COMP. RATIO = 8.5	REAR AXLE RATIO= 3.25									
HUMIDITY = 40.0 PERCENT	CLOSED THROTTLE=10.0	SPECIFIC GRAVITY = .721	VISCOSITY = .556 CS	VALVE FLOW AREA=6.82 IN2	TIRE REVS/MILE = 775.0									
DENSITY = .0704 LBM/FT3														

CARBURETOR-ENGINE OPERATION AT CONSTANT THROTTLE OPENING-VARIABLE ENGINE SPEED														
ENGINE RPM	THROT ANGLE	THROT FLOW AREA	INTAKE MAN. PRESS	MOIST AIR FLOW	DRY AIR FLOW	TOTAL MIXT. FLOW	THROT PLATE FLOW	THROT MACH NO.	MAIN F/A RATIO	TOTAL F/A RATIO	MIXT. CP/CV RATIO	THROT TOTAL PRESS	THROT TOTAL TEMP	THROT PLATE COEFF N
500.0	10.0	.0179	11.73	42.67	42.13	47.68	29.35	1.0000	.0000	.1188	1.406	29.277	92.0	.700
600.0	10.0	.0179	10.35	42.76	42.21	47.89	29.35	1.0000	.0000	.1216	1.406	29.277	92.0	.700
700.0	10.0	.0179	9.33	42.74	42.20	47.97	29.35	1.0000	.0000	.1239	1.406	29.277	92.0	.700
800.0	10.0	.0179	8.56	42.73	42.18	48.03	29.35	1.0000	.0000	.1257	1.406	29.277	92.0	.700
900.0	10.0	.0179	7.95	42.72	42.17	48.09	29.35	1.0000	.0000	.1273	1.406	29.277	92.0	.700
1000.0	10.0	.0179	7.47	42.71	42.17	48.13	29.35	1.0000	.0000	.1286	1.406	29.277	92.0	.700
1200.0	10.0	.0179	6.77	42.69	42.14	48.19	29.35	1.0000	.0000	.1305	1.406	29.277	92.0	.700
1400.0	10.0	.0179	6.32	42.72	42.17	48.28	29.35	1.0000	.0000	.1319	1.406	29.277	92.0	.700
1600.0	10.0	.0179	5.97	42.71	42.16	48.31	29.35	1.0000	.0000	.1330	1.406	29.277	92.0	.700
1800.0	10.0	.0179	5.70	42.70	42.15	48.34	29.35	1.0000	.0000	.1338	1.406	29.277	92.0	.700
2000.0	10.0	.0179	5.48	42.69	42.15	48.36	29.35	1.0000	.0000	.1345	1.406	29.277	92.0	.700
2200.0	10.0	.0179	5.30	42.69	42.14	48.38	29.35	1.0000	.0000	.1351	1.406	29.277	92.0	.700
2400.0	10.0	.0179	5.15	42.68	42.14	48.40	29.35	1.0000	.0000	.1356	1.406	29.277	92.0	.700
2600.0	10.0	.0179	5.03	42.68	42.14	48.41	29.35	1.0000	.0000	.1361	1.406	29.277	92.0	.700
2800.0	10.0	.0179	4.92	42.67	42.13	48.42	29.35	1.0000	.0000	.1364	1.406	29.277	92.0	.700
3000.0	10.0	.0179	4.82	42.67	42.13	48.44	29.35	1.0000	.0000	.1368	1.406	29.277	92.0	.700
3200.0	10.0	.0179	4.74	42.67	42.13	48.44	29.35	1.0000	.0000	.1371	1.406	29.277	92.0	.700
3400.0	10.0	.0179	4.66	42.58	42.04	48.36	29.35	1.0000	.0000	.1374	1.406	29.277	92.0	.700
3600.0	10.0	.0179	4.59	42.61	42.07	48.40	29.35	1.0000	.0000	.1378	1.406	29.277	92.0	.700
3800.0	10.0	.0179	4.54	42.63	42.09	48.43	29.35	1.0000	.0000	.1378	1.406	29.277	92.0	.700
4000.0	10.0	.0179	4.49	42.76	42.21	48.58	29.35	1.0000	.0000	.1380	1.406	29.277	92.0	.700
4200.0	10.0	.0179	4.44	42.70	42.16	48.53	29.35	1.0000	.0000	.1382	1.406	29.277	92.0	.700
4400.0	10.0	.0179	4.39	42.68	42.14	48.51	29.35	1.0000	.0000	.1383	1.406	29.277	92.0	.700

TABLE XVIII  
SIMULATION PREDICTIONS FOR A CONSTANT THROTTLE  
ANGLE ANALYSIS (26°)

CARBURETOR-ENGINE OPERATION AT CONSTANT THROTTLE OPENING-VARIABLE ENGINE SPEED															
ENGINE RPM	THROT ANGLE	THROT FL/W AREA	INTAKE MAN. PRESS	MOIST AIR FLOW	DRY AIR FLOW	TOTAL MIXT. FLOW	THROT PLATE FLOW	THROT MACH NO.	MAIN F/A RATIO	TOTAL F/A RATIO	MIXT. CP/CV RATIO	THROT TOTAL PRESS	THROT TOTAL TEMP	THROT PLATE C/VEFF	N
500.0	26.0	.1568	28.07	136.74	134.99	141.58	135.24	.2438	.0299	.0359	1.397	29.256	85.0	.900	3
600.0	26.0	.1568	27.62	156.22	154.23	165.70	158.80	.2882	.0584	.0614	1.389	29.247	78.4	.900	9
700.0	26.0	.1568	27.09	176.24	174.00	188.75	181.37	.3336	.0716	.0719	1.385	29.237	75.3	.900	17
800.0	26.0	.1568	26.51	196.02	193.52	209.73	201.51	.3777	.0709	.0709	1.385	29.227	75.5	.900	14
900.0	26.0	.1568	25.89	214.30	211.56	228.89	220.01	.4210	.0690	.0690	1.386	29.217	75.9	.900	8
1000.0	26.0	.1568	25.26	230.75	227.81	246.02	236.41	.4625	.0670	.0670	1.386	29.207	76.4	.900	8
1200.0	26.0	.1568	23.94	258.94	255.64	275.05	264.31	.5420	.0630	.0630	1.387	29.189	77.3	.900	7
1400.0	26.0	.1568	22.61	280.90	277.32	297.82	286.21	.6169	.0610	.0610	1.388	29.174	77.8	.900	8
1600.0	26.0	.1568	21.34	296.97	293.19	314.86	302.62	.6854	.0610	.0610	1.388	29.161	77.8	.900	8
1800.0	26.0	.1568	20.15	308.73	304.79	327.32	314.55	.7487	.0610	.0610	1.388	29.151	77.8	.900	7
2000.0	26.0	.1558	19.04	316.88	312.84	335.95	322.96	.8071	.0610	.0610	1.388	29.145	77.8	.900	5
2200.0	26.0	.1568	18.02	322.43	318.32	341.84	328.55	.8609	.0610	.0610	1.388	29.140	77.8	.900	5
2400.0	26.0	.1568	17.09	325.87	321.72	345.48	331.95	.9106	.0607	.0609	1.388	29.137	77.9	.900	5
2600.0	26.0	.1568	16.25	327.91	323.73	347.57	333.58	.9559	.0593	.0607	1.388	29.135	78.2	.900	4
2800.0	26.0	.1568	15.48	328.53	324.34	348.21	334.02	.9983	.0582	.0607	1.389	29.135	78.4	.900	4
3000.0	26.0	.1568	14.80	328.86	324.67	348.56	333.92	1.0000	.0572	.0607	1.389	29.134	78.7	.900	5
3200.0	26.0	.1558	14.20	329.03	324.84	348.78	333.84	1.0000	.0563	.0608	1.389	29.134	78.9	.900	5
3400.0	26.0	.1558	13.67	329.18	324.98	348.98	333.76	1.0000	.0556	.0609	1.389	29.134	79.1	.900	5
3600.0	26.0	.1558	13.19	329.20	325.01	349.06	333.70	1.0000	.0549	.0611	1.390	29.134	79.2	.900	4
3800.0	26.0	.1568	12.77	329.34	325.15	349.26	333.64	1.0000	.0544	.0613	1.390	29.134	79.3	.900	4
4000.0	26.0	.1568	12.38	329.47	325.27	349.46	333.59	1.0000	.0539	.0615	1.390	29.133	79.4	.900	4
4200.0	26.0	.1568	12.03	329.57	325.37	349.64	333.54	1.0000	.0534	.0617	1.390	29.133	79.6	.900	4
4400.0	26.0	.1568	11.71	329.67	325.47	349.81	333.50	1.0000	.0530	.0619	1.390	29.133	79.6	.900	4
4600.0	26.0	.1568	11.41	329.75	325.55	349.97	333.46	1.0000	.0526	.0621	1.390	29.133	79.7	.900	4
4800.0	26.0	.1568	11.14	329.83	325.63	350.11	333.43	1.0000	.0523	.0623	1.390	29.133	79.8	.900	4
5000.0	26.0	.1568	10.89	329.90	325.70	350.26	333.40	1.0000	.0520	.0625	1.391	29.133	79.9	.900	4

were the actual nominal dimensions of the carburetor. Table 17 shows the simulation predictions for the case of completely closed throttle ( $\Theta = 10^\circ$ ). Note that the throttle plate flow is choked at all engine speeds, and that the main fuel system is not operating. The fuel-air ratio is very rich, and becomes richer as the engine speed is increased. This results from the increase in the intake manifold vacuum with engine speed, even though the air mass flow rate is constant. This was discussed in the analysis presented in Chapter 2.

Table 18 shows the simulation predictions for a throttle angle of  $26^\circ$ . It is immediately obvious that the flow conditions are significantly different from the previous case. The air flow rates are 3 to 8 times those at  $10^\circ$ , and the throttle plate flow does not choke until an engine speed of 3000 RPM is reached.

## 2. Carburetor-Engine Operating Map

A complete carburetor-engine operating map can be generated by performing the constant engine speed analysis for many RPM values, and the constant throttle angle analysis for many  $\Theta$  values. If this is done, all possible operating points can be shown on a single graph. This type of analysis was made available within the carburetor simulation program. When it is specified, a series of constant RPM and constant  $\Theta$  analyses are performed, and the results plotted as shown in Figure 69. This is a very informative graph since it immediately gives the minimum possible air flow rate and intake manifold pressure.



# CARBURETOR-ENGINE OPERATING MAP

$P_0 = 29.28^H$  HG       $T_0 = 92.0^{\circ}$  F      HUMIDITY = 40.0 %  
 DISPLACEMENT = 288.5 IN.<sup>3</sup>      COMP. RATIO = 9.30

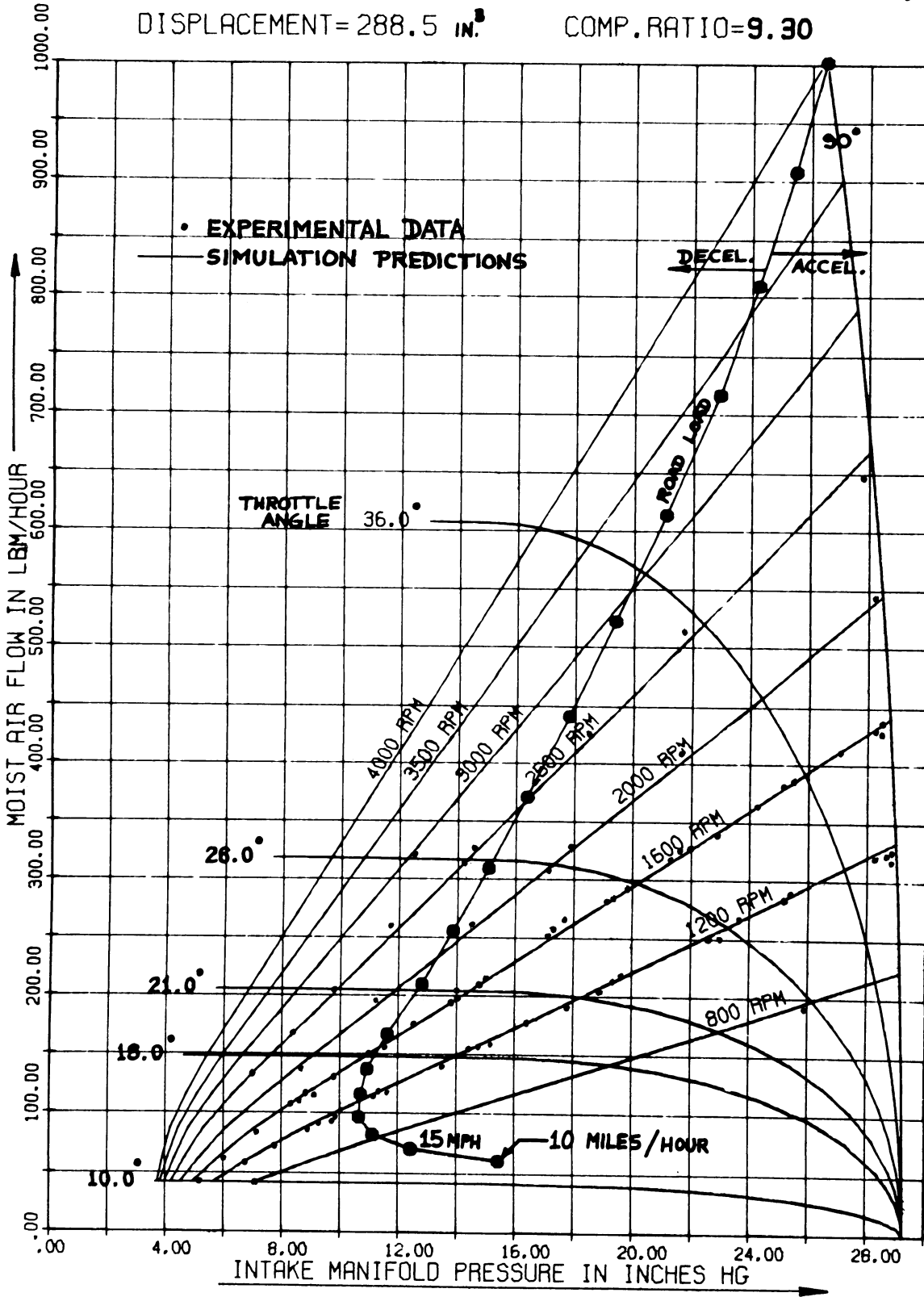


Figure 69. Carburetor - Engine - Vehicle Operating Map

Using this type of computer plot it is possible to quickly determine the air flow rate and intake manifold pressure for any throttle angle and engine speed. For example it may be quickly noted that if the throttle angle is  $21^{\circ}$ , and the engine speed is increased from 1600 to 3000 RPM, the measured air flow rate will remain constant at 205 pounds per hour.

Another interesting feature of this operating map is the relation of the operating points to the road load conditions. (The method of obtaining the road load operating line will be discussed in the next section.) Combinations of engine speed and throttle angle which lie upon the road load operating line correspond to road load operating points. Operating points to the right of the road load line would result in vehicle acceleration or steady operation on an uphill grade. Conversely, operation at points on the left of the road load line would result in vehicle deceleration or steady operation on a downhill grade. The further away from the road load line, the greater the acceleration or deceleration conditions. Thus, for this particular carburetor, engine, and vehicle, a throttle angle of  $21^{\circ}$  and an engine speed of 1900 RPM will yield steady vehicle speeds of 45 miles per hour. A throttle angle of  $21^{\circ}$  and an engine speed of 3500 RPM obviously corresponds to a heavy deceleration condition.

### 3. Accuracy of the Simulation Predictions

The agreement between the simulation predictions and the experimental data was very good, as may be seen in Figure 69. The small points represent actual experimental data from Tables 9 and 10, and the lines represent the simulation predictions. The predicted air mass flow

rates and intake manifold pressures were within 8% of the experimental values in nearly all cases, and generally were within 3 or 4%. In numerous runs the experimental points corresponded precisely with the simulation predictions. The fuel flow rate and fuel-air ratio predictions were also quite good, being within 7 or 8% of the actual experimental data in nearly all cases, with the majority of the predictions being within 5% of the experimental values. Thus, actual data trends over a wide operating range, such as from 1600 RPM, closed throttle, to 1600 RPM, wide open throttle, were predicted quite accurately.

The boost and primary venturii suction were similarly predicted quite accurately. The predicted values were within about 8% of the measured values, with the predictions usually being slightly lower than the actual data. This is to be expected since the actual boost venturi suction is not uniform at the given section, but decreases with distance from the inner wall. The experimental values were given in figure 36 on page 184, and the predicted values for a typical venturii geometry will be presented later in this chapter.

#### 4. Available Computer Plots

With the large amount of information predicted in a complete carburetor-engine operating map analysis, many other computer plots may be obtained. There are eleven distinct computer plots available within the simulation, each available in four different scales. These plots are listed on the third page of the main program in Appendix I. Various combinations of two or more of these plots may also be specified.

One type of plot that may be obtained for a series of constant RPM analyses is presented in Figure 70. This is the variation in overall (total) fuel-air ratio with air flow, at various engine speeds. This is a very useful plot, since it corresponds to the standard flow box test of a carburetor. However, it has the distinct advantage of directly involving the engine variables, whereas a flow box curve does not. This type of plot immediately indicates how a proposed carburetor design will perform over a wide speed and load range. Note that the abrupt increase in fuel-air ratio for each engine speed corresponds to the opening point of the enrichment valve. This plot also verifies a statement made in Chapter 2, that there are an infinite number of fuel-air ratios for a given air flow rate, depending on the engine speed and intake manifold vacuum.

A computer plot of the predicted main system fuel flow rate, as a function of the metering signal, is given in Figure 71. (The data correspond to the same set of conditions as Figure 70). This type of plot may be obtained whenever the main fuel flow is to be examined in detail. Note that the main fuel flow does not begin until the boost venturi suction exceeds the spill point value, and also that the main fuel flow rate is not always the same at a given value of the metering signal.

It was previously mentioned that each computer plot was available in four different scales. An excellent example of the practical use of this feature is Figure 72. This shows the carburetor-engine operating map for one of the other scales available. By comparing this plot with the one shown in Figure 69, it will be seen that the region of smaller

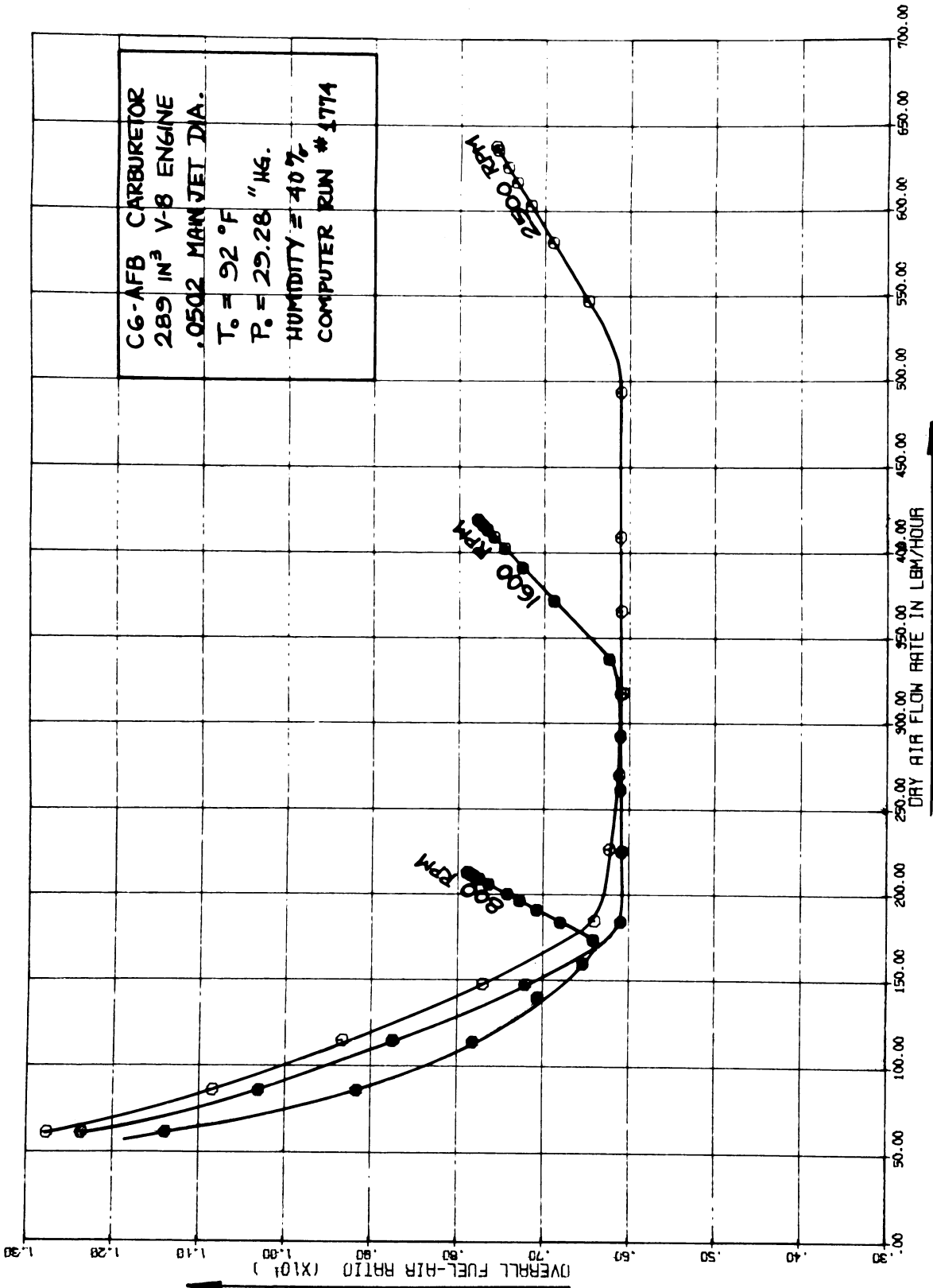


Figure 70. Predicted Fuel-Air Ratio Variations

## COMPUTER PREDICTION OF FUEL FLOW RATE

MAIN ORIFICE NUMBER = F-50

FUEL TEMPERATURE = 80.0 °F

RUN NUMBER = 1/1/68

FUEL = STANDARD GAS.

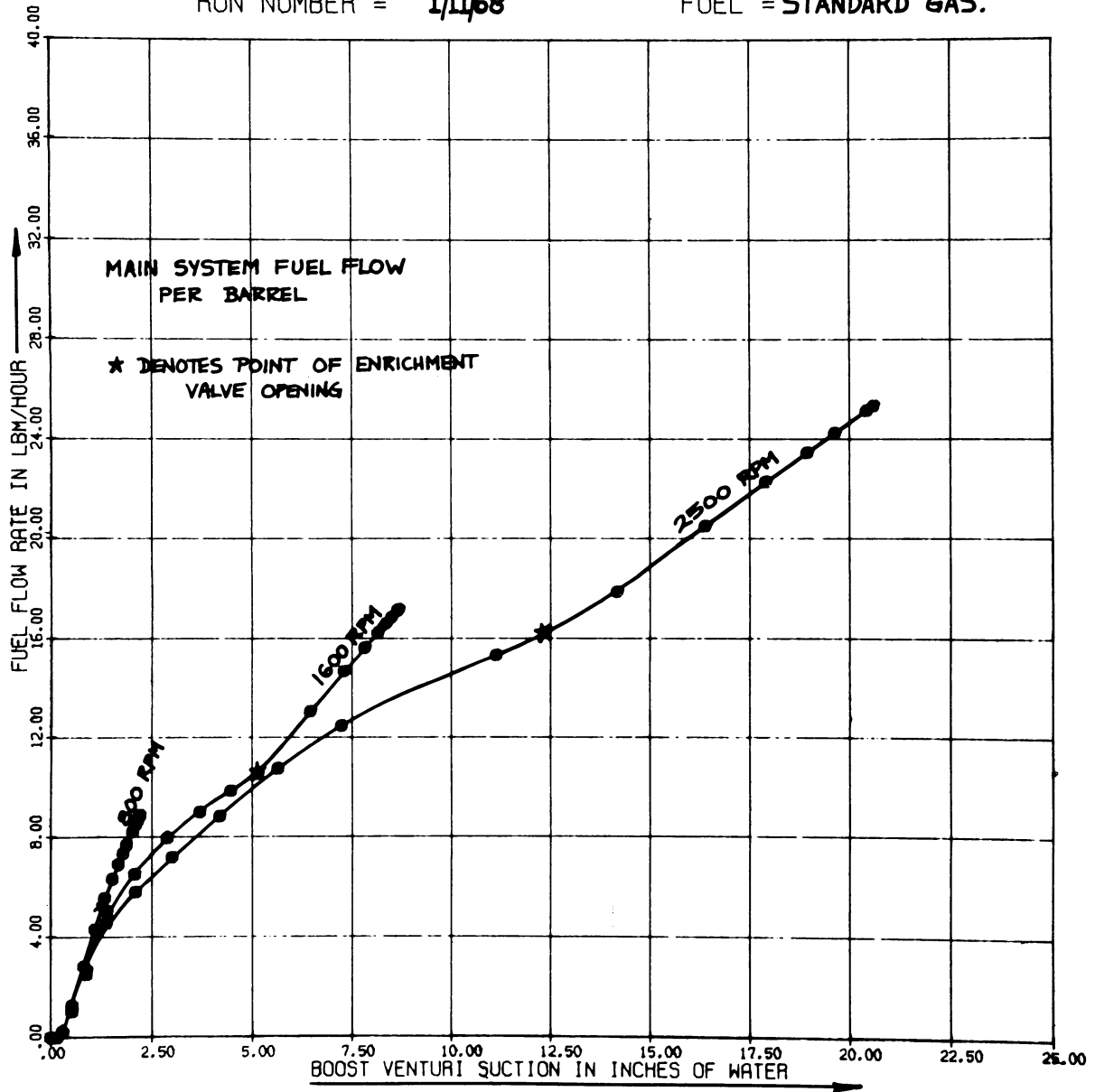


Figure 71. Predicted Main Fuel Flow Rate Variations

# CARBURETOR-ENGINE OPERATING MAP

$P_0 = 29.18'' \text{ HG}$      $T_0 = 92.0^\circ \text{ F}$     HUMIDITY = 25.0 %  
 DISPLACEMENT = 289.2  $\text{in}^3$     COMP. RATIO = 9.30

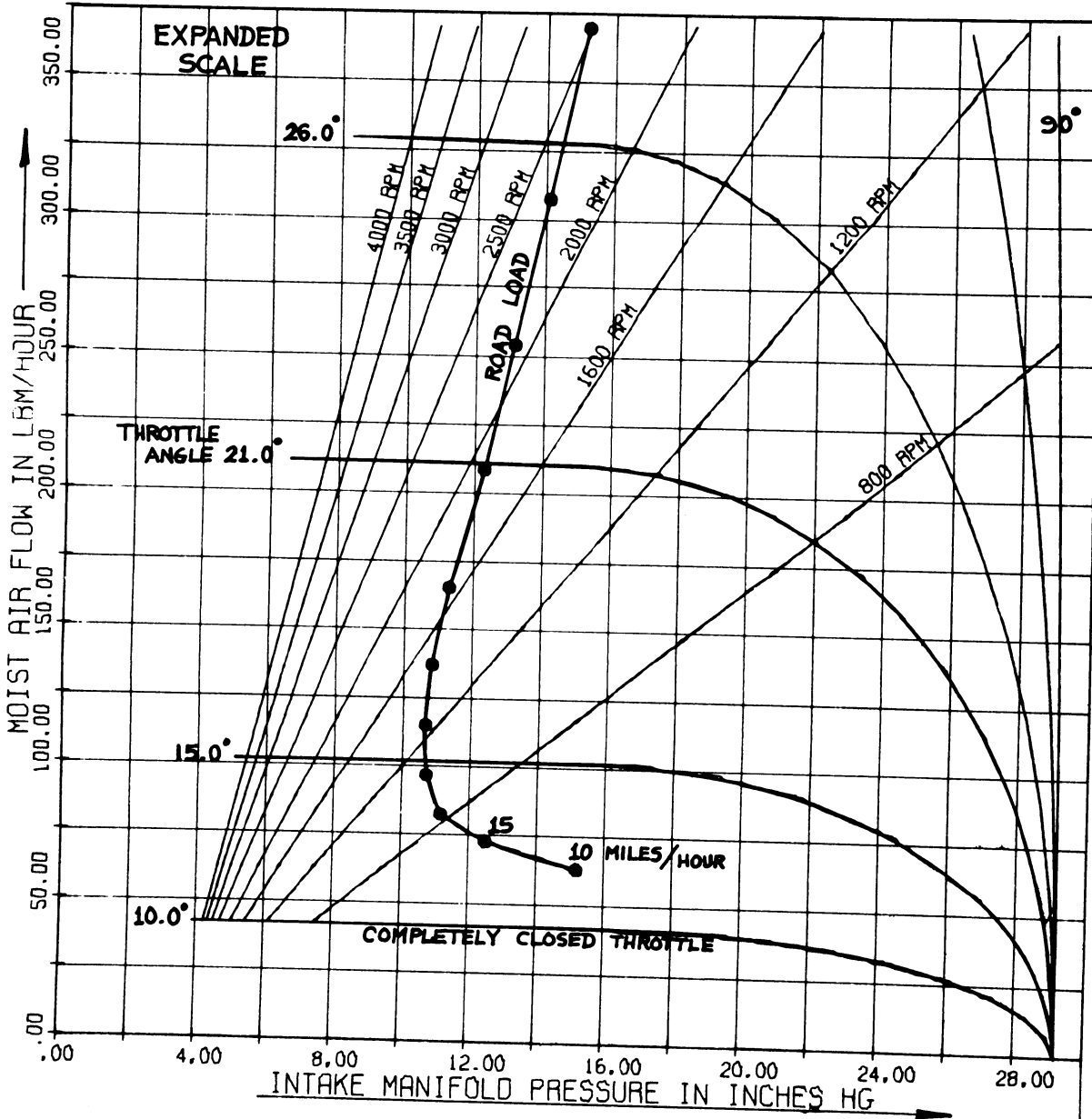


Figure 72. Carburetor - Engine - Vehicle Operating Map With Expanded Scale

4-44  
NIM D7-4

throttle angles has been expanded. (The specified ambient conditions and fuel temperature were different in the two simulation runs, thus one is not merely an expansion of the other.)

#### E. CARBURETOR ANALYSIS AT ROAD LOAD OPERATING CONDITIONS

One very important feature of this simulation program is that a proposed carburetor design may be analyzed for a sequence of operating points that correspond to road load operation with a specified engine and vehicle. This is accomplished by varying the vehicle velocity in five mile per hour increments and calculating the required throttle angle and engine speed. Obtaining the throttle angle is a reasonably complex procedure, and was discussed in Chapter 6. Once this value has been obtained however, the values of the carburetor, engine, and vehicle parameters corresponding to that particular vehicle speed are calculated iteratively. This includes such important variables as the engine air flow rate, brake horsepower, brake specific fuel consumption, fuel-air ratio, and miles per gallon of fuel.

The simulation predictions for a road load analysis of a typical carburetor-engine-vehicle combination are listed in Table 19. The input data was for a Ford C6AF-9510-B carburetor, utilizing Standard regular gasoline at 80° F. The ambient temperature and pressure were 80° F and 29.28 inches of mercury respectively. The engine and vehicle input data are listed in Tables 20 and 21. Note in the road load simulation predictions that the throttle angle increases very little at the lower vehicle speeds, but must be opened substantially at speeds greater than



65 miles per hour. Note also the variations in air flow rate and intake manifold pressure. It is these points that can be plotted on the operating map grids to obtain the road load operating point line, in the manner shown in Figures 69 and 72.

The accuracy of the predictions made for the carburetor analysis under road load conditions was generally quite good. Actual road load data were not obtained in this study, therefore available proving ground data were utilized. The simulation runs were made for the carburetor, engine, and vehicle specifications corresponding to the proving ground tests. In this manner the simulation predictions could be compared to the actual data. The vehicle miles per gallon values are shown in Figure 73 for both the simulation run and the actual road load test. Although the experimental data were obtained only for vehicle speeds in the 30 to 70 miles per hour range, the simulation predictions agreed very well with these values. Not only did the actual and predicted miles per gallon peak at the same speed, but the predicted maximum value was within 4% of the actual value.

The importance of the road load analysis portion of the overall carburetor simulation may be summarized as follows:

1. It permits the theoretical evaluation of carburetor performance for various engine-vehicle combinations
2. The influence of any one of hundreds of carburetor variables (or fuel, ambient, engine, or vehicle variables) on the road load fuel-air ratio and mileage can be predicted

TABLE XIX  
SIMULATION PREDICTIONS FOR CARBURETOR OPERATION  
AT ROAD LOAD CONDITIONS

ROAD LOAD CARBURETOR-ENGINE-VEHICLE PERFORMANCE

THE FOLLOWING VALUES ARE CALCULATED FOR A TRANSMISSION GEAR RATIO OF 1.000

CAR MPH	ENGINE RPM	THROT ANGLE	MOIST AIRFLO	BHP	IHP	MAN. PRESS.	AC	F/A RATIC	ENGINE ISFC	ENGINE BSFC	FUEL RATE	MPG	NN
10.0	387.5	11.75	59.30	1.73	3.51	15.91	35.51	.1043	1.7484	3.5441	6.13	9.808	5
15.0	581.3	12.54	68.42	2.83	5.60	12.69	36.91	.1015	1.2266	2.4303	6.87	13.124	6
20.0	775.0	13.35	78.47	4.20	8.06	11.25	33.31	.0968	.9313	1.7866	7.51	16.015	4
25.0	968.7	14.38	82.19	5.95	10.95	10.69	31.13	.0930	.7745	1.4256	8.48	17.724	5
30.0	1162.5	15.59	109.75	8.16	14.34	10.68	30.03	.0868	.6563	1.1524	9.41	19.175	6
35.0	1356.2	16.87	129.95	10.95	18.31	10.91	27.30	.0792	.5563	.9308	10.15	20.660	5
40.0	1550.0	18.38	155.88	14.40	22.98	11.43	21.96	.0694	.4655	.7425	10.70	22.490	6
45.0	1743.8	20.47	195.63	18.62	28.50	12.63	18.38	.0613	.4169	.6375	11.88	22.779	5
50.0	1937.5	22.46	238.32	23.73	35.13	13.69	18.45	.0609	.4085	.6047	14.35	20.951	5
55.0	2131.2	24.67	287.62	29.84	42.93	14.86	18.49	.0607	.4023	.5788	17.27	19.149	5
60.0	2325.0	27.00	344.60	37.07	52.06	16.15	18.49	.0607	.3978	.5587	20.71	17.423	5
65.0	2518.7	29.61	409.87	45.53	62.66	17.57	18.43	.0610	.3946	.5431	24.73	15.808	5
70.0	2712.5	32.66	485.54	55.36	74.83	19.17	18.43	.0610	.3917	.5294	29.31	14.362	5
75.0	2906.3	36.41	572.09	66.69	88.65	20.90	18.43	.0610	.3894	.5176	34.52	13.067	5
80.0	3100.0	41.39	669.32	79.66	104.23	22.77	18.43	.0610	.3875	.5070	40.39	11.912	5
85.0	3293.7	46.90	758.94	94.41	121.71	24.15	18.16	.0636	.3925	.5060	47.77	10.700	4
90.0	3487.5	54.80	851.86	111.10	141.16	25.43	20.46	.0676	.4034	.5125	56.94	9.506	4
95.0	3681.2	85.42	952.80	125.88	162.70	26.78	23.66	.0717	.4171	.5225	67.86	8.418	14

THE MAXIMUM VEHICLE SPEED HAS BEEN ATTAINED.....THIS SPEED IS 95.0 MILES PER HOUR

A ROAD LOAD LINE WAS PLOTTED WITH 18 POINTS

TABLE XX  
ENGINE INPUT DATA FOR ROAD LOAD ANALYSIS

IHP AND FMEP INPLT DATA FOR THE 1966 FORD 289 V-8 ENGINE

MEASURED AIR FLOW RATE = 200.0 LBM/HOUR			MEASURED AIR FLOW RATE = 432.0 LBM/HOUR		
PCINT	F/A RATIO	I-F-P1	POINT	F/A RATIO	IHP2
1	.0000	.00	1	.0000	.00
2	.0050	.00	2	.0050	.00
3	.0100	.00	3	.0100	.00
4	.0150	.00	4	.0150	.00
5	.0200	.00	5	.0200	.00
6	.0250	.00	6	.0250	.00
7	.0300	.00	7	.0300	.00
8	.0350	2.00	8	.0350	5.00
9	.0400	5.00	9	.0400	12.00
10	.0450	14.00	10	.0450	34.50
11	.0500	21.60	11	.0500	49.60
12	.0550	26.10	12	.0550	59.80
13	.0600	29.00	13	.0600	66.10
14	.0650	30.50	14	.0650	69.50
15	.0700	31.00	15	.0700	71.50
16	.0750	31.20	16	.0750	72.70
17	.0800	31.20	17	.0800	73.20
18	.0850	31.10	18	.0850	73.50
19	.0900	31.00	19	.0900	73.30
20	.0950	30.60	20	.0950	72.90
21	.1000	29.90	21	.1000	72.10
22	.1050	29.00	22	.1050	71.10
23	.1100	27.60	23	.1100	68.70
24	.1150	26.20	24	.1150	65.50
25	.1200	23.80	25	.1200	60.50
26	.1250	20.80	26	.1250	51.40
27	.1300	16.40	27	.1300	38.00
28	.1350	10.05	28	.1350	22.80
29	.1400	4.00	29	.1400	10.00
30	.1450	1.00	30	.1450	2.50
31	.1500	.00	31	.1500	.00
32	.1550	.00	32	.1550	.00
33	.1600	.00	33	.1600	.00
34	.1650	.00	34	.1650	.00
35	.1700	.00	35	.1700	.00

FMEP AT WIDE OPEN THROTTLE

PCINT	ENGINE RPM	FMEP1
1	.0	13.40
2	400.0	10.95
3	800.0	10.16
4	1200.0	10.82
5	1600.0	11.48
6	2000.0	13.45
7	2400.0	16.32
8	2800.0	19.30
9	3200.0	21.55
10	3600.0	24.00
11	4000.0	25.58
12	4400.0	27.00

FMEP AT CLOSED THROTTLE

PCINT	ENGINE RPM	FMEP2
1	.0	13.40
2	400.0	14.09
3	800.0	15.30
4	1200.0	16.18
5	1600.0	17.10
6	2000.0	18.40
7	2400.0	19.86
8	2800.0	21.60
9	3200.0	23.20
10	3600.0	24.72
11	4000.0	26.06
12	4400.0	27.18

13	4800.0	28.35	13	4800.0	28.85
14	5200.0	29.65	14	5200.0	30.20

TABLE XXI  
VEHICLE INPUT DATA FOR ROAD LOAD ANALYSIS

VEHICLE INPUT DATA FOR THE 1966 FORD FAIRLANE 500

VEHICLE FRONTAL AREA = 30.70 FT2  
 VEHICLE CURB WEIGHT = 3435 LBM  
 ROLLING RESISTANCE FACTOR = .01500 LBF/LBM  
 WIND RESISTANCE FACTOR = .00121 LBF/MPH FT2  
 TIRE REVOLUTIONS PER MILE = 775.0  
 REAR AXLE RATIO = 3.000  
 LOW GEAR RATIO = 1.000  
 SECOND GEAR RATIO = 1.000  
 HIGH GEAR RATIO = 1.000

INPUT DATA FOR GRIFICE COEFFICIENTS OF DISCHARGE

POINT	RE	F-50	C.100	0.616	1.426	3.629	4.726	7.230	10.58	RE	F-50 L
1	0	.000	.000	.000	.000	.000	.000	.000	.000	0	.000
2	500	.577	.663	.690	.737	.674	.623	.570	.525	100	.361
3	1000	.656	.665	.720	.766	.715	.680	.647	.620	200	.467
4	1500	.702	.654	.677	.770	.735	.710	.688	.660	300	.513
5	2000	.734	.648	.668	.774	.755	.727	.711	.685	400	.550
6	2500	.761	.644	.700	.788	.768	.741	.724	.703	500	.577
7	3000	.783	.641	.675	.790	.772	.750	.729	.712	600	.597
8	3500	.804	.638	.677	.790	.776	.756	.730	.720	700	.614
9	4000	.820	.635	.675	.793	.775	.761	.734	.726	800	.629
10	4500	.832	.633	.670	.796	.781	.764	.739	.729	900	.643
11	5000	.840	.631	.678	.798	.783	.766	.743	.732	1000	.656
12	5500	.848	.625	.658	.800	.785	.768	.746	.734	1100	.665
13	6000	.854	.627	.666	.802	.786	.770	.747	.736	1200	.675
14	6500	.860	.626	.676	.804	.787	.771	.749	.737	1300	.684
15	7000	.865	.625	.713	.805	.788	.772	.751	.738	1400	.693
16	7500	.869	.624	.705	.806	.785	.773	.753	.739	1500	.702
17	8000	.873	.623	.700	.807	.790	.774	.755	.740	1600	.709
18	8500	.876	.622	.650	.808	.791	.775	.757	.741	1700	.716
19	9000	.879	.621	.682	.809	.792	.776	.759	.742	1800	.722
20	9500	.881	.620	.680	.810	.793	.777	.760	.743	1900	.728
21	10000	.883	.620	.680	.810	.793	.778	.761	.743	2000	.734

COMPUTER PREDICTION OF ROAD LOAD FUEL ECONOMY

CARBURETOR : CGAF 2 BARREL  
 ENGINE : 289 IN<sup>3</sup> V-8  
 VEHICLE : 1966 FORD FAIRLANE - 4DR.

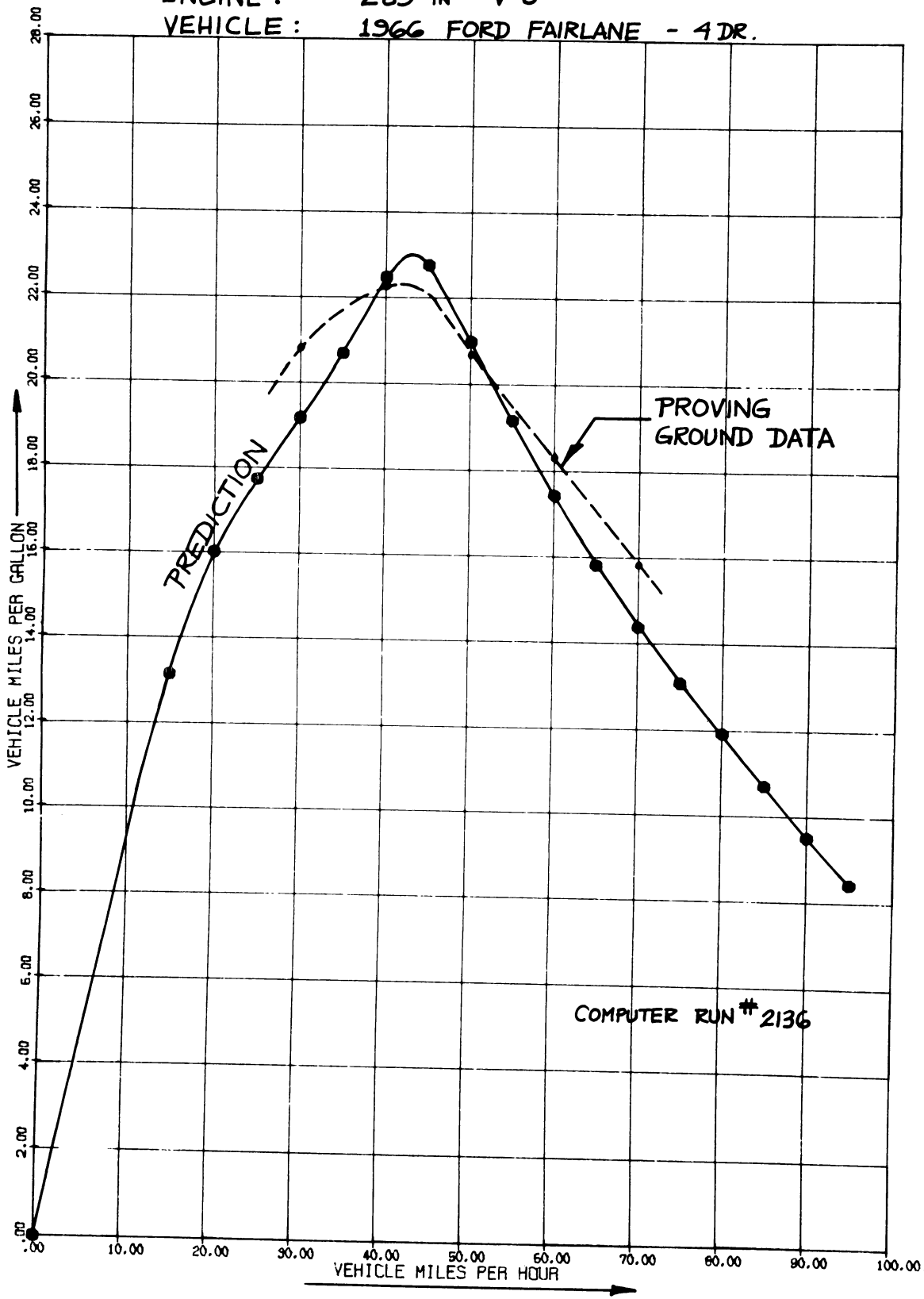


Figure 73. Predicted And Experimental Road Load Fuel Economy Values

## F. CARBURETOR ANALYSIS WITH PRODUCTION VARIATIONS IN DIMENSIONS

A very useful feature of the overall carburetor simulation is that the effects of production tolerances on carburetor performance may be evaluated theoretically. In effect, numerous "computer carburetors" may be constructed and tested, each having a random set of dimensions within the production limits. In this manner the fuel-air ratio spread to be expected among production carburetors, with specified sets of dimensions and tolerances, can be determined. The tolerances can then be perturbed, if desired, to determine the critical elements. The more critical tolerances could then be tightened, and the less critical tolerances increased, resulting in a lower fuel-air ratio spread among production carburetors, and a possible decrease in the average cost per unit.

The dimensional variations among production carburetors are simulated by utilizing the arrays of dimensions and tolerances which are read in initially. Each dimension that is read in, such as the throttle bore diameter or the main metering orifice diameter, will have a corresponding tolerance read in as data also. This will be the  $\pm 3 \sigma$  value for the dimension, or 3 standard deviations allowable on either side of the nominal dimension. Thus, if the blueprint specification for a given element diameter is  $1.000 \pm 0.001$ , the nominal dimension is 1.000, the tolerance is 0.001, and the standard deviation is 0.00033.

When the production dimension analysis is requested, the number of units to be "built", and the manner in which they are all to be

evaluated, is specified. The simulation then processes each nominal carburetor dimension in the input data, and assigns a random value to it, according to the specified tolerance. This is accomplished by calling on a random number generation subroutine, RANDND, which provides a random dimension within the tolerance band, on the basis of a Gaussian distribution of values. After this has been performed for each dimension, the carburetor is analyzed in any manner specified, and another carburetor is then "built". This continues until the desired number of units have been evaluated.

A typical simulation output for this type of analysis is shown in Table 22. This run was performed to check the operation of the technique, and all of the nominal dimensions and tolerances were obtained from the blueprints for a Ford C6AF-9510-B carburetor. Twelve production carburetors were "built", and their performances were evaluated at one operating point, that of 1600 RPM and  $26^{\circ}$  throttle angle. All of the nominal dimensions, as well as the dimensions of a typical production carburetor, are listed. The first carburetor was assigned the production dimensions listed in the table, and the middle carburetor (number 6) was assigned the nominal values. Note that all performance variations listed in the simulation printout are due to variations in dimensions from one production carburetor to the next. It can be seen that the total fuel-air ratio variation (at this operating point) is from 0.0603 to 0.0628, or a spread of 0.0025. More units could, of course, be built in order to establish the standard deviation of the fuel-air ratio.

TABLE XXII  
 SIMULATION PREDICTIONS FOR THE EFFECTS OF PRODUCTION  
 TOLERANCES ON CARBURETOR PERFORMANCE

UNIVERSITY OF MICHIGAN  
 MECHANICAL ENGINEERING DOCTORAL THESIS  
 DIGITAL SIMULATION OF CARBURETOR METERING  
 CARBURETOR-ENGINE-VEHICLE OPERATING MAP

DAVID L. HARRINGTON

THE TYPE OF ANALYSIS REQUESTED IS.....SPECIFIED INPUT POINT  
 THE TYPE OF PLOT(S) REQUESTED ARE.....NO PLOTS REQUESTED  
 THIS SIMULATION PERFORMED ON.....12 MAR 1969  
 PURPOSE OF THIS SIMULATION RUN.....TO SIMULATE PRODUCTION VARIATIONS IN CARBURETOR DIMENSIONS

AMBIENT CONDITIONS	CARBURETOR	FUEL	ENGINE	VEHICLE
PRESSURE = 29.00 INCHES HG TEMPERATURE = 80.0 DEGREES F HUMIDITY = 50.0 PERCENT DENSITY = .0713 LBM/FT3	FORD 2 BBL. C6AF-9510-R MAIN JET = F-50 MAIN VENTURI=1.145 IN. CLOSED THROTTLE=10.0	STANDARD REG. GASOLINE TEMPERATURE = 80.0 F SPECIFIC GRAVITY = .721 VISCOSITY = .556 CS	1966 FORD 289 V-R DISPLACEMENT=289.2 C.I. COMP. RATIO = 9.3 VALVE FLOW AREA=6.82 IN2	1966 FORD FAIRLANE VEHICLE WEIGHT=3435.0 REAR AXLE RATIO= 3.00 TIRE REVS/MILE =775.0

INPUT DATA FOR THE FORD 2 BBL. C6AF-9510-R CARBURETOR.  
 \*\*\*NOMINAL DIMENSIONS\*\*\*

MAIN METERING ORIFICE TYPE F-50  
 MAIN METERING ORIFICE DIAMETER = .0502 INCH  
 MAIN METERING ORIFICE LENGTH = .1830 INCH  
 MAIN METERING ORIFICE L/D RATIO = 3.6454  
 NUMBER OF MAIN METERING ORIFICES = 2  
 COMPLETELY CLOSED THROTTLE ANGLE = 10.000 DEGREES  
 THROTTLE BORE DIAMETER = 1.4370 INCHES  
 THROTTLE SHAFT DIAMETER = .3750 INCH  
 INITIAL SPILL POINT OF MAIN SYSTEM = .140 INCH  
 MAIN VENTURI THROAT DIAMETER = 1.1450 INCHES

THROTTLE PLATE BYPASSES

TRANSFER TUBE DIAMETER = .0730 INCH  
 CHOKE BLEED RESTRICTION DIAMETER = .0000 INCH  
 ENRICHMENT BLEED RESTRICTION DIAMETER = .0730 INCH

GEOMETRIC RELATION BETWEEN BOOST AND MAIN VENTURI

XMV1 = 1.2500 INCHES  
 XMV2 = 1.0000 INCHES  
 XBV = .7800 INCHES  
 XMB = .0700 INCHES



TABLE XXII (continued)

MAIN VENTURI ELEMENT		DIAMETER	FUEL CHANNEL ELEMENT		L/D RATIO	ORIFICE TYPE
1	1.930 INCHES		1	.183 INCH	3.645	1.0
2	1.930 INCHES		2	.312 INCH	1.668	.0
3	1.145 INCHES		3	.106 INCH	1.309	3.0
4	1.160 INCHES		4	.125 INCH	.400	.0
5	1.400 INCHES		5	.390 INCH	2.500	2.0
			6	.206 INCH	1.526	.0
			7	.125 INCH	4.464	2.0
			8	.938 INCH	6.378	.0
			9	.250 INCH	.859	.0
			10	1.000 INCH	6.329	.0
			11	.340 INCH	1.259	.0
			12	.812 INCH	5.075	.0
			13	.135 INCH	.600	2.0
			14	1.930 INCH	31.639	.0
			15	.094 INCH	3.608	2.0
			16	.706 INCH	5.043	.0
			17	.780 INCH	8.298	.0
			18	.106 INCH	2.524	2.0
			19	2.000 INCH	21.277	.0
			20	.0590 INCH	1.797	3.0
			21	.0310 INCH	4.032	2.0
			22	.0446 INCH	.700	2.0
			23	.0270 INCH	5.185	2.0
			24	.0390 INCH	3.205	2.0
			25	.0350 INCH	3.029	2.0

TABLE XXII (continued)

DIMENSIONS OF A TYPICAL PRODUCTION CARBURETOR

MAIN METERING ORIFICE TYPE F-50  
 MAIN METERING ORIFICE DIAMETER = .0499 INCH  
 MAIN METERING ORIFICE LENGTH = .1830 INCH  
 MAIN METERING ORIFICE L/D RATIO = 3.6651  
 NUMBER OF MAIN METERING ORIFICES = 2  
 COMPLETELY CLOSED THROTTLE ANGLE = 10.056 DEGREES  
 THROTTLE RORE DIAMETER = 1.4370 INCHES  
 THROTTLE SHAFT DIAMETER = .3750 INCH  
 INITIAL SPILL POINT OF MAIN SYSTEM = .140 INCH  
 MAIN VENTURI THROAT DIAMETER = 1.1453 INCHES

THROTTLE PLATE RYPASSES

TRANSFER TUBE DIAMETER = .0725 INCH  
 CHOKE BLEED RESTRICTION DIAMETER = .0000 INCH  
 ENRICHMENT BLEED RESTRICTION DIAMETER = .0735 INCH

GEOMETRIC RELATION BETWEEN BOOST AND MAIN VENTURI

XMV1 = 1.2501 INCHES  
 XMV2 = .9954 INCHES  
 XBV = .7798 INCHES  
 XMB = .0692 INCHES

MAIN VENTURI ELEMENT

ELEMENT	DIAMETER
1	1.930 INCHES
2	1.930 INCHES
3	1.145 INCHES
4	1.160 INCHES
5	1.400 INCHES

BOOST VENTURI ELEMENT

ELEMENT	DIAMETER
1	1.030 INCHES
2	.875 INCHES
3	.538 INCHES
4	.596 INCHES
5	.650 INCHES
6	.750 INCHES

FUEL CHANNEL ELEMENT

ELEMENT	DIAMETER	LENGTH	L/D RATIO	ORIFICE TYPE
1	.0499 INCH	.183 INCH	3.665	1.0
2	.1680 INCH	.312 INCH	1.660	.0
3	.0817 INCH	.106 INCH	1.298	3.0
4	.3125 INCH	.125 INCH	.400	.0
5	.1558 INCH	.390 INCH	2.504	2.0
6	.1353 INCH	.206 INCH	1.522	.0
7	.0276 INCH	.125 INCH	4.524	2.0
8	.1469 INCH	.938 INCH	6.383	.0

TABLE XXII (continued)

9	.2932 INCH	.250 INCH	.853	.0
10	.1576 INCH	1.000 INCH	6.347	.0
11	.2689 INCH	.340 INCH	1.265	.0
12	.1592 INCH	.812 INCH	5.099	.0
13	.2239 INCH	.135 INCH	.603	.0
14	.0601 INCH	1.930 INCH	32.091	.0
15	.0258 INCH	.094 INCH	3.642	.0
16	.1403 INCH	.706 INCH	5.033	.0
17	.0954 INCH	.780 INCH	8.179	.0
18	.0419 INCH	.106 INCH	2.530	.0
19	.0936 INCH	.000 INCH	21.376	.0
20	.0596 INCH	.106 INCH	1.778	3.0
21	.0313 INCH	.125 INCH	3.980	.0
22	.0447 INCH	.031 INCH	.698	.0
23	.0271 INCH	.140 INCH	5.159	.0
24	.0392 INCH	.125 INCH	3.188	.0
25	.0346 INCH	.106 INCH	3.062	.0

**SIMULATE 12 PRODUCTION CARBURETORS**

CARBURETOR-ENGINE OPERATION FOR SPECIFIC OPERATING POINTS (RPM AND THETA SUPPLIED AS INPUT DATA)

ENGINE RPM	THROTTLE ANGLE	THROT FLOW AREA	INTAKE MAN. PRESS	MOIST AIR FLOW	DRY AIR FLOW	BOOST VENTURI SUCTION	MAIN VENTURI SUCTION	THROT MACH NO.	MAIN F/A RATIO	TOTAL F/A RATIO	TOTAL FUEL FLOW	MAIN FUEL FLOW	THROT TOTAL TEMP	AIR BLEED FLOW	J
		IN <sup>2</sup>	INCHES Hg	LBM/HR	LBM/HR	INCHES H <sub>2</sub> O	INCHES H <sub>2</sub> O				LBM/HR	LBM/HR	°F	LBM/HR	
1600.0	26.0	.1566	19.91	298.87	295.59	3.69	1.94	.7507	.0505	.0606	17.912	14.938	68.2	.413	3
1600.0	26.0	.1568	19.91	299.00	295.72	3.67	1.95	.7509	.0517	.0615	18.186	15.275	68.0	.396	3
1600.0	26.0	.1565	19.89	298.80	295.52	3.69	1.94	.7521	.0521	.0623	18.399	15.396	67.9	.408	3
1600.0	26.0	.1566	19.90	298.88	295.60	3.70	1.94	.7514	.0519	.0617	18.238	15.355	67.9	.409	3
1600.0	26.0	.1567	19.91	299.03	295.75	3.70	1.95	.7506	.0511	.0611	18.083	15.119	68.1	.404	3
1600.0	26.0	.1566	19.91	298.95	295.68	3.68	1.94	.7508	.0509	.0611	18.065	15.050	68.1	.405	3
1600.0	26.0	.1569	19.92	299.29	296.01	3.69	1.95	.7500	.0516	.0615	18.218	15.277	68.0	.403	3
1600.0	26.0	.1565	19.88	298.69	295.42	3.65	1.94	.7524	.0524	.0621	18.360	15.494	67.8	.400	3
1600.0	26.0	.1566	19.90	298.80	295.53	3.69	1.94	.7510	.0507	.0608	17.967	14.983	68.2	.401	3
1600.0	26.0	.1568	19.90	299.13	295.85	3.70	1.94	.7514	.0526	.0628	18.575	15.567	67.7	.402	3
1600.0	26.0	.1567	19.93	299.12	295.84	3.70	1.95	.7496	.0501	.0602	17.808	14.826	68.3	.396	3
1600.0	26.0	.1566	19.93	299.05	295.78	3.70	1.94	.7499	.0506	.0603	17.841	14.959	68.2	.413	3

## G. AUXILIARY SUBROUTINE PRINTOUTS

It should perhaps be emphasized here that the individual subroutines were written to do significantly more than return a needed number to the main program. Each subroutine performs a comprehensive analysis of one component of the carburetor, and thus makes available a complete set of parameters for each operating point. An example of this is subroutine SIGNAL, which performs a complete analysis of the flow within the main and boost venturii for any specified geometry and air flow rate. Although the chief function of this subroutine is to supply the boost venturi suction to the main program, all of the other venturi parameters are also available. Thus, if this particular function of the carburetor is to be studied in detail, an auxiliary printout may be requested which will contain such variables as the Mach numbers, pressures, velocities, mass flow rates, and temperatures at each station within the main and boost venturii.

One of these auxiliary printouts is shown in Table 23, for the entire air flow range of the venturii system. Note that the maximum possible air mass flow rates are given for both the primary and boost venturii (for the specified geometry and stagnation conditions). Note also that the boost venturi chokes at a total air flow rate per barrel of about 750 pounds per hour, after which the metering signal is constant. The total air flow rate can increase further because the primary venturi is not choked. When the air flow rate supplied to SIGNAL exceeds the capacity of the venturii system, the subroutine prints out this fact along with the

TABLE XXIII

COMPUTER PREDICTION OF MAIN AND BOOST VENTURI PARAMETERS  
VALUES PREDICTED BY SUBROUTINES SIGNAL AND SOLVE

MAIN AIR FRACT.	JUTLET PRESS. ERROR	TOTAL AIR FLOW	PRIMARY VENTURI FLOW	BOOST VENTURI FLOW	PRIMARY THROAT MACH NO	BOOST VENTURI MACH NO	PRIMARY VENTURI SIGNAL	BOOST VENTURI SIGNAL	BOOST OUTLET PRESS.	BOOST TOTAL PRESS.	BOOST TOTAL TEMP.	BOOST THROAT SUCTION	MAX. PRIMARY FLOW	MAX. BOOST FLOW	J
.6348	.0000	50.00	15.87	9.13	.0130	.0198	.051	.113	28.996	29.000	80.00	.109	708.0	266.4	3
.6348	.0000	100.00	31.74	18.26	.0259	.0397	.203	.452	28.986	28.999	80.00	.437	708.0	266.4	3
.6348	.0001	150.00	47.61	27.39	.0389	.0596	.457	1.019	28.968	28.997	80.00	.984	707.9	266.4	3
.6348	.0001	200.00	63.48	36.54	.0519	.0796	.814	1.815	28.942	28.995	80.00	1.753	707.9	266.4	3
.6349	.0001	250.00	79.36	45.64	.0650	.0997	1.273	2.843	28.912	28.993	80.00	2.746	707.8	266.3	4
.6349	.0000	300.00	95.23	54.77	.0781	.1199	1.836	4.108	28.870	28.990	80.00	3.967	707.7	266.3	4
.6349	.0000	350.00	111.11	63.89	.0912	.1404	2.503	5.613	28.823	28.986	80.00	5.420	707.6	266.3	4
.6349	.0000	400.00	126.99	73.01	.1044	.1610	3.276	7.366	28.768	28.982	80.00	7.111	707.5	266.2	4
.6350	.0000	450.00	142.87	82.13	.1177	.1820	4.156	9.371	28.706	28.977	80.00	9.046	707.4	266.2	4
.6350	.0000	500.00	158.75	91.25	.1311	.2032	5.144	11.639	28.636	28.971	80.00	11.233	707.3	266.1	4
.6350	.0000	550.00	174.64	100.36	.1446	.2248	6.243	14.179	28.558	28.965	80.00	13.683	707.1	266.1	4
.6351	.0000	600.00	190.53	109.47	.1582	.2467	7.453	17.003	28.473	28.958	80.00	16.404	706.9	266.0	4
.6351	.0000	650.00	206.42	118.58	.1719	.2692	8.778	20.124	28.379	28.950	80.00	19.412	706.8	265.9	4
.6352	.0000	700.00	222.32	127.68	.1857	.2921	10.220	23.559	28.277	28.942	80.00	22.720	706.6	265.9	4
.6353	.0000	750.00	238.23	136.77	.1997	.3157	11.781	27.328	28.177	28.933	80.00	26.347	706.3	265.8	4
.6353	.0001	800.00	254.14	145.86	.2139	.3400	13.465	31.454	28.048	28.923	80.00	30.315	706.1	265.7	4
.6354	.0000	850.00	270.06	154.94	.2282	.3650	15.276	35.966	27.920	28.913	80.00	34.649	705.9	265.6	4
.6355	.0000	900.00	285.98	164.02	.2427	.3911	17.217	40.897	27.783	28.901	80.00	39.382	705.6	265.5	4
.6356	.0000	950.00	301.91	173.09	.2575	.4182	19.293	46.290	27.637	28.889	80.00	44.552	705.3	265.4	4
.6357	.0000	1000.00	317.86	182.14	.2725	.4466	21.510	52.199	27.481	28.875	80.00	50.208	705.0	265.3	4
.6358	.0000	1050.00	333.81	191.19	.2877	.4765	23.872	58.693	27.314	28.861	80.00	56.411	704.7	265.1	4
.6360	.0000	1100.00	349.78	200.22	.3033	.5084	26.387	65.861	27.137	28.845	80.00	63.241	704.4	265.0	4
.6361	.0000	1150.00	365.77	209.23	.3191	.5426	29.063	73.828	26.949	28.828	80.00	70.807	704.1	264.8	4
.6363	.0000	1200.00	381.78	218.22	.3354	.5798	31.907	82.769	26.749	28.810	80.00	79.259	703.7	264.7	4
.6365	.0001	1250.00	397.82	227.18	.3520	.6211	34.932	92.950	26.537	28.789	80.00	88.818	703.4	264.5	4
.6368	.0000	1300.00	413.89	236.11	.3691	.6681	38.150	104.809	26.311	28.766	80.00	99.838	703.0	264.3	4
.6371	.0001	1350.00	430.02	244.98	.3867	.7241	41.577	119.171	26.071	28.740	80.00	112.939	702.6	264.0	4
.6375	.0000	1400.00	446.25	253.75	.4049	.7971	45.239	138.047	25.815	28.709	80.00	129.456	702.2	263.7	5
.6382	.0001	1450.00	462.70	262.30	.4239	.9323	49.189	172.458	25.540	28.667	80.00	153.742	701.7	263.3	4
.6490	.0020	1500.00	486.72	263.28	.4530	.9998	55.427	188.962	25.105	28.660	80.00	157.889	701.1	263.3	3
.6603	.0020	1550.00	511.72	263.28	.4851	.9998	62.587	188.962	24.609	28.660	80.00	157.889	700.3	263.3	3
.6709	.0020	1600.00	536.72	263.28	.5196	.9998	70.549	188.962	24.059	28.660	80.00	157.889	699.6	263.3	3
.6809	.0020	1650.00	561.72	263.28	.5571	.9998	79.478	188.962	23.447	28.660	80.00	157.889	698.8	263.3	3
.6903	.0020	1700.00	586.72	263.28	.5985	.9998	89.629	188.962	22.757	28.660	80.00	157.889	697.9	263.3	3
.6991	.0020	1750.00	611.72	263.28	.6455	.9998	101.412	188.962	21.967	28.660	80.00	157.889	697.0	263.3	3
.7075	.0020	1800.00	636.72	263.28	.7011	.9998	115.581	188.962	21.039	28.660	80.00	157.889	696.1	263.3	3
.7154	.0020	1850.00	661.72	263.28	.7724	.9998	133.882	188.962	19.896	28.660	80.00	157.889	695.2	263.3	3
.7229	.0020	1900.00	686.72	263.28	.8895	.9998	163.666	188.962	18.327	28.660	80.00	157.889	694.2	263.3	3
.7266	.0020	1950.00	708.00	266.40	.9998	1.0000	186.529	186.583	18.062	29.000	80.00	157.889	708.0	266.4	0
.7266	.0020	2000.00	708.00	266.40	.9998	1.0000	186.529	186.583	18.062	29.000	80.00	157.889	708.0	266.4	0

THE AIR FLOW SUPPLIED TO SIGNAL EXCEEDS THE VENTURI FLOW CAPACITY  
THE AIR FLOW SUPPLIED TO SIGNAL EXCEEDS THE VENTURI FLOW CAPACITY

maximum values.

#### H. COMPUTER TIMES REQUIRED

The complete carburetor simulation program, consisting of the main program and 12 subroutines, was run on an IBM 7090 computer. Some subroutine debugging was performed using an IBM 360-65, however no complete simulation runs were performed on that machine. The computer plots were generated on a CALCOMP Model 763 digital incremental plotter. The times required for these operations varied considerably with the type of analysis requested within the simulation, and with the number and type of plots to be generated. A brief summary of these times is given in the following table.

TABLE XXIV  
REQUIRED COMPUTER TIMES (APPROXIMATE)

<u>OPERATION</u>	<u>TIME</u>
Compilation time on FASTRAN and MAD compilers	2.2 minutes
Execution time for a typical constant RPM or constant $\Theta$ run	1.5 minutes
Execution time for a carburetor- engine operating map	9 minutes
Execution time for a road load analysis	5 minutes
Execution time for a production dimension analysis (12 units)	4 minutes
Execution time for a complete carburetor- engine-vehicle operating map	13 minutes
Plotting time for all graphs except operating map	2.5 minutes
Plotting time for operating map	4.5 minutes

## CHAPTER IX

### APPLICATIONS OF THE COMPLETE CARBURETOR SIMULATION

#### A. GENERAL APPLICATIONS

The discussions given in the preceding chapter were concerned with the various analysis types that may be specified within the carburetor simulation. The topic to be considered in this chapter is that of possible applications of the complete simulation, utilizing one or more of the available analyses. Two of the obvious general applications have been mentioned previously; that of the evaluation of a proposed carburetor design by predicting the performance, and evaluating the effect of the production tolerances on the fuel-air ratio spread among carburetors. Other, perhaps less obvious, applications will now be considered, and suitable examples presented.

#### B. SINGLE VARIABLE EFFECTS

One of the most useful applications of the complete carburetor simulation is that of predicting single variable effects. This may be accomplished by performing the simulation a number of times, each time incrementing only the independent variable being investigated. The significance of this technique is that the independent variable under investigation may be any one of hundreds of carburetor, fuel, ambient, engine, or vehicle variables. Its effect on any of the dependent variables in the analysis could be predicted with just a few simulation runs.

The number of permutations and combinations that are possible is enormous. A few of these possible combinations are:

1. The effect of ambient pressure on the metering signal.
2. The effect of ambient temperature on the delivered fuel-air ratio.
3. The effect of fuel temperature on the delivered fuel-air ratio.
4. The effect of main venturi diameter on the road load miles per gallon.
5. The effect of throttle bore diameter on the road load throttle angle.
6. The effect of engine displacement on the delivered fuel-air ratio.
7. The effect of vehicle differential gear ratio on the road load fuel-air ratio values.

The list could be extended considerably, however it should be obvious that there are many single variable effect applications.

#### C. ADDITIONAL APPLICATIONS

The simulation has numerous other useful applications in addition to the multitude of single variable effect situations. One group of applications is in comparing designs or parameters. A few examples of this utilization of the simulation are:

1. To evaluate various proposed carburetor designs by comparing their predicted fuel-air ratio curves.
2. To evaluate the mating of a particular engine with various proposed carburetors by comparing the resulting predictions for the road load BSFC values.
3. To evaluate various proposed venturi geometries by comparing the resulting predictions for the metering signal curve.

Other applications are abundant, and are concerned with optimization of systems, and the sizing of components to comply with desired performance specifications.



#### D. EXAMPLES OF SINGLE VARIABLE EFFECTS

Actual simulation runs were performed on numerous occasions in order to determine the influence of various independent variables. The results of two of these runs will be presented in this section as examples of the carburetor simulation applicability.

The first example represents the results of a simulation run to determine the effects of a reduced ambient pressure, corresponding to an altitude of 6000 feet above sea level. A complete carburetor-engine-vehicle operating map analysis was requested, and the simulation predictions are listed in Table 25, and plotted in Figure 74. The corresponding predictions for the sea level case were listed previously in Table 16, and plotted in Figure 69.

The results of three constant engine speed analyses for the simulated altitude of 6000 feet are shown in Table 25. The 1600 RPM run at altitude may be compared to the 1600 RPM run at sea level (Table 16) with the resulting conclusions:

1. At altitude, the predicted air flow rate and intake manifold pressure are lower with the same throttle angle.
2. At altitude, the predicted boost and primary venturi suction are larger for the same air mass flow rate.
3. At altitude, the predicted fuel-air ratio values are generally richer.

One item that should be noted is that the fuel flow rate in the sea level run is the value for both barrels, whereas in the altitude run it is per barrel. Figure 74 shows the operating map for the altitude conditions. Note that it is significantly different from the sea level operating map. The minimum air mass flow rate and intake manifold

TABLE XXV  
SIMULATION PREDICTIONS FOR CARBURETOR PERFORMANCE  
AT ALTITUDE

UNIVERSITY OF MICHIGAN  
MECHANICAL ENGINEERING DOCTORAL THESIS  
DIGITAL SIMULATION OF CARBURETOR METERING  
CARBURETOR-ENGINE-VEHICLE OPERATING MAP

DAVID L. HARRINGTON

THE TYPE OF ANALYSIS REQUESTED IS.....COMPLETE OPERATING MAP  
THE TYPE OF PLOT(S) REQUESTED ARE.....COMPLETE OPERATING MAP  
THIS SIMULATION PERFORMED ON.....07 FEB 1968  
PURPOSE OF THIS SIMULATION RUN.....TO CHECK THE EFFECT OF ALTITUDE ON THE OPERATING MAP

AMBIENT CONDITIONS			CARBURETOR			FUEL			ENGINE			VEHICLE			
PRESSURE = 24.00 INCHES HG	FORC 2 8BL. G6AF-9510-B	STANDARD REG. GASOLINE	1966 FORC 285 V-8												
TEMPERATURE = 70.0 DEGREES F	MAIN JET = F-50	TEMPERATURE = 80.0 F	DISPLACEMENT=289.2 C.I.												
HUMIDITY = 40.0 PERCENT	MAIN VENTURI=1.145 IN.	SPECIFIC GRAVITY= .721	COMP. RATIO = 9.3												
DENSITY = .0601 LBM/FT3	CLOSED THROTTLE=10.0	VISCOSITY = .556 CS	VALVE FLOW AREA=6.82 IN2												

CARBURETOR-ENGINE OPERATION AT CONSTANT ENGINE SPEED-VARIABLE THROTTLE OPENING

ENGINE RPM	THROT ANGLE	THROT FLOW AREA	INTAKE MAN. PRESS	MOIST AIR FLOW	DRY AIR FLOW	BOOST VENTURI SUCTION	MAIN VENTURI SUCTION	THROT MACH NO.	MAIN F/A RATIO	TOTAL F/A RATIO	TOTAL FUEL FLOW	MAIN FUEL FLOW	THROT TOTAL TEMP	THROT PLATE COEFF	J
800.0	10.0	.0179	5.48	34.93	34.66	.05	.03	1.0000	.0000	.1208	2.093	.000	70.0	.683	3
800.0	12.0	.0287	7.27	51.49	51.10	.11	.06	1.0000	.0000	.1163	2.972	.000	70.0	.721	2
800.0	14.0	.0413	9.75	72.34	71.79	.23	.12	1.0000	.0000	.0940	3.374	.000	70.0	.757	3
800.0	16.0	.0559	12.76	96.64	95.91	.43	.23	.9931	.0128	.0824	3.549	.612	67.0	.790	3
800.0	18.0	.0724	15.65	120.22	119.31	.67	.36	.8057	.0270	.0760	4.536	1.612	63.7	.817	3
800.0	20.0	.0907	17.88	138.54	137.49	.90	.48	.6617	.0381	.0711	4.850	2.621	61.1	.838	3
800.0	22.0	.1109	19.53	151.40	150.26	1.09	.58	.5504	.0494	.0623	4.684	3.713	58.4	.854	3
800.0	24.0	.1329	20.63	160.70	159.49	1.23	.65	.4694	.0583	.0636	5.075	4.650	56.4	.859	3
800.0	26.0	.1567	21.43	167.82	166.55	1.35	.72	.4042	.0654	.0675	5.617	5.448	54.7	.865	3
800.0	28.0	.1822	22.01	173.14	171.83	1.45	.77	.3517	.0709	.0715	6.140	6.092	53.4	.871	3
800.0	30.0	.2095	22.44	177.12	175.78	1.52	.81	.3083	.0746	.0746	6.553	6.553	52.5	.876	2
800.0	35.0	.2848	23.12	183.03	181.64	1.63	.86	.2270	.0766	.0766	6.558	6.558	52.1	.850	2
800.0	40.0	.3700	23.46	185.99	184.58	1.69	.90	.1742	.0776	.0776	7.165	7.165	51.8	.500	2
800.0	45.0	.4641	23.64	187.59	186.17	1.72	.91	.1381	.0782	.0782	7.279	7.279	51.7	.511	2
800.0	50.0	.5662	23.74	188.50	187.08	1.74	.92	.1125	.0785	.0785	7.344	7.344	51.6	.520	2
800.0	55.0	.6749	23.80	189.06	187.63	1.76	.93	.0939	.0787	.0787	7.383	7.383	51.6	.527	2
800.0	60.0	.7884	23.84	189.40	187.97	1.76	.94	.0801	.0788	.0788	7.408	7.408	51.5	.532	2
800.0	70.0	1.0134	23.89	189.77	188.34	1.77	.94	.0619	.0790	.0790	7.435	7.435	51.5	.540	2
800.0	80.0	1.0894	23.90	189.85	188.41	1.78	.94	.0575	.0790	.0790	7.440	7.440	51.5	.543	1

THE OPERATING MAP GRID HAS BEEN DRAWN  
A LINE WAS PLOTTED WITH 19 POINTS

TABLE XXV (continued)

**ALTITUDE EFFECTS**

CARBURETOR-ENGINE OPERATION AT CONSTANT ENGINE SPEED-VARIABLE THROTTLE OPENING

ENGINE RPM	THROTTLE ANGLE	THROTTLE FLOW AREA	INTAKE MAN. PRESS	MOIST AIR FLOW	DRY AIR FLOW	BOOST VENTURI SUCTION	MAIN VENTURI SUCTION	THROTTLE MACH NO.	MAIN F/A RATIO	TOTAL F/A RATIO	TOTAL FUEL FLOW	MAIN FUEL FLOW	THROTTLE TOTAL TEMP	THROTTLE PLATE COEFF	J
1600.0	10.0	.0179	3.63	34.92	34.65	.05	.03	1.0000	.0000	.1249	2.164	.000	70.0	.683	3
1600.0	12.0	.0287	4.50	51.60	51.21	.11	.06	1.0000	.0000	.1218	3.118	.000	70.0	.721	2
1600.0	14.0	.0413	5.59	72.41	71.87	.23	.12	1.0000	.0000	.1013	3.639	.000	70.0	.757	2
1600.0	16.0	.0559	7.03	96.83	96.10	.43	.23	1.0000	.0113	.0885	4.253	.545	67.3	.750	3
1600.0	18.0	.0724	8.74	124.54	123.60	.72	.38	1.0000	.0272	.0772	4.774	1.684	63.6	.817	3
1600.0	20.0	.0907	10.63	155.07	153.90	1.13	.60	1.0000	.0464	.0669	5.145	3.571	59.1	.838	4
1600.0	22.0	.1109	12.67	188.41	186.99	1.69	.89	1.0000	.0610	.0610	5.703	5.703	55.7	.854	3
1600.0	24.0	.1329	14.66	221.50	219.83	2.35	1.25	.8699	.0610	.0610	6.705	6.705	55.7	.859	2
1600.0	26.0	.1567	16.39	250.29	248.39	3.03	1.60	.7577	.0610	.0610	7.576	7.576	55.7	.865	2
1600.0	28.0	.1822	17.82	274.06	271.99	3.65	1.93	.6639	.0610	.0610	8.296	8.296	55.7	.871	2
1600.0	30.0	.2095	18.95	293.46	291.25	4.21	2.22	.5869	.0639	.0635	9.304	9.304	55.0	.876	3
1600.0	35.0	.2848	20.90	327.21	324.74	5.28	2.78	.4410	.0698	.0698	11.338	11.338	53.7	.890	3
1600.0	40.0	.3700	22.00	346.40	343.78	5.95	3.13	.3423	.0732	.0732	12.580	12.580	52.9	.900	3
1600.0	45.0	.4641	22.63	357.54	354.84	6.36	3.35	.2730	.0751	.0751	13.329	13.329	52.4	.911	2
1600.0	50.0	.5662	23.01	364.19	361.44	6.61	3.48	.2232	.0763	.0763	13.787	13.787	52.1	.920	2
1600.0	55.0	.6749	23.25	368.29	365.50	6.77	3.56	.1867	.0770	.0770	14.072	14.072	52.0	.927	2
1600.0	60.0	.7884	23.39	370.90	368.10	6.88	3.62	.1594	.0775	.0775	14.255	14.255	51.9	.932	2
1600.0	70.0	1.0134	23.56	373.74	370.91	6.99	3.68	.1235	.0779	.0779	14.455	14.455	51.8	.940	2
1600.0	80.0	1.0894	23.59	374.33	371.51	7.02	3.69	.1145	.0780	.0780	14.498	14.498	51.7	.943	2

A LINE WAS PLOTTED WITH 19 POINTS  
A LINE WAS PLOTTED WITH 19 POINTS

TABLE XXV (continued)

ALTITUDE EFFECTS

CARBURETOR-ENGINE OPERATION AT CONSTANT ENGINE SPEED-VARIABLE THROTTLE OPENING

ENGINE RPM	THROTTLE ANGLE	THROTTLE FLOW AREA	INTAKE MAN. PRESS	MCIST AIR FLOW	DRY AIR FLOW	BOOST VENTURI SUCTION	MAIN VENTURI SUCTION	THROTTLE MACH NO.	MAIN F/A RATIO	TOTAL F/A RATIO	TOTAL FUEL FLOW	MAIN FUEL FLOW	THROTTLE TOTAL TEMP	THROTTLE PLATE COEFF	J
2500.0	10.0	.0179	2.98	34.92	34.65	.05	.03	1.0000	.0000	.1265	2.192	.000	70.0	.683	3
2500.0	12.0	.0287	3.52	51.62	51.23	.11	.06	1.0000	.0000	.1241	3.178	.000	70.0	.721	2
2500.0	14.0	.0413	4.12	72.38	71.83	.23	.12	1.0000	.0000	.1045	3.753	.000	70.0	.757	3
2500.0	16.0	.0559	4.99	96.84	95.11	.43	.23	1.0000	.0108	.0920	4.422	.520	67.5	.790	3
2500.0	18.0	.0724	6.06	124.65	123.71	.72	.38	1.0000	.0256	.0803	4.567	1.584	64.0	.817	3
2500.0	20.0	.0907	7.29	155.34	154.17	1.14	.60	1.0000	.0428	.0684	5.274	3.302	60.0	.838	3
2500.0	22.0	.1109	8.62	189.12	187.69	1.70	.90	1.0000	.0555	.0605	5.711	5.245	56.9	.854	3
2500.0	24.0	.1329	10.02	225.35	223.65	2.44	1.29	1.0000	.0575	.0607	6.784	6.474	56.4	.859	2
2500.0	26.0	.1567	11.54	265.02	263.02	3.40	1.80	1.0000	.0603	.0609	8.004	7.524	55.9	.865	2
2500.0	28.0	.1822	13.17	307.31	304.99	4.60	2.43	.9656	.0610	.0610	9.302	9.302	55.7	.871	2
2500.0	30.0	.2095	14.71	347.43	344.81	5.93	3.12	.8627	.0610	.0610	10.517	10.517	55.7	.876	2
2500.0	35.0	.2848	17.75	427.61	424.38	9.13	4.78	.6582	.0610	.0610	12.544	12.544	55.7	.850	2
2500.0	40.0	.3700	19.74	480.06	476.43	11.63	6.07	.5187	.0663	.0663	15.759	15.795	54.5	.500	3
2500.0	45.0	.4641	20.98	513.70	509.82	13.43	6.99	.4178	.0701	.0701	17.870	17.870	53.6	.511	3
2500.0	50.0	.5662	21.77	535.10	531.06	14.65	7.61	.3436	.0725	.0725	19.251	19.251	53.0	.920	3
2500.0	55.0	.6749	22.27	548.83	544.68	15.47	8.03	.2884	.0740	.0740	20.162	20.162	52.7	.927	2
2500.0	60.0	.7884	22.60	557.76	553.55	16.02	8.30	.2469	.0750	.0750	20.766	20.766	52.4	.532	2
2500.0	70.0	1.0134	22.96	567.68	563.39	16.65	8.62	.1918	.0761	.0761	21.447	21.447	52.2	.540	2
2500.0	80.0	1.0894	23.04	569.80	565.49	16.78	8.69	.1780	.0764	.0764	21.553	21.553	52.1	.543	2

A LINE WAS PLOTTED WITH 19 POINTS  
 A LINE WAS PLOTTED WITH 19 POINTS  
 A LINE WAS PLOTTED WITH 19 POINTS  
 A LINE WAS PLOTTED WITH 19 POINTS

TABLE XXV (continued)

ROAD LOAD CARBURETOR-ENGINE-VEHICLE PERFORMANCE

6000 FEET ALTITUDE

THE FOLLOWING VALUES ARE CALCULATED FOR A TRANSMISSION GEAR RATIO OF 1.000

CAR MPH	ENGINE RPM	THROT ANGLE	MOIST AIRFLO	BHP	IHP	MAN. PRESS.	AO	F/A RATIO	ENGINE ISFC	ENGINE BSFC	FUEL RATE	MPG	AN
10.0	387.5	12.81	58.10	1.73	3.47	15.02	38.57	.1033	1.7147	3.4405	5.95	10.102	5
15.0	581.3	13.34	65.01	2.83	5.56	11.69	33.81	.0976	1.1298	2.2222	6.28	14.352	5
20.0	775.0	14.21	74.78	4.20	8.01	10.37	30.19	.0905	.8417	1.6035	6.74	17.835	4
25.0	968.7	15.49	90.11	5.95	10.87	10.09	30.01	.0863	.7107	1.2580	7.72	19.467	5
30.0	1162.5	16.81	107.39	8.16	14.23	10.11	28.19	.0812	.6081	1.0600	8.65	20.847	4
35.0	1356.2	18.24	128.02	10.55	18.18	10.33	25.52	.0749	.5239	.8704	9.53	22.094	5
40.0	1550.0	19.97	154.26	14.40	22.80	10.89	19.78	.0670	.4505	.7136	10.27	23.415	4
45.0	1743.8	22.33	194.49	18.62	28.27	12.07	18.43	.0610	.4165	.6322	11.77	22.986	4
50.0	1937.5	24.55	235.49	23.73	34.87	13.03	18.43	.0610	.4089	.6008	14.26	21.085	4
55.0	2131.2	27.02	283.90	29.84	42.65	14.15	18.43	.0610	.4031	.5760	17.19	19.241	4
60.0	2325.0	29.92	340.68	37.07	51.76	15.44	18.43	.0610	.3984	.5564	20.62	17.455	4
65.0	2518.7	33.40	406.63	45.53	62.35	16.87	18.43	.0610	.3947	.5405	24.61	15.882	3
70.0	2712.5	37.60	477.72	55.36	74.54	18.28	18.31	.0619	.3936	.5255	25.34	14.349	3
75.0	2906.3	42.28	547.57	66.69	88.44	19.41	18.70	.0653	.4013	.5322	35.45	12.708	4
80.0	3100.0	49.26	625.97	79.66	104.08	20.66	21.71	.0691	.4126	.5351	42.94	11.203	4
85.0	3293.7	64.46	714.19	94.41	121.58	22.03	24.63	.0733	.4273	.5503	51.95	9.839	6
90.0	3487.5	85.00	764.55	111.10	141.05	22.25	25.02	.0739	.4281	.5437	60.41	8.960	14

THE MAXIMUM VEHICLE SPEED HAS BEEN ATTAINED.....THIS SPEED IS 90.0 MILES PER HOUR

THE HIGH GEAR ROAD LOAD LINE WAS PLOTTED

# CARBURETOR-ENGINE OPERATING MAP

$P_0 = 24.00$  "HG       $T_0 = 70.0^\circ$ F      HUMIDITY = 40.0%  
 DISPLACEMENT = 289.2 IN<sup>3</sup>      COMP. RATIO = 9.30

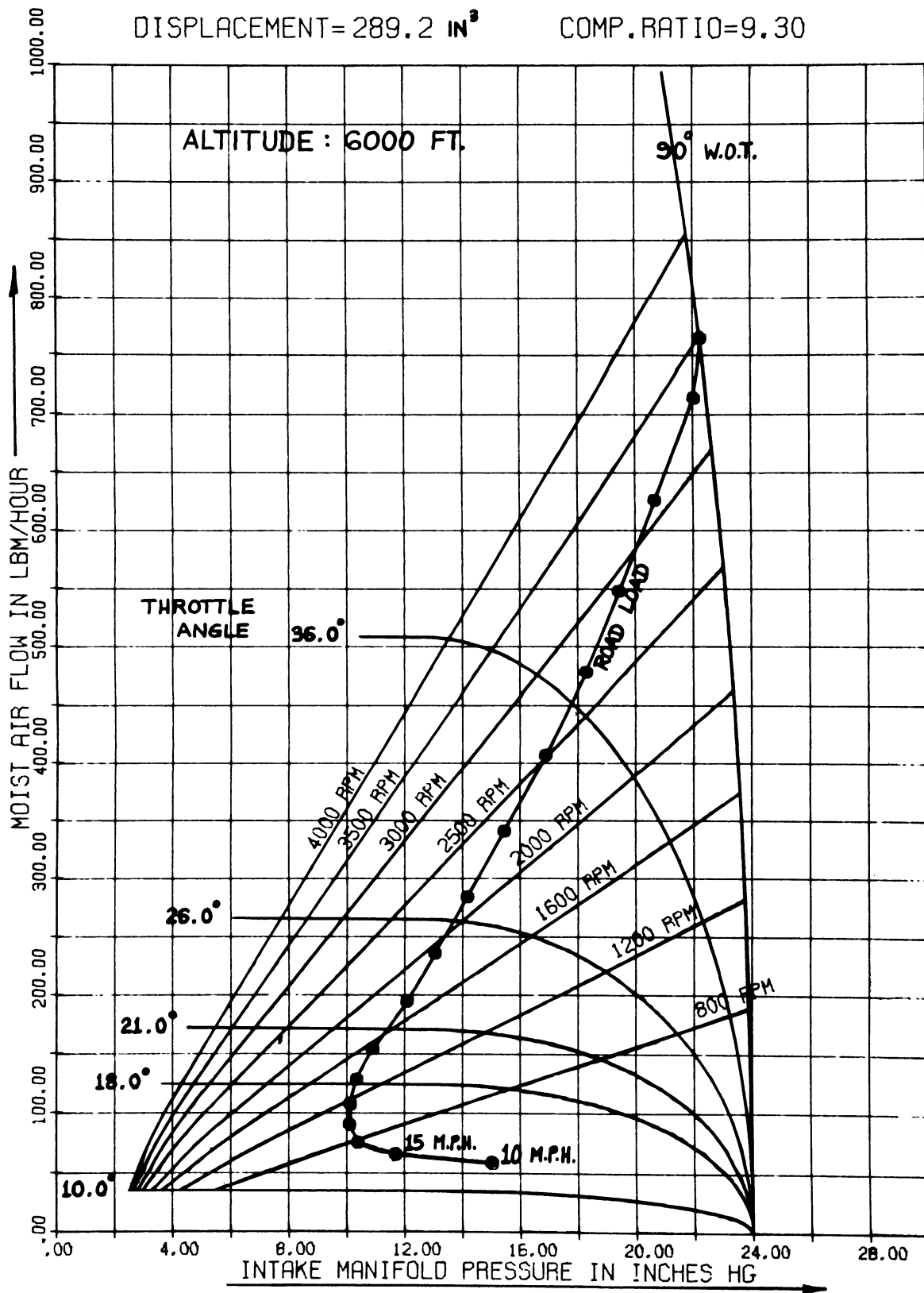


Figure 74. Carburetor - Engine - Vehicle Operating Map At Altitude

pressure are less at the altitude condition, as is the air flow rate for each throttle angle. One important item to notice however, is that the road load operating line is affected very little, except that the top speed of the vehicle is decreased (the intersection of the road load line with the wide open throttle line.)

The second example represents the results of a simulation run to determine the effects of a reduced ambient temperature, in this case  $0^{\circ}$  F. Again a complete carburetor-engine-vehicle operating map analysis was utilized. The fuel temperature specified for this simulation run was  $30^{\circ}$  F, which represented a reasonable float bowl temperature under these ambient conditions. The simulation predictions for the cold inlet air case are listed in Table 26, and are plotted in Figure 75.

If these results are compared to the corresponding results for normal ambient conditions (Figure 69 and Table 16), the following conclusions may be drawn:

1. The air mass flow rate is greater at the same throttle angle for the cold inlet air case.
2. The boost and primary venturi suction are less at the same air mass flow rate for the cold inlet air case.
3. The fuel-air ratios for the cold inlet air case are leaner than for normal inlet air temperatures at some air flow rates, and richer at other air flow rates.
4. The minimum air flow rate is greater, and the minimum intake manifold pressure is less for the cold inlet air case.

TABLE XXVI  
SIMULATION PREDICTIONS FOR CARBURETOR PERFORMANCE  
WITH REDUCED AMBIENT TEMPERATURE

UNIVERSITY OF MICHIGAN  
MECHANICAL ENGINEERING DOCTORAL THESIS  
DIGITAL SIMULATION OF CARBURETOR METERING  
CARBURETOR-ENGINE-VEHICLE OPERATING MAP  
DAVID L. HARRINGTON

THE TYPE OF ANALYSIS REQUESTED IS.....COMPLETE OPERATING MAP  
THE TYPE OF PLOT(S) REQUESTED ARE.....COMPLETE OPERATING MAP  
THIS SIMULATION PERFORMED ON .....19 FEB 1968  
PURPOSE OF THIS SIMULATION RUN .....TO CHECK THE EFFECT AMBIENT TEMPERATURE ON THE OPERATING MAP

AMBIENT CONDITIONS		CARBURETOR		FUEL		ENGINE		VEHICLE	
PRESSURE = 29.28 INCHES HG	FGRD 2 BBL. C6AF-9510-B STANFORD REG. GASOLINE	1966 FORD 289 V-8						1966 FORD FAIRLANE	
TEMPERATURE = 40.0 PERCENT HUMIDITY = 40.0 PERCENT DENSITY = .0845 LB/M/FT <sup>3</sup>	MAIN JET = F-50 MAIN VENTURI=1.145 IN. VISCOSITY = .752 CLOSED THROTTLE=10.0	TEMPERATURE = 30.0 F SPECIFIC GRAVITY = .752 VALVE FLOW AREA=6.82 IN <sup>2</sup>						VEHICLE WEIGHT=3435.0 REAR AXLE RATIO= 3.00 TIRE REVS/MILE =775.0	

CARBURETOR-ENGINE OPERATION AT CONSTANT ENGINE SPEED-VARIABLE THROTTLE OPENING

ENGINE RPM	THROT ANGLE	THROT FLOW AREA	INTAKE		MOIST AIR FLOW		DRY AIR FLOW		BCCST VENTURI SUCTION		MAIN VENTURI SUCTION		THROT MACH NO.	MAIN F/A RATIO	TOTAL F/A RATIO	TOTAL FUEL FLOW		MAIN FUEL FLOW		THROT TOTAL TEMP	THROT PLATE COEFF J	
			MAN. PRESS	AREA	AIR FLOW	MOIST AIR FLOW	AIR FLOW	VENTURI SUCTION	BCCST VENTURI SUCTION	MAIN VENTURI SUCTION	F/A RATIO	F/A RATIO				FUEL FLOW	FUEL FLOW					
800.0	10.0	.0175	6.26	.0175	45.51	45.51	45.51	.03	.06	.03	.03	1.0000	.0000	.1321	3.031	.000	.000	.000	.000	.0	.683	3
800.0	12.0	.0286	8.34	.0286	67.49	67.49	67.49	.07	.14	.07	.07	1.0000	.0000	.1109	3.742	.000	.000	.000	.000	.0	.721	3
800.0	14.0	.0413	11.27	.0413	94.15	94.15	94.15	.15	.28	.15	.15	1.0000	.0101	.0909	4.281	.474	.474	.474	.474	-2.4	.757	3
800.0	16.0	.0559	14.83	.0559	125.49	125.49	125.49	.27	.52	.27	.27	1.0000	.0289	.0759	4.764	1.813	1.813	1.813	1.813	-6.8	.790	3
800.0	18.0	.0724	18.38	.0724	157.47	157.47	157.47	.44	.83	.44	.44	.8439	.0503	.0657	5.176	3.561	3.561	3.561	3.561	-11.8	.817	3
800.0	20.0	.0907	21.25	.0907	183.51	183.51	183.51	1.15	1.15	1.15	1.15	.6929	.0610	.0610	5.597	5.597	5.597	5.597	5.597	-14.4	.838	3
800.0	22.0	.1109	23.37	.1109	203.28	203.28	203.28	1.42	1.42	1.42	1.42	.5759	.0613	.0613	6.229	6.229	6.229	6.229	6.229	-14.4	.854	3
800.0	24.0	.1325	24.80	.1325	217.27	217.27	217.27	1.63	1.63	1.63	1.63	.4912	.0656	.0656	7.131	7.131	7.131	7.131	7.131	-15.5	.859	3
800.0	26.0	.1567	25.87	.1567	227.75	227.75	227.75	1.80	1.80	1.80	1.80	.4220	.0689	.0689	7.645	7.645	7.645	7.645	7.645	-16.2	.865	3
800.0	28.0	.1822	26.64	.1822	235.41	235.41	235.41	1.94	1.94	1.94	1.94	.3662	.0712	.0712	8.386	8.386	8.386	8.386	8.386	-16.8	.871	2
800.0	30.0	.2094	27.21	.2094	241.08	241.08	241.08	2.04	2.04	2.04	2.04	.3203	.0730	.0730	8.799	8.799	8.799	8.799	8.799	-17.2	.876	2
800.0	35.0	.2848	28.09	.2848	249.83	249.83	249.83	2.20	2.20	2.20	2.20	1.15	.0757	.0757	5.453	5.453	5.453	5.453	5.453	-17.8	.890	2
800.0	40.0	.3699	28.55	.3699	254.24	254.24	254.24	2.29	2.29	2.29	2.29	1.813	.0770	.0770	9.791	9.791	9.791	9.791	9.791	-18.2	.900	2
800.0	45.0	.4640	28.77	.4640	256.62	256.62	256.62	2.34	2.34	2.34	2.34	1.439	.0778	.0778	9.977	9.977	9.977	9.977	9.977	-18.3	.911	2
800.0	50.0	.5660	28.91	.5660	258.00	258.00	258.00	2.37	2.37	2.37	2.37	1.24	.0782	.0782	10.085	10.085	10.085	10.085	10.085	-18.4	.920	2
800.0	55.0	.6747	28.99	.6747	258.63	258.63	258.63	2.38	2.38	2.38	2.38	1.25	.0784	.0784	10.150	10.150	10.150	10.150	10.150	-18.5	.927	2
800.0	60.0	.7882	25.05	.7882	259.35	259.35	259.35	2.40	2.40	2.40	2.40	1.25	.0834	.0786	10.191	10.191	10.191	10.191	10.191	-18.5	.932	2
800.0	70.0	1.0131	25.10	1.0131	259.91	259.91	259.91	2.41	2.41	2.41	2.41	1.26	.0645	.0788	10.235	10.235	10.235	10.235	10.235	-18.6	.940	2
800.0	80.0	1.0889	25.11	1.0889	260.02	260.02	260.02	2.41	2.41	2.41	2.41	1.26	.0599	.0788	10.244	10.244	10.244	10.244	10.244	-18.6	.943	1

THE OPERATING MAP GRID HAS BEEN DRAWN  
A LINE WAS PLOTTED WITH 19 POINTS



TABLE XXVI (continued)

A LINE WAS PLOTTED WITH 19 FCINIS

CARBURETOR-ENGINE OPERATION AT CONSTANT ENGINE SPEED-VARIABLE THROTTLE OPENING

ENGINE RPM	THRUT ANGLE	THRUT FLOW		INTAKE MAN. PRESS		MCIST AIR FLCW		DRY AIR FLCW		BCCST VENTURI SUCTION		MAIN VENTURI SUCTION		IFROT MACH NC.	MAIN F/A RATIO	TOTAL F/A RATIO	ICTAL FUEL FLOW	MAIN FUEL FLOW	THRGT TOTAL TEMP	THRCT PLATE COEFF	J
		AREA	AREA	AREA	AREA	AREA	AREA	AREA	AREA	AREA	AREA	AREA	AREA								
1600.0	10.0	.0175	4.24	45.55	45.95	.06	.03	1.0000	.0000	.1385	.0000	.1385	3.191	.000	.000	.000	.000	.0	.683	3	
1600.0	12.0	.0286	5.06	67.52	67.52	.14	.07	1.0000	.0000	.1205	.0000	.1205	4.669	.000	.000	.000	.000	.0	.721	3	
1600.0	14.0	.0413	6.37	94.39	94.39	.25	.15	1.0000	.0000	.1018	.0000	.1018	4.805	.431	.431	.431	.431	-2.2	.757	3	
1600.0	16.0	.0559	8.09	125.81	125.81	.52	.27	1.0000	.0000	.0850	.0248	.0850	5.349	1.562	1.562	1.562	1.562	-5.8	.790	3	
1600.0	18.0	.0724	10.13	161.66	161.66	.88	.46	1.0000	.0000	.0681	.0443	.0681	5.506	3.581	3.581	3.581	3.581	-10.4	.817	3	
1600.0	20.0	.0907	12.39	202.63	202.63	1.40	.73	1.0000	.0539	.0615	.0539	.0615	6.226	5.458	5.458	5.458	5.458	-12.7	.838	3	
1600.0	22.0	.1105	14.85	248.13	248.13	2.12	1.11	1.0000	.0572	.0607	.0572	.0607	7.530	7.101	7.101	7.101	7.101	-13.5	.854	2	
1600.0	24.0	.1325	17.25	292.89	292.89	2.98	1.56	.9018	.0610	.0610	.0610	.0610	8.532	8.927	8.927	8.927	8.927	-14.4	.859	2	
1600.0	26.0	.1567	19.42	333.01	333.01	3.88	2.03	.7861	.0610	.0610	.0610	.0610	10.157	10.157	10.157	10.157	10.157	-14.4	.865	2	
1600.0	28.0	.1822	21.22	366.46	366.46	4.72	2.47	.6892	.0610	.0610	.0610	.0610	11.177	11.177	11.177	11.177	11.177	-14.4	.871	2	
1600.0	30.0	.2094	22.69	393.77	393.77	5.48	2.86	.6076	.0610	.0610	.0610	.0610	12.010	12.010	12.010	12.010	12.010	-14.4	.876	2	
1600.0	35.0	.2848	25.17	441.75	441.75	6.57	3.62	.4569	.0668	.0668	.0668	.0668	14.748	14.748	14.748	14.748	14.748	-15.7	.890	3	
1600.0	40.0	.3699	26.58	469.52	469.52	7.91	4.11	.3552	.0710	.0710	.0710	.0710	16.680	16.680	16.680	16.680	16.680	-16.7	.900	3	
1600.0	45.0	.4640	27.39	485.75	485.75	8.50	4.41	.2837	.0735	.0735	.0735	.0735	17.863	17.863	17.863	17.863	17.863	-17.3	.911	3	
1600.0	50.0	.5660	27.88	495.52	495.52	8.57	4.60	.2320	.0750	.0750	.0750	.0750	18.593	18.593	18.593	18.593	18.593	-17.7	.920	2	
1600.0	55.0	.6747	28.19	501.55	501.55	9.10	4.72	.1942	.0760	.0760	.0760	.0760	19.050	19.050	19.050	19.050	19.050	-17.9	.927	2	
1600.0	60.0	.7882	28.38	505.40	505.40	9.26	4.80	.1658	.0766	.0766	.0766	.0766	19.345	19.345	19.345	19.345	19.345	-18.0	.932	2	
1600.0	70.0	1.0131	28.59	509.59	509.59	9.42	4.88	.1285	.0772	.0772	.0772	.0772	19.669	19.669	19.669	19.669	19.669	-18.2	.940	2	
1600.0	80.0	1.0885	28.63	510.46	510.46	9.46	4.90	.1192	.0773	.0773	.0773	.0773	19.737	19.737	19.737	19.737	19.737	-18.2	.943	2	

A LINE WAS PLOTTED WITH 19 FCINIS

TABLE XXVI (continued)

CARBURETOR-ENGINE OPERATION AT CONSTANT ENGINE SPEED-VARIABLE THROTTLE OPENING

ENGINE RPM	THROTTLE ANGLE	THROTTLE FLOW AREA		INTAKE MAN. PRESS		PCIST AIR FLOW		DRY AIR FLOW		BCCST VENTURI SUCTION		MAIN VENTURI SUCTION		THROTTLE MACH NO.	MAIN F/A RATIO	TOTAL F/A RATIO	TOTAL FUEL FLOW		MAIN FUEL FLOW	THROTTLE TOTAL TEMP	THROTTLE COEFF	J
		THROTTLE FLOW AREA	INTAKE MAN. PRESS	PCIST AIR FLOW	DRY AIR FLOW	BCCST VENTURI SUCTION	MAIN VENTURI SUCTION	TOTAL FUEL FLOW	MAIN FUEL FLOW													
2500.0	10.0	.0179	3.54	45.64	45.84	.06	.03	1.0000	.0000	.1416	3.246	.000	.000	1.0000	.0000	.1416	3.246	.000	.000	.0	.683	4
2500.0	12.0	.0286	3.94	67.53	67.53	.14	.07	1.0000	.0000	.1246	4.207	.000	.000	1.0000	.0000	.1246	4.207	.000	.000	.0	.721	3
2500.0	14.0	.0413	4.67	94.25	94.29	.28	.15	1.0000	.0000	.1071	5.050	.414	.414	1.0000	.0088	.1071	5.050	.414	.414	-2.1	.757	3
2500.0	16.0	.0555	5.70	125.55	125.95	.52	.27	1.0000	.0237	.0907	5.709	1.491	1.491	1.0000	.0237	.0907	5.709	1.491	1.491	-5.6	.790	3
2500.0	18.0	.0724	7.00	162.02	162.02	.88	.46	1.0000	.0415	.0728	5.501	3.365	3.365	1.0000	.0415	.0728	5.501	3.365	3.365	-9.8	.817	3
2500.0	20.0	.0907	8.46	203.27	203.27	1.41	.74	1.0000	.0493	.0652	6.631	5.006	5.006	1.0000	.0493	.0652	6.631	5.006	5.006	-11.6	.838	3
2500.0	22.0	.1105	10.04	248.99	248.99	2.13	1.12	1.0000	.0510	.0633	7.880	6.352	6.352	1.0000	.0510	.0633	7.880	6.352	6.352	-12.0	.854	2
2500.0	24.0	.1329	11.70	296.72	296.72	3.05	1.60	1.0000	.0530	.0619	9.180	7.864	7.864	1.0000	.0530	.0619	9.180	7.864	7.864	-12.5	.859	2
2500.0	26.0	.1567	13.50	348.81	348.81	4.25	2.22	1.0000	.0553	.0610	10.634	9.653	9.653	1.0000	.0553	.0610	10.634	9.653	9.653	-13.0	.865	2
2500.0	28.0	.1822	15.42	404.39	404.39	5.77	3.01	.9984	.0581	.0607	12.267	11.744	11.744	.9984	.0581	.0607	12.267	11.744	11.744	-13.7	.871	3
2500.0	30.0	.2094	17.30	458.52	458.92	7.48	3.89	.8941	.0610	.0610	13.997	13.997	13.997	.8941	.0610	.0610	13.997	13.997	13.997	-14.4	.876	3
2500.0	35.0	.2848	21.14	570.31	570.31	11.74	6.08	.6833	.0610	.0610	17.395	17.395	17.395	.6833	.0610	.0610	17.395	17.395	17.395	-14.4	.890	2
2500.0	40.0	.3695	23.65	643.66	643.66	15.15	7.81	.5360	.0621	.0621	19.992	19.992	19.992	.5360	.0621	.0621	19.992	19.992	19.992	-14.7	.900	2
2500.0	45.0	.4640	25.20	691.05	691.09	17.63	9.05	.4327	.0668	.0668	23.097	23.097	23.097	.4327	.0668	.0668	23.097	23.097	23.097	-15.8	.911	3
2500.0	50.0	.5660	26.18	721.54	721.54	19.33	9.90	.3563	.0699	.0699	25.202	25.202	25.202	.3563	.0699	.0699	25.202	25.202	25.202	-16.5	.920	3
2500.0	55.0	.6747	26.82	741.16	741.16	20.48	10.47	.2993	.0718	.0718	26.605	26.605	26.605	.2993	.0718	.0718	26.605	26.605	26.605	-16.9	.927	3
2500.0	60.0	.7882	27.23	753.99	753.99	21.26	10.85	.2563	.0731	.0731	27.542	27.542	27.542	.2563	.0731	.0731	27.542	27.542	27.542	-17.2	.932	3
2500.0	70.0	1.0131	27.69	768.27	768.27	22.15	11.29	.1992	.0745	.0745	28.602	28.602	28.602	.1992	.0745	.0745	28.602	28.602	28.602	-17.5	.940	3
2500.0	80.0	1.0889	27.79	771.31	771.31	22.34	11.38	.1850	.0748	.0748	28.830	28.830	28.830	.1850	.0748	.0748	28.830	28.830	28.830	-17.6	.943	2

A LINE WAS PLOTTED WITH 19 PCINIS  
A LINE WAS PLOTTED WITH 18 PCINIS  
A LINE WAS PLOTTED WITH 16 PCINIS

# CARBURETOR-ENGINE OPERATING MAP

$P_0 = 29.28'' \text{ HG}$      $T_0 = 0.0^\circ \text{ F}$     HUMIDITY = 40.0 %  
 DISPLACEMENT = 289.2  $\text{IN}^3$     COMP. RATIO = 9.30

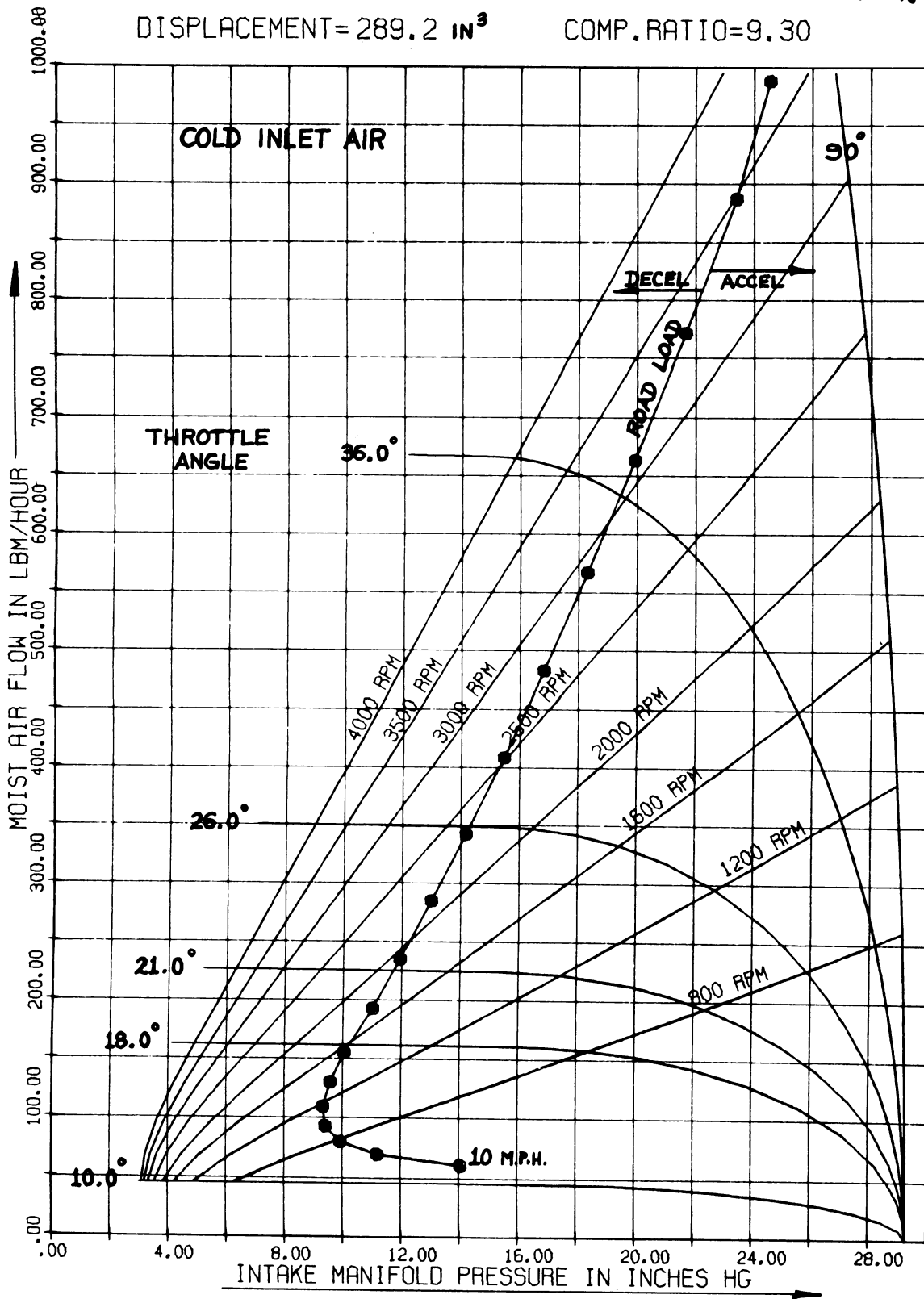


Figure 75. Carburetor - Engine - Vehicle Operating Map For Reduced Ambient Temperature

## CHAPTER X

### RECOMMENDATIONS

Although the simulation as written provides a reasonable description of carburetor performance over a wide operating range, there are nevertheless many areas in which further investigations are needed. Some of these areas will be discussed briefly.

The fuel channel model should be extended to include fuel vaporization and temperature changes within the channel network. The current model utilizes a constant fuel temperature throughout the channel, and does not include the flow of fuel vapor. The ASTM distillation curve for each possible fuel type should be made available in the analysis. The residence time of the fuel-air mixture within the fuel channel and the changing volume flow rate of the bubbles should both be considered. The volume flow rate of the gas phase will be affected by the following factors:

1. Fuel vaporization along the channel.
2. Pressure and temperature changes along the channel.
3. Changing gas phase composition.
4. Condensation of bleed air moisture.

Another important area of further study is that of pulsating flow. Basic analyses should be performed on the air pulses within the carburetor, and upon the resulting fluid pulsations within the fuel channel. The pulses should be described in terms of the engine and carburetor variables, and the damping effect of the throttle plate analyzed. The effect of fluid pulsation frequency and waveform on the discharge

coefficient of orifices should also be investigated.

There are numerous additional areas which could and should be studied in the future. This includes the effects of back or reverse flow within the fuel channel, the improved description and prediction of fuel drop size distributions, and the extension of the simulation to air valve carburetors.

APPENDIX A

ADDITIONAL SIMULATION PREDICTIONS

LOG-LOG PLOT OF CARBURETOR FLOW PARAMETERS

MAIN ORIFICE NUMBER= F-50

FUEL TEMPERATURE = 80.0 °F

RUN NUMBER = 1/11/68

FUEL = STANDARD GASOLINE

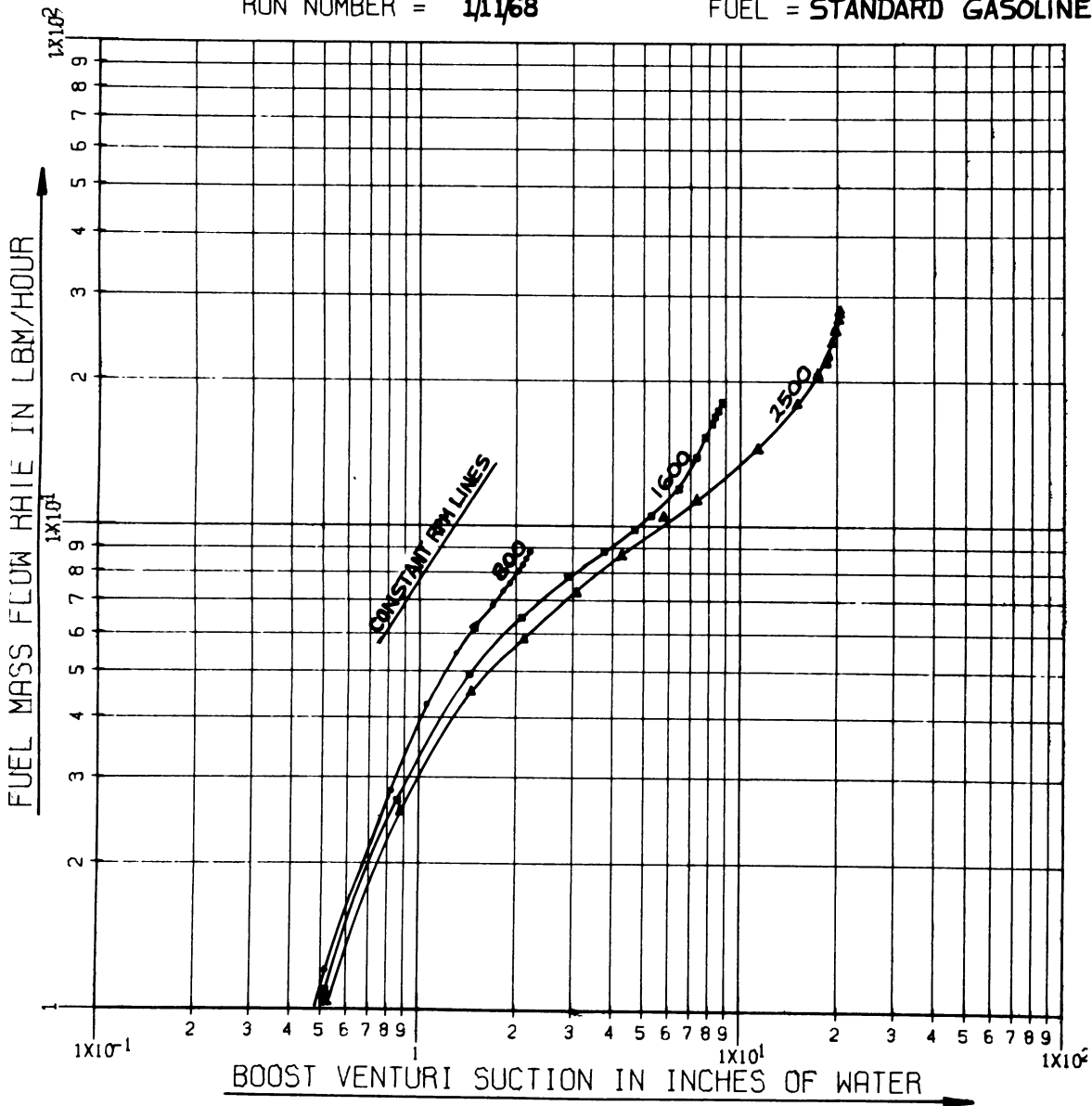


Figure 76. Simulation Predictions Of Main Fuel Flow Rates

TABLE XXVII  
 SIMULATION PREDICTIONS FOR THE EFFECTS OF PRODUCTION  
 TOLERANCES ON CARBURETOR PERFORMANCE (FORD  
 C4AFB-91 CARBURETOR

UNIVERSITY OF MICHIGAN  
 MECHANICAL ENGINEERING DOCTORAL THESIS  
 DIGITAL SIMULATION OF CARBURETOR METERING  
 CARBURETOR-ENGINE-VEHICLE OPERATING MAP

DAVID L. HARRINGTON

THE TYPE OF ANALYSIS REQUESTED IS.....SPECIFIED INPUT POINT  
 THE TYPE OF PLOTS REQUESTED ARE.....NO PLOTS REQUESTED  
 THIS SIMULATION PERFORMED ON.....05 MAR 1968  
 PURPOSE OF THIS SIMULATION RUN.....TO SIMULATE PRODUCTION VARIATIONS IN CARBURETOR DIMENSIONS

AMBIENT CONDITIONS	CARBURETOR	FUEL	ENGINE	VEHICLE
PRESSURE = 29.90 INCHES HG	FORD 2 BARREL C4AFB-91	STANDARD REG. GASOLINE	1966 FORD 289 V-8	1966 FORD FAIRLANE
TEMPERATURE = 80.0 DEGREES F	MAIN JET = F-50	TEMPERATURE = 80.0 F	DISPLACEMENT=289.2 C.I.	VEHICLE WEIGHT=3435.0
HUMIDITY = 50.0 PERCENT	MAIN VENTURI=1.145 IN.	SPECIFIC GRAVITY= .721	COMP. RATIO = 9.3	REAR AXLE RATIO= 3.00
DENSITY = .0713 LBM/FT <sup>3</sup>	CLOSED THROTTLE= 5.0	VISCOSITY = .556 CS	VALVE FLOW AREA=6.82 IN <sup>2</sup>	TIRE REVS/MILE =775.0

INPUT DATA FOR THE FORD 2 BARREL C4AFB-91 CARBURETOR.  
 \*\*\*NOMINAL DIMENSIONS\*\*\*

MAIN METERING ORIFICE TYPE F-50  
 MAIN METERING ORIFICE DIAMETER = .0502 INCH  
 MAIN METERING ORIFICE LENGTH = .1830 INCH  
 MAIN METERING ORIFICE L/D RATIO = 3.6454  
 NUMBER OF MAIN METERING ORIFICES = 2  
 COMPLETELY CLOSED THROTTLE ANGLE = 5.000 DEGREES  
 THROTTLE MORE DIAMETER = 1.4370 INCHES  
 THROTTLE SHAFT DIAMETER = .3750 INCH  
 INITIAL SPILL POINT OF MAIN SYSTEM = .200 INCH  
 MAIN VENTURI THROAT DIAMETER = 1.1450 INCHES

THROTTLE PLATE BYPASSES

TRANSFER TUBE DIAMETER = .0730 INCH  
 CHOKE BLEED RESTRICTION DIAMETER = .0000 INCH  
 ENRICHMENT BLEED RESTRICTION DIAMETER = .0730 INCH

GEOMETRIC RELATION BETWEEN BOOST AND MAIN VENTURI

XWV1 = 1.2500 INCHES  
 XWV2 = 1.0000 INCHES  
 XBV = .7800 INCHES  
 XMB = .0700 INCHES



TABLE XXVII (continued)

DIMENSIONS OF A TYPICAL PRODUCTION CARRURETOR

MAIN METERING ORIFICE TYPE F-50  
 MAIN METERING ORIFICE DIAMETER = .0500 INCH  
 MAIN METERING ORIFICE LENGTH = .1830 INCH  
 MAIN METERING ORIFICE L/D RATIO = 3.6573  
 NUMBER OF MAIN METERING ORIFICES = 2  
 COMPLETELY CLOSED THROTTLE ANGLE = 5.002 DEGREES  
 THROTTLE ROPE DIAMETER = 1.4375 INCHES  
 THROTTLE SHAFT DIAMETER = .3745 INCH  
 INITIAL SPILL POINT OF MAIN SYSTEM = .200 INCH  
 MAIN VENTURI THROAT DIAMETER = 1.1450 INCHES

THROTTLE-PLATE BYPASSES

TRANSFER TUBE DIAMETER = .0730 INCH  
 CHECK BLEED RESTRICTION DIAMETER = .0000 INCH  
 ENRICHMENT BLEED RESTRICTION DIAMETER = .0732 INCH

GEOMETRIC RELATION BETWEEN ROOST AND MAIN VENTURI

XWV1 = 1.2468 INCHES  
 XWV2 = 1.0002 INCHES  
 XRV = .7769 INCHES  
 XMR = .0095 INCHES

MAIN VENTURI ELEMENT		DIAMETER	LENGTH	L/D RATIO	ORIFICE TYPE
1		1.030 INCHES	.183 INCH	3.657	1.0
2		1.930 INCHES	.312 INCH	1.664	.0
3		1.145 INCHES	.106 INCH	1.311	3.0
4		1.160 INCHES	.125 INCH	.399	.0
5		1.400 INCHES	.390 INCH	2.498	2.0
ROOST VENTURI ELEMENT		DIAMETER	LENGTH	L/D RATIO	ORIFICE TYPE
1		1.030 INCHES	.183 INCH	3.657	1.0
2		.875 INCHES	.312 INCH	1.664	.0
3		.538 INCHES	.106 INCH	1.311	3.0
4		.596 INCHES	.125 INCH	.399	.0
5		.650 INCHES	.390 INCH	2.498	2.0
6		.750 INCHES	.206 INCH	1.527	.0
FUEL CHANNEL ELEMENT		DIAMETER	LENGTH	L/D RATIO	ORIFICE TYPE
1		.0500 INCH	.183 INCH	3.657	1.0
2		.1875 INCH	.312 INCH	1.664	.0
3		.0800 INCH	.106 INCH	1.311	3.0
4		.3133 INCH	.125 INCH	.399	.0
5		.1561 INCH	.390 INCH	2.498	2.0
6		.1349 INCH	.206 INCH	1.527	.0
7		.0282 INCH	.125 INCH	4.438	2.0
8		.1471 INCH	.938 INCH	6.372	.0

TABLE XXVII (continued)

MATN VENTURI ELEMENT	DIAMETER	DIAMETER	LFNGTH	L/D RATIO	ORIFICE TYPE
1	1.930 INCHES	.502 INCH	.183 INCH	3.645	1.0
2	1.930 INCHES	.1870 INCH	.312 INCH	1.668	.0
3	1.145 INCHES	.0810 INCH	.106 INCH	1.309	3.0
4	1.160 INCHES	.3125 INCH	.125 INCH	.400	.0
5	1.400 INCHES	.1560 INCH	.390 INCH	2.500	2.0
		.1350 INCH	.206 INCH	1.526	.0
		.0280 INCH	.125 INCH	4.464	2.0
		.1470 INCH	.038 INCH	6.378	.0
		.2910 INCH	.250 INCH	.859	.0
		.1580 INCH	1.000 INCH	6.329	.0
		.2700 INCH	.340 INCH	1.259	.0
		.1600 INCH	.012 INCH	5.075	.0
		.2250 INCH	.135 INCH	.600	2.0
		.0610 INCH	1.930 INCH	31.639	.0
		.0260 INCH	.094 INCH	3.608	2.0
		.1400 INCH	.706 INCH	5.043	.0
		.0940 INCH	.780 INCH	8.298	.0
		.0420 INCH	.106 INCH	2.524	2.0
		.0940 INCH	2.000 INCH	21.277	.0
		.0590 INCH	.106 INCH	1.797	3.0
		.0310 INCH	.125 INCH	4.032	2.0
		.0446 INCH	.031 INCH	.700	2.0
		.0270 INCH	.140 INCH	5.185	2.0
		.0390 INCH	.125 INCH	3.205	2.0
		.0350 INCH	.106 INCH	3.029	2.0

BOOST VENTURI  
ELEMENT

DIAMETER
1.030 INCHES
.875 INCHES
.538 INCHES
.504 INCHES
.650 INCHES
.750 INCHES

FUEL CHANNEL  
ELEMENT

FUEL CHANNEL ELEMENT	DIAMETER	DIAMETER	LFNGTH	L/D RATIO	ORIFICE TYPE
1	.502 INCH	.502 INCH	.183 INCH	3.645	1.0
2	.1870 INCH	.1870 INCH	.312 INCH	1.668	.0
3	.0810 INCH	.0810 INCH	.106 INCH	1.309	3.0
4	.3125 INCH	.3125 INCH	.125 INCH	.400	.0
5	.1560 INCH	.1560 INCH	.390 INCH	2.500	2.0
6	.1350 INCH	.1350 INCH	.206 INCH	1.526	.0
7	.0280 INCH	.0280 INCH	.125 INCH	4.464	2.0
8	.1470 INCH	.1470 INCH	.038 INCH	6.378	.0
9	.2910 INCH	.2910 INCH	.250 INCH	.859	.0
10	.1580 INCH	.1580 INCH	1.000 INCH	6.329	.0
11	.2700 INCH	.2700 INCH	.340 INCH	1.259	.0
12	.1600 INCH	.1600 INCH	.012 INCH	5.075	.0
13	.2250 INCH	.2250 INCH	.135 INCH	.600	2.0
14	.0610 INCH	.0610 INCH	1.930 INCH	31.639	.0
15	.0260 INCH	.0260 INCH	.094 INCH	3.608	2.0
16	.1400 INCH	.1400 INCH	.706 INCH	5.043	.0
17	.0940 INCH	.0940 INCH	.780 INCH	8.298	.0
18	.0420 INCH	.0420 INCH	.106 INCH	2.524	2.0
19	.0940 INCH	.0940 INCH	2.000 INCH	21.277	.0
20	.0590 INCH	.0590 INCH	.106 INCH	1.797	3.0
21	.0310 INCH	.0310 INCH	.125 INCH	4.032	2.0
22	.0446 INCH	.0446 INCH	.031 INCH	.700	2.0
23	.0270 INCH	.0270 INCH	.140 INCH	5.185	2.0
24	.0390 INCH	.0390 INCH	.125 INCH	3.205	2.0
25	.0350 INCH	.0350 INCH	.106 INCH	3.029	2.0

TABLE XXVII (continued)

10	.2904 INCH	.861	.750 INCH	.0
11	.1583 INCH	6.316	1.000 INCH	.0
12	.2720 INCH	1.250	.340 INCH	.0
13	.1600 INCH	5.074	.812 INCH	.0
14	.2243 INCH	.602	1.135 INCH	2.0
15	.0609 INCH	31.687	1.930 INCH	.0
16	.0260 INCH	3.614	.094 INCH	2.0
17	.1193 INCH	5.068	.706 INCH	.0
18	.0940 INCH	8.297	.780 INCH	.0
19	.0419 INCH	2.534	1.06 INCH	2.0
20	.0952 INCH	21.006	2.000 INCH	.0
21	.0310 INCH	1.794	1.104 INCH	3.0
22	.0443 INCH	4.032	.125 INCH	2.0
23	.0273 INCH	.705	.031 INCH	2.0
24	.0349 INCH	5.121	.140 INCH	2.0
25	.0351 INCH	3.214	.125 INCH	2.0
		3.016	.106 INCH	2.0

CAPTURED-ENGINE OPERATION FOR SPECIFIC OPERATING POINTS (RPM AND THETA SUPPLIED AS INPUT DATA)

ENGINE RPM	THRUST ANGLE	THRUST FLOW AREA	INTAKE MAN. PRESS	MOIST AIR FLOW	DRY AIR FLOW	ROOST VENTURI SUCTION	MAIN VENTURI SUCTION	THRUST MACH NO.	MAIN F/A RATIO	TOTAL F/A RATIO	TOTAL FUEL FLOW	MAIN FUEL FLOW	THRUST TOTAL TEMP	AIR BLEED FLOW	J
1600.0	30.0	.2153	23.30	354.82	350.94	5.26	2.76	.5626	.0629	.0629	22.091	22.091	65.3	.416	2
1600.0	30.0	.2152	23.28	354.82	350.93	5.27	2.77	.5633	.0637	.0637	22.352	22.352	65.1	.416	2
1600.0	30.0	.2151	23.28	354.78	350.90	5.27	2.78	.5636	.0640	.0640	22.447	22.447	65.1	.412	2
1600.0	30.0	.2150	23.27	354.66	350.77	5.24	2.75	.5638	.0637	.0637	22.333	22.333	65.1	.420	2
1600.0	30.0	.2152	23.29	354.74	350.86	5.25	2.76	.5631	.0632	.0632	22.172	22.172	65.2	.415	2
1600.0	30.0	.2151	23.28	354.84	350.95	5.24	2.77	.5635	.0641	.0641	22.487	22.487	65.0	.423	2
1600.0	30.0	.2152	23.27	354.82	350.94	5.27	2.77	.5639	.0644	.0644	22.615	22.615	65.0	.408	2
1600.0	30.0	.2152	23.27	354.82	350.93	5.26	2.76	.5639	.0644	.0644	22.590	22.590	65.0	.415	2
1600.0	30.0	.2152	23.29	354.82	350.94	5.28	2.76	.5629	.0633	.0633	22.216	22.216	65.2	.419	2
1600.0	30.0	.2151	23.27	354.79	350.90	5.27	2.76	.5639	.0643	.0643	22.573	22.573	65.0	.411	2
1600.0	30.0	.2152	23.29	354.89	351.00	5.24	2.75	.5630	.0637	.0637	22.370	22.370	65.1	.409	2
1600.0	30.0	.2150	23.28	354.70	350.81	5.26	2.76	.5636	.0636	.0636	22.294	22.294	65.2	.414	2

## APPENDIX B

### THROTTLE FLOW AREA

The throttle plate-shaft combination will be analyzed geometrically to obtain the throttle flow area as a function of throttle angle, plate and shaft diameters, and throttle closing angle. This flow area corresponds to the throat area of the converging nozzle which is used as the throttle plate model.

The symbols used in this analysis are:

$D$  = throttle bore diameter

$d$  = throttle shaft diameter

$\theta$  = throttle angle

$\theta_0$  = throttle angle in completely closed position

$A$  = area

Figure 77 illustrates the variables involved in the throttle flow analysis. Note that the minimum possible throttle angle is  $\theta_0$  and that the throttle shaft constitutes a variable restriction which depends on the throttle angle. (It contributes very little at small throttle angles and is the entire restriction at wide open throttle.)

Note that the throttle bore area is  $\pi D^2/4$  and that the throttle restriction area is:

$$\frac{\pi}{4} D^2 \left( \frac{\cos \theta}{\cos \theta_0} \right)$$

If the throttle shaft were negligibly small, the flow area would be;

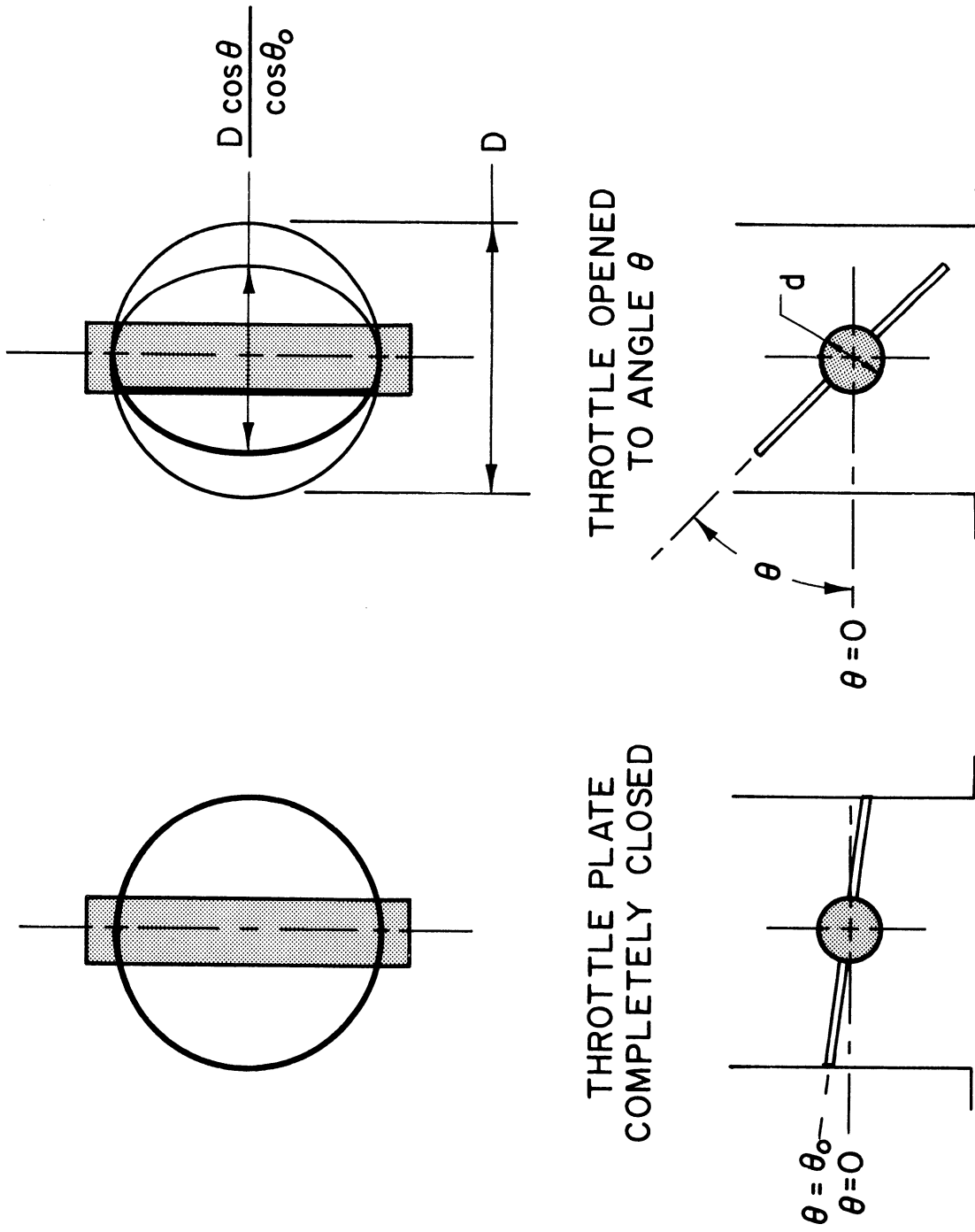
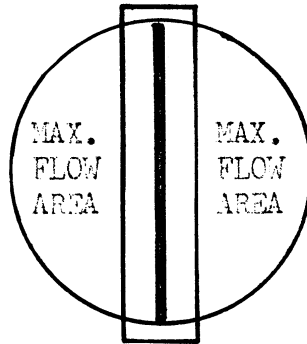


Figure 77. Variables In The Throttle Plate Flow Analysis

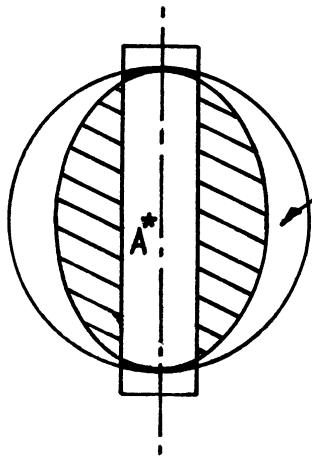
$$A_{\text{flow}} = \frac{\pi D^2}{4} - \frac{\pi D^2}{4} \left[ \frac{\cos \theta}{\cos \theta_0} \right] = \frac{\pi D^2}{4} \left[ 1 - \frac{\cos \theta}{\cos \theta_0} \right]$$

However, the shaft is usually so large that its effects may not be neglected.

Note that the maximum flow area is shown in the sketch:



Thus, in the general case of an angle  $\theta$ , the flow area will be given by determining what portion of the ellipse is not adding to the restriction, but is only blocking a region already blocked by the shaft.



Thus:

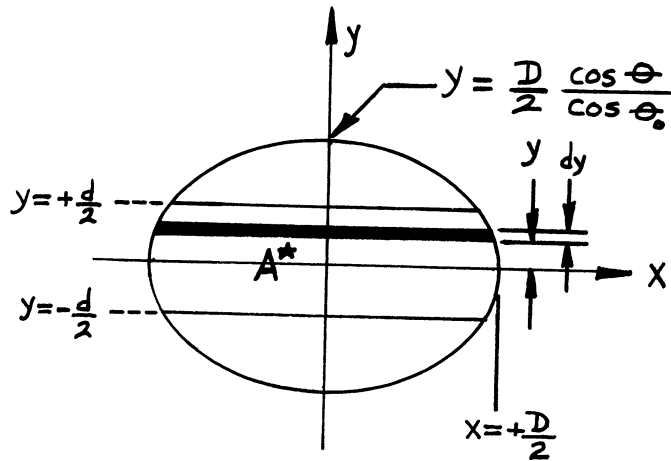
$$\left\{ \begin{array}{l} \text{Flow area} \\ \text{Bore Area} \end{array} \right. = \text{Throttle area} - \text{Shaft area} - \text{Cross hatched region of ellipse}$$

Note also that the shaft area is not a simple rectangle but is rounded at the ends.

or if  $A^*$  is the region shown in the above sketch, then:

$$\text{Net Flow Area} = \text{Throttle bore area} - \text{Total area of ellipse} + A^* - A_{\text{shaft}}$$

The determination of  $A^*$ , the portion of the ellipse which is blocked by the throttle shaft, involves the evaluation of an elliptic integral.



$$dA = 2x \, dy$$

$$A^* = 2 \int_{y=0}^{y=d/2} dA = 2 \int_{y=0}^{y=d/2} 2x \, dy$$

But the equation of the throttle plate ellipse above is:

$$\frac{4x^2}{D^2} + \frac{4y^2}{D^2 \frac{\cos^2 \theta}{\cos^2 \theta_0}} = 1 \quad \text{EQN B1}$$

or: 
$$x = \sqrt{\frac{D^2}{4} - \frac{y^2 \cos^2 \theta_0}{\cos^2 \theta}}$$

thus: 
$$A^* = 4 \int_{y=0}^{y=d/2} \left[ \frac{D^2}{4} - \frac{y^2 \cos^2 \theta_0}{\cos^2 \theta} \right]^{1/2} dy$$

For convenience, let:

$$R = \frac{D}{2} \quad \text{thus: } \sqrt{\frac{D^2}{4} - \frac{y^2 \cos^2 \theta_0}{\cos^2 \theta}} = \frac{1}{\cos \theta} \sqrt{B^2 - y^2 \cos^2 \theta_0}$$

$$B = R \cos \theta$$

therefore:

$$A^* = \frac{4}{\cos \theta} \int_{y=0}^{y=d/2} [B^2 - y^2 \cos^2 \theta_0]^{1/2} dy$$

Integrating:

$$A^* = \frac{2}{\cos \theta \cos \theta_0} \left[ y \cos \theta_0 \sqrt{B^2 - y^2 \cos^2 \theta_0} + B^2 \sin^{-1} \left( \frac{y \cos \theta_0}{B} \right) \right]_0^{d/2}$$

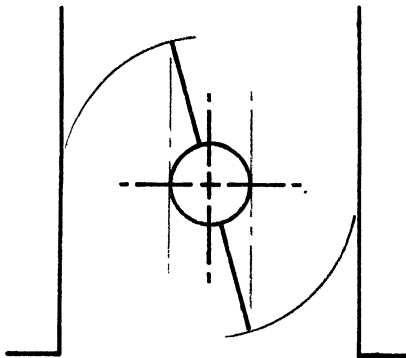
Or:

$$A^* = \frac{2}{\cos \theta \cos \theta_0} \left[ \frac{d}{2} \cos \theta_0 \sqrt{\frac{D^2}{4} \cos^2 \theta - \frac{d^2}{4} \cos^2 \theta_0} + \frac{D^2}{4} \cos^2 \theta \sin^{-1} \left( \frac{d \cos \theta_0}{D \cos \theta} \right) \right]$$

EQN B2

A restriction resulting from the integration is that;  $d \cos \theta_0 / D \cos \theta \leq 1$

$$\text{or that; } \cos \theta \geq \frac{d}{D} \cos \theta_0$$



This corresponds to the physical situation shown in the sketch to the left.

Note that the throttle plate is not reducing the flow area for this (or larger) values of the throttle angle  $\theta$ .

Thus simplifying:

$$A^* = \frac{d}{2 \cos \theta} \sqrt{D^2 \cos^2 \theta - d^2 \cos^2 \theta_0} + \frac{D^2 \cos \theta}{2 \cos \theta_0} \sin^{-1} \left( \frac{d \cos \theta_0}{D \cos \theta} \right) \text{EQN B3}$$



In a similar manner, the cross sectional area of the shaft is found to be:

$$A_{\text{shaft}} = \frac{d}{2} \sqrt{D^2 - d^2} + \frac{D^2}{2} \sin^{-1} \left( \frac{d}{D} \right) \quad \text{EQN B4}$$

A simple check may be made here: when  $d = D$  ;

$$A_{\text{shaft}} \text{ should equal } \frac{\pi D^2}{4}$$

Check:

$$A_{\text{shaft}} = \frac{D}{2} \sqrt{0} + \frac{D^2}{2} \sin^{-1} (1) = \frac{\pi}{2} \cdot \frac{D^2}{2}$$

Thus :

$$A_{\text{flow}} = \frac{\pi D^2}{4} \left[ 1 - \frac{\cos \theta}{\cos \theta_0} \right] + A^* - A_{\text{shaft}} \quad \text{EQN B5}$$

Now substituting the relationships for  $A^*$  and  $A_{\text{shaft}}$ , the final equation for the throttle flow area is:

$$A_{\text{flow}} = \frac{\pi D^2}{4} \left[ 1 - \frac{\cos \theta}{\cos \theta_0} \right] + \frac{d}{2 \cos \theta} \sqrt{D^2 \cos^2 \theta - d^2 \cos^2 \theta_0} \\ + \frac{D^2 \cos \theta}{2 \cos \theta_0} \sin^{-1} \left( \frac{d \cos \theta_0}{D \cos \theta} \right) - \frac{d}{2} \sqrt{D^2 - d^2} + \frac{D^2}{2} \sin^{-1} \left( \frac{d}{D} \right)$$

EQN B6

This obviously requires a computer subroutine to evaluate AFLOW for any  $\theta$ ,  $D$ ,  $d$ , and  $\theta_0$ .

In the subroutine THROTL the following symbols have been defined:

THETA	=	$\theta$	in degrees	RTHETA	=	$\theta$	in radians
THETAO	=	$\theta_o$	in degrees	RTHETO	=	$\theta_o$	in radians
DT	=	D	in inches	ASTAR	=	$A^*$	in inches <sup>2</sup>
DS	=	d	in inches	ASHAFT	=	$A_{\text{shaft}}$	in inches <sup>2</sup>

For a typical carburetor used in this study, the variables have the following values:

$$D = 1.438 \text{ inch} \quad d = 0.375 \text{ inch} \quad \theta_o = 0.70^\circ$$

Actually the closing angle  $\theta_o$  is  $5.0^\circ$  but, as discussed in Chapter II, to have the above equation yield the throttle plate leakage area when  $\theta = 5.0^\circ$  (completely closed), a smaller value of  $\theta_o$  is used. This is far superior to neglecting the leakage area, especially for small throttle openings.

## APPENDIX C

### IDLE NEEDLE FLOW AREA

A large proportional of the pressure loss in the idle flow channel is across the idle needle screw. This screw has a tapered section which projects through a drilled hole on the downstream side of the throttle plate. Since this idle needle flow area is very influential in determining the idle fuel flow, it must be known in terms of the needle geometry.

The symbols used in this analysis are:

$d_i$  = Idle discharge port diameter in inches

$d_n$  = Idle needle diameter blocking the port in inches

$N_{th}$  = Number of threads per inch on idle screw

$\alpha$  = Included angle of idle needle in degrees

TURNS = Number of turns of needle screw from fully closed position

The geometric arrangement of the idle needle and port is illustrated in Figure 78. Note that one turn of the idle screw from the fully closed position will move it  $1/N_{th}$  inches. This opens up the annular flow area between diameters  $d_n$  and  $d_i$ . It is this annular flow area that we wish to calculate. Note that from the right triangle formed by the portion of the idle needle projecting into the port we obtain:

$$\text{TAN} (\alpha / 2) = \frac{\Delta \text{RADIUS}}{1/N_{th}} \quad \text{EQN C1}$$

Where  $\Delta \text{RADIUS}$  is  $1/2$  of the difference between  $d_i$  and  $d_n$ . Thus the change in diameter or  $(d_i - d_n)$  per turn is given by:

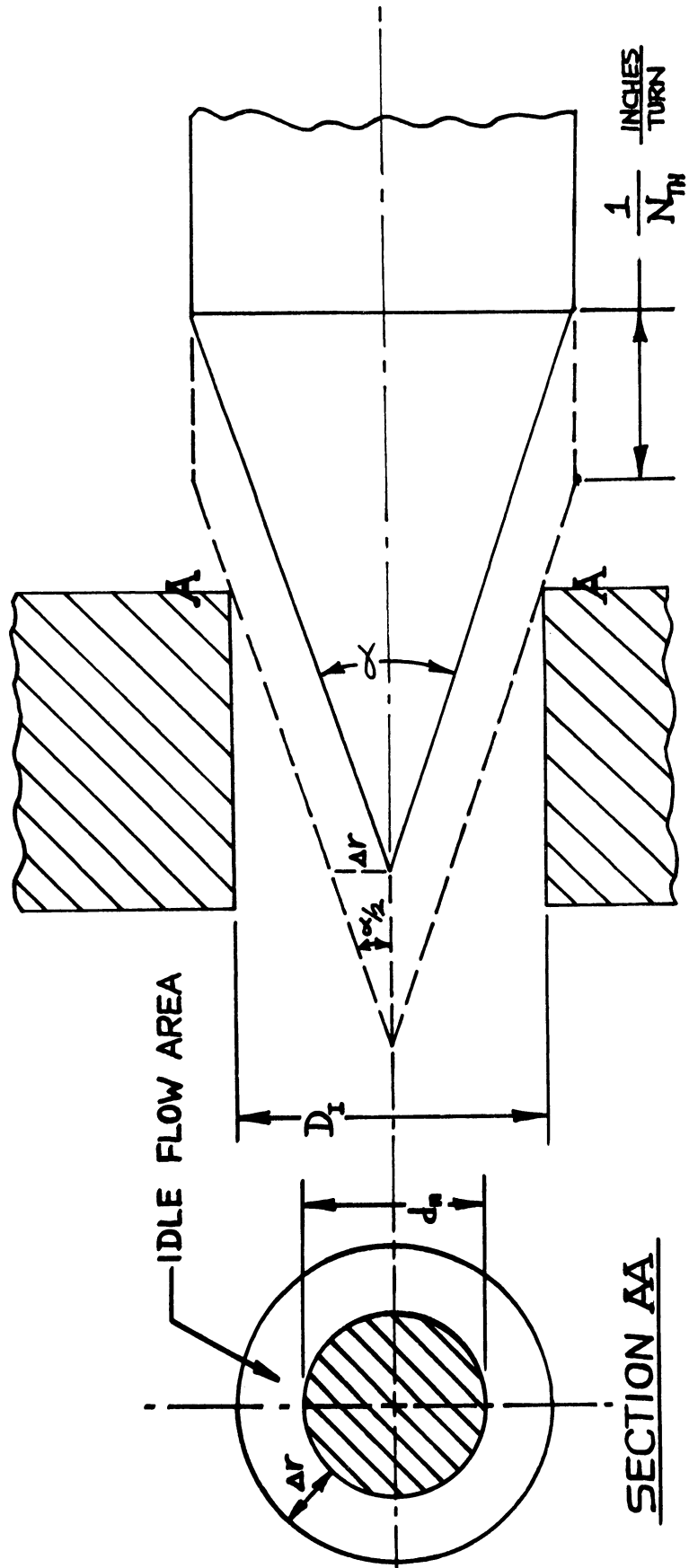


Figure 78. Idle Needle Flow Area Variables

$$\Delta \text{ DIAMETER} = (d_i - d_n) = \frac{2}{N_{th}} \text{ TAN}(\alpha/2) [\text{TURNS}] \quad \text{EQN C2}$$

Thus:

$$d_n = d_i - \frac{2 (\text{TURNS})}{N_{th}} \text{ TAN}(\alpha/2) \quad \text{EQN C3}$$

$$\text{or: Annular Idle Flow area} = \frac{\pi d_i^2}{4} - \frac{\pi}{4} \left[ d_i - \frac{2 (\text{TURNS})}{N_{th}} \text{ TAN}(\alpha/2) \right]^2 \quad \text{EQN C4}$$

For the typical values of:

$$\alpha = 25^\circ \quad N_{th} = 32 \text{ threads/inch}$$

$$d_i = 0.060 \text{ inch} \quad \text{TURNS} = 2$$

$$\text{AIDLE} = 0.002827 - 0.7854 \left[ 0.060 - \frac{(4.0)(0.2217)}{32.0} \right]^2$$

or

$$\text{AIDLE} = 0.002006 \text{ in}^2$$

## APPENDIX D

### THERMODYNAMIC PROPERTIES\* OF AN AIR, WATER VAPOR, AND FUEL VAPOR MIXTURE

\* Molecular weight, specific heats, and specific heat ratio of a multi-component mixture of ideal gases.

Subscripts: 1 = fuel vapor  
2 = air  
3 = water vapor

#### VARIABLES:

n = number of moles

m = mass of component

W = molecular weight

y = mole fraction

FAMAIN = main system fuel-air ratio by weight

FATOTL = total fuel-air ratio by weight (main + idle)

$\omega$  = water vapor-air mass fraction

$\phi$  = relative humidity

T = temperature °F

P = Pressure - psia

The number of moles of component i is given by

$$n_i = \frac{m_i}{W_i} \quad \text{EQN D1}$$

and the mole fraction is then:

$$y = \frac{n_i}{\sum_i n_i} \quad \text{EQN D2}$$

The molecular weight of the multi-component mixture is given by:

$$W_{\text{total}} = \sum_i y_i W_i = y_1 W_1 + y_2 W_2 + y_3 W_3 \quad \text{EQN D3}$$

By using equation (2),  $W_{\text{total}}$  may be expressed as:

$$W_{\text{total}} = \frac{n_1 W_1 + n_2 W_2 + n_3 W_3}{n_{\text{total}}} \quad \text{EQN D4}$$

But :

$$n_{\text{total}} = \frac{m_1}{W_1} + \frac{m_2}{W_2} + \frac{m_3}{W_3}$$

Therefore :

$$W_{\text{total}} = \frac{m_1 + m_2 + m_3}{\frac{m_1}{W_1} + \frac{m_2}{W_2} + \frac{m_3}{W_3}} = \frac{\frac{m_1}{m_2} + 1 + \frac{m_3}{m_2}}{\frac{1}{m_2} \left[ \frac{m_1}{W_1} + \frac{m_2}{W_2} + \frac{m_3}{W_3} \right]}$$

EQN D5

But the mass fractions have the following meanings:

$$\frac{m_1}{m_2} = \text{fuel-air ratio} \quad \frac{m_3}{m_2} = \omega$$

Where  $\omega$  is related to the partial pressure of the water and the relative humidity by the following relationship:<sup>71</sup>

$$\omega = \frac{0.622 P_3 \phi}{P_{\text{total}}}$$

$P_3$  is the vapor pressure of the water at the temperature of the mixture and is correlated very well by the equation:

$$P_3 = 1.302 \left( \frac{T}{100} \right)^3 - 0.765 \left( \frac{T}{100} \right) + 0.413 \left( \frac{T}{100} \right) \text{ psia}$$

EQN D6

over a temperature range from 20°F to 120°F. Thus the expression for the molecular weight of the mixture becomes:

$$W_{\text{total}} = \frac{1 + F/A + \omega}{\frac{F/A}{W_{\text{fuel}}} + \frac{1}{W_{\text{air}}} + \frac{\omega}{W_{\text{H}_2\text{O}}}}$$

EQN D7

Since fuel may be introduced at two points in the air flow path, the thermodynamic properties of the mixture must be calculated using the local fuel-air ratio. Noting that the total mixture ratio is given by:

FATOTL = FAMAIN + FAIDLE, the fuel-air ratio to be used is as

follows:

- a) before boost venturi;  $F/A = 0$
- b) between boost venturi and idle discharge;  $F/A = \text{FAMAIN}$   
(including throttle plate)
- c) between idle port and engine cylinder;  $F/A = \text{FATOTL}$

Therefore, for an analysis of flow at the throttle plate, the molecular weight to be used is:

$$W_{\text{MOLEC}} = \frac{1 + \text{FAMAIN} + \text{OMEGA}}{\frac{\text{FAMAIN}}{\text{FUELM}} + \frac{1.0}{28.95} + \frac{\text{OMEGA}}{18.016}}$$

EQN D8

and for an analysis of flow from the carburetor to the engine cylinder

the molecular weight is:

$$W_{\text{MOLEC}} = \frac{1 + \text{FATOTL} + \text{OMEGA}}{\frac{\text{FATOTL}}{\text{FUELM}} + \frac{1.0}{28.95} + \frac{\text{OMEGA}}{18.016}}$$

EQN D9

where the computer variables names have been introduced.



SPECIFIC HEATS:

$$C_p (\text{mix}) = \frac{m_1}{m_{\text{total}}} (C_p)_1 + \frac{m_2}{m_{\text{total}}} (C_p)_2 + \frac{m_3}{m_{\text{total}}} (C_p)_3$$

EQN D10

But:

$$m_{\text{total}} = m_{\text{fuel vapor}} + m_{\text{air}} + m_{\text{water vapor}}$$

or:

$$m_{\text{total}} = m_1 + m_2 + m_3$$

$$C_p (\text{mix}) = \frac{m_1 (C_p)_1 + m_2 (C_p)_2 + m_3 (C_p)_3}{m_1 + m_2 + m_3}$$

EQN D11

But  $m_{\text{total}}$  is not convenient for carburetor work, therefore divide by  $m_2$  instead of  $m_{\text{total}}$ :

thus :

$$C_p (\text{mix}) = \frac{\frac{m_1}{m_2} (C_p)_1 + (C_p)_2 + \frac{m_3}{m_2} (C_p)_3}{\frac{m_1}{m_2} + 1 + \frac{m_3}{m_2}}$$

$$\text{But } \frac{m_3}{m_2} = \text{OMEGA} = \omega \quad \text{and} \quad \frac{m_1}{m_2} = F/A$$

Therefore:

$$C_p (\text{mix}) = \frac{(C_p)_{\text{air}} + \omega (C_p)_{\text{H}_2\text{O}} + (F/A) (C_p)_{\text{fuel}}}{1 + \omega + F/A}$$

EQN D12

Similarly:

$$C_v (\text{mix}) = \frac{(C_v)_{\text{air}} + \omega (C_v)_{\text{H}_2\text{O}} + (F/A) (C_v)_{\text{fuel}}}{1 + \omega + F/A}$$

EQN D13

Or in computer nomenclature:

$$C_v(\text{mix}) = \frac{CVAIR + OMEGA*CVH2O + FATOTL*CVFUEL}{1.0 + OMEGA + FATOTL}$$

the specific heat ratio is given by:

$$K_{\text{mix}} = \frac{(C_p)_{\text{mix}}}{(C_v)_{\text{mix}}} = \frac{(C_p)_{\text{air}} + \omega (C_p)_{\text{H}_2\text{O}} + (F/A)(C_p)_{\text{fuel}}}{(C_v)_{\text{air}} + \omega (C_v)_{\text{H}_2\text{O}} + (F/A)(C_v)_{\text{fuel}}}$$

EQN D14

Program values used to evaluate the mixture values are:

$$(C_p)_{\text{air}} = .240 \qquad (C_p)_{\text{water vapor}} = .445 \text{ btu/lbm } ^\circ\text{R}$$

$$(C_v)_{\text{air}} = .171 \qquad (C_v)_{\text{water vapor}} = .335$$

TYPICAL FUELS

	Normal Octane	Iso Octane	Ethyl Alcohol	Gasoline	Methyl Alcohol
$(C_p)_{\text{fuel vapor}}$	.400	.400	.460	.400	.410
$(C_v)_{\text{fuel vapor}}$	.381	.381	.407	.381	.370

## APPENDIX E

### EXPLANATION OF SUBROUTINES

#### 1. THROTL

Subroutine THROTL operates on the geometric data for the throttle plate and shaft and returns a throttle flow area. For a specified throttle bore diameter, throttle shaft diameter, completely closed throttle angle, and throttle plate opening, this subroutine evaluates the equations resulting from the elliptic integral (Appendix B) and returns a throttle flow area. This area is per barrel and is in square inches.

#### 2. ASSUME

This subroutine provides reasonable initial guesses for the main, idle, enrichment, and total fuel rates and also for the main, idle, and total fuel-air ratios. Any iteration in the main program which requires an initial guess for a fuel rate or fuel-air ratio may call on ASSUME with an air flow rate and intake manifold vacuum. On the basis of typical carburetor curves of fuel-air ratio versus air flow rate, reasonable values are assigned to the initial guesses. This greatly reduces the number of iterations required, since the values are in the correct range initially.

#### 3. FLOW

This subroutine determines all important parameters associated with flow in the fuel channels. With the fuel properties, complete channel geometry, air bleed sizes, metering signal, and intake manifold

vacuum specified, subroutine FLOW iteratively evaluates the Reynolds number dependent flow network which constitutes the fuel channel. Total pressure losses due to orifices, bends, sudden expansions and contractions, two-phase flow, and viscous friction are evaluated. Fuel and air flow rates in each of the twenty five elements in the five branches of the flow network are adjusted according to the pressure loss error in each element until convergence is obtained. When this occurs, the system parameters are known for each element. These include flow rate, velocity, total and static pressures, and Reynolds numbers. Thus, the overall fuel system parameters such as main, idle, and enrichment fuel flow rates, and air bleed flow rates are known.

#### 4. AIRMAS

This subroutine operates on engine-throttle plate input data and returns mixture flow rates and intake manifold pressure to the main program. Thus the main function of AIRMAS is to theoretically determine the dry air, water vapor, and fuel vapor flow rates in pounds per hour, and the intake manifold pressure in inches of mercury. The ambient conditions, engine specifications, and needed carburetor geometry are first supplied to the subroutine. Then, for any engine speed and throttle flow area, AIRMAS simultaneously evaluates the exhaustor (engine) and nozzle (throttle plate) flow equations and, by repeated iteration, obtains the mixture and component flow rates and intake manifold pressure which satisfy the equations. The moist air flow rate, or the sum of the dry air and water vapor flow rates, is of particular interest

since this is the quantity measured in an engine air flow test.

The iteration method is basically as follows. For any assumed intake manifold pressure two moist air flow rates are calculated. These flow rates result from the exhauster and nozzle flow equations respectively. Equation 2.19 yields a moist air flow rate which satisfies the exhauster flow conditions and equation 2.10 gives a flow rate which satisfies the compressible mixture flow through the converging nozzle (throttle plate). This is shown in Figure 5. Continuity, of course, requires that the moist air flow rate to the engine be the sum of the moist air flows through and around the nozzle. Accounting is made of the fact that air, water vapor, and fuel vapor are flowing and that multiple bypasses exist around the throttle plate. The iteration then proceeds until the error parameter is within a specified value.

## 5. SIGNAL

This subroutine evaluates all aspects of the compressible mixture flow through the primary and secondary venturii. Its chief function is to calculate the theoretical metering signal (the boost venturi vacuum at the fuel discharge nozzle in inches of water) based on the geometry and flow conditions which have been supplied. After the total mixture flow rate has been obtained by AIRMAS, subroutine SIGNAL iteratively determines what fraction of the moist air flows through the main venturi, and what fraction flows through the boost venturi. Then, with the flow rates known, the Mach numbers, pressures, and temperatures

are calculated at each station of the venturii. Interacting phenomena such as increased mixture flow rate in the boost venturi due to fuel vaporization, and changing mixture properties with distance are included. The analysis is performed for any fuel type, temperature, and flow rate as specified by the main program.

## 6. SOLVE

Subroutine SOLVE evaluates the Mach number for any compressible flow situation. That is, if the flow conditions at any station are supplied, the Mach number will be returned by SOLVE. Thus, if the flow area, local stagnation conditions, mixture molecular weight, mixture specific heat ratio, and mass flow rate are specified, a Mach number can be iteratively obtained. The Newton-Rhapson iterations are required because the compressible flow relationships are not explicit in the Mach number. This is discussed in detail in Chapter II. Subroutine SOLVE incorporates certain other features including checks to determine if the specified conditions result in a valid flow situation, and accurate initial guesses for the Mach number based on linearizing the flow equations. This reduces the number of iterations required for a given error level.

## 7. XMIX

The function of XMIX is to provide the thermodynamic properties of a mixture of air, water vapor, and fuel vapor. These properties are determined for the relative proportions of each component in the mixture.

These proportions are related to the fuel-air ratio and relative humidity of the mixture, which are specified in the subroutine list. Thus, for a given fuel type, air temperature, fuel-air ratio, and relative humidity at a given carburetor station, subroutine XMIX will calculate the mixture molecular weight, specific heats, and specific heat ratio, and return them to the main program.

#### 8. STERL

This subroutine is essentially a generalized Mth degree interpolation program which is utilized many times in the overall simulation. When supplied with a set of data (for anything) and an X argument, STERL will return a corresponding Y value to the calling program. Basically this subroutine operates on the N data points supplied to it and generates a difference table. It utilizes Sterling's technique, which is the sum of the Gauss forward difference and the Gauss backward difference, to obtain an Mth degree interpolation value, with M less than or equal to N-1 (For complete information see Appendix F). Thus, for discharge coefficient data, engine IHP data, etc., accurate interpolated values can be obtained for specified values of the abscissa.

#### 9. FPROP

Subroutine FPROP contains property correlations for numerous fluids and supplies the property values to the main program whenever it is called. The fluid properties correlated as a function of temperature include specific gravity, viscosity, and surface tension. The temperature

range in most cases is 20<sup>o</sup> F to 110<sup>o</sup> F although some data extends to slightly higher temperatures. Values are also supplied for liquid specific heat, constant pressure and constant volume specific heats of the vapor, molecular weight, lower heating value, and latent heat of vaporization. All of this is available for nine fluids of interest in carburetor work. These include iso-octane, four brands of gasoline, ethyl alcohol, mineral spirits, air, and water. Thus, any property value of any of these fluids can be supplied to the main program by FPROP.

#### 10. CALCOMP PLOTTING

There are three separate CALCOMP plotting subroutines or external functions. They provide the detailed instructions and formatting required to produce eleven different plots automatically. The plotting portion of the simulation is specific to the University of Michigan system, that is, the plotting instructions have meaning only in that particular system and in any other computer system they would have to be modified. The three plotting subroutines are written in the MAD language.

The eleven plots available will not be given here since they are listed early in the main computer program in Appendix I. Most of the common plots encountered in carburetor work are available in the plotting routines if desired. The naming scheme within these routines is illustrated by considering the first two entries, which are CALMAP and CALMVH. The CAL in all cases indicates a CALCOMP plot and the last



three letters indicate the type of plot. In the first case it is a complete operating map (carburetor-engine-vehicle) and in the second it is a plot of fuel mass flow rate versus head.

The main purpose of these routines is to provide for automatic computer plotting of the simulation predictions, which presents the results in a familiar form and reduces the man-hours required to evaluate a computer run.

## APPENDIX F

### MULTI-PURPOSE INTERPOLATION SUBROUTINE

A general purpose subroutine was written to accurately perform all needed data interpolations within the simulation. These interpolations are performed on actual data many times per operating point iteration, and are required for the following reasons:

1. to obtain an orifice  $C_d$  value for a specific  $R_e$  argument
2. to obtain a throttle plate  $C_d$  value for a specific  $\theta$  argument
3. to obtain an engine IHP value for a specific F/A argument
4. to obtain an engine FMEP value for a specified RPM argument

The interpolation scheme utilized in subroutine STERL is basically a generalized form of Sterling's method, which uses a combination of the Gauss forward difference technique (GFF) and the Gauss backward difference technique (GBF). These techniques begin by first generating a difference table from the X and Y data arrays supplied to the subroutine. This table is generated by determining the difference between consecutive values in the next lower order, starting with the Y values. Figure 79 shows the difference table corresponding to nine data points which represent the variation in  $C_d$  with Reynolds number for a square-edged orifice with an L/D ratio of 3.629. Note that the number of data points is N, and that the divided difference columns are designated by  $\delta_M$ , where M is the divided difference order. This order corresponds to the degree of interpolation desired, which is the degree of a polynomial that is passed through the data points in the vicinity of the X argument.

I	X(I) REYNOLDS NUMBER	f [X(I)] C <sub>d</sub>	$\delta_1$	$\delta_2$	$\delta_3$	$\delta_4$	$\delta_5$	$\delta_6$	$\delta_7$	$\delta_8$
0	0.0	0.000	0.674	-0.633	0.616	-0.603	0.583	-0.562	0.539	-0.519
1	500.0	0.674	0.041	-0.017	0.013	-0.020	0.021	-0.023	0.020	
2	1000.0	0.715	0.024	-0.004	-0.007	0.001	-0.002	-0.003		
3	1500.0	0.739	0.020	-0.011	0.006	-0.001	-0.005			
4	2000.0	0.759	0.009	-0.005	0.005	-0.001	-0.005			
5	2500.0	0.768	0.004	-0.000	0.005	-0.006				
6	3000.0	0.772	0.004	-0.001	-0.001					
7	3500.0	0.776	0.003							
8	4000.0	0.779								

Figure 79. Sample Difference Table Using Actual Square-Edged Orifice Data

The interpolated value can be related to the values in the difference table by the GFF and GBF. First let us define the following symbols which appear in these functions:

- N = number of data points
- M = desired interpolation degree ( $M \leq N-1$ )
- XARG = X argument for which an interpolation is desired
- DX = increment of X data points
- Xstart = the X data point used to start the interpolation.  
(in most cases the closest one to XARG).
- $\delta_M f(Xstart)$  =  $M^{\text{th}}$  order divided difference of f (XSTART)

A convenient interpolation parameter can be defined in terms of the above variables.

This is:

$$\alpha = \frac{XARG - XSTART}{DX} \quad \text{EQN F1}$$

The Gauss forward and backward functions can be expressed in terms of the above variables and the divided differences in the table<sup>69</sup>.

GFF:

$$f(XARG) = f(XSTART) + \alpha \delta_1 f(XSTART + DX/2) + \frac{\alpha(\alpha-1) \delta_2 f(XSTART)}{2!} + \frac{\alpha(\alpha-1)(\alpha+1) \delta_3 f(XSTART + DX/2)}{3!} + \dots \quad \text{EQN F2}$$

GBF:

$$f(XARG) = f(XSTART) + \alpha \delta_1 f(XSTART - DX/2) + \frac{\alpha(\alpha+1) \delta_2 f(XSTART)}{2!} + \frac{\alpha(\alpha+1)(\alpha-1) \delta_3 f(XSTART - DX/2)}{3!} + \dots \quad \text{EQN F3}$$

Sterling's interpolation technique utilizes the sum of the GFF and GBF to obtain the desired interpolated value,  $f(XARG)$ :

$$STERL = \frac{GFF + GBF}{2} \quad \text{EQN F4}$$

Combining equations F2 and F3, the resulting relationship for Sterling's interpolation method is:

$$f(XARG) = f(XSTART) + \frac{\alpha}{2} \left[ \delta_1 f(XSTART + DX/2) + \delta_1 f(XSTART - DX/2) \right] + \frac{\alpha^2 \delta_2 f(XSTART)}{2!} + \frac{\alpha(\alpha+1)(\alpha-1)}{2 \cdot 3!} \left[ \delta_3 f(XSTART + DX/2) + \delta_3 f(XSTART - DX/2) \right] + \dots \quad \text{EQN F5}$$

A simple example of this interpolation technique can be given for the data shown in Figure 79. If the X argument is 2200.0, what is the interpolated value,  $f(XARG)$ ? Let the desired interpolation degree M be equal to 2 (for simplicity). Thus:

$$XARG = 2200.0 \quad XSTART = 2000.0$$

$$M = 2 \quad \alpha = 0.40$$

$$f(XARG) = 0.759 + \frac{0.40}{2} (0.009 + 0.020) + \frac{(0.40)^2}{2} (-0.011)$$

$$f(XARG) = 0.759 + 0.0058 - 0.00088 = 0.76398$$

$$\text{or: } f(XARG) = 0.7640$$

## APPENDIX G

### GENERAL CONVERGENCE TECHNIQUE

A general convergence technique which was utilized extensively in this simulation will be discussed. The simulation contains a very large number of trial and error (iterative) solutions which have very complex error terms. A rapid and stable method of obtaining the required solutions was obviously needed. The following technique adequately met this need. First consider the familiar Newton-Rhapson iteration technique which is commonly used to obtain the roots of a polynomial,  $f(x)$ . Figure 80 illustrates the derivation of the simple relationship for obtaining the next guess,  $X_{i+1}$ , after one arbitrary initial guess,  $X_i$ .

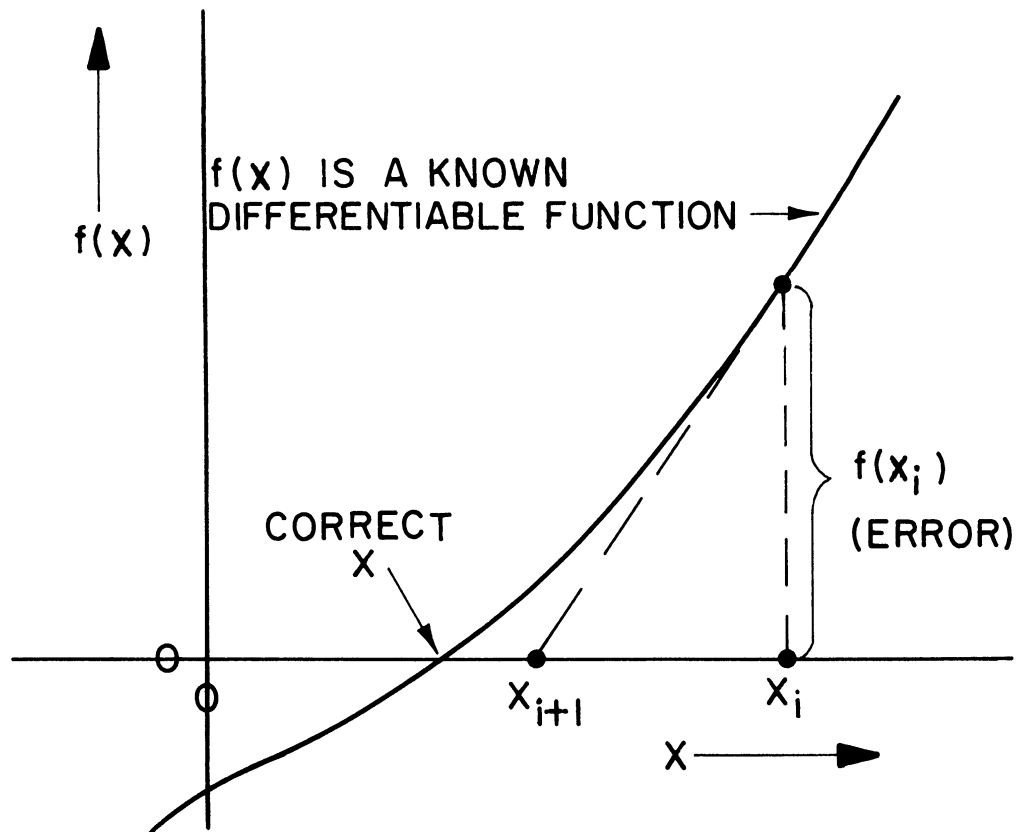


Figure 80. Illustration of the Newtonian iteration technique

$$\frac{df(x)}{dx} = \frac{f(x_i) - f(x_{i+1})}{x_i - x_{i+1}} \quad \text{or} \quad x_{i+1} = x_i - \frac{f(x_i)}{\frac{df(x_i)}{dx}} \quad \text{EQN G1}$$

But what if the function to be minimized is a complex relationship which cannot be expressed analytically and which therefore cannot be differentiated?

Such is the case in figure 81 where a generalized error,  $E(Z)$ , is shown as a function of the parameter  $Z$ .

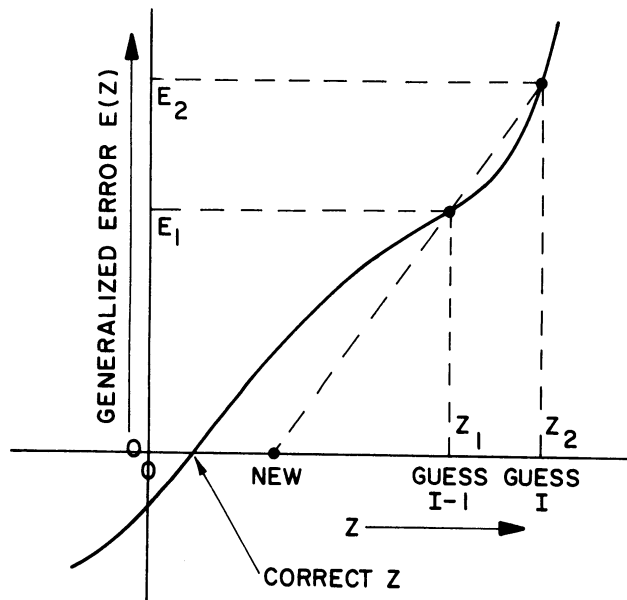


Figure 81. Illustration Of Generalized Convergence Technique

This error function can be related to many variables and may be so complex that it can only be generated by trying values of  $Z$ . For example,  $Z$  may be a fuel flow rate, and the iterative error parameter,  $E(Z)$ , may be the difference between pressure losses predicted by different sub-routines. In any case, the problem is to continuously change  $Z$  and reduce  $E(Z)$  to a small value. This method begins with a completely

arbitrary guess for  $Z$  and, no matter how complex the calculation, a resulting value for the error,  $E_1$ . Next, another arbitrary guess is made for  $Z$  (usually a small distance from  $Z_1$ ) and a different error value,  $E_2$ , results. Now the next iterative value for  $Z$  can be obtained by similar triangles:

$$\frac{Z_2 - Z_i}{E_2} = \frac{Z_2 - Z_1}{E_2 - E_1} \quad \text{or} \quad Z_i = Z_2 - \left[ \frac{E_2 (Z_2 - Z_1)}{E_2 - E_1} \right] \quad \text{EQN G2}$$

Equation G2 gives the next iterative value,  $Z_i$ , as a function of the values and errors of the two previous guesses. This worked extremely well in all cases and gave fairly rapid convergence for a wide range of functions.



## APPENDIX H

### ANALYTICAL PREDICTION OF FUEL VAPORIZATION WITHIN THE CARBURETOR

Consider the steady state vaporization of a single spherical droplet in an infinite gaseous environment. The droplet temperature does not vary within the drop or with time. This corresponds to the period in time following  $t^*$ . (illustrated in Figure 9.) The variables to be used in this analysis and their respective units are given in the following list:

$P_{\infty}$  = ambient pressure in psia

$T_f$  = fuel droplet temperature in  $^{\circ}\text{R}$

$P_{\text{surf}}$  = fuel vapor pressure at  $T_f$  in psia

$P_{v\infty}$  = fuel vapor pressure at  $\infty$  in psia

$m$  = droplet mass in lbm

$\dot{m}$  = droplet vaporization rate in lbm/sec

$t$  = time in seconds

$d_f$  = droplet diameter in microns

$d_s$  = sauter mean diameter in microns

$W_f$  = fuel molecular weight in lbm per lb mol

$D_v$  = mass diffusivity of fuel vapor in air -  $\text{Ft}^2$  per hour

$\bar{R}$  = Universal gas constant in  $\text{Ft lbf per lb mol } ^{\circ}\text{R}$

$A$  = area in  $\text{ft}^2$

$g_c$  = mass conversion factor -  $\text{ft lbf per lbm sec}^2$

$\rho_f$  = fuel density in lbm per cubic ft.

$V_{\text{rel}}$  = relative velocity between droplet and air in feet per sec.

$\mu_{\text{air}}$  = absolute viscosity of air in lfb sec per Ft<sup>2</sup>

First considering zero relative velocity between the drop and the surrounding medium, the diffusional mass transfer process can be described by the Stephan diffusion equation for spherical geometry:<sup>17</sup>

$$\frac{dm}{dt} = \frac{\pi d_f^2 P_\infty D_v W_f}{\bar{R} T_f} \frac{d}{dr} \left[ \log_e \left( 1 - \frac{P_s}{P_\infty} \right) \right] \quad \text{EQN H1}$$

now integrating on the drop radius from  $r=r$  to  $r=\infty$  we obtain:

$$\frac{dm}{dt} = \frac{2\pi d_f D_v W_f}{\bar{R} T_f} (P_s - P_v) \left( \frac{P}{P_{bm}} \right) \quad \text{EQN H2}$$

where  $P_{bm}$  is the log mean partial pressure. The ratio of  $P_\infty/P_{bm}$  is usually close to unity<sup>15</sup> unless the partial pressure of the fuel vapor is a significant portion of the total pressure  $P_\infty$ . Letting this ratio be unity, and noting that the mass of the droplet,  $m$ , may be written as;

$$\pi \rho_f d_f^3 / 6 \text{ and that } dm \text{ is negative (mass is leaving the drop-}$$

let) we obtain:

$$-d(d_f^3) = \frac{(6)(2)\pi D_v W_f d_f}{\pi \rho_f \bar{R} T_f} (P_s - P_{v\infty}) dt$$

or

$$-(3 d_f) d(d_f) = \frac{12 D_v W_f}{\rho_f \bar{R} T_f} (P_s - P_{v\infty}) dt$$

or integrating from  $t = 0$  to  $t = t$  and from the initial diameter

$$d_s \text{ to } d_f: \quad -3 \int_{d_s}^{d_f} d_f d(d_f) = \int_0^t \frac{12 D_v W_f}{\rho_f \bar{R} T_f} (P_s - P_{v\infty}) dt$$

or in the correct units:

$$d_f^2 = d_s^2 - (12192)(304800) \frac{8 D_v W_f}{\rho_f \bar{R} T_f} (P_s - P_{v\text{sat}}) t \text{ microns}^2 \quad \text{EQN H3}$$

equation H3 gives the droplet diameter as a function of time for zero relative velocity. The vaporization rate in the correct units can be obtained by rearranging equation H2 and noting that the droplet surface area  $A$  is  $\pi d_f^2$ .

$$\frac{\dot{m}}{A} = (12192.0) \frac{2 D_v W_f}{\bar{R} T_f d_f} (P_s - P_{v\text{sat}}) \frac{\text{lbm}}{\text{sec ft}^2} \quad \text{EQN H4}$$

(The conversion between microns and feet has been used in the above two equations; 304,800 microns per foot.)

Now for mass transfer in the presence of a relative velocity between the drop and the surroundings, the quiescent equations will be modified by a mass transfer Nusselt number,  $(Nu)_m$ . This dimensionless number is a function of the Reynolds and Schmidt numbers which are defined as:

$$R_e = \text{Droplet Reynolds number} = \frac{(\mathbf{v}_{\text{rel}}) (d_f) (\rho_{\text{air}})}{\mu_{\text{air}}}$$

$$S_c = \text{Schmidt number} = \frac{\mu_{\text{air}}}{(\rho_{\text{air}}) (D_v)}$$

Ranz and Marshall<sup>20</sup> offered the following mass transfer correlation:

$$(Nu)_m = 2.0 + 0.6 (R_e)^{1/2} (S_c)^{1/3}$$

Since the mass transfer consists of a quiescent contribution and a convective contribution, the Nusselt correlation modifies equation H4 in the following manner:

$$\frac{\dot{m}}{A} = (12192.0) \frac{D_v W_f}{R T_f d_f} (P_s - P_{v\infty}) \left[ 2.0 + 0.6(R_e)^{1/2} (S_c)^{1/3} \right] \frac{\text{lbm}}{\text{sec ft}^2}$$

EQN H5

which reduces to equation H4 for zero relative velocity (Zero Reynolds Number.)

At this point the spray characteristics must be introduced. If the total vaporization rate of the spray is desired, then  $d_f$  and  $A$  must be parameters which describe the entire spray. This was accomplished in Chapter 2 where the Sauter mean diameter was discussed. Thus, for a spray mass flow rate of  $\dot{m}(\text{spray})$  lbm/sec, the total spray surface area is:

$$A_{\text{spray}} = \frac{(6)(304,800) \dot{m}_{\text{spray}}}{(\rho_f) (d_s)} \text{ ft}^2/\text{second} \quad \text{EQN H6}$$

and the number of drops formed per second is given by:

$$\frac{\text{drops}}{\text{second}} = \frac{(6)(304,800)^3 \dot{m}_{\text{spray}}}{\pi \rho_f d_s^3} \quad \text{EQN H7}$$

The fraction of the spray vaporized in a time  $\Delta t$  is an important parameter and can be obtained by considering equation H5 and the expression for the droplet mass. In a short time increment  $\Delta t$ , the droplet of initial size  $d_s$  will lose a small amount of mass,  $m_{\text{loss}}$ . The fraction lost will be;

$$\text{FRACT} = m_{\text{loss}}/m_{\text{initial}}$$

but the initial droplet mass is:

$$m_{\text{initial}} = \frac{\rho_f \pi d_s^3}{(6)(304,800)^3} \text{lbm} \quad \text{EQN H8}$$

and the droplet surface area is:

$$A_{\text{drop}} = \frac{\pi d_s^2}{(304,800)^2} \text{ ft}^2 \quad \text{EQN H9}$$

the mass lost can be obtained by substituting the droplet area into equation H5 and noting that the droplet diameter  $d_f$  will be equal to  $d_s$ .

$$m_{\text{loss}} = (A_{\text{drop}}) (12192.0) \frac{D_v W_f}{\bar{R} T_f d_s} (P_s - P_{v\infty}) (Nu)_m \Delta t \text{ lbm}$$

thus in a small time interval  $\Delta t$ :

$$\text{FRACT} = \frac{m_{\text{loss}}}{m_{\text{initial}}} = \frac{\pi d_s^2 (6) (304,800)^3}{(304,800)^2 \rho_f \pi d_s^3} (12192.0) \frac{D_v W_f}{\bar{R} T_f d_s} (P_s - P_v) (Nu)_m \Delta t$$

or simplifying:

$$\text{FRACT} = \frac{(6) (304,800) (12192)}{\rho_f \bar{R} T_f d_s} \frac{D_v W_f}{2} (P_s - P_{v\infty}) \left[ 2.0 + 0.6 (Re)^{1/2} (Sc)^{1/3} \right] \Delta t$$

EQN H10

This is valid only for the first 20 to 25% of the mass vaporized since it was assumed that the droplet diameter did not change greatly from  $d_s$ . Larger percentage vaporizations could be handled by taking small time steps and recalculating  $d_f$  and  $Re$  for each step.

It is now advantageous to express the fraction vaporized as a function of the downstream distance in the carburetor,  $\Delta z$ . In order to eliminate  $\Delta t$ , an expression for the time required for the droplet to travel a distance  $\Delta z$  inches must be obtained, and this entails an analysis of the droplet motion after it enters the air stream.

The force acting on the drop will be  $F = C_{\text{drag}} A_p \left[ \frac{\rho_{\text{air}} V_{\text{rel}}^2}{2 g_c} \right]$  EQN H11

Where  $C_{\text{drag}}$  is the drag coefficient and  $A_p$  is the projected area of the drop. This force will result in a z motion with time described by:

$$F = \frac{m}{g_c} \frac{d^2 z}{dt^2} \quad \text{EQN H12}$$

If we restrict our analysis to the initial acceleration of the droplet (not in the portion where the relative velocity is nearly zero), then over the short time interval of interest here:

$$Z = \frac{g_c F_{\text{ave}} t^2}{2m} \quad \text{or} \quad t = \sqrt{\frac{2mZ}{g_c F_{\text{ave}}}}$$

where  $F_{\text{ave}}$  is the average force acting on the droplet in the interval from  $t = 0$  to  $t = t$ .

$$\text{but: } m = \frac{\rho_f \pi d_s^3}{6} \quad \text{and} \quad A_p = \frac{\pi d_s^2}{4}$$

$$\text{thus: } \Delta t = \sqrt{\frac{2 \rho_f \pi d_s^3 (4) g_c (2) \Delta Z}{6 g_c C_{\text{drag}} \pi d_s^2 \rho_{\text{air}} V_{\text{rel}}^2}}$$

or simplifying and introducing the correct units:

$$\Delta t = \sqrt{\frac{2 \rho_f d_s \Delta Z}{(304,800) \rho_{\text{air}} C_d V_{\text{rel}}^2}} \text{ sec.} \quad \text{EQN H13}$$

In the Reynolds number range less than 1.0, the drag coefficient is given by Stokes Law :

$$C_{\text{drag}} = \frac{24}{Re} = \frac{(24) (304,800) \mu_{\text{air}} g_c}{\rho_{\text{air}} V_{\text{rel}} d_s} \quad \text{EQN H14}$$

Thus, in the Stokes Law range, the time to go a distance  $\Delta Z$  is given by substituting equation H14 into equation H13:

$$\Delta t = \frac{d_s}{304,800} \sqrt{\frac{\rho_f \Delta Z}{(108) \mu_{\text{air}} V_{\text{rel}} g_c}} \text{ seconds} \quad \text{EQN H15}$$

It is quite doubtful that the droplet Reynolds number would be less than 1.0 for the region of interest which is the brief time period after the fuel enters the air stream. This is the time of maximum relative velocity and droplet diameter and hence, Reynolds number. Thus  $C_{\text{drag}}$  was obtained by an equation approximating the drag coefficient curve for spheres<sup>29</sup>.

Thus the mass fraction vaporized in the distance  $\Delta Z$  inches (restricted to  $\Delta Z$  values which do not give over approximately 25% vaporized) is:

$$\text{FRACT} = (12192) \sqrt{304,800} \sqrt{8} \left[ \frac{D_v W_f (P_s - P_{v\infty})}{\rho_f \bar{R} T_f d_s^2} \right] \sqrt{\frac{\rho_f d_s \Delta Z}{\rho_{\text{air}} C_{\text{drag}} V_{\text{rel}}^2}} \cdot \left[ 2.0 + 0.6 (R_e)^{1/2} (S_c)^{1/3} \right]$$

EQN H16

APPENDIX I  
LISTING OF MAIN PROGRAM

MAIN PROGRAM:

RANDOM DIMENSIONS

SPECIFIED INPUT POINT ANALYSIS

CONSTANT ENGINE SPEED ANALYSIS

ROAD LOAD ANALYSIS

CONSTANT THROTTLE ANGLE ANALYSIS

CARBURETOR - ENGINE OPERATING MAP

CARBURETOR - ENGINE - VEHICLE OPERATING MAP



\$ COMPIL FASTRAN, EXECUTE, PUNCH OBJECT

DIGITAL SIMULATION OF AN AIR-BLED, BOOST VENTURI CARBURETOR

```

C
C
C
DIMENSION ONAM(10),SCRACH( 45),PMAN(30),WETA(30)
DIMENSION FMEP1 ( 35), FMEP2 ( 35),XMPG( 21),SPEED( 21)
DIMENSION DCHAN(25),XLCHAN(25),CTYPE(25),DMV(10),DBV( 6)
DIMENSION DCHNOM(25),DMVNOM(10),DBVNOM( 6)
DIMENSION CD1(21),CD2(21), CD3(21),CD4(21)
DIMENSION CD5(21),CD6(21),CD7(21),CD8(21),CD9(21)
DIMENSION ANAME(4),FNAME(4),PNAME(4),ENAME(4)
DIMENSION ANGLC(25),DCHTOL(25),DMVTOL(10),DBVTOL( 6),XLD(25)
DIMENSION VNAME(4),CNAME(4),WHY(12)
DIMENSION ACHAN(25),AMV(10),ABV( 6),DIHP1(35),DIHP2(35)
DIMENSION TRANS( 5), CTHROT( 15),BHPP(21)
DIMENSION CD(21), RE(21), XIHP(21),BOOSTW(21),TOTLFA(21)
DIMENSION FLOWTP(21),FLOWMP(21), DRYAP(21),BSFCP(21)

```

```

C
COMMON ORDER,PRINTF,REJET,CDJET,DELXJ,DELXJL,DELXSE,XNCDJ,
1 XNCDJL,XNCDSE,URNS,SPILL1,RPM,DISPL,CR,DBLEED,DTRANS,
2 DCHOKE,PRINTA,XMACHT,TOTF,ACHAN,XLD,CTYPE,ANGLC,CD1,CD2,
3 CD3,CD4,CD5,CD6,CD7,CD8,CD9,SCRACH

```

```

C
C
C
READ INPUT TAPE 7,211,XNCDJ,XNCDJL,XNCDSE,DELXJ,DELXJL,DELXSE
NCDJ=XNCDJ
NCDJL=XNCDJL
NCDSE=XNCDSE
READ INPUT TAPE 7,209,ONAM(1),(CD1(I),I=1,NCDJ )
READ INPUT TAPE 7,209,ONAM(2),(CD2(I),I=1,NCDJL )
READ INPUT TAPE 7,209,ONAM(3),(CD3(I),I=1,NCDSE )
READ INPUT TAPE 7,209,ONAM(4),(CD4(I),I=1,NCDSE )
READ INPUT TAPE 7,209,ONAM(5),(CD5(I),I=1,NCDSE )
READ INPUT TAPE 7,209,ONAM(6),(CD6(I),I=1,NCDSE )
READ INPUT TAPE 7,209,ONAM(7),(CD7(I),I=1,NCDSE )
READ INPUT TAPE 7,209,ONAM(8),(CD8(I),I=1,NCDSE )
READ INPUT TAPE 7,209,ONAM(9),(CD9(I),I=1,NCDSE )
1 READ INPUT TAPE 7,203,VNAME(1),VNAME(2),VNAME(3),VNAME(4),
WEIGHT,AREA,TIREN,ROLL,DRAG
READ INPUT TAPE 7,204,RATIOD,TRANS(1),TRANS(2),TRANS(3)
1 READ INPUT TAPE 7,201,ENAME(1),ENAME(2),ENAME(3),ENAME(4),
BORE,STROKE,CYL
READ INPUT TAPE 7,205,CR,DMAN,VALVED,VSTEM,BORTOL,STOL,CRTOL
READ INPUT TAPE 7,210,AIRFL1,AIRFL2,XNIHP,XMINR,DELXR,XNFMEP,
1 XMINS,DELXS
NFMEP=XNFMEP
NIHP=XNIHP
READ INPUT TAPE 7,205,(FMEP1(I),I=1,NFMEP)

```

## DIGITAL SIMULATION OF AN AIR-BLED, BOOST VENTURI CARBURETOR

```

READ INPUT TAPE 7,205,(FMEP2(I),I=1,NFMEP)
READ INPUT TAPE 7,205,(DIHP1(I),I=1,NIHP )
READ INPUT TAPE 7,205,(DIHP2(I),I=1,NIHP )
READ INPUT TAPE 7,207,XNTHET,XMINT,DELXT,NMV,NBV,NCHAN
NTHETA=XNTHET
READ INPUT TAPE 7,205, (CTHROT(I),I=1,NTHETA)
READ INPUT TAPE 7,205,(DCHNOM(I),I=1,NCHAN )
READ INPUT TAPE 7,205,(DCHTOL(I),I=1,NCHAN )
READ INPUT TAPE 7,205,(XLCHAN(I),I=1,NCHAN )
READ INPUT TAPE 7,205,(CTYPE(I),I=1,NCHAN )
READ INPUT TAPE 7,205,( ANGLC(I),I=1,NCHAN )
READ INPUT TAPE 7,205,(DMVNOM(I),I=1,NMV )
READ INPUT TAPE 7,205,(DMVTOL(I),I=1,NMV )
READ INPUT TAPE 7,205,(DBVNOM(I),I=1,NBV )
READ INPUT TAPE 7,205,(DBVTOL(I),I=1,NBV )
READ INPUT TAPE 7,210,XM1NOM,XM2NOM,XBVNOM,XMBNOM,XM1TOL,
1 XM2TOL,XBVTOL,XMBTOL
20 READ INPUT TAPE 7,213,(WHY(I),I=1,11)
READ INPUT TAPE 7,208,CNAME(1),CNAME(2),CNAME(3),CNAME(4),
1 ORNAM,BBLS,JETS,THONOM,DTNOM,DSNOM
READ INPUT TAPE 7,205,SPILL1,SPILL2,THOTOL,DTTOL,DSTOL,OPENE
1 TURNS
READ INPUT TAPE 7,211,DBLNOM,DTRNOM,DCNOM,DBTOL,DTRTOL,DCTOL
READ INPUT TAPE 7,201,FNAME(1),FNAME(2),FNAME(3),FNAME(4),
1 FTYPE,TFUEL,FRACT
READ INPUT TAPE 7,200,POHG,TOF,HUMID
READ INPUT TAPE 7,214,RANVAR,XNUNIT,NUNITS
READ INPUT TAPE 7,201,ANAME(1),ANAME(2),ANAME(3),ANAME(4),
1 ATYPE,PRINT1,ORDER
READ INPUT TAPE 7,202,PNAME(1),PNAME(2),PNAME(3),PNAME(4),
1 PTYPE,SCALE
READ INPUT TAPE 7,204,PRINTA,PRINTF,PRINTS,DEBUGA

```

C  
C  
C  
C  
C

```

200 FORMAT (3F10.4)
201 FORMAT (4A6,6X,3F10.4)
202 FORMAT (4A6,6X,2F10.4)
203 FORMAT (4A6,6X,5F10.4)
204 FORMAT (4F10.4)
205 FORMAT (7F10.4)
206 FORMAT ( 7I5)
207 FORMAT (3F10.4,3I5 )
208 FORMAT (5A6,5F10.4)
209 FORMAT (1A6,4X,7F10.4,/, (7F10.4))
210 FORMAT (8F10.4)
211 FORMAT (6F10.4)
212 FORMAT ( 9I5)
213 FORMAT (11A6)
214 FORMAT (2F10.4,I5 )
215 FORMAT (5F10.4)

```

C  
C  
C  
C

## DIGITAL SIMULATION OF AN AIR-BLED, BOOST VENTURI CARBURETOR

AType INDICATES THE CONDITIONS UNDER WHICH THE CARBURETOR IS TO BE ANALYZED

AType=1.0 ..... ANALYSIS OF ONE OPERATING POINT (RPM AND THETA)  
 AType=2.0 ..... CONSTANT ENGINE SPEED-VARIABLE THROTTLE ANGLE  
 AType=3.0 ..... CONSTANT THROTTLE ANGLE-VARIABLE ENGINE SPEED  
 AType=4.0 ..... CARBURETOR-ENGINE OPERATING MAP  
 AType=5.0 ..... CARBURETOR ANALYSIS UNDER ROAD LOAD CONDITIONS  
 AType=6.0 ..... CARBURETOR-ENGINE-VEHICLE OPERATING MAP

PTYPE INDICATES THE TYPE OR TYPES OF CALCOMP PLOTS DESIRED

PTYPE=0.0 ..... NO PLOTS  
 PTYPE=1.0 ..... MAIN JET DISCHARGE COEFFICIENT VS. REYNOLDS NO.  
 PTYPE=2.0 ..... MAIN SYSTEM FUEL FLOW VS. BOOST VENTURI SUCTION  
 PTYPE=3.0 ..... MAIN SYSTEM FUEL FLOW VS. BOOST SUCTION (LOG-LOG)  
 PTYPE=4.0 ..... MAIN JET DISCHARGE COEFFICIENT VS. BOOST SUCTION  
 PTYPE=5.0 ..... MAIN JET DISCHARGE COEFFICIENT VS. TOTAL FUEL FLOW  
 PTYPE=6.0 ..... TOTAL F/A RATIO VS. AIR FLOW RATE  
 PTYPE=7.0 ..... VEHICLE MILES PER GALLON VS. MILES PER HOUR  
 PTYPE=8.0 ..... ENGINE BSFC VS. ENGINE BHP  
 PTYPE=9.0 ..... ENGINE IHP VS. AIR FLOW RATE  
 PTYPE=10.0 ..... ENGINE IHP VS. TOTAL F/A RATIO  
 PTYPE=11.0 ..... COMPLETE CARBURETOR-ENGINE-VEHICLE OPERATING MAP  
 PTYPE=12.0 ..... CURVES 11.0 AND 2.0  
 PTYPE=13.0 ..... CURVES 11.0 AND 6.0  
 PTYPE=14.0 ..... CURVES 11.0 AND 7.0

CTYPE INDICATES THE TYPE OF PASSAGE WHICH COMPOSES THE I-TH FUEL CHANNEL ELEMENT. THIS WILL BE USED TO INDICATE WHETHER DISCHARGE COEFFICIENTS MUST BE CALCULATED FOR THAT ELEMENT

CTYPE(I)=0.0 ..... NOT AN ORIFICE  
 CTYPE(I)=1.0 ..... A STANDARD CARBURETOR MAIN METERING ORIFICE  
 CTYPE(I)=2.0 ..... A SQUARE-EDGED ORIFICE  
 CTYPE(I)=3.0 ..... A VARIABLE AREA ORIFICE SUCH AS AN ENRICHMENT VALVE OR IDLE NEEDLE

PRINT1 INDICATES WHICH INPUT DATA SHOULD BE PRINTED OUT

PRINT1=0.0 ..... NO INPUT DATA PRINTED  
 PRINT1=1.0 ..... ONLY THE INITIAL HEADING PRINTED  
 PRINT1=2.0 ..... HEADING PLUS CARBURETOR INPUT DATA PRINTED  
 PRINT1=3.0 ..... HEADING PLUS CARBURETOR AND ENGINE DATA PRINTED  
 PRINT1=4.0 ..... HEADING, CARBURETOR, ENGINE, VEHICLE DATA PRINTED  
 PRINT1=5.0 ..... ALL INPUT DATA PRINTED

WRITE OUTPUT TAPE 6,22

FORMAT (1H1)

WRITE OUTPUT TAPE 6,1

FORMAT (1H ,49X,24H UNIVERSITY OF MICHIGAN /,1H ,41X,

1 40H MECHANICAL ENGINEERING DOCTORAL THESIS /,1H ,41X,

## DIGITAL SIMULATION OF AN AIR-BLED, BOOST VENTURI CARBURETOR

```

2      43H DIGITAL SIMULATION OF CARBURETOR METERING /,1H ,42X,
3      41H CARBURETOR-ENGINE-VEHICLE OPERATING MAP ,23X,
4      21H DAVID L. HARRINGTON /,1H )
WRITE OUTPUT TAPE 6,6,ANAME(1),ANAME(2),ANAME(3),ANAME(4)
6      FORMAT (1H ,10X,40H THE TYPE OF ANALYSIS REQUESTED IS.....
1      4A6 )
WRITE OUTPUT TAPE 6,7,PNAME(1),PNAME(2),PNAME(3),PNAME(4)
7      FORMAT (1H ,10X,40H THE TYPE OF PLOT(S) REQUESTED ARE.....
1      4A6 )
CALL TODAY (DATE1,DATE2)
WRITE OUTPUT TAPE 6,5,DATE1,DATE2,WHY(1),WHY(2),WHY(3),
1      WHY(4),WHY(5),WHY(6),WHY(7),WHY(8),WHY(9),WHY(10),WHY(11)
5      FORMAT (1H ,10X,40H THIS SIMULATION PERFORMED ON .....
12A6,/,11X, 40H PURPOSE OF THIS SIMULATION RUN ..... ,11A6 )
WRITE OUTPUT TAPE 6,47
WRITE OUTPUT TAPE 6,2
2      FORMAT (1H ,130H      AMBIENT CONDITIONS          CARBURE
1R      FUEL          ENGINE
2      VEHICLE      )
WRITE OUTPUT TAPE 6,3
3      FORMAT (1H ,130H -----
1-----
2----- )
C
C      PO IS IN PSIA      TO IS IN DEGREES RANKINE
C      DISPLACEMENT IS IN CUBIC INCHES
C
      PO=POHG*0.4912
      TOR=TOF + 459.6
      PCH=100.0*HUMID
      AMDENS=14.696*144.0*POHG/(29.92*53.34*TOR)
      DISPL=C.785398*BORE*BORE*STROKE*CYL
      AVALVE=C.7854*CYL*((VALVED-0.150)*(VALVED-0.150)-VSTEM*VSTE
1      /8BLS
      DUMTHO=THONOM
      CALL FPROP (FTYPE,TFUEL,TFUEL,SGFUEL,VISKM,CORR,CLIQ,CPFUEL,
1      CVFUEL,WMOLEC,HVAPOR,SIGMA,HEATV )
DO 171 I=1,NCHAN,1
171    XLD(I)=XLCHAN(I)/DCHNOM(I)
      RNO=C.C
C
C
24    IF(PRINT1-0.0) 25,25,24
CONTINUE
WRITE OUTPUT TAPE 6,4,POHG,CNAME(1),CNAME(2),CNAME(3),
1    CNAME(4),FNAME(1),FNAME(2),FNAME(3),FNAME(4),ENAME(1),
2    ENAME(2),ENAME(3),ENAME(4),VNAME(1),VNAME(2),VNAME(3),
3    TOF,ORNAM,TFUEL,DISPL,WEIGHT,PCH,DMVNOM(3),SGFUEL,
4    CR,RATIOD,AMDENS,DUMTHO,VISKM,AVALVE,TIREN
4    FORMAT (1H ,11H PRESSURE =,F6.2,16H INCHES HG ,4A6,4A6
1    2X,4A6,3X,3A6/,1H ,14H TEMPERATURE =,F5.1,24H DEGREES F MAI
2    2JET =,1A6,7X,14H TEMPERATURE =,F5.1, 21H F      DISPLACEMENT=,F5
3    ,24H C.I.      VEHICLE WEIGHT=,F6.1/,1H ,11H HUMIDITY =,F5.1,
4    30H PERCENT      MAIN VENTURI=,F5.3,23H IN.      SPECIFIC GRAV
5    5Y=,F5.3,17H      COMP. RATIO =,F4.1,9X,17H REAR AXLE RATIO=,F5.2/,
6    1H ,10H DENSITY =,F7.4,32H LBM/FT3      CLOSED THROTTLE=,F4.
7    15H      VISCOSITY =,F6.3,25H CS      VALVE FLOW AREA=,F4.2,23H

```

## DIGITAL SIMULATION OF AN AIR-BLED, BOOST VENTURI CARBURETOR

```

82   TIRE REVS/MILE =,F5.1/ )
    IF (PRINT1-2.0) 185,170,170
C   PRINT THE CARBURETOR INPUT DATA
170  WRITE OUTPUT TAPE 6,172,CNAME(1),CNAME(2),CNAME(3),CNAME(4)
    WRITE OUTPUT TAPE 6,173,ORNAM,DCHNOM(1),XLCHAN(1),XLD(1),
1    JETS,THONOM,DTNOM,DSNOM,SPILL1,DMVNOM(3)
    WRITE OUTPUT TAPE 6,174,DTRNOM,DCNOM,DBLNOM,XM1NOM,XM2NOM,
1    XBVNOM,XMBNOM
    WRITE OUTPUT TAPE 6,175
    WRITE OUTPUT TAPE 6,176
    DO 236 I=1,NMV,1
236  WRITE OUTPUT TAPE 6,177,I,DMVNOM(I)
    WRITE OUTPUT TAPE 6,179
    WRITE OUTPUT TAPE 6,176
    DO 237 I=1,NBV,1
237  WRITE OUTPUT TAPE 6,177,I,DBVNOM(I)
    WRITE OUTPUT TAPE 6,181
    WRITE OUTPUT TAPE 6,182
    DO 238 I=1,NCHAN,1
238  WRITE OUTPUT TAPE 6,183,I,DCHNOM(I),XLCHAN(I),XLD(I),CTYPE(I)
172  FORMAT(1H0, 5X,20H INPUT DATA FOR THE ,4A6,11H CARBURETOR. /,
1    1H ,19X,27H ***NOMINAL DIMENSIONS*** // )
173  FORMAT (1H ,10X,28H MAIN METERING ORIFICE TYPE =,A6 /,
1    11X,33H MAIN METERING ORIFICE DIAMETER = ,F7.4,6H INCH /,
2    11X,31H MAIN METERING ORIFICE LENGTH = ,F7.4,6H INCH /,
3    11X,34H MAIN METERING ORIFICE L/D RATIO = ,F7.4, /,
4    11X,35H NUMBER OF MAIN METERING ORIFICES =,F3.0, /,
5    11X,35H COMPLETELY CLOSED THROTTLE ANGLE =,F6.3,9H DEGREES /,
6    11X,25H THROTTLE BORE DIAMETER = ,F7.4,8H INCHES /,
7    11X,25H THROTTLE SHAFT DIAMETER= ,F7.4,6H INCH /,
8    11X,37H INITIAL SPILL POINT OF MAIN SYSTEM =,F5.3,6H INCH /,
9    11X,31H MAIN VENTURI THROAT DIAMETER = ,F7.4,8H INCHES // )
174  FORMAT ( 5X,25H THROTTLE PLATE BYPASSES //,
1    11X,25H TRANSFER TUBE DIAMETER =,F6.4,6H INCH /,
2    11X,35H CHOKE BLEED RESTRICTION DIAMETER =,F6.4,6H INCH /,
3    11X,40H ENRICHMENT BLEED RESTRICTION DIAMETER =,F6.4,6H INCH // ,
4    5X,51H GEOMETRIC RELATION BETWEEN BOOST AND MAIN VENTURI //,
5    11X, 7H XMV1 =,F7.4,8H INCHES /,
6    11X, 7H XMV2 =,F7.4,8H INCHES /,
7    11X, 7H XBV =,F7.4,8H INCHES /,
8    11X, 7H XMB =,F7.4,8H INCHES // )
175  FORMAT (1H4,9X,15H MAIN VENTURI /,14X, 9H ELEMENT ,10X,10H D
    DIAMETER )
176  FORMAT (11X,14H ----- ,6X,14H ----- )
177  FORMAT (11X,18,10X,F9.3,8H INCHES )
179  FORMAT (1H0,9X,15H BOOST VENTURI/,14X, 9H ELEMENT ,10X,10H D
    DIAMETER )
181  FORMAT (1H0,12X,13HFUEL CHANNEL ,79X,9H ORIFICE /,14X,
1    9H ELEMENT ,13X,10H DIAMETER ,13X,10H LENGTH ,13X,
2    11H L/D RATIO ,10X,10H TYPE )
182  FORMAT (11X,14H ----- ,9X,14H ----- ,9X,
1    14H ----- ,9X,14H ----- ,9X,13H -----)
183  FORMAT (11X,19,12X,F9.4,5H INCH,9X,F9.3,5H INCH,11X,F10.3,
1    13X,F9.1 )
185  CONTINUE
C   IF (PRINT1-3.0) 192,186,186

```

## DIGITAL SIMULATION OF AN AIR-BLED, BOOST VENTURI CARBURETOR

```

C      PRINT THE ENGINE INPUT DATA (IHP VS. F/A AND FMFP VS. RPM)
186    WRITE OUTPUT TAPE 6,187,ENAME(1),ENAME(2),ENAME(3),ENAME(4)
      WRITE OUTPUT TAPE 6,188,AIRFL1,AIRFL2
      WRITE OUTPUT TAPE 6,189
      WRITE OUTPUT TAPE 6,230
      WRITE OUTPUT TAPE 6,231
      DUMFR=XMINR-DELXR+0.0000001
      DO 190 I=1,NIHP,1
      DUMFR=DUMFR+DFLXR
190    WRITE OUTPUT TAPE 6,191,I,DUMFR,DIHP1(I),I,DUMFR,DIHP2(I)
      WRITE OUTPUT TAPE 6,232
      WRITE OUTPUT TAPE 6,233
      WRITE OUTPUT TAPE 6,231
      DUMRPM=XMINR-DELXS+0.0000001
      DO 235 I=1,NFMFP,1
      DUMRPM=DUMRPM+DELXS
235    WRITE OUTPUT TAPE 6,234,I,DUMRPM,FMFP1(I),I,DUMRPM,FMFP2(I)
187    FORMAT (1H4,25X,33H IHP AND FMFP INPUT DATA FOR THE ,4A6,
1      7H ENGINE // )
188    FORMAT (1H ,10X,25H MEASURED AIR FLOW RATE =,F6.1,10H LBM/H
1R ,20X,25H MEASURED AIR FLOW RATE =,F6.1,10H LBM/HOUR )
189    FORMAT (11X,41H-----
1      20X,41H----- )
230    FORMAT (11X,6H POINT,8X,11H F/A RATIO ,7X,9H IHP1 ,
1      20X,6H POINT,8X,11H F/A RATIO ,7X,9H IHP2 )
231    FORMAT (11X,6H -----,8X,11H-----,7X,9H----- ,
1      20X,6H -----,8X,11H-----,7X,9H----- )
191    FORMAT (10X,I5,10X,F8.4,10X,F6.2,22X,I5,10X,F8.4,10X,F6.2 )
232    FORMAT (1H /,1H0,16X,28H FMFP AT WIDE OPEN THROTTLE ,33X,
1      25H FMFP AT CLOSED THROTTLE /)
233    FORMAT (11X,6H POINT,8X,12H ENGINE RPM ,5X,8H FMFP1 ,
1      22X,6H POINT,7X,12H ENGINE RPM ,6X,8H FMFP2 )
234    FORMAT (10X,I5,10X,F8.1,10X,F6.2,22X,I5,10X,F8.1,10X,F6.2 )
192    CONTINUE
C
      IF (PRINT1-4.0) 169,163,163
C      PRINT THE VEHICLE INPUT DATA
163    WRITE OUTPUT TAPE 6,167,VNAME(1),VNAME(2),VNAME(3),VNAME(4)
      WRITE OUTPUT TAPE 6,168,AREA,WEIGHT,ROLL,DRAG,TIREN,RATIOD,
1      TRANS(1),TRANS(2),TRANS(3)
167    FORMAT (1H4, 5X,28H VEHICLE INPUT DATA FOR THE ,4A6, /// )
168    FORMAT (1H ,10X,23H VEHICLE FRONTAL AREA =,F6.2,5H FT2 /,
1      11X,22H VEHICLE CURB WEIGHT = ,F6.0,5H LBM /,
2      11X,28H ROLLING RESISTANCE FACTOR = ,F6.5,9H LBF/LBM /,
3      11X,25H WIND RESISTANCE FACTOR = ,F6.5,13H LBF/MPH FT2 /,
4      11X,28H TIRE REVOLUTIONS PER MILE = ,F6.1, /,
5      11X,18H REAR AXLE RATIO = ,F6.3 /,
6      11X,17H LOW GEAR RATIO = ,F6.3 /,
7      11X,20H SECOND GEAR RATIO = ,F6.3 /,
8      11X,18H HIGH GEAR RATIO = ,F6.3 / )
169    CONTINUE
C
      IF (PRINT1-5.0) 25,193,193
C      PRINT THE ORIFICE COEFFICIENT INPUT DATA
193    WRITE OUTPUT TAPE 6,194
      WRITE OUTPUT TAPE 6,196,ONAM(1),(ONAM(I),I=3,9),ONAM(2)
      WRITE OUTPUT TAPE 6,197

```

## DIGITAL SIMULATION OF AN AIR-BLED, BOOST VENTURI CARBURETOR

```

DUM1=-DELXJ + 0.000001
DUM2=-DELXJL + 0.000001
DO 198 I=1,NCDJ,1
DUM1=DUM1+DELXJ
DUM2=DUM2 + DELXJL

```

```

198 WRITE OUTPUT TAPE 6,199,I,DUM1,CD1(I),CD3(I),CD4(I),
1 CD5(I),CD6(I),CD7(I),CD8(I),CD9(I),DUM2,CD2(I)
199 FORMAT (I9,F9.0,8F9.3,8X,F8.0,F10.3 )
194 FORMAT (1H2,34X,50H INPUT DATA FOR ORIFICE COEFFICIENTS OF DI
ISCHARGE // )
196 FORMAT (5X,13H POINT RE,4X,A6,3X,A6,3X,A6,3X,A6,3X,A6,3X,
1 A6,3X,A6,3X,A6,11X,4H RE,5X,A6 )
197 FORMAT (117H -----
1-----
2-- )
25 CONTINUE
AMAX=995.0
SET=2.0
PTHETA=0.0
IF (PTYPE-11.0) 14,158,158
158 IF (SCALE-2.0) 13,12,13
12 AMAX=740.00
DX= +30.00/7.50
DY= +750.00/7.50
GO TO 14
13 IF (SCALE-3.0) 66,65,65
65 AMAX=370.00
DX=+30.00/7.500
DY=375.00/7.500
GO TO 14
66 CONTINUE
AMAX=995.0
DX= +30.00/6.375
DY=1000.00/8.500
14 CONTINUE
SET=2.0

```

```

C
C SET CONTROLS THE PLOTTING SUBROUTINES
C

```

```

C SET=0.0.....SET GRID,PLOT POINTS,END PLOT
C SET=1.0..... PLOT POINTS,END PLOT
C SET=2.0.....SET GRID,PLOT POINTS
C SET=3.0..... PLOT POINTS

```

```

C
C NOW BUILD CARBURETORS WITH PRODUCTION VARIATIONS IN DIMENSIONS
C

```

```

8 CARBNO=0.0
: GENERATE PRODUCTION DIMENSIONS FOR AIR AND FUEL PASSAGES
243 CARBNO=CARBNO+1.0
DO 9 J=1,NCHAN,1

```

```

C
C SIGMA IS THE STANDARD DEVIATION OF THE POPULATION OF DIMENSIONS
C

```

```

C RANDND IS A LIBRARY SUBROUTINE WHICH PRODUCES RANDOM NUMBERS
C WITH A GIVEN NOMINAL (MEAN) VALUE AND STANDARD DEVIATION

```

## DIGITAL SIMULATION OF AN AIR-BLED, BOOST VENTURI CARBURETOR

```

C
      SIGMA=DCHTOL(J)/3.0
      DCHAN(J)=RANDND(DCHNOM(J),SIGMA,RND)
9     XLD(J)=XLCHAN(J)/DCHAN(J)
      DO 10 J=1,NMV,1
      SIGMA=DMVTOL(J)/3.0
10    DMV(J)=RANDND(DMVNOM(J),SIGMA,RND)
      DO 11 J=1,NBV,1
      SIGMA=DBVTOL(J)/3.0
11    DBV(J)=RANDND(DBVNOM(J),SIGMA,RND)
      SIGMA=XM1TOL/3.0
      XMV1 =RANDND(XM1NOM,SIGMA,RND)
      SIGMA=XM2TOL/3.0
      XMV2 =RANDND(XM2NOM,SIGMA,RND)
      SIGMA=XBVTOL/3.0
      XBV  =RANDND(XBVNOM,SIGMA,RND)
      SIGMA=XMBTOL/3.0
      XMB  =RANDND(XMBNOM,SIGMA,RND)
      SIGMA=THOTOL/3.0
      THETAO=RANDND(THONOM,SIGMA,RND)
      SIGMA= DTTOL/3.0
      DT    =RANDND(DTNOM ,SIGMA,RND)
      SIGMA= DSTOL/3.0
      DS    =RANDND(DSNOM ,SIGMA,RND)
      SIGMA=DRTOL /3.0
      DBLEED=RANDND(DBLNOM,SIGMA,RND)
      SIGMA=DTRTOL/3.0
      DTRANS=RANDND(DTRNOM,SIGMA,RND)
      SIGMA=DCTOL /3.0
      DCHOKE=RANDND(DCNOM ,SIGMA,RND)
225   IF (CARBNO-1.0) 19,225,19.
226   IF (PRINT1-2.0) 19,226,226
224   WRITE OUTPUT TAPE 6,224
      FORMAT (1H1,5X,48H DIMENSIONS OF A TYPICAL PRODUCTION CARBU
1TOR  // )
      WRITE OUTPUT TAPE 6,173,ORNAM,DCHAN(1),XLCHAN(1),XLD(1),JET
1     THETAO,DT,DS,'SPILL1,DMV(3)
      WRITE OUTPUT TAPE 6,174,DTRANS,DCHOKE,DBLEED,XMV1,XMV2,XBV,
1     XMB
      WRITE OUTPUT TAPE 6,175
      WRITE OUTPUT TAPE 6,176
      DO 178 I=1,NMV,1
178   WRITE OUTPUT TAPE 6,177,I,DMV(I)
      WRITE OUTPUT TAPE 6,179
      WRITE OUTPUT TAPE 6,176
      DO 180 I=1,NBV,1
180   WRITE OUTPUT TAPE 6,177,I,DBV(I)
      WRITE OUTPUT TAPE 6,181
      WRITE OUTPUT TAPE 6,182
      DO 184 I=1,NCHAN,1
184   WRITE OUTPUT TAPE 6,183,I,DCHAN(I),XLCHAN(I),XLD(I),CTYPE(I)
C
C     NOW ALL THE DIMENSIONS HAVE BEEN GIVEN PRODUCTION VALUES
C
19    CONTINUE
      DO 223 J=1,NBV,1
223   ABV(J)=0.785398*DBV(J)*DBV(J)

```



## DIGITAL SIMULATION OF AN AIR-BLED, BOOST VENTURI CARBURETOR

```
CALL THROTL (90.00, THETA0, DT, DS, AWOT )
```

```
AMV(1)=0.785398*DMV(1)*DMV(1)
```

```
AMV(2)=0.785398*DMV(2)*DMV(2) -ABV(2)
```

```
AMV(3)=0.785398*DMV(3)*DMV(3) -ABV(6)
```

```
AMV(4)=0.785398*DMV(4)*DMV(4) -ABV(6)
```

```
AMV(5)=0.785398*DMV(5)*DMV(5)
```

```
AMV(6)=AWOT
```

```
AMV(7)=0.785398*DMAN*DMAN*CYL/BRLS
```

```
AMV(8)=AVALVE
```

```
DO 15 J=1, NCHAN, 1
```

```
15 ACHAN(J)=0.785398*DCHAN(J)*DCHAN(J)
```

```
C
C THE FOLLOWING VALUE OF THETA0 ACCOUNTS FOR THE LEAKAGE AREA
C WHEN THE THROTTLE IS COMPLETELY CLOSED
```

```
DUMTHO=THETA0
```

```
THETA0=THETA0 - 3.800 -0.1000*THETA0
```

```
IF (THETA0) 150,151,151
```

```
150 THETA0=0.010
```

```
151 CONTINUE
```

```
IF (ATYPE-1.0) 221,245,221
```

```
245 CONTINUE
```

```
IF (CARBNO-1.0) 227,30,227
```

```
C
C
C CALCULATE SPECIFIED OPERATING POINTS
C
```

```
30 WRITE OUTPUT TAPE 6,45
```

```
45 FORMAT (1H4,16X,98H CARBURETOR-ENGINE OPERATION FOR SPECIFIC
10OPERATING POINTS (RPM AND THETA SUPPLIED AS INPUT DATA) //)
```

```
WRITE OUTPUT TAPE 6,164
```

```
WRITE OUTPUT TAPE 6,165
```

```
WRITE OUTPUT TAPE 6,166
```

```
WRITE OUTPUT TAPE 6,146
```

```
77 READ INPUT TAPE 7,23,RPM,THETA,PRINTO,STOP
```

```
23 FORMAT (4F10.4)
```

```
227 IF (STOP) 263,263,262
```

```
262 IF (XNUNIT-CARBNO) 271,271,263
```

```
271 SET=1.0
```

```
263 CONTINUE
```

```
I=0
```

```
K=0
```

```
VACMAN=12.0
```

```
GO TO 268
```

```
270 IF (RANVAR) 241,241,242
```

```
242 IF (XNUNIT-CARBNO) 241,241,243
```

```
241 CONTINUE
```

```
IF (STOP) 244,244,20
```

```
244 CARBNO=1.0
```

```
GO TO 77
```

```
C
221 IF (ATYPE-2.0) 31,79,31
```

```
31 IF (ATYPE-4.0) 88,79,88
```

```
88 IF (ATYPE-6.0) 70,79,70
```

```
79 CONTINUE
```

```
C
C
```

## DIGITAL SIMULATION OF AN AIR-BLED, BOOST VENTURI CARBURETOR

```

C
C          CALCULATE CONSTANT RPM LINES
C
      IF (PRINT1-1.0) 32,32,222
222     CONTINUE
      WRITE OUTPUT TAPE 6,22
      WRITE OUTPUT TAPE 6,2
      WRITE OUTPUT TAPE 6,3
      WRITE OUTPUT TAPE 6,4,POHG,CNAME(1),CNAME(2),CNAME(3),
1       CNAME(4),FNAME(1),FNAME(2),FNAME(3),FNAME(4),ENAME(1),
2       ENAME(2),ENAME(3),ENAME(4),VNAME(1),VNAME(2),VNAME(3),
3       TOF,ORNAM,TFUEL,DISPL,WEIGHT,PCH,DMVNOM(3),SGFUEL,
4       CR,RATIO0,AMDENS,DUMTHO,VISKM,AVALVE,TIREN
32     READ INPUT TAPE 7,23,RPM,RPMLIM,PRINTO
      IF (PRINTO)149,149,148
148     WRITE OUTPUT TAPE 6,47
      WRITE OUTPUT TAPE 6,144
144     FORMAT (1H4,16X,82H CARBURETOR-ENGINE OPERATION AT CONSTANT
ENGINE SPEED-VARIABLE THROTTLE OPENING //)
      WRITE OUTPUT TAPE 6,164
      WRITE OUTPUT TAPE 6,165
      WRITE OUTPUT TAPE 6,166
      WRITE OUTPUT TAPE 6,146
164     FORMAT (132H
1DRY      BOOST      MAIN      THROT      INTAKE      MOIST
2THROT    AIR        )
165     FORMAT (132H ENGINE      THROT      FLOW      MAN.      AIR
1AIR     VENTURI    VENTURI    MACH      F/A       F/A       FUEL     FUEL
2TOTAL   BLEED      )
166     FORMAT (132H RPM      ANGLE      AREA      PRESS      FLOW
1LOW     SUCTION    SUCTION    NO.       RATIO     RATIO     FLOW     FLOW
2TEMP    FLOW      J )
146     FORMAT (132H -----
1-----
2-----)
149     CONTINUE
      I=0
      K=0
      PLOTN=0.0
      PLOTI=0.0
      DUMA=0.0
      SWITCH=0.00
      VACMAN=21.00 + RPM/800.0
268     CONTINUE
      GUESS=VACMAN
      XGUESS=0.65
      C8=0.400*1.25*1545.4*585.0*(CR-1.0)/(28.95*CR*0.4912)
      C9=(CR-0.5)/CR
      DRYA2=DISPL*RPM*(POHG*C9-VACMAN)/(C8*1.0620)
      CALL ASSUME (DRYA2,VACMAN,OPENE,FAMAIN,FATOTL,FARICH,
1       FLOWM,FLOWT,FLOWE )
      RATEMF=2.0*FLOWM
C     NOW INITIAL GUESSES HAVE BEEN MADE FOR EACH NEEDED PARAMETER
      OLDA1=FATOTL
      OLDA2=FAMAIN
      OLDAIR=DRYA2
      IF (ATYPE-1.0) 260,18,260

```

## DIGITAL SIMULATION OF AN AIR-BLED, BOOST VENTURI CARBURETOR

```

260      THETA=DUMTHO
246      DUMA=DUMA + 2.0
          IF ( DUMA-DUMTHO-0.10 ) 246,246,247
247      CONTINUE
16       IF ( I-1 ) 29,248,249
248      THETA=DUMA
          GO TO 29
249      IF ( THETA-29.9 ) 27,27,28
27       THETA=THETA+2.000
          GO TO 29
28       IF ( THETA-59.9 ) 257,257,258
257      THETA=THETA+5.000
          GO TO 29
258      THETA=THETA + 10.0
29       CONTINUE
          IF ( THETA - 84.00 ) 18,17,17
18       I=I+1
          CALL THROTL ( THETA, THETA0, DT, DS, AFLOW )
          AMV(6)=AFLOW
          OPEN=THETA-THETA0
          CALL STERL ( CTHROT, XMINT, DELXT, ORDER, XNTHET, SCRACH, OPEN, CDT,
1          0.0 )
          J=0
250      CONTINUE
          IF ( J-15 ) 253,254,254
254      WRITE OUTPUT TAPE 6,255
255      FORMAT (46H NO FUEL-AIR CONVERGENCE WITHIN MAIN PROGRAM )
          GO TO 261
253      J=J+1
          CALL AIRMAS ( POHG, TOF, HUMID, THETA, CDT, AFLOW, FTYPE, TFUEL,
1          FRACT, GUESS, FAMAIN, FATOTL, VACMAN, DRYAIR, WETAIR, VENFLO )
          GUESS=VACMAN
          CALL SIGNAL ( POHG, TOF, HUMID, VENFLO, FTYPE, TFUEL, RATEMF,
1          AMV, ABV, XMV1, XMV2, XBV, XMB, BBLS, FRACT, XGUESS, PRINTS,
2          XFV, BVFLO, PVFLO, BVMACH, PVMACH, BVSUCW, PVSUCW )
          RATEMF=BBLS*FLOWM
          XGUESS=XFV
          CALL FLOW ( POHG, TOF, HUMID, BVSUCW, VACMAN, OPENE, FTYPE,
1          TFUEL, NCHAN, FLOWM, FLOWT, FLOWE, FLOWJ, FLOWI, SUMAIR )
          FAMAIN=BBLS*FLOWM/DRYAIR
          FATOTL=BBLS*FLOWT/DRYAIR
          DELFA1=FATOTL-OL DFA1
          DELFA2=FAMAIN-OL DFA2
          DELAIR=DRYAIR-OL DAIR
          OL DFA1=FATOTL
          OL DFA2=FAMAIN
          OL DAIR=DRYAIR
          IF ( ABSF( DELFA1 ) - 0.00020 ) 251,251,250
251      IF ( ABSF( DELFA2 ) - 0.00020 ) 252,252,250
252      IF ( ABSF( DELAIR ) - 0.250 ) 261,261,250
261      CONTINUE
          PRESS=POHG-VACMAN
          PMAN(I)= PRESS
          WETA(I)=WETAIR
          CD(I)=CDJET
          RE(I)=REJET
          BOOSTW(I)=BVSUCW

```

## DIGITAL SIMULATION OF AN AIR-BLED, BOOST VENTURI CARBURETOR

```

FLOWTP(I)=FLOWT
FLOWMP(I)=FLOWM
TOTLFA(I)=FATOTL
DRYAP(I)=DRYAIR
DUMFT=BBLS*FLOWT
DUMFM=BBLS*FLOWM
SUMAIR=BBLS*SUMAIR
IF (PRINTO) 239,239,259
259 1 WRITE OUTPUT TAPE 6,256,RPM,THETA,AFLOW,PRESS,WETAIR,DRYAIR
256 1 BVSUCW,PVSUCW,XMACHT,FAMAIN,FATOTL,DUMFT,DUMFM,TOTF,SUMAIR
1 FORMAT (F8.1,F9.1,F9.4,F9.2,3F9.2,F8.2,F9.4,F9.4,F8.4,F8.3,
239 1 F8.3,F8.1,F7.3,I4 )
239 CONTINUE
IF (ATYPE-1.0) 264,78,264
264 1 IF (SWITCH-0.0) 61,61,26
61 CONTINUE
C
IF (WETAIR-AMAX) 26,26,50
50 K=I
PLOTI=I
SWITCH=1.0
26 CONTINUE
GO TO 16
17 CONTINUE
C PLOT A CONSTANT RPM LINE
IF (PTYPE-0.0) 40,40,91
91 CONTINUE
IF (ATYPE-2.00) 78,84,78
84 IF (RPMLIM-RPM) 85,85,78
85 SET=1.0
78 CONTINUE
TYPEL=-1.0
PLOTN=I
IF (PTYPE-1.0) 301,300,301
300 DXCR=10.00/7.50
DYCR=0.500/7.50
CALL CALCVR ( RE,CD,PLOTN,0.0,DXCR,0.50,DYCR,1.0,SET,1.0,
1 1.0,1.0,TYPEL, 68.0,TFUEL,0.0 )
SET=3.0
GO TO 40
301 IF (PTYPE-2.0) 303,302,303
302 DXMH=25.00/7.50
DYM=40.00/7.50
CALL CALMVH (BOOSTW,FLOWMP,PLOTN,0.0,DXMH,0.0,DYM,1.0,SET,
1 1.0,1.0,1.0,+1.00, 68.00,TFUEL,1.0 )
SET=3.0
GO TO 40
303 IF (PTYPE-3.0) 305,304,305
304 XEXP=-1.0
DXLL=3.00/7.50
YEXP=-1.0
DYLL=3.00/7.50
DO 315 J=1,I,1
IF (BOOSTW(J)-0.100) 317,316,316
317 BOOSTW(J)=0.100
316 IF (FLOWMP(J)-0.100) 318,315,315
318 FLOWMP(J)=0.100

```

## DIGITAL SIMULATION OF AN AIR-BLED, BOOST VENTURI CARBURETOR

```

315     CONTINUE
      CALL CALLOG (BOOSTW, FLOWMP, PLOTN, XEXP, DXLL, YEXP, DYLL, 1.0,
1       SET, 1.0, 1.0, 1.0, TYPEL, 68.00, TFUEL, 1.0 )
      SET=3.0
      GO TO 40
305     IF (PTYPE-4.0) 307,306,307
306     DXCH=25.00/7.50
      DYCH=0.500/7.50
      CALL CALCVH (BOOSTW, CD , PLOTN, 0.0, DXCH, 0.50, DYCH, 1.0, SET,
1       1.0, 1.0, 1.0, +1.00, 68.00, TFUEL, 1.0 )
      SET=3.0
      GO TO 40
307     IF (PTYPE-5.0) 309,308,309
308     DXCM=25.00/7.50
      DYCM=0.500/7.50
      CALL CALCVH (FLOWTP, CD , PLOTN, 0.0, DXCM, 0.50, DYCM, 1.0, SET,
1       1.0, 1.0, 1.0, TYPEL, 68.00, TFUEL, 0.0 )
      SET=3.0
      GO TO 40
309     IF (PTYPE-6.0) 311,310,311
310     DXFA=700.00/8.925
      DYFA=0.100/6.375
      CALL CALFVA (DRYAP, TOTLFA, PLOTN, 0.0, DXFA, 0.0300, DYFA, 1.0, SET,
1       1.0, 2.0, 2.0, +1.00, 1.0, TFUEL, 1.0 )
      SET=3.0
      GO TO 40
311     IF (PTYPE-11.0) 40,86,86
86     CONTINUE
      IF (ATYPE-1.0) 265,266,265
266     K=I
      PLOTI=I
      GO TO 267
265     IF (SET - 2.50) 43,43,46
46     XSTART=1.00 + (PMAN(1) - 00.00)/DX
      YSTART= 1.0 + (WETA(1) - 0.00)/DY
      CALL PENUP (XSTART, YSTART)
43     CONTINUE
      PMAN(I+1)=PMAN(I)
      WETA(I+1)=WETA(I)
      IF (K-0) 55,55,56
55     K=I
      PLOTI=I
56     IF (WETA(K) - AMAX -3.000) 80,80,81
81     PMAN(K)=PMAN(K)-(WETA(K)-AMAX)*((PMAN(K)-PMAN(K-1)) /
1       (WETA(K)-WETA(K-1)))
      WETA(K)=AMAX
80     CONTINUE
69     IF (SCALE-3.0) 67,68,68
68     MH=(K+1)/2 + 3
      GO TO 76
67     MH=(I+1)/2
76     CONTINUE
      IF (RPM-1900.0) 63,64,64
63     MH=MH-1
64     CONTINUE
72     IF (PMAN(MH)-23.00) 73,73,71
71     MH=MH- 1

```

## DIGITAL SIMULATION OF AN AIR-BLED, BOOST VENTURI CARBURETOR

```

73      GO TO 72
        CONTINUE
        ML=MH - 1
C
        ANGLR=ATAN((DX*(WETA(MH)-WETA(ML)))/(DY*(PMAN(MH)-PMAN(ML)))
        ANGLD=ANGLR*180.00/3.1415926
        YVAL=1.060 + WETA(MH)/DY
        XVAL=1.000 + PMAN(MH)/DX
        CALL PSYMB ( XVAL ,YVAL,-0.100,9H      RPM,ANGLD,9 )
        CALL PFNMBR (XVAL,YVAL,-0.100,RPM,ANGLD,6H(F5.0))
267     CALL CALMAP (PMAN,WETA,PLOTI,00.0,DX,00.0,DY,POHG,SET,PCH ,
1       1.00,1.00, CR ,DISPL, TOF ,SCALE )
        SET=3.0
        IF (ATYPE-1.0) 272,270,272
272     WRITE OUTPUT TAPE 6,152,PLOTI
152     FORMAT (39H      A LINE WAS PLOTTED WITH ,F4.0,
1       8H POINTS )
        CALL PENUP (2.000,1.125)
40      CONTINUE
        IF (ATYPE-1.0) 269,270,269
269     IF (PTHETA) 108,108,75
108     IF (RPMLIM-RPM) 70,70,32
70      CONTINUE
        IF (ATYPE-5.00) 89,21,89
89      IF (ATYPE-6.00) 136,90,136
21      SET=0.0
90      CONTINUE
C
C
C      CALCULATE CARBURETOR-ENGINE-VEHICLE PARAMETERS ALONG A
C      ROAD LOAD CURVE
C
141     WRITE OUTPUT TAPE 6,141
        FORMAT (1H1,40X,51H ROAD LOAD CARBURETOR-ENGINE-VEHICLE PER
1       1RMANCE //)
        NGEAR=1
        CALL THROTL (90.00,THETA0,DT,DS,AWOT )
133     RATIOI=TRANS(NGEAR)
        WRITE OUTPUT TAPE 6,139,RATIOI
139     FORMAT (1H0,71H THE FOLLOWING VALUES ARE CALCULATED FOR A
1       1ANSMISSION GEAR RATIO OF ,F5.3//)
        L=0
        WRITE OUTPUT TAPE 6,145
        WRITE OUTPUT TAPE 6,142
        WRITE OUTPUT TAPE 6,143
145     FORMAT (132H      CAR      ENGINE      THROT      MOIST
1       1      MAN.      BLEED      F/A      ENGINE      ENGINE      FUEL
2       2      )
142     FORMAT (132H      MPH      RPM      ANGLE      AIRFLO      BHP
1       1 IHP      PRESS.      AIR      RATIO      ISFC      BSFC      RATE
2       2 MPG      NN      )
143     FORMAT (132H      -----      -----      -----      -----      -----
1       1-----      -----      -----      -----      -----      -----
2       2-----      -----      )
104     VMPPH=5.00
        DEBUG=0.0

```

## DIGITAL SIMULATION OF AN AIR-BLED, BOOST VENTURI CARBURETOR

```

PRINTO=0.0
EPS2=0.200
THSTEP=2.0
RPM=TIREN*RATIOD*RATIOT*10.0/60.0
VACMAN=14.1
GUFSS=VACMAN
XGUFSS=0.65
C8=0.400*1.25*1545.4*585.0*(CR-1.0)/(28.95*CR*0.4912)
C9=(CR-0.5)/CR
DRYA2=DISPL*RPM*(POHG*C9-VACMAN)/(C8*1.0620)
CALL ASSUME (DRYA2,VACMAN,OPENE,FAMAIN,FATOTL,FARICH,
1 FLOWM,FLOWT,FLOWE )
RATEMF=2.0*FLOWM

```

C NOW INITIAL GUESSES HAVE BEEN MADE FOR EACH NEEDED PARAMETER

C

```

134 L=L+1
105 VMPH=VMPH + 5.000
ROADHP=(VMPH/375.0)*(ROLL*WEIGHT+DRAG*AREA*VMPH*VMPH)
DRIVEN=0.8600-(VMPH/1210.00)-(VMPH*VMPH/333300.00)
BHP=ROADHP/DRIVEN
RPM=TIREN*RATIOD*RATIOT*VMPH/60.00
CALL STERL (FMPE1,XMINS,DELXS,ORDER,XNFMEP,SCRACH,RPM,FMIN,
1 DEBUG )
CALL STERL (FMPE2,XMINS,DELXS,ORDER,XNFMEP,SCRACH,RPM,FMAX,
1 DEBUG )
CHANGE=0.0
NN=0

```

C MAKE AN INITIAL GUESS FOR THE THROTTLE PLATE OPENING

```
THETA=DUMTHO+5.700+46.50*VMPH*VMPH/10000.00
```

```

120 CONTINUE
NN=NN+1
IF (NN-33) 121,121,122
122 WRITE OUTPUT TAPE 6,123
123 FORMAT (1H0,32H NO THROTTLE ANGLE CONVERGENCE )
GO TO 113
121 IF (NN-14) 159,219,159
219 IF (AWOT*0.99-AFLOW) 113,113,159
159 IF (NN-21) 153,154,153
154 WRITE OUTPUT TAPE 6,155
155 FORMAT (61H 20 ROAD LOAD ITERATIONS HAVE BEEN ATTEMPTED.....T
1RY 12 MORE )

```

```

138 WRITE OUTPUT TAPE 6,138
FORMAT (80H THIS IS A ROAD LOAD DEBUGGING PRINTOUT TO CHEC
1K THROTTLE ANGLE CONVERGENCE )
EPS2=1.000
CHANGE=0.0
THETA=16.0

```

```

153 THSTEP=34.00
CONTINUE
CALL THROTL (THETA,THETAO,DT,DS,AFLOW )
AMV(6)=AFLOW
OPEN=THETA-THETAO
CALL STERL (CTHROT,XMINT,DELXT,ORDER,XNTHET,SCRACH,OPEN,CDT,
1 0.0 )
CALL AIRMAS (POHG,TOF,HUMID,THETA,CDT,AFLOW,FTYPE,TFUEL,
1 FRACT,GUESS,FAMAIN,FATOTL,VACMAN,DRYAIR,WETAIR,VENFLO )
GUESS=VACMAN

```

## DIGITAL SIMULATION OF AN AIR-BLED, BOOST VENTURI CARBURETOR

```

CALL SIGNAL (POHG,TOF,HUMID,VENFLO,FTYPE,TFUEL,RATEMF,
1      AMV,ABV,XMV1,XMV2,XBV,XMB,BBLS,FRACT,XGUESS,PRINTS,
2      XFV,BVFLO,PVFLO,BVMACH,PVMACH,BVSUCW,PVSUCW )
RATEMF=BBLS*FLOWM
XGUESS=XFV
CALL FLOW (POHG,TOF,HUMID,BVSUCW,VACMAN,OPENE,FTYPE,
1      TFUEL,NCHAN, FLOWM, FLOWT, FLOWE, FLOWJ, FLOWI,SUMAIR )
FAMAIN=BBLS*FLOWM/DRYAIR
FATOTL=BBLS*FLOWT/DRYAIR
CALL STERL (DIHP1,XMINR,DELXR,ORDER,XNIHP,SCRACH,FATOTL,
1      XIHP1,DEBUG )
CALL STERL (DIHP2,XMINR,DELXR,ORDER,XNIHP,SCRACH,FATOTL,
1      XIHP2,DEBUG )
109      IF (XIHP1) 109,127,127
127      XIHP1=000.0
128      IF (XIHP2) 128,129,129
128      XIHP2=00.10
129      CONTINUE
XIMEP1=5252.0*150.8*XIHP1/(RPM*DISPL)
XIMEP2=5252.0*150.8*XIHP2/(RPM*DISPL)
SLOPE=(XIHP2-XIHP1)/(AIRFL2-AIRFL1)
AO=AIRFL2 - XIHP2/SLOPE
PM = POHG - VACMAN
FMEP=FMIN+(FMAX-FMIN)*(POHG- PM)/(POHG-3.000)
TORQF=FMEP*DISPL/150.8
FHP=TORQF*RPM/5252.0
XIHP=BHP+FHP
AIRFLO=AO + XIHP/SLOPE
FUELR=FATOTL*AIRFLO
XISFC=FUELR/XIHP
BSFC=FUELR/BHP
IF (CHANGE ) 112,111,112
111      ERR1=DRYAIR-AIRFLO
IF (ABSF(ERR1)-EPS2) 113,113,125
125      THOLD=THETA
THETA=THETA-THSTEP*ABSF(ERR1)/ERR1
CHANGE=1.00
GO TO 110
112      ERR2=DRYAIR-AIRFLO
IF (ABSF(ERR2)-EPS2 ) 113,113,114
114      SAVE1=THETA
IF (ABSF(ERR2-ERR1)-0.005 ) 229,229,195
229      THETA=THETA - ERR2*0.10
GO TO 228
195      CONTINUE
THETA=THETA+ERR2*(THETA-THOLD)/(ERR1-ERR2)
228      IF (THETA-DUMTHD) 115,116,116
115      THETA=DUMTHD
GO TO 117
116      IF (THETA-90.00) 117,117,118
118      THETA=85.00
117      CONTINUE
THOLD=SAVE1
ERR1=ERR2
110      CONTINUE
IF (EPS2-1.000) 120,124,120
124      WRITE OUTPUT TAPE 6,106,NN,VMPH,RPM,THOLD,THETA,AIRFLO,DRY

```



## DIGITAL SIMULATION OF AN AIR-BLED, BOOST VENTURI CARBURETOR

```

1      ,WETAIR,ERR1,FATOTL,XIHP,BHP
106   FORMAT (I5,7F10.1,2F10.4,2F10.3)
      GO TO 120
113   WETA(L)=WETAIR
      PMAN(L)=POHG-VACMAN
      XMPG(L)=VMPH*SGFUEL*231.0*62.400/(1728.0*BSFC*BHP)
      SPEED(L)=VMPH
      CD(L)=CDJET
      RE(L)=REJET
      BOOSTW(L)=RVSUCW
      FLOWTP(L)=FLOWT
      FLOWMP(L)=FLOWM
      TOTLFA(L)=FATOTL
      DRYAP(L)=DRYAIR
      BSFCP(L)=BSFC
      BHPP(L)=BHP
      XIHPP(L)=XIHP
      SUMAIR=BBL S*SUMAIR
130   WRITE OUTPUT TAPE 6,131,VMPH,RPM,THETA,WETAIR,BHP,XIHP,
1      PMAN(L),SUMAIR,FATOTL,XISFC,BSFC,FUELR,XMPG(L),NN
131   FORMAT (2F 9.1,6F 9.2,3F10.4,F10.2,F9.3,I6 )
      IF (AFLOW-0.99*AWOT) 160,162,162
162   WRITE OUTPUT TAPE 6,161,VMPH
161   FORMAT (1H0, 5X,65H THE MAXIMUM VEHICLE SPEED HAS BEEN ATTAIN
1ED.....THIS SPEED IS ,F5.1,16H MILES PER HOUR //)
      GO TO 137
160   IF (RPM-3900.0) 119,119,137
119   IF (WETAIR-AMAX + 30.0) 134,134,137
137   CONTINUE
      IF (PTYPE-0.0) 92,92,93
93    CONTINUE
C    ALL PTYPE CHECKS WILL GO HERE
      PLOTI=L
      TYPEL=-1.0
      PLOTN=L
      IF (PTYPE-1.0) 351,350,351
350   DXCR=10.00/7.50
      DYCR=0.500/7.50
      CALL CALCVR ( RE,CD,PLOTN,0.0,DXCR,0.50,DYCR,1.0,SET,1.0,
1      1.0,1.0,TYPEL, 68.0,TFUEL,0.0 )
      SET=3.0
      GO TO 375
351   IF (PTYPE-2.0) 353,352,353
352   DXMH=25.00/7.50
      DYM=40.00/7.50
      CALL CALMVH (BOOSTW, FLOWMP, PLOTN,0.0,DXMH,0.0,DYM,1.0,SET,
1      1.0,1.0,1.0,+1.00, 68.00,TFUEL,1.0 )
      SET=3.0
      GO TO 375
353   IF (PTYPE-3.0) 355,354,355
354   XEXP=-1.0
      DXLL=3.00/7.50
      YEXP=-1.0
      DYLL=3.00/7.50
      DO 376 J=1,L,1
      IF (BOOSTW(J)-0.100) 378,377,377
378   BOOSTW(J)=0.100

```

## DIGITAL SIMULATION OF AN AIR-BLED, BOOST VENTURI CARBURETOR

```

377     IF (FLOWMP(J)-0.100) 379,376,376
379     FLOWMP(J)=0.100
376     CONTINUE
      CALL CALLOG (BOOSTW,FLOWMP,PLOTN,XEXP,DXLL,YEXP,DYLL,1.0,
1       SET,1.0,1.0,1.0,TYPEL, 68.00,TFUEL,1.0 )
      SET=3.0
      GO TO 375
355     IF (PTYPE-4.0) 357,356,357
356     DXCH=25.00/7.50
      DYCH=0.500/7.50
      CALL CALCVH (BOOSTW, CD ,PLOTN,0.0,DXCH,0.50,DYCH,1.0,SET,
1       1.0,1.0,1.0,TYPEL, 68.00,TFUEL,1.0 )
      SET=3.0
      GO TO 375
357     IF (PTYPE-5.0) 359,358,359
358     DXCM=25.00/7.50
      DYCM=0.500/7.50
      CALL CALCVM (FLOWTP, CD ,PLOTN,0.0,DXCM,0.50,DYCM,1.0,SET,
1       1.0,1.0,1.0,TYPEL, 68.00,TFUEL,0.0 )
      SET=3.0
      GO TO 375
359     IF (PTYPE-6.0) 361,360,361
360     DXFA=700.00/8.925
      DYFA=0.100/6.375
      CALL CALFVA (DRYAP,TOTLFA,PLOTN,0.0,DXFA,0.0300,DYFA,1.0,SE
1       1.0,2.0,2.0,+1.00,1.0,TFUEL,1.0 )
      SET=3.0
      GO TO 375
361     IF (PTYPE-7.0) 363,362,363
362     DXMS=100.00/6.375
      DYMS=28.00/8.925
      CALL CALMVS (SPEED,XMPG,PLOTN,0.0,DXMS,0.0,DYMS,1.0,SET,1.0
1       2.0,2.0,-1.0,1.0,TFUEL,1.0 )
      SET=3.0
      GO TO 375
363     IF (PTYPE-8.0) 365,364,365
364     DXBB=100.00/10.00
      DYBB=2.00/10.00
      DO 373 J=1,L,1
      IF (BSFCP(J)-2.500) 373,373,372
372     BSFCP(J)=2.500
373     CONTINUE
      CALL CALBVB (BHPP,BSFCP,PLOTN,0.0,DXBB,0.4,DYBB,1.0,SET,1.0
1       2.0,2.0,+1.00,1.0,TFUEL,1.0 )
      SET=3.0
      GO TO 375
365     IF (PTYPE-9.0) 367,366,367
366     DXIA=700.00/8.925
      DYIA=100.00/6.375
      CALL CALIVA (DRYAP,XIHPP,PLOTN,0.0,DXIA,0.0,DYIA,1.0,SET,
1       1.0,2.0,2.0,+1.00,1.0,TFUEL,1.0 )
      SET=3.0
      GO TO 375
367     IF (PTYPE-10.0) 369,368,369
368     DXIF=0.1400/8.925
      DYIF=100.00/6.375
      CALL CALIVF (TOTLFA,XIHPP,PLOTN,0.0,DXIF,0.0,DYIF,1.0,SET,

```

## DIGITAL SIMULATION OF AN AIR-BLED, BOOST VENTURI CARBURETOR

```

1      1.0,2.0,2.0,TYPE1,1.0,TFUEL,1.0 )
      SET=3.0
      GO TO 375
369   IF (PTYPE-11.0) 375,370,370
370   IF (RATIOT-1.0001) 140,140,92
140   CONTINUE
      WRITE OUTPUT TAPE 6,132
132   FORMAT (44H THE HIGH GEAR ROAD LOAD LINE WAS PLOTTED )
      CALL CALMAP (PMAN ,WETA ,PLOTI,00.0,DX,00.0,DY,POHG,SET,-1.0,
1      1.00,1.00, CR ,DISPL, TOF,SCALE )
      SET=3.0
375   CONTINUE
92    CONTINUE
      IF (RATIOT-1.0001) 136,136,135
135   NGEAR=NGEAR+1
      GO TO 133
136   CONTINUE
C
      IF (ATYPE-3.0) 240,96,240
240   IF (ATYPE-4.0) 95,99,95
95    IF (ATYPE-6.0) 62,99,62
96    SET=2.0
99    CONTINUE
C
C
C
C
C      CALCULATE CONSTANT THROTTLE LINES
C
      IF (PRINT1-0.0) 39,39,87
87    WRITE OUTPUT TAPE 6,22
      WRITE OUTPUT TAPE 6,2
      WRITE OUTPUT TAPE 6,3
      WRITE OUTPUT TAPE 6,4,POHG,CNAME(1),CNAME(2),CNAME(3),
1      CNAME(4),FNAME(1),FNAME(2),FNAME(3),FNAME(4),ENAME(1),
2      ENAME(2),ENAME(3),ENAME(4),VNAME(1),VNAME(2),VNAME(3),
3      TOF,ORNAM,TFUEL,DISPL,WEIGHT,PCH,DMVNOM(3),SGFUEL,
4      CR,RATIOT,AMDENS,DUMTHO,VISKM,AVALVE,TIREN
39    READ INPUT TAPE 7,23,THETA,THETAL,PRINTO
      IF (PRINTO)157,157,156
156   WRITE OUTPUT TAPE 6,47
      WRITE OUTPUT TAPE 6,147
147   FORMAT (1H4,16X,82H CARBURETOR-ENGINE OPERATION AT CONSTANT T
      HROTTLE OPENING-VARIABLE ENGINE SPEED //)
      WRITE OUTPUT TAPE 6,164
      WRITE OUTPUT TAPE 6,165
      WRITE OUTPUT TAPE 6,166
      WRITE OUTPUT TAPE 6,146
157   CONTINUE
47    FORMAT (1H //)
      SWITCH=0.0
      K=0
      PLOTN=0.0
      DEBUG=0.0
      PTHETA=1.0
      PLOTI=0.0
      RPM=000.0
      IF (THETA-25.0) 54,54,51

```

## DIGITAL SIMULATION OF AN AIR-BLED, BOOST VENTURI CARBURETOR

```

51      IF (THETA-64.0) 52,52,53
52      RPM=50.00
        GO TO 54
53      RPM=100.00
54      CONTINUE
        PMAN(1) = POHG
        WETA(1)=0.000
        VACMAN=0.10
        GUESS=VACMAN
        XGUESS=0.65
        C8=0.400*1.25*1545.4*585.0*(CR-1.0)/(28.95*CR*0.4912)
        C9=(CR-0.5)/CR
        DRYA2=DISPL*RPM*(POHG*C9-VACMAN)/(C8*1.0620)
        CALL ASSUME (DRYA2,VACMAN,OPENE,FAMAIN,FATOTL,FARICH,
1         FLOWM,FLOWT,FLOWE )
        RATEMF=2.0*FLOWM
C      NOW INITIAL GUESSES HAVE BEEN MADE FOR EACH NEEDED PARAMETER
        OLDA1=FATOTL
        OLDA2=FAMAIN
        OLDAIR=DRYA2
        DO 33 I=2,28,1
34      IF (RPM-199.0) 34,34,35
48      IF (THETA-15.0) 48,48,49
48      RPM=RPM + 25.00
        GO TO 38
49      RPM=RPM + 50.00
        GO TO 38
35      IF (RPM-999.0) 36,36,37
36      RPM=RPM+100.0
        GO TO 38
37      RPM=RPM+250.0
38      CONTINUE
        CALL THROTL (THETA,THETA0,DT,DS,AFLOW )
        AMV(6)=AFLOW
        OPEN=THETA-THETA0
        CALL STERL (CTHROT,XMINT,DELXT,ORDER,XNTHET,SCRACH,OPEN,CDT,
1         0.0 )
        J=0
320     CONTINUE
        IF (J-15) 323,324,324
324     WRITE OUTPUT TAPE 6,325
325     FORMAT (46H NO FUEL-AIR CONVERGENCE WITHIN MAIN PROGRAM
        GO TO 331
323     J=J+1
        CALL AIRMAS (POHG,TOF,HUMID,THETA,CDT,AFLOW,FTYPE,TFUEL,
1         FRACT,GUESS,FAMAIN,FATOTL,VACMAN,DRYAIR,WETAIR,VENFLO )
        GUESS=VACMAN
        CALL SIGNAL (POHG,TOF,HUMID,VENFLO,FTYPE,TFUEL,RATEMF,
1         AMV,ABV,XMV1,XMV2,XBV,XMB,BBLS,FRACT,XGUESS,PRINTS,
2         XFV,BVFLO,PVFLO,BVMACH,PVMACH,BVSUCW,PVSUCW )
        RATEMF=BBLS*FLOWM
        XGUESS=XFV
        CALL FLOW (POHG,TOF,HUMID,BVSUCW,VACMAN,OPENE,FTYPE,
1         TFUEL,NCHAN, FLOWM, FLOWT, FLOWE, FLOWJ, FLOWI,SUMAIR )
        FAMAIN=BBLS*FLOWM/DRYAIR
        FATOTL=BBLS*FLOWT/DRYAIR
        DELFA1=FATOTL-OLDA1

```

## DIGITAL SIMULATION OF AN AIR-BLED, BOOST VENTURI CARBURETOR

```

DELFA2=FAMAIN-OL DFA2
DELAIR=DRYAIR-OLDAIR
OL DFA1=FATOTL
OL DFA2=FAMAIN
OLDAIR=DRYAIR

```

```

321 IF (ABSF(DELFA1)-0.00060) 321,321,320

```

```

322 IF (ABSF(DELFA2)-0.00060) 322,322,320

```

```

331 IF (ABSF(DELAIR)-0.750 ) 331,331,320

```

```

CONTINUE

```

```

PRESS=POHG-VACMAN

```

```

PMAN(I)= PRESS

```

```

WETA(I)=WETAIR

```

```

CD(I)=CDJET

```

```

RE(I)=REJET

```

```

BOOSTW(I)=BVSUCW

```

```

FLOWTP(I)=FLOWT

```

```

FLOWMP(I)=FLOWM

```

```

TOTLFA(I)=FATOTL

```

```

DRYAP (I)=DRYAIR

```

```

DUMFT=BRLS*FLOWT

```

```

DUMFM=BRLS*FLOWM

```

```

SUMAIR=BRLS*SUMAIR

```

```

DUMPR=PRINTO

```

```

IF (RPM-490.0) 103,103,102

```

```

103 PRINTO=0.0

```

```

102 IF (RPM-5010.0) 100,100,101

```

```

101 PRINTO=0.0

```

```

100 CONTINUE

```

```

IF (PRINTO) 347,347,348

```

```

348 WRITE OUTPUT TAPE 6,256,RPM,THETA,AFLOW,PRESS,WETAIR,DRYAIR,
1 BVSUCW,PVSUCW,XMACHT,FAMAIN,FATOTL,DUMFT,DUMFM,TOTF,SUMAIR,J

```

```

347 CONTINUE

```

```

PRINTO=DUMPR

```

```

IF (SWITCH-0.0) 60,60,33

```

```

60 CONTINUE

```

```

IF (WETAIR- AMAX) 33,33,57

```

```

57 K=I

```

```

PLOTI=I

```

```

SWITCH=1.00

```

```

33 CONTINUE

```

```

C

```

```

C

```

```

C

```

```

PLOT A CONSTANT THROTTLE ANGLE LINE

```

```

IF (PTYPE-0.0) 75,75,94

```

```

94 CONTINUE

```

```

C ALL PTYPE CHECKS WILL GO HERE

```

```

44 IF (THETAL-THETA) 42,42,41

```

```

42 SET=1.0

```

```

41 CONTINUE

```

```

XSTART= 1.0 + (PMAN(1) - 00.00)/DX

```

```

YSTART= 1.0 + (WETA(1) - 0.00)/DY

```

```

CALL PENUP (XSTART,YSTART)

```

```

IF (K-0) 58,58,59

```

```

58 K=I

```

```

PLOTI=I

```

```

59 IF (WETA(K) - AMAX -3.000) 82,82,83

```

```

83 PMAN(K)=PMAN(K)-(WETA(K)-AMAX)*((PMAN(K)-PMAN(K-1)) /

```

## DIGITAL SIMULATION OF AN AIR-BLED, BOOST VENTURI CARBURETOR

```
1      (WETA(K)-WETA(K-1))
      WETA(K)=AMAX
82     CONTINUE
      CALL CALMAP (PMAN,WETA,PLOTI,00.0,DX,00.0,DY,POHG,SET,PCH
1      1.00,1.00, CR ,DISPL, TOF ,SCALE )
      SET=3.0
      ALIMIT=0.900*AMAX
      IF (WETA(K) - ALIMIT) 74,74,75
74     XVAL=PMAN(K)/DX - 0.480 + 1.000
      YVAL=WETA(K)/DY - 0.040 + 1.000
      CALL PFNMBR (XVAL,YVAL,-0.100,THETA,0.000,6H(F4.1))
75     CONTINUE
      IF (THETA1-THETA) 62,62,39
62     CONTINUE
      GO TO 20
      END
```

APPENDIX J  
LISTING OF SUBROUTINES

SUBROUTINES:

THROTL

ASSUME

FLOW

AIRMAS

SIGNAL

SOLVE

XMIX

STERL

FPROP

PLOTTING ROUTINE 1

PLOTTING ROUTINE 2

PLOTTING ROUTINE 3

\$

## COMPILE FASTRAN, PUNCH OBJECT

PAGE 1

SUBROUTINE THROTL (THETA, THETAO, DT, DS, AFLOW )

```

C
C   THIS SUBROUTINE CALCULATES THE FLOW AREA AT THE THROTTLE
C   RESTRICTION FOR ANY VALUE OF THETA, THETO, THROTTLE BORE DIAMETER
C   AND THROTTLE SHAFT DIAMETER.
C
C
201  IF (THETA-THETAO) 200,201,201
212  THETA= 180.0 - THETA
202  CONTINUE
      RTHETA=3.1415926*THETA/180.0
      RTHETO=3.1415926*THETAO/180.0
      DUM1=COS(RTHETA)
      DUM2=DUM1*DUM1
      DUM3=COS(RTHETO)
      DUM4=DUM3*DUM3
      DUM5=DS*DUM3/(DT*DUM1)
      DUM6=DUM1/DUM3
      DUM7=DS/DT
203  IF (DT-DS) 200,203,203
      DUM8=DUM7*DUM3
      ANG1= ARCSIN (DUM7)
      DUM9=DT*DT-DS*DS
      ASHAFT=0.5*SQRT(DUM9)*DS + 0.5*DT*DT*ANG1
204  IF (DUM1-DUM8) 204,205,205
      CONTINUE
      ASTAR=0.785398*DT*DT*DUM6
      AFLOW=0.785398*DT*DT - ASHAFT
      GO TO 209
205  ANG=ARCSIN(DUM5)
      ASTAR=DS*SQRT(DT*DT*DUM2-DS*DS*DUM4)*0.50/DUM1 + ANG*DT*DT*DUM1*
1      0.50/DUM3
      AFLOW=0.785398*DT*DT*(1.0-DUM6)+ASTAR-ASHAFT
      GO TO 209
200  CONTINUE
210  WRITE OUTPUT TAPE 6,206
206  FORMAT (47H THETA NOT WITHIN LIMITS OR DS GREATER THAN DT )
      THETA=THETAO
      GO TO 202
209  CONTINUE
208  RETURN
      END

```



\$ COMPILÉ FASTRAN,PUNCH OBJECT

1

1 SUBROUTINE ASSUMF (DRYA2,VACMAN,OPENE,FAMAIN,FATOTL,FARICH,  
FLOWM, FLOWT, FLOWE )

C  
C  
C  
C  
C

THESE ARE APPROXIMATE TYPICAL VALUES FOR THE FUEL-AIR RATIOS  
DELIVERED BY THE MAIN AND IDLE SYSTEMS. THIS IS USED ONLY TO  
GENERATE INITIAL GUESSES FOR THE FUEL FLOW RATES IN EACH SYSTEM

FARICH=0.0000

IF (DRYA2-50.00) 51,51,52

51 FAIDLE=0.1100

FAMAIN=0.0000

GO TO 60

52 IF (DRYA2- 75.0) 53,53,54

53 FAIDLE=0.1100-0.1100\*(DRYA2-50.00)/125.0

FAMAIN=0.0000

GO TO 60

54 IF (DRYA2-175.0) 55,55,56

55 FAIDLE=0.1100-0.1100\*(DRYA2-50.00)/125.0

FAMAIN=0.0610\*(DRYA2-75.00)/100.00

GO TO 60

56 FAIDLE=0.0000

FAMAIN=0.0610

60 IF (VACMAN-OPENE) 57,57,58

57 FAIDLE=FAIDLE\*VACMAN/(12.00-VACMAN)

DUM8=FAMAIN

FAMAIN=FAMAIN\*(20.00+OPENE-VACMAN)/20.00

FARICH=FAMAIN-DUM8

GO TO 61

58 IF (VACMAN-12.00) 61,59,59

59 FAIDLE=FAIDLE + 0.0420\*(VACMAN-12.00)/(44.00-VACMAN)

62 FAMAIN=FAMAIN\*37.0/(VACMAN+25.00)

61 FATOTL=FAMAIN + FAIDLE

C THESE ARE THE SYSTEM FLOW RATES PER BARREL

C

FLOWM=0.5\*FAMAIN\*DRYA2

FLOWT=0.5\*FATOTL\*DRYA2

FLOWE=0.5\*FARICH\*DRYA2

C

C END OF FUEL-AIR RATIO APPROXIMATION FOR INITIALIZATION PURPOSES

C

RETURN

END

PAGE 1

```

SUBROUTINE FLOW (POHG,TOF,HUMID,BVSUCW,VACMAN,OPENE,FTYPE,
1   TFUEL,NCHAN,XFLOWM,XFLOWT,XFLOWE,XFLOWJ,XFLOWI,SUMAIR )
C   THIS SUBROUTINE CALLS ON FPROP AND STERL
DIMENSION CD1(21),CD2(21),CD3(21),CD4(21),CD5(21),CD6(21)
DIMENSION CD7(21),CD8(21),CD9(21),ACHAN(25),XLD(25),CTYPE(25)
DIMENSION D(25),DUMR(25),DELPTW(25),DUMLD(10),S( 45),VEL(25)
DIMENSION ANGLC(25),SKIP(25),DN(25),CBLEED(5)
DIMENSION RE(25),VHEADW(25)
COMMON ORDER,PRINTF,REJET,CDJET,DELXJ,DELXJL,DELXSE,XNCDJ,
1   XNCDJL,XNCDSE,URNS,SPILL1,RPM,DISPL,CR,DBLEED,DTRANS,
2   DCHOK,PRINTA,XMACHT,TOTF,ACHAN,XLD,CTYPE,ANGLC,CD1,CD2,
3   CD3,CD4,CD5,CD6,CD7,CD8,CD9,S
SAVE3=XLD( 3)
SAVE4=XLD(20)
SAVE5=ACHAN( 3)
SAVE6=ACHAN(20)
SAVEI1=0.000
SAVEI2=0.000
CALL FPROP (FTYPE,TFUEL,TFUEL,SGFUEL,VISKM,CORR,CLIQ,CPFUEL,
1   CVFUEL,WFUEL,HVAPOR,GAMMA,HEATV )
GAMMA=0.000001
DENSF=SGFUEL*62.34
TOR=TOF + 459.6
AMDENS=POHG*0.4912*144.0/(53.34*TOR)
VISKE=VISKM/92903.0
VISAG=VISKE*DENSF
VISAE=VISAG/32.174
AVISKM=12.0774 + 4.6452*TOF/100.0
AVISKE=AVISKM/92903.0
DPEJET=0.0
SETUP=1.0
VACW=13.594*VACMAN
VACM=VACMAN
IF (VACM) 46,46,47
46   VACM=+0.010
VACW=13.594*VACM
47   CONTINUE
DX=DELXSE
XN=XNCDSE
ARICH=ACHAN(3)
D(20)=SQRT(ACHAN(20)/0.7854)
AIDLE=ACHAN(20)-0.7854*((D(20)-0.4430*0.0312*URNS)**2)
IF (AIDLE-0.0000001) 48,49,49
48   AIDLE=0.0000001
SETUP=0.0
49   IF (AIDLE-ACHAN(20)) 89,89,88
88   AIDLE=ACHAN(20)
89   CONTINUE

```

2

```

ITERI=0
ITERE=0
ITERJ=0
EDUM=1.0
XMDUM=1.0
DUMMYP=PRINTF
DUMLD(3)=0.100
DUMLD(4)=0.616
DUMLD(5)= 1.420
DUMLD(6)= 3.630
DUMLD(7)= 4.730
DUMLD(8)= 7.230
DUMLD(9)= 10.56
DUMLD(10)=10.56
CBLEED(1)=0.600
CBLEED(2)=0.600
CBLEED(3)=0.600
CBLEED(4)=0.600
CBLEED(5)=0.600
FLOWT=XFLOWT
FLOWM=XFLOWM
FLOWE=XFLOWE
FLOWJ=FLOWT-FLOWE
FLOWI=FLOWT-FLOWM
DO 9 I=1,NCHAN,1
SKIP(I)=0.0
IF (ACHAN(I)-0.0000002) 112,111,111
112 ACHAN(I)=0.0000002
SKIP(I)=1.0
111 CONTINUE
DELPTW(I)=0.0
VEL(I)=0.0
VHEADW(I)=0.0
DN(I)=DENSF
9 D(I)=SQRT(ACHAN(I)/0.785398)
DN(21)=AMDENS
DN(22)=AMDENS
DN(23)=AMDENS
DN(24)=AMDENS
DN(25)=AMDENS

```

C

```

C NOW CALCULATE THE ENRICHMENT VALVE OPENING
IF (VACM-OPENE) 6,5,5
5 ARICH=0.0000001
FLOWE=0.0
DO 74 I=3,7,1
74 SKIP(I)=1.0
FLOWJ=FLOWT
EDUM=0.0
GO TO 8
6 IF (FLOWE) 100,100,101
100 FLOWE=1.00
FLOWT=FLOWT+1.0
FLOWM=FLOWT
FLOWI=0.0
101 IF (VACM-OPENE/3.000 ) 43,43,7
7 ARICH=ARICH*(OPENE-VACM)*(OPENE-VACM)/(0.4444*OPENE*OPENE)

```

PAGE 3

```

AIDLE=0.0000001
SETUP=0.0
BVSMIN=SPILL1*SGFUEL+GAMMA/D(13)
IF (BVSUCW-BVSMIN) 81,81,8
43 AIDLE=0.0000001
SETUP=0.0
BVSMIN=SPILL1*SGFUEL+GAMMA/D(13)
IF (BVSUCW-BVSMIN) 81,81,8
8 CONTINUE
D( 3)=SQRT(ARICH/0.785398)
D(20)=SQRT(AIDLE/0.785398)
XLD( 3)=XLD( 3)*SQRT(ACHAN( 3)/0.7854)/D( 3)
XLD(20)=XLD(20)*SQRT(ACHAN(20)/0.7854)/D(20)
ACHAN( 3)=ARICH
ACHAN(20)=AIDLE
IF (SETUP) 91,91,90
90 FLOWM=0.0
DO 72 I=10,13,1
72 SKIP(I)=1.0
SKIP(21)=1.0
SKIP(22)=1.0
SKIP(23)=1.0
FLOWI=FLOWT
XMDUM=0.0
CBLEED(1)=0.000001
CBLEED(2)=0.000001
CBLEED(3)=0.000001
91 IF ( AIDLE -0.000002 ) 127,127,128
127 FLOWI=0.0
DO 71 I=14,20,1
71 SKIP(I)=1.0
SKIP(24)=1.0
SKIP(25)=1.0
CBLEED(4)=0.000001
CBLEED(5)=0.000001
IF (XMDUM) 81,81,82
81 AIRM1=0.0
AIRM2=0.0
AIRI1=0.0
AIRI2=0.0
FLOWM=0.0
FLOWT=0.0
FLOWE=0.0
FLOWJ=0.0
RE(1)=0.0
CDJ=0.0
DELPTW(1)=0.0
SETUP=0.0
VHEADW(1)=0.0
ITER=0
GO TO 149
82 CONTINUE
FLOWM=FLOWT
XIDUM=0.0
128 C8=3600.0*SQRT((14.696*2.0*32.174/(406.62*144.0))
AIRM1=C8*ACHAN(21)*CBLEED(1)*SQRT(AMDENS*BVSUCW*0.68)
AIRM2=C8*ACHAN(23)*CBLEED(3)*SQRT(AMDENS*BVSUCW*0.90)

```

4

```

AIRI1=C8*ACHAN(24)*CBLEED(4)*SQRT(AMDENS*VACW*0.060 )
AIRI2=C8*ACHAN(25)*CBLEED(5)*SQRT(AMDENS*VACW*0.250 )
IF (SAVEI2) 179,179,178

```

178

```

AIRI1=SAVEI1
AIRI2=SAVEI2

```

179

```

SUMAIR=AIRM1+AIRM2

```

C

C

```

NOW LOGICAL GUESSES HAVE BEEN MADE FOR THE FUEL AND AIR BLEED
FLOW RATES IN EACH SYSTEM

```

C

C

```

FLOWJ=FLOWT-FLOWE
FLOWI=FLOWT-FLOWM

```

C

C

C

C

C

C

C

C

C

C

C

```

DUMR(I) IS THE FUEL FLOW RATE THRU FUEL CHANNEL ELEMENT I
FLOWJ IS THE FUEL FLOW RATE THRU THE MAIN METERING ORIFICE
FLOWE IS THE FUEL FLOW RATE THRU THE MAIN ENRICHMENT VALVE ORIFICE
FLOWI IS THE FUEL FLOW RATE THRU THE MAIN IDLE CHANNEL
FLOWM IS THE FUEL FLOW RATE THRU THE MAIN MAIN DELIVERY CHANNEL
FLOWT IS THE TOTAL FUEL FLOW RATE PER CARBURETOR BARREL
AIRM1 IS THE AIR BLEED FLOW RATE THRU THE FIRST MAIN AIR BLEED
AIRM2 IS THE AIR BLEED FLOW RATE THRU THE SECOND MAIN AIR BLEED
AIRI1 IS THE AIR BLEED FLOW RATE THRU THE FIRST IDLE AIR BLEED
AIRI2 IS THE AIR BLEED FLOW RATE THRU THE SECOND IDLE AIR BLEED

```

```

XISW=0.0

```

```

DUMDP=0.0

```

```

C1=128.0*1728.0*406.62/(3.14159*3600.0*2116.62 )

```

```

C2=8.0*144.0*406.62/(3.14159*3.14159*3600.0*3600.0*14.696)

```

```

C3=406.62/(2116.6*2.0*32.174)

```

```

C4=406.62*144.0/(3600.0*3600.0*14.696*2.0*32.174)

```

118

```

CONTINUE

```

```

XJSW=0.0

```

```

ITERJ=0

```

120

```

DUMR(1)=FLOWJ

```

```

DUMR(2)=FLOWJ

```

```

ESW=0.0

```

```

ITERE=0

```

```

DUMR(8)=FLOWT

```

```

DUMR(9)=FLOWT

```

```

DUMR(10)=FLOWM

```

```

DUMR(11)=FLOWM+AIRM1

```

```

DUMR(12)=FLOWM+AIRM1+AIRM2

```

```

DUMR(13)=FLOWM+AIRM1+AIRM2

```

```

DO 11 K=14,16,1

```

11

```

DUMR(K)=FLOWI

```

```

DUMR(17)=FLOWI+AIRI1

```

```

DUMR(18)=FLOWI+AIRI1

```

```

DUMR(19)=FLOWI+AIRI1+AIRI2

```

```

DUMR(20)=FLOWI+AIRI1+AIRI2

```

```

DUMR(21)=AIRM1

```

```

DUMR(22)=AIRM1

```

```

DUMR(23)=AIRM2

```

```

DUMR(24)=AIRI1

```

```

DUMR(25)=AIRI2

```

```

SUMAIR=AIRM1+AIRM2

```

```

AIDENS=(POHG-VACMAN*0.500)*0.4912*144.0/(53.34*(TFUEL+459.6))

```

```

IF (SKIP(13)) 103,103,104

```

103

```

DN(11)=(AIRM1+FLOWM)/(AIRM1/AMDENS+FLOWM/DENSF)

```

```

DN(12)=(SUMAIR+FLOWM)/(SUMAIR/AMDENS+FLOWM/DENSF)
DN(13)=DN(12)
104 IF (SKIP(20)) 105,105,106
105 DN(17)=(AIRI1+FLOWI)/(AIRI1/AIDENS+FLOWI/DENSF)
DN(18)=DN(17)
DN(19)=(AIRI1+AIRI2+FLOWI)/((AIRI1+AIRI2)/AIDENS+FLOWI/DFENS)
DN(20)=DN(19)
106 CONTINUE
55 DO 10 K=3,6,1
10 DUMR(K)=FLOWE*2.0
DUMR(7)=FLOWE
DO 51 I=1,NCHAN,1
IF (SKIP(I)) 76,76,51
76 CONTINUE
VEL(I)=144.0*DUMR(I)/(DN(I)*3600.0*ACHAN(I))
RE(I)=VEL(I)*D(I)/(12.0*VISKE)
VHEADW(I)=406.62*DN(I)*VEL(I)*VEL(I)/(2116.6*2.0*32.174)
IF (I-20) 107,107,108
108 RE(I)=VEL(I)*D(I)/(12.0*AVISKE)
107 CONTINUE
IF (RE(I)) 99,102,102
99 WRITE OUTPUT TAPE 6,180,I,DUMR(I),VEL(I),RE(I)
180 FORMAT (33H NEGATIVE REYNOLDS NUMBER IN FLOW ,I10,3F10.3 )
DUMR(I)=0.001
VEL(I) =0.001
RE(I)=10.00
102 IF (CTYPE(I)-1.0) 12,13,14
C THIS CHANNEL ELEMENT IS A SIMPLE PASSAGE
C
C CALCULATE THE SUDDEN EXPANSION OR CONTRACTION LOSS
C
12 IF (I-14) 25,26,25
26 CC=0.62 + 0.38*(ACHAN(14)/ACHAN(9))**3
F1=((1.0/CC - 1.0)*(VEL(14)/VEL(13)))**2
GO TO 21
25 IF (I-8) 171,170,171
170 F1=((1.0-ACHAN(7)/ACHAN(8))*(FLOWE/FLOWT))**2
GO TO 21
171 IF (ACHAN(I)-ACHAN(I-1)) 19,20,18
18 F1=(1.0-ACHAN(I-1)/ACHAN(I))**2
GO TO 21
19 CC=0.62 + 0.38*(ACHAN(I)/ACHAN(I-1))**3
F1=((1.0/CC-1.0)*(ACHAN(I-1)/ACHAN(I)))**2
GO TO 21
20 F1=0.0
C NOW CALCULATE THE BEND LOSS
C
21 ANG=ANGLC(I)*3.14159/180.0
F2=0.900-0.900*COS(ANG)
FACTOR=F1 + F2
DPENTR=C3*DN(I)*VEL(I-1)*VEL(I-1)*FACTOR
IF (I-2) 168,167,168
167 DPEJET=DPENTR
168 CONTINUE
IF (RE(I) - 2100.0 ) 15,15,16
15 FDARCY=64.0/RE(I)
DPW=FDARCY*XLD(I)*VHEADW(I)

```

6

```

GO TO 17
16 FDARCY=0.3164/(RE(I)**0.250)
DPW=FDARCY*XLD(I)*VHEADW(I)
17 DELPTW(I)=DPENTR + DPW
GO TO 50

```

C THIS CHANNEL ELEMENT IS A MAIN METERING ORIFICE

```

13 DEBUG=0.0
IF (RE(I)-10000.0) 86,85,85
85 RE(I)=10000.0
GO TO 23
86 CONTINUE
IF (RE(I) - 2000.0) 22,22,23
22 CALL STERL (CD2,0.0,DELXJL,ORDER,XNCDJL,S,RE(I),CDJ ,DEBUG)
GO TO 24
23 CALL STERL (CD1,0.0,DELXJ,ORDER,XNCDJ,S,RE(I),CDJ ,DEBUG)
24 CONTINUE
CDUM=1.0-CDJ*CDJ
ADUM=1.0
IF (CDJ-0.005) 119,119,155
119 DELPTW(I)=0.0
GO TO 50
155 DELPTW(I)=C4*DUMR(I)*DUMR(I)*ADUM*CDUM/(DENSF*ACHAN(I)*
1 ACHAN(I)*CDJ*CDJ )
GO TO 50

```

C

C

THIS CHANNEL ELEMENT IS A SQUARE EDGED ORIFICE

C

```

14 IF (RE(I)-10000.0) 84,84,83
83 REDUM=10000.0
GO TO 92
84 REDUM=RE(I)
92 DO 27 J=3,10,1
IF (XLD(I)-DUMLD(J)) 28,28,27
27 CONTINUE
28 DEBUG=0.0
IF (J-4) 29,30,31
29 CALL STERL (CD3,0.0,DX,ORDER,XN,S,REDUM,CDSE ,DEBUG)
GO TO 41
30 CALL STERL (CD3,0.0,DX,ORDER,XN,S,REDUM,CDSE1,DEBUG)
CALL STERL (CD4,0.0,DX,ORDER,XN,S,REDUM,CDSE2,DEBUG)
GO TO 40
31 IF (J-6 ) 32,33,34
32 CALL STERL (CD4,0.0,DX,ORDER,XN,S,REDUM,CDSE1,DEBUG)
CALL STERL (CD5,0.0,DX,ORDER,XN,S,REDUM,CDSE2,DEBUG)
GO TO 40
33 CALL STERL (CD5,0.0,DX,ORDER,XN,S,REDUM,CDSE1,DEBUG)
CALL STERL (CD6,0.0,DX,ORDER,XN,S,REDUM,CDSE2,DEBUG)
GO TO 40
34 IF (J-8 ) 35,36,37
35 CALL STERL (CD6,0.0,DX,ORDER,XN,S,REDUM,CDSE1,DEBUG)
CALL STERL (CD7,0.0,DX,ORDER,XN,S,REDUM,CDSE2,DEBUG)
GO TO 40
36 CALL STERL (CD7,0.0,DX,ORDER,XN,S,REDUM,CDSE1,DEBUG)
CALL STERL (CD8,0.0,DX,ORDER,XN,S,REDUM,CDSE2,DEBUG)
GO TO 40
37 IF (J-10) 38,39,39
38 CALL STERL (CD8,0.0,DX,ORDER,XN,S,REDUM,CDSE1,DEBUG)

```

PAGE 7

```

CALL STERL (CD9,0.0,DX,ORDER,XN,S,REDUM,CDSE2,DEBUG)
GO TO 40
39 CALL STERL (CD9,0.0,DX,ORDER,XN,S,REDUM,CDSE ,DEBUG)
GO TO 41
40 CONTINUE
X=DUMLD(J)-DUMLD(J-1)
Y=CDSE2-CDSE1
CDSE=CDSE1+(XLD(I)-DUMLD(J-1))*Y/X
41 CDUM=1.0-CDSE*CDSE
IF (I-20) 110,110,109
109 L=I-20
CBLEED(L)=CDSE
GO TO 50
110 CONTINUE
IF (ACHAN(I-1)-ACHAN(I)) 44,45,45
44 CC=0.62 + 0.38*(ACHAN(I)/ACHAN(I-1))**3
FACTOR=((1.0/CC-1.0)*(ACHAN(I-1)/ACHAN(I)))**2
DELPTW(I)=C3*DN(I)*VEL(I-1)*VEL(I-1)*FACTOR
GO TO 50
45 CONTINUE
ADUM=1.0-(ACHAN(I)/ACHAN(I-1))**2
DELPTW(I)=C4*DUMR(I)*DUMR(I)*ADUM*CDUM/(DN(I)*ACHAN(I)*
1 ACHAN(I)*CDSE*CDSE )
C
C NOW THE PRESSURE DROP ACROSS THIS PARTICULAR ORIFICE IS KNOWN
C
50 CONTINUE
C
IF (VACM -OPENE) 58,61,61
58 IF (I-7) 61,80,61
80 DUMV2=144.0*DUMR(2)/(DENSF*3600.0*ACHAN(2))
DUMVH2=406.62*DENSF*DUMV2*DUMV2/(2116.6*2.0*32.174)
SUMDPJ=DELPTW(1) + DELPTW(2) +DUMVH2
IF (ESW) 52,52,53
52 SUMDPE=DELPTW(3)+DELPTW(4)+DELPTW(5)+DELPTW(6)+DELPTW(7)+
1 VHEADW(7)
ERRE1=SUMDPE-SUMDPJ
ITERE=1
EPSE=0.015
IF (ABSF(ERRE1)-0.100 ) 42,42,54
54 CONTINUE
OLDFE=FLOWE
FLOWE=FLOWE-0.100*ABSF(ERRE1)/ERRE1
IF (FLOWE) 181,182,182
181 FLOWE=0.0005
182 FLOWJ=FLOWT - FLOWE
DUMR(1)=FLOWJ
DUMR(2)=FLOWJ
ESW=1.0
GO TO 55
53 ITERE=ITERE+1
IF (ITERE-10) 116,115,116
115 EPSE=0.160
116 IF (ITERE-16) 122,122,60
122 CONTINUE
SUMDPE=DELPTW(3)+DELPTW(4)+DELPTW(5)+DELPTW(6)+DELPTW(7)+
1 VHEADW(7)

```



8

```

ERRE2=SUMDPE-SUMDPJ
IF ( ABSF(ERRE2)-EPSE ) 42,42,56

```

56

```

SAVE=FLOWE
FLOWE=FLOWE+ERRE2*(FLOWE-OLDFE)/(ERRE1-ERRE2)
IF ( FLOWE ) 59,57,57

```

59

```
FLOWE=0.0005
```

57

```

OLDFE=SAVE
ERRE1=ERRE2
FLOWJ=FLOWT - FLOWE
DUMR(1)=FLOWJ
DUMR(2)=FLOWJ

```

```
GO TO 55
```

42

```
CONTINUE
```

50

```

FLOWJ=FLOWT - FLOWE
DUMR(1)=FLOWJ
DUMR(2)=FLOWJ

```

51

```
CONTINUE
```

52

```
IF ( I-13 ) 75,62,75
```

53

```

IF ( XJSW ) 63,63,64
SUMDPM=DELPTW(1)+DELPTW(2)+SPILL1*SGFUEL+VHEADW(13)+
0.1*GAMMA/D(13)

```

1

```
DO 65 L=8,13,1
```

55

```
SUMDPM=SUMDPM+DELPTW(L)
```

```
ERRJ1=SUMDPM-BVSUCW
```

```
ITERJ=1
```

```
EPSJ=0.0150
```

56

```
IF ( ABSF(ERRJ1)-0.1000 ) 164,164,66
```

```
CONTINUE
```

```
OLDFJ=FLOWJ
```

```
FLOWJ=FLOWJ-0.250*ABSF(ERRJ1)/ERRJ1
```

```
IF ( FLOWJ ) 175,176,176
```

75

```
FLOWJ=0.100
```

76

```
CONTINUE
```

```
FLOWE=FLOWE*FLOWJ/OLDFJ
```

```
XJSW=1.0
```

```
FLOWT=FLOWJ+FLOWE
```

```
FLOWM=FLOWT-FLOWI
```

```
IF ( FLOWM ) 87,87,120
```

4

```
ITERJ=ITERJ+1
```

```
IF ( ITERJ-10 ) 117,121,117
```

21

```
EPSJ=0.160
```

17

```
IF ( ITERJ-16 ) 124,124,125
```

25

```
WRITE OUTPUT TAPE 6,126
```

26

```
FORMAT (34H NO MAIN CONVERGENCE WITHIN FLOW )
```

```
GO TO 73
```

24

```
CONTINUE
```

```
SUMDPM=DELPTW(1)+DELPTW(2)+SPILL1*SGFUEL+VHEADW(13)+
```

1

```
0.1*GAMMA/D(13)
```

```
DO 67 L=8,13,1
```

7

```
SUMDPM=SUMDPM+DELPTW(L)
```

```
ERRJ2=SUMDPM-BVSUCW
```

```
IF ( ABSF(ERRJ2)-EPSJ ) 164,164,68
```

8

```
SAVE=FLOWJ
```

```
FLOWJ=FLOWJ+ERRJ2*(FLOWJ-OLDFJ)/(ERRJ1-ERRJ2)
```

```
IF ( FLOWJ ) 69,70,70
```

9

```
FLOWJ=+0.100
```

0

```
OLDFJ=SAVE
```

```

FLOWE=FLOWE*FLOWJ/OLDFJ
ERRJ1=ERRJ2
FLOWT=FLOWJ+FLOWE
FLOWM=FLOWT-FLOWI
IF (FLOWM) 87,87,120
87    FLOWM=0.0
      AIRM1=0.0
      AIRM2=0.0
      FLOWI=FLOWT
      GO TO 120
164   OLDAM1=AIRM1
      OLDAM2=AIRM2
      DELPMB=DELPTW(1)+DELPTW(2)+DELPTW(8)+DELPTW(9)+DELPTW(10)+
1     VHEADW(10)
      DELPTW(23)=DELPTW(1)+DELPTW(2)+DELPTW(8)+DELPTW(9)+DELPTW(10)+
1     DELPTW(11)+VHEADW(12)
      AIRM2=C8*ACHAN(23)*CBLEED(3)*SQRT(AMDENS*DELPTW(23))
C
IF (SKIP(21)) 113,113,114
113   DUM21=1.0/(ACHAN(21)*ACHAN(21)*CBLEED(1)*CBLEED(1))
      DUM22=1.0/(ACHAN(22)*ACHAN(22)*CBLEED(2)*CBLEED(2))
      AIRM1=C8*SQRT(AMDENS*DELPMB)/SQRT(DUM21+DUM22)
      DELPTW(21)=DELPMB/(1.0+ACHAN(21)*ACHAN(21)*CBLEED(1)*
1     CBLEED(1)/(ACHAN(22)*ACHAN(22)*CBLEED(2)*CBLEED(2)))
      DELPTW(22)=DELPMB-DELPTW(21)
114   IF (ABSF(AIRM1-OLDAM1)-0.005) 165,165,118
165   IF (ABSF(AIRM2-OLDAM2)-0.005) 73,73,118
73    FLOWT=FLOWJ+FLOWE
      FLOWM=FLOWT-FLOWI
75    CONTINUE
      IF (AIDLE-0.000002) 130,129,129
129   IF (I-25) 130,131,130
131   CONTINUE
      IF (XISW) 132,132,133
132   SUMDPI=DELPTW(1)+DELPTW(2)+DELPTW(8)+DELPTW(9)+VHEADW(20)
      DO 134 L=14,20,1
134   SUMDPI=SUMDPI+DELPTW(L)
      ERR11=SUMDPI-VACW
      XISW=1.0
      ITERI=1
      EPSI=0.150
      IF (ABSF(ERR11)-0.750) 162,162,135
135   CONTINUE
      OLDFI=FLOWI
      FLOWI=FLOWI-0.500*ABSF(ERR11)/ERR11
      IF (FLOWI) 143,144,144
143   FLOWI=0.0005
      AIR11=0.0
      AIR12=0.0
144   CONTINUE
      IF (SKIP(13)) 148,148,147
147   FLOWM=0.0
      AIRM1=0.0
      AIRM2=0.0
      FLOWT=FLOWI
      FLOWJ=FLOWT-FLOWE
      GO TO 118

```

10

```

148      RATIO=(DELPTW(1)+DELPTW(2)+DELPTW(8)+DELPTW(9))/BVSUCW
        IF (RATIO-0.950) 96,96,95
95      RATIO=0.950
96      CONTINUE
        IF (RATIO*(OLDFI-FLOWI)+FLOWM) 156,156,157
156     FLOWM=0.100*FLOWM
        GO TO 158
157     FLOWM=FLOWM+RATIO*(OLDFI-FLOWI)
158     CONTINUE
        FLOWT=FLOWI+FLOWM
        FLOWJ=FLOWT-FLOWE
        GO TO 118
133     ITERI=ITERI+1
        IF (ITERI-10) 172,123,172
123     EPSI=1.000
172     IF (ITERI-16) 136,136,137
137     WRITE OUTPUT TAPE 6,138
138     FORMAT (39H NO IDLE CONVERGENCE WITHIN FLOW )
        GO TO 149
136     CONTINUE
        SUMDPI=DELPTW(1)+DELPTW(2)+DELPTW(8)+DELPTW(9)+VHEADW(20)
        DO 139 L=14,20,1
139     SUMDPI=SUMDPI+DELPTW(L)
        ERRI2=SUMDPI-VACW
        IF (ABS(ERRI2)-EPSI) 162,162,140
140     SAVE=FLOWI
        FLOWI=FLOWI+ERRI2*(FLOWI-OLDFI)/(ERRI1-ERRI2)
        IF (FLOWI-15.00) 146,146,145
145     FLOWI=15.00
146     CONTINUE
        IF (FLOWI) 141,142,142
141     FLOWI=0.0005
        AIRI1=0.0
        AIRI2=0.0
142     OLDFI=SAVE
        ERRI1=ERRI2
        IF (SKIP(13)) 154,154,153
153     FLOWM=0.0
        AIRM1=0.0
        AIRM2=0.0
        FLOWT=FLOWI
        FLOWJ=FLOWT-FLOWE
        GO TO 118
154     RATIO=(DELPTW(1)+DELPTW(2)+DELPTW(8)+DELPTW(9))/BVSUCW
        IF (RATIO-0.990) 98,98,97
97      RATIO=0.990
98      CONTINUE
        IF (RATIO*(OLDFI-FLOWI)+FLOWM) 159,159,160
159     FLOWM=0.100*FLOWM
        GO TO 161
160     FLOWM=FLOWM+RATIO*(OLDFI-FLOWI)
161     CONTINUE
        FLOWT=FLOWI+FLOWM
        FLOWJ=FLOWT-FLOWE
        GO TO 118
130     CONTINUE
51      CONTINUE

```

PAGE 11

```

162      OLDAI1=AIRI1
        OLDAI2=AIRI2
        IF (SKIP(20)) 169,169,149
169      CONTINUE
        DELPTW(24)=DELPTW(1)+DELPTW(2)+DELPTW(8)+DELPTW(9)+DELPTW(14)
        +DELPTW(15)+VHEADW(16)
        DELPTW(25)=DELPTW(1)+DELPTW(2)+DELPTW(8)+DELPTW(9)+DELPTW(14)
        +DELPTW(15)+DELPTW(16)+DELPTW(17)+DELPTW(18)+VHEADW(19)
        AIRI1=C8*ACHAN(24)*CBLEED(4)*SQRT(AIDENS*DELPTW(24))
        AIRI2=C8*ACHAN(25)*CBLEED(5)*SQRT(AIDENS*DELPTW(25))
        IF (ABSF(AIRI1-OLDAI1)-0.008) 163,163,166
163      IF (ABSF(AIRI2-OLDAI2)-0.008) 149,149,166
166      XISW=0.0
        ITERI=C
        GO TO 118

C
149      SUMAIR=AIRM1+AIRM2
        IF (SETUP) 94,94,93
93      BVSMIN= SPILL1*SGFUEL*1.08 + GAMMA/D(13) + (DELPTW(1) +
1      DELPTW(2)+DELPTW(8)+DELPTW(9))
        SAVEI1=AIRI1
        SAVEI2=AIRI2
        SETUP=0.0
        IF (BVSUCW-BVSMIN ) 94,94,89
94      XFLOWT=FLOWT
        XFLOWM=FLOWM
        XFLOWE=FLOWE
        XFLOWJ=FLOWJ
        XFLOWI=FLOWI
        REJET=RE(1)
        CDJET=CDJ
        DPJET=DELPTW(1) + VHEADW(1) + DPEJET
        IF (SKIP(20)) 77,77,78
77      ITER=ITERI
        GO TO 79
78      ITER=ITERJ
79      CONTINUE
        IF (DUMMYP) 150,150,151
151     WRITE OUTPUT TAPE 6,152,BVSUCW,VACM ,FLOWM,FLOWT,FLOWJ,
1      FLOWE,FLOWI,CDJET,DPJET,ITER,ITERE,ITERJ,ITERI,
2      AIRM1,AIRM2,AIRI1,AIRI2
152     FORMAT (1H0,/,9F8.3,4I5,4F8.3,/)
150     CONTINUE
        XLD( 3)=SAVE3
        XLD(20)=SAVE4
        ACHAN( 3)=SAVE5
        ACHAN(20)=SAVE6
        RETURN
        END

```



```

TOR=TOF + 459.6
TOTR=TOR
TOTF=TOF
DUMHU=HUMID
DUMMYP=DEBUG
DUMPA=PRINTA
CDBL=0.840
CDTR=0.840
VCL=DISPL/(CR-1.0)
ABLEED=0.785398*DBLEED*DBLEED
ATRANS=0.785398*DTRANS*DTRANS
ACHOKE=0.785398*DCHOKE*DCHOKE
SWITCH=0.0
TF=TOF/100.0
PMAW=1.302*TF*TF*TF-0.765*TF*TF+0.413*TF
OMEGA=0.622*HUMID*PMAW/PO
C GET THE PROPERTIES OF THE MOIST AIR
FA=0.0000
1 CALL XMIX (TOF,POHG,HUMID,FTYPE,TFUEL,FA,WMOIST,CPWET,CVWET
GKWET )
1 CALL XMIX (TOTF,PTHG,DUMHU,FTYPE,TFUEL,FATOTL,WMOLEM,CPMIX,
CVMIX,GKMIX )
DUMFA=FAMAIN*FRACT
1 CALL XMIX (TOTF,PTHG,DUMHU,FTYPE,TFUEL,DUMFA,WMOLET,CPMAIN,
CVMAIN,GK )
C GET THE FUEL PROPERTIES
1 CALL FPROP (FTYPE,TFUEL,TFUEL,SGFUEL,VISKM,CORR,CLIQ,CPFUEL
CVFUEL,WFUEL,HVAPOR,SIGMA,HEATV )
FAIDLE=FATOTL-FAMAIN
TOTR=TOR + FRACT*FAMAIN*HVAPOR/CPWET
TOTF=TOTR-459.6
TMAN= TOR +FATOTL*HVAPOR/CPWET + EXHEAT*60.0
TMANF=TMAN-459.6
44 IF (FATOTL-0.0400) 44,44,45
TCLR=650.0 + 700.0*FATOTL/0.0400
GO TO 50
45 IF (FATOTL-0.0800) 47,46,46
46 TCLR=1350.0-700.0*(FATOTL-0.0800)/0.0700
IF (TCLR-650.0) 48,50,50
48 TCLR=650.0
GO TO 50
47 TCLR=1350.0
50 CONTINUE
TCYLR=TMAN+TCLR/9.00
C5=TCYLR/TMAN
C6=TCLR/TMAN
C7=C5/C6
C8=0.400*C5*1545.4*TMAN*(CR-1.0)/(WMOLEM*CR*0.4912)
C9=(CR-C7)/CR
C10=(GKWET-1.0)/GKWET
C11=(GKWET+1.0)/(2.0*GKWET)
C12=3600.0*SQRT(GKWET*WMOIST*32.174/1545.4)*ABLEED*PO*
1 SQRT(2.0/(GKWET-1.0))/SQRT(TOTR)
C13=3600.0*SQRT(GKWET*WMOIST*32.174/1545.4)*ACHOKE*PO*
1 SQRT(2.0/(GKWET-1.0))/SQRT(TOTR)
PRBMAX=1.0/((2.0/(GKWET+1.0))*((GKWET/(GKWET-1.0))))

```

3

```

10  CONTINUE
    N=N+1
    IF ( N - 21) 71,72,71
72  EPS=0.80
    SWITCH=0.0
    VACMAN=8.0
    DUMHU=HUMID
    WRITE OUTPUT TAPE 6,14
14  FORMAT (1H ,65H 20 ITERATIONS HAVE BEEN PERFORMED WITHIN AIRM
IAS.....TRY 8 MORE )
    IF (PRINTA) 71,71,56
56  DUMMYP=1.0
71  CONTINUE
    GASM2=DISPL*RPM*(POHG*C9-VACMAN)/C8
C
    DUMMY1=GASM2/1000.0
C
    PT=STAGNATION PRESSURE AT THROTTLE PLATE IN PSIA
C
    PTHG=STAGNATION PRESSURE AT THROTTLE PLATE IN INCHES HG
C
    CORRELATED PO LOSS IN VENTURI IS 1.0 INCH HG FOR 912.0 LB/HOUR
    PT=PO - 1.200*0.4912*DUMMY1*DUMMY1
    PTHG=PT/0.4912
    DUMHU=PT*OMEGA/(0.622*PMAXW)
C
    VLIMIT=(PO-PT)/0.4912
    IF (VACMAN-VLIMIT) 61,61,62
61  VACMAN=VLIMIT + 0.0001
    GO TO 71
62  CONTINUE
    PR=PT/(PO-VACMAN*0.4912)
    PRMAX=1.0/((2.0/(GK+1.0))*(GK/(GK-1.0)))
    IF (PR-PRMAX) 12,11,11
11  PR=PRMAX
12  CONTINUE
    C1=2.0*3600.0*SQRT(GK*WMOLET*32.174/1545.4)*AFLOW*PT*
1  SQRT(2.0/(GK-1.0))/SQRT(TOTR)
    C2=(GK-1.0)/GK
    C3=(GK+1.0)/(2.0*GK)
    CHECK=PR**C2
    IF (CHECK-1.00) 63,64,64
63  WRITE OUTPUT TAPE 6,65
65  FORMAT (1H0,40H THE PRESSURE RATIO IS LESS THAN 1.000 )
    WRITE OUTPUT TAPE 6,66,PR,PO,PT,VACMAN,VLIMIT,PRMAX,N
66  FORMAT (6F15.6,I15 )
    PR= 1.0040
64  CONTINUE
    GASMT=C1*SQRT(PR**C2 - 1.0)*CDT/(PR**C3)
    PRBL=PO/(PO - VACMAN*0.4912)
    IF (PRBL-PRBMAX) 67,68,68
68  PRBL=PRBMAX
67  CONTINUE
    AIRMB=CDBL*C12*SQRT(PRBL**C10-1.00)/(PRBL**C11)
    AIRMC=CDBL*C13*SQRT(PRBL**C10-1.00)/(PRBL**C11)
    GASMTR=CDTR*C1*(ATRANS/AFLOW)*SQRT(PR**C2-1.0)/(PR**C3)
    GASM1=GASMT+AIRMB+GASMTR+AIRMC
; CHOKED FLOW FOR GK=1.4 WILL BE 1914.40*2.0*AFLOW*PT/SQRT(TOTR)+ 13.0
    IF (SWITCH-0.0) 33,34,33
34  WETA2=GASM2*(1.0+OMEGA)/(1.0 + OMEGA + FATOTL)

```

PAGE 4

```

WETA1=GASM1*(1.0+OMEGA)/(1.0 + OMEGA + FAMAIN)
E1=WETA1-WETA2
  IF (ABSF(E1)-EPS ) 13,13,39
39  CONTINUE
  VOLD=VACMAN
  VACMAN=VACMAN - 0.0500*ABSF(E1)/E1
  SWITCH=1.0
  GO TO 36
33  WETA2=GASM2*(1.0+OMEGA)/(1.0 + OMEGA + FATOTL)
  WETA1=GASM1*(1.0+OMEGA)/(1.0 + OMEGA + FAMAIN)
  E2=WETA1-WETA2
  IF (ABSF(E2)-EPS) 13,13,35
35  SAVE=VACMAN
  IF (E1) 40,13,41
40  STEP=1.100
  GO TO 42
41  STEP=0.900
42  CONTINUE
  VACMAN=VACMAN+E2*(VACMAN-VOLD)*STEP/(E1-E2)
  VOLD=SAVE
  E1=E2
36  CONTINUE
  IF (DUMMYP) 17,17,15
15  WRITE OUTPUT TAPE 6,16,N,RPM,THETA,VOLD,WETA2,WETA1,E1,
1  VACMAN,FAMAIN,FATOTL,PTHG,TMANF
16  FORMAT (I4,2F10.1,F10.2,2F10.1,2F10.2,2F10.4,F10.2,F10.1 )
17  CONTINUE
  IF (N - 29) 31,30,30
30  WRITE OUTPUT TAPE 6,32
32  FORMAT (1H0,46H NO MANIFOLD VACUUM CONVERGENCE WITHIN AIRMAS )
  GO TO 13
31  CONTINUE
  IF (VACMAN-VLIMIT) 27,27,28
27  VACMAN=VLIMIT + 0.0001
  GO TO 10
28  IF (VACMAN-POHG*C9) 10,29,29
29  VACMAN=POHG*C9 - 0.010
  GO TO 10
13  WETAIR=WETA2
  GASFLO=GASM2
  VENFLO=WETAIR-AIRMB
  DRYAIR=WETAIR/(1.0 + OMEGA)
  XMACHT=SQRT(2.0/(GK-1.0))*SQRT(PR**((GK-1.0)/GK)-1.000)
  PMAN=POHG-VACMAN
  VACM=VACMAN
  XMAINR=FAMAIN
  XTOTLR=FATOTL
  IF (DUMPA ) 76,76,75
75  WRITE OUTPUT TAPE 6,77,RPM,THETA,AFLOW,PMAN,WETAIR,DRYAIR,
1  GASFLO,GASMT,XMACHT,FAMAIN,FATOTL,GK,PTHG,TOTF,CDT,N
77  FORMAT (F8.1,F9.1,F9.4,F9.2,3F9.2,F8.2,F9.4,F9.4,F8.4,F8.3
1  F8.3,F8.1,F7.3,I4 )
76  CONTINUE
  RETURN
  END

```



COMPILE FASTRAN,PUNCH OBJECT

1

```

SUBROUTINE SIGNAL (POHG,TOF,HUMID,VENFLO,FTYPE,TFUEL,RATEMF,
1     AMV,ABV,XMV1,XMV2,XBV,XMB,BBLS,FRACT,XGUESS,PRINTS,
2     XFV,BVFLO,PVFLO,BVMACH,PVMACH,BVSUCW,PVSUCW )
DUMMYP=PRINTS
DIMENSION AMV(10),ABV(10)
DUMFLO=VENFLO/BBLS
CALL FPROP (FTYPE,TFUEL,TFUEL,SGFUEL,VISKM,CORR,CLIQ,CPFUEL,
1     CVFUEL,WFUEL,HVAPOR,GAMMA,HEATV )
FRACTR=FRACT*0.400
EPS=0.00012
TOR=TOF+459.6
TOMR=TOR
TOBR=TOR
TOMF=TOF
TOBF=TOF
PO=POHG*0.4912
POMHG=POHG
POBHG=POHG
POM=PO
POB=PO
C
GET THE PROPERTIES OF THE MOIST AIR IN THE PRIMARY VENTURI
CALL XMIX (TOF,POHG,HUMID,FTYPE,TFUEL,0.0,WMOIST,CPWET,
1     CVWET,GKWET )
C1=SQRT(GKWET*32.174*WMOIST/(1545.4*TOR))
C2=2.0*32.174*144.0*0.4912
C3=0.50*(GKWET + 1.0)
C4=0.50*(GKWET + 1.0)/(GKWET-1.0)
C5=C3**C4
C6=3600.0*PO*C1/C5
FMAXB=C6*ABV(3)
FMAXM=C6*AMV(3)
FMAXT=FMAXM+FMAXB
IF (FMAXT-DUMFLO) 28,29,29
28 WRITE OUTPUT TAPE 6,30
30 FORMAT (1H ,67H THE AIR FLOW SUPPLIED TO SIGNAL EXCEEDS THE V
VENTURI FLOW CAPACITY )
J=0
GO TO 51
29 CONTINUE
J=0
SWITCH=0.0
IF (XGUESS) 11,11,10
10 XF=XGUESS
GO TO 12
11 XF=0.800*AMV(3)/(AMV(3)+ABV(3))
12 CONTINUE
J=J+1
IF (J-12) 53,54,53

```

PAGE 2

```

54      EPS=0.00028
        GO TO 15
53      IF (J-15) 55,56,55
56      SWITCH=0.0
        EPS=0.00100
        XF=0.650
        FMAXB=C6*ABV(3)
        FMAXM=C6*AMV(3)
        FMAXT=FMAXM+FMAXB
        GO TO 15
55      CONTINUE
13      IF (J-25) 15,13,13
13      WRITE OUTPUT TAPE 6,14
14      FORMAT (1H0,33H NO XF CONVERGENCE WITHIN SIGNAL /)
        GO TO 23
15      RATEM=XF*DUMFLO
        RATEB=DUMFLO-RATEM
        IF (FMAXB-RATEB) 26,36,36
36      CONTINUE
C      GET THE TOTAL PRESSURE LOSS IN THE BOOST VENTURI
        CALL SOLVE (POHG,TOF, POHG,TOF,HUMID,ABV(3),RATEB,WMOIST,
1      GKWET,FMAXB3,RHOB3,PBHG3,TRF3,BMACH3,SUCWB3 )
        IF (FMAXB3-RATEB) 37,38,38
37      DUMRB=FMAXB3
        GO TO 39
38      DUMRB=RATEB
39      CONTINUE
        VELB3=DUMRB*144.0/(RHOB3*ABV(3)*3600.0)
        POBHG=POHG-RHOB3*VELB3*VELB3*((1.0-ABV(3)/ABV(4))**2)/C2
C      GET THE BOOST VENTURI SUCTION AT THE FUFL DISCHARGE NOZZLE
        CALL SOLVE (POHG,TOF,POBHG,TOF,HUMID,ABV(3),RATEB,WMOIST,
1      GKWET,FMAXB4,RHOB4,PBHG4,TRF4,BMACH4,SUCWB4 )
C      TRY ABV(3) HERE IF BOOST SUCTIONS ARE TOO LOW
        FMAXB=FMAXB4
        IF (FMAXB-RATEB) 26,27,27
26      RATEB=FMAXB
        RATEM=DUMFLO-RATEB
        XF=RATEM/DUMFLO
        GO TO 36
27      CONTINUE
C
C
C      FLVAPB IS THE FUEL VAPOR MASS FLOW RATE AT THE BOOST VENTURI EX
C      FLLIQB IS THE LIQUID FUEL MASS FLOW RATE AT THE BOOST VENTURI EX
C      BFA IS THE F/A RATIO OF THE VAPOR MIXTURE LEAVING THE BOOST VENT
C
        FLVAPB=0.5*RATEMF*FRACTB
        FLLIQB=0.5*RATEMF*(1.0-FRACTB)
        BFA=FLVAPB/RATEB
        FLMIXB=RATEB+FLVAPB
C      GET THE PROPERTIES OF THE MIXTURE LEAVING THE BOOST VENTURI
        TOBR=TOR+BFA*HVAPOR/CPWET
        TORF=TOBR-459.6
        CALL XMIX (TOBF,POBHG,HUMID,FTYPE,TFUEL,BFA,WMIXB,CPMIX,
1      CVMIX,GKMIX )
C      FIND THE MAIN VENTURI MACH NUMBER AT STATION 4
        DUMMYM=RATEM/1000.0

```

3

```

      POMHG=POHG-1.200*DUMMYM*DUMMYM
C     GET THE PRIMARY VENTURI THROAT SUCTION
      CALL SOLVE (POHG,TOF,POMHG,TCMF,HUMID,AMV(3),RATEM,WMOIST,
1      GKWET,FMAXM3,RHOM3,PMHG3,TMF3,PMACH3,SUCWM3 )
      FMAXM=FMAXM3
      CALL SOLVE (POHG,TOF,POMHG,TCMF,HUMID,AMV(4),RATEM,WMOIST,
1      GKWET,FMAXM4,RHOM4,PMHG4,TMF4,PMACH4,SUCWM4 )
      PM4W=13.594*PMHG4
C     FIND THE MACH NUMBER AT THE BOOST VENTURI OUTLET
      CALL SOLVE (POHG,TOF,POBHG,TOBF,HUMID,ABV(5),FLMIXB,WMIXB,
1      GKMIX,FMAXB5,RHOB5,PBHG5,TBF5,BMACH5,SUCWB5 )
      PB5W=13.594*PBHG5
      FMAXT=FMAXM+FMAXB
      IF (FMAXT-DUMFLO) 44,43,43
44     WRITE OUTPUT TAPE 6,30
51     RATEB=FMAXB
      RATEM=FMAXM
      XF=RATEM/(RATEM+RATEB)
      DUMMYP=1.0
      GO TO 22
43     CONTINUE
41     IF (FMAXM-RATEM) 24,42,42
24     RATEM=FMAXM
      XF=RATEM/DUMFLO
      RATEB=DUMFLO-RATEM
      GO TO 36
42     IF (SWITCH) 16,16,17
16     E1=PB5W-PM4W
      IF (ABSF(E1)-EPS ) 23,23,33
33     CONTINUE
      XF1=XF
      SWITCH=1.0
      XF=XF - 0.010*ABSF(E1)/E1
      GO TO 32
17     E2=PB5W-PM4W
      IF (ABSF(E2)-EPS ) 23,23,18
18     SAVE=XF
      IF (BMACH4-0.999) 45,45,46
46     IF (E2) 45,23,47
47     RATEB=FMAXB
      RATEM=DUMFLO-RATEB
      XF=RATEM/DUMFLO
      GO TO 22
45     IF (PMACH3-0.999) 48,48,49
49     IF (E2) 50,23,48
50     RATEM=FMAXM
      RATEB=DUMFLO-RATEM
      XF=RATEM/DUMFLO
      GO TO 22
48     CONTINUE
      XF=XF-E2*(XF1-XF)/(E1-E2)
      XF1=SAVE
      E1=E2
32     CONTINUE
      IF (XF-0.0500) 19,12,20
19     XF=0.0500
      GO TO 12

```

PAGE 4

20 IF (XF-0.9500) 12,12,21  
 21 XF=0.9500  
 GO TO 12

C

C NOW THE FRACTION OF THE AIR FLOW PASSING THROUGH EACH VENTURI  
 C AND THE BOOST VENTURI SUCTION ARE KNOWN  
 C

22 CONTINUE  
 CALL SOLVE (POHG,TOF,POBHG,TOF,HUMID,ABV(3),RATEB,WMOIST,  
 1 GKWET,FMAXB4,RHOB4,PBHG4,TBF4, BMACH4, SUCWB4 )  
 CALL SOLVE (POHG,TOF,POMHG,TOMF,HUMID,AMV(3),RATEM,WMOIST,  
 1 GKWET,FMAXM3,RHOM3,PMHG3,TMF3, PMACH3, SUCWM3 )  
 CALL SOLVE (POHG,TOF,POMHG,TOMF,HUMID,AMV(4),RATEM,WMOIST,  
 1 GKWET,FMAXM4,RHOM4,PMHG4,TMF4, PMACH4, SUCWM4 )  
 CALL SOLVE (POHG,TOF,POBHG,TOBF,HUMID,ABV(5),FLMIXB,WMIXB,  
 1 GK MIX,FMAXB5,RHOB5,PBHG5,TBF5, BMACH5, SUCWB5 )  
 E2=13.594\*(PBHG5-PMHG4)  
 IF (E2-0.0100) 23,23,57

57 E2=0.0020  
 23 PVFLO=RATEM  
 BVFLO=RATEB  
 PVMACH=PMACH3  
 BVMACH=BMACH4  
 PVSUCW=SUCWM3  
 BVSUCW=SUCWB4  
 Xfv=XF

C

IF (DUMMYP) 40,40,34  
 34 WRITE OUTPUT TAPE 6,35,Xfv,E2,VENFLO,PVFLO,BVFLO,PVMACH,  
 1 BVMACH,PVSUCW,BVSUCW,PMHG4,POBHG,TOBF,SUCWB3,FMAXM,  
 2 FMAXB,J  
 35 FORMAT(F8.4,F10.4,F9.2,F9.2,F9.2,F9.4,F9.4,F8.3,F9.3,F9.3,  
 1 F8.3,F8.2,F8.3,F8.1,F7.1,I4 )  
 40 RETURN  
 END

\$ COMPILER FASTRAN, PUNCH OBJECT

1

SUBROUTINE SOLVE (POHG, TOF, POLHG, TOLF, HUMID, A, FLO, WMOLEC, GK,  
1 FLOMAX, RHOL, PLHG, TLF, XMACH, XSUC )

C

BB1F(X)=1.0/X  
 BB2F(X) = ( ABSF(X) )\*\* 2  
 BB3F(X)=X\*A14  
 BB4F(X)=BB2F(X)\*A14  
 BB5F(X)=1.0 + A15\*BB2F(X)  
 BB6F(X)=A8\*BB5F(X)  
 BB7F(X)=1.0+GK\*BB2F(X)  
 BR8F(X)=A2/BB7F(X)  
 BB9F(X)=(1.0-BB2F(X))/(GK\*BB2F(X))  
 B10F(X)=BB2F(X)/A8  
 B11F(X)=ELOG(BB2F(X))  
 B12F(X)=BB2F(X)/A7 - 1.0/A4  
 B13F(X)=BB2F(X)/A7 - 1.0  
 B14F(X)=A8/BB2F(X) - 1.0/A4  
 B15F(X)=BB2F(X) + A11  
 B16F(X)=A13\*BB2F(X) - 1.0  
 B17F(X)=A7 \* ELOG(BB6F(X))  
 B18F(X)=SQRT (BB6F(X))  
 B19F(X)=SQRT (BB5F(X))/(A8\*\*A9)  
 B20F(X)=1.0/(GK\*BB2F(X))  
 B21F(X) = A17\*BB2F(X) / BB5F(X)  
 B22F(X)=BB5F(X)\*\*A9  
 B23F(X)=BB5F(X)\*\*A16

C THE FOLLOWING FUNCTIONS ARE USED WITH NEWTONS METHOD

TOPF(X)=C3\*B22F(X) - X  
 BOTF(X)=A17\*C3\*X\*B23F(X) - 1.0  
 YTOPF(X) = BB9F(X)+A7\*ELOG(B21F(X)) - HH  
 YBOTF(X) = -2.0\*BB1F(X)\*(B20F(X)-A7/BB5F(X))  
 QTOPF(X)=X\*B19F(X)-Q  
 QBOTF(X)=(BB5F(X)+A15\*BR2F(X)) \* (A8\*\*(-A9))/SQRT (BB5F(X))

C

A1 =GK-1.0  
 A2 =GK+1.0  
 A3 =1.0/A1  
 A4 =A2/A1  
 A5 =GK/A1  
 A6 =SQRT (GK)  
 A7 =A2/(2.0\*GK)  
 A8 =2.0/A2  
 A9 =A2/(2.0\*A1)  
 A10=A2\*\*2  
 A11=2.0\*A3  
 A12=SQRT (2.0\*A2)

PAGE 2

A13=2.0\*A5  
 A14=GK/2.0  
 A15=A1/2.0  
 A16=(3.0-GK)\*.5/A1  
 A17=A2/2.0  
 A18=1.0/A6

C

Q=1.0  
 HH=1.0  
 AGAIN=0.0  
 PO=POHG\*0.4912  
 POL=POLHG\*0.4912  
 TOP=TOF+459.6  
 TOLR=TOLF+459.6  
 RHOLZ=144.0\*POL\*WMOLEC/(1545.4\*TOLR)  
 C1=SQRT(GK\*32.174\*WMOLEC/(1545.4\*TOLR))  
 C2=3600.0\*A\*POL\*C1  
 C3=FLO/C2  
 FLOMAX=C2/B22F(1.00)  
 C4=1.0 + (B22F(1.0)-1.0)\*FLO/FLOMAX  
 IF (FLOMAX-FLO) 7,9,9

7

XMACH=1.0

GO TO 19

9

CONTINUE

EPSLON=0.000050

C

THIS IS AN INITIAL GUESS FOR THE MACH NUMBER

DUMACH=C4\*C2

ITER=0

10

CHANGE=TOPF(DUMACH)/BOTF(DUMACH)

SAVE=DUMACH

DUMACH=DUMACH - CHANGE

ITER=ITER+1

IF (AGAIN) 23,23,24

24

WRITE OUTPUT TAPE 6,25,ITER,SAVE,CHANGE,DUMACH

25

FORMAT (30X,I8,3F12.6)

23

CONTINUE

40

IF (ITER-18) 13,13,11

11

WRITE OUTPUT TAPE 6,12

12

FORMAT (1H0,41H NO MACH NUMBER CONVERGENCE WITHIN SOLVE )

IF (AGAIN) 21,21,14

21

AGAIN=1.0

GO TO 9

13

CONTINUE

IF (DUMACH-1.000) 16,16,15

15

DUMACH=1.0000

GO TO 10

16

IF (DUMACH) 17,17,18

17

DUMACH=0.00001

GO TO 10

18

CONTINUE

IF (ABS(CHANGE) - EPSLON) 14,14,10

14

XMACH=DUMACH

19

PLHG=POLHG/(BB5F(XMACH)\*\*A5)

XSUC=13.594\*(POHG-PLHG)

TLR=TOLR/BB5F(XMACH)

TLF=TLR-459.6

RHOL=RHOLZ/(BB5F(XMACH)\*\*A3)

3

---

20

RETURN  
END

\$ ..... COMPILF FASTRAN, PUNCH OBJECT

PAGE 1

1 SUBROUTINE XMIX (TOF,POHG,HUMID,FTYPE,TFUEL,FA,WMOL,  
CPMIX,CVMIX,GKMIX )

C  
C THIS SUBROUTINE CALCULATES THE THERMODYNAMIC PROPERTIES OF AN  
C IDEAL GAS MIXTURE CONSISTING OF AIR, WATER VAPOR, AND FUEL VAPOR  
C THIS IS DONE FOR ANY SPECIFIED FUEL, FUEL-AIR RATIO, PRESSURE,  
C TEMPERATURE, AND HUMIDITY  
C

PO=POHG\*0.4912  
TOR=TOF + 459.6  
TF=TOF/100.0  
PMAW=1.302\*TF\*TF\*TF - 0.765\*TF\*TF + 0.413\*TF  
OMEGA=0.622\*HUMID\*PMAW/PO

C  
C GET AIR PROPERTIES  
C

FLUID=8.0  
CALL FPROP (FLUID,TOF,TOF,DENSM,VISKM,CORR,CLIQ,CPAIR,CVAIR,  
1 WAIR,HVAPOR,SIGMA,HEATV )

C  
C GET WATER VAPOR PROPERTIES  
C

FLUID=2.0  
CALL FPROP (FLUID,TOF,TOF,DENSM,VISKM,CORR,CLIQ,CPH20,CVH20,  
1 WH20,HVAPOR,SIGMA,HEATV )

C  
C GET FUEL PROPERTIES  
C

CALL FPROP (FTYPE,TFUEL,TFUEL,DENSM,VISKM,CORR,CLIQ,CPFUEL,  
1 CVFUEL,WFUEL,HVAPOR,SIGMA,HEATV )

C  
C4=1.0 +FA +OMEGA  
C5=FA/WFUEL + 1.0/WAIR + OMEGA/WH20  
WMOL=C4/C5  
CPMIX=(CPAIR+OMEGA\*CPH20+FA\*CPFUEL)/C4  
CVMIX=(CVAIR+OMEGA\*CVH20+FA\*CVFUEL)/C4  
GKMIX=CPMIX/CVMIX  
RETURN  
END



\$ ..... COMPILER MAD,PUNCH OBJECT

17 MAY 1967 VERSION) PROGRAM LISTING ... ..

EXTERNAL FUNCTION (Y,XXMIN,DELTAX,FM,FN,SCRACH,XARG,YEST,  
1       DEBUG )

INTEGER I,J,M,N,ISTART,MAXM,ME,MO  
INTEGER R,NPOINT,NX,K,KO,KE,NDP,COUNT,NDUM  
DIMENSION X(250)

ENTRY TO STERL.

M=FM

DUM1=FN

DUM1=DUM1 - 1.0

N=DUM1

      FIRST CHECK FOR OBVIOUS ERRORS

WHENEVER N.L. 1

PRINT RESULTS N

N=1

M=1

END OF CONDITIONAL

WHENEVER M.G.N

PRINT COMMENT \$0    M EXCEEDS N                    \$

PRINT COMMENT \$0    M WILL BE SET EQUAL TO N            \$

PRINT RESULTS M,N

M=N

END OF CONDITIONAL

WHENEVER M.L.1

PRINT COMMENT \$0 M WAS LESS THAN 1 SO M WAS SET EQUAL TO 1 \$

PRINT RESULTS M

M=1

END OF CONDITIONAL

THROUGH SETUP, FOR I=0,1,I.G.N

DUM2=I

SETUP

X(I)=XXMIN + DUM2\*DELTAX

WHENEVER XARG .L. X(0)

PRINT COMMENT \$0 THE X ARGUMENT IS SMALLER THAN THE MINIMUM \$

YEST=Y(1)-(X(1)-XARG)\*(Y(1)-Y(0))/(X(1)-X(0))

PRINT COMMENT \$    AN EXTRAPOLATION HAS BEEN MADE    \$

XMIN=XXMIN

XMAX=X(N)

XVALUE=XARG

YVALUE=YEST

PRINT RESULTS XMIN,XMAX,XVALUE,YVALUE

TRANSFER TO DONE

END OF CONDITIONAL

WHENEVER XARG.G. X(N)

PRINT COMMENT \$0 THE X ARGUMENT IS LARGER THAN THE MAXIMUM \$

YEST=Y(N)-(XARG-X(N))\*(Y(N)-Y(N-1))/(X(N)-X(N-1))

PRINT COMMENT \$    AN EXTRAPOLATION HAS BEEN MADE    \$

XMIN=XXMIN

XMAX=X(N)

XVALUE=XARG

YVALUE=YEST

PRINT RESULTS XMIN,XMAX,XVALUE,YVALUE

TRANSFER TO DONE

END OF CONDITIONAL

```

WHENEVER DEBUG .E. 1.00
PRINT FORMAT NVAL,N
VECTOR VALUES NVAL=$1H0,S40,23H THIS DATA SET HAS N = 14
PRINT FORMAT ATITLE
VECTOR VALUES ATITLE=$1H0,S39,32HI X(I)
THROUGH LIST, FOR I=0,1,I.G.N
LIST PRINT FORMAT NEAT,I,X(I),Y(I)
VECTOR VALUES NEAT=$1H ,S30,I10,F15.3,F15.3 *$
END OF CONDITIONAL

BEGIN THE INTERPOLATION BY SETTING UP THE DIFFERENCE TABLE

FIND THE Y(I) VALUE WHICH IS CLOSEST TO XARG AND USE THIS
AS THE CENTRAL DIFFERENCE STARTING POINT UNLESS M EXCEEDS
MMAX FOR THIS STARTING POINT

WHENEVER XARG.G.X(0).AND.(XARG-X(0)).LE.((X(1)-X(0))/2.0)
ISTART=1
TRANSFER TO TESTM
END OF CONDITIONAL
WHENEVER XARG.L.X(N).AND.(XARG-X(N-1)).GE.((X(N)-X(N-1))/2.0)
ISTART=N-1
TRANSFER TO TESTM
END OF CONDITIONAL
THROUGH SCAN, FOR I=0,1,I.G.N
WHENEVER .ABS.(XARG-X(I)).L.(0.00001*(X(N)-X(N-1)))
ISTART=I
YFST=Y(I)
TRANSFER TO DONE
END OF CONDITIONAL
WHENEVER XARG .L. X(I) , TRANSFER TO WHERE
SCAN CONTINUE
WHERE WHENEVER (X(I)+X(I-1))-2.0*XARG).G.(0.0)
ISTART=I-1
OR WHENEVER .ABS.(X(I)+X(I-1))-2.0*XARG).L.(0.005*(X(I)-X(I-1))) .AND.I.GE.(N/2)
1 ISTART=I-1
OTHERWISE
ISTART=I
END OF CONDITIONAL

NOW THE OPTIMUM STARTING POINT,Y(ISTART),IS KNOWN

NOW CHECK TO SEE IF THE DIFFERENCE TABLE,STARTING AT
Y(ISTART), EXTENDS OUT TO THE DESIRED M VALUE

TESTM WHENEVER ISTART.LE.(N/2)
MAXM=ISTART*2
OTHERWISE
MAXM=(N-ISTART)*2
END OF CONDITIONAL

THUS, FOR THIS XARG, WE NOW KNOW THE MAXIMUM POSSIBLE
VALUE OF M WHICH MAY BE SPECIFIED.
CHECK TO SEE IF A LARGER M HAS BEEN SPECIFIED

WHENEVER M.G.MAXM.AND.ISTART.LE.(N/2)
ISTART=(M+1)/2
TRANSFER TO MOVEUP
END OF CONDITIONAL

```

```

WHENEVER M.G.MAXM
I START=N - ((M+1)/2)
END OF CONDITIONAL
MOVEUP CONTINUE

```

THE FOLLOWING TWO FUNCTIONS MAKE CONVENIENT USE OF  
INTEGER DIVISION

```

R=(M+1)/2
NPOINT=(2*R)+1
NPOINT IS THE NUMBER OF DATA POINTS REQUIRED FOR AN
M-TH DEGREE EVALUATION USING STIRLING'S FORMULA

```

```

ZERO THIS MERELY ASSURES THAT THE SCRACH ARRAY IS INITIALLY ZERO
THROUGH ZERO, FOR I=0,1,I.G.N
SHIFT SCRACH(I)=0.0
THROUGH SHIFT, FOR I=0,1,I.G.(NPOINT-1)
SCRACH(I)=Y(I START-R+I)
NOW TEST TO SEE IF M IS AN ODD OR EVEN DIFFERENCE
BECAUSE THE ITERATION TECHNIQUE DEPENDS ON THIS

```

```

ODEVEN=(-1).P.M
WHENEVER ODEVEN.G. 0
ME=M
MO=M-1
NDUM=0
OTHERWISE
ME=M-1
MO=M
NDUM=1
END OF CONDITIONAL
NX=2*N-1

```

NX IS THE MAXIMUM SUBSCRIPT FOR THE SCRACH ARRAY

COUNT IS AN INDEX WHICH COUNTS THE NUMBER OF CENTRAL  
DIFFERENCES THAT ARE SAVED IN THE SCRACH ARRAY

```

K=0
KO=0
KE=0
COUNT=0
THROUGH BETA, FOR J=NPOINT-1,-1,J.F.NDUM
K=K+1
EVENOD=(-1).P.K

```

EVENOD IS A VARIABLE WHICH INDICATES WHETHER THE CURRENT  
DIFFERENCE COLUMN IS ODD (FIRST COLUMN) OR EVEN (SECOND  
COLUMN). THIS IS NEEDED BECAUSE WE RETAIN TWO VALUES  
FOR THE ODD CASE AND ONE VALUE FOR THE EVEN CASE.

```

ODD THROUGH ODD, FOR I=0,1,I.E.J
SCRACH(I)=SCRACH(I+1) - SCRACH(I)
WHENEVER EVENOD.L. 0
KO=KO+1
SCRACH(NX-3*KO+3)=SCRACH(R-KO+1)
SCRACH(NX-3*KO+2)=SCRACH(R-KO)
COUNT=COUNT+2
OTHERWISE
KE=KE+1
SCRACH(NX-3*KE+1)=SCRACH(R-KE)

```

```

COUNT=COUNT+1
END OF CONDITIONAL
BETA CONTINUE
      SWITCH TAKES THE DIFFERENCE VALUES FROM THE UPPER PART OF
      THE SCRACH ARRAY AND PLACES THEM IN THE LOWERMOST PORTION
      THROUGH SWITCH, FOR I=0,1,I.E.COUNT
SWITCH SCRACH(I) =SCRACH(2*N-COUNT+I)
      SCRACH(COUNT)=Y(ISTART)

      THE SCRACH ARRAY IS NOW IN ITS FINAL ORDERED FORM, WITH
      SCRACH(0) CONTAINING THE HIGHEST FORWARD DIFFERENCE

      NOW COMPUTE ALPHA AND EVALUATE THE INTERPOLATING
      POLYNOMIAL FOR THIS VALUE OF XARG.
ALPHA=(XARG-X(ISTART))/(X(ISTART+1)-X(ISTART))
E=SCRACH(2*(M-ME))
      THROUGH ETERM, FOR I=ME,-2,I.L.2
ETERM 1 E=E*((ALPHA+(I-2)/2.0)*(ALPHA-(I-2)/2.0))/(I*(I-1))
      +SCRACH(3*((ME-I+2)/2)+2*(M-ME))

      NOW ALL OF THE EVEN TERMS HAVE BEEN EVALUATED, INCLUDING
OD=(SCRACH(M-MO)+SCRACH(M-MO+1))/2.0
      THROUGH OTERM, FOR I=MO,-2,I.L.3
OTERM 1 OD=OD*((ALPHA+(I-1)/2.0)*(ALPHA-(I-1)/2.0))/(I*(I-1))
      2 +((SCRACH(3*((MO-I+2)/2)+(M-MO))+SCRACH(3*((MO-I+2)/2)
      +(M-MO+1)))/2.0

      OD=ALPHA*OD
      NOW ALL OF THE ODD TERMS HAVE BEEN EVALUATED
YEST=E+OD
DONE CONTINUE
      WHENEVER DEBUG .E. 1.00
      PRINT COMMENT $ STERLING HAS COMPLETED AN INTERPOLATION
      PRINT RESULTS M,N,XARG,YEST
      END OF CONDITIONAL
      FUNCTION RETURN
      END OF FUNCTION

```

1

SUBROUTINE FPROP (FLUID,TEMP,TMAN,DENSM,VISKM,CORR,CLIQ,  
1 CPFUEL,CVFUEL,WMOLEC,HVAPOR,SIGMA,HEATV )

C  
C SIGMA IS THE SURFACE TENSION OF THE FLUID IN CONTACT  
C WITH AIR IN DYNES/CM  
C

C BEST FIT CURVES FOR SPECIFIC GRAVITY AND VISCOSITY  
C

C ISO-OCTANE ..... FLUID=0.0  
C STANDARD REGULAR...FLUID=1.0  
C WATER ..... FLUID=2.0  
C ETHYL ALCOHOL.....FLUID=3.0  
C SHELL PREMIUM..... FLUID=4.0  
C CLARK 100 ..... FLUID=5.0  
C MARATHON REG ..... FLUID=6.0  
C MINERAL SPIRITS....FLUID=7.0  
C AIR.....FLUID=8.0  
C

SWITCH=0.0

20 IF (FLUID - 0.0) 21,30,21  
30 SWITCH=1.0  
DENSM=0.7219-0.00043826\*TEMP  
VISKM=-0.4378 + 313.3462/(TEMP +200.0)  
CORR=SQRT ((0.7219-0.00043826\*TMAN)/DENSM)  
CLIQ = 0.4800  
CPFUEL= 0.4000  
CVFUEL= 0.3810  
WMOLEC= 114.00  
HVAPOR= -141.0  
SIGMA= 22.2000 - 0.050 \* TEMP  
HEATV=19080.0

GO TO 10

21 IF (FLUID - 1.0) 22,31,22  
31 SWITCH=1.0  
DENSM=24720.0/(TEMP +6270.0)-3.172  
VISKM=135.79/(TEMP +132.5)-0.0830  
CORR=SQRT ((24720.0/(TMAN+6270.0)-3.17)/DENSM)  
CLIQ = 0.5810  
CPFUEL= 0.4000  
CVFUEL= 0.3810  
WMOLEC= 126.00  
HVAPOR= -142.0  
SIGMA= 24.1000 - 0.048 \* TEMP  
HEATV=19000.0

GO TO 10

22 IF (FLUID - 2.0) 23,32,23  
32 SWITCH=1.0  
DENSM=1.000-0.000133\*TEMP

PAGE 2

```

VISKM=-0.1570+102.0/(TEMP +20.0)
CORR=SQRT ((1.00-0.000133*TMAN)/DENSM)
IF (TEMP-32.0) 14,14,15
14 VISKM=100000.0
15 CONTINUE
CLIQ = 1.0000
CPFUEL= 0.4600
CVFUEL= 0.3600
WMOLEC= 18.016
HVAPOR= -1125.0+1.5625*TEMP
SIGMA= 72.7
HEATV=00000.0
GO TO 10
23 IF (FLUID - 3.0) 24,33,24
33 SWITCH=1.0
DENSM=0.830-0.000340*TEMP
VISKM=-0.0890+346.0/(TEMP +190.0)
CORR=SQRT ((0.830-0.000340*TMAN)/DENSM)
CLIQ = 0.4800
CPFUEL= 0.4600
CVFUEL= 0.4070
WMOLEC= 46.000
HVAPOR= -361.0
SIGMA= 26.86 - 0.046 * TEMP
HEATV=11550.0
GO TO 10
24 IF (FLUID - 4.0) 25,34,25
34 SWITCH=1.0
DENSM=0.7893-0.000472*TEMP
VISKM=0.7710-0.002440*TEMP
CORR=SQRT ((0.7893-0.000472*TMAN)/DENSM)
CLIQ = 0.4800
CPFUEL= 0.4000
CVFUEL= 0.3810
WMOLEC= 126.00
HVAPOR= -142.0
SIGMA= 27.20 - 0.052 * TEMP
HEATV=19000.0
GO TO 10
25 IF (FLUID - 5.0) 26,35,26
35 SWITCH=1.0
DENSM=0.7480-(0.00040)*TEMP
VISKM=0.6740-(0.001933)*TEMP
CORR=SQRT ((0.7480-(0.000400)*TMAN)/DENSM)
CLIQ = 0.4800
CPFUEL= 0.4000
CVFUEL= 0.3810
WMOLEC= 126.00
HVAPOR= -142.0
SIGMA= 25.30 - 0.052 * TEMP
HEATV=19000.0
GO TO 10
26 IF (FLUID - 6.0) 27,36,27
36 SWITCH=1.0
DENSM=2328.56812/(TEMP *1.8+32.-2074.76544)+2.03898
VISKM=118.12441/(TEMP *1.8+32.+77.16928)-.07321
CORR=1.0

```

3

CLIQ = 0.5150  
 CPFUEL= 0.4000  
 CVFUEL= 0.3810  
 WMOLEC= 126.00  
 HVAPOR= -142.0

SIGMA= 24.80 - 0.049 \* TEMP  
 HEATV=19000.0

GO TO 10

27 IF (FLUID - 7.0) 28,37,28

37 SWITCH=1.0

DENSM=0.6409 + 41.88/(TEMP +215.0)

VISKM= -0.1250 + 201.0/(TEMP +65.30)

CORR=SQRT ((0.6409+41.88/(TMAN+215.0))/DENSM)

CLIQ=1.0

CPFUEL=0.5

CVFUEL=0.4

WMOLEC=100.0

HVAPOR= -100.0

SIGMA= 38.60 - 0.078 \* TEMP

HEATV=19000.0

GO TO 10

28 IF (FLUID - 8.0) 10,38,10

38 SWITCH=1.0

DENSM=0.6360/(TEMP +459.6)

VISKM=12.0774+4.6452\*TEMP /100.0

CORR=1.0

CLIQ = 0.0000

CPFUEL= 0.2410

CVFUEL= 0.1710

WMOLEC= 28.950

HVAPOR= -000.0

SIGMA= 0.0000

HEATV=00000.0

10 IF (SWITCH) 11,11,12

11 WRITE OUTPUT TAPE 6,13,FLUID

13 FORMAT (1H4,68H THE VALUE OF FLUID IS NOT BETWEEN 0.0 AND 8.0  
 1 THE VALUE IS,F10.3 )

FLUID=1.0

GO TO 20

12 CONTINUE

RETURN

END

---

 COMP ILE MAD
 

---

(1967 VERSION) PROGRAM LISTING ... ..

---

```

EXTERNAL FUNCTION (XX,YY,POINTS,XMIN,GX,YMIN,GY, VAR1 ,SAMEX,
1      FSYMB,XO,YO,FTYPE,FRUN,TEMP,MAIN )
INTEGER SYMBOL,NPOINT,J,T,TYPE,RUN
INTEGER K
ENTRY TO CALMAP.
SAMAX=SAMEX

```

---

```

SAMAX=0.0 .....SET GRID,END PLOT
SAMAX=1.0 ...END PLOT ONLY
SAMAX=2.0 ...SFT GRID ONLY
SAMAX=3.0 ...NFITHER

```

---

```

XORG=XO
YORG=Y0
DX=GX
DY=GY

```

---

CHANGE TO INTEGER FORM

---

```

NPOINT=POINTS
RUN=FRUN
SYMBOL=FSYMB
TYPE=FTYPE
PLTREC.

```

---

```

PLTSIZ. (1.000)
WHENEVER SAMAX.E.1.0.OR.SAMAX.E.3.0,TRANSFER TO NEXT4

```

---

```

BEGIN A PLOT
DRAW THE X AND Y AXES

```

---

```

WHENEVER MAIN .G. 1.50
PAXIS.(XORG,YORG,YMPT,+28,7.50,90.0,YMIN,DY,0.500)
PENUP. (0.670,6.400)
PENDN. (0.670,7.500)
PENDN. (0.670,6.400)
PAXIS.(XORG,YORG,XMPT,-38,7.50,0.0,XMIN,DX,0.500)
PENUP. (2.500,0.570)
PENDN. (7.500,0.570)
PENDN. (2.500,0.570)
PLTOFS. (XMIN,DX,YMIN,DY,XORG,YORG )
PGRID.(XORG,YORG,0.50,0.50,15,15 )
PSYMB. (1.70,9.50,0.20,HEADM,0.00,33 )
PENUP. (1.700,9.450)
PENDN. (7.300,9.450)
PENDN. (1.700,9.450)
PSYMB.(1.90,9.00,0.14,TESTM,0.00,48 )
PSYMB.(2.1,8.70,0.14,MAPINF,0.00,38 )
PNUMBR.(2.60,9.00,0.14,VAR1,0.00,$F5.2*$)
PNUMBR.(3.70,8.70,0.14,FRUN,0.00,$F5.1*$)
PNUMBR.(6.97,9.00,0.14,FSYMB,0.00,$F5.1*$)
PNUMBR.(6.55,8.70,0.14,FTYPE,0.0,$F4.2*$ )
PNUMBR.(4.45,9.00,0.14,TEMP,0.0,$F5.1*$ )
END OF CONDITIONAL

```

---



WHENEVER MAIN .L. 1.50

PAXIS.( XORG,YORG,YMAPT,+28,8.500,90.0,YMIN,DY,0.4250)

PENUP.(0.700,6.650)

PENDN.(0.700,8.000)

PENDN.(0.700,6.650)

PAXIS.( XORG,YORG,XMAPT,-38,6.375,0.0,XMIN,DX,0.4250 )

PENUP.(2.250,0.610)

PENDN.(6.600,0.610)

PENDN.(2.250,0.610)

PLTOFS. ( XMIN,DX,YMIN,DY,XORG,YORG )

PGRID.( XORG,YORG,0.4250,0.4250,15,20 )

PSYMB. (1.20,10.5,0.20,HEADM,0.00,33 )

PENUP.(1.200,10.45)

PENDN.(6.800,10.45)

PENDN.(1.200,10.45)

PSYMB.(1.40,10.0,0.14,TESTM,0.00,48 )

PSYMB.(1.6,9.70,0.14,MAPINF,0.00,38 )

PNUMBR.(2.10,10.0,0.14,VAR1,0.00,\$F5.2\*\$)

PNUMBR.(3.20,9.70,0.14,FRUN,0.00,\$F5.1\*\$)

PNUMBR.(6.47,10.0,0.14,FSYMB,0.00,\$F5.1\*\$ )

PNUMBR.(6.05,9.70,0.14,FTYPE,0.0,\$F4.2\*\$ )

PNUMBR.(3.95,10.0,0.14,TEMP,0.00,\$F5.1\*\$ )

END OF CONDITIONAL

PRINT FORMAT SPACE

VECTOR VALUES SPACE =\$1H0 \*\$

WHENEVER NPOINT .G.35,NPOINT=35

K=0

PRINT COMMENT \$ THE OPERATING MAP GRID HAS BEEN DRAWN \$

THROUGH CHECK, FOR J=0,1,J.E.NPOINT

WHENEVER XX(J).L. 1.0 .OR. XX(J).G. 35.0 ,K=K+1

CONTINUE

NPOINT=NPOINT-K

VECTOR VALUES XMAPT=\$ INTAKE MANIFOLD PRESSURE IN INCHES HG \$

VECTOR VALUES YMAPT=\$ MOIST AIR FLOW IN LBM/HOUR \$

VECTOR VALUES HEADM=\$ CARBURETOR-ENGINE OPERATING MAP \$

VECTOR VALUES TESTM=\$ PO= HG TO= F HUMIDITY= \$

VECTOR VALUES MAPINF=\$DISPLACEMENT= COMP.RATIO= \$

XS=XORG + (XX(1) - 00.00)/DX

YS=YORG+(YY(1)-0.00)/DY

PENUP.(XS,YS)

PLOT THE DATA POINTS

CONTINUE

NPOINT= -NPOINT

SYMBOL=+1

T=0

WHENEVER FSYMB .L. 0.0, T=+1

PLINE.(XX(0),YY(0),NPOINT,1,T,SYMBOL,1)

NPOINT= -NPOINT

PLINE.(XX(0),YY(0),NPOINT,1,T,SYMBOL,1)

WHENEVER SAMAX.G. 1.50,TRANSFER TO EXTR4

PLTEND.

CONTINUE

FUNCTION RETURN

ENTRY TO CALMVH.

XORG=X0

YORG=Y0

SAMAX=SAMEX

DX=GX

```

DY=GY
NPOINT=POINTS
RUN=FRUN
SYMBOL=FSYMB
TYPE=FTYPE
PLTRFC.
WHENEVER SAMAX.E.1.0.OR.SAMAX.E.3.0,TRANSFER TO NEXT

```

```

BEGIN A PLOT

```

```

DRAW THE X AND Y AXIS

```

```

MAIN=0.0 INDEPENDENT PLOTTING VARIABLE IS MAIN JET LOSS
MAIN=1.0 INDEPENDENT PLOTTING VARIABLE IS BOOST SUCTION
MAIN=2.0 INDEPENDENT PLOTTING VARIABLE IS ENRICH. LOSS

```

```

WHENEVER MAIN .E. 0.0
PAXIS.(XORG,YORG,XTITLD,-43,7.50,00.0,XMIN,DX,0.75 )
VECTOR VALUES XTITLD=$ MAIN JET PRESSURE DROP IN INCHES OF WATER
END OF CONDITIONAL
WHENEVER MAIN .E. 1.0
PAXIS.(XORG,YORG,XTITLE,-42,7.50,00.0,XMIN,DX,0.75 )
VECTOR VALUES XTITLE=$ BOOST VENTURI SUCTION IN INCHES OF WATER $
END OF CONDITIONAL
WHENEVER MAIN .E. 2.0
PAXIS.(XORG,YORG,XTITLE,-53,7.50,00.0,XMIN,DX,0.75 )
VECTOR VALUES XTITLE=$ ENRICHMENT ORIFICE PRESSURE DROP IN INCHES
1 TER $
END OF CONDITIONAL
PAXIS.(XORG,YORG,YTITL ,+32,7.50,90.0,YMIN,DY,0.75 )
VECTOR VALUES YTITL =$ FUEL FLOW RATE IN LBM/HOUR $
PLTDFS.(XMIN,DX,YMIN,DY,XORG,YORG)
PGRID.(XORG,YORG,0.75,0.75,10,10 )
PSYMB.(1.7,9.50,0.20,HEADN ,0.0,38 )
VECTOR VALUES HEADN =$COMPUTER PREDICTION OF FUEL FLOW RATE $
PSYMB.(1.8,9.00,0.14,TEST2,0.0,49)
VECTOR VALUES TEST2=$ MAIN ORIFICE NUMBER= FUEL TEMPERATU
PSYMB.(2.0,8.70,0.14,INFOR ,0.0,14)
VECTOR VALUES INFOR =$ RUN NUMBER = $
PSYMB.(5.4,8.70,0.14,LIQUID,0.0,14)
VECTOR VALUES LIQUID=$ FUEL = $
PNUMBR.(3.6,8.700,0.14,RUN,0.0,$I7*$ )
PNUMBR.(7.4, 9.00,0.14,TEMP,0.0,$F5.1*$ )

```

```

PLOT THE DATA POINTS

```

```

NEXT PLINE.(XX(1),YY(1),NPOINT,1,TYPE,SYMBOL,1)
WHENEVER SAMAX .G. 1.5,TRANSFER TO EXTRY
PLTEND.

```

```

EXTRY CONTINUE
FUNCTION RETURN
ENTRY TO CALLOG.

```

```

XORG=X0
YORG=Y0
SAMAX=SAMEX
DX=GX
DY=GY

```

```

NPOINT=POINTS
RUN=FRUN
SYMBOL=FSYMB
TYPE=FTYPE
WHENEVER SAMAX.E.1.0.OR.SAMAX.E.3.0,TRANSFER TO NEXT3

```

## DRAW THE X AND Y AXIS

WHENEVER MAIN .E. 0.0

PLGAXS.(XORG,YORG,XTITLM,-43,7.50,00.0,XMIN,DX )

VECTOR VALUES XTITLM=\$ MAIN JET PRESSURE DROP IN INCHES OF WATER \$

END OF CONDITIONAL

WHENEVER MAIN .E. 1.0

PLGAXS.(XORG,YORG,XTITLN,-42,7.50,00.0,XMIN,DX )

VECTOR VALUES XTITLN=\$ BOOST VENTURI SUCTION IN INCHES OF WATER \$

END OF CONDITIONAL

WHENEVER MAIN .E. 2.0

PLGAXS.(XORG,YORG,XTITLO,-53,7.50,00.0,XMIN,DX )

VECTOR VALUES XTITLO=\$ ENRICHMENT ORIFICE PRESSURE DROP IN INCHES OF WATER \$

END OF CONDITIONAL

PLGAXS.(XORG,YORG,YTITL3,+33,7.50,90.0,YMIN,DY )

VECTOR VALUES YTITL3=\$ FUEL MASS FLOW RATE IN LBM/HOUR \$

PLTOFS.(XMIN,DX,YMIN,DY,XORG,YORG)

XD=1.0/DX

YD=1.0/DY

PLGGRD.(XORG,YORG,XD,7.50,+7.50,0.0)

PLGGRD.(XORG,YORG,YD,7.50,-7.50,90.0)

PSYMB.(1.5,9.50,0.20,HEAD3,0.0,49)

VECTOR VALUES HEAD3=\$ PREDICTION OF MAIN FUEL FLOW PARAMETERS \$

PSYMB.(1.8,9.00,0.14,TEST6,0.0,49)

VECTOR VALUES TEST6=\$ MAIN ORIFICE NUMBER= FUEL TEMPERATURE = \$

PSYMB.(2.0,8.70,0.14,INFOR3,0.0,14)

VECTOR VALUES INFOR3=\$ RUN NUMBER = \$

PSYMB.(5.4,8.70,0.14,LIQUID,0.0,14)

VECTOR VALUES LIQUID=\$ FUEL = \$

PNUMBR.(3.6,8.700,0.14,RUN,0.0,\$I7\*\$ )

PNUMBR.(7.6,9.000,0.14,TEMP,0.0,\$F5.1\*\$ )

## PLOT THE DATA POINTS

PLTLOG.(3)

PLINE.(XX(1),YY(1),NPOINT,1,TYPE,SYMBOL,1)

PLTREC.

WHENEVER SAMAX .G. 1.5,TRANSFER TO EXTR3

PLTEND.

TRANSFER TO EXTR6

CONTINUE

CONTINUE

FUNCTION RETURN

ENTRY TO CALAVH.

XORG=X0

YORG=Y0

SAMAX=SAMEX

DX=GX

DY=GY

NPOINT=POINTS

RUN=FRUN

SYMBOL=FSYMB

TYPE=FTYPE

PLTREC.

WHENEVER SAMAX.E.1.0 .OR.SAMAX.F.3.0,TRANSFER TO NEXTA

PAXIS.(XORG,YORG,XAIRT,-42,7.50,00.0,XMIN,DX,0.75 )

PAXIS.(XORG,YORG,YAIRT,+33,7.50,90.0,YMIN,DY,0.75 )

VECTOR VALUES XAIRT=\$ BOOST VENTURI SUCTION IN INCHES OF WATER \$

VECTOR VALUES YAIRT=\$ AIR BLEED FLOW RATE IN LBM/HOUR \$

PLTOFS.(XMIN,DX,YMIN,DY,XORG,YORG )

PGRID.(XORG,YORG,0.75,0.75,10,10 )

PSYMB.(1.5,9.50,0.20,AHEAD,0.0,49 )

```
VECTOR VALUES AHEAD=$ COMPUTER PREDICTION OF AIR BLEED FLOW RATE
PSYMB.(1.8,9.00,0.14,ATEST,0.0,49)
VECTOR VALUES ATEST=$ AIR BLEED DIAMETERS= FUEL TEMPERATUR
PSYMB.(2.0,8.70,0.14,ANFORM,0.0,14 )
VECTOR VALUES ANFORM=$ RUN NUMBER = $
PSYMB. (5.4,8.70,0.14,FLOAIR,0.0,14)
VECTOR VALUES FLOAIR=$ FUEL = $
PNUMBR.(3.6,8.700,0.14,RUN,0.0,$I7*$ )
PNUMBR.(7.4,9.000,0.14,TEMP,0.0,$F5.1*$ )
PLOT THE DATA POINTS
NEXTA PLINE.(XX(1),YY(1),NPOINT,1,TYPE,SYMBOL,1)
WHENEVER SAMAX .G. 1.5,TRANSFER TO AEXTR
PLTEND.
AEXTR CONTINUE
FUNCTION RETURN
END OF FUNCTION
```

COMPILE MAD

MAY 1967 VERSION) PROGRAM LISTING ... ..

```

EXTERNAL FUNCTION (XX,YY,POINTS,XMIN,GX,YMIN,GY, VARI ,SAMEX,
1      FSYMB,XO,YO,FTYPE,FRUN,TEMP,MAIN )
INTEGER SYMBOL,NPOINT,J,T,TYPE,RUN
ENTRY TO CALCVR.
XORG=XO
YORG=YO
-----
SAMAX=SAMEX
DX=GX
DY=GY
NPOINT=POINTS
RUN=FRUN
SYMBOL=FSYMB
-----
TYPE=FTYPE
PLTREC.
WHENEVER SAMAX.F.1.0.OR.SAMAX.E.3.0,TRANSFER TO NXTPLT
  BEGIN A PLOT
  DRAW THE X AND Y AXIS
  WHENEVER MAIN .E. 0.0
PAXIS.(XORG,YORG,YTITLA,+35,7.50,90.0,YMIN,DY,0.75 )
VECTOR VALUES YTITLA=$ MAIN JET COEFFICIENT OF DISCHARGE $
PSYMB.(1.3,9.50,0.20,HEADNA,00.0,44 )
VECTOR VALUES HEADNA=$ MAIN METERING ORIFICE CHARACTERISTIC CURVE $
END OF CONDITIONAL
WHENEVER MAIN .F. 1.0
PAXIS.(XORG,YORG,YTITLB,+39,7.50,90.0,YMIN,DY,0.75 )
VECTOR VALUES YTITLB=$ MAIN CHANNEL COEFFICIENT OF DISCHARGE $
PSYMB.(1.3,9.50,0.20,HEADNB,00.0,35 )
VECTOR VALUES HEADNB=$ MAIN CHANNEL CHARACTERISTIC CURVE $
END OF CONDITIONAL
WHENEVER MAIN .E. 2.0
PAXIS.(XORG,YORG,YTITLC,+45,7.50,90.0,YMIN,DY,0.75 )
VECTOR VALUES YTITLC=$ ENRICHMENT ORIFICE COEFFICIENT OF DISCHARGE $
PSYMB.(1.3,9.50,0.20,HEADNC,00.0,41 )
VECTOR VALUES HEADNC=$ ENRICHMENT ORIFICE CHARACTERISTIC CURVE $
END OF CONDITIONAL
PAXIS.(XORG,YORG,XTITLR,-34,7.50,0.0,XMIN,DX,0.75 )
VECTOR VALUES XTITLR=$ REYNOLDS NUMBER OVER ONE THOUSAND$
PLTOFS.(XMIN,DX,YMIN,DY,XORG,YORG)
PGRID.(XORG,YORG,.75,.75,10,10)
PSYMB.(1.8,9.00,0.14,TEST1,0.0,49 )
VECTOR VALUES TEST1=$ MAIN ORIFICE NUMBER=          FUEL TEMPERATURE = $
PSYMB.(2.0,8.70,0.14,INFORM,0.0,14 )
VECTOR VALUES INFORM=$ RUN NUMBER = $
PSYMB.(5.4,8.70,0.14,LIQUID,0.0,14)
VECTOR VALUES LIQUID=$ FUEL =          $
PNUMBR.(3.6,8.700,0.14,RUN,0.0,$I7*$ )
PNUMBR.(7.4,9.000,0.14,TEMP,0.0,$F5.1*$ )
  PLOT THE DATA POINTS
-----
PLINE.(XX(1),YY(1),NPOINT,1,TYPE,SYMBOL,1)
WHENEVER SAMAX .G. 1.5,TRANSFER TO EXTRA
PLTEND.
CONTINUE
FUNCTION RETURN

```

ENTRY TO CALCVM.

XORG=XO

YORG=YO

SAMAX=SAMEX

DX=GX

DY=GY

NPOINT=POINTS

RUN=FRUN

SYMBOL=FSYMB

TYPE=FTYPE

PLTREC.

WHENEVER SAMAX.E.1.0.OR.SAMAX.E.3.0,TRANSFER TO NEXT2  
DRAW THE X AND Y AXIS

WHENEVER MAIN .E. 0.0

PAXIS.(XORG,YORG,YTITLJ,+32,7.50,90.0,YMIN,DY,0.75 )

VECTOR VALUES YTITLJ=\$ MAIN JET DISCHARGE COEFFICIENT \$

PSYMB.(1.3,9.50,0.20,HEADJ,00.0,45 )

VECTOR VALUES HEADJ=\$ MAIN JET DISCHARGE COEFFICIENT VS FLOW RATE  
END OF CONDITIONAL

WHENEVER MAIN .E. 1.0

PAXIS.(XORG,YORG,YTITLK,+41,7.50,90.0,YMIN,DY,0.75 )

VECTOR VALUES YTITLK=\$ MAIN FLOW CHANNEL DISCHARGE COEFFICIENT \$

PSYMB.(1.3,9.50,0.20,HEADK,00.0,45 )

VECTOR VALUES HEADK=\$ CHANNEL DISCHARGE COEFFICIENT VS FLOW RATE  
END OF CONDITIONAL

WHENEVER MAIN .E. 2.0

PAXIS.(XORG,YORG,YTITLL,+42,7.50,90.0,YMIN,DY,0.75 )

VECTOR VALUES YTITLL=\$ ENRICHMENT ORIFICE DISCHARGE COEFFICIENT \$

PSYMB.(1.3,9.50,0.20,HEADL,00.0,45 )

VECTOR VALUES HEADL=\$ ENRICHMENT ORIFICE COEFFICIENT VS FLOW RATE  
END OF CONDITIONAL

PAXIS.(XORG,YORG,XTITL2,-33,7.50,0.0,XMIN,DX,0.75 )

VECTOR VALUES XTITL2=\$ FUEL FLOW RATE IN LBM/HOUR \$

PLTOFS.(XMIN,DX,YMIN,DY,XORG,YORG)

PGRID.(XORG,YORG,0.75,0.75,10,10 )

PSYMB.(1.8,9.00,0.14,TEST5,0.0,49 )

VECTOR VALUES TEST5=\$ MAIN ORIFICE NUMBER= FUEL TEMPERATU

PSYMB.(2.0,8.70,0.14,INFOR2,0.0,14)

VECTOR VALUES INFOR2=\$ RUN NUMBER = \$

PSYMB.(5.4,8.70,0.14,LIQUID,0.0,14)

VECTOR VALUES LIQUID=\$ FUEL = \$

PNUMBR.(3.6,8.700,0.14,RUN,0.0,\$I7\*\$ )

PNUMBR.(7.4,9.000,0.14,TEMP,0.0,\$F5.1\*\$ )

PLOT THE DATA POINTS

NEXT 2 PLINE.(XX(1),YY(1),NPOINT,1,TYPE,SYMBOL,1)

WHENEVER SAMAX .G. 1.5,TRANSFER TO EXTR2

PLTEND.

EXTR 2 CONTINUE

FUNCTION RETURN

ENTRY TO CALCVH.

XORG=XO

YORG=YO

SAMAX=SAMEX

DX=GX

DY=GY

NPOINT=POINTS

RUN=FRUN

SYMBOL=FSYMB

TYPE=FTYPE

PLTREC.

WHENEVER SAMAX.E.1.0.OR.SAMAX.E.3.0,TRANSFER TO NEX1

DRAW THE X AND Y AXIS

WHENEVER MAIN .E. 0.0

PAXIS.(XORG,YORG,XTITLG,-47,7.50,00.0,XMIN,DX,0.75 )

PAXIS.(XORG,YORG,YTITLG,+32,7.50,90.0,YMIN,DY,0.75 )

PSYMB.(1.1,9.50,0.20,HEADG,00.0,49 )

VECTOR VALUES XTITLG=\$ MAIN ORIFICE PRESSURE DROP IN INCHES OF WATER \$

VECTOR VALUES YTITLG=\$ MAIN JET DISCHARGE COEFFICIENT \$

VECTOR VALUES HEADG=\$ MAIN JET DISCHARGE COEFFICIENT VS PRESSURE LOSS \$

END OF CONDITIONAL

WHENEVER MAIN .E. 1.0

PAXIS.(XORG,YORG,XTITLH,-42,7.50,00.0,XMIN,DX,0.75 )

PAXIS.(XORG,YORG,YTITLG,+32,7.50,90.0,YMIN,DY,0.75 )

PSYMB.(1.1,9.50,0.20,HEADH,00.0,49 )

VECTOR VALUES XTITLH=\$ BOOST VENTURI SUCTION IN INCHES OF WATER \$

VECTOR VALUES YTITLH=\$ MAIN FLOW CHANNEL DISCHARGE COEFFICIENT \$

VECTOR VALUES HEADH=\$ CHANNEL DISCHARGE COEFFICIENT VS BOOST SUCTION \$

END OF CONDITIONAL

WHENEVER MAIN .E. 2.0

PAXIS.(XORG,YORG,XTITLI,-53,7.50,00.0,XMIN,DX,0.75 )

PAXIS.(XORG,YORG,YTITLI,+42,7.50,90.0,YMIN,DY,0.75 )

PSYMB.(1.1,9.50,0.20,HEADI,00.0,49 )

VECTOR VALUES XTITLI=\$ ENRICHMENT ORIFICE PRESSURE DROP IN INCHES OF WA

1 TER \$

VECTOR VALUES YTITLI=\$ ENRICHMENT ORIFICE DISCHARGE COEFFICIENT \$

VECTOR VALUES HEADI=\$ ENRICHMENT ORIFICE COEFFICIENT VS PRESSURE LOSS \$

END OF CONDITIONAL

PLTOFS.(XMIN,DX,YMIN,DY,XORG,YORG)

PGRID.(XORG,YORG,0.75,0.75,10,10 )

PSYMB.(1.8,9.00,0.14,TEST4,0.0,49 )

VECTOR VALUES TEST4=\$ MAIN ORIFICE NUMBER=

FUEL TEMPERATURE = \$

PSYMB.(2.0,8.70,0.14,INFOR1,0.0,14)

VECTOR VALUES INFOR1=\$ RUN NUMBER = \$

PSYMB.(5.4,8.70,0.14,LIQUID,0.0,14)

VECTOR VALUES LIQUID=\$ FUEL = \$

PNUMBR.(3.6,8.700,0.14,RUN,0.0,\$I7\*\$ )

PNUMBR.(7.4,9.000,0.14,TEMP,0.0,\$F5.1\*\$ )

PLOT THE DATA POINTS

PLINE.(XX(1),YY(1),NPOINT,1,TYPE,SYMBOL,1)

WHENEVER SAMAX .G. 1.5,TRANSFER TO EXTR1

PLTEND.

CONTINUE

FUNCTION RETURN

END OF FUNCTION

1

COMPILE MAL

(17 MAY 1967 VERSION) PROGRAM LISTING ... ..

```

EXTERNAL FUNCTION (XX,YY,POINTS,XMIN,GX,YMIN,GY, VARI ,SAMEX,
1      FSYMB,XO,YO,FTYPE,FRUN,TEMP,MAIN )
INTEGER SYMBOL,NPOINT,TYPE,RUN
ENTRY TO CALIVA.
XORG=XO
YORG=YO
-----
SAMAX=SAMEX
DX=GX
DY=GY
NPOINT=POINTS
RUN=FRUN
SYMBOL=FSYMB
-----
TYPE=FTYPE
PLTREC.
WHENEVER SAMAX.E. 1.0 .OR. SAMAX.E. 3.0,TRANSFER TO NEXTIA
  BEGIN A PLOT
  DRAW THE X AND Y AXIS
  XT=8.925/14.00
-----
  YT=6.375/10.00
  PAXIS. (XORG,YORG,YTITL5,+22,6.375,90.0,0.0,DY,YT )
  PLTOFS. (0.0,DX,0.0,DY,XORG,YORG)
  VECTOR VALUES YTITL5=$ INDICATED HORSEPOWER      $
  PAXIS. (XORG,YORG,XTITL5,-33,8.925,0.0,0.0,DX,XT )
  VECTOR VALUES XTITL5=$ DRY AIR FLOW RATE IN LBM/HOUR      $
-----
  PGRID. (XORG,YORG,XT,YT,14,10)
  PSYMB. (3.0,9.125,0.200,HEAD5,0.0,43 )
  VECTOR VALUES HEAD5=$ SIMULATION OF CARBURETOR-ENGINE OPERATION
NEXTIA  PLINE. (XX(1),YY(1),NPOINT,1,TYPE,SYMBOL,1 )
  WHENEVER SAMAX .G. 1.50,TRANSFER TO EXTRIA
  PLTEND.
-----
EXTRIA  CONTINUE
  FUNCTION RETURN
  ENTRY TO CALIVF.
  XORG=XO
  YORG=YO
  SAMAX=SAMEX
-----
  DX=GX
  DY=GY
  NPOINT=POINTS
  RUN=FRUN
  SYMBOL=FSYMB
  TYPE=FTYPE
-----
  PLTREC.
  WHENEVER SAMAX.E. 1.0 .OR. SAMAX.E. 3.0,TRANSFER TO NEXTFI
  BEGIN A PLOT
  DRAW THE X AND Y AXIS
  XT=8.925/14.00
-----
  YT=6.375/10.00
  PAXIS. (XORG,YORG,YTITL3,+22,6.375,90.0,0.0,DY,YT )
  PLTOFS. (0.0,DX,0.0,DY,XORG,YORG)
  VECTOR VALUES YTITL3=$ INDICATED HORSEPOWER      $
  PAXIS. (XORG,YORG,XTITL3,-27,8.925,0.0,0.0,DX,XT )
  VECTOR VALUES XTITL3=$ OVERALL FUEL-AIR RATIO      $

```



PGRID. (XORG,YORG,XT,YT,14,10)

PSYMB. (3.0,9.125,0.200,HEAD3,0.0,43 )

VECTOR VALUES HEAD3=\$ SIMULATION OF CARBURETOR-ENGINE OPERATION \$

FI PLINE. (XX(1),YY(1),NPOINT,1,TYPE,SYMBOL,1 )

WHENEVER SAMAX .G. 1.50,TRANSFER TO EXTRFI

PLTEND.

FI CONTINUE

FUNCTION RETURN

ENTRY TO CALBVR.

XORG=X0

YORG=Y0

SAMAX=SAMEX

DX=GX

DY=GY

NPOINT=POINTS

RUN=FRUN

SYMBOL=FSYMB

TYPE=FTYPE

PLTREC.

PLTSIZ. (0.750)

WHENEVER SAMAX.E. 1.0 .OR. SAMAX.E. 3.0,TRANSFER TO NEXTBB

BEGIN A PLOT

DRAW THE X AND Y AXIS

PAXIS. (XORG,YORG,YTITL1,+47,10.0,90.0,0.30,0.10,1.00 )

PLTOFS. (0.0,10.0,0.30,0.10,XORG,YORG)

VECTOR VALUES YTITL1=\$ BRAKE SPECIFIC FUEL CONSUMPTION IN LBM/BHP HR \$

PAXIS. (XORG,YORG,XTITL1,-27,10.0,0.0,0.0,10.0,1.00 )

VECTOR VALUES XTITL1=\$ ENGINE BRAKE HORSEPOWER \$

PGRID. (XORG,YORG,1.0,1.0,10,10)

PSYMB. (3.30,12.90,0.20,HEAD1,0.0,43 )

VECTOR VALUES HEAD1=\$ SIMULATION OF CARBURETOR-ENGINE OPERATION \$

PSYMB. (4.30,12.40,0.20,HEAD2,0.0,23 )

VECTOR VALUES HEAD2=\$ ROAD LOAD BSFC VALUES \$

BB PLINE. (XX(1),YY(1),NPOINT,1,TYPE,SYMBOL,1 )

WHENEVER SAMAX .G. 1.50,TRANSFER TO EXTRBB

PLTEND.

BB CONTINUE

FUNCTION RETURN

ENTRY TO CALFVA.

XORG=X0

YORG=Y0

SAMAX=SAMEX

DX=GX

DY=GY

NPOINT=POINTS

RUN=FRUN

SYMBOL=FSYMB

TYPE=FTYPE

PLTREC.

WHENEVER SAMAX.E. 1.0 .OR. SAMAX.E. 3.0,TRANSFER TO NEXTFA

BEGIN A PLOT

DRAW THE X AND Y AXIS

XT=8.925/14.00

YT=6.375/10.00

PAXIS. (XORG,YORG,YTITL4,+24,6.375,90.0,0.0300,DY,YT )

PLTOFS. (0.0,DX,0.0300,DY,XORG,YORG)

VECTOR VALUES YTITL4=\$ OVERALL FUEL-AIR RATIO \$

PAXIS. (XORG,YORG,XTITL4,-33,8.925,0.0,0.0,DX,XT )

VECTOR VALUES XTITL4=\$ DRY AIR FLOW RATE IN LBM/HOUR \$

PGRID. (XORG,YORG,XT,YT,14,10)

```

PSYMB. (3.0,9.125,0.200,HEAD4,0.0,43 )
VECTOR VALUES HEAD4=$ PREDICTED FUEL-AIR RATIO VS. DRY AIR FLOW
NEXTFA PLINE. (XX(1),YY(1),NPOINT,1,TYPE,SYMBOL,1 )
        WHENEVER SAMAX .G. 1.50,TRANSFER TO EXTRFA
        PLTEND.
EXTRFA CONTINUE
        FUNCTION RETURN
        ENTRY TO CALMVS.
        XORG=XD
        YORG=YD
        SAMAX=SAMEX
        DX=GX
        DY=GY
        NPOINT=POINTS
        RUN=FRUN
        SYMBOL=FSYMB
        TYPE=FTYPE
        PLTREC.
        WHENEVER SAMAX.E. 1.0 .OR. SAMAX.E. 3.0,TRANSFER TO NEXTMS
        BEGIN A PLOT
        DRAW THE X AND Y AXIS
        XT=6.375/10.00
        YT=8.925/14.00
        PAXIS. (XORG,YORG,YTITL6,+27,8.925,90.0,0.0,DY,YT )
        PLTOFS. (0.0,DX,0.0,DY,XORG,YORG)
        VECTOR VALUES YTITL6=$ VEHICLE MILES PER GALLON      $
        PAXIS. (XORG,YORG,XTITL6,-25,6.375,0.0,0.0,DX,XT )
        VECTOR VALUES XTITL6=$ VEHICLE MILES PER HOUR        $
        PGRID. (XORG,YORG,XT,YT,10,14)
        PSYMB. (2.05,11.75,0.150,HEAD6,0.0,39 )
        VECTOR VALUES HEAD6=$ PREDICTED ROAD LOAD FUEL ECONOMY  $
NEXTMS PLINE. (XX(1),YY(1),NPOINT,1,TYPE,SYMBOL,1 )
        WHENEVER SAMAX .G. 1.50,TRANSFER TO EXTRMS
        PLTEND.
EXTRMS CONTINUE
        FUNCTION RETURN
        END OF FUNCTION

```

APPENDIX K

ADDITIONAL FLOW MODEL CURVES AND  
DATA UTILIZED WITHIN THE SIMULATION

TABLE XXVIII  
 REDUCED DATA FOR A LUCITE FLOW MODEL  
 TEST USING HOT MINERAL SPIRITS

LUCITE FLOW MODEL TEST

THIS DATA IS FOR TEST NUMBER 1011671 THIS TEST IS FOR MINERAL SPIRITS AT A MEAN TEMPERATURE OF 135.0

THE JET HAS A DIAMETER OF .0502 INCHES AND A LENGTH OF .1830 INCHES  
 THE FLUID VISCOSITY IN CENTIPOISES IS .878  
 THE FLUID SPECIFIC GRAVITY IS .761  
 THE MAIN JET IS OPEN  
 THE LOWER MAIN AIR BLEED IS OPEN  
 THE UPPER MAIN AIR BLEED IS OPEN  
 THE INDEPENDENT PLOTTING VARIABLE IS THE BCCST VENTURI SUCTION  
 THE REYNOLDS NUMBER IS BASED ON THE MAIN CRIFICE DIAMETER

\*\*\* PROGRAM RESULTS FOR THIS RUN \*\*\*

RUN	BLEDP	FATEPH	RE	CCCFAN	RVSUCH	CDJET	PDRPW	DELPRM	DELPM	FMULW	PFFCFN
1	.211	6.68	1258.0	.5563	3.23	.7362	2.12	.13	-.03	1.24	53.6
2	.278	8.46	1593.3	.6463	4.40	.7794	3.03	.17	-.03	1.56	57.7
3	.348	10.36	1951.1	.6663	6.21	.7776	4.56	.25	-.02	1.32	63.9
4	.386	11.49	2162.8	.6656	7.63	.7903	5.43	.28	-.02	2.44	62.5
5	.429	13.23	2490.9	.6960	9.28	.8106	6.84	.40	-.02	2.70	65.6
6	.464	14.14	2662.0	.6959	10.60	.8141	7.75	.50	-.01	3.15	65.4
7	.488	14.75	2777.9	.6943	11.60	.8076	8.57	.47	.00	3.42	66.6
8	.528	16.07	3025.3	.7160	12.94	.8246	9.75	.57	.01	3.62	68.3
9	.567	17.10	3220.9	.7198	14.51	.8277	10.97	.57	.02	4.10	68.9
10	.592	18.07	3401.8	.7194	16.20	.8267	12.27	.68	.03	4.48	68.4
11	.588	18.12	3412.1	.7251	16.05	.8346	12.11	.67	.02	4.48	65.0
12	.612	18.87	3552.7	.7262	17.34	.8395	12.98	.72	.03	4.87	68.6

RUN	QCOTF	KATICM	RATICV	GCCTA	AIRVEL	VIDELA	WIDELA	SUMERR	DELAW	CDAIR	REAIRB
1	.14	31.61	20.81	2.93	54.5	114.1	.44	-.14	2.21	.477	1426.1
2	.18	30.42	21.62	3.85	71.7	134.2	.52	-.16	3.06	.534	1876.7
3	.22	29.80	22.07	4.82	89.6	161.2	.63	-.18	4.41	.556	2345.9
4	.24	29.78	22.08	5.34	99.4	177.8	.69	-.15	5.36	.559	2602.2
5	.28	30.84	21.32	5.94	110.5	197.1	.77	-.09	6.59	.561	2894.0
6	.30	30.49	21.57	6.42	119.4	210.4	.82	.00	7.52	.568	3127.9
7	.31	30.21	21.76	6.76	125.8	220.2	.85	.04	8.23	.571	3294.3
8	.34	30.45	21.59	7.31	135.9	233.2	.91	.11	9.23	.583	3599.3
9	.36	30.19	21.78	7.85	146.0	246.8	.96	.19	10.34	.591	3823.0
10	.38	30.50	21.56	8.20	152.6	261.1	1.01	.25	11.57	.584	3995.6
11	.38	30.79	21.35	8.15	151.6	259.7	1.01	.23	11.45	.584	3970.0
12	.40	30.83	21.33	8.48	157.7	269.9	1.05	.21	12.37	.584	4128.8

TABLE XXIX  
 REDUCED DATA FOR A LUCITE FLOW MODEL  
 TEST USING COLD MINERAL SPIRITS

LUCITE FLOW MODEL TEST

THIS DATA IS FOR TEST NUMBER 1110671 THIS TEST IS FOR LAB GAS AT A MEAN TEMP OF 32.0 F NO AIR BLEEDS

THE JET HAS A DIAMETER OF .0502 INCHES AND A LENGTH OF .1830 INCHES  
 THE FLUID VISCOSITY IN CENTISTOKES IS .742  
 THE FLUID SPECIFIC GRAVITY IS .751  
 THE MAIN JET IS OPEN  
 THE INDEPENDENT PLOTTING VARIABLE IS THE MAIN JET PRESSURE DRCP  
 THE REYNOLDS NUMBER IS BASED ON THE MAIN CRIFICE DIAMETER

\*\*\* PROGRAM RESULTS FOR THIS RUN \*\*\*

RUN	HVSUC	KATEPH	RE	CCCCAN	BVSUCM	CELPW	DELBPW	DELPXW	EMULW	CDJET	PERCFW
1	1.01	3.44	776.4	.6433	.74	.66	.01	.03	.04	.6815	52.6
2	2.14	5.57	1258.0	.7160	1.58	1.47	.05	.06	.09	.7407	73.4
3	3.03	6.86	1548.6	.7408	2.23	2.10	.14	.10	.11	.7638	76.6
4	3.88	7.94	1793.3	.7581	2.86	2.70	.24	.10	.14	.7794	78.9
5	5.13	9.40	2121.8	.7800	3.78	3.68	.27	.09	.18	.7909	83.2
6	6.05	10.38	2343.7	.7934	4.46	4.37	.34	.07	.18	.8014	84.9
7	6.93	11.13	2513.0	.7948	5.11	5.00	.35	.10	.24	.8030	85.7
8	7.90	11.97	2702.9	.8007	5.82	5.73	.41	.10	.25	.8074	86.8
9	8.25	13.17	2873.9	.8142	6.82	6.74	.46	.10	.29	.8186	88.1
10	10.62	14.25	3216.3	.8218	7.83	7.74	.54	.13	.32	.8264	88.6
11	12.64	15.65	3532.3	.8273	9.31	9.23	.63	.13	.38	.8309	89.7
12	13.91	16.50	3724.2	.8314	10.25	10.17	.69	.15	.39	.8347	90.2
13	13.87	16.50	3724.2	.8326	10.22	10.15	.69	.16	.39	.8353	90.3
14	15.05	17.26	3895.7	.8361	11.09	11.05	.76	.18	.39	.8375	90.9
15	16.73	18.35	4141.9	.8431	12.33	12.27	.82	.16	.43	.8452	91.2
16	18.21	19.17	4327.6	.8444	13.42	13.33	.85	.19	.44	.8472	91.3
17	19.08	20.20	4560.0	.8555	14.50	14.37	.86	.23	.43	.8472	91.3
18	21.44	21.19	4783.2	.8601	15.80	15.59	.94	.21	.49	.8598	91.3
19	21.53	21.13	4770.4	.8560	15.86	15.62	.97	.14	.52	.8658	91.0
20	23.15	21.94	4953.6	.8572	17.06	16.81	.99	.35	.39	.8627	91.0
21	24.55	22.76	5138.3	.8635	18.09	17.83	1.02	.31	.54	.8636	91.3
22	25.99	23.28	5255.7	.8584	19.15	18.77	1.01	.53	.54	.8697	91.5
23	27.94	24.30	5486.3	.8642	20.59	20.19	1.13	.27	.77	.8671	91.5

## LOG-LOG PLOT OF SYSTEM FLOW PARAMETERS

MAIN ORIFICE NUMBER= **F-50** AVERAGE TEMP = 32.0 °F  
 RUN NUMBER = 1110671 TEST FLUID = **STANDARD REG. GASOLINE**

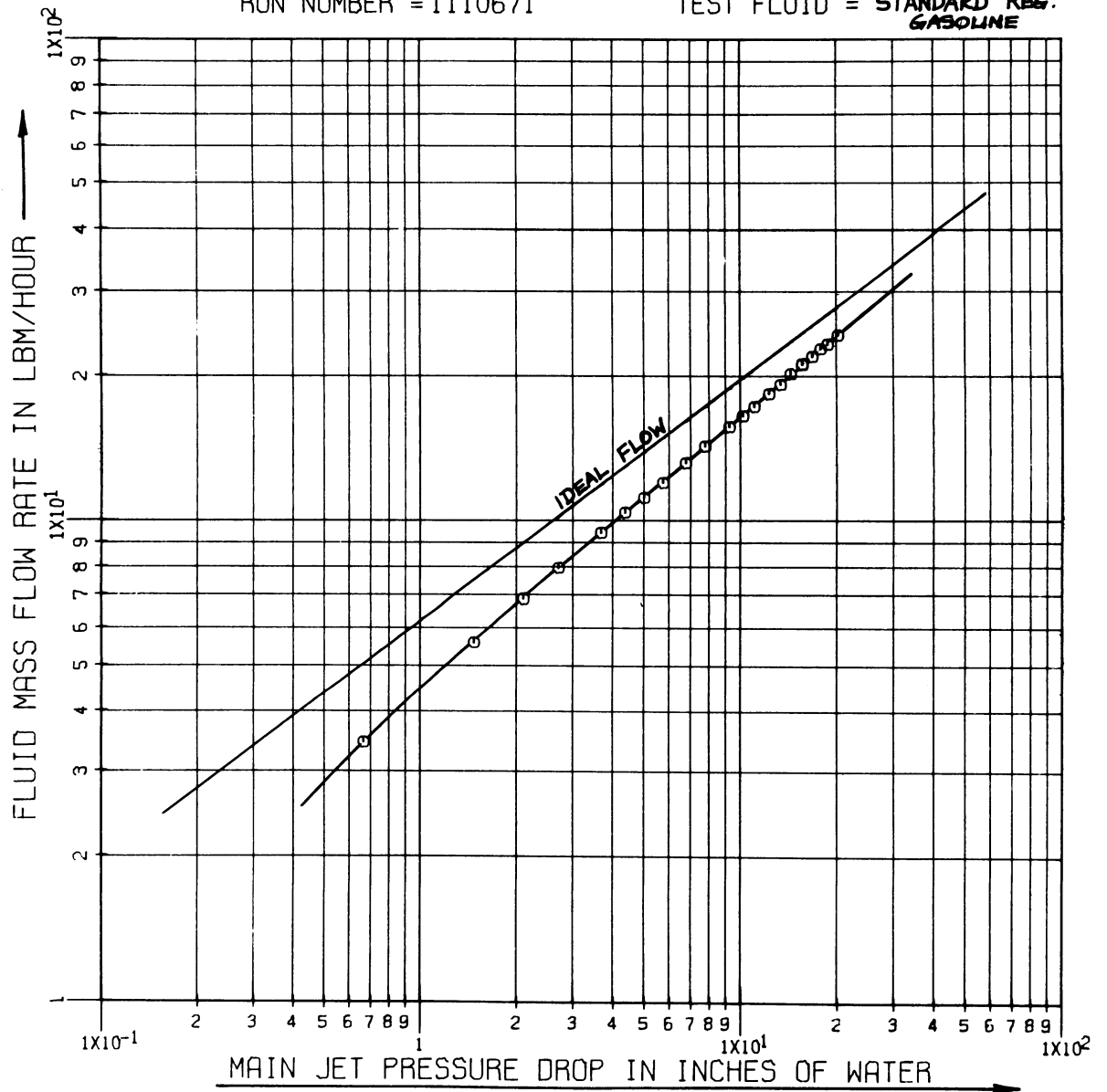


Figure 82. Fuel Mass Flow Rate As A Function Of The Main Metering Orifice Pressure Differential In The Lucite Flow Model

### MAIN CHANNEL CHARACTERISTIC CURVE

MAIN ORIFICE NUMBER = **F-50**    AVERAGE TEMP = 100.0 °F  
RUN NUMBER = 621671            TEST FLUID = **MIN.SPIRITS**

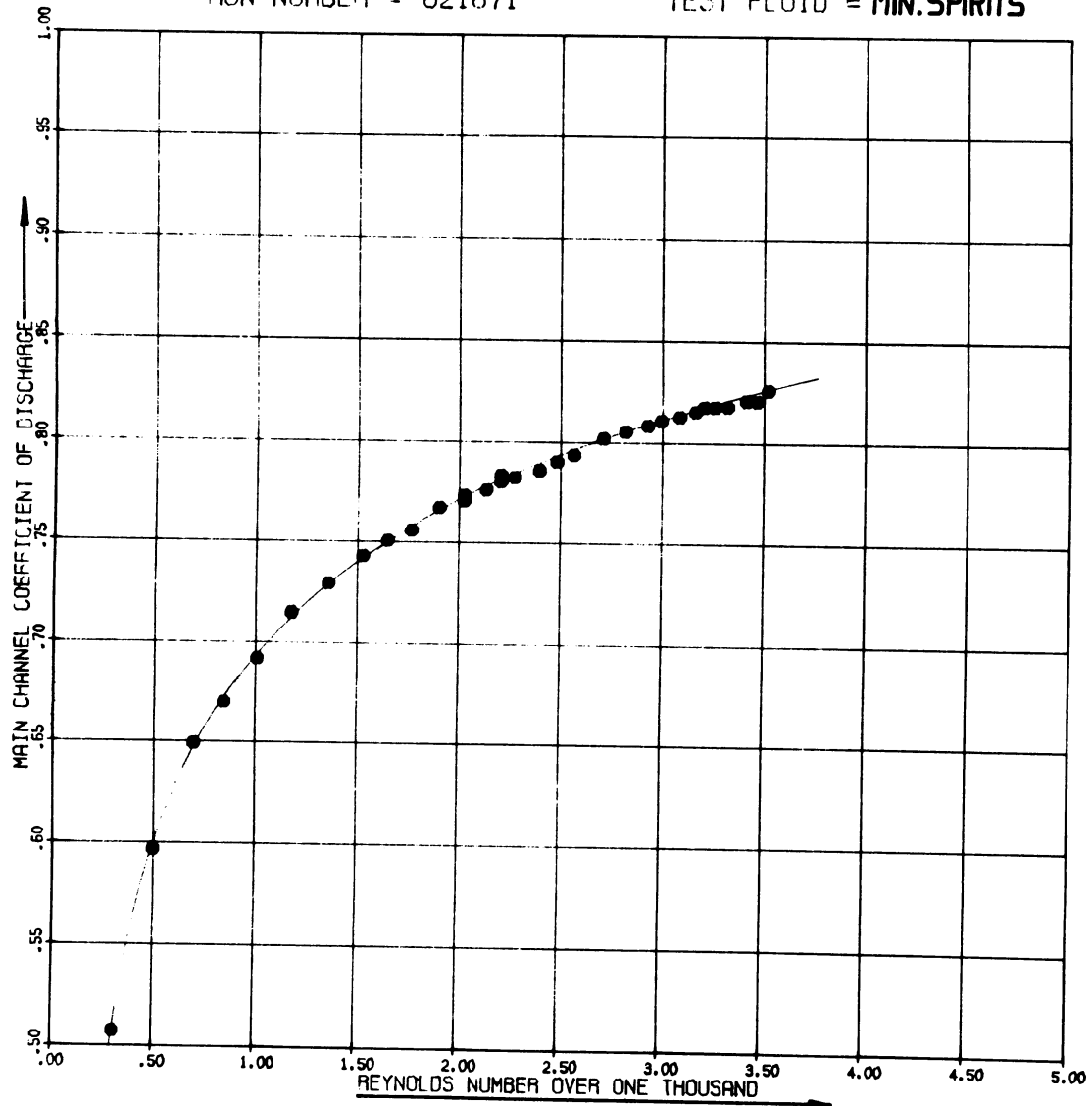


Figure 83. Main Fuel Channel Discharge Coefficient Curve

## FLUID FLOW RATE VS PRESSURE DROP

MAIN ORIFICE NUMBER = **F-50**      AVERAGE TEMP = 135.0°F  
 RUN NUMBER = 919671                      TEST FLUID = **MIN. SPIRITS**

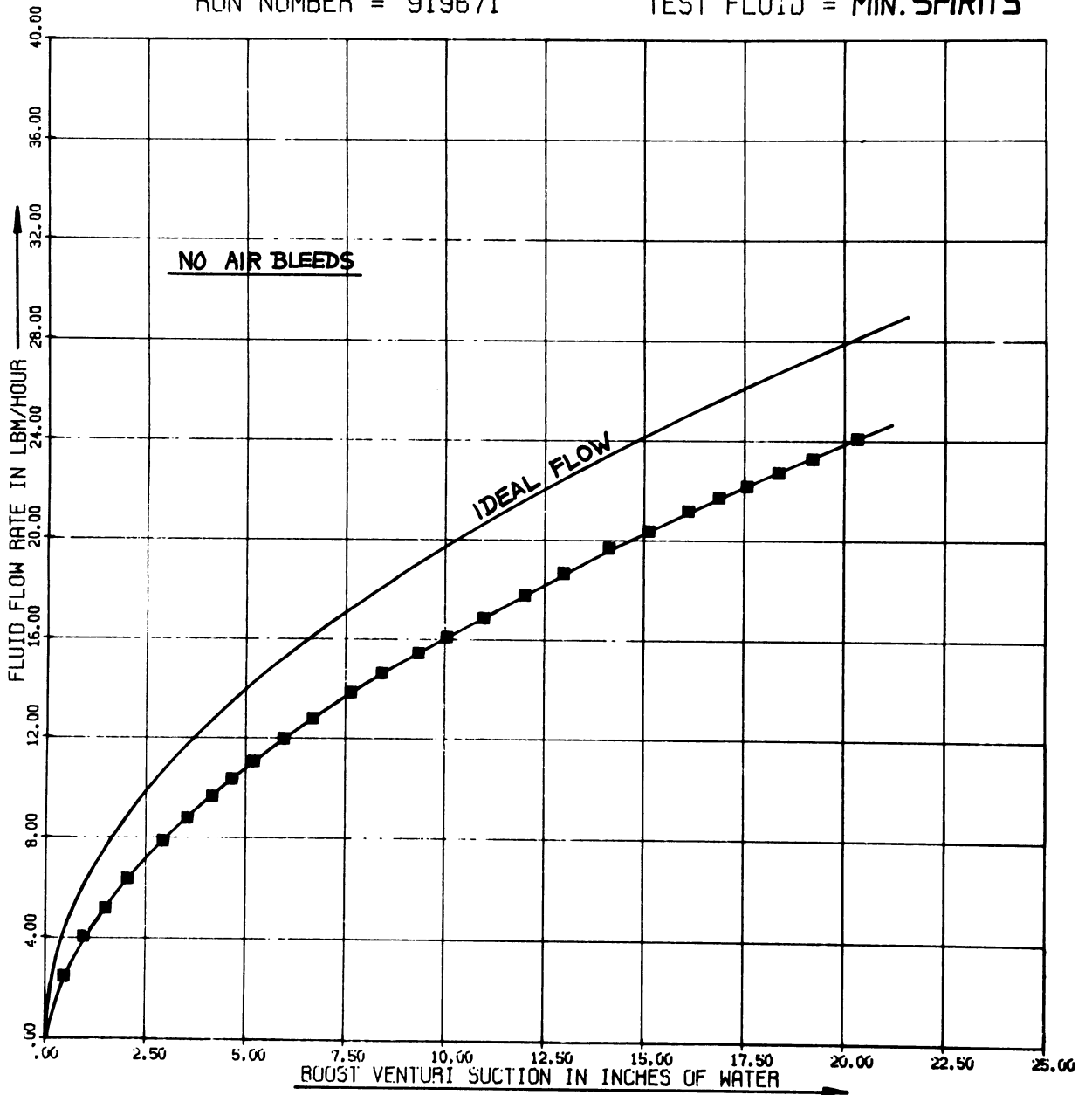


Figure 84. Mass Flow Rate Of Hot Test Fluid Within The Lucite Flow Model



TABLE XXX  
 SPECIFICATIONS AND EXPERIMENTAL VALUES  
 FOR A TYPICAL TEST CARBURETOR

Carburetor Model: C6AF-9510-B

Carburetor Type: Ford 2-barrel, fixed jet, air bled, 1 boost venturi

Main venturi throat diameter = 1.1450 inches

Throttle bore diameter = 1.4370 inches

Boost venturi throat diameter = 0.538 inches

Boost venturi outer diameter = 0.750 inches

Throttle plate shaft diameter = 0.375 inches

Main venturi area = 1.0257 in<sup>2</sup> (per venturi)

Throttle bore area = 1.6211 in<sup>2</sup> (per bore)

Maximum throttle flow area = 1.0910 in<sup>2</sup> (per bore)

Boost venturi throat area = 0.2273 in.<sup>2</sup> (per venturi)

Net main venturi throat flow area = 0.5787 in<sup>2</sup> (area external to boost venturi)

Ratio of:  $\frac{\text{Net main venturi area}}{\text{Boost venturi throat area}} = 2.586$

Total venturi throat flow area = 0.8442 in<sup>2</sup> (per barrel)

Throttle angle (fully opened) = 85.0°

Throttle angle (fully closed) = 10.0°

Throttle angle (normal idle) = 12.5°

#### EXPERIMENTAL AIR FLOW VALUES

Throttle plate leakage (throttle closed) = 13.90 lbm air/hr (per barrel)

Maximum transfer tube flow = 4.40 lbm air/hr (per tube)

TABLE XXX (continued)

Maximum enrichment valve air bleed flow = 4.35 lbm air/hr.

Total air flow with closed throttle =  $2(13.90) + 2(4.40) + 4.35 = 41.0$  lbm/hr.  
(both barrels)

Idle air flow (typical value) = 64.0 lbm air/hr. (both barrels).

TABLE XXXI

VISCOSITY CONVERSIONS UTILIZED  
IN THE SIMULATION

	ENGLISH SYSTEM			METRIC SYSTEM		
	NAME	PROGRAM NAME	UNITS	NAME	PROGRAM NAME	UNITS
ABSOLUTE VISCOSITY	None	VISAE	$\frac{\text{lbf sec}}{\text{ft}^2} = \frac{\text{slug}}{\text{ft sec}}$	Poise or Centipoise	VISAM (centipoise)	$\frac{\text{dyne sec}}{\text{cm}^2} = \frac{\text{gm}}{\text{cm sec}}$
KINEMATIC VISCOSITY	None	VISKE	$\frac{\text{ft}^2}{\text{sec}}$	Stoke or centistoke	VISKM (centistoke)	$\frac{\text{cm}^2}{\text{sec}}$
ABSOLUTE CONVERSIONS	$1 \frac{\text{lbf sec}}{\text{ft}^2} = 4.79 (10)^4 \text{ centipoise}$ VISAE = $4.79 (10)^4$ VISAM			$1 \text{ centipoise} = 1/4.79(10)^4$ VISAM = $1/4.79(10)^4$		$\frac{\text{lbf sec}}{\text{ft}^2}$ VISAE
KINEMATIC CONVERSIONS	$1 \frac{\text{ft}^2}{\text{sec}} = 92903.0 \text{ centistokes}$ VISKE = 92903.0 VISKM			$1 \text{ centistoke} = 1/92903.0$ VISKM = 1/92903.0		$\frac{\text{ft}^2}{\text{sec}}$ VISKE

An additional useful quantity within the simulation is VISAG, which is defined as:

$$\text{VISAG} = 32.174 \cdot \text{VISAE} \cdot \frac{\text{lbm}}{\text{ft sec}}$$

TABLE XXXII

## CONSTANTS UTILIZED IN THE SIMULATION

Standard atmosphere =  $14.6959 \text{ lbf/in}^2 = 2116.62 \text{ lbf/ft}^2 = 29.92 \text{ "Hg}$ .

Standard atmosphere =  $406.857 \text{ in. H}_2\text{O at } 39^\circ \text{ F}$

Standard atmosphere =  $407.787 \text{ in. H}_2\text{O at } 60^\circ \text{ F}$

Standard atmosphere =  $557.086 \text{ in. gasoline of } 0.732 \text{ SG}$

Density of water (sat. at  $32^\circ \text{ F}$ ) =  $62.4142 \text{ lbm/ft}^3$

Density of water (sat. at  $60^\circ \text{ F}$ ) =  $62.286 \text{ lbm/ft}^3$

Density of water ( $1 \text{ gm/cm}^3$ ) =  $62.428335 \text{ lbm/ft}^3$

Air density at  $60^\circ \text{ F}$  and  $14.696 \text{ psia}$  =  $0.07636 \text{ lbm/ft}^3$

Air density at  $70^\circ \text{ F}$  and  $14.696 \text{ psia}$  =  $0.07492 \text{ lbm/ft}^3$

$1 \text{ lbm} = 453.59237 \text{ grams}$

$1 \text{ in}^3 = 16.387162 \text{ cm}^3$

$1 \text{ inch} = 2.540005 \text{ cm}$

$1 \text{ cm} = .393700 \text{ inch (definition)}$

Density of Mercury =  $13.5951 \text{ gm/cm}^3$  at  $32.0^\circ \text{ F}$

Density of Mercury =  $13.5458 \text{ gm/cm}^3$  at  $68.0^\circ \text{ F}$

$\bar{R}$  (universal gas constant) =  $1545.4 \frac{\text{ft lbf}}{\text{lb mol } ^\circ\text{R}}$

$R$  (air constant) =  $53.34 \frac{\text{ft lb}}{\text{lbm } ^\circ\text{R}}$ .

## APPENDIX L

### EXPLANATION OF SYMBOLS USED IN THE SIMULATION

The meanings of the primary variables in the simulation are listed here for reference purposes. The variables used for indexing, switching, substituting, and temporarily saving values are listed but the meanings are not given. The symbols have been arranged in alphabetical order, in the following categories:

1. non-subscripted variables in the simulation
2. subscripted variables in the simulation
3. non-subscripted variables related to the plotting and interpolation routines
4. subscripted variables related to the plotting and interpolation routines
5. symbols associated with constants and dummy variables, and with indexing and switching
6. variables related only to initiating plots and constructing axes

#### 1. NON-SUBSCRIPTED VARIABLES IN THE SIMULATION

<u>SYMBOL</u>	<u>MEANING</u>
ABLEED	Flow area of enrichment valve vacuum bleed orifice
ACHOKE	Flow area of choke restriction orifice
ADUM	Approach velocity factor for fuel channel orifices
AFLOW	Throttle flow area
AIDENS	Density of bleed air in idle system
AIDLE	Flow area at idle needle screw

<u>SYMBOL</u>	<u>MEANING</u>
AIRFL1	Air mass flow rate for first engine IHP data set
AIRFL2	Air mass flow rate for second engine IHP data set
AIRFLO	Air mass flow rate which will give the required IHP for the current iterative fuel-air ratio
AIRI1	Mass flow rate of first idle air bleed
AIRI2	Mass flow rate of second idle air bleed
AIRM1	Mass flow rate of first main air bleed
AIRM2	Mass flow rate of second main air bleed
AIRMB	Air flow rate through enrichment valve bleed orifice
AIRMC	Air flow rate through choke orifice
AMDENS	Ambient air density
AO	Air flow rate intercept on IHP plot
AREA	Vehicle frontal area
ARICH	Enrichment valve flow area
ASHAFT	Transverse cross-sectional area of throttle shaft
ASTAR	Throttle flow area parameter
ATRANS	Flow area of throttle bypass orifice
ATYPE	Control variable specifying the type of analysis to be performed
AVALVE	Total intake valve flow area
AVISKE	Kinematic viscosity of bleed air in English units
AVISKM	Kinematic viscosity of bleed air in centistokes
AWOT	Maximum throttle flow area per barrel
BBLS	Number of carburetor barrels

<u>SYMBOL</u>	<u>MEANING</u>
BFA	Fuel-air ratio of mixture leaving boost venturi
BHP	Engine brake horsepower
BMACH3	Mach number at boost venturi station 3
BMACH4	Mach number at boost venturi station 4
BMACH5	Mach number at boost venturi station 5
BORE	Engine cylinder bore diameter
BORTOL	Tolerance of the engine bore diameter
BSFC	Engine brake specific fuel consumption
BVFLO	Air mass flow rate in one boost venturi
BVMACH	Boost venturi throat Mach number
BVS MIN	Minimum boost suction to initiate main system fuel flow
BVSUCW	Boost venturi suction
CARBNO	Current carburetor being built for the production dimension analysis
CC	Vena contracta coefficient
CDBL	Discharge coefficient of the enrichment vacuum bleed orifice
CDJ	Iterative main metering orifice discharge coefficient
CDJET	Predicted main metering orifice discharge coefficient
CDSE	Discharge coefficient of square-edged fuel channel orifice
CDSE1	Iterpolated $C_d$ for next lowest known L/D ratio
CDSE2	Iterpolated $C_d$ for next highest known L/D ratio
CDT	Throttle plate discharge coefficient
CDTR	Discharge coefficient of throttle bypass orifice

<u>SYMBOL</u>	<u>MEANING</u>
CDUM	Total pressure loss factor for fuel channel orifices
CLIQ	Liquid fuel specific heat
CORR	Correction factor for fuel head variations with density
CPAIR	Constant pressure specific heat of dry air
CPH2O	Constant pressure specific heat of water vapor
CPMAIN	Constant pressure specific heat of the mixture at the throttle plate
CPMIX	Constant pressure specific heat of the mixture in general
CPWET	Constant pressure specific heat of moist air
CPFUEL	Constant pressure specific heat of fuel vapor
CR	Engine compression ratio
CRTOL	Engine compression ratio tolerance
CVAIR	Constant volume specific heat of dry air
CVFUEL	Constant volume specific heat of fuel vapor
CVH2O	Constant volume specific heat of water vapor
CVMAIN	Constant volume specific heat of the mixture at the throttle plate
CVMIX	Constant volume specific heat of the mixture in general
CVWET	Constant volume specific heat of moist air
CYL	Number of cylinders in engine
DBLEED	Production diameter of enrichment valve vacuum bleed
DBLNOM	Nominal diameter of enrichment valve vacuum bleed
DBTOL	Tolerance on the enrichment valve vacuum bleed diameter
DCHOKE	Production diameter of choke bleed restriction



<u>SYMBOL</u>	<u>MEANINGS</u>
DCNOM	Nominal diameter of choke bleed restriction
DCTOL	Tolerance on the choke bleed restriction diameter
DELAIR	Change in engine air mass flow rate for the current iteration
DELFA1	Change in total fuel-air ratio for the current iteration
DELFA2	Change in main fuel-air ratio since the last iteration
DELXJ	Reynolds number increment used in main metering orifice data
DELXJL	Reynolds number increment used in low head data for the main metering jet
DELXR	Fuel-air ratio increment used in engine IHP data
DELXS	RPM increment used in engine FMEP data
DELXSE	Reynolds number increment used in square-edged orifice data
DELPMB	Static pressure differential across first main system air bleed
DELXT	Throttle angle increment used in throttle $C_d$ data
DENSF	Fuel density in pounds per cubic foot
DENSM	Fuel density in grams per cubic centimeter
DISPL	Engine displacement in cubic inches
DMAN	Effective average diameter of intake manifold runner
DPEJET	Exit pressure loss for the main metering orifice
DPENTR	Entrance pressure loss for a fuel channel element
DPJET	Predicted static pressure differential of main metering orifice
DPW	Element total pressure loss due to fluid friction
DRAG	Vehicle air resistance coefficient
DRIVEN	Total vehicle drive train efficiency
DRYA2	Initial guess for the engine dry air flow rate

SYMBOL	MEANINGS
DRYAIR	Total dry air mass flow rate to engine
DS	Production diameter of throttle shaft
DSNOM	Nominal diameter of throttle shaft
DSTOL	Tolerance on the throttle shaft diameter
DT	Production diameter of throttle bore
DTRANS	Production diameter of throttle bypass orifice
DTNOM	Nominal diameter of throttle bore
DTRNOM	Nominal diameter of throttle bypass orifice
DTRTOL	Tolerance on the throttle bypass orifice diameter
DTTOL	Tolerance on the throttle bore diameter
DUMACH	Iterative venturi Mach number
E1	General error of the previous iteration
E2	General error of the current iteration
EPS	General maximum allowable convergence error
EPS2	Maximum allowable air mass flow rate error
EPSE	Maximum allowable enrichment pressure drop error
EPSI	maximum allowable idle system pressure drop error
EPSJ	Maximum allowable main jet pressure drop error
EPSLON	Maximum allowable Mach number error
ERR1	Air mass flow rate error on the previous iteration (see Figure 5)
ERR2	Air mass flow rate error on the current iteration (see Figure 5)
ERRE1	Pressure error on previous enrichment flow iteration

<u>SYMBOL</u>	<u>MEANINGS</u>
ERRE2	Pressure error on current enrichment flow iteration
ERRI1	Pressure error on previous idle system flow iteration
ERRI2	Pressure error on current idle system flow iteration
ERRJ1	Pressure error on previous main jet flow iteration
ERRJ2	Pressure error on current main jet flow iteration
EXHEAT	Intake manifold heat parameter
F1	Sudden expansion or contraction pressure loss factor
F2	Bend pressure loss factor
FA	General fuel-air ratio
FACTOR	Sum of F1 and F2
FAIDLE	That portion of the total fuel-air ratio due to idle fuel flow
FAMAIN	Main system fuel-air ratio
FARICH	Initial guess for the total fuel-air ratio with the enrichment system functioning
FATOTL	Total (overall) fuel-air ratio
FDARCY	Darcy friction factor
FHP	Friction horsepower of engine
FLLIQB	Liquid fuel mass flow rate leaving each boost venturi
FLMIXB	Mass flow rate of air, water vapor, and fuel vapor leaving each boost venturi
FLOWE	Fuel mass flow rate in enrichment system
FLOWI	Fuel mass flow rate in idle system
FLOWJ	Fuel mass flow rate through main metering orifice
FLOWM	Fuel mass flow rate in main system

<u>SYMBOL</u>	<u>MEANINGS</u>
FLOWT	Total fuel mass flow rate per barrel
FLUID	Fluid type code
FLVAPB	Mass flow rate of fuel vapor leaving boost venturi
FMAX	Maximum engine FMEP at a given RPM
FMAXB	Maximum possible moist air mass flow rate through one boost venturi
FMAXB3	Maximum possible moist air mass flow rate at the boost venturi throat
FMAXB4	Maximum possible moist air mass flow rate at boost venturi station 4
FMAXB5	Maximum possible moist air mass flow rate at boost venturi station 5
FMAXM	Maximum possible moist air mass flow rate through one main venturi
FMAXM3	Maximum possible moist air mass flow rate at main venturi station 5
FMAXM4	Maximum possible moist air mass flow rate at the main venturi throat
FMAXT	Maximum possible moist air flow rate through one carburetor barrel
FMEP	Friction mean effective pressure of engine
FMIN	Minimum FMEP at the specified engine speed
FRACT	Initial guess for the fraction of the main fuel flow vaporized between the boost venturi and the throttle plate
FRACTB	Initial guess for the fraction of the main fuel vaporized within the boost venturi
FTYPE	Variable denoting the fuel type code
FUELR	Total fuel mass flow rate for all barrels

<u>SYMBOL</u>	<u>MEANINGS</u>
GAMMA	Fuel surface tension
GASFLO	Total mixture mass flow rate to the engine
GASM1	Iterative air flow rate from nozzle equations
GASM2	Iterative air flow rate from exhauster equation
GASMTR	Air mass flow rate through throttle bypass orifice
GASMT	Mixture mass flow rate at throttle plate
GK	General Specific heat ratio
GKMIX	Specific heat ratio of mixture at throttle plate
GKWET	Specific heat ratio of moist air
GUESS	Initial guess for the intake manifold vacuum
HEATV	Lower heating value of fuel
HUMID	Fractional relative humidity
HVAPOR	Latent heat of vaporization of the fuel
JETS	Number of main metering orifices
NBV	Number of boost venturi stations in the analysis
NCDJL	Number of points in the low head main metering orifice $C_d$ data
NCDJ	Number of points in the main metering orifice $C_d$ data
NCDSE	Number of points in the square-edged orifice $C_d$ data
NCHAN	Number of elements in the fuel channel
NFMEP	Number of points in the engine FMEP data
NGEAR	Number of transmission gear ratios in the road load analysis
NIHP	Number of points in the engine IHP data
NMV	Number of main venturi stations in the analysis

<u>SYMBOL</u>	<u>MEANINGS</u>
NTHETA	Number of points in the throttle plate $C_d$ data
NUNITS	Number of carburetors to be built for the production dimension analysis
OLDFE	Enrichment fuel flow rate for the previous iteration
OLDF1	Idle system fuel flow rate for the previous iteration
OLDFJ	Main jet fuel flow rate for the previous iteration
OMEGA	Water vapor to air mass ratio
OPENE	Vacuum at which the enrichment valve begins to open
ORDER	The interpolation degree utilized by STERL
PB5W	Boost venturi outlet pressure in inches of water
PBHG3	Boost venturi throat pressure in inches of mercury
PBHG4	Pressure at boost venturi station 4 in inches of mercury
PBHG5	Boost venturi outlet pressure in inches of mercury
PCH	Per cent relative humidity
PM4W	Pressure at main venturi station 4 in inches of water
PMACH3	Mach number at main venturi throat
PMACH4	Mach number at main venturi station 4
PMAN	Intake manifold pressure in inches of mercury
PMAXW	Vapor pressure of water for 100% humidity
PMHG3	Main venturi throat pressure in inches of water
PMHG4	Pressure at main venturi station in inches of mercury
PO	Ambient pressure in PSIA
POB	Stagnation pressure at boost venturi inlet
POBHG	Stagnation pressure at boost venturi outlet in inches of mercury

<u>SYMBOL</u>	<u>MEANINGS</u>
POHG	Ambient pressure in inches of mercury
POL	Local stagnation pressure in general
POM	Stagnation pressure at main venturi inlet
POMHG	Stagnation pressure at main venturi station 4 in inches of mercury
PR	Pressure ratio across throttle plate
PRBL	Pressure ratio across throttle bypass orifice
PRBMAX	Maximum possible pressure ratio for throttle bypass orifice
PRESS	Intake manifold pressure in inches of mercury
PRINT1	Variable which controls data printout within main program
PRINTA	Variable which controls auxiliary printout by subroutine AIRMAS
PRINTF	Variable which controls auxiliary printout by subroutine FLOW
PRINTO	Variable which controls auxiliary printout of road load values
PRINTS	Variable which controls auxiliary printout by subroutine SIGNAL
PRMAX	Pressure ratio for choked throttle FLOW
PT	Stagnation pressure of mixture at throttle plate in PSIA
PTHG	Stagnation pressure of mixture at throttle plate in inches of mercury
PTYPE	Variable which controls the type of CALCOMP plot obtained
PVFLO	Air mass flow rate in one primary venturi
PVMACH	Primary venturi throat Mach number
PVSUCW	Primary venturi suction
RANVAR	Variable which indicates whether a production dimension analysis is to be performed
RATEB	Moist air mass flow rate in each boost venturi

<u>SYMBOL</u>	<u>MEANINGS</u>
RATEM	Moist air mass flow rate in each main venturi
RATEMF	Total main system fuel flow rate for all barrels
RATIOD	Vehicle differential gear ratio
RATIOP	Fraction of the boost venturi suction lost in elements 1 to 9
RATIO T	Current vehicle transmission gear ratio
REJET	Reynolds number of the main metering orifice fuel FLOW
RHOB3	Air density at boost venturi throat
RHOB4	Mixture density at boost venturi station 4
RHOB5	Mixture density at boost venturi outlet
RHOM3	Air density at main venturi throat
RHOM4	Air density at main venturi station 4
RHOLZ	Local mixture density in general
ROADHP	Required rear wheel horsepower at a given vehicle speed
ROLL	Rolling resistance factor for vehicle
RPM	Engine speed in revolutions per minute
RPMLIM	Maximum engine speed for which an operating map is desired
RTHETA	Throttle angle in radians
RTHETO	Completely closed throttle angle in radians
SGFUEL	Fuel specific gravity
SIGMA	Standard deviation of carburetor dimensions, also fuel surface tension
SLOPE	Current slope of the IHP versus air mass flow rate curve
SPILL1	Initial spill point of carburetor
SPILL2	Secondary spill point of carburetor



<u>SYMBOL</u>	<u>MEANINGS</u>
STOL	Tolerance for the engine stroke
STROKE	Engine stroke
SUCWB3	Suction at boost venturi throat in inches of water
SUCWB4	Suction at boost venturi station 4 in inches of water
SUCWB5	Suction at boost venturi outlet in inches of water
SUCWM3	Suction at main venturi throat in inches of water
SUCWM4	Suction at main venturi station 4 in inches of water
SUMAIR	Total air bleed mass flow rate for the main system
SUMDPE	Sum of the pressure differentials in the enrichment system
SUMDPI	Sum of the pressure differentials in the idle system
SUMDPJ	Sum of the pressure differentials for elements 1 and 2
SUMDPM	Sum of the pressure differentials for the main system
TBF3	Static temperature at boost venturi throat in $^{\circ}\text{F}$
TBF4	Static temperature at boost venturi station 4 in $^{\circ}\text{F}$
TBF5	Static temperature at boost venturi outlet in $^{\circ}\text{F}$
TCLR	Absolute temperature of the gases in the cylinder clearance volume when exhaust valve closes
TCYLR	Absolute temperature of the mixture in the cylinder when the intake valve closes
TEMP	Fuel temperature in degrees Fahrenheit
TFUEL	Fuel temperature in degrees Fahrenheit
THETAL	Maximum throttle angle for which an operating map is desired
THETAO	Production value for the completely closed throttle angle
THETA	General throttle angle

<u>SYMBOL</u>	<u>MEANINGS</u>
THONOM	Nominal value for the completely closed throttle angle
THOTOL	Angular tolerance for the completely closed throttle angle
THSTEP	The throttle angle increment used in the road load analysis
TIREN	Tire revolutions per mile
TLR	Local static temperature in degrees Rankine
TMAN	Absolute temperature of mixture leaving the intake manifold runner in $^{\circ}\text{F}$
TMANF	Temperature of mixture leaving the intake manifold runner in $^{\circ}\text{F}$
TMF3	Static temperature at the main venturi throat in $^{\circ}\text{F}$
TMF4	Static temperature at main venturi station 4 in $^{\circ}\text{F}$
TOBF	Stagnation temperature at boost venturi inlet in $^{\circ}\text{F}$
TOBR	Stagnation temperature at boost venturi inlet in $^{\circ}\text{R}$
TOF	Ambient temperature in degrees Fahrenheit
TOMF	Stagnation temperature at main venturi inlet in $^{\circ}\text{F}$
TOMR	Stagnation temperature at main venturi inlet in $^{\circ}\text{R}$
TORQF	Friction torque of the engine
TOR	Ambient temperature in degrees Rankine
TOTF	Total temperature of the mixture at the throttle plate ( $^{\circ}\text{F}$ )
TOTR	Total temperature of the mixture at the throttle plate ( $^{\circ}\text{R}$ )
TURNS	Number of turns of the idle needle screw from the completely closed position
VACM	Intake manifold vacuum in inches of mercury
VACMAN	Iterative intake manifold vacuum in inches of mercury
VALVED	Intake valve seat diameter

<u>SYMBOL</u>	<u>MEANINGS</u>
VCL	Total clearance volume of engine
VELB3	Velocity of moist air at boost venturi throat
VENFLO	Total moist air mass flow rate per venturi stack
VISAE	Absolute viscosity of fuel in English units
VISAM	Absolute viscosity of fuel in centipoise
VISKE	Kinematic viscosity of fuel in English units
VISKM	Kinematic viscosity of fuel in centistokes
VLIMIT	Lower bound for intake manifold vacuum
VMPH	Vehicle velocity in miles per hour
VOLD	Intake manifold vacuum for the previous iteration
VSTEM	Valve stem diameter
WAIR	Molecular weight of dry air
WEIGHT	Vehicle curb weight
WETA1	Moist air flow portion of GASM1
WETA2	Moist air flow portion of GASM2
WETAIR	Total moist air mass flow rate to engine
WFUEL	Molecular weight of fuel being used
WH20	Molecular weight of water vapor
WMIXB	Molecular weight of mixture leaving boost venturi
WMOIST	Molecular weight of moist air in general
WMOL	Molecular weight of a mixture in general
WMOLEC	Molecular weight of fuel in general
WMOLEM	Molecular weight of mixture in engine cylinder

<u>SYMBOL</u>	<u>MEANINGS</u>
WMOLET	Molecular weight of mixture at throttle plate
XBVNOM	Nominal venturi dimension (see Figure 2)
XBV	Production venturi dimension (see Figure 2)
XBVTOL	Tolerance of venturi dimension (see Figure 2)
XF	Fraction of the total venturi air flow that does not flow through the boost venturi
XF1	Value of XF for the previous iteration
XFV	Value of XF for the previous air flow value
XGUESS	Initial guess for XF
XFLOWE	Predicted enrichment system fuel mass flow rate
XFLOWI	Predicted idle system fuel mass flow rate
XFLOWJ	Predicted main metering orifice fuel mass flow rate
XFLOWM	Predicted main system fuel mass flow rate
XFLOWT	Predicted total fuel mass flow rate per barrel
XIHP1	Indicated horsepower from high air flow data set
XIHP2	Indicated horsepower from low air flow data set
XIHP	Indicated horsepower corresponding to the current iterative air flow and fuel-air ratio
XIMEP1	Indicated mean effective pressure corresponding to XIHP1
XIMEP2	Indicated mean effective pressure corresponding to XIHP2
XISFC	Engine indicated specific fuel consumption
XMACHT	Mach number of the mixture flow at the throttle plate
XMAINR	Fuel-air ratio based on main fuel flow and venturi air flow
XM1NOM	Nominal venturi dimension (see Figure 2)

<u>SYMBOL</u>	<u>MEANINGS</u>
XM1TOL	Tolerance of venturi dimension (see Figure 2)
XM2NOM	Nominal venturi dimension (see Figure 2)
XM2TOL	Tolerance of venturi dimension (see Figure 2)
XMB	Production venturi dimension (see Figure 2)
XMBNOM	Nominal venturi dimension (see Figure 2)
XMBTOL	Tolerance of venturi dimension (see Figure 2)
XMINR	Fuel-air ratio of first point in the engine IHP data
XMINS	Engine speed at first point in the engine FMEP data
XMINT	Throttle angle at first point in the throttle $C_d$ data
XMV1	Production venturi dimension (see Figure 2)
XMV2	Production venturi dimension (see Figure 2)
XNCDJ	Same as NCDJ except floating point
XNCDJL	Same as NCDJL except floating point
XNCDSE	Same as NCDSE except floating point
XNFMEP	Same as NFMEP except floating point
XNIHP	Same as NIHP except floating point
XNTHET	Same as NTHETA except floating point
XNUNIT	Same as NUNITS except floating point
XTOTLR	Total fuel-air ratio of mixture leaving intake manifold

## 2. SUBSCRIPTED VARIABLES IN THE SIMULATION

<u>SYMBOL</u>	<u>MEANING</u>
ABV	Boost venturi flow area
ACHAN	Fuel channel element flow areas
AMV	Main venturi flow areas
ANAME	Description of analysis
ANGLC	Angles between the current fuel channel element and the preceding one
BHPP	Engine brake horsepower values for plotting
BOOSTW	Boost venturi suction values for plotting
BSFCP	Brake specific fuel consumption values for plotting
CBLEED	Air bleed orifice discharge coefficients
CD	Main metering orifice $C_d$ values for plotting
CD1	$C_d$ data for main metering orifice being used
CD2	$C_d$ data (low head) for main metering orifice
CD3	$C_d$ data for square-edged orifice with $L/D = 0.100$
CD4	$C_d$ data for square-edged orifice with $L/D = 0.616$
CD5	$C_d$ data for square-edged orifice with $L/D = 1.426$
CD6	$C_d$ data for square-edged orifice with $L/D = 3.629$
CD7	$C_d$ data for square-edged orifice with $L/D = 4.726$
CD8	$C_d$ data for square-edged orifice with $L/D = 7.230$
CD9	$C_d$ data for square-edged orifice with $L/D = 10.58$
CNAME	Carburetor description
CTHROT	Throttle plate discharge coefficient values

<u>SYMBOL</u>	<u>MEANING</u>
CTYPE	Type codes for fuel channel elements
D	Fuel channel element diameters
DBV	Boost venturi production diameters
DBVNOM	Boost venturi nominal diameters
DBVTOL	Tolerances for boost venturi diameters
DCHAN	Production diameters for fuel channel elements
DCHNOM	Nominal diameters for fuel channel elements
DCHTOL	Tolerances for fuel channel element diameters
DELPTW	Total pressure loss of fuel channel elements
DIHP1	Indicated horsepower values at the lower air flow
DIHP2	Indicated horsepower values at the higher air flow
DMV	Production diameters of the main venturi
DMVNOM	Nominal diameters of the main venturi
DMVTOL	Tolerances for the main venturi diameters
DN	Density of the fluid within the fuel channel elements
DRYAP	Dry air mass flow rate values for plotting
ENAME	Engine description
FLOWMP	Main system fuel flow rates for plotting
FLOWTP	Total fuel flow rates for plotting
FMEP1	Friction mean effective pressure values at full throttle
FMEP2	Friction mean effective pressure values at closed throttle
FNAME	Fuel description
ONAM	Orifice descriptions

<u>SYMBOL</u>	<u>MEANING</u>
PMAN	Intake manifold pressure
PNAME	Plot description
RE	Fuel channel element Reynolds numbers
SCRACH	Work area for subroutine STERL
SKIP	Array used to indicate whether flow exists in a fuel channel element
SPEED	Vehicle speed
TOTLFA	Total fuel-air ratio values for plotting
TRANS	Transmission gear ratios
VEL	Velocity of the fluid within the fuel channel elements
VHEADW	Velocity head of the fluid within the fuel channel elements
VNAME	Vehicle description
WETA	Total moist air mass flow rate for plotting
WHY	Description of the simulation run
XIHPP	Engine indicated horsepower values for plotting
XLCHAN	Fuel channel element length
XLD	L/D ratio of fuel channel elements
XMPG	Vehicle miles per gallon

### 3. NON-SUBSCRIPTED VARIABLES RELATED TO THE PLOTTING AND INTERPOLATION ROUTINES

<u>SYMBOL</u>	<u>MEANING</u>
ALPHA	General interpolation parameter
DELTA X	X spacing of data supplied to interpolation routine
FM	Degree of interpolation to be used



<u>SYMBOL</u>	<u>MEANING</u>
FN	Number of data points supplied to interpolation routine
FRUN	Run number for the simulation plots
FSYMB	Plotting symbol to be used
FTYPE	Type of line plot desired
GX	Grid line spacing for X axis
GY	Grid line spacing for Y axis
MAIN	Variable which determines the plot scale
POINTS	Number of points to be plotted
SAMEX	Variable which controls the number of curves plotted on one grid
TEMP	Temperature to be printed on plot
VARI	A number to be printed on plot
XARG	The X argument for which an interpolated Y value is desired
XMIN	The X value at the plot origin
XO	X Coordinate of the plot origin
XXMIN	Minimum value of the X data supplied to the interpolation routine
YEST	Interpolated Y value
YMIN	The Y value at the plot origin
YO	Y coordinate of the plot origin

4. SUBSCRIPTED VARIABLES RELATED TO THE PLOTTING AND INTERPOLATION ROUTINES

<u>SYMBOL</u>	<u>MEANING</u>
XX	General array of values associated with the X axis of a plot
Y	General array of data supplied to interpolation routine
YY	General array of values associated with the Y axis of a plot

5. SYMBOLS ASSOCIATED WITH CONSTANTS AND DUMMY VARIABLES, AND WITH INDEXING AND SWITCHING

A1 to A18	DUMLD	J	RNO
AGAIN	DUMMY1	K	SAVE
ANG	DUMMYM	L	SAVE1
ANG1	DUMMYP	M	SAVE5
C1 to C13	DUMPA	MH	SAVE6
CHANGE	DUMPR	ML	SAVE11
DATE1	DUMR	N	SAVE12
DATE2	DUMRB	NN	SETUP
DEBUG	DUMRPM	OLDAI1	STEP
DEBUGA	DUMTHO	OLDAI2	STOP
DUM1 to DUM22	DUMV2	OLDAIR	SWITCH
DUMA	DUMVH2	OLDAM1	TF
DUMDP	EDUM	OLDAM2	THOLD
DUMFA	ESW	OLDFA1	X
DUMFLO	HH	OLDFA2	XIDUM
DUMFM	I	OPEN	XISW
DUMFR	ITER	ORNAM	XJSW
DUMFT	ITERE	PM	XMDUM
DUMGAM	ITERI	Q	XN
DUMHU	ITERJ	REDUM	Y

6. VARIABLES RELATED ONLY TO INITIATING PLOTS AND CONSTRUCTING AXES

ALIMIT	DXFA	DYCM	PLOTN
AMAX	DXIA	DYCR	SCALE
ANGLD	DXIF	DYFA	SET
ANGLR	DXLL	DYIA	XEXP
DX	DXMH	DYIF	XSTART
DXBB	DXMS	DYLL	XVAL
DXCH	DY	DYMH	YEXP
DXCM	DYBB	DYMS	YSTART
DXCR	DYCH	PLOTI	YVAL

## BIBLIOGRAPHY

### COMPRESSIBLE MIXTURE FLOW

1. Dodson, J. E., Booth, C. T., and Metsger, A. B., "An Investigation of the Air Metering Characteristics of Various Combinations of Carburetor Elements", M. S. thesis, M.I.T., 1940.
2. Fries, B. A., Davis, F. J., and Hull, D. E., "Engine Air Flow by the Total Count Method", SAE Preprint 85, 1959.
3. Gerhart, R. V., et al, "Thermodynamic Properties of Air", Mechanical Engineering, April, 1942, pp. 270-272.
4. Hwa, W. Z., "A Study of Double Venturis for Aircraft Carburetors", M.I.T. thesis, Oct., 1941.
5. Mirsky, W., and Bolt, J. A., "A Preliminary Literature Survey of the Fuel Metering and Induction Processes for Spark-Ignited Engines", University of Michigan Research Institute paper, project 2813, 1958.
6. Newhall, H. K., and Starkman, E. S., "Thermodynamic Properties of Octane and Air for Engine Performance Calculations", SAE paper 633G, 1963.
7. Oppenheim, A. K., and Chilton, E. G., "Pulsating Flow Measurement - A Literature Survey", ASME paper 53-A-157, 1953.
8. Prien, W. F., "A Study of the Effect of Air Pulsations on the Operation of A Carburetor", M.I.T. thesis, May 1954.
9. Rogowski, A. R., "Elements of Internal Combustion Engines", McGraw-Hill, New York, 1953.
10. Shapiro, A. H., "The Dynamics and Thermodynamics of Compressible Fluid Flow", The Ronald Press Co., New York, 1953, Chap. 4, 6, 7 and 8.

### ATOMIZATION AND VAPORIZATION

11. Bahr, D. W., "Evaporation and Spreading of Isooctane Sprays in High-Velocity Air Streams", NACA Report RM E53I14, 1953.

12. Benson, G. M., et al, "The Determination of Cross-Sectional Drop-Size Distributions of Liquid Sprays by a Fluorescent Technique", University of Wisconsin research report, June, 1958.
13. Consiglio, J. A., "The Effect of Operating Variables on Sprays Produced by a Pressure-Type Nozzle", Ph.D. thesis, University of Michigan, 1961.
14. Fuchs, N. A., "Evaporation and Droplet Growth in Gaseous Media", Pergamon Press, New York, 1949.
15. Graves, C. G., and Bahr, D. W., "Atomization and Evaporation of Liquid Fuels, "NACA report 1300, 1957, Chapter I.
16. Ingebo, R. D., "Vaporization Rates and Drag Coefficients for Isooctane Sprays in Turbulent Air Streams", NACA report TN3265, 1954.
17. Jakob, M., "Heat Transfer", Vol. I, John Wiley and Sons, Inc., 1949.
18. Marshall, W. R., "Atomization and Spray Drying", Chem. Eng. Prog. Monograph Series, No. 2, Vol. 50, 1954.
19. Nukiyama, S., and Tanasawa, Y., "Experiments on the Atomization of Liquids in an Air Stream, Reports 1, 2, and 4, Defense Res. Board, Ottawa, March, 1950 (Translated from Trans. Jap. Soc. Mech. Eng., Vol. 4, No. 14, Feb. 1938. pp. 86-93).
20. Ranz, W. E., and Marshall, W. R. Jr., "Evaporation from Drops", Chem. Eng. Prog., Vol. 48, No. 3, March, 1952, pp. 141-146; No. 4, April, 1952, pp. 173-180.
21. Rice, E. J., "The Effect of Selected Fluid Parameters on Spatial Drop Size Distribution", Ph.D. thesis, University of Wisconsin, 1966.

#### FUEL AND AIR BLEED FLOW

22. Baker, O., "Simultaneous Flow of Oil and Gas," The Oil and Gas Journal, July 26, 1954, pp. 183-186.
23. Daily, J. W., and Harleman, D. R. F., "Fluid Dynamics", Addison-Wesley Pub. Co., Inc., Reading, Mass., 1966, Chapt. 13 and 14.
24. Huey, C. T., and Bryant, R. A. A., "A Theory for Froth Flow in Horizontal Pipes", ASME paper 65-WA/FE-5, 1965.

25. Ishikawa, M. and Ito, M., "The Effect of Temperature on Carburation and its Compensation", Journal Soc. Mech. Engr., Vol. 31, No. 140, Dec. 1928.
26. Kay, J. M., "Fluid Mechanics and Heat Transfer", Cambridge University Press, London, 1963, Chap. 6, 15, and 18.
27. Langhaar, H. L., "Steady Flow in the Transition Length of a Straight Tube", Journal of Applied Mechanics, Trans. ASME, Vol. 64, 1942, p pp. A-55-58.
28. Lockhart, R. W. and Martinelli, R. C., "Proposed Correlation of Data for Isothermal Two-Phase Two-Component Flow in Pipes", Chem. Eng. Prog., Vol. 45, 1949, pp. 39-48.
29. Streeter, V. L., "Fluid Mechanics", McGraw-Hill, Inc., New York, 1958, Chapters 4, 6 and 10.
30. Ting, C. H., "Analysis of Air Bleeds and Several Typical Idling Systems for Carburetors", M.I.T. thesis, 1946.
31. Weir, A., "Two and Three-Dimensional Flow of Air Through Square-Edged Sonic Orifices", Ph.D. thesis, University of Michigan, 1954.

#### ORIFICE FLOW

32. Bond, W. N., "The Effect of Viscosity on Orifice Flows", Proc. Royal Soc., Nov. 1921, pp. 225-230.
33. Earles, S. W. E., and Zarek, J. M., "Use of Sharp-Edged Orifices for Metering Pulsating Flow", Proc. Inst. Mech. Engr., 1963, Vol. 177, No. 37, p. 997.
34. Greenland, L. S., "Fluid Flow Through Restrictions", Aircraft Engr., June, 1943.
35. Hall, G. W., "Analytical Determination of the Discharge Characteristics of Cylindrical-Tube Orifices", Jour. Mech. Eng. Science, Vol. 5, No. 1, 1963, pp. 91-97.
36. Kastner, L. J., and McVeigh, J. C., "A Reassessment of Metering Orifices for Low Reynolds Numbers", Proc. Instn. Mech. Engrs., Vol. 180, Part 1, No. 13, 1965, pp. 331-355.
37. Kreith, Frank, and Eisenstadt, Raymond, "Pressure Drop and Flow Characteristics of Short Capillary Tubes at Low Reynolds Numbers", ASME paper 56-SA-15, June, 1956.

38. Lichtarowicz, A., Duggins, R. K., and Markland, E., "Discharge Coefficients for Incompressible Non-Cavitating Flow Through Long Orifices", Jour. Mech. Eng. Science, Vol. 7, No. 2, 1965, pp. 210-219.
39. Mirsky, W. and Bolt, J. A., "Flow Characteristics of the Carter Type 120 Carburetor Metering Jet", Project 2813 final report, U. of Mich. Research Institute, Aug. 1960.
40. Nakayama, Y., "Action of the Fluid in the Air Micrometer", Japanese Soc. of Mech. Eng., Vol. 4, No. 15, 1961, pp. 507-515.
41. Spikes, R. H. and Pennington, G. A., "Discharge Coefficient of Small Submerged Orifices," Inst. Mech. Engrs., pp. 9-13.
42. Starrett, P. S., Nottage, H. B. and Halfpenny, P. F., "Survey of Information Concerning the Effects of Nonstandard Approach Conditions upon Orifice and Venturi Meters", ASME paper 65-WA/FM-5, 1965.
43. Zucrow, M. J., "Discharge Characteristics of Submerged Jets", Purdue Research Bulletin No. 31, June 1928.

#### CARBURETOR DESIGN AND TESTING

44. Bolt, Jay A. and Boerma, M., "The Influence of Inlet Air Conditions on Carburetor Metering", SAE paper 660119, 1966.
45. Carnell, N. W., "The Flow Box - An Instrument to Measure Fuel Metering Devices for Internal Combustion Engines", General Motors Eng. Jour., March 1960, pp. 30-36.
46. Freeman, J. H. and Stahman, R. C., "Vehicle Performance and Exhaust Emission, Carburetion Versus Timed Fuel Injection", SAE paper 650863, 1965.
47. Goetsch, E., et al, "Actual Pressure Differentials in the Main Metering System of a Fore 2-V Carburetor", Ford Motor Co. Internal Report, April, 1965.
48. Muller, H. L., Kay, R. E., and Wagner, T. O., "Determining the Amount and Composition of Evaporative Losses from Automotive Fuel Systems", SAE paper No. 660407, 1966.

49. Robinson, J. E., and Wagner, R. W., "Part Throttle Vapor Lock Test Development", SAE paper 956A, 1965.
50. Shaffer, E. S., "Nozzle and Venturi Design Criteria for 4MC Carburetor", Rochester Products Internal Report, March, 1964.
51. Smith, S. B., "Effect of Change in Fuel Specifications on Carburetion", Bendix Corporation Internal Report 4190, Dec., 1944.
52. Stoltman, Donald, "The Design Evolution of the Quadrajet Carburetor", SAE paper 660127, 1966.
53. Sytz, W. E., and Harkins, J., "The Effect of Increasing Gasoline Viscosity on Engine Performance", California Research Corp. Report, April, 1961.
54. Tice, P. S., "Theory Governing Carburetor with Intake Throttle," Automotive Industries, November, 1923, pp. 1099-1101.
55. Yu, T. C., "Fuel Distribution Studies - A New Look at an Old Problem", SAE Trans., P. 610, 1963.
56. Wahrenbrock, R. J., "The Effect of Fuel Density on Carburetion", Ethyl Corp., Research Memo ERM-H13, April, 1953.

#### ENGINE AND VEHICLE TESTS

57. Bolt, J. A. and Holkeboer, D. H., "Lean Fuel-Air Mixtures for High-Compression Spark-Ignited Engines," SAE Trans., Vol. 70, 1962, pp. 195-202.
58. Bigley, H. A., Jr., Domke, C. J., and Niles, H. T., "CRC Looks at Cars, Fuels, and Vapor Lock", SAE paper 650860, 1965.
59. Cleveland, A. E., and Bishop, I. N., "Fuel Economy", SAE Journal, Aug. 1960, pp. 27-33.
60. Fuchs, E. J., "Laboratory Engine Method for Measurement of Detergency Effectiveness of Gasoline Additives on Carburetor Throttle Body Deposits," SAE paper 379D, 1961.
61. "Fuel Economy Tests at Steady Speed", Ford Motor Company Internal Reports, 1965-67.
62. Kerley, R. V. and Thurston, K. W., "The Indicated Performance of Otto-Cycle Engines", Ethyl Corp. Research paper 61-17, Nov. 1961.

AUTOMOTIVE SIMULATION TECHNIQUES

63. Huber, P., and Brown, J. R., "Computation of Instantaneous Air Flow and Volumetric Efficiency", SAE paper 812 B, 1964.
64. McAulay, K. J., Borman, G. L., et al, "Development and Evaluation of the Simulation of the Compression-Ignition Engine", SAE paper 650451, May, 1965.

FUEL PROPERTIES

65. Hurd, B. L., Jr., "Fuels for High Compression Engines", SAE preprint 260B, 1960.
66. Maxwell, J. B., "Data Book on Hydrocarbons", Van Nostrand Co., Inc., 1950.
67. Rossini, F. D., et al, "Selected Values of Physical and Thermodynamic Properties of Hydrocarbons and Related Compounds", Carnegie Press, Pittsburgh, 1953.
68. Van Duyne, R. J., "Measurement of Dynamic Surface Tension Changes in Froth-Forming Aqueous Solutions", Ph.D. thesis, University of Michigan, 1961.

GENERAL REFERENCES

69. Carnahan, B., Luther, H. A., and Wilkes, J. O., "Applied Numerical Methods", Volumes I and II, John Wiley and Sons, Inc., New York, 1964.
70. Taylor, C. F., and Taylor, E. S., "The Internal Combustion Engine", Int'l Textbook Co., 2nd Edition, 1962.
71. Van Wylen, G. J., and Sonntag, R. E., "Fundamentals of Classical Thermodynamics", John Wiley and Sons, Inc., New York, 1966.